ADVANCES AND TRENDS IN DEVELOPMENT OF PLANT FACTORIES

EDITED BY: Alejandro Isabel Luna-Maldonado, Juan Antonio Vidales-Contreras and Humberto Rodríguez-Fuentes

PUBLISHED IN: Frontiers in Plant Science

frontiers Research Topics

frontiers

ISSN 1664-8714
ISBN 978-2-88945-139-5
DOI 10.3389/978-2-88945-139-5

About Frontiers

Frontiers is more than just an open-access publisher of scholarly articles: it is a pioneering approach to the world of academia, radically improving the way scholarly research is managed. The grand vision of Frontiers is a world where all people have an equal opportunity to seek, share and generate knowledge. Frontiers provides immediate and permanent online open access to all its publications, but this alone is not enough to realize our grand goals.

Frontiers Journal Series

The Frontiers Journal Series is a multi-tier and interdisciplinary set of open-access, online journals, promising a paradigm shift from the current review, selection and dissemination processes in academic publishing. All Frontiers journals are driven by researchers for researchers; therefore, they constitute a service to the scholarly community. At the same time, the Frontiers Journal Series operates on a revolutionary invention, the tiered publishing system, initially addressing specific communities of scholars, and gradually climbing up to broader public understanding, thus serving the interests of the lay society, too.

Dedication to Quality

Each Frontiers article is a landmark of the highest quality, thanks to genuinely collaborative interactions between authors and review editors, who include some of the world's best academicians. Research must be certified by peers before entering a stream of knowledge that may eventually reach the public - and shape society; therefore, Frontiers only applies the most rigorous and unbiased reviews.
Frontiers revolutionizes research publishing by freely delivering the most outstanding research, evaluated with no bias from both the academic and social point of view.
By applying the most advanced information technologies, Frontiers is catapulting scholarly publishing into a new generation.

What are Frontiers Research Topics?

Frontiers Research Topics are very popular trademarks of the Frontiers Journals Series: they are collections of at least ten articles, all centered on a particular subject. With their unique mix of varied contributions from Original Research to Review Articles, Frontiers Research Topics unify the most influential researchers, the latest key findings and historical advances in a hot research area! Find out more on how to host your own Frontiers Research Topic or contribute to one as an author by contacting the Frontiers Editorial Office: **researchtopics@frontiersin.org**

ADVANCES AND TRENDS IN DEVELOPMENT OF PLANT FACTORIES

Topic Editors:
Alejandro Isabel Luna-Maldonado, Autonomous University of Nuevo Leon, Mexico
Juan Antonio Vidales-Contreras, Autonomous University of Nuevo Leon, Mexico
Humberto Rodríguez-Fuentes, Autonomous University of Nuevo Leon, Mexico

Growing lettuce plants in a Pilot Plant Factory at the Faculty of Agriculture of Autonomous University of Nuevo León.
Photo by Prof. Humberto Rodríguez-Fuentes

The plant factory is a facility that aids the steady production of high-quality vegetables all year round by artificially controlling the cultivation environment (e.g., light, temperature, humidity, carbon dioxide concentration, and culture solution), allowing growers to plan production. By controlling theinternal environment,plant factories can produce vegetables about two to four times faster than by typical outdoor cultivation. In addition, as multiple cultivation shelves (a multi-shelf system) are used, the mass production of vegetables in a small space is facilitated. This research topic presents some new trends on intelligent measuring systems; environment controlled and optimization; flavonoids; phenylpropanoids, transcriptomes, and bacteria.

Citation: Luna-Maldonado, A. I., Vidales-Contreras, J. A., Rodríguez-Fuentes, H., eds. (2017). Advances and Trends in Development of Plant Factories. Lausanne: Frontiers Media.
doi: 10.3389/978-2-88945-139-5

Table of Contents

Pharmaceuticals

Genetic engineering

Biofertilizers

frontiers in Plant Science

EDITORIAL
published: 09 December 2016
doi: 10.3389/fpls.2016.01848

Editorial: Advances and Trends in Development of Plant Factories

*Alejandro I. Luna-Maldonado *, Juan A. Vidales-Contreras * and Humberto Rodríguez-Fuentes **

Department of Agricultural and Food Engineering, Faculty of Agriculture, Autonomous University of Nuevo Leon, Nuevo Leon, Mexico

Keywords: plant factories, intelligent systems, environment controlled and optimization, pharmaceuticals, genetic engineering, biofertilizers

Editorial on Research Topic

Advances and Trends in Development of Plant Factories

The plant factory is a facility that aids the steady production of high-quality vegetables all year round by artificially controlling the cultivation environment (e.g., light, temperature, humidity, carbon dioxide concentration, and culture solution), allowing growers to plan production. By controlling the internal environment, plant factories can produce vegetables about two to four times faster than by typical outdoor cultivation. In addition, as multiple cultivation shelves (a multi-shelf system) are used, the mass production of vegetables in a small space is facilitated.

This research topic presents some new trends on intelligent measuring systems; environment controlled and optimization; flavonoids; phenylpropanoids, transcriptomes, and bacteria.

Among some of the new findings on intelligent measuring systems, Chen et al. developed an automated measurement system to measure and record the plant weight during plant growth in plant factory. They found that plant weights measured by the weight measurement device are highly correlated with the weights estimated by the stereo-vision imaging system. Moriyuki and Fukuda devised a novel high-throughput diagnosis system using the measurement of chlorophyll fluorescence forming an image of 7200 seedlings acquired by a CCD camera and an automatic transferring machine. They used machine learning in order to extract biological indices and predict plant growth. Previously, Hashimoto et al. (2001) applied an intelligent control system consisting of a decision system based on neuronal networks and genetic algorithms to optimize the growth of hydroponic tomato plants during the seedling stage. Hwang et al. (2014) also proposed a plant factory automatic control system to collect crop image information (illuminance, temperature, humidity, EC, pH, and CO2) and provided crop environment control and service suitable for crop growth step (crop shape, size, color, and length).

Related to environment controlled and optimization, Zheng et al. explored the effects of different density treatments on potato spatial distribution and yield in spring and fall. They concluded that increased density significantly increased potato yield, but the degree of influence associated with different growing seasons differed slightly. In Japan, there were 165 plant factories with artificial lighting (Kozai et al., 2015). Wang et al. added an air exchanger for cooling in plant production systems with artificial light (PPAL). They found that using air exchanger to introduce outdoor cold air is as an effective way to reduce electric-energy consumption with little effects on plant growth in a PPAL. Besides, the cultivation methods in a plant factory with artificial lighting (PFLA) were studied by Zhang et al., retarded senescence of outer leaves of lettuce and found white LEDs are more appropriate for lettuce growth than red or blue LEDs. In another research, Li et al. applied LED lighting [LED with zoom lenses (Z-LED) and conventional non-lenses LED (C-LED)]. The improvement saved over half of the light source electricity, while the temperature and rate of photosynthesis abruptly decreased, causing reductions in plant yield and nitrate content, while

OPEN ACCESS

Edited and reviewed by:
Diego Rubiales, Spanish National Research Council, Spain

****Correspondence:***
Alejandro I. Luna-Maldonado
alejandro.lunaml@uanl.edu.mx
Juan A. Vidales-Contreras
juan.vidalescn@uanl.edu.mx
Humberto Rodríguez-Fuentes
humberto.rodriguezfn@uanl.edu

Specialty section:
This article was submitted to Crop Science and Horticulture, a section of the journal Frontiers in Plant Science

Received: *31 October 2016*
Accepted: *23 November 2016*
Published: *09 December 2016*

Citation:
Luna-Maldonado AI, Vidales-Contreras JA and Rodríguez-Fuentes H (2016) Editorial: Advances and Trends in Development of Plant Factories. Front. Plant Sci. 7:1848. doi: 10.3389/fpls.2016.01848

having no negative effects on morphological parameters and photosynthetic pigment contents. About nighttime supplemental LED inter-lighting, Tewolde et al. found nighttime LED inter-lighting can effectively improve tomato plant growth and yield with lower energy cost compared with daytime both in summer and winter. Moreover, Cao et al. achieved that tomato inside of a solar greenhouse increased their fresh weight with the increase of RL NB frequencies. On the other hand, Wang et al. found that leaf photosynthetic capacity and photosynthetic rate increased with decreasing Red/Blue lights ratio until 1. However, shoot dry weight increased with increasing Red/Blue lights ratio with the greatest value under Red/Blue = 12 treatment. They concluded that quantitative Blue light could promote photosynthetic performance or growth by stimulating morphological and physiological responses. Miyagi et al. (2017) found that synergistic effects of monochromic LED combined with high CO_2 and nutrients would be beneficial alternatives for cultivation of lettuce in the plant factory. Shimokawa et al. (2014) concluded that simultaneous red and blue irradiation promote plant growth more effectively than monochromatic and fluorescent light irradiation. They also found that alternating red and blue light accelerated plant growth significantly even when the total light intensity per day was the same as with simultaneous irradiation. The fresh weight of the plant doubles compared to normal LED cultivation methods. The plant factory can increase harvests and sales using this this method (Showa, 2016).

The production of pharmaceuticals in a plant factory represents an opportunity for health benefits from plants. Flavonoids are a group of plant metabolites thought to provide health benefits through cell signaling pathways and antioxidant effects (Spencer, 2016). Dong et al. studied soluble flavonoids and found that "Xiangfen 1" banana can be a rich source of natural antioxidants in human diets. Jeong et al. (2015) characterized the polyphenolic contents of lettuce leaves grown under different night-time temperatures and cultivation. Plant-derived phenylpropanoids (PPPs) compose the largest group of secondary metabolites produced by higher plants (Korkina et al., 2011). Dwivedi et al. reviewed the progress for accessing variation in PPPs in germplasm collections. PPPs are a diverse chemical class with immense health benefits that are biosynthesized from the aromatic amino acid L-phenylalanine.

Genetic engineering of plants deals on the creation of plants to resist herbicides and pests, but also to improve the quality of the crops in terms of consumers (Sévenier et al., 2002). Xing et al. found complex regulatory mechanisms involved in floral induction, flower bud formation, and flowering characteristics, which might reflect the genetic variation of the flowering gene and their data provided a foundation for the further exploration of apple diversity and gene–phenotype relationships, and for future research on molecular breeding to improve apple and related species. Higashi et al. studied circadian oscillation of the lettuce transcriptome under constant light and light–dark conditions and found gene expression pattern is related to photosynthesis and optical response performs normally in lettuce. Higashi et al. detected diurnal variation of tomato transcriptome through the molecular timetable method in a sunlight-type plant factory. They found circadian clock mediate the optimization for fluctuating environments in the field and it has possibilities to enhance resistibility to stress and floral induction by controlling circadian clock through light supplement and temperature control. Tanigaki et al. (2016) in their research suggested that the regulation of gating stomata does not depend predominantly on TOC1 and significantly reflects the extracellular environment. Besides, Zhang et al. studied transcriptome analysis of *Dendrobium officinale* and its application to the identification of genes associated with polysaccharide synthesis valuable clues for identifying candidate genes involved in polysaccharide biosynthesis and elucidating the mechanism of polysaccharide biosynthesis. On the other hand, Hiwasa-Tanase and Ezura reviewed on molecular breeding to create optimized crops: From genetic manipulation to potential applications in plant factories and found that Cost-effectiveness is improved from the use of cultivars that are specifically optimized for closed system cultivation. Lai et al. studied two LcbHLH transcription factors interacting with LcMYB1 in regulating late structural genes of anthocyanin biosynthesis in *Nicotiana and Litchi chinensis* during anthocyanin accumulation and found LcbHLH1 and LcbHLH3 are essential partner of LcMYB1 in regulating the anthocyanin production in tobacco and probably also in litchi. The LcMYB1-LcbHLH complex enhanced anthocyanin accumulation may associate with activating the transcription of DFR and ANS.

Bacterial biofertilizers can improve plant growth through several different mechanisms: (i) the synthesis of plant nutrients or phytohormones, which can be absorbed by plants, (ii) the mobilization of soil compounds, making them available for the plant to be used as nutrients, (iii) the protection of plants under stressful conditions, thereby counteracting the negative impacts of stress, or (iv) defense against plant pathogens, reducing plant diseases or death (García-Fraile et al., 2015). Kifle and Laing isolated and screened bacteria for their diazotrophic potential and their influence on growth promotion of maize seedlings in greenhouses. They identified that isolates showed significant effect on at least two growth parameters were at species or genera level.

AUTHOR CONTRIBUTIONS

All authors listed have made substantial, direct, and intellectual contribution to the work, and approved it for publication.

FUNDING

AL acknowledges support from PAYCIT UANL 2015. JV acknowledges support from CONACYT. HF acknowledges support from Administration of Faculty of Agriculture, Autonomous University of Nuevo Leon.

ACKNOWLEDGMENTS

As the topic editors, we would like to thank all our colleagues who contributed their articles. We would also like to express our gratitude to the numerous colleagues who contributed to

the success of this Research topic by acting as reviewers or editors. We are especially grateful for excellent technical support provided by the editorial office and the chief editors. Finally, we dedicate this book to the memory of Kei Nakaji, Emeritus Professor at Kyushu University, whose devotion to his students and agricultural ecology will be always remembered.

REFERENCES

García-Fraile, P., Menéndez, E., and Rivas, R. (2015). Role of bacterial biofertilizers in agriculture and forestry. *AIMS Bioeng.* 2, 183–205. doi: 10.3934/bioeng.2015.3.183

Hashimoto, Y., Murase, H., Morimoto, T., and Torii, T. (2001). Intelligent systems for agriculture in Japan. *IEEE Control Syst.* 21, 71–85. doi: 10.1109/37.954520

Hwang, J., Jeong, H., and Yoe, H. (2014). Study on the plant factory automatic control system according to each crop growth step. *Adv. Sci. Technol. Lett.* 49, 174–179. doi: 10.14257/astl.2014.49.33

Jeong, S. W., Kim, G. S., Lee, W. S., Kim, Y. H., Kang, N. J., Jin, J. S., et al. (2015). The effects of different night-time temperatures and cultivation durations on the polyphenolic contents of lettuce: application of principal component analysis. *J. Adv. Res.* 6, 493–499. doi: 10.1016/j.jare.2015.01.004

Korkina, L., Kostyuk, V., De Luca, C., and Pastore, S. (2011). Plant phenylpropanoids as emerging anti-inflammatory agents. *Mini Rev. Med. Chem.* 11, 823–835. doi: 10.2174/138955711796575489

Kozai, T., Niu, G., and Takagaki, M. (eds.) (2015). *Plant Factory: An Indoor Vertical Farming System for Efficient Quality Food Production*. Academic Press.

Miyagi, A., Uchimiya, H., and Kawai-Yamada, M. (2017). Synergistic effects of light quality, carbon dioxide and nutrients on metabolite compositions of head lettuce under artificial growth conditions mimicking a plant factory. *Food Chem.* 218, 561–568. doi: 10.1016/j.foodchem.2016.09.102

Sévenier, R., van der Meer, I. M., Bino, R., and Koops, A. J. (2002). Increased production of nutriments by genetically engineered crops. *J. Am. Coll. Nutr.* 21(Suppl. 3), 199S–204S. doi: 10.1080/07315724.2002.10719266

Shimokawa, A., Tonooka, Y., Matsumoto, M., Ara, H., Suzuki, H., Yamauchi, N., et al. (2014). Effect of alternating red and blue light irradiation generated by light emitting diodes on the growth of leaf lettuce. *bioRxiv*, 003103. doi: 10.1101/003103. Available online at: http://biorxiv.org/content/early/2014/02/28/003103.full.pdf+html

Showa, D. (2016). *The Shigyo Method for Cultivation. LED Irradiation Optimized for Plant Growth Facilities.* Available online at: http://www.sdk.co.jp/english/products/160/164/13978.html

Spencer, M. (2016). *The Need for Balance – Dealing with the Causes of Meniere's. 1st Edn*. Smashwords Edition.

Tanigaki, Y, Higashi, T, Takayama, K, Nagano, A. J., Honjo, M. N., and Fukuda, H. (2016). Transcriptome analysis of plant hormone-related tomato (*Solanum lycopersicum*) genes in a sunlight-type plant *Factory*. *PLoS One* 11:e0150788. doi: 10.1371/journal.pone.0150788

Conflict of Interest Statement: The authors declare that the research was conducted in the absence of any commercial or financial relationships that could be construed as a potential conflict of interest.

frontiers in Plant Science

ORIGINAL RESEARCH
published: 31 March 2016
doi: 10.3389/fpls.2016.00392

An Automated and Continuous Plant Weight Measurement System for Plant Factory

*Wei-Tai Chen, Yu-Hui F. Yeh, Ting-Yu Liu and Ta-Te Lin**

Department of Bio-Industrial Mechatronics Engineering, National Taiwan University, Taipei, Taiwan

In plant factories, plants are usually cultivated in nutrient solution under a controllable environment. Plant quality and growth are closely monitored and precisely controlled. For plant growth evaluation, plant weight is an important and commonly used indicator. Traditional plant weight measurements are destructive and laborious. In order to measure and record the plant weight during plant growth, an automated measurement system was designed and developed herein. The weight measurement system comprises a weight measurement device and an imaging system. The weight measurement device consists of a top disk, a bottom disk, a plant holder and a load cell. The load cell with a resolution of 0.1 g converts the plant weight on the plant holder disk to an analog electrical signal for a precise measurement. The top disk and bottom disk are designed to be durable for different plant sizes, so plant weight can be measured continuously throughout the whole growth period, without hindering plant growth. The results show that plant weights measured by the weight measurement device are highly correlated with the weights estimated by the stereo-vision imaging system; hence, plant weight can be measured by either method. The weight growth of selected vegetables growing in the National Taiwan University plant factory were monitored and measured using our automated plant growth weight measurement system. The experimental results demonstrate the functionality, stability and durability of this system. The information gathered by this weight system can be valuable and beneficial for hydroponic plants monitoring research and agricultural research applications.

Keywords: growth curve modeling, fresh weight, hydroponics, vegetables, plant growth, load cell

OPEN ACCESS

Edited by:
Alejandro Isabel Luna-Maldonado, Universidad Autónoma de Nuevo León, Mexico

Reviewed by:
Hao Peng, Washington State University, USA
Chong Zhang, University of Maryland–Baltimore, USA

****Correspondence:***
Ta-Te Lin
m456@ntu.edu.tw

Specialty section:
This article was submitted to Crop Science and Horticulture, a section of the journal Frontiers in Plant Science

Received: *31 January 2016*
Accepted: *14 March 2016*
Published: *31 March 2016*

Citation:
Chen W-T, Yeh Y-HF, Liu T-Y and Lin T-T (2016) An Automated and Continuous Plant Weight Measurement System for Plant Factory. Front. Plant Sci. 7:392. doi: 10.3389/fpls.2016.00392

INTRODUCTION

A plant factory is an indoor cultivation space where the growing environment of plants is carefully controlled, including factors such as light, temperature, carbon dioxide, and nutrient solution. Hydroponics is a cultivation method commonly used in plant factories, where plants are grown without soil, but rather with nutrient solution. Compared with soil cultivation, hydroponics has the advantages of conservation of water and nutrients, as well as more complete control of the environmental factors affecting plant growth (Jones, 2004). A plant factory is intended to achieve the stable and optimized production of plants by controlling the growing environment. Therefore, growing plants in a plant factory also becomes a control problem in engineering. Plant growth is responsive to the environmental parameters. Therefore, by manipulating the growing environment, plant growth can be controlled as expected. There already exist different sensors

for measuring environment parameters, such as photometer, thermometer, humidity sensor, and electrolyte analyzer. In order to measure plant responses to the environment, various approaches have been developed to quantify plant features such as leaf area and plant weight as affected by different growing conditions.

To quantify plant growth, plant weight is an important feature. However, the traditional method for plant weight measurement, which measures plant weights manually by picking plants up and measuring weight using an electronic balance, is not only destructive but also laborious. Sase et al. (1988) measured the weight and leaf area of lettuce under different sources of light. The results showed no significant difference in fresh weight, dry weight and plant area between lettuce grown under high-pressure sodium lamps and metal halide lamps. Therefore, the research indicated that spectral power radiation from lamps has no influence on fresh or dry weight on a specific range of photosynthetic photon flux (Sase et al., 1988). Van Henten and Bontsema (1995) showed a linear relation between the leaf area and the dry weight of lettuce through examining the results from image processing methods and destructive plant weight measurements; they indicated the possibility of a non-destructive plant growth measurement method using the plant leaf area to estimate the plant dry weight. As there are too many input environmental parameters to be adjusted in a plant factory, the traditional weight measurement method can hardly be applied due to its time and labor costs. Therefore, an automatic plant weight measurement instrument which can measure plant weight continuously during plant growing period is needed for plant factory.

Some automated plant weight measurement instruments have been developed. Takaichi et al. (1996) developed an instrument which automatically measures tomato plant fresh weight using two electronic balances. A tomato plant growing in a pot with nutrient solution was suspended. The total weight of the pot was measured using one electronic balance, while the weight of nutrient solution was measured using the other electronic balance. This instrument automatically and continuously realizes plant weight measurement for hydroponics (Takaichi et al., 1996). However, the instrument can only be applied in the laboratory, as it requires two electronic balances to measure a single plant's weight. Baas and Slootweg (2004) developed an on-line plant monitoring equipment for horticulture, which measures the weight of a group of Gerbera using multiple load cells. A group of Gerbera was growing on the Rockwool slab. The weight system mounted with load cells was put under the Rockwool slab to automatically measure the total weight of plants (Baas and Slootweg, 2004). This instrument achieves automated plant weight measurements in real cultivational space; however, it can only measure the total weight of a group of Gerbera, not a single plant's weight. In order to build a plant growth monitoring model which is responsive to environment changes, the environment parameters must stay consistent for all growing plants, which is difficult to achieve. Therefore, an instrument made for single plant measurement is still desired. Helmer et al. (2005) developed a system called CropAssist, which can automatically measure plant weight and transpiration for vine crops, such as tomatoes and cucumbers, using pairs of load cells and a trough system. CropAssist is a commercial system which can measure plant weights and transpiration rates of single or multiple plants using two load cells. The weights of vine plants were measured by the upper load cell which suspends the vine plants. The transpiration rates were estimated by the lower load cell which measures weight changes of growing media (Helmer et al., 2005). However, this system can only work for vine crops and not suitable for leafy vegetables, because it is not convenient to hang leafy vegetables and leafs touching the ground can introduce notable errors to CropAssist system. Furthermore, considering space efficiency, CropAssist system is too bulky to use in plant factories.

In the present research, an automated and continuous plant weight monitoring system is proposed. This system includes two main parts: an automated plant weight measurement instrument and a stereo-vision imaging system. Since the plant weight measurement instrument consists of two acrylic plates and a load cell, it is easy to build and apply in practice. Hydroponic plants were grown on our instrument from budding to harvesting. During the plant growth period, the weight of the plants was measured using this weight measurement instrument, and compared with imaging features captured by the cameras in the stereo-vision imaging system. These instruments were applied to measure weight growth of Boston lettuce and coral lettuce cultivated in the National Taiwan University plant factory. Also, destructive measurements were carried out to validate the measurement accuracy of this system. Finally, continuous plant weights were measured by both this weight measurement instrument and the imaging system.

MATERIALS AND METHODS

Instrument Design

The sensor used to measure plant weight in our weight measurement instrument is a load cell. A load cell is a transducer which converts a force signal into an electric signal. In this research, LDB-2 kg load cells (Esense Scientific Ltd., Taiwan) were used, with a measuring resolution of 0.1 g, and capability to measure weight from 0 to 2 kg. Our automated weight measurement instrument has four components: a top disk, a bottom disk, a plant holder and a load cell. As **Figure 1** illustrates, the plant is fixed on the sponge block, which is clinched by the plant holder. The plant holder is hung on the top disk, which

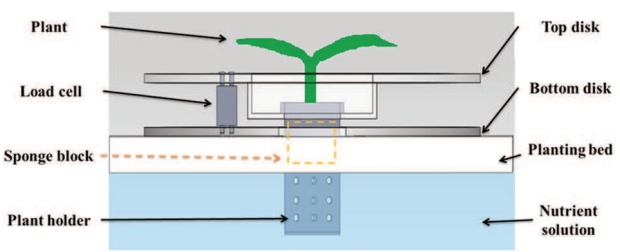

FIGURE 1 | The design of weight measurement instrument.

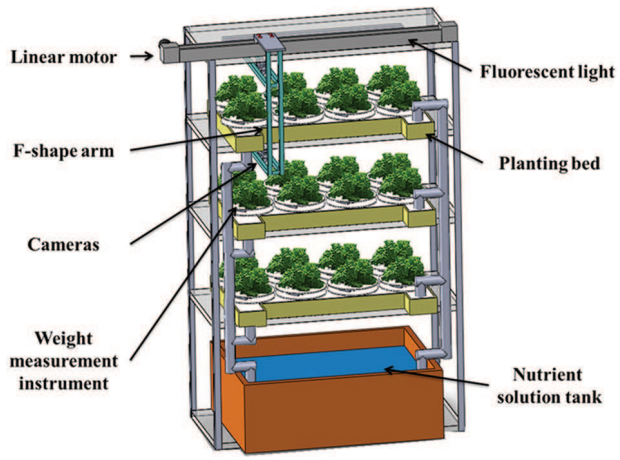

FIGURE 2 | System schematic diagram in a plant factory.

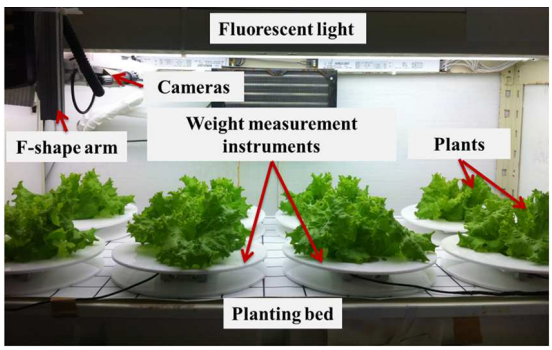

FIGURE 3 | Real scene in National Taiwan University plant factory.

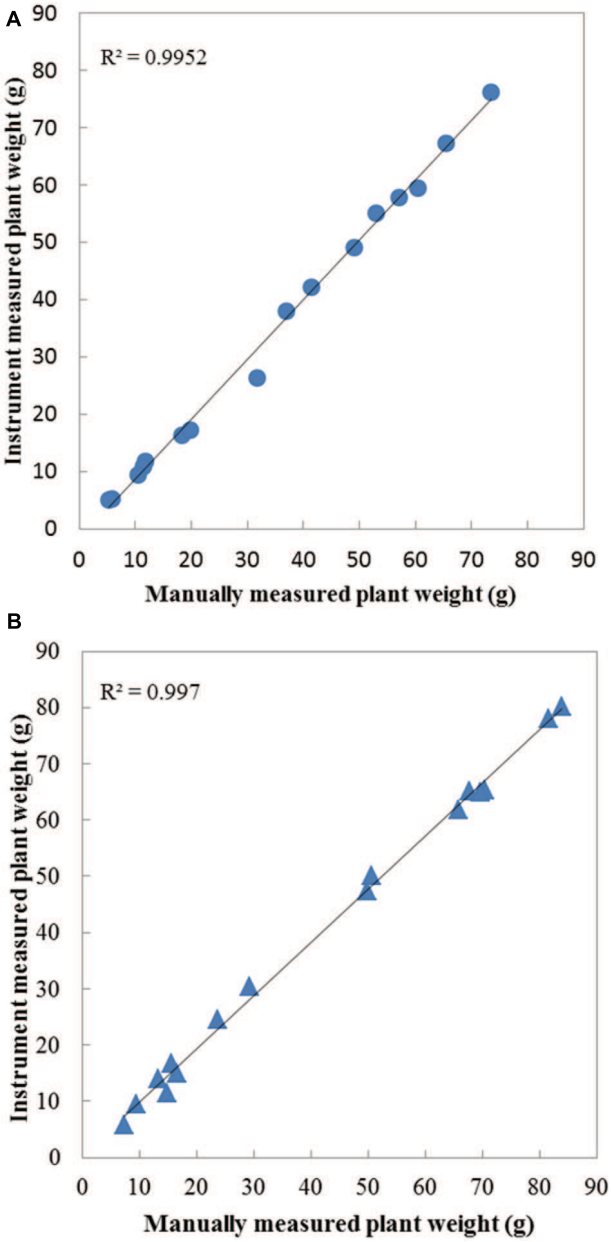

FIGURE 4 | Weight measurement accuracy validation for (A) Boston lettuces (circle) and (B) coral lettuces (triangle).

is also fixed with one top end of the load cell. The bottom disk is fixed on the bottom of the other end of the load cell. Since the load cell connects the top disk and the bottom disk, and the bottom disk is placed on the planting bed for support, the total weight on the top disk creates a downward force onto the load cell which is then converted to an analog electric signal. The load cell is connected to a amplifier and conditioner module (Model: JS300, Jihsense Ltd., Taiwan) which amplifies and converts the electric signal to a proportional weight value. This weight signal is then sent to the computer via RS232 connector. The plant to be measured is fixed and grown on the plant holder. Therefore, as the plant grows, the weight change can be measured continuously by the load cell. The plant weight measured by the instrument is only the plant shoot, since the plant root is immersed in the nutrient solution and the weight is canceled out by the buoyant force. The top disk and bottom disk both have an opening hole in the middle, so the shoot part can grow upward through the top disk, and the root can grow downward and immerse in a nutrient solution of the hydroponics system. The top disk is designed in a bowl shape to lower the plant holder, so the root can immerse into the nutrient solution even during the budding period. The plant holder is designed as an enclosure with holes to avoid roots tangling with other plants, and to ensure circulation of nutrient solution.

System Setup and Cultivation Environment

All experiments were carried out in the National Taiwan University plant factory. This pilot plant factory is an indoor hydroponics environment. The environmental conditions, including light, temperature and nutrient solution, are artificial, and controllable. The light source is provided by the fluorescent

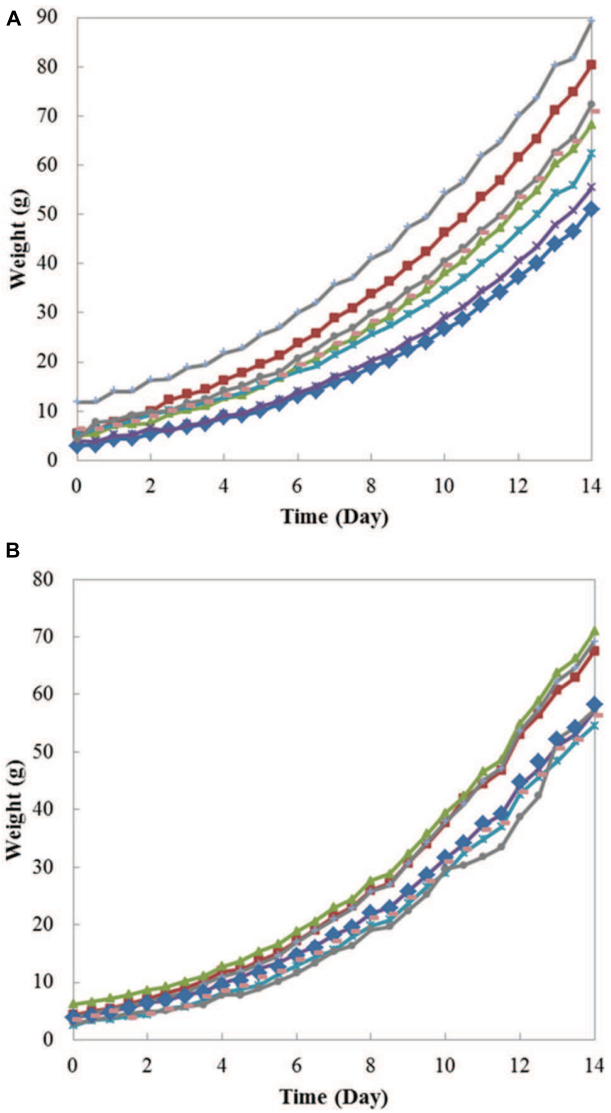

FIGURE 5 | Plant weight growth curves of (A) eight Boston lettuces and (B) eight coral lettuces.

light instead of sunlight, so the light intensity and light period is controllable. The average light intensity on the planting bed is 169 μmole/s.m^2. The temperature in the planting bed is stably controlled and monitored by an air conditioner and a temperature sensor. The day and night temperature were set at 23 and 19°C, respectively, with 16 h of light per day. The light period starts at 8:00 and the dark period starts at 0:00. The typical CO_2 concentration in the plant factory ranges from 300 to 500 ppm in 1 day timeframe. The nutrient solution is an A–B bottle mixed solution containing Magnesium carbonate, Calcium carbonate, Potassium carbonate, chelated iron, boric acid, Sodium molybdate, Copper sulfate, Manganese sulfate, Potassium chloride, Potassium phosphate, and Zinc sulfate, provided by the Department of Horticulture and Landscape Architecture of National Taiwan University.

This weight monitoring system was set up in the planting room of the National Taiwan University plant factory, as shown in **Figures 2** and **3** shows the real scene of one planting bed. There are multiple vertically arranged planting beds in one growing shelf stand. For each planting bed, there are T5 fluorescent lights to provide illumination, and circulating essential nutrient solution for the plants. The nutrient solution is circulated with the nutrient tank at the bottom of the growing shelf stand to ensure a stable supply of the nutrient. There are eight holes uniformly distributed on the 110 cm × 50 cm planting bed, with one weight measuring instrument in each hole, so eight plants can be monitored concurrently in one planting bed. The opening of the weight measurement instrument bottom disk is aligned with the hole of the planting bed to ensure that the root can immerse in nutrient solution. The plant weight's analog electric signal provided by the load cell is transferred to a computer via an analog-digital converter for recording purpose. A user interface program was developed to record and display the plant weight in real time. In order to compare plant weight measured by load cell with those measured by the stereo-vision method, an imaging system is used to simultaneously measure geometric features of plants. Cameras mounted on the F-shape arm are driven by a motor to take images above the same plant bed. Geometric features of measured plants are calculated based on the stereo-vision approach. The details of the imaging system and algorithms are proposed and provided in a previous paper (Yeh et al., 2014).

In this research, two species of lettuce, Boston lettuce (Known-you seed Co., Ltd. LS-047) and coral lettuce (Known-you seed Co., Ltd. LS-005) were grown and measured using this weight monitoring system and the imaging system. The plants were grown in nursery pots for 14 days for germination. After the roots of the plants were long enough to immerse in the nutrient solution, the plants were transplanted to the weight measurement instrument's plant holders to grow on the planting bed. In each experiment, weight measurement instruments with plants in the plant holder were arranged carefully on the planting bed. The nutrient solution was circulating between the planting beds and storage tank with a pump to ensure that the nutrition is uniform during the experiments.

RESULTS

Weight Measurement Validation

In order to validate the accuracy of our weight measurement instrument, 16 Boston lettuces and 16 coral lettuces which were grown were picked up and measured destructively using an electronic balance across the 14 day growing period. **Figure 4** shows the results of plant weight measurement validation of the Boston and coral lettuces. The vertical axis represents the last weight measurement recorded by the instrument before destructive measurement. The horizontal axis is the weight of the plant shoot part measured by an electronic balance, which is regarded as the ground truth. Since the weight of the plant root was canceled out by the buoyant force, as the density of roots is very close to nutrient solution, an average density of

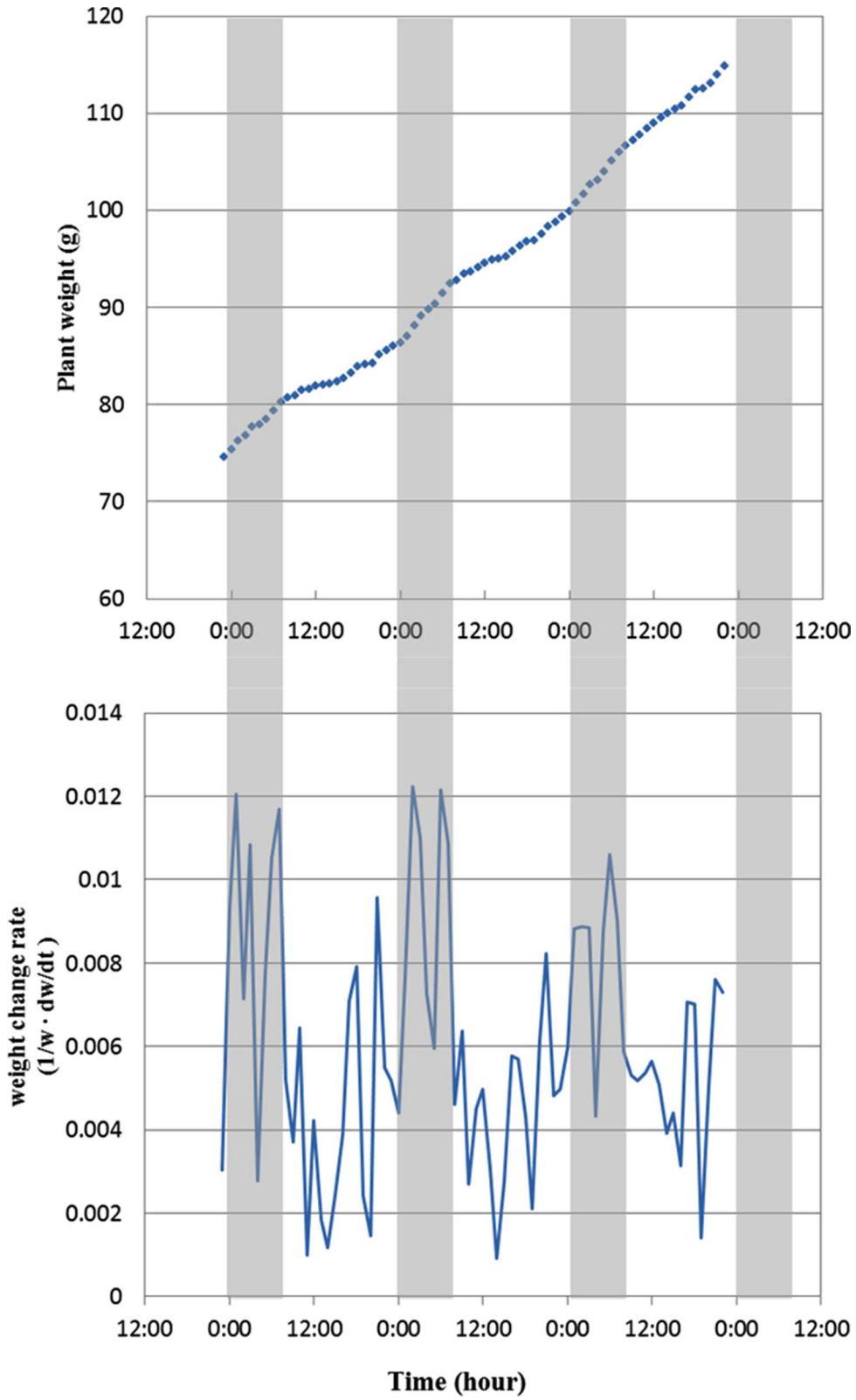

FIGURE 6 | Diurnal change of plant weight (top) and weight change rate (bottom) from day 15 to day 18 of the growing period. The gray area indicates the dark period, and white area is light period. The weight change rates are calculated as the weight difference between previous and current hour over current hour weight.

0.98 g/cm^3 for lettuces and 0.99 g/cm^3 for the nutrient solution. The plant weight measured using this instrument is close to the shoot part only. The average error between the instrument's weight measurement and electronic balance's measurement for the Boston lettuce is 5.66, and 6.99% for the coral lettuce.

Since this weight measurement instrument is designed not to affect plant growth, one round of cultivation experiment was carried out to confirm this design principle. In this validation experiment, 16 Boston lettuces were monitored for 24 days, eight of them were grown with the weight measurement instrument on the planting bed and the other eight were grown without the instrument. At the end of the experiment, the plant weights were measured by the electronic balance; eight Boston lettuces grown on our instrument had an average weight of 202.1 g with a standard deviation of 19.2 g. The other eight Boston lettuces grown solely on a planting bed had an average weight of 201.3 g with a standard deviation of 26.4 g. It is clear that the plant weights with and without the weight measurement instrument are close and the appearance is alike, which proves that the instrument does not affect the plant growth.

Continuous Weight Measurement

This weight measurement instrument measures individual plant's weight non-destructively and continuously in a hydroculture environment. Therefore, the growth of individual plants during the growth period can be monitored and recorded using this instrument. **Figure 5** shows the weight growth curves of eight Boston lettuces and eight coral lettuces measured. Each point on the figure is the average weight measured in that particular hour. It can be seen that both Boston lettuce and coral lettuce show similar weight growing pattern. At the beginning, the weight changes were relatively small, since the plants were just transplanted onto the planting bed. This is the root growing period. The weight changed faster as the plants grew larger.

Based on plant growth curve, further information can be extracted and analyzed. **Figure 6** shows the diurnal change of a Boston lettuce in weight from day 15 to day 18 of the growing period. The weight change rates are calculated as the weight difference between previous and current hour over current hour weight. The result shows a diurnal pattern of plant weight change rates. The change rates are all positive but smaller at the beginning of the light period and larger at the end of light period. The plant weight change rates remain large during the dark period. This phenomenon coincides with other researches which show plants grow rhythmically in association with light accessibility (Normann et al., 2007; Nozue et al., 2007). This result shows that the weight measurement precision is sufficient to detect plant growth rhythm due to light accessibility; thus, the system provides another useful function for plant physiological research.

Plant Weight Measurement Instrument and Imaging Measurement System

In this monitoring system, there is another method to measure plant weight, the stereo-vision imaging system. The weight and imaging feature of plants obtained show high correlation

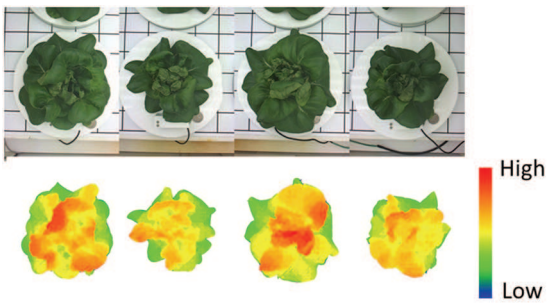

FIGURE 7 | The (top) is the raw image of Boston lettuces and the (bottom) is the corresponding pseudo-color depth image calculated by stereo-vision algorithm.

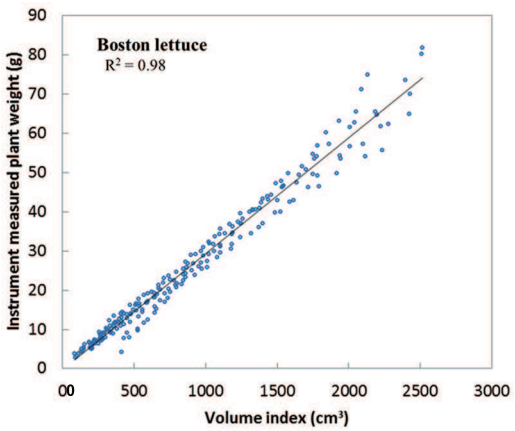

FIGURE 8 | Linear model built between plant weight and plant volume index.

across plant growing periods. Eight Boston lettuces were grown and measured by both the weight measurement instrument and the stereo-vision imaging system. By applying stereo-vision techniques, the plant volumes can be calculated from captured plant images, as shown in **Figure 7**. In **Figure 7**, the top is the raw image of Boston lettuces and the bottom is the corresponding pseudo-color depth image calculated by stereo-vision algorithm. The plant volume index can be further derived based on the depth image of the plants. Since both weight and vision measurement were taken continuously during the plant growth period, the relationship between plant weight and plant volume index can be found. **Figure 8** shows that a linear model existed between plant weight and plant volume index based on this round of experiment, and a high R-square of 0.98 was obtained. Based on this linear model, plant weights can then be estimated based on the volume index data, as shown in **Figure 9**. As the weight and volume index of plants have a linear relationship between them, the growth curves of weight estimated by the volume index would have the same pattern as the volume index ones as shown in **Figures 9A,C**. The errors between predicted weight and measured weight across the growth period are plotted in **Figure 9D**. It is clear that the errors are within 1.5 g for the first

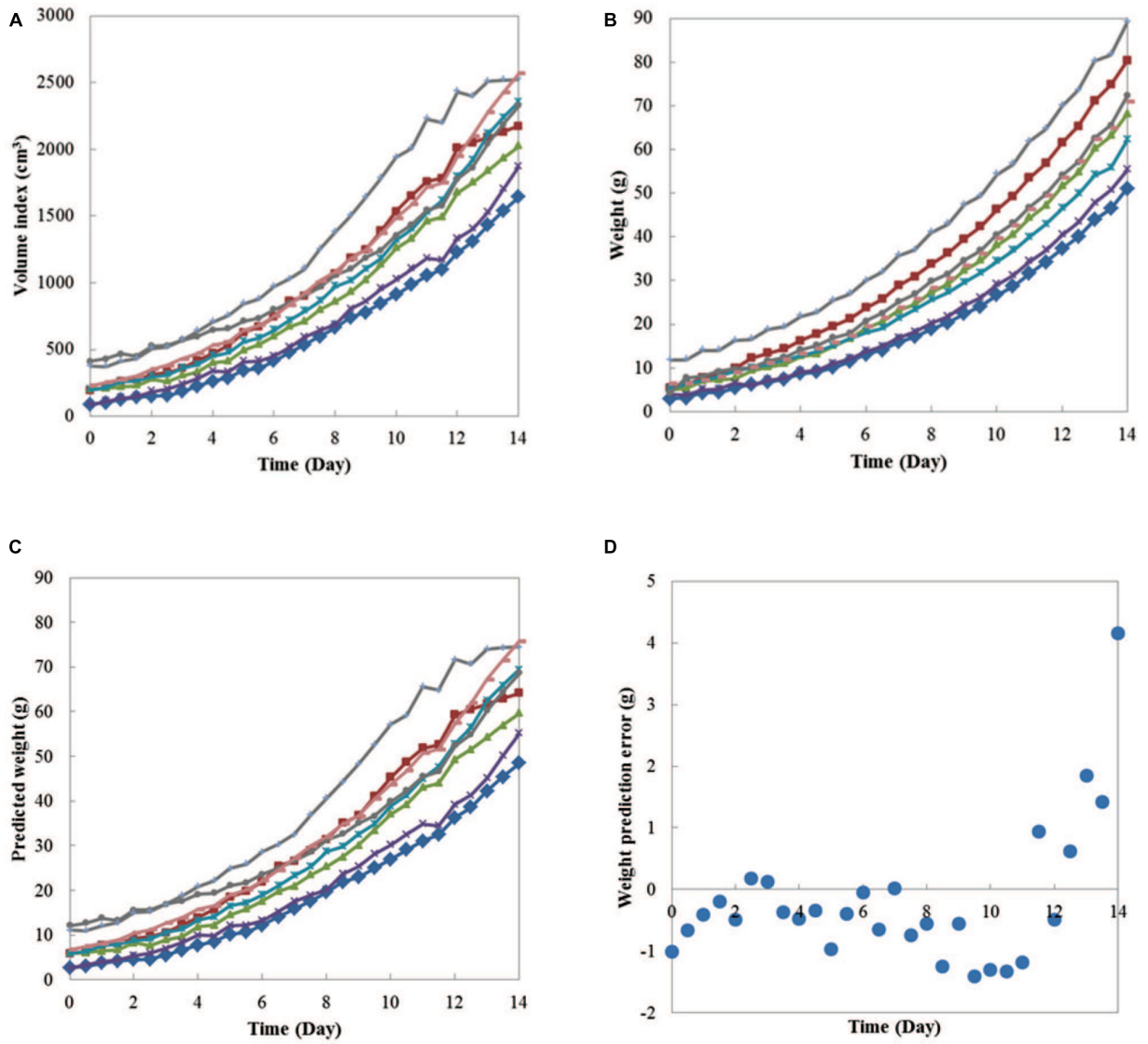

FIGURE 9 | Growth curves of eight Boston lettuces. (A) volume index measured by the imaging system; **(B)** weight measured by the weight measurement instrument; **(C)** weight predicted from the volume index measured; and **(D)** the prediction error over the growth period.

10 days and relatively larger at the later part of the growth period. This is understandable: as the plant grows bigger, the error of volume estimation from the image becomes greater due to void space in the plant volume. Hence, the weight estimated by the volume index is affected by this cumulative error. However, this estimation error is still much below 1% of the actual weight. The result shows the possibility and capability of estimating plant weight from the volume measurement using a simple imaging system.

DISCUSSIONS

For both the Boston lettuce and coral lettuce, compared with the traditional destructive measurement method, the weight measured by our instrument has minor error; however, automated and non-destructive measurement is achieved. Furthermore, the result shows that the weight measurement instrument can be applied to hydroponic leafy plants which can be of different geometric shapes. In our weight measurement instrument design, the top disk is used to support hanging down leaf. For different plant species, the diameter of top disk can to be changed accordingly in order to support all hanging down leaf of plant. Also, the hole on the top disk and bottom disk can be modified to the size for stems and roots to fit.

From the results presented, the weights between plants disperse due to the spatial non-uniformity of light intensity, as well as temperature variation to each plant. The plants grew faster with the higher light intensity supplied. The difference between Boston lettuce and coral lettuce can also be pointed

out via comparing two figures in **Figure 5**. The coral lettuces generally have lighter weights than the Boston ones with smaller variance in weight between plants. This result shows that the instrument can measure plant weight continuously during the growth period. In a plant factory, small variation of plant weight is to be expected. Thus, besides the final plant weight, the variability of plant weight is an indicator for the growers to adjust their operations and environmental parameters. Using the current measurement system, a couple of plant growth curves can be acquired spontaneously and concurrently. Compared with traditional destructive measurements, which require 100s of manual measurements to get same amount of data, our instrument can reduce labor and save time for experiments. Hence, this continuous weight measurement system is an efficient tool for plant factories to obtain optimum growing condition of crops.

Comparing the plant weight instrument and the imaging system, the automated weight measurement system is required to calibrate the imaging system. Hence, the imaging system cannot be applied solely at the beginning. For different growing environment and different species of crop, the calibration needs to be retained again. Therefore, both the automated imaging system and weight measurement system are needed at the set up phase of the system. The automated weight measurement system is more compact and portable to fit different hydroponic environment. Furthermore, the automated weight instrument provides direct measurements, no calibration required. On the other hand, the main advantage of using imaging information is that the weights of multiple plants only need to be measured once after the calibration model between plant weight and volume index is determined. The imaging measurement system is equipped with moving cameras, so only a few cameras are required to measure the plant weight of numerous plants by converting the volume index to estimated plant weight using the calibration model. It is therefore worth noting that the weight measurement instrument exhibits another important functionality to efficiently build a calibration model between image features (projected leaf area, volume index, etc.) and the plant weight for specific plants. This kind of calibration model was usually difficult to build and could only be obtained using destructive method.

Nevertheless, in the future study, we aim to build an instrument based on this design to measure the weight of whole plant, including the shoot weight and the root weight separately. The hole on the disk is large enough for the stem of lettuce to grow throughout the entire growth period. In addition, the hole do not affect the stand stability of lettuces, since the plant is not supported by the hole of disk but fixed on the sponge block, which is clamped by the plant holder. For root weight measurement, it is possible by draining out the nutrient solution to measure the whole plant weight and thus to obtain the root weight.

CONCLUSION

In this research, an automated, non-destructive plant weight measurement system for hydroponic plants is developed, which includes a self-developed weight measurement instrument and a stereo-vision imaging system. The weight measurement instrument made of a load cell and acrylic plates is able to continuously measure the weight of the plant shoot part not specific to any hydroponic plant. The accuracy of the instrument is validated by comparing instrument results with electronic balance readings with an average of 6% measurement error. The experiment's results also show that plant growth is not affected by the attachment of the instrument to the plant. Successful measurements of growth curves of Boston lettuce and coral lettuce in a plant factory were demonstrated. Furthermore, the diurnal pattern of plant weight change rate in light and dark periods can be observed through this system. There is another approach to retrieve plant weight during plant growth period, which is to use plant weight and imaging measurement to find a calibration model between them. Once the calibration model is found, only the image information of plants is needed to estimate plant weight during the plant growth period. Below 1% error in weight estimation across the whole growth period is demonstrated. This research shows the functionality of this automated weight measurement system and the possibility of future contribution in practical applications for plant factories, as well as for various plant physiological researches.

AUTHOR CONTRIBUTIONS

W-TC, T-TL: conception, design, and implementation of the research; W-TC, Y-HY, T-YL, T-TL: acquisition and analysis of the data; WC, T-TL: interpretation of data; WC, Y-HY, T-TL: drafting the manuscript.

ACKNOWLEDGMENT

This work was supported by the Council of Agriculture (grant no. 104AS-16.4.1-ST-A6, to TL).

REFERENCES

Baas, R., and Slootweg, C. (2004). On-line acquisition of plant related and environmental parameters (plant monitoring) in gerbera: determining plant responses. *Acta Hortic.* 654, 139–146. doi: 10.17660/ActaHortic.2004.654.14

Helmer, T., Ehret, D. L., and Bittman, S. (2005). CropAssist, an automated system for direct measurement of greenhouse tomato growth and water use. *Comput. Electron. Agric.* 48, 198–215. doi: 10.1016/j.compag.2005.04.005

Jones, J. B. Jr. (2004). *Hydroponics: A Practical Guide for the Soilless Grower*, 2nd Edn. Boca Raton, FL: CRC Press.

Normann, J., Vervliet-Scheebaum, M., Albrechtová, J. T. P., and Wagner, E. (2007). "Rhythmic stem extension growth and leaf movements as markers of plant behaviour: the integral output from endogenous and environmental signals," in *Rhythms in Plants: Phenomenology, Mechanisms, and Adaptive*

Significance, eds S. Mancuso and S. Shabala (New York, NY:Springer), 199–217.

Nozue, K., Covington, M. F., Duek, P. D., Lorrain, S., Fankhauser, C., Harmer, S. L., et al. (2007). Rhythmic growth explained by coincidence between internal and external cues. *Nature* 448, 358–361. doi: 10.1038/nature05946

Sase, S., Ikeda, H., and Takezono, T. (1988). Plant production in the artificial environment. *Acta Hortic*. 230, 323–328. doi: 10.17660/ActaHortic.1988.230.42

Takaichi, M., Shimaji, H., and Higashide, T. (1996). Monitoring of the change in fresh weight of plants grown in water culture. *Acta Hortic*. 440, 413–418. doi: 10.17660/ActaHortic.1996.440.72

Van Henten, E. J., and Bontsema, J. (1995). Non-destructive crop measurements by image processing for crop growth control. *J. Agr. Eng. Res.* 61, 97–105. doi: 10.1006/jaer.1995.1036

Yeh, Y. H. F., Lai, T. C., Liu, T. Y., Liu, C. C., Chung, W. C., and Lin, T. T. (2014). An automated growth measurement system for leafy vegetables. *Biosyst. Eng.* 117, 43–50. doi: 10.1016/j.biosystemseng.2013.08.011

Conflict of Interest Statement: The authors declare that the research was conducted in the absence of any commercial or financial relationships that could be construed as a potential conflict of interest.

frontiers in Plant Science

ORIGINAL RESEARCH
published: 30 March 2016
doi: 10.3389/fpls.2016.00270

Performance of Introducing Outdoor Cold Air for Cooling a Plant Production System with Artificial Light

Jun Wang[1,2], *Yuxin Tong*[1,2]*, *Qichang Yang*[1,2] and *Min Xin*[1,2]

[1] Institute of Environment and Sustainable Development in Agriculture, Chinese Academy of Agricultural Science, Beijing, China, [2] Key Laboratory of Energy Conservation and Waste Management of Agricultural Structures, Ministry of Agriculture, Beijing, China

The commercial use of a plant production system with artificial light (PPAL) is limited by its high initial construction and operation costs. The electric-energy consumed by heat pumps, applied mainly for cooling, accounts for 15–35% of the total electric-energy used in a PPAL. To reduce the electric-energy consumption, an air exchanger with low capacity (180 W) was used for cooling by introducing outdoor cold air. In this experiment, the indoor air temperature in two PPALs (floor area: 6.2 m^2 each) was maintained at 25 and 20°C during photoperiod and dark period, respectively, for lettuce production. A null CO_2 balance enrichment method was used in both PPALs. In one PPAL ($PPAL_e$), an air exchanger (air flow rate: 250 $m^3 \cdot h^{-1}$) was used along with a heat pump (cooling capacity: 3.2 kW) to maintain the indoor air temperature at the set-point. The other PPAL ($PPAL_c$) with only a heat pump (cooling capacity: 3.2 kW) was used for reference. Effects of introducing outdoor cold air on energy use efficiency, coefficient of performance (COP), electric-energy consumption for cooling and growth of lettuce were investigated. The results show that: when the air temperature difference between indoor and outdoor ranged from 20.2 to 30.0°C: (1) the average energy use efficiency of the air exchanger was 2.8 and 3.4 times greater than the COP of the heat pumps in the $PPAL_e$ and $PPAL_c$, respectively; (2) hourly electric-energy consumption for cooling in the $PPAL_e$ reduced by 15.8–73.7% compared with that in the $PPAL_c$; (3) daily supply of CO_2 in the $PPAL_e$ reduced from 0.15 to 0.04 kg compared with that in the $PPAL_c$ with the outdoor air temperature ranging from −5.6 to 2.7°C; (4) no significant difference in lettuce growth was observed in both PPALs. The results indicate that using air exchanger to introduce outdoor cold air should be considered as an effective way to reduce electric-energy consumption for cooling with little effects on plant growth in a PPAL.

Keywords: coefficient of performance, energy saving, heat pump, lettuce, plant factory

OPEN ACCESS

Edited by:
Alejandro Isabel Luna-Maldonado, Universidad Autónoma de Nuevo León, Mexico

Reviewed by:
Hao Peng, Washington State University, USA
Chong Zhang, University of Maryland Baltimore County, USA

***Correspondence:**
YuxinTong
tongyuxin@caas.cn

Specialty section:
This article was submitted to Crop Science and Horticulture, a section of the journal Frontiers in Plant Science

Received: *01 December 2015*
Accepted: *21 February 2016*
Published: *30 March 2016*

Citation:
Wang J, Tong Y, Yang Q and Xin M (2016) Performance of Introducing Outdoor Cold Air for Cooling a Plant Production System with Artificial Light. Front. Plant Sci. 7:270. doi: 10.3389/fpls.2016.00270

INTRODUCTION

Recently, plant production systems with artificial light (PPAL) have been gradually used for plant growth in Asian countries, like China and Japan, due to their incomparable advantages of year round scheduled high-quality plant production, high resources use efficiencies, little environmental pollutions, etc. (Kozai, 2012; Fang, 2013). Unlike a greenhouse, the wall of a PPAL is constructed

with opaque thermal insulated materials and artificial lighting is the sole light source for plant growth (Kozai et al., 2006; Li et al., 2012). Heat pumps are often used to remove extra heat generated from artificial lighting to maintain an optimum air temperature. Therefore, the operation cost of a PPAL is high and the commercial use of PPAL is limited. The cost of electric-energy consumed by artificial lighting and heat pumps, accounts for more than 30% of the total operation cost in a PPAL (Fang, 2013). The electric-energy consumed by heat pumps, accounts for 15–35% of the total electric-energy consumption in a PPAL, is mainly used for cooling (Nishimura et al., 2001; Ohyama et al., 2001). Therefore, reducing the electric-energy consumption of heat pumps would be helpful for reducing the operation cost of a PPAL.

Several methods were investigated to reduce the electric-energy consumed by heat pumps for cooling: (1) employing light devices with low heat generation, such as light emitting diode (e.g., Poulet et al., 2014), for reducing heat load in a PPAL, (2) changing light intensity at different plant growth stages (e.g., Tong and Yang, 2014), (3) employing movable light systems (e.g., Li et al., 2014), and (4) introducing seasonal ice storage system for cooling (Yang et al., 2012), etc. However, few studies have been reported on reducing electric-energy consumption for cooling by improving the coefficient of performance (COP) or shortening the operation time of heat pumps working with low COP. It has been reported that high COP for cooling is usually achieved when cooling load is 60–80% of the cooling capacity of a heat pump (Tong et al., 2013). Too low/high heat load reduces the COP. Low heat load also causes frequent ON/OFF operation of heat pumps, which reduces the COP. Outdoor air, whenever its temperature is below the air temperature in the PPAL, is a potential cold source for cooling the air temperature in a PPAL. And therefore direct air exchange may be more energy-efficient than using a heat pump. The main drawback of direct air exchange is that CO_2 utilization efficiency would decrease when indoor CO_2 concentration needs to be kept at high levels (e.g., 1000 μmol mol^{-1}) because some of the injected CO_2 would be lost during the air exchange process (Tingey et al., 2000). Without CO_2 enrichment, CO_2 depletion (50–200 μmol mol^{-1}) could occur during photoperiod, even with natural ventilation (Sanchez-Guerrero et al., 2005). Under such conditions, CO_2 concentration may become a limiting environmental factor for photosynthesis (Thongbai et al., 2010). Therefore, a null CO_2 balance enrichment method, where CO_2 concentration is maintained at the same as outdoor level, is proposed to keep high utilization efficiency of supplied CO_2 when the outdoor cold air is introduced into a PPAL (Kozai, 2009).

In this study, we investigated air exchanging aided by a heat pump as a primary cooling method. The performance of the cooling method was compared with the cooling method that depended solely on a heat pump. To avoid CO_2 depletion and keep a high CO_2 utilization efficiency, the null CO_2 balance enrichment method was used. Two PPALs employed each of the two cooling methods. The objectives of this study are: (1) to analyze the feasibility of saving electric-energy by exchanging air with outdoor cool air in comparison with using only the heat pump; (2) to examine whether air exchanging would impact the amount of supplied CO_2 if null CO_2 balance enrichment method is used; and (3) to determine whether introducing outdoor air would have any negative effects on plant growth.

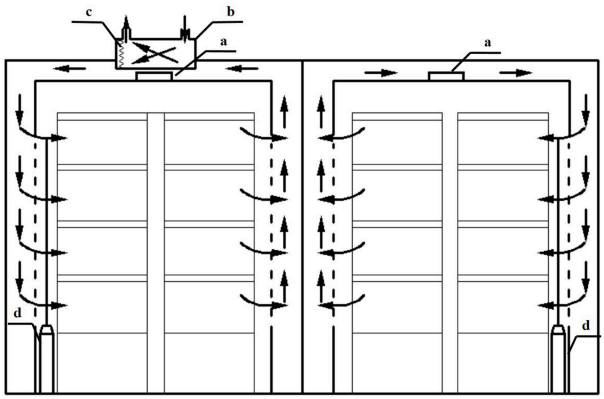

FIGURE 1 | Schematic diagram of the plant factories used in the experiment. a: heat pump installed inside the PPAL; b: air exchanger installed inside the ceiling of the PPAL; c: air filter; d: CO_2 gas cylinder.

MATERIALS AND METHODS

Plant Production System with Artificial Light (PPAL)

Two PPALs were used in this experiment. Each PPAL with a volume of 11.7 m^3 (2.2 m wide, 2.8 m long and 1.9 m high) was built in 2012 and located in China Academy of Agricultural Sciences, Beijing. The Plan view of the PPALs is shown in **Figure 1**. Each PPAL was installed two plant cultivation modules with three layers. The dimension of the plant cultivation modules was 2.1 × 0.7 × 1.8 m. Each layer was equipped with a cultivation bed (2.0 m long, 0.6 m wide, and 0.06 m deep) and fluorescent lamps (24 W, NVC-YZ24-T5, Guangdong, China), 0.4 m above the cultivation bed. In the culture beds, nutrient solution was circulated continuously by water pumps. Styrofoam boards were floated on the nutrient solution to support lettuce plants. Each PPAL was equipped with an air source heat pump for cooling (cooling capacity: 3.2 kW, FTXN32KV2C, Daikin, Industries. Ltd, Japan) and a CO_2 gas cylinder for CO_2 enrichment. On the ceiling of the experimental PPAL ($PPAL_e$), one air exchanger (capacity: 180 W, air flow rate: 250 $m^3 \cdot h^{-1}$, FY-25LD2C, Guangdong, China) and an air filter (FY-BFG062C, Panasonic Ecology Systems Guangdong Co., Ltd) was installed for exchanging indoor warm and humid air with outdoor cold and dry air. Another PPAL ($PPAL_c$) with only the heat pump was used as reference.

Plant Materials and Growth Conditions

Lettuce plants (*Lactuca* sativa var.) were grown in the PPALs during the experiment. Lettuce seeds were sown in a plastic tray under LED light (80 μmol $\cdot m^{-2} \cdot s^{-1}$) and irrigated with tap water once a day. Fifteen days after sowing, uniform seedlings were transplanted into the styrofoam boards with a density of 25 plants $\cdot m^{-2}$ and grown hydroponically using modified

Notation	
Symbols	
Variables	
COP	Coefficient of performance for heating
C	Daily use of CO_2, kg
EUE	Energy use efficiency
E	Electricity consumption rate of air exchanger, W
i	Enthalpy, kJ kg^{-1}
P	Electricity consumption rate of heat pump, W
Q	Heat energy, W
q	Air flow rate, $m^3 \cdot s^{-1}$
R	Reduction in daily use of CO_2
SHF	Sensible heat factor
T	Air temperature, °C
Constants	
ρ	Specific weight of air density of dry air, $kg \cdot m^{-3}$
λ	Latent heat of water vaporization, $J \cdot Kg^{-1}$
Subscripts	
ax	Air exchanger
c	In the $PPAL_c$
d	At the air discharge
e	In the $PPAL_e$
h	heat energy
hp	Heat pump
l-hp	Latent heat extracted by heat pump
l-ax	Latent heat extracted by air exchanger
i	Indoor air
o	Outdoor air
s	At the air suction

Hoagland's solution, whose chemical composition was as follows ($mg \cdot L^{-1}$): $Ca(NO_3)_2 \cdot 4H_2O$, 945; KNO_3, 607; $NH_4H_2PO_4$, 115; $MgSO_4 \cdot 7H_2O$, 495; Na_2Fe-EDTA, 30; $MnSO_4 \cdot H_2O$, 1.61; $CuSO_4 \cdot 5H_2O$, 0.08; $ZnSO_4 \cdot 7H_2O$, 0.22; $(NH4)_6Mo_7O_{24} \cdot 4H_2O$, 0.02; H_2BO_3, 2.86. The nutrient solution was renewed once a week and the electrical conductivity of the solution was adjusted to 2.0 $dS \cdot m^{-1}$. Nutrient solution pH was maintained at 6.0 to 6.5. During the experiment, indoor air temperature was set at 25 and 20°C during photoperiod and dark period, respectively. Photosynthetic photon flux (*PPF*) measured at a distance of 10 cm up from cultivation beds was 150 $\mu mol \cdot m^{-2} \cdot s^{-1}$ with a photoperiod of 12 $h \cdot d^{-1}$ (dark period: 21:00–09:00). Indoor CO_2 concentration was always kept at the same as outdoor level.

Experimental Setup

In the $PPAL_e$, indoor air temperature (T_i) was allowed to maintain at around the set point of 25 and 20°C during photoperiod and dark period, respectively, within the range from T_l to T_h, where the T_l was the low air temperature set point and T_h was the high temperature set point. T_l was 23 and 18°C during photoperiod and dark period, respectively; T_h was 27 and 22°C during photoperiod and dark period, respectively. The air temperature dead band was configured to avoid frequent ON/OFF operation of the air exchanger and heat pump for cooling. T_i in the $PPAL_e$ was controlled by the air exchanger aided by the heat pump. When the outdoor air temperature (T_o) was lower than T_l, and T_i was higher than the temperature set point, the outdoor cold and dry air was introduced by the air exchanger for cooling. If T_i went above T_h, the air exchanger was turned off, and the heat pump started to operate for cooling until T_i decreased to the set temperature. If T_i dropped below T_l, the air exchanger was also automatically turned off. If T_o was higher than T_h, the heat pump was operated for cooling. In the $PPAL_c$, only the heat pump was used to maintain the indoor air temperature at the set point of 25 and 20°C during photoperiod and dark period, respectively.

During photoperiod, a null CO_2 balance enrichment method was employed in both PPALs. The CO_2 supply system consisted of a CO_2 gas cylinder, an electronic mass flow meter (CMS 0020/0050), CO_2 distribution perforated plastic tubes (3 mm, polyethylene) network. The CO_2 distribution plastic tubes reached out to each layer to distribute CO_2 uniformly. In the $PPAL_e$, CO_2 was supplemented by outdoor air when the air exchanger was operating. But whenever the indoor CO_2 concentration was 50 $\mu mol \cdot mol^{-1}$ lower than outdoor due to reduced operation of air exchanger, the CO_2 from the gas cylinder was released into the $PPAL_e$. While in the $PPAL_c$, only the CO_2 from the gas cylinder was used to keep the indoor CO_2 concentration at the same as outdoor level. The experiment was conducted from November 13th to December 18th in 2014.

Calculations

Coefficient Of Performance (COP) for Cooling of the Heat Pump

COP of the heat pump for cooling a PPAL was defined as:

$$COP = \frac{Q_{hp}}{P} \tag{1}$$

where Q_{hp}: heat energy removed rate by the heat pump (W), P: electric-energy consumption rate of the heat pump (W).

Heat energy removed rate by the heat pump was calculated by the general known equation:

$$Q_{hp} = q \cdot \rho \cdot (i_s - i_d) \tag{2}$$

where q: air flow rate of the heat pump ($m^3 \cdot s^{-1}$); ρ: density of dry air (kg (D.A.)$\cdot m^{-3}$); i_s: enthalpy at the air suction of the internal unit of the heat pump ($J \cdot kg^{-1}$ (D.A.)); i_d: enthalpy at the discharge ports of the internal unit of the heat pump ($J \cdot kg^{-1}$ (D.A.)).

The sensible heat factor of the heat pump (SHF_{hp}) was defined as:

$$SHF_{hp} = 1 - \frac{Q_{l-hp}}{Q_{hp}} \tag{3}$$

where

$$Q_{l-hp} = \lambda \cdot q \cdot \rho \cdot (x_s - x_d) \tag{4}$$

is the latent heat load (W), with λ: latent heat of water vaporization (2.5×10^6 $J \cdot kg^{-1}$ at 20°C; ASHRAE, 2001); x_s, x_d: absolute humidity at the air suction and discharge ports of the internal unit of the heat pump ($kg \cdot kg^{-1}$ (D.A.)).

Electric-Energy Use Efficiency of the Air Exchanger

The electric-energy use efficiency of air exchanger (EUE) was defined as:

$$EUE = \frac{Q_{ax}}{E} \tag{5}$$

where Q_{ax}: heat energy removed rate by the air exchanger (W), E: electricity consumption rate of the air exchanger (W).

Heat energy removed rate by the air exchanger was calculated similar to Equation (2):

$$Q_{ax} = q \cdot \rho \cdot (i_i - i_o) \tag{6}$$

where i_i: enthalpy of the indoor air (J·kg^{-1} (D.A.)); i_o: enthalpy of the outdoor air(J·kg^{-1} (D.A.)).

The sensible heat factor of air exchanger (SHF_{ax}) can be estimated by:

$$SHF_{ax} = 1 - \frac{Q_{l-ax}}{Q_{ax}} \tag{7}$$

Where

$$Q_{l-ax} = \lambda \cdot q \cdot \rho \cdot (x_i - x_o) \tag{8}$$

is the latent heat load (W); x_i: absolute humidity of the air expelled from the $PPAL_e$ (kg·kg^{-1} (D.A.)); x_o: absolute humidity of the outdoor air entering the $PPAL_e$ (kg·kg^{-1} (D.A.)).

Reduction in the Amount of Supplied CO_2

The reduction in the amount of supplied CO_2(R) was calculated by:

$$R = C_c - C_e \tag{9}$$

Where C_c: daily amount of CO_2 supplemented to the PPALc (kg); and C_e: daily amount of CO_2 supplemented to the $PPAL_e$ (kg).

Measurements

Environmental Conditions Inside and Outside the PPALs

The inside air temperature and relative humidity of both the $PPAL_e$ and $PPAL_c$ were measured by sensors (TR-72WF, T&D, Co. Japan; precision: air temperature ±0.3°C, relative humidity ±3%). Three sensors were set at a height of 1.5 m from the ground at three measuring points in the middle of each PPAL. The air temperature and relative humidity at the air suction and air discharge ports of the internal unit of each heat pump were measured using sensors (TR-72WF, T&D, Co. Japan; precision: air temperature ±0.3°C, relative humidity ±3%). Vapor pressure deficit (VPD) was determined from the measurements of the air temperature and relative humidity, as the method described in Prenger and Ling (2001). The inside CO_2 concentration was measured by an infrared type CO_2 analyzer (GMT 222, Vaisala Oyj, Helsinki, Finland). The CO_2 analyzer was set at 1.5 m above floor level in the middle of each PPAL. All the above data were automatically recorded every minute with a wireless data collection system. The air flow rate at the air discharge port of the internal unit of each heat pump was measured manually once every second using an air flow meter (Model 6533, Kanomax, Japan).

The outdoor air temperature, relative humidity (TR-72WF, T&D, Co. Japan; precision: air temperature ±0.3°C, relative humidity ±3 %) and CO_2 concentration(GMT 222, Vaisala Oyj, Helsinki, Finland) were recorded every minute in a small weather station 5 m away from the experimental PPAL. All the data were recorded every minute.

Energy Consumption in Both PPALs

The electric-energy consumption rates of heat pumps and air exchanger were measured by wattmeters (KWm8115, Panasonic Electric Works, Japan) and recorded every minute.

Daily Use of CO_2 Supplemented to Both PPALs

Daily use of CO_2 supplemented to both PPALs were determined from continuously measurement of the weight of the CO_2 cylinders, using electronic scales (FZ-TCS50, Julin, Instruments, Co., Xiamen, China).

Measurement of Lettuce Plant Growth and Chlorophyll Concentration

At the 25 and 35 days after transplanting, lettuce plants were randomly sampled to measure their growth. Fifteen plants from each PPAL were harvested each time to measure their fresh weights. Dry weights were measured after being dried at 80°C for 72 h.

Samples were excised from the leaves of 10 plants at a similar position for each treatment. Leaves were weighed out in 0.1–0.2 g (fresh weight). The extractions were performed using 10 ml (V) of 80% acetone until the leaf turned white. The optical density was measured with UV-1800 spectrophotometer (Shimadzu, Japan) at 663 nm (OD663) and at 645 nm (OD645) for chlorophyll a (Chl a) and chlorophyll b (Chl b). The chlorophyll concentrations (Chl) were determined as the method described in Lichtenthaler and Wellburn (1983).

Statistical analysis

Statistical differences among the treatments were analyzed by the least significant difference (LSD) test ($p < 0.05$) when analysis of variance (ANOVA) by SPSS software (SPSS for Windows, SPSS Inc., USA) indicated treatment significance.

RESULTS

Energy Use Efficiencies of Air Exchanger and Heat Pumps

Both the EUE of air exchanger and the COP of heat pumps for cooling increased with the increase in air temperature difference between indoor and outdoor. When the air temperature difference between indoor and outdoor ranged from 20.2 to 30.0°C, the EUE of the air exchanger for cooling the $PPAL_e$ ranged from18.6 to 32.9 with an average of 25.6, the COP of the heat pump in the $PPAL_e$ ranged from 4.2 to 18.2 with an average of 9.0, and the COP of the heat pump in the $PPAL_c$ ranged from 1.6 to 16.8 with an average of 7.5 (**Figure 2**). The average EUE of

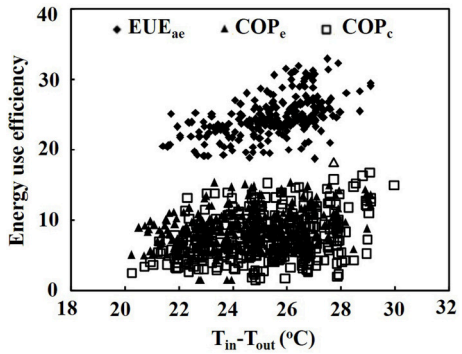

FIGURE 2 | Energy use efficiency of the air exchanger and heat pumps as affected by the air temperature difference between indoor and outdoor. EUE, energy use efficiency of the air exchanger; COP_e, energy use efficiency of the heat pump in the $PPAL_e$; COP_c, energy use efficiency of the heat pump in the $PPAL_c$.

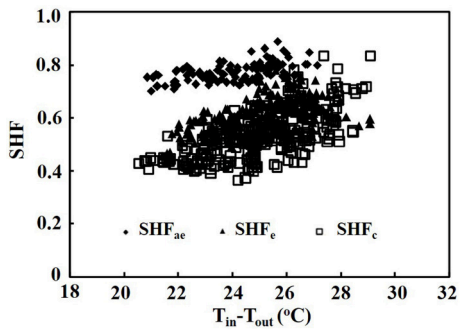

FIGURE 3 | Sensible heat factor (SHF) of the air exchanger and heat pumps as affected by the air temperature difference between indoor and outdoor. SHF_{ae}, sensible heat factor of the air exchanger; SHF_e, sensible heat factor of the heat pump in the $PPAL_e$; SHF_c, sensible heat factor of the heat pump in the $PPAL_c$.

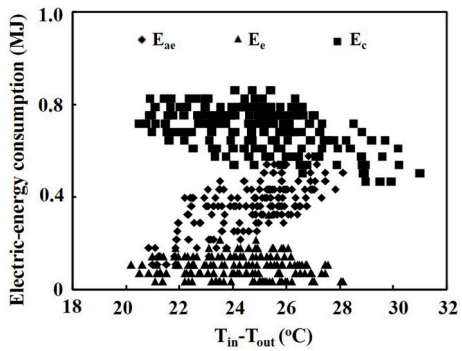

FIGURE 4 | Electric-energy consumption of the air exchanger and heat pumps as affected by the air temperature difference between indoor and outdoor. E_{ae}, electric-energy consumption of the air exchanger; E_e, electric-energy consumption of the heat pump in the $PPAL_e$; E_c, electric-energy consumption of the heat pump in the $PPAL_c$.

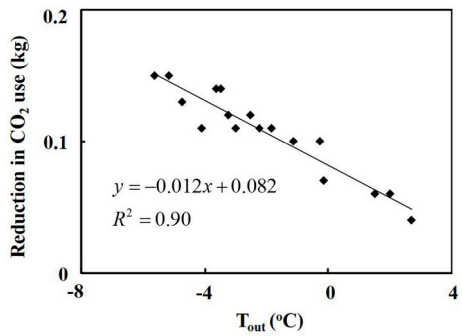

FIGURE 5 | Reduction of daily CO_2 supplied in the $PPAL_e$ compared with that in the $PPAL_c$ as affected by outdoor air temperature.

air exchanger was 2.8 and 3.4 times greater than the average COP of the heat pumps in the $PPAL_e$ and $PPAL_c$, respectively.

SHF of Air Exchanger and Heat Pumps

When the air temperature difference between indoor and outdoor ranged from 20.2 to 30.0°C, the SHF of the air exchanger ranged from 0.7 to 0.9, the SHF of the heat pump in the $PPAL_e$ ranged from 0.5 to 0.7, while the SHF of the heat pump in the $PPAL_c$ ranged from 0.4 to 0.8 (**Figure 3**).

Electric-Energy Consumption of Air Exchanger and Heat Pumps

When the air temperature difference between indoor and outdoor ranged from 20.2 to 35.7°C, the hourly electric-energy consumption of the air exchanger ranged from 0.11 MJ to 0.58 MJ, while that of the heat pump in the $PPAL_e$ ranged from 0.32 to 0.04 MJ, and that of the heat pump in the $PPAL_c$ ranged from 0.86 to 0.47 MJ (**Figure 4**). The hourly electric-energy consumption in the $PPAL_e$ was 15.8–73.7% lower than that in the $PPAL_c$.

Reduction in the Use of Supplemental CO_2

The $PPAL_e$ required 0.04–0.15 kg less CO_2 per day to replenish the CO_2 depletion than the $PPAL_c$, when the daily average outdoor air temperature ranged from −5.6 to 2.7°C (**Figure 5**).

Environmental Conditions in Both PPALS

The air temperature inside both PPALs could be controlled within the acceptable ranges (23 to 27°C during photoperiod and 18 to 22°C during dark period, respectively). The air temperature inside the $PPAL_e$ was lower than that of $PPAL_c$ with a highest different value of 4.7°C. The high fluctuation of air temperature inside the $PPAL_e$ was observed especially during lower outdoor air temperature (**Figure 6A**).

The VPD in the $PPAL_e$ ranged from 0.5 to 1.8 kPa during photoperiod and from 0.2 to 1.0 kPa during dark period. While the VPD in the $PPAL_c$ ranged from 0.2 to 1.8 kPa during photoperiod and from 0.2 to 1.0 kPa during dark period (**Figure 6B**).

CO_2 concentration during photoperiod in both PPALs could be maintained at around outdoor level in this experiment. Average CO_2 concentration during photoperiod

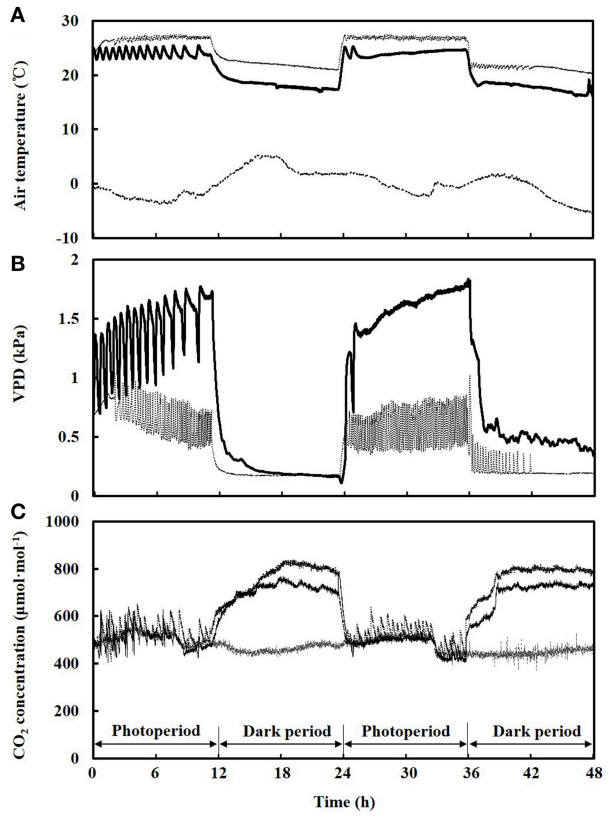

FIGURE 6 | Time course of air temperature (A), vapor pressure deficit (VPD) (B) and CO_2 concentration (C). ___: environmental conditions in the $PPAL_e$; .....: environmental conditions in the $PPAL_c$; - - -: outdoor environmental conditions.

was 493 and 510 μmol mol^{-1} in the $PPAL_e$ and $PPAL_c$, respectively, while the average outdoor CO_2 concentration was 498 μmol mol^{-1} (**Figure 6C**). During dark period, CO_2 concentration in the $PPAL_e$ increased from 472 to 769 μmol·mol^{-1}, while that in the $PPAL_c$ increased from 522 to 841 μmol·mol^{-1}. CO_2 concentration during dark period was lower in the $PPAL_e$ than that in the $PPAL_c$ during this experiment.

Lettuce Growth in Both PPALS

The growth images of lettuce on DAT15 and DAT30 in PPALe and PPALc were showed in **Figures 7A,B**, respectively. **Figure 8** presents the fresh and dry weights measured at 25 and 35 days after transplanting. No significant differences of fresh or dry weight of lettuce plants were found between the two PPALs. By calculating from data used in **Figure 8**, the ratio of shoot fresh weight to dry weight in $PPAL_e$ and $PPAL_c$ were 16.4 and 16.3 g·g^{-1}, respectively, while the ratio of root fresh weight to dry weight in $PPAL_e$ and $PPAL_c$ were 29.1 and 32.3 g·g^{-1}, respectively. There were no significant differences between the two PPALs. Photosynthetic pigments of lettuce plants in both PPALs also showed no significant difference (**Figure 9**).

DISCUSSION

Feasibility of Saving Electric-Energy by Air Exchanging with Outdoor Air for Cooling

In the present experiment, the high EUE of air exchanger indicates that air exchanger with a low capacity is more energy-efficient for cooling in a PPAL than the heat pump with a high capacity under the experimental conditions. In the present experiment, both the EUE of air exchanger and the COP of heat pumps for cooling increased with decreasing outdoor air temperature when the indoor air temperature could be maintained at around the set point, which agrees with previous reports (e.g., Tong et al., 2013). The reason of higher EUE of the air exchanger in comparison with the COP of the heat pumps probably was that the outdoor air with low temperature and humidity was introduced into indoor directly by using air exchanger with low capacity. The COP of the heat pump in the $PPAL_e$ was slightly higher than the COP of heat pump in the $PPAL_c$, probably because the operation time of the heat pump in the $PPAL_e$ in low heat load was reduced by introducing outdoor cold air.

In **Figure 2**, the scattered data for EUE of the air exchanger and COP of both heat pumps were probably because the EUE and COP were not only affected by the air temperature but also affected by the relative humidity of indoor and outdoor air (Tong et al., 2010).Thus, the air exchanger and heat pump not only extracted sensible heat but also latent heat from the PPALs. The SHF value represents the ratio of the sensible heat energy to the total heat energy removed from the PPALs by air exchanger and heat pumps. The higher SHF value of the air exchanger indicated that mainly sensible heat contributed to the total heat energy extracted from the $PPAL_e$, because introducing outdoor dry air reduced indoor-outdoor relative humidity difference. The SHF of the heat pump in the $PPAL_c$ was slightly lower than that in the $PPAL_e$ (**Figure 3**), probably because the higher indoor relative humidity increased the ratio of latent heat energy to the total heat energy extracted from the $PPAL_c$.

Saving Electric-Energy by Using the Air Exchanger

Hourly electric-energy consumption of the air exchanger and heat pumps as affected by air temperature difference between indoor and outdoor is shown in **Figure 4**. The electric-energy consumption of the heat pump both in the $PPAL_c$ and the $PPAL_e$ decreased with increasing air temperature difference between indoor and outdoor due to the increased COP. The hourly electric-energy consumption of the heat pump in the $PPAL_e$ was much lower than that of the heat pump in the $PPAL_c$. Compared with the heat pump in the $PPAL_c$, saving-energy of the heat pump in the $PPAL_e$ became more pronounced with increasing air temperature difference between indoor and outdoor. The above results indicated that the operation time of the heat pump in the $PPAL_e$ was significantly shortened, particularly under large air temperature difference. The hourly electric-energy consumption of air exchanger increased with increasing air temperature difference between indoor and outdoor although the EUE increased. This was because with decreasing outdoor air

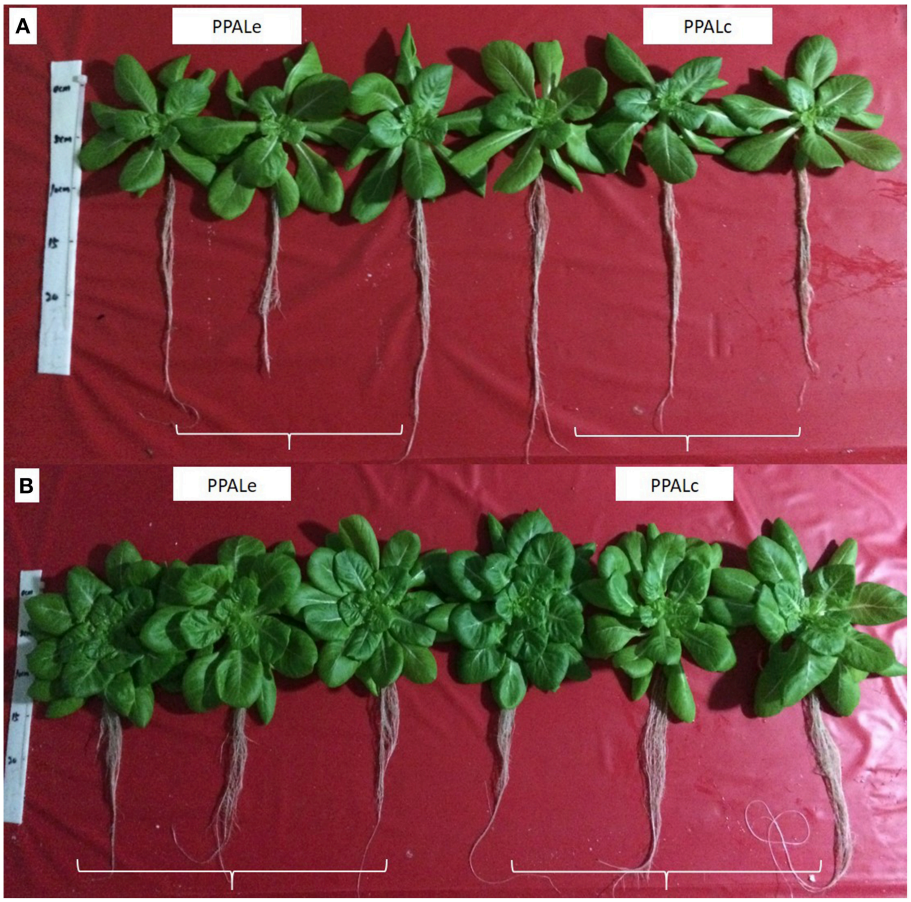

FIGURE 7 | Growth images of lettuce on DAT15 (A) and DAT30 (B) in the $PPAL_e$ and $PPAL_c$.

temperature, operation time of the air exchanger increased since the indoor air temperature could be controlled at the set point using only air exchanger for cooling.

Reduction in the Use of Supplemental CO_2

In the experiment, to avoid high CO_2 depletion and low CO_2 utilization efficiency, CO_2 concentration was replenished to keep the concentration at outside level. The reduction in daily supply of CO_2 in the $PPAL_e$ was because CO_2 gas from outdoor air was supplied to the indoor air when the air exchanger was used and the pure CO_2 was used whenever the indoor CO_2 concentration could not be kept at outside level, while in the $PPAL_c$, only pure CO_2 was used to keep the indoor CO_2 concentration at outside level. Increasing operation time of the air exchanger for introducing outdoor cold air could save CO_2 supplied into a PPAL with the null CO_2 balance enrichment method. With increasing outdoor air temperature the operation time of the air exchanger decreased as shown in **Figure 4**, so then more pure CO_2 was needed.

Environmental Conditions in Both PPALS

Time course of air temperatures inside both PPALs shown in **Figure 6A** indicates that the air exchanger could be used for cooling in most of the time since the heat pump was operated for cooling when the indoor air temperature could not be controlled below 27 and 22°C during photoperiod and dark period, respectively. The fluctuation of air temperature inside the $PPAL_e$ was because different control strategies of the air exchanger and heat pumps were employed in this experiment. Heat pumps employed a proportional-integral-derivative (PID) control method, while the air exchanger employed a simple ON/OFF control method.

CO_2 concentration during photoperiod in both PPALs could be maintained at around outdoor level in this experiment, with the reasonable fluctuations of CO_2 concentration in both PPALs caused by ON/OFF operation of the CO_2 supplemental devices. To reduce the fluctuations in CO_2 concentration, PID control method should be employed instead of ON/OFF control method. Compared to CO_2 concentration in the $PPAL_c$, lower CO_2 concentration in the $PPAL_e$ during dark period was caused by the amount of CO_2 leakage increasing with increasing air exchange rate due to the operation of the air exchanger.

Lettuce Growth in Both PPALS

No significant differences of fresh/dry weights and photosynthetic pigments of lettuce plants were found despite of

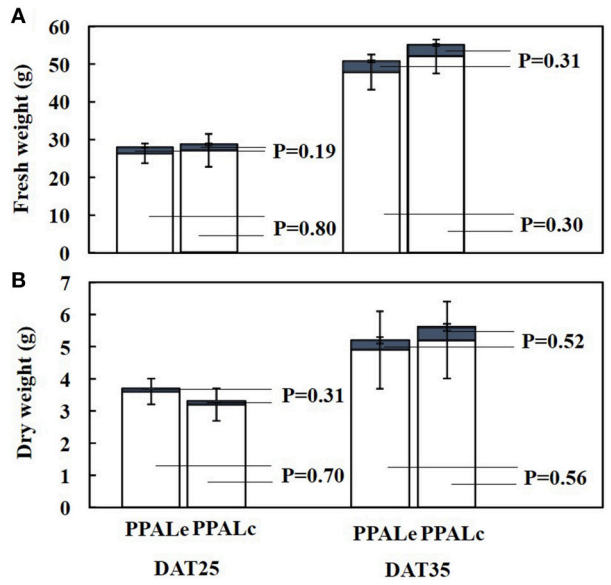

FIGURE 8 | Fresh (A) and dry weights (B) of lettuce on DAT25 and DAT35 in $PPAL_e$ and $PPAL_c$. Open and filled bars respect shoot weight and root weight, respectively. Values were the means of six replicates with standard errors shown by vertical bars. Statistical differences among the treatments were analyzed by LSD test ($p < 0.05$).

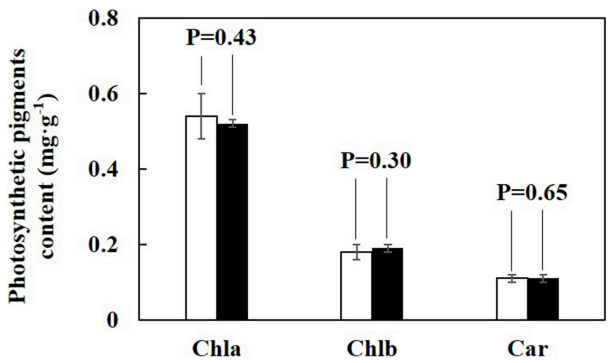

FIGURE 9 | Photosynthetic pigments (chlorophyll and carotenoid) contents of harvested lettuce on DAT35 in both PPALs. Open and filled bars respect photosynthetic pigments content of lettuce in the $PPAL_e$ and $PPAL_c$, respectively. Values were the means of six replicates with standard errors shown by vertical bars. Statistical differences among the treatments were analyzed by LSD test ($p < 0.05$).

the differences in environmental conditions of the two PPALs. The air temperatures inside both PPALs were controlled within the optimum ranges recommended (Li et al., 2012; Chen et al., 2014; Tong and Yang, 2014), but the air temperature inside the $PPAL_c$ was slightly higher than that inside the $PPAL_e$. High air temperature during photoperiod significantly improved plant growth, while high air temperature during dark period had adverse effects on plant growth because it would enhance dark respiration (Peet and Bartholomew, 1996; Morales et al., 2003).

A similar VPD ranged from 0.2 to 1.0 kPa was observed in both PPALs during dark period. Grange and Hand (1987) quoted that a VPD in the range of 0.2–1.0 kPa has little effect on the physiology and development of crops, while during photoperiod, the VPD in the $PPAL_e$ was much higher than that in the $PPAL_c$, because the very dry outdoor air was introduced into the $PPAL_e$ when the air exchanger was used. According to Hoffman (1979), an increase in VPD from 1 to 1.8 kPa determines the major reduction in plant growth on several crops, and this could be probably due to the depression of photosynthesis (Xu et al., 1991), related to the reduction of stomatal conductance (Grange and Hand, 1987). In contrast, some studies reported that low VPD positively affects dry matter accumulation and can also promote the incidence of calcium related physiological disorders in leaves (Janse and Welles, 1984; Holder and Cockshull, 1990; Kreij, 1996; Dorais et al., 2004).

The average CO_2 concentration in both PPALs was maintained at approximately the same as outdoor level during photoperiod, although CO_2 concentration in the $PPAL_c$ was slightly higher than that in the $PPAL_e$ during dark period. Based on above discussion, the lettuce plants growth in this experiment might be affected by different environmental conditions, but positive effects because of higher air temperature during photoperiod were all offset by negative effects of higher air temperature during dark period and lower VPD in the $PPAL_c$.

Economic Benefit Analysis of Introducing Outdoor Cold Air for Cooling Together with Null CO_2 Balance Enrichment Method

Costs for electric-energy consumed by the air exchanger and heat pumps were analyzed based on an industrial electricity cost of 0.81 RMB·kWh^{-1} and data in **Figure 4**. Electric-energy cost for cooling in the $PPAL_e$ ranged from 0.10 to 1.89 RMB·h^{-1}, with an average of 1.14 RMB·h^{-1}, while the electric-energy cost for cooling in the $PPAL_c$ ranged from 1.36 to 2.52 RMB·h^{-1}, with an average of 2.04 RMB·h^{-1}, when the air temperature difference between indoor and outdoor ranged from 20.2 to 35.7°C. The above results indicated that about 0.9 RMB·h^{-1} on average could be saved in the $PPAL_e$ than that in the $PPAL_c$ under the experimental conditions.

Cost for reduction in CO_2 supplied in both PPALs was analyzed based on CO_2 (purity of 99.9%) cost of 0.71 RMB·kg^{-1} and data in **Figure 5**. Reduction in CO_2 cost ranged from 0.03 to 0.11 RMB·d^{-1}, with an average of 0.08 RMB·d^{-1}, when the daily average outdoor air temperature ranged from −5.6 to 2.7°C.

As discussed in sections of "Saving electric-energy by using the air exchanger" and "Reduction in the use of supplemental CO_2," the economic benefit of introducing outdoor cold air for cooling together with null CO_2 balance enrichment method was significantly affected by the indoor and outdoor environmental conditions. Greater economic benefit can be achieved with increasing operation time of the air exchanger. Furthermore, the present experiment was conducted in a model PPAL with a small volume of 11.7 m^3, while the volume of a commercial used PPAL is usually larger than 1000 m^3. Thus, in a commercial used PPAL with a volume of 1000 m^3, the saved electric energy and CO_2 cost can be 76.92 RMB·h^{-1} and 6.84 RMB·d^{-1}, respectively. However, the actual economic benefit in a commercial PPAL should be further confirmed in future researches.

CONCLUSION

To reduce the electric-energy consumption for cooling in a PPAL, an air exchanger was employed aided by a heat pump for cooling by introducing outdoor air whenever the indoor air temperature was lower than outdoor air temperature. To avoid a high depletion of CO_2 concentration and keep a high supplied CO_2 utilization efficiency, a null CO_2 balance enrichment method was used in this experiment. Experimental results showed that when the air temperature difference between indoor and outdoor ranged from 20.2 to 30.0°C: (1) the average EUE of the air exchanger was 2.8 and 3.4 times greater than the COP of the heat pumps in the $PPAL_e$ and $PPAL_c$, respectively; (2) the hourly electric-energy consumption in the $PPAL_e$ was reduced by 15.8–73.7% compared with that in the $PPAL_c$; (3) the daily use of supplemental CO_2 in the $PPAL_e$ was greatly reduced from 0.15 to 0.04 kg compared with that in the $PPAL_c$. Operating the air exchanger did not affect the growth of lettuce. Overall, introducing cold air by air exchanger proved to be an effective cooling method for PPALs, however, auxiliary cooling devices are needed (such as heat pump) whenever air exchanger could not meet the cooling demand.

AUTHOR CONTRIBUTIONS

JW carried out the measurements, data analysis and drafted the manuscript. MX participated in part of measurements and data analysis. YT and QY made substantial guide about experiment design, and critically revised the manuscript.

ACKNOWLEDGMENTS

We are grateful for the financial support from the National High Technology Research and Development Plan of China (863 Project, grant No. 2013AA103007).

REFERENCES

ASHRAE (2001). *2001ASHRAE Fundamentals Handbook (SI)*. Atlanta, GA: American Society of Heating, Refrigerating and Air-conditioning Engineers, Inc.

Chen, X. L., Guo, W. Z., Xue, X. Z., Wang, L. C., and Qiao, X. J. (2014). Growth and quality responses of 'Green Oak Leaf' lettuce as affected by momochromic or mixed radiation provided by fluorescent lamp (FL) and light-emitting diode (LED). *Sci. Hortic.* 172, 168–175. doi: 10.1016/j.scienta.2014.04.009

Dorais, M., Demers, D. A., Papadopoulos, A. P., and Van Ieperen, W. (2004). Greenhouse tomato fruit cuticle cracking. *Hortic. Rev.* 30, 163–184. doi: 10.1002/9780470650837

Fang, W. (2013). Quantification of performance in plant factory. *Technol. Adv. Prot. Hortic.* 64–71.

Grange, R. I., and Hand, D. W. (1987). A review of the effects of atmospheric humidity on the growth ofhorticultural crops. *J. Hortic. Sci.* 62, 125–134.

Hoffman, G. J. (1979). "Humidity," in *Controlled Environment Guidelines for Plant Research,* eds T. W. Tibbits and T. T. Kozlowski (London: Academic Press), 141–172.

Holder, R., and Cockshull, K. E. (1990). Effects of humidity on the growth and yield of glasshouse tomatoes. *J. Hortic. Sci.* 65, 31–39.

Janse, J., and Welles, G. W. H. (1984). Effects of energy saving measures on keeping quality of tomatoand cucumber fruits. *Acta Hortic.* 163, 261–269. doi: 10.17660/ActaHortic.1984.163.29

Kozai, T. (2009). *Solar Assisted Plant Factory, 1st Edn*. Tokyo: Ohmsha.

Kozai, T. (2012). *Plant Factory with Artificial Light*. Toyko: Ohmsha.

Kozai, T., Ohyama, K., and Chun, C. (2006). Commercialized closed systems with artificial lighting for plant production. *Acta Hortic.* 711, 61–70. doi: 10.17660/ActaHortic.2006.711.5

Kreij, C. (1996). Interactive effects of air humidity, calcium and phosphate on blossom-end rot, leaf deformation, production and nutrient content of tomato. *J. Plant Nutr.* 19, 361–377. doi: 10.1080/01904169609365127

Li, K., Yang, Q. C., Tong, Y. X., and Cheng, R. F. (2014). Using movable light-emitting diodes for electricity savings in a plant factory growing lettuce. *Horttechnology* 24, 546–553.

Li, M., Kozai, T., Ohyama, K., Shimamura, D., Gonda, K., and Sekiyama, T. (2012). CO_2 balance of a commercial closed system with artificial lighting for producing lettuce plants. *Hortscience* 47, 1257–1260.

Lichtenthaler, H. K., and Wellburn, A. R. (1983). Determination of total carotenoids and chlorophylls a and b of leaf extracts in different solvents. *Biochem. Soc. Trans.* 603, 591–592. doi: 10.1042/bst0110591

Morales, D., Rodriguez, P., Dell'Amico, J., Nicolas, E., Torrecillas, A., and Sanchez-Blanco, M. J. (2003). High-temperature preconditioning and thermal shock imposition affects water relations, gas exchange and root hydraulic conductivity in Tomato. *Biol. Plant.* 47, 6–12.

Nishimura, M., Kozai, T., Kubota, C., and Chun, C. (2001). Analysis of electric energy consumption and its cost for a closed-type transplant production system. *J. Soc. High Technol. Agric.* 13, 204–209. doi: 10.2525/jshita.13.204

Ohyama, K., Fujiwara, M., Kozai, T., and Chun, C. (2001).Consumption of electric energy and water for eggplant plug transplant production in a closed-type transplant production system. *J. Soc. High Technol. Agric.* 13, 1–6. doi: 10.2525/jshita.13.1

Peet, M. M., and Bartholomew, M. (1996). Effect of night temperature on pollen characteristics, growth and fruit set in tomato (Lycopersiconesculentum Mill). *J. Am. Soc. Hortic. Sci.* 121, 514–519.

Poulet, L., Massa, G. D., Morrow, R. C., Bourget, C. M., Wheeler, R. M., and Mitchell, C. A. (2014). Significant reduction in energy for plant-growth lighting in space using targeted LED lighting and spectral manipulation. *Life Sci. Space Res.* 2, 43–53. doi: 10.1016/j.lssr.2014.06.002

Prenger, J. J., and Ling, P. P. (2001). *Greenhouse Condensation Control Understanding and Using Vapor Pressure Deficit (VPD)*. Available online at: http://citeseerx.ist.psu.edu/viewdoc/summary?

Sanchez-Guerrero, M. C., Lorenzo, P., Medrano, E., Castilla, N., Soriano, T., and Baille, A. (2005). Effect of variable CO_2 enrichment on greenhouse production in mild winter climates. *Agric. For. Meteorol.* 132, 244–252. doi: 10.1016/j.agrformet.2005.07.014

Thongbai, P., Koai, T., and Ohyama, K. (2010). CO2 and air circulation effects on photosynthesis and transpiration of tomato seedlings. *Sci. Hortic.* 126, 338–344. doi: 10.1016/j.scienta.2010.07.018

Tingey, D. T., Waschmann, R. S., Phillips, D. L., and Olszyk, D. M. (2000). The carbon dioxide leakage from chambers measured using sulfur hexafluoride. *Environ. Exp. Bot.* 43, 101–110. doi: 10.1016/S0098-8472(99)00051-9

Tong, Y., Kozai, T., and Ohyama, K. (2013). Performance of household heat pumps for nighttime cooling of a tomato greenhouse during the summer. *Appl. Eng. Agric.* 29, 415–422. doi: 10.13031/aea.29.9984

Tong, Y., Kozai, T., Ohyama, K., and Nishiyoga, M. (2010). Greenhouse heating using heat pumps with a high coefficient of performance (COP). *Biosyst. Eng.* 106, 405–411. doi: 10.1016/j.biosystemseng.2010.05.003

Tong, Y., and Yang, Q. C. (2014). Analysis of electric-energy utilization efficiency in a plant factory with artificial light for lettuce production. *Acta Hort*. 1037, 277–284. doi: 10.17660/ActaHortic.2014.1037.32

Xu, H. L., Yamagishi, T., and Wada, Y. (1991). Interactive effect of soil water regime with above-ground conditions on photosynthesis in wheat plants. *Crop Sci. Soc. Jpn*. 60, 515–522. doi: 10.1626/jcs.60.515

Yang, Q. C., Wei, L. L., Liu, W. K., and Cheng, R. F. (2012). *Plant Factories: Systems and Practice*. Beijing: Chemical Industry Pub. Co.

Conflict of Interest Statement: The authors declare that the research was conducted in the absence of any commercial or financial relationships that could be construed as a potential conflict of interest.

frontiers in Plant Science

ORIGINAL RESEARCH
published: 22 April 2016
doi: 10.3389/fpls.2016.00527

Effects of Red Light Night Break Treatment on Growth and Flowering of Tomato Plants

Kai Cao[1,2†], Lirong Cui[1,2†], Lin Ye[1,2,3], Xiaoting Zhou[1,2], Encai Bao[1,2], Hailiang Zhao[1,2] and Zhirong Zou[1,2]*

[1] State Key Laboratory of Crop Stress Biology for Arid Areas, College of Horticulture, Northwest A&F University, Yangling, China, [2] Key Laboratory of Protected Horticultural Engineering in Northwest, Ministry of Agriculture, Yangling, China, [3] Agriculture College, Ningxia University, Yinchuan, China

Compact and healthy young plants increase crop production and improve vegetable quality. Adverse climatic conditions and shading can cause young plants to become elongated and spindly. We investigated the effects of night break (NB) treatments on tomato plants using red light (RL) with an intensity of 20 $\mu mol \cdot m^2 \cdot s^{-1}$. Tomato plants were subjected to NB treatments with different frequencies ranging from every 1, 2, 3, and 4 h, and plant growth, flowering, and yield were monitored. The results showed that with the increase of RL NB frequency, plant height decreased, stem diameter increased, and flower initiation delayed, the content of indole-3-acetic acid (IAA) and gibberellin 3 (GA_3) in the leaf and stem declined. When the RL NB frequency was every 1 h, the heights of tomato plant decreased by 32.73% compared with the control, the diameter of tomato plants increased by 27.09% compared with the control, the number of leaves produced before flowering increased to 11, compared with 8 in the control, the contents of IAA and GA_3 in the leaf decreased by 33.3 and 41.29% respectively compared with the control, the contents of IAA and GA_3 in the stem decreased by 56.04 and 57.14% respectively compared with the control. After RL NB treatments, tomato plants were transplanted into a solar greenhouse to evaluate tomato yield. When tomato plants pre-treated with RL NB, per tomato fresh weight of the first spica increased with the increase of RL NB frequencies. These results indicate that more compact and healthier tomato plants could be gotten by RL NB treatments and improve tomato early yield.

Keywords: flowering, fruit fresh weight, hormone, night break, stem elongation, tomato

OPEN ACCESS

Edited by:
Alejandro Isabel Luna-Maldonado, Universidad Autónoma de Nuevo León, Mexico

Reviewed by:
Miyako Kusano, University of Tsukuba, Japan
Fisun G. Çelikel, Ondokuz Mayis University, Turkey

***Correspondence:**
Zhirong Zou
zouzhirong2005@hotmail.com

† These authors have contributed equally to this work.

Specialty section:
This article was submitted to Crop Science and Horticulture, a section of the journal Frontiers in Plant Science

Received: *08 January 2016*
Accepted: *04 April 2016*
Published: *22 April 2016*

Citation:
Cao K, Cui L, Ye L, Zhou X, Bao E, Zhao H and Zou Z (2016) Effects of Red Light Night Break Treatment on Growth and Flowering of Tomato Plants. Front. Plant Sci. 7:527. doi: 10.3389/fpls.2016.00527

INTRODUCTION

The seedling growth period is crucial for vegetable production. This period has important effects on plant growth and development,harvest time, total yield efficiency, and fruit numbers per plant. Seedling optimization can increase production yield and improve the quality of vegetable crops. If plants grow too tall, they become troublesome during propagation, transport, and planting. However, adverse environmental conditions, high humidity, and greenhouse shading often degrade seedling quality (Zhan et al., 2003). To prevent plants from becoming spindly, growers often control seedling height by application of growth retardants such as B-nine (daminozide), Bonzi (paclobutrazol), and Cycocel (chlormequat chloride) (Nourai and Harris, 1983; Berova and Zlatev, 2000; Haque et al., 2007). However, these growth retardants

excessively attenuate plant height and slow plant growth after transplanting. Restrictions on the use of growth regulating chemicals have been set on vegetable crops because of potential health risks to workers and consumers. Therefore, identification of a non-chemical alternative to control greenhouse crop height is increasingly important.

Light quality, specifically red light (RL) and far-red light (FRL), affects plant growth. In many morphological studies, high RL:FRL ratio strongly inhibits stem elongation, whereas low RL:FRL ratio enhanced stem elongation (Alokam et al., 2002; Kurepin et al., 2007). Phytochromes are important photoreceptors that sense RL and FRL. Phytochromes are photochromic proteins that have two photo-interconvertible isomeric forms: the red-light-absorbing form (Pr) is biologically inactive, whereas the far-red-light-absorbing form (Pfr) is biologically active (Hughes and Lamparter, 1999; Smith, 2000). The conversion between Pr and Pfr synchronizes plant development with the light environment. In daylight, phytochromes exist predominantly in the Pfr form, which results in the suppression of genes involved in elongation growth. During the night, Pfr undergoes dark recovery and slowly converts into the inactive Pr form, which increases the expression of genes involved in elongation growth (Nozue et al., 2007; Soy et al., 2012). Phytochromes also are involved in flowering, long-day-plants such as *Arabidopsis* (Mockler et al., 1999) and pea (Weller and Reid, 1993), and short-day-plants such as sorghum (Childs et al., 1997) and rice (Izawa et al., 2002), showed early flowering and reduced photoperiodic sensitivities in their *phy* mutants.

A short exposure to light in the middle of the night inhibits or promotes plant growth and flowering. This phenomenon is called night break (NB), which has been used extensively as a tool to study photoperiodic control of growth and flowering. In *Eustoma grandiflorum* and *Cymbidium*, NB treatment by high RL:FRL ratio reduces stem elongation (Yamada et al., 2009; Kim et al., 2011). NB treatment promotes flowering of long-day plants and inhibits flowering of short-day plants (Goto et al., 1991; Ishikawa et al., 2005). NB treatment with RL change phytochromes from the Pr form to the Pfr form during the night. However, the effect of NB treatment on stem elongation and flowering in a day-neutral plant such as tomato was unknown.

Light-emitting diode (LED) is a new light source with several unique advantages, including narrow bandwidth, relatively cool emitting surface, minimum heating, and the ability to control spectral composition and wavelength specificity (Bourget, 2008). These solid-state light sources are therefore ideal for use in plant lighting experiments to influence plant morphology and metabolism (Massa et al., 2008; Morrow, 2008). In this study, we investigated the effects of NB treatment on tomato growth, flowering, and fresh fruit weight using red LED light. The basic knowledge gained by these experiments provides useful information for the development of seedling management practices using specific light manipulation protocols in commercial operations.

MATERIALS AND METHODS

Plant Materials and Treatments

The tomato (*Solanum lycopersicum*) cultivar Jinpeng No.1 was used as experimental material. Tomato seeds were soaked in 50% bleach for 30 min, rinsed thoroughly in running water, and then placed directly on moistened filter paper and incubated at 25°C. After germination, seeds were sown onto culture substrate and placed in a growth chamber with a day/night temperature regime of 25°C/18°C, 12 h photoperiod, and 60–75% relative humidity. When the first leaf fully expanded, the same-sized plants were selected and transplanted to plastic pots (pot size 5 × 5 × 8 cm, one seedling per pot) filled with culture substrate. Then, plants were placed in an environmentally controlled greenhouse at Northwest A&F University, Yangling, Shaanxi, China. The greenhouse was completely enclosed in glass and equipped with pad-and-fan cooling and water heating systems; therefore, the greenhouse could be maintained at a temperature of 25–30°C during the day and 15–18°C during the night, with 60–75% relative humidity. The plants were irrigated every week with Yamasaki nutrient solution (pH 6.5 ± 0.1, electrical conductivity 1.4–1.8 $dS{\cdot}m^{-1}$) containing 4 $mmol{\cdot}L^{-1}$ NO_3-N, 0.7 $mmol{\cdot}L^{-1}$ NH_4-N, 0.7 $mmol{\cdot}L^{-1}$ P, 4 $mmol{\cdot}L^{-1}$ K, 1.0 $mmol{\cdot}L^{-1}$ Mg, 1.7 $mmol{\cdot}L^{-1}$ Ca, 2.7 $mmol{\cdot}L^{-1}$ S, and micronutrients.

The environmentally controlled greenhouse was divided into five sections. Plants (n = 45) were placed in each section and covered with opaque black cardboard box to prevent light contamination. A LED panel (339 × 350 mm, model ISL-RFGB, CCS Inc., Kyoto, Japan) with red LEDs (peak illumination at 658 nm) was horizontally placed 20 cm above the plants inside the opaque cardboard box. The photosynthetic photon flux density of RL was measured by a spectroradiometer (PAR-NIR, Apogee Instruments Inc., Logan, UT). The RL intensity and spectrum are shown in **Figure 1**. The daily RL NB treatment occurred from 20:00 to 08:00 h, lasting for 10 min at an intensity of 20 $\mu mol{\cdot}m^2{\cdot}s^{-1}$ inside the opaque cardboard box, with frequencies ranging from every 1, 2, 3, and 4 h. The experiments were conducted in 1–4 black opaque cardboard boxes during the night. The control plants did not receive any NB treatment; they were kept in the fifth black opaque cardboard box during the night, which prevented any light contamination. NB treatments finished when all tomato plants flowered.

Measurement of Plant Growth and Development during the NB treatment Period

Plant height and stem diameter were measured weekly for 10 plants during the NB treatment period. Plant height was measured using a ruler with 0.01 cm accuracy; stem diameter was measured at the first internode using a digital caliper with 0.01 mm accuracy (Digimatic Caliper, Shengli Co., Ltd., Beijing, China). When the plants flowered, 10 plants in each treatment were harvested separately for measurement of leaf, stem, and root dry matter weight (DM). DM was determined after drying tissue at 70°C for 2 days, and then weight was recorded using a balance with 0.01 g accuracy. The time to the start of first inflorescence

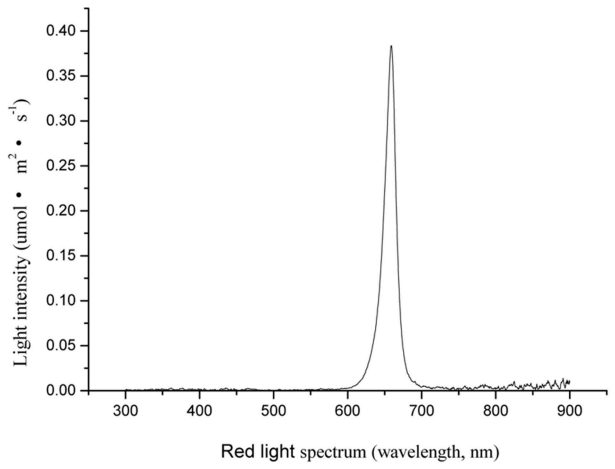

FIGURE 1 | Spectral distribution characteristics of red LED used for night break (NB) treatment.

and the number of leaves below the first inflorescence were recorded.

Measurement of Hormone Contents in Leaves and Stems

To measure the contents of indole-3-acetic acid (IAA) and gibberellin (GA), the third leaf of 3 tomato plants from the top, and the stems of 3 tomato plants were harvested quickly at 08.00 h when RL NB treatments were finished, and were preserved in liquid nitrogen. Approximately 1 g of leaves and stem were extracted with 10 mL of pre-cooled 80% methanol for 24 h at 4°C. The samples were centrifuged at 15,000 × g for 20 min at 4°C, the supernatant was collected, and concentrated into the aqueous phase by placing in a 40°C water bath with rotary evaporator (RE-205, Huayi Instrument Co., Ltd., Shanghai, China). The organic phase was treated with 0.2–0.3 g of polyvinylpolypyrrolidone (PVPP). After another centrifugation at 15,000 × g for 20 min at 4°C, the supernatant was adjusted to pH 2.5–3.0, extracted three times with an equal volume of ethyl acetate, and finally evaporated to dryness with a rotary evaporator at 40°C as described above.

The dried samples containing IAA and GA_3 were dissolved in chromatography grade methanol with 0.1 M glacial acetic acid as the mobile phase. The flow rate for all analyses was adjusted to 1 mL/min. Samples (100 μL) were subjected to high performance liquid chromatography (HPLC) analysis (Dobrev and Vankova, 2012; Yang et al., 2014). Detection and analysis were performed using a Waters 2498/UV Visible Detector (Shaanxi, China) (Djilianov et al., 2013). The analysis of IAA and GA_3 contents were repeated with 3 biological replicates, and each sample was assayed in triplicate by HPLC.

Measurement of Plant Growth, Development, and Yield after NB Treatment

NB treatments were finished when all plants began flowering. Then, tomato plants were transplanted into a solar greenhouse at the Experimental Station of Horticulture Department, Northwest A&F University P.R. China. The greenhouse is 76 m long and 8 m wide, with a planting area of 405 m^2. Construction of the solar greenhouse was described by Qiu et al. (2011). For each NB treatment group, 30 tomato plants were evenly transplanted along the edge of the furrow side with row spacing of 0.35 m and interplant spacing of 0.35 m. Plant height, stem diameter, and dry mass were determined at 2, 5, and 8 weeks after 10 tomato plants were transplanted into the solar greenhouse. Fresh fruit yield per plant and individual fruit weights were measured for each plant of 10 plants measured at harvest.

Statistical Analysis

Data were analyzed with ANOVA and Duncan's multiple range tests using the SAS software package (version 8.0, SAS Institute Cary, NC, USA). Graphing was performed in Excel 2007 or OriginPro (version 8.0, Origin Lab, MA, USA).

RESULTS

Effects of RL NB Treatments on Tomato Vegetative Growth

To study the effect of NB treatments on tomato seedling stem elongation, we first determined the RL NB treatments that were most effective to inhibit stem elongation in tomato plants. When the first leaf expanded, The RL NB treatments were applied to tomato plants when the first leaf expanded, were scheduled to last for 10 min, and recurred with a frequency of 1, 2, 3, and 4 h from 20:00 to 08:00 h. **Figure 2A** shows that all RL NB treatments inhibited stem elongation of tomato plants. The RL-treated plants were shorter than the control plants. After 56 days of RL NB treatments, the heights of tomato plants exposed to RL NB every 1, 2, 3, and 4 h decreased by 32.73, 31.44, 20.44, and 13.00%, respectively, compared with those of the control plants (**Figure 2B**).

The stem diameters of tomato plants were strongly affected by RL NB treatments (**Figure 2C**). After 56 days of treatments, the stem diameters of tomato plants subjected to RL NB every 1, 2, 3, and 4 h increased by 27.09, 25.08, 10.22, and 6.07%, respectively, compared with those of control plants (**Figure 2D**). No differences in total dry weight of tomato plants were observed between the RL NB treatment groups and the control group (**Table 1**). However, the leaf dry weight significantly increased and the stem dry weight significantly decreased in plants subjected to RL NB treatment every 1 and 2 h compared with those of the control plants (**Table 1**).

Effects of RL NB Treatments on Flowering of Tomato Plants

The transition from vegetative growth to reproductive growth is a major event in the plant cycle. The RL NB treatments delayed the flowering time of tomato plants. Control plants produced 8 leaves on the main stem before flowering; however, plants treated with RL NB every 1 and 2 h produced 11 leaves before flowering (**Figure 3A**), and those treated with RL NB every 3 h produced an average of 9 leaves before flowering (**Figure 3A**). There were no differences in the number of leaves produced before flowering in

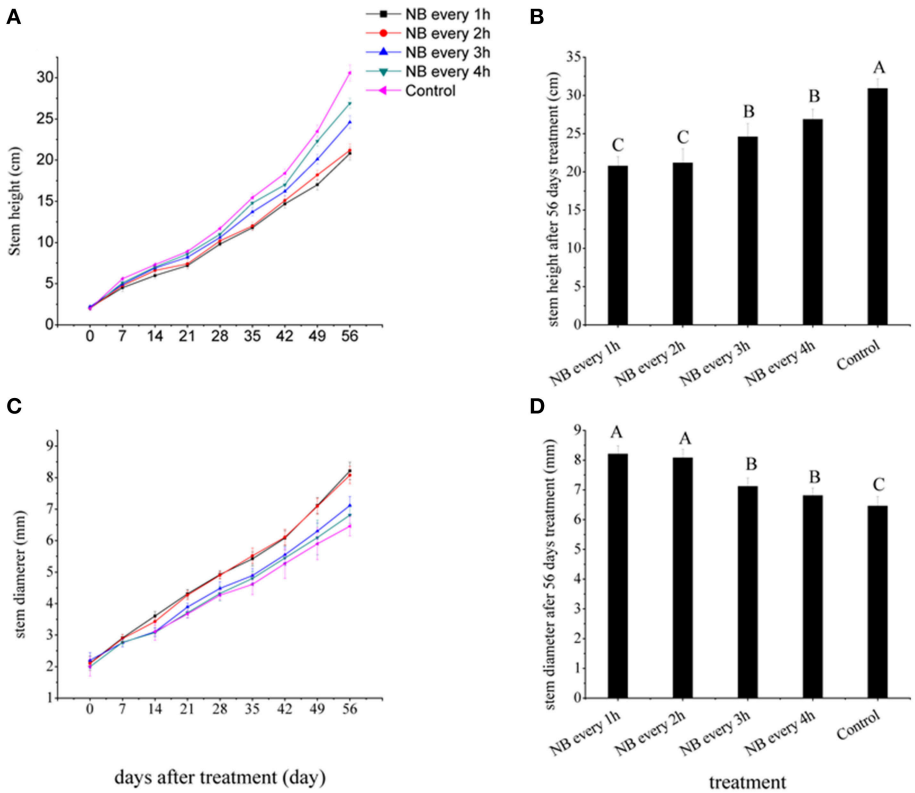

FIGURE 2 | Effects of red light (RL) night break (NB) treatment on tomato plant height and stem diameter. (A) Plant height was measured weekly after RL NB treatments every 1, 2, 3, and 4 h. **(B)** Plant height was measured after 56 days of RL NB treatments every 1, 2, 3, and 4 h. **(C)** Stem diameter was measured weekly after RL NB treatments every 1, 2, 3, and 4 h. **(D)** Stem diameter after 56 days of RL NB treatments every 1, 2, 3, and 4 h. Vertical bars represent SE ($n = 10$). Bars with different letters are significantly different at the level of $P = 0.01$ (Duncan's multiple range test).

TABLE 1 | Effect of red light night break (NB) on the dry weight of tomato leaf, stem, and root.

Treatment	Leaf dry weight (g)	Stem dry weight (g)	Root dry weight (g)	Total dry weight (g)
NB every 1 h	0.86^{A}	0.37^{B}	0.15^{A}	1.39^{A}
NB every 2 h	0.84^{A}	0.38^{B}	0.14^{A}	1.36^{A}
NB every 3 h	0.77^{B}	0.44^{AB}	0.13^{A}	1.34^{A}
NB every 4 h	0.75^{B}	0.48^{A}	0.13^{A}	1.36^{A}
Control	0.72^{B}	0.53^{A}	0.12^{A}	1.37^{A}

Different letters in a column represent significance at the 0.01 level (Duncan's multiple range test).

plants subjected to RL NB treatment every 4 h and control plants. The time from the start of the experiment to flowering was 39 days for control plants. The time to flowering for tomato plants subjected to RL NB treatment every 1, 2, 3, and 4 h increased to 56, 53, 49, and 42 days, respectively (**Figure 3B**).

Effects of RL NB Treatments on IAA and GA_3 Contents

IAA and GA have important roles in plant growth and development. We measured the contents of IAA and GA_3 in leaves and stems of tomato plants subjected to RL NB treatment for 56 days. The results showed that IAA and GA_3 contents in both leaves and stems decreased after RL NB treatment (**Figures 4A,B**). Treatment of tomato plants with RL NB every 1, 2, 3, and 4 h reduced the IAA contents in leaves by 33.3, 29.93, 15.31, and 8.50%, respectively, and reduced the GA_3 content in leaves by 41.29, 40.74, 24.07, and 9.26%, respectively, compared with those of control plants (**Figures 4A,B**). The RL NB treatment every 1, 2, 3, and 4 h reduced the IAA and GA_3 contents in stem by 56.04, 51.09, 24.17, and 7.69%, respectively, and 57.14, 46.71, 28.57, and 14.28%, respectively, compared with those of control plants (**Figures 4A,B**).

Effects of RL NB Treatments on Mature Tomato Plant Growth and Fresh Fruit Weight

The quality of plants and young plants is important for plant growth and yield. Two weeks after the young tomato plants were transplanted into the solar greenhouse, the stem diameter and leaf dry mass of tomato plants treated with RL NB every 1 and 2 h increased significantly, whereas plant height and stem dry weight decreased, and root dry weight did not change compared with control plants (**Table 2**). No significant differences in plant height, stem diameter, leaf dry mass, and stem dry mass were

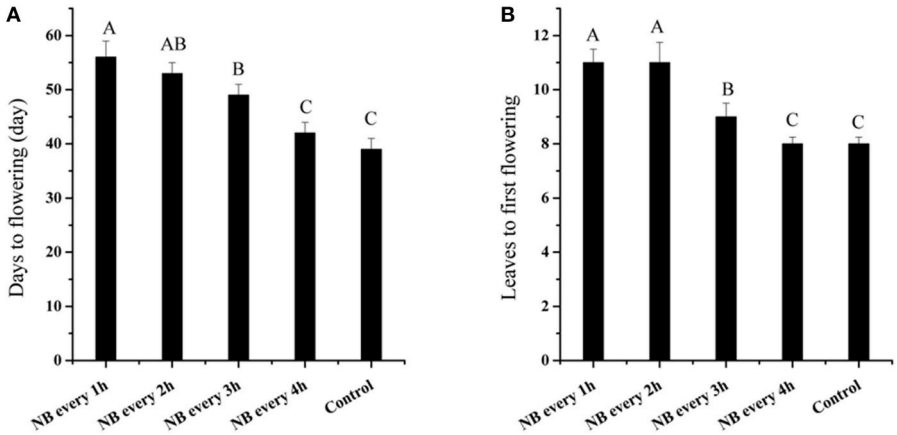

FIGURE 3 | Effects of red light (RL) night break (NB) on flowering of tomato plants. (A) Effects of RL NB treatment every 1, 2, 3, and 4 h on the number of days to flowering. **(B)** Effects of RL NB treatment every 1, 2, 3, and 4 h on the number of leaves to flowering. Vertical bars represent SE ($n = 3$). Bars with different letters are significantly different at the level of $P = 0.01$ (Duncan's multiple range test).

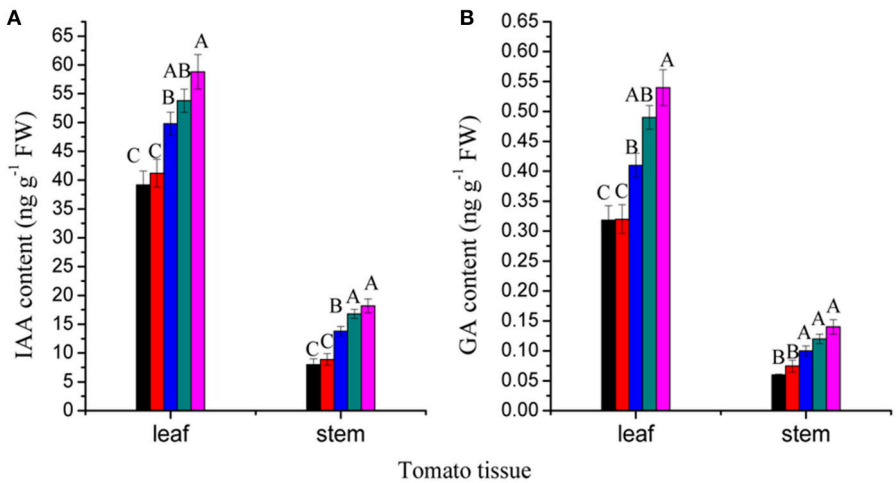

FIGURE 4 | Effects of red light (RL) night break (NB) on phytohormone contents in leaves and stems of tomato plants. (A) Effects of RL NB treatment every 1, 2, 3, and 4 h on IAA contents in tomato leaves and stems. **(B)** Effects of RL NB treatment every 1, 2, 3, and 4 h on GA contents in tomato leaves and stems. Vertical bars represent SE ($n = 3$). Bars with different letters are significantly different at the level of $P = 0.01$ (Duncan's multiple range test).

TABLE 2 | Growth and development of tomato plants in the solar greenhouse after red light night break (NB) treatment of plants and young plants up until flowering.

Treatment	2 weeks in solar greenhouse					5 weeks in solar greenhouse					8 weeks in solar greenhouse				
	Plant height (cm)	Stem diameter (cm)	Dry mass (g)			Plant height (cm)	Stem diameter (cm)	Dry mass (g)			Plant height (cm)	Stem diameter (cm)	Dry mass (g)		
			Leaf	Stem	Root			Leaf	Stem	Root			Leaf	Stem	Root
NB every 1 h	48.12^{B}	11.96^{A}	6.18^{A}	2.36^{A}	1.36^{A}	92.12^{A}	14.58^{A}	18.66^{A}	8.34^{A}	2.09^{A}	157.82^{A}	16.21^{A}	34.81^{A}	14.88^{A}	4.44^{A}
NB every 2 h	49.02^{B}	10.72^{A}	6.07^{A}	2.22^{A}	1.32^{A}	92.19^{A}	14.45^{A}	18.52^{A}	7.95^{A}	1.99^{A}	155.71^{A}	15.99^{A}	33.78^{A}	15.03^{A}	4.71^{A}
NB every 3 h	54.42^{AB}	9.77^{B}	5.34^{B}	2.18^{AB}	1.18^{A}	90.18^{A}	13.18^{A}	16.93^{A}	7.92^{A}	2.11^{A}	157.23^{A}	15.38^{A}	30.77^{A}	14.92^{A}	4.55^{A}
NB every 4 h	55.58^{A}	8.55^{C}	4.85^{C}	2.11^{B}	1.26^{A}	90.14^{A}	13.08^{A}	17.18^{A}	7.83^{A}	1.98^{A}	153.35^{A}	15.62^{A}	33.34^{A}	14.55^{A}	4.18^{A}
Control	57.85^{A}	8.08^{C}	4.46^{C}	1.99^{B}	1.10^{A}	89.95^{A}	12.99^{A}	17.11^{A}	7.99^{A}	2.06^{A}	150.59^{A}	15.41^{A}	33.41^{A}	13.72^{A}	4.62^{A}

Different letters in a column represent significance at the 0.01 level (Duncan's multiple range test).

TABLE 3 | Effect of red light night break (NB) on tomato growth, development, and fruit yield.

Treatment	Per fruit mass of first spica (g)	Per fruit mass of second spica (g)	Per fruit mass of third spica (g)	Fresh fruit mass per plant (kg)
NB every 1 h	215.561^{A}	211.232^{A}	204.522^{A}	2.62^{A}
NB every 2 h	207.348^{A}	219.311^{A}	198.451^{A}	2.51^{A}
NB every 3 h	178.145^{B}	207.431^{A}	211.072^{A}	2.38^{AB}
NB every 4 h	146.235^{B}	207.174^{A}	209.812^{A}	2.23^{B}
Control	138.036^{C}	203.321^{A}	216.216^{A}	2.12^{B}

Different letters in a column represent significance at the 0.01 level (Duncan's multiple range test).

detected 5 weeks after tomato plants were transplanted into the solar greenhouse.

After the tomato plants pre-treated with RL NB treatment every 1, 2, 3, and 4 h, the per tomato fresh weight increased by 23.58, 18.39, 12.26, and 9.43%, respectively, compared with control plants (**Table 3**). The increased fresh weight per tomato plant is due to the increased fresh weight of the first spica. There were no differences in the fresh weights of the second and third spica for plants subjected to RL NB treatments and control plants (**Table 3**).

DISCUSSION

Previous studies on stem elongation kinetics indicated that stem elongation was not constant during a 24 h day/night cycle, in many plant species, stem elongation rate was higher in dark conditions than in the light (Bertram and Karlsen, 1994; Tutty et al., 1994). Therefore, one of the effective ways to control plant height is to control the light condition in the dark period. Recent studies report that RL or high R: Fr light can make phytochromes exist more in Pfr form which inhibit plant stem elongation, whereas FRL or low R: Fr light can make phytochromes exist more in Pr form which can promote plant stem elongation (Behringer and Davies, 1992; Van Tuinen et al., 1999; Smith, 2000). Tomato contains five phytochromes, designated PHYA, PHYB1, PHYB2, PHYE, and PHYF, the five phytochromes can sense RL and FRL to control tomato plant growth (Hauser et al., 1997). It has been concluded that PHYB1 is mainly responsible for mediating the de-etiolation response of seedlings to RL as quantified by the inhibition of hypcotyl elongation, enhancement of anthocyanin accumulation, and end-of-day FRL responses (Kerckhoffs et al., 1997). Tomato plants subjected to light environments with low R:FR ratio or end-of-day FRL treatment displayed no differences in leaf area expansion, but had significantly increased stem elongation (Chia and Kubota, 2010; Kurepin et al., 2010). In the current study, we use RL NB treatment to prevent tomato plants from becoming spindly. RL NB can quickly change phytochromes from the Pr form to the Pfr form during the night and inhibit tomato stem elongation. The results showed that with the increase of RL NB frequency, plant height decreased. When the RL NB frequency was every 1 h, the heights of tomato plant decreased by 32.73% compared with the control (**Figures 2A,B**).

Before entering dark conditions, phytochromes exist predominantly in the Pfr form. After entering dark conditions, Pfr undergoes dark recovery and slowly converts into the inactive Pr form. 10 min RL NB can quickly change phytochromes from the Pr form to the Pfr form. When RL NB frequency is every 4 h, the tomato plants will enter dark period 4 h after 10 min RL NB which will lead phytochromes undergoes dark recovery and slowly converts into the inactive Pr form during the 4 h dark period. Therefore, the inhibition of tomato stem elongation by RL NB every 4 h is limited. However, when RL NB frequencies is every 1 h, the tomato plants will enter dark period 1 h after 10 min RL NB which will not enough for dark recovery. Therefore, the inhibition of tomato stem elongation by RL NB every 1 h is significant.

Light and phytohormones did not always independently regulate plant growth. This study showed that IAA and GA_3 contents decreased in both leaf and stem after treatment with RL NB, which reduced tomato stem elongation. Similar results have been reported by Steindler et al. (1999), who observed that inhibition of auxin transport alone was sufficient to abolish hypocotyl elongation in *Arabidopsis* plants grown under low R:FR ratio. Behringer and Davies (1992) reported that end-of-day FRL treatment increased IAA levels and stem elongation in the third internode of *Pisum sativum* plants. Kurepin et al. (2010) reported that stem elongation and endogenous GA levels increased when tomato plants were grown under low R:FR ratio conditions. Van Tuinen et al. (1999) demonstrated that tomato plants subjected to end-of-day FRL treatment elongated significantly more than control plants which could be due to the fact that phytochromes exist more in the Pr form during the night after end-of-day FRL treatment. In this study, RL NB treatment caused rapid conversion of the phytochromes from the Pr form to the Pfr form, which reduced the expression of genes involved in hormone synthesis, decreased the content of IAA and GA_3 in tomato leaf and stem, and inhibited tomato stem elongation (Nozue et al., 2007; Soy et al., 2012).

Tomato is a photoperiod-insensitive plant. The primary shoot is terminated by an inflorescence, and subsequent upright growth of tomato plants manifests as an apparent linear shoot consisting of consecutive sympodial units, each producing three leaves before terminating in a compound inflorescence. Tomato flowering time was evaluated by the number of leaves produced in the initial segment. Flower initiation was earlier and inflorescence development was superior under short-day conditions than under long-day conditions (Kinet, 1977). The NB treatments affected flowering of both long-day (Goto et al., 1991) and short-day plants (Ishikawa et al., 2005), but the effects were more evident in short-day plants, in which flowering was inhibited by a very short exposure to light during the night (Ishikawa et al., 2005). In the present study, the number of leaves to the first inflorescence increased from 8 in the control to 11 after tomato plants suffer from RL NB treatment every 1 and 2 h, but the number of inflorescences and florets did not differ from those of control plants. The sympodial unit morphologies of tomato plants subjected to RL NB treatments were the same as

those of control plants, with each producing three leaves before terminating in a compound inflorescence (data not shown). Daily exposure to 1 h of light in the middle of the night resulted in early flowering in *Arabidopsis* (Goto et al., 1991). Treatment of rice (*Oryza sativa*) with RL NB for 10 min clearly affected flowering when applied for different numbers of days (Ishikawa et al., 2005). In *Eustoma grandiflorum*, NB treatment using light with R:FR ratio above 5.3 delayed flowering, whereas light with R:FR ratio below 5.3 promoted earlier flowering (Yamada et al., 2009; Kim et al., 2011). In the future tomato growth, we can control the number of leaves to flowering through RL NB treatments.

Tomato is widely grown worldwide, and its production is economically and culturally important. The production of compact and heathier tomato plants could ultimately increase plant yield. This study showed that the fresh weight of the first spica increased after RL NB treatment. This resulted from an increase in the number of leaves from 8 to 11 in response to RL NB treatment every 1 and 2 h. The model developed by Heuvelink (1996) proposes that dry matter distribution in fruiting vegetable crops is regulated primarily by organ sink strength. Fruit development is an important event that significantly changes the sink load. From the time of inception, tomato fruit may account for as much as 90% of the total increase in plant dry weight (Nielsen and Veierskov, 1988). The RL NB treatment delayed flowering time in tomato plants, and plants produced more leaves, which increased leaf dry matter distribution, enhanced photosynthesis, and accelerated plant growth. This resulted in higher fresh weight of the first spica after treatment of tomato plants with RL NB.

LED is a new light source with several unique advantages, the use of LED in protected agriculture will become more and more popular. Therefore, the research of the precision utilization of LED in protected horticulture is very important for energy-saving and accuracy control in protected vegetable growth. Based on the results we obtained in this study, R LED could be used as a non-chemical alternative to control tomato height. More compact and healthier tomato plants could be gotten by NB using R LED and improve tomato early yield.

AUTHOR CONTRIBUTIONS

ZZ conceived and designed research; KC, LC, LY, XZ, and HZ conducted the experiments and write this manuscript, EB revised the language.

ACKNOWLEDGMENTS

This research was supported by the Key Laboratory of Protected Horticultural Engineering in Northwest, Ministry of Agriculture, PR China, by the State Key Laboratory of Crop Stress Biology for Arid Areas, NWAFU, PR China, and by the Agriculture Research System in China (No. CARS-25-D-02).

REFERENCES

Alokam, S., Chinnappa, C., and Reid, D. M. (2002). Red/far-red light mediated stem elongation and anthocyanin accumulation in Stellaria longipes: differential response of alpine and prairie ecotypes. *Can. J. Bot.* 80, 72–81. doi: 10.1139/b01-137

Behringer, F. J., and Davies, P. J. (1992). Indole-3-acetic acid levels after phytochrome-mediated changes in the stem elongation rate of dark-and light-grown Pisum seedlings. *Planta* 188, 85–92. doi: 10.1007/BF01160716

Berova, M., and Zlatev, Z. (2000). Physiological response and yield of paclobutrazol treated tomato plants (*Lycopersicon esculentum* Mill.). *Plant Growth Regul.* 30, 117–123. doi: 10.1023/A:1006300326975

Bertram, L., and Karlsen, P. (1994). Patterns in stem elongation rate in chrysanthemum and tomato plants in relation to irradiance and day/night temperature. *Sci. Hortic.* 58, 139–150. doi: 10.1016/0304-4238(94)90134-1

Bourget, C. M. (2008). An introduction to light-emitting diodes. *HortScience* 43, 1944–1946.

Chia, P.-L., and Kubota, C. (2010). End-of-day far-red light quality and dose requirements for tomato rootstock hypocotyl elongation. *HortScience* 45, 1501–1506.

Childs, K. L., Miller, F. R., Cordonnier-Pratt, M.-M., Pratt, L. H., Morgan, P. W., and Mullet, J. E. (1997). The sorghum photoperiod sensitivity gene, Ma3, encodes a phytochrome B. *Plant Physiol.* 113, 611–619. doi: 10.1104/pp.113.2.611

Djilianov, D. L., Dobrev, P. I., Moyankova, D. P., Vankova, R., Georgieva, D. T., Gajdošová, S., et al. (2013). Dynamics of endogenous phytohormones during desiccation and recovery of the resurrection plant species Haberlea rhodopensis. *J. Plant Growth Regul.* 32, 564–574. doi: 10.1007/s00344-013-9323-y

Dobrev, P. I., and Vankova, R. (2012). "Quantification of abscisic acid, cytokinin, and auxin content in salt-stressed plant tissues," in *Plant Salt Tolerance*, eds S. Shabala and T. A. Cuin (Sydney, NSW: Springer), 251–261.

Goto, N., Kumagai, T., and Koornneef, M. (1991). Flowering responses to light-breaks in photomorphogenic mutants of *Arabidopsis thaliana*, a long-day plant. *Physiol. Plant.* 83, 209–215. doi: 10.1111/j.1399-3054.1991.tb02144.x

Haque, S., Farooqi, A., Gupta, M., Sangwan, R., and Khan, A. (2007). Effect of ethrel, chlormequat chloride and paclobutrazol on growth and pyrethrins accumulation in Chrysanthemum cinerariaefolium Vis. *Plant Growth Regul.* 51, 263–269. doi: 10.1007/s10725-007-9170-6

Hauser, B. A., Pratt, L. H., and Cordonnier-Pratt, M.-M. (1997). Absolute quantification of five phytochrome transcripts in seedlings and mature plants of tomato (*Solanum lycopersicum* L.). *Planta* 201, 379–387. doi: 10.1007/s004250050080

Heuvelink, E. (1996). Dry matter partitioning in tomato: validation of a dynamic simulation model. *Ann. Bot.* 77, 71–80. doi: 10.1006/anbo.1996.0009

Hughes, J., and Lamparter, T. (1999). Prokaryotes and phytochrome. The connection to chromophores and signaling. *Plant Physiol.* 121, 1059–1068. doi: 10.1104/pp.121.4.1059

Ishikawa, R., Tamaki, S., Yokoi, S., Inagaki, N., Shinomura, T., Takano, M., et al. (2005). Suppression of the floral activator Hd3a is the principal cause of the night break effect in rice. *Plant Cell* 17, 3326–3336. doi: 10.1105/tpc.105.037028

Izawa, T., Oikawa, T., Sugiyama, N., Tanisaka, T., Yano, M., and Shimamoto, K. (2002). Phytochrome mediates the external light signal to repress FT orthologs in photoperiodic flowering of rice. *Genes Dev.* 16, 2006–2020. doi: 10.1101/gad.999202

Kerckhoffs, L., Schreuder, M., Tuinen, A. V., Koornneef, M., and Kendrick, R. (1997). Phytochrome control of anthocyanin biosynthesis in tomato seedlings: analysis using photomorphogenic mutants. *Photochem. Photobiol.* 65, 374–381. doi: 10.1111/j.1751-1097.1997.tb08573.x

Kim, Y. J., Lee, H. J., and Kim, K. S. (2011). Night interruption promotes vegetative growth and flowering of *Cymbidium*. *Sci. Hortic.* 130, 887–893. doi: 10.1016/j.scienta.2011.08.031

Kinet, J. (1977). Effect of light conditions on the development of the inflorescence in tomato. *Sci. Hortic.* 6, 15–26. doi: 10.1016/0304-4238(77)90074-7

Kurepin, L. V., Walton, L. J., and Reid, D. M. (2007). Interaction of red to far red light ratio and ethylene in regulating stem elongation of Helianthus annuus. *Plant Growth Regul.* 51, 53–61. doi: 10.1007/s10725-006-9147-x

Kurepin, L. V., Yip, W.-K., Fan, R., Yeung, E. C., and Reid, D. M. (2010). The roles and interactions of ethylene with gibberellins in the far-red enriched light-mediated growth of *Solanum lycopersicum* seedlings. *Plant Growth Regul.* 61, 215–222. doi: 10.1007/s10725-010-9465-x

Massa, G. D., Kim, H.-H., Wheeler, R. M., and Mitchell, C. A. (2008). Plant productivity in response to LED lighting. *HortScience* 43, 1951–1956.

Mockler, T. C., Guo, H., Yang, H., Duong, H., and Lin, C. (1999). Antagonistic actions of Arabidopsis cryptochromes and phytochrome B in the regulation of floral induction. *Development* 126, 2073–2082.

Morrow, R. C. (2008). LED lighting in horticulture. *HortScience* 43, 1947–1950.

Nielsen, T. H., and Veierskov, B. (1988). Distribution of dry matter in sweet pepper plants (*Capsicum annuum* L.) during the juvenile and generative growth phases. *Sci. Hortic.* 35, 179–187. doi: 10.1016/0304-4238(88)90111-2

Nourai, A., and Harris, G. (1983). Effects of growth retardants on inflorescence development in tomato. *Sci. Hortic.* 20, 341–348. doi: 10.1016/0304-4238(83)90148-6

Nozue, K., Covington, M. F., Duek, P. D., Lorrain, S., Fankhauser, C., Harmer, S. L., et al. (2007). Rhythmic growth explained by coincidence between internal and external cues. *Nature* 448, 358–361. doi: 10.1038/nature05946

Qiu, R., Kang, S., Li, F., Du, T., Tong, L., Wang, F., et al. (2011). Energy partitioning and evapotranspiration of hot pepper grown in greenhouse with furrow and drip irrigation methods. *Sci. Hortic.* 129, 790–797. doi: 10.1016/j.scienta.2011.06.012

Smith, H. (2000). Phytochromes and light signal perception by plants—an emerging synthesis. *Nature* 407, 585–591. doi: 10.1038/35036500

Soy, J., Leivar, P., González-Schain, N., Sentandreu, M., Prat, S., Quail, P. H., et al. (2012). Phytochrome-imposed oscillations in PIF3 protein abundance regulate hypocotyl growth under diurnal light/dark conditions in Arabidopsis. *Plant J.* 71, 390–401. doi: 10.1111/j.1365-313x.2012.04992.x

Steindler, C., Matteucci, A., Sessa, G., Weimar, T., Ohgishi, M., Aoyama, T., et al. (1999). Shade avoidance responses are mediated by the ATHB-2 HD-zip protein, a negative regulator of gene expression. *Development* 126, 4235–4245.

Tutty, J. R., Hicklenton, P. R., Kristie, D. N., and McRae, K. B. (1994). The influence of photoperiod and temperature on the kinetics of stem elongation in Dendranthema grandiflorum. *J. Am. Soc. Hortic. Sci.* 119, 138–143.

Van Tuinen, A., Peters, A., Kendrick, R., Zeevaart, J., and Koornneef, M. (1999). Characterisation of the procera mutant of tomato and the interaction of gibberellins with end-of-day far-red light treatments. *Physiol. Plant.* 106, 121–128. doi: 10.1034/j.1399-3054.1999.106117.x

Weller, J. L., and Reid, J. B. (1993). Photoperiodism and photocontrol of stem elongation in two photomorphogenic mutants of *Pisum sativum* L. *Planta* 189, 15–23. doi: 10.1007/BF00201338

Yamada, A., Tanigawa, T., Suyama, T., Matsuno, T., and Kunitake, T. (2009). Red: far-red light ratio and far-red light integral promote or retard growth and flowering in *Eustoma grandiflorum* (Raf.) Shinn. *Sci. Hortic.* 120, 101–106. doi: 10.1016/j.scienta.2008.09.009

Yang, R., Yang, T., Zhang, H., Qi, Y., Xing, Y., Zhang, N., et al. (2014). Hormone profiling and transcription analysis reveal a major role of ABA in tomato salt tolerance. *Plant Physiol. Biochem.* 77, 23–34. doi: 10.1016/j.plaphy.2014.01.015

Zhan, J., Huang, W., and Wang, L. (2003). Research of weak light stress physiology in plants. *Chinese Bull. Bot.* 20, 43–50. doi: 10.3969/j.issn.1674-3466.2003.01.005

Conflict of Interest Statement: The authors declare that the research was conducted in the absence of any commercial or financial relationships that could be construed as a potential conflict of interest.

frontiers in Plant Science

ORIGINAL RESEARCH
published: 31 March 2016
doi: 10.3389/fpls.2016.00394

High-Throughput Growth Prediction for *Lactuca sativa* L. Seedlings Using Chlorophyll Fluorescence in a Plant Factory with Artificial Lighting

Shogo Moriyuki[1] *and Hirokazu Fukuda*[1,2]*

[1] Department of Mechanical Engineering, Graduate School of Engineering, Osaka Prefecture University, Osaka, Japan,
[2] Japan Science and Technology Agency, PRESTO, Saitama, Japan

Poorly grown plants that result from differences in individuals lead to large profit losses for plant factories that use large electric power sources for cultivation. Thus, identifying and culling the low-grade plants at an early stage, using so-called seedlings diagnosis technology, plays an important role in avoiding large losses in plant factories. In this study, we developed a high-throughput diagnosis system using the measurement of chlorophyll fluorescence (CF) in a commercial large-scale plant factory, which produces about 5000 lettuce plants every day. At an early stage (6 days after sowing), a CF image of 7200 seedlings was captured every 4 h on the final greening day by a high-sensitivity CCD camera and an automatic transferring machine, and biological indices were extracted. Using machine learning, plant growth can be predicted with a high degree of accuracy based on biological indices including leaf size, amount of CF, and circadian rhythms in CF. Growth prediction was improved by addition of temporal information on CF. The present data also provide new insights into the relationships between growth and temporal information regulated by the inherent biological clock.

Keywords: circadian clock, chlorophyll fluorescence, diagnosis system, imaging, lettuce, machine learning

OPEN ACCESS

Edited by:
Alejandro Isabel Luna-Maldonado, Universidad Autónoma de Nuevo León, Mexico

Reviewed by:
Hao Peng, Washington State University, USA
Chong Zhang, University of Maryland Baltimore County, USA

***Correspondence:**
Hirokazu Fukuda
fukuda@me.osakafu-u.ac.jp

Specialty section:
This article was submitted to Crop Science and Horticulture, a section of the journal Frontiers in Plant Science

Received: *29 January 2016*
Accepted: *14 March 2016*
Published: *31 March 2016*

Citation:
Moriyuki S and Fukuda H (2016) High-Throughput Growth Prediction for Lactuca sativa L. Seedlings Using Chlorophyll Fluorescence in a Plant Factory with Artificial Lighting. Front. Plant Sci. 7:394. doi: 10.3389/fpls.2016.00394

INTRODUCTION

A plant factory using artificial light offers the potential of stably producing vegetables under constant cultivation year-round, and production can be increased by using vertical multi-cultivating racks (Kozai et al., 2015). However, this approach is more costly than production of outdoor-grown vegetables under sunlight, because the initial costs, and running costs of the equipment are higher. To reduce these costs, reduction of energy costs, development of more efficient environmental control systems, and more effective cultivation protocols are required. Thus, these plant factories require precise environmental control (Morimoto et al., 1995; Kozai et al., 2015). Recently, Li et al. (2016) and Murase et al. (2015) examined the effect of light quality on plant growth. Moreover, Okamura et al. (2014) investigated the optimal harvesting time for vaccine-producing transgenic lettuce and Takahashi et al. (2012) assessed the effect of air flow on production of a vaccine protein against swine edema disease in transgenic lettuce.

Poorly grown plants that do not meet the quality required for sale cause serious losses, reducing the profit of plant factories (Kozai et al., 2015). Poor growth inevitably occurs due to individual differences, even when the same varieties and seeds are cultivated. Thus, identifying and culling

low-grade plants at an early stage, using so-called seedling diagnosis technology, is an important process for making plant factories profitable. This technology predicts growth using biological information from seedlings and disposes of seedlings that are predicted to grow poorly (Fukuda et al., 2011).

In large-scale plant factories, statistical values for biological information are stable (Ninness, 2000), because the statistical population of plants is over 1000 every day. Therefore, the accuracy of growth predictors has improved as automatic data acquisition systems and databases to store the biological data have been constructed. In general, multiple visual inspections of leaf size, color, and shape of every seedling provide indices for the assessment of plant growth in commercial factories.

Recently, imaging of chlorophyll fluorescence (CF) has been used as a highly efficient means of visually inspecting plants to assess photosynthetic capacity and degree of stress (Takayama et al., 2014). CF is due to the emission of red light from chlorophyll α pigments (Krause and Weis, 1991; Govindjee, 1995) when residual light energy is not used for photosynthetic reactions. Accurate measurement of CF emission thus allows the evaluation of photosynthetic functions, both the photosynthetic photochemical reactions and the status of heat dissipation processes, without any need for physical contact with the plant (Maxwell and Johnson, 2000; Takayama and Nishina, 2009). The technique of imaging CF, originally developed by Omasa et al. (1987) and Daley et al. (1989), has been used to evaluate the heterogeneous distribution of photosynthetic activities over a leaf surface and thus to detect photosynthetic dysfunctions caused by biotic and abiotic stress factors. Recently, CF imaging has been scaled up to a whole plant (Takayama et al., 2010), a tree canopy (Nichol et al., 2012), and tomato crops cultivated in a large-scale greenhouse (Takayama et al., 2011a,b,c).

CF also exhibits an inherent circadian rhythm, resulting from the regulation of expression of photosynthesis-associated genes by the circadian clock with an approximately 24 h period, and Gould et al. (2009) measured circadian rhythm by the CF in *Arabidopsis thaliana*. Clock genes, which generate circadian rhythms, also regulate growth (Dodd et al., 2005, 2015; Harmer, 2009; Farré and Weise, 2012; Higashi et al., 2014, 2015; Voß et al., 2015). In a previous study of seedling diagnosis, we verified the effectiveness of growth prediction based on the circadian rhythm using a bioluminescent reporter gene assay for transgenic *A. thaliana* carrying the *CCA1*::*LUC* construct, in which the promoter of the *CCA1* clock gene has been fused to a modified firefly luciferase (*LUC*) gene (Fukuda et al., 2011). This study clarified that growth in biomass is correlated with the amount of *CCA1* clock gene expression that was measured via luciferase bioluminescence under various light conditions. In addition, we have investigated features of the circadian rhythm in lettuce cultivars using a similar luciferase-based bioluminescent assay to that of *AtCCA1*::*LUC* (Ukai et al., 2012; Higashi et al., 2014) and evaluated the growth rate of lettuce plants when the circadian rhythm is regulated by conditions of a non-24 h period (Higashi et al., 2015). We speculated that measurement of circadian rhythms will lead to improved plant growth prediction.

Hence, CF monitoring has a practical advantage for simultaneous capture of multiple types of biological information, improving the accuracy of seedling diagnosis. However, there are two tasks needed for construction of a seedling diagnosis system: development of equipment that can measure a time course of CF for a large number of seedlings simultaneously and assessment of the effectiveness of growth prediction based on indices related to the circadian rhythm.

We developed a high-throughput growth prediction methodology for *Lactuca sativa* L. seedlings using CF in a commercial large-scale plant factory, which produces about 5000 lettuce plants every day. The CF of each seedling was measured 6 times every 4 h at 6 days after sowing to detect the circadian rhythm. Multiple types of biological information (six variables including leaf area and the amplitude of the circadian rhythm) were obtained from CF imaging. Finally, we assessed the ability of each variable to predict growth and then combined the variables by machine learning to explore superior indices for seedling diagnosis.

MATERIALS AND METHODS

Plant Material and Growth Conditions

Experiments were carried out using lettuce seeds (*L. sativa* L. cv. Frillice and SB555GL, fixed lines of lettuce cultivars from Snow Brand Seed Co., Ltd., Sapporo, Japan).

Two rooms were used for cultivation (rooms A and B); room A was designed for germination and greening of seed cotyledons, and room B was designed for raising seedlings. Room A was equipped with a carrier machine for a greening panel, a white light emitting diode (LED) for greening (LIFELED'S; NEC Lighting, Ltd., Tokyo, Japan), and our seedling diagnosis system. Room B was equipped with LED units for raising seedlings (with blue, white, red, and far-red LEDs, GreenPower LED production module DR/W/FR 120, Philips, Amsterdam, Netherlands).

In room A, first, each plant was seeded in a greening panel (60 × 60 cm; **Figure 1C**) allowing 600 plants to be seeded to a urethane sponge sheet (each sponge block was 25 × 25 mm) with 5 L tap water and fertilizer ($N:P_2O_5$: K_2O:CaO:MgO = 10:8:27:0:4 and $N:P_2O_5:K_2O$:CaO:MgO = 11:0:0:23:0, Otsuka House No. 1 and 2, respectively; Otsuka Chemical Co., Ltd., Osaka, Japan) at pH 6.0 and EC 0.6. Secondly, the greening panel was laid in the dark at 25°C for 2 days in a growth chamber for germination. Thirdly, plants were cultivated 4 days under white LED light under 15-h light: 9-h dark conditions. Finally, CF of each seedling was measured 6 times every 4 h at 6 days after sowing seeds (see next section). After this measurement, the seedlings were transplanted in a raising panel (60 × 90 cm; **Figure 1D**) with 153 plantation holes. These seedlings were then raised in room B under 15-h light: 9-h dark conditions at 22°C for 11 days.

To investigate prediction accuracy, we measured fresh weight W_i of 153 Frillice plants and 148 SB555GL plants at 17 days after sowing. We considered the fresh weight of whole plant of Frillice including the sponge and root, whereas fresh weight of SB555GL was weight after removing sponge and root. There was no influence of sponge part: its weight was 0.228 ± 0.002 g.

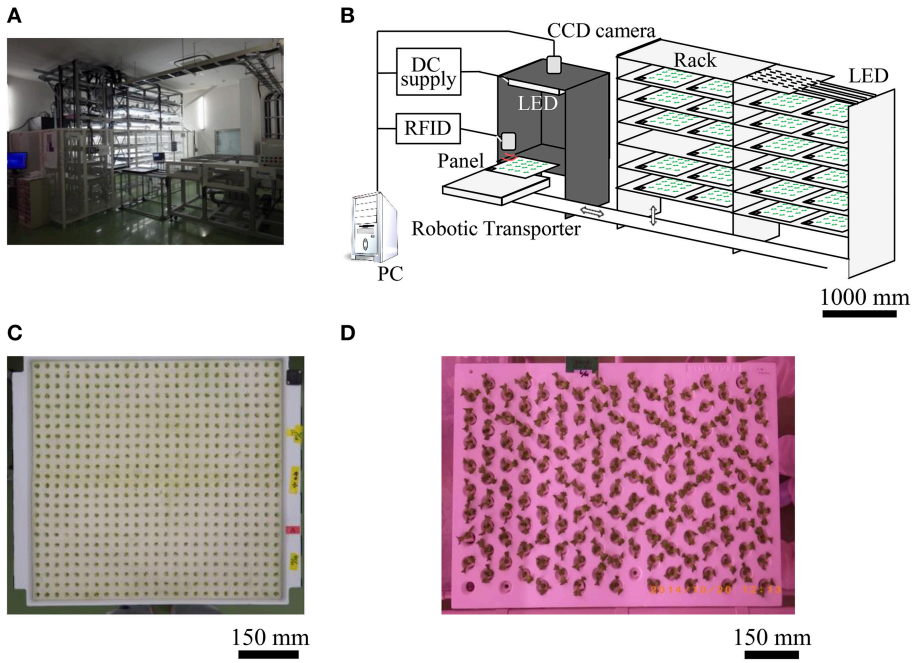

FIGURE 1 | Seedling diagnostics system and individual panels. Shown are photographs of **(A)** room A, system chart **(B)**, greening panel **(C)**, and raising panel **(D)**.

Automatic Chlorophyll Fluorescent Measurement System

In a large-scale plant factory, automation is required for seedling diagnosis and transplantation of plants. Thus, we developed a seedling diagnosis system (**Figures 1A,B**) which can diagnose over 7200 seedlings every day in such a factory. This seedling diagnosis system has a carrier robot for greening panels, a seedling diagnosis apparatus, and a transplanting robot.

The diagnosis apparatus is made up mainly of a dark box (900 mm in width, 900 mm in depth, and 1200 mm in height), a highly sensitive charge coupled device (CCD) camera (Hamamatsu ORCA-Flash4.0; Hamamatsu Photonics KK, Shizuoka, Japan) in the upper dark box, 8 blue LED panels [λ_p = 470 nm, 150 × 150 mm at the base; 4 ISL-150X150-HBB blue panels (CCS Inc., Kyoto, Japan), and 4 VBL-SL150 blue panels (Valore Corp., Kyoto, Japan)] in the dark box to excite the chlorophyll of the seedling. In addition, it included a PC-controlled CCD camera, LED controller, RFID system (V680-CA5D02-V2; OMRON Corporation, Kyoto, Japan), digital input/output unit (DIO-6464L-USB; CONTEC Co., Ltd., Osaka, Japan), and automatic acquisition/analysis program for leaf area, CF, and circadian rhythms.

In the seedling diagnosis system, at the time of seedling diagnosis on day 6 after sowing, the greening panel carrier robot automatically carried a target panel to the dark box. Immediately, seedlings were illuminated with blue LED light (30 μmol m^{-2} s^{-1}) for 2 s to excite chlorophyll. Then, a CF image, such as in **Figure 2A**, was obtained by CCD camera immediately after the blue LED was turned off. The exposure time of the CCD camera was set to 2 s and the CF image was captured 14 times sequentially for 30 s in one measurement. This measurement was repeated 6 times every 4 h.

We also utilized an RFID system to input seedling diagnosis results, and a digital input/output unit to control opening and closing of the shutter that the dark box was equipped with. Based on the results, we were able to transplant only superior seedlings from the greening panel to the raising panel by a transplant robot automatically.

Methods of Calculating Leaf Area and Circadian Rhythms

To calculate leaf area, the grayscale image acquisition CCD camera captures the distribution of fluorescence intensity between sponge and seedling simultaneously. Discriminant analysis is a method to separate the seedling distribution from intensity distribution mechanically (Phan and Cichocki, 2010). Using this method, we could automatically obtain the threshold k^* that corresponds to the maximum value of the separation metric $f(k)$ that compares between-class variance and within-class variance. The separation metric $f(k)$ is described by:

$$f(k^*) = \max_{0 \le k < L} f(k) = \max_{0 \le k < L} \frac{n_1(k) \cdot \left(\mu_1(k) - \mu_0\right)^2 + n_2(k) \cdot \left(\mu_2(k) - \mu_0\right)^2}{n_1(k) \cdot \sigma_1^2(k) + n_2(k) \cdot \sigma_2^2(k)}$$

where $n_1(k)$, $\mu_1(k)$, and $\sigma_1^2(k)$ are the number of pixels, the average, and the variance of fluorescence distribution that was less than k (sponge distribution in **Figure 2B**), respectively. On the other hand, $n_2(k)$, $\mu_2(k)$, and $\sigma_2^2(k)$ are the number of pixels,

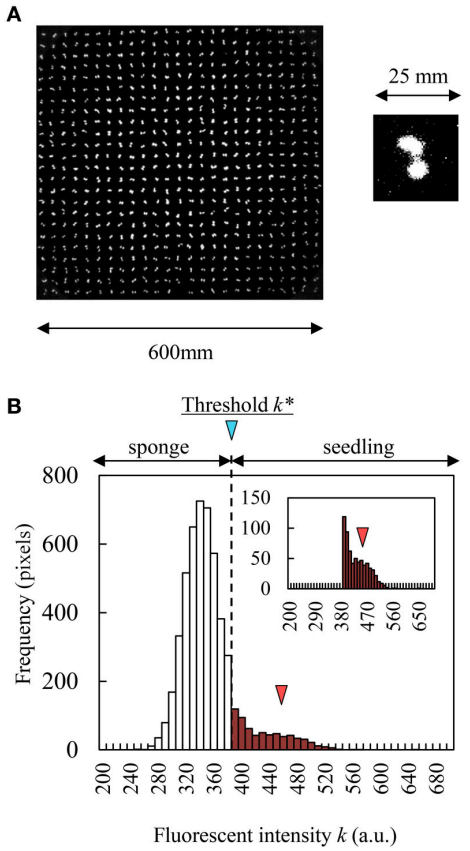

FIGURE 2 | CF obtained by CCD camera and histogram of fluorescent intensity in a seedling and sponge image. (A) Grayscale CF image of 600 seedlings (contrast changed). **(B)** Histogram of fluorescent intensity of sponge (white bars) and a seedling (red bar). Red triangle indicates the peak of histogram in a seedling.

the average, and the variance of fluorescence distribution that was greater than k (seedling distribution in **Figure 2B**), respectively. μ_0 is the average of the whole distribution, and L is the maximum number of k ($L = 2^{16}$). If the fluorescence intensity from a pixel was greater than k^*, this pixel was determined as belonging to the leaf area, and if not, to the sponge block region. We calculated k^* in each sponge block region (71 × 72 pixels).

Next, to calculate the circadian rhythm of CF, sequential CF images were captured every 2 s 14 times with a 2 s exposure time to measure the delay curve of CF (**Figure 3A**); this imaging was performed 6 times every 4 h. For a defined leaf area, we obtained the CF per seedling $C_{ij}(\kappa)$, where κ means time, i means seedling ID, and j means the number of measurement times. The CF decreased in time immediately after blue LED turn-off, and the light intensity converged to the constant value C'_{ij} (**Figure 3A**). We defined the amount of CF as $I_{ij}(t)$ normalized by C'_{ij} as follows:

$$I_{ij}(t) = \int_0^{\kappa^*} \left(\frac{C_{ij}(\kappa) - C'_{ij}}{C'_{ij}} \right) d\kappa$$

where $\kappa = 0$ means the time of blue LED turn-off in the dark box, and the constant value C'_{ij} occurs at $\kappa = \kappa^*$.

We obtained $I_{ij}(t)$ for each seedling 6 times ($n = 6$) every 4 h. We calculated the amplitude a_i and the peak phase φ_i ($0 \leq \varphi_i < 2\pi$) that corresponds to the maximum value of the determination coefficient (Halberg et al., 1972) as follows:

$$y_i(t) = a_i \cos\left(2\pi \frac{t}{T} - \varphi_i\right) + \frac{1}{n}\sum_{j=1}^{n} I_{ij}(t)$$

$$A_i = a_i / \frac{1}{n}\sum_{j=1}^{n} I_{ij}(t)$$

In our study, when $t = 0$, the white LED used for greening was turned on in room A. T is the light period (in this case, 24 h). In addition, we defined the normalized amplitude A_i as the seedling diagnosis index.

RESULTS

Correlation between CF and Fresh Weight

Figure 3A shows that the CF decreased over time immediately after blue LED turn-off and then converged to a constant value C'_{ij} of about 30 s. **Figures 3B,C** show histograms of the fresh weight of Frillice and SB555GL, respectively. Both distributions were nearly Gaussian. **Figures 3D,E** shows the alteration of $I_{ij}(t)$ during a day from one morning to the next. As the average of the fresh weight W_i is μ_w and its standard variation is σ_w, we separated plants into four categories based on these values: 1 ($\mu_w + \sigma_w < W_i$), 2 ($\mu_w < W_i \leq \mu_w + \sigma_w$), 3 ($\mu_w - \sigma_w < W_i \leq \mu_w$), and 4 ($W_i \leq \mu_w - \sigma_w$). From these results, we found that both cultivars strongly emitted CF at night. Moreover, CF decreased with higher weight over a threshold ($W_i > 7.6$ g) in Frillice; on the other hand, SB555GL did not show such a tendency (**Figures 3F,G**). The vertical axis in **Figures 3F,G** mean the average of CF from 10 plants for fresh weight.

Correlation between Indices of Circadian Rhythms and Fresh Weight

Figures 4A,B,D,E show the relationship between W_i and the amplitude A_i and peak phase φ_i. Based on these results, we found that these indices of circadian rhythm did not have any correlation with W_i; that is, the correlation coefficient R was low. In **Figures 4B,E**, the center value and range of φ_i differed depending on the cultivar. Hence, we also defined a baseline $\overline{\varphi_i}$ for peak phase φ_i, and obtained phase φ_i' to consider the environmental synchrony.

$$\varphi_i' = \overline{\varphi_i} + |\overline{\varphi_i} - \varphi_i|$$

$\overline{\varphi_i}$ for Frillice and SB555GL was 1.70π rad and 1.66π rad, respectively. **Figures 4C,F** shows the correlation between phase φ_i' and W_i, for which a weak correlation was observed in SB555GL. It seems that growth prediction may be improved by considering the phase of the circadian rhythm.

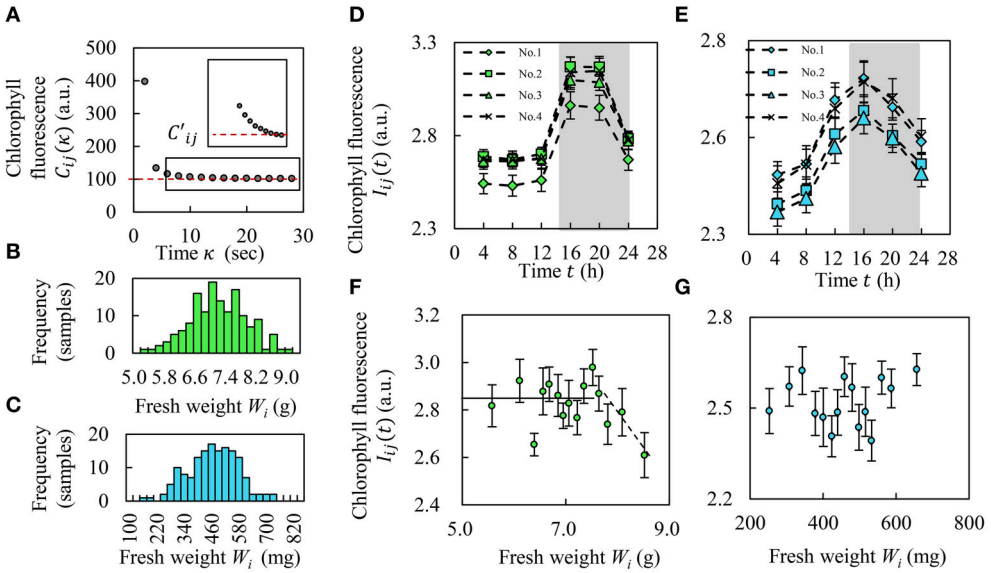

FIGURE 3 | Amount of chlorophyll and relationship between CF and fresh weight. (A) Red line shows convergence value, C'_{ij}. **(B,C)** Histograms of fresh weight in Frillice **(B)** and SB555GL **(C)**. **(D,E)** Alteration of CF $I_{ij}(t)$ over the course of a day in Frillice **(D)** and SB555GL **(E)**, averaging $I_{ij}(t)$ into four categories (see Results Section). The white and gray background colors indicate light and dark conditions. **(F,G)** Relationship between the average value of fresh weight W_i and the average of CF from each top 10 plants for fresh weight of Frillice **(F)** and SB555GL **(G)**. All error bars mean standard error.

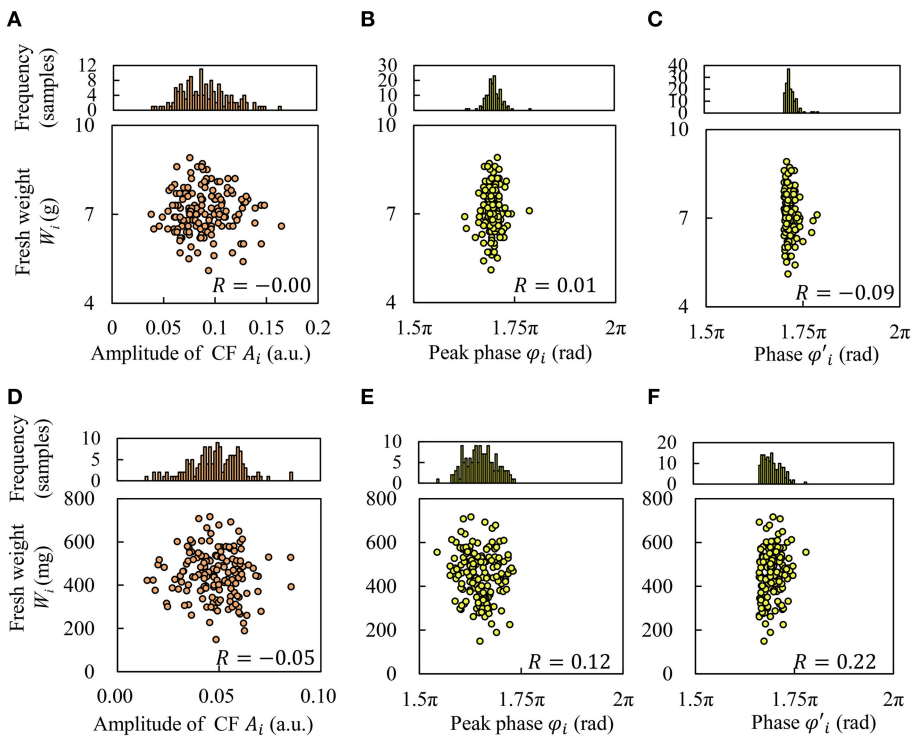

FIGURE 4 | Correlation between fresh weight and index of circadian rhythms of CF. Frillice: **(A–C)**; SB555GL: **(D–F)**. **(A,D)** Amplitude A_i, **(B,E)** peak phase φ_i, and **(C,F)** phase φ'_i.

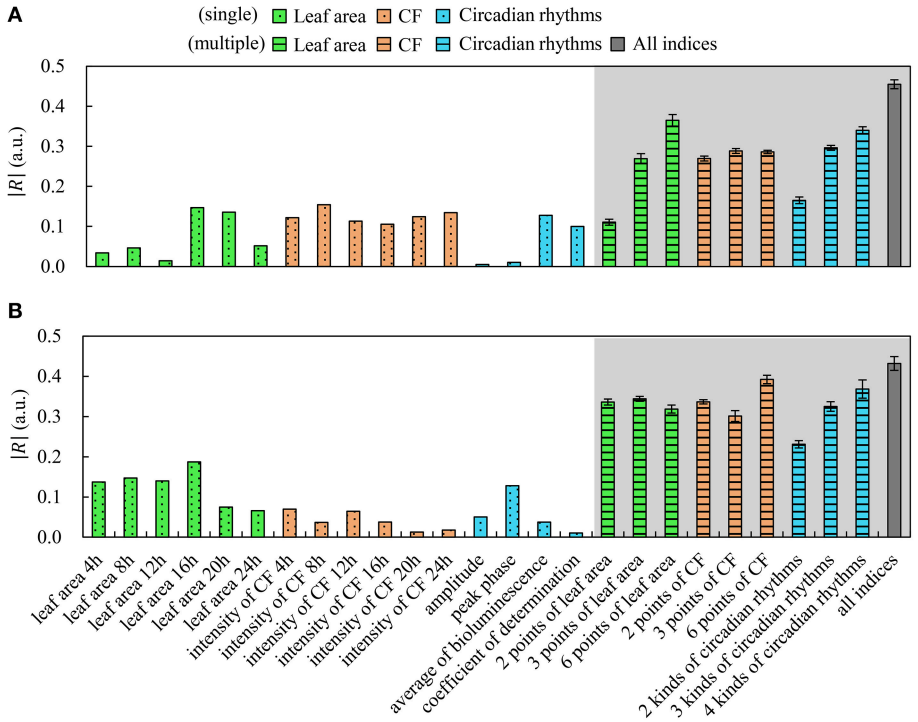

FIGURE 5 | Correlation between indices and fresh weight using machine learning. Frillice **(A)**; SB555GL **(B)**. White background indicates a single index, and gray background indicates multiple indices. All error bars indicate standard error.

Growth Prediction Using Machine Learning

Neural networks have the inherent capability of learning unknown nonlinear properties (Chen et al., 1990). Morimoto and Hashimoto (2009) used neural networks to control environmental factors in plant factories, and Hendrawan and Murase (2011) used neural networks to predict water content of moss using RGB intensity. In our study, we predicted plant growth using a neural network based on biological information, including 6 time measurements of leaf area and CF (e.g., at 4, 8, 12, 16, 20, and 24 h), and 4 circadian rhythm features. These circadian rhythm features are amplitude A_i, peak phase φ_i, average of CF ($< I_i >= \frac{1}{n}\sum_{j=1}^{n} I_{ij}(t)$), and the determination coefficient of curve approximation $y_i(t)$. We created a neural network containing up to 16 kinds of biological information in an input layer and W_i in an output layer using 70% of all plant data as training data by a back-propagation method. We used neural networks 40 times with several types of input data, and estimated the average correlation coefficient R and standard error. **Figure 5** shows the magnitude of the correlation coefficient $|R|$ between each index and W_i . The white background in **Figure 5** indicates a single index; that is, single data points were used for leaf area at each time, CF at each time, amplitude, peak phase, average of CF, and determination coefficient. The gray background in **Figure 5** indicates multiple indices: leaf area (2, 3, and 6 points), CF (2, 3, and 6 points), circadian rhythms (2, 3, and 4 kinds), and all biological indices. We defined 2 points of leaf area and CF as meaning data acquired 2 times (at 12 and 24 h) and 3 points of leaf area as meaning data acquired 3 times (at 8, 16, and 24 h). In addition, we defined 2 kinds of circadian rhythms by A_i and φ_i, 3 kinds of circadian rhythms by A_i, φ_i, and $< I_i >$, and 4 kinds of circadian rhythms by all of them plus the determination coefficient. We found that growth was better predicted by multiple indices over a single index.

DISCUSSION

In this study, we found that the fresh weight of Frillice and SB555GL showed Gaussian distributions based on the Kolmogorov-Smirnov test. **Figures 3D,E** shows that Frillice and SB555GL have circadian rhythms and a peak of CF in the evening for all plants, supporting the results of Gould et al. (2009). We have succeeded in developing a seedling diagnostics system that automatically measures CF and circadian rhythms of each plant at an early stage simultaneously. **Figure 3F** shows fresh weight in Frillice decreases with increase of CF, up to a certain threshold based on fresh weight. In other words, when this seedling is under a certain threshold value of CF, its growth is better. This observation suggests that seedlings that use a lot of light energy in photochemical reactions, which would decrease the CF, have higher growth potential.

As can be seen in **Figure 4**, it would appear that growth prediction can be improved by considering environmental synchrony. It is known that the dry weight increase of *A. thaliana* in a 24 h light cycle is better than in a 20 or 28 h cycle (Dodd et al., 2005; Fukuda et al., 2011), suggesting that the relationship of phase between circadian rhythms and environmental cycles

strongly affect plant growth. Thus, we introduced the peak baseline φ_i' to investigate the effect of the relationship of phase between circadian rhythms and environmental cycles. The peak baseline φ_i' was slightly better than the original peak phase φ_i for growth prediction, as shown in **Figure 4F**. Moreover, the blue LED light pulses for excitation of chlorophyll would provide no effect on the circadian rhythms. In our previous work (Ohara et al., 2015a,b), it was investigated how plant circadian clock responds to light pulse perturbations. The phase shift of circadian rhythm became maximally to 0.4 rad/2π (∼9.6 h) by a blue LED light pulse (80 μmol m^{-2} s^{-1} for 2 h). Based on this knowledge, the phase shift by our diagnostic lighting could be estimated as very small.

As shown in **Figure 5**, by increasing the number of measurements, the correlation coefficient R was improved. An increased number of measurements about leaf area led to improved prediction of growth in Frillice. In contrast, only two measurements of leaf area tended to effectively improve prediction of growth in SB555GL. Therefore, the optimal set of predictive indices depends on cultivar and/or dataset. In addition, using indices of circadian rhythms, no significant difference was observed for combinations of circadian rhythms and leaf area, or for circadian rhythms and CF. For growth prediction using all biological indices, it was significantly different from growth prediction using other indices inferred by machine learning in Frillice; on the other hand, the growth prediction using all biological indices was significantly different from indices other than the 6 time points for CF and the 4 kinds of circadian rhythms in SB555GL. Therefore, it is necessary to decide whether to acquire information on circadian rhythm, and we suggest that the research goal may depend on whether growth prediction can be based on circadian rhythms.

Fukuda et al. (2011) referred to improvement of plant productivity under several LED light conditions by selection of a threshold for an index I using the correlation coefficient R between production P and index I. In our study, I is the data output by neural networks, and R is the correlation coefficient between fresh weight W_i and the data output by neural networks. Therefore, as suggested by **Figure 5**, improving the value of R would lead to improvements in productivity; thus, we expect this seedling diagnosis system will be useful.

In conclusion, we developed a seedling diagnosis system that automatically identifies and selects plants showing poor growth based on biological information obtained at an early stage. We expect that this system will decrease operational cost in plant factories due to individual differences in plants. Using this system, we automatically obtained leaf area, CF, and information on circadian rhythms and suggested improvements to the prediction of growth by machine learning. We found that the system predicted plant growth with a high degree of accuracy; however, the mechanisms of plant growth have yet to be clearly identified. Future research will focus on predicting growth with additional accuracy by the use of environmental information in plant factory.

AUTHOR CONTRIBUTIONS

HF and SM designed the experiments, and developed a high-throughput diagnosis system. SM performed biological data analysis. SM and HF wrote the manuscript. All authors discussed the results and implications and commented on the manuscript.

ACKNOWLEDGMENTS

We are grateful to Tsubakimoto Chain Co. for constructing our diagnosis system and Green Clocks Co. for cultivation. This study was supported by a Ministry of Education, Science, Sports and Culture, Grant-in-Aid for Scientific Research (No. 25712029 to HF) and by PRESTO, JST.

REFERENCES

Chen, S., Billings, S. A., and Grant, P. M. (1990). Non-linear system identification using neural networks. *Int. J. Control* 51, 1191–1214. doi: 10.1080/00207179008934126

Daley, P. F., Raschke, K., Ball, J. T., and Berry, J. A. (1989). Topography of photosynthetic activity of leaves obtained from video images of chlorophyll fluorescence. *Plant Physiol.* 90, 1233–1238. doi: 10.1104/pp.90.4.1233

Dodd, A. N., Belbin, F. E., Frank, A., and Webb, A. A. (2015). Interactions between circadian clocks and photosynthesis for the temporal and spatial coordination of metabolism. *Front. Plant Sci.* 6:245. doi: 10.3389/fpls.2015.00245

Dodd, A. N., Salathia, N., Hall, A., Kévei, E., Tóth, R., Nagy, F., et al. (2005). Plant circadian clocks increase photosynthesis, growth, survival, and competitive advantage. *Science* 309, 630–633. doi: 10.1126/science.1115581

Farré, E. M., and Weise, S. E. (2012). The interactions between the circadian clock and primary metabolism. *Plant Biol.* 15, 293–300. doi: 10.1016/j.pbi.2012.01.013

Fukuda, H., Ichino, T., Kondo, T., and Murase, H. (2011). Early diagnosis of productivity through a clock gene promoter activity using a Luciferase bioluminescence assay in *Arabidopsis thaliana*. *Environ. Control Biol.* 49, 51–60. doi: 10.2525/ecb.49.51

Gould, P. D., Diaz, P., Hogben, C., Kusakina, J., Salem, R., Hartwell, J., et al. (2009). Delayed fluorescence as a universal tool for the measurement of circadian rhythms in higher plants. *Plant J.* 58, 893–901. doi: 10.1111/j.1365-313X.2009.03819.x

Govindjee, E. (1995). Sixty-three years since Kautsky: chlorophyll α fluorescence. *Aust. J. Plant Physiol.* 22, 131–160. doi: 10.1071/PP9950131

Halberg, F., Johnson, E. A., Nelson, W., Runge, W., and Sothern, R. (1972). Autorhythmometry-procedures for physiologic self-measurements and their analysis. *Physiol. Teacher* 1, 1–11.

Harmer, S. L. (2009). The circadian system in higher plants. *Ann. Rev. Plant Biol.* 60, 357–377. doi: 10.1146/annurev.arplant.043008.092054

Hendrawan, Y., and Murase, H. (2011). Determining an ANN pre-treatment algorithm to predict water content of moss using RGB intensities. *EAEF* 4, 95–105. doi: 10.1016/s1881-8366(11)80008-x

Higashi, T., Kamitamari, A., Okamura, N., Ukai, K., Okamura, K., Tezuka, T., et al. (2014). Characterization of circadian rhythms through a bioluminescence reporter assay in *Lactuca sativa* L. *Environ. Control Biol.* 52, 21–27. doi: 10.2525/ecb.52.21

Higashi, T., Nishikawa, S., Okamura, N., and Fukuda, H. (2015). Evaluation of growth under non-24 h period lighting conditions in *Lactuca sativa* L. *Environ. Control Biol.* 53, 7–12. doi: 10.2525/ecb.53.7

Kozai, T., Niu, G., and Takagaki, M. (2015). *Plant Factory, -an Indoor Vertical Farming System for Efficient Quality Foor Production, 1st Edn* Cambridge, CA:Massachusetts: Academic press.

Krause, G. H., and Weis, E. (1991). Chlorophyll fluorescence and photosynthesis: the basics. *Annu. Rev. Plant Physiol. Plant Mol.* 42, 313–349. doi: 10.1146/annurev.pp.42.060191.001525

Li, K., Li, Z., and Yang, Q. (2016). Improving light distribution by zoom lens for electricity savings in a plant factory with light-emitting diodes. *Front. Plant Sci.* 7:92. doi: 10.3389/fpls.2016.00092

Maxwell, K., and Johnson, G. N. (2000). Chlorophyll fluorescence - a practical guide. *J. Exp. Bot.* 51, 659–668. doi: 10.1093/jexbot/51.345.659

Morimoto, T., and Hashimoto, Y. (2009). Speaking plant/fruit approach for greenhouses and plant factories. *Environ. Control Biol.* 47, 55–72. doi: 10.2525/ecb.47.55

Morimoto, T., Torii, T., and Hashimoto, Y. (1995). Optimal control of physiological processes of plants in a green plant factory. *Control Eng. Practice* 3, 505–511. doi: 10.1016/0967-0661(95)00022-M

Murase, H., Helm, B., and Oke, S. (2015). Investigation of a scanning laser projector as an energy-efficient light source in plant production. *Environ. Control Biol.* 53, 71–76. doi: 10.2525/ecb.53.71

Nichol, C. J., Pieruschka, R., Takayama, K., Förster, B., Kolber, Z., Rascher, U., et al. (2012). Canopy conundrums: building on the biosphere 2 experience to scale measurements of inner and outer canopy photoprotection from the leaf to the landscape. *Funct. Plant Biol.* 39, 1–24. doi: 10.1071/FP11255

Ninness, B. (2000). Strong laws of large numbers under weak assumptions with application. *IEEE Trans. Automat. Control.* 45, 2117–2122. doi: 10.1109/9.887637

Ohara, T., Fukuda, H., and Tokuda, I. T. (2015a). An extended mathematical model for reproducing the phase response of *Arabidopsis thaliana* under various light conditions. *J. Theor. Biol.* 382, 337–344. doi: 10.1016/j.jtbi.2015.07.016

Ohara, T., Fukuda, H., and Tokuda, I. T. (2015b). Phase response of the *Arabidopsis thaliana* circadian clock to light pulses of different wavelengths. *J. Biol. Rhythms* 30, 95–103. doi: 10.1177/0748730415576426

Okamura, K., Matsuda, Y., Igari, K., Fukuda, H., and Murase, H. (2014). The optimal harvesting time of vaccine-producing transgenic lettuce cultivated in a closed plant factory. *Environ. Control Biol.* 52, 57–61. doi: 10.2525 ecb.52/.57.

Omasa, K., Shimazaki, K., Aiga, I., Larcher, W., and Onoe, M. (1987). Image analysis of chlorophyll fluorescence transients for diagnosing the photosynthetic system of attached leaves. *Plant Physiol.* 84, 748–752. doi: 10.1104/pp.84.3.748

Phan, A. H., and Cichocki, A. (2010). Tensor decompositions for feature extraction and classification of high dimensional datasets. *IEICE Nonlinear Theory Appl.* 1, 37–68. doi: 10.1587/nolta.1.37

Takahashi, N., Okamura, K., Matsuda, Y., Igari, K., Kato, K., Asao, H., et al. (2012). Effects of air flow on production of vaccine protein against swine edema disease in transgenic lettuce. *Environ. Control Biol.* 50, 135–141. doi: 10.2525/ecb.50.135

Takayama, K., Hirota, R., Takahashi, N., Nishina, H., Arima, S., Yamamoto, K., et al. (2014). Development of chlorophyll fluorescence imaging robot for practical use in commercial greenhouse. *Acta Hortic.* 1037, 671–676. doi: 10.17660/ActaHortic.2014.1037.86

Takayama, K., and Nishina, H. (2009). Chlorophyll fluorescence imaging of the chlorophyll fluorescence induction phenomenon for plant health monitoring. *Environ. Control Biol.* 47, 101–109. doi: 10.2525/ecb.47.101

Takayama, K., Nishina, H., Arima, S., Hatou, K., Ueka, Y., and Miyoshi, Y. (2011a). "Early detection of drought stress in tomato plants with chlorophyll fluorescence imaging -practical application of the speaking plant approach in a greenhouse," in *Preprints of the 18th IFAC World Congress* (Milano), 1785–1790.

Takayama, K., Nishina, H., Mizutani, K., Arima, S., Hatou, K., and Miyoshi, Y. (2011b). Chlorophyll fluorescence imaging for health condition monitoring of tomato plants in greenhouse. *Acta Hortic.* 893, 333–339. doi: 10.17660/ActaHortic.2011.893.29

Takayama, K., Nishina, H., Mizutani, K., Iyoko, S., Arima, S., Hatou, K., et al. (2011c). Evaluation of photosynthetic functions of tomato plants in greenhouse with chlorophyll fluorescence induction imaging system. *Acta Hortic.* 907, 337–342. doi: 10.17660/ActaHortic.2011.907.55

Takayama, K., Sakai, Y., Oizumi, T., and Nishina, H. (2010). Assessment of photosynthetic dysfunction in a whole tomato plant with chlorophyll fluorescence induction imaging. *Environ. Control Biol.* 48, 151–159. doi: 10.2525/ecb.48.151

Ukai, K., Inai, K., Nakamichi, N., Ashida, H., Yokota, A., Hendrawan, Y., et al. (2012). Traveling waves of circadian gene expression in lettuce. *Environ. Control Biol.* 50, 237–246. doi: 10.2525/ecb.50.237

Voß, U., Wilson, M. H., Kenobi, K., Gould, P. D., Robertson, F. C., Peer, W. A., et al. (2015). The circadian clock rephases during lateral root organ initiation in *Arabidopsis thaliana*. *Nat. Commun.* 6, 7641. doi: 10.1038/ncomms8641

Conflict of Interest Statement: The authors declare that the research was conducted in the absence of any commercial or financial relationships that could be construed as a potential conflict of interest.

frontiers in Plant Science

ORIGINAL RESEARCH
published: 09 February 2016
doi: 10.3389/fpls.2016.00092

Improving Light Distribution by Zoom Lens for Electricity Savings in a Plant Factory with Light-Emitting Diodes

Kun Li[1,2†], Zhipeng Li[1,2†] and Qichang Yang[1,2]*

[1] Institute of Environment and Sustainable Development in Agriculture, Chinese Academy of Agricultural Science, Beijing, China, [2] Key Lab of Energy Conservation and Waste Management of Agricultural Structures, Ministry of Agriculture, Beijing, China

The high energy consumption of a plant factory is the biggest issue in its rapid expansion, especially for lighting electricity, which has been solved to a large extent by light-emitting diodes (LED). However, the remarkable potential for further energy savings remains to be further investigated. In this study, an optical system applied just below the LED was designed. The effects of the system on the growth and photosynthesis of butterhead lettuce (*Lactuca sativa* var. capitata) were examined, and the performance of the optical improvement in energy savings was evaluated by comparison with the traditional LED illumination mode. The irradiation patterns used were LED with zoom lenses (Z-LED) and conventional non-lenses LED (C-LED). The seedlings in both treatments were exposed to the same light environment over the entire growth period. The improvement saved over half of the light source electricity, while prominently lowering the temperature. Influenced by this, the rate of photosynthesis sharply decreased, causing reductions in plant yield and nitrate content, while having no negative effects on morphological parameters and photosynthetic pigment contents. Nevertheless, the much higher light use efficiency of Z-LEDs makes this system a better approach to illumination in a plant factory with artificial lighting.

Keywords: reserved growing space, principles during transplanting, precise illuminating, zoom, light use efficiency

OPEN ACCESS

Edited by:
Alejandro Isabel Luna Maldonado, Universidad Autónoma de Nuevo León, Mexico

Reviewed by:
Hao Peng, Washington State University, USA
Hui Li, Mount Sinai Hospital, USA

***Correspondence:**
Qichang Yang
yangqichang@caas.cn

† These authors are joint first authors.

Specialty section:
This article was submitted to Crop Science and Horticulture, a section of the journal Frontiers in Plant Science

Received: *11 August 2015*
Accepted: *18 January 2016*
Published: *09 February 2016*

Citation:
Li K, Li Z and Yang Q (2016) Improving Light Distribution by Zoom Lens for Electricity Savings in a Plant Factory with Light-Emitting Diodes. Front. Plant Sci. 7:92. doi: 10.3389/fpls.2016.00092

INTRODUCTION

A plant factory is regarded as an ideal candidate for precision agriculture (Murase, 2000) due to the observability and controllability of most of its environmental factors, in which artificial lights play an important part. Plant factories with artificial lighting have been applied in many fields (Ting et al., 1993; Watanabe, 2009; Kato et al., 2010, 2011; Shimizu et al., 2011; Christou, 2013; Pamungkas et al., 2014). However, the technology has met difficulties in entering the market due to the large investment in facilities and high operating costs involved (Ohyama et al., 2001; Kwon et al., 2014), precluding large-scale application. With the enormous potential demand, research on the energy consumption of plant factories has become increasingly important and attracted widespread attention.

Several possible solutions for reducing the energy consumption have been studied. Hashimoto (1991) proposed that the computer-integrated plant growth factory for agriculture and horticulture should be expected to be the most effective system in the coming generation. After many years of

research, higher levels of environmental management and control techniques were introduced, bringing the plant factory into full play with respect to optimizing the energy efficiency (Seo and Choi, 2011; Ijaz et al., 2012; Wu et al., 2012; Kwon et al., 2014). The power source options of plant factories were also greatly expanded by the development of clean energy technology. Hyun et al. (2014) analyzed various unused energy heat sources such as air source, power plant waste heat, seawater, river, and geothermal heat, and found that the coefficient of performance of the heat pump applied in the study was the highest using power plant waste heat. Waste heat from coal-fired thermal power plants was also introduced to nearby plant factories, reducing fuel oil consumption by 16.05 TJ per year and total CO_2 emissions by 1204 tons per year (Togawa et al., 2014).

For further energy conservation, electricity consumption should be cut down, especially that used in artificial lighting, which makes up 45% of the total (Ikeda et al., 1992); its use could be reduced by 50% by improving the efficiency of the lighting (Nishimura et al., 2001; Bülow-Hübe, 2008). The application of new types of light source might be the most effective method of energy saving. Previous studies have indicated that among these newly developed artificial lighting technologies, the light-emitting diode (LED) has already been widely used for plant growth (Li and Kubota, 2009; Hogewoning et al., 2010; Li et al., 2010, 2012; Johkan et al., 2012; Samuolienė et al., 2012) for its tailorable spectral composition, wavelength specificity, narrow bandwidth, and foremost, high energy efficiency compared with conventional plant cultivation artificial light sources such as mercury tungsten lamps (Austin, 1965), high-pressure sodium lamps (Sager et al., 1982; Tibbitts et al., 1983), and fluorescent lamps (Andersen, 1986). In recent years, complementary to inorganic LEDs, highly efficient flexible organic light-emitting diodes (OLED) have been characterized by laboratories and found to have an energy efficiency of 30 lm/W at 1000 cd/m^2, which is two to three times higher than that of common incandescent bulbs (Holst Centre, 2012). Advanced cultivation techniques also play a crucial role in the full exploitation of potential artificial lighting technologies. Yamada et al. (2000) found that stepwise photosynthetic photon flux (PPF) control is a useful method for reducing the electricity consumption of lighting and increasing the electricity utilization efficiency. The lighting consumption has been reported to decrease by 18.4% under a vertical and horizontal movable system, halving the initial light source input while maintaining the yield (Li et al., 2014). Poulet et al. (2014) showed that 50% less energy per unit dry biomass accumulated was used for lettuce crops grown with a targeted LED lighting system.

The elimination of occupied energy on reserved growing space without reducing the photosynthetic yield has drawn our attention as well. Different from the research of Poulet et al. (2014), to find an accurate and effective method to reduce the unnecessary illumination between the gaps between adjacent lettuces in practical application was the focus of our research. On the basis of understanding the transplanting process, two principles were put forward:

(i) Space will always be reserved for plants development until the next transplanting;
(ii) Transplanting will be executed as long as the plant canopies contact with the adjacent leaves.

To explore the potential and effectiveness of this approach, a precise illuminating system involving zoom lenses was built, and its benefits were evaluated by analyzing the electricity consumption of the lighting as well as the plant growth, plant physiology, and phytochemical accumulation of the lettuce grown under different lighting modes. The objective of this research was to develop a lighting system for lettuce production in a plant factory by dynamically focusing the irradiation on the plant canopy, providing a high PPF with low electricity consumption while maintaining the lettuce yield and quality.

MATERIALS AND METHODS

Plant Materials and Growth Conditions

Butterhead lettuce seeds (Flandria RZ, Rijk Zwaan, De Lier, The Netherlands) were sown in a plastic seedling tray (57 cm × 23.5 cm × 4 cm) and germinated in a 50 m^{-2} computer-controlled fully closed plant factory at the Chinese Academy of Agricultural Science (CAAS), Beijing, China (latitude 39°57′40.2″N, longitude 116°19′34.6″E) under dim LED light (50 $\mu mol \cdot m^{-2} \cdot s^{-1}$) and irrigated with tap water once per day. Approximately 15 day after sowing, 16 uniform seedlings were transplanted onto cultivation boards (polyethylene, 68 cm × 72 cm × 1.4 cm, 32 plants/m^2) and were cultivated with the deep flow technique (Hu et al., 2008) for 25 day under a 16-h photoperiod on a 24-h light/dark cycle. The air temperature measured at the top of the canopy was maintained at 23 ± 0.5°C during the daytime and 20 ± 0.5°C at night. The relative humidity was 60 ± 5%, and the concentration of carbon dioxide was kept at 400 ± 10 ppm. Modified Hoagland nutrient solution [(±SE) pH6.3 ± 0.1, EC 1.6 ± 0.2 $mS \cdot cm^{-1}$] was used, and half dose nutrient solution (EC 1.0 ± 0.2 $mS \cdot cm^{-1}$) was employed during the seeding stage. The air temperature and humidity were measured twice per day, and the parameters of the nutrient solution were monitored daily.

Light Treatments

A precise illumination system was built (**Figure 1**) that was composed of 16 multi-chip LEDs (**Figure 2A**, WenLiang Electronics CO., Shenzhen, China). Two red (peak at 630 nm) chips and a blue (peak at 460 nm) chip were fixed on strip form aluminum heat sinks and located right above each plant to form a lighting array (**Figure 3**, 72 cm × 68 cm) as the light source of the zoom LED treatment (Z-LED). The lighting array was placed horizontally 30 cm above the seedlings inside the plant factory to achieve the illumination schedule described below. The rated power for each chip is 3 W, while the output power can be regulated individually by adjusting the current and voltage output of the alternating current to direct current power source (DPS-3005D; ZhaoXin

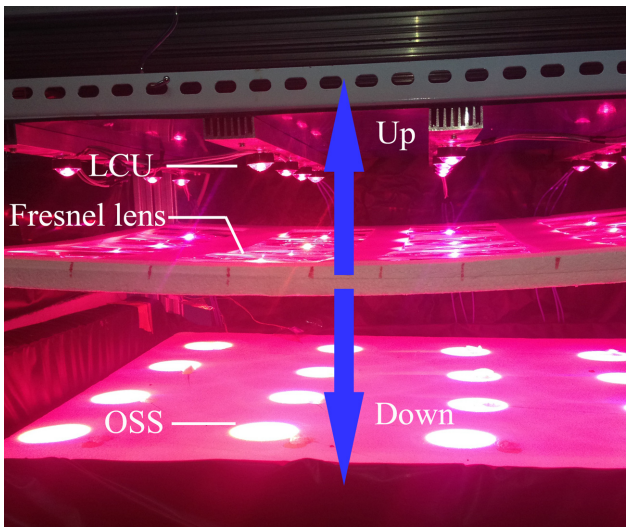

FIGURE 1 | The precise illuminating system used in this study. The multi-chip light- emitting diode – convex lens units (LCUs) were located 30 cm away from the seedlings as the light sources. The Fresnel lens array was located between the LCUs and the seedlings, while able to be moved in the directions of the blue arrows to manually adjust the diameters of the orbicular spectrum spots (OSSs).

Electronic Instrument Equipment Co., Shenzhen, China) connected to each LED chip. As the optical accessories, 16 convex lenses (**Figure 2B**, 24.50 mm × 14.00 mm, transmittance 93%, HengZheng Optics Technology Co., Ltd., Dongguan, China) were tightly attached to their corresponding LEDs. Directly below the multi-chip LED – convex lens unit (LCU, **Figure 2C**), 16 Fresnel lenses (**Figure 2D**, 120 mm × 120 mm, transmittance 95%, YuYing Optical Instrument CO., LTD, ShanDong, China) were fixed in a horizontal plane frame structure (high-density foam polystyrene), which could be manually moved vertically along the axial direction of the LCU (**Figure 1**).

The photosynthetic quantum in the Z-LED was accumulated by the LCUs as much as possible before irradiation onto the plant canopy, while the diameters of the orbicular spectrum spots (OSS) were adjusted by manually regulating the distance between the Fresnel lens frame and the LCU to adapt the dimensions of the plant canopy (**Figure 1**).

Different from the Z-LED treatment, four custom-manufactured LED panels (60 cm × 25 cm × 1.2 cm; FHT Co., Shenzhen, China) with red (peak at 630 nm) and blue (peak at 460 nm) LEDs were used as the main light source in the conventional non-lens LED (C-LED) treatment and were placed horizontally 30 cm above the seedlings inside the plant factory to achieve the illumination.

The red–blue ratio (R/B) for both treatments was kept at 8:1 (Wen, 2009). Each treatment covered 0.5 m^2 (completely covering the growing area of the plants below) was carefully isolated by black films to prevent light contamination from each other during the experiment. The PPF on the plant canopies of the treatments were kept at 70 $\mu mol \cdot m^{-2} \cdot s^{-1}$ by adjusting the luminous intensity of the individual LEDs for the first 10 days, allowing it to rise to 120 $\mu mol \cdot m^{-2} \cdot s^{-1}$ for the following 15 days. The illumination time was 16 h per day (0800 to 2400 HR). The spectral energy distribution scans were recorded at 400 to 800 nm with 2-nm steps of the LEDs (**Figure 4**) with a calibrated fiber optic spectrometer (AvaSpec-2048; Avantes, Apeldoorn, The Netherlands) placed horizontally under the light sources used for the experiments.

Measurements

Once the seedlings were transplanted onto the cultivation board, the diameters of the plant canopies were measured daily. A vernier caliper was employed to gage the length between the central leaf and the edge of the projection of the longest leaf, representing the maximum radius of the OSS of the plant.

The ambient temperatures of the growth were recorded using a data acquisition system (Model CR1000, Campbell Scientific, Inc., North Logan, UT, USA) at 10 min intervals. The temperature was measured using Type T thermocouples (accuracy was ±0.2°C). All thermocouples were measured for 25 days at each point and kept immobile. The leaf temperature was measured by thermocouple, following (Luján et al., 2009).

The plant photosynthetic data were measured on the last day of the growth. The leaf photosynthesis was measured with a portable gas exchange device equipped with a leaf chamber fluorometer (LI-6400; LI-COR). Measurements were carried out between 0900 and 1200 HR, and the samples of two treatments were conducted alternatingly. For the measurements, six mature leaves from different plants were selected. The PPF was 120 $\mu mol \cdot m^{-2} \cdot s^{-1}$; the measurements were taken when the photosynthesis rate reached steady state (after approximately 10 min). The vapor pressure deficit in the leaf chamber was maintained below 1 kPa; the leaf temperature and CO_2 concentration in the measurement chamber were maintained at 20°C and 400 ppm, respectively.

Twenty-five days after transplanting, the plants were harvested to measure their growth and to analyze their phytochemical concentrations. The fresh weight (FW), dry weight (DW), plant height, number of leaves, leaf length, leaf area, and leaf chlorophyll (Chl) concentrations were measured after harvest. The leaf areas were measured by the cut-paper weighing method, following Minaxi and Saxena (2010). The plant height, leaf length and leaf width were measured using a vernier caliper (Wu et al., 2007). The leaves were packaged in plastic bags and preserved in an ultralow temperature refrigerator, prepared to be homogenized and used in the determination of ascorbic acid, protein, nitrate and soluble sugar concentrations.

An electricity meter (LCDG-ZJ120-01; LiChuang Science and Technology Co., Laiwu, China) was employed to measure the electricity consumption of the illumination (the energy costs for cooling, ventilation and the recirculation of the nutrient solution were not accounted for in our experiments). The light utilization efficiency [LUE (grams per kilowatt hour)] of each treatment was determined [LUE = leaf FW (grams per plant) · 32 plants/m^2/electric energy consumption of lighting (kilowatts per hour)].

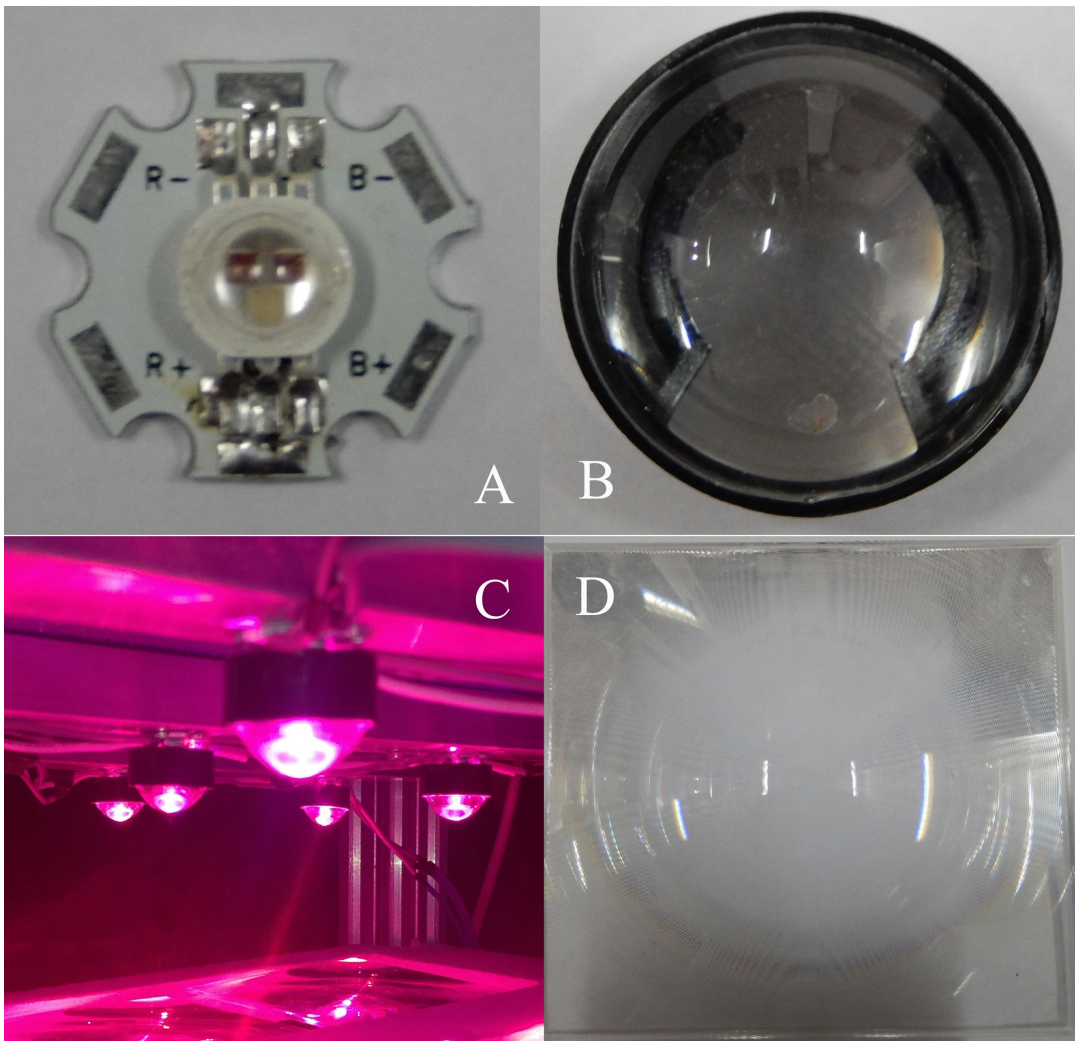

FIGURE 2 | Multi-chip light-emitting diodes (LEDs) (A) have three chips (two red chips and one blue chip) to satisfy the spectrum demand of the lettuce; each chip's rated power is 3 W. Combined with the convex lens **(B)**, they form the multi–chip LED – convex lens unit (LCU, **C**), hanging 30 cm over the top of the cultivation boards to accumulate the photosynthetic quantum as much as possible to irradiate the Fresnel lens **(D)**, which focuses the photosynthetic quantum again to illuminate the plants.

The weighed fresh leaf tissue (2 g) was extracted in 96% alcohol/water (v/v) (50 ml for each gram). The extract was centrifuged (3K15; Sigma Laborzentrifugen, Osterode am Harz, Germany) at 10,000 *g* for 10 min. The supernatant was separated, and the absorbance was read at 400–700 nm on a spectrophotometer (UV-1800; SHIMADZU Co., Kyoto Japan) at wavelengths of 663 nm (A663) and 646 nm (A646), respectively. The chlorophyll a (Chl a) and chlorophyll b (Chl b) concentrations were measured by spectrophotometry and calculated according to the following equations of Lichtentaler and Wellburn (1983): Chl a = (12.21 × A663–2.81 × A646) × 20/1000/2 and Chl b = (20.13 × A646 –5.03 × A663) × 20/1000/2.

The nitrate content was determined as described by Cataldo et al. (1975). Freeze-dried samples (2 g) were homogenized in 15 ml water and buffer solution to 25 ml volume. The homogenates were filtered, and the filtrates were centrifuged at 10,000 *g* for 15 min. The supernatants were decanted and saved for analysis. A quadruple volume of salicylic acid [5% (w/v)] was mixed, and the pH value was controlled to above 12 by the addition of 9.5 ml 8% sodium hydroxide. The liquid supernatant was measured by spectrophotometry at a 410 nm wavelength to determine the nitrate content.

Protein solutions were prepared in 0.15 M sodium chloride. Freeze-dried samples (0.3 g) were extracted in 5 ml solvent and then centrifuged at 3,000 gn for 10 min. Coomassie brilliant blue G-250 [(5 mL, 0.01%(w/v)] was added into 1 ml of the supernatant and was shaken frequently for 2 min before the spectrophotometric detection at 595 nm wavelength. The protein content was measured following Bradford (1976).

Soluble sucrose content was determined as described by Beck and Bibby (1961). Freeze sample (0.3 g) were extracted

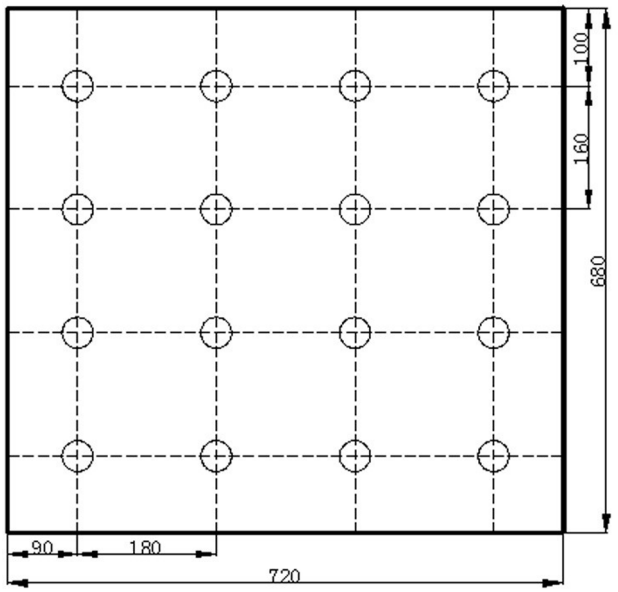

FIGURE 3 | The position arrangement of the multi–chip LED–LCUs over the cultivation board, indicating the allocation of positions for lettuce seedlings. All dimensions were in millimeters.

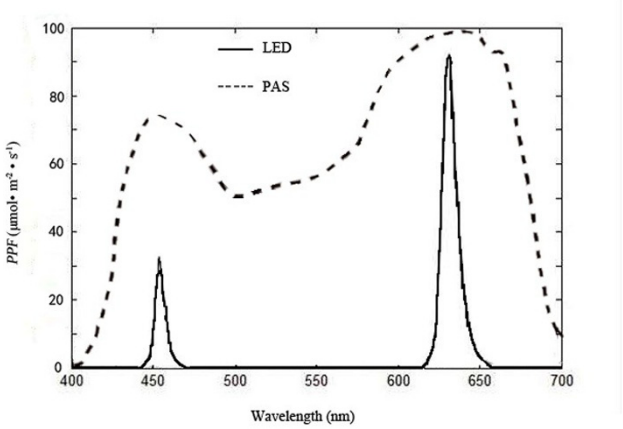

FIGURE 4 | Spectral distributions of light from multi-chip LEDs, measured with a fiber optic spectrometer (AvaSpec-2048; Avantes, Apeldoorn, The Netherlands), and plant absorption spectrum (PAS) reported by Sager et al. (1982); PPF = photosynthetic photon flux.

in 10 mL of water, 0.5 ml anthrone ethyl acetate, and 0.5 ml concentrated sulfuric acid before incubated in a boiling water bath for 10 min. After constant volume to 25 ml, samples were read in the spectrophotometric at 630 nm wavelength. All the phytochemical concentration experiments were repeated 5 times for error reduction.

Experimental Design and Statistical Analysis

The experiment was performed twice. Statistical analysis was performed using SAS software (version 9.2; SAS Institute, Cary, NC, USA). Variance analyses within treatments were used, and different letters within the column indicate significant differences at $P \leq 0.05$ according to the least significant difference test.

Experiment 1: Establishing Lettuce Growth Curve at Experimental Irradiance

For the growth curve experiment, 36 plants were cultured under such circumstances as described before in Plant materials and growth conditions while exposed under the light environment described above in Light treatments by C-LED. To maintain the designed light quality and PPF under the constantly changing canopies, the luminous intensity of the individual LEDs were set up every 5 days by adjusting the output of the power supply. The diameters of the lettuces were examined every day for 25 days from seedling to final harvest. We can obtain the detailed diameter of the lettuce in **Figure 5** to find the reasonable size of the OSS. We also calculate the theoretical energy savings.

Experiment 2: Growth and Energy Consumption Comparison Between Z-LED and C-LED

According to the preliminary experiment's result, an appropriate Fresnel lens array was employed in Z-LED, combined with suitable LCUs (**Figure 2C**), so that the OSS that fell on the plant canopy could be adjusted to match the diameter of the growing plants by manually adjusting the distance between the Fresnel lens array and the multi-chip LEDs every day. The diameter of the OSS decreased (zoom out) with the increasing of the distance, while the diameter increased (zoom in) with the decreasing of the distance. The physiological and biochemical parameters were determined by using the methodology described above in Measurements. To avoid the unwanted variation of the light environment parameters with the growth of the diameter and height of the plants in both treatments, the light sources were located at an identical height (30 cm) above the cultivation boards, while the luminous intensity of the individual LEDs and the diameter of OSS were adjusted by regulating the output of the power supply and the distance between the Fresnel lens array and LCUs, respectively.

Experiment 3: Effects of Z-LED on the Ambient Temperature of Plant Growth

Considering the tremendous diversities between Z-LED and C-LED, the environmental parameters, more specifically, a temperature of three sampling point (plant leaf, nutrient solution, and gap on cultivation board between OSS) arrangement was designed for both treatments. The temperatures from all six sampling points were monitored through the entire experiment. The data acquired at 1200 HR everyday were used for analysis. This was chosen because the sampling points had been warmed up by the light source irradiation for 4 h, gradually reaching

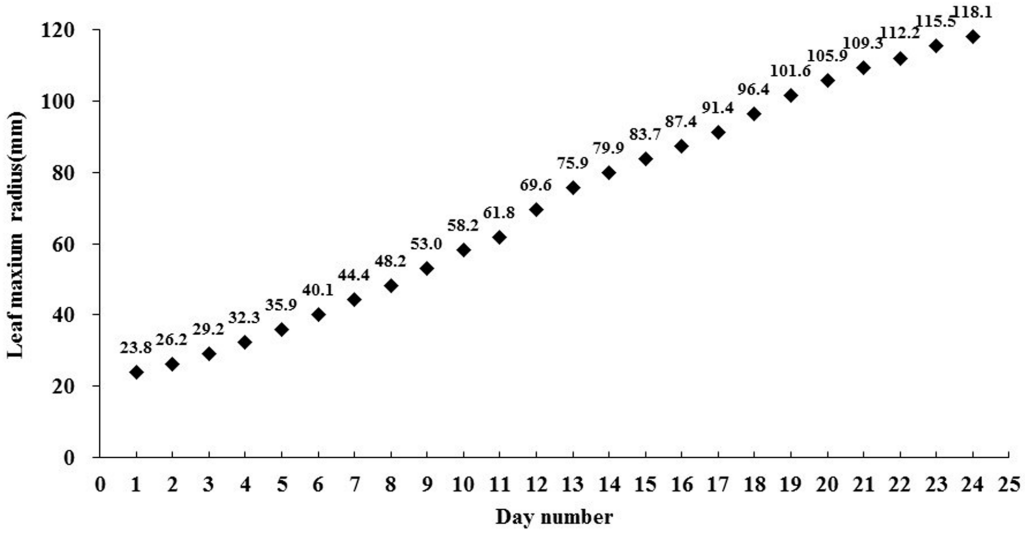

FIGURE 5 | The curve of the average leaf maximum radius from 36 lettuce plants during 25 days of growth under the conventional non-zoom LED case.

TABLE 1 | Electricity consumption of lighting, plant yields and light utilization efficiencies (LUEs) of lettuce under zoom lens lighting-emitting diode (Z-LED), and conventional non-lens LED (C-LED).

Energy parameters	Z-LED	C-LED
Electricity consumption (kWh/m^2)	23.73	49.51
Plant yields (g/m^2)	1130.72 ± 12.19b	1496.93 ± 25.04a
LUEs (g/kWh)	94.38 ± 1.02a	60.64 ± 1.03b

The electricity consumptions were recorded with an electricity meter. Light utilization efficiencies were estimated by dividing the yield (g/m^{-2}) by the electricity consumption of lighting per area. Data were analyzed by analysis of variance, and different letters within the column indicate significant differences at $P \leq 0.05$ according to the least significant difference test.

the equilibrium state and were also not affected by the nutrient solution circulation.

RESULTS

Performance Characteristics and Electric-Energy Consumption of the Lighting Systems

Based on the growth surveillance of the lettuce under the scheduled light environment, the radius curve of projection area of plant on the cultivation board was established (**Figure 5**), which indicated the expanded tendency that the OSS should follow. During 25 days' growth, the leaf radius increased at a varying velocity from 23.8 to 118.1 mm. With the closed observation during the experiment, 14 days after transplanting, when the radius reached 79.9 mm, the contiguous OSSs were tangent to each other during expansion. The optical component parameters of the precise illumination system were determined. High-power (9 W) multi-chip LEDs were employed, and the heat sinking was fully considered. The convex lenses were confirmed to possess an emission angle of 60°. The optical characteristics of the Fresnel lenses used were a focal length of 100 mm, a focus diameter of 4 mm, and dimensions of 120 mm × 120 mm.

As a result, when used as an alternative to conventional LED lights, the Z-LED consumed much less (52.06%) electricity (**Table 1**), but, the plant yield decreased significantly (**Table 2**). Despite this, by benefitting from the excellent energy saving effect, the Z-LED achieved a 55.64% increase in LUE relative to the C-LED (**Table 1**), allowing the plants to obtain the desired illumination with minimal energy consumption.

Influence on Temperature

There were significant differences in temperature on the plant leaf, cultivation board, and nutrient solution between two treatments. As shown in **Figure 6A**, there was a large

TABLE 2 | Lettuce fresh weight (FW), dry weight (DW), leaf area, plant height, true leaf number, leaf length and leaf width for lettuce under Z-LED and C-LED.

Growth parameter	Z-LED	C-LED
Leaf FW (g)	37.68 ± 2.04b	45.23 ± 5.69a
Leaf DW (g)	1.31 ± 0.21b	1.89 ± 0.45a
Leaf area (cm^2)	1.22 × 10^3 ± 185.52a	1.22 × 10^3 ± 150.73a
Plant high (mm)	68.56 ± 11.62a	75.01 ± 9.06a
True leaf number	29.10 ± 1.52a	28 ± 2.45a
Leaf length (mm)	142.87 ± 4.35a	141.57 ± 4.12a
Leaf width (mm)	83.85 ± 6.72a	84.65 ± 7.72a

Data were analyzed by analysis of variance, and different letters within the column indicate significant differences at $P \leq 0.05$ according to the least significant difference test.

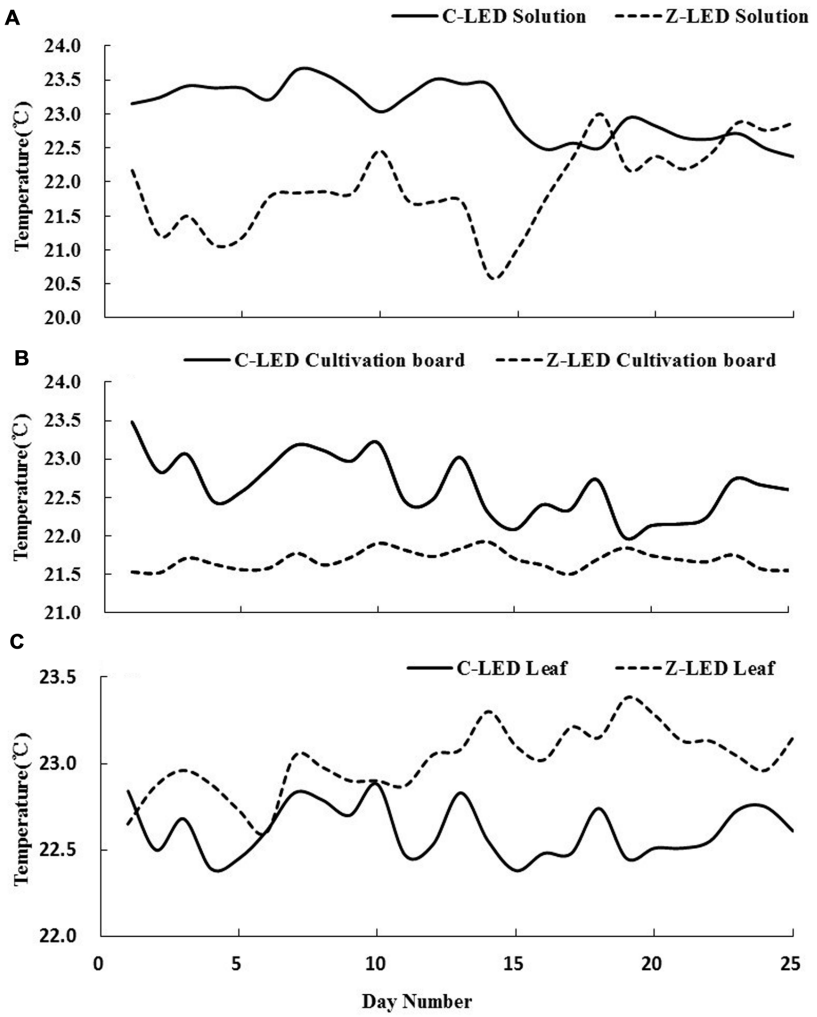

FIGURE 6 | Temperature of nutrient solutions (A), cultivation boards (B), and leaves (C) from zoom lens lighting-emitting diode (Z-LED) and conventional non-lens LED (C-LED), measured from transplanting to harvest (25 days). All data were acquired from 1150 to 1210 HR every day.

gap in the temperature of the nutrient solution before day 10. The temperatures were approximately 23 and 21.5°C in the C-LED and Z-LED, respectively. Subsequently, the curve rapidly coincided at 22.5°C just after day 10 and maintained this level until the final day. The cultivation board temperature of the Z-LED was 21.5°C throughout the entire experiment, while a descent could be observed from approximately 23 to 22.5°C in the C-LED treatment after the tenth day (**Figure 6B**). Unlike the tendency of the data in the cultivation board and nutrient solution, the canopy temperature of Z-LED (**Figure 6C**) notably increased compared with the C-LED, despite the massive amount of heat energy that had been removed from its system. In addition, the Z-LED canopy temperature manifested a further elevation to approximately 23.5°C on the 10th day, while its counterpart was maintained at 22.5°C throughout the whole experiment period.

Plant Growth

The lettuce growth was significantly affected by the different light modes in the treatments (**Table 2**). However, unexpectedly, notable negative effects were observed in the Z-LED treatment, leading to 23.07 and 30.68% decreases in the leaf FW and DW, respectively. The difference is not evident in physiological parameters such as plant height, true leaf number, leaf area, leaf length, and leaf width. The C-LED treatment exhibits an apparent improvement in all photosynthetic parameters compared with that of the Z-LED (**Table 3**), with increases of 68.01, 75, 60, and 12.16% for net photosynthesis, stomatal conductance, intercellular CO_2 concentration, and transpiration rate, respectively.

Phytochemical Accumulation

The phytochemical concentrations in the lettuce leaves were significantly affected by the different light treatments (**Table 4**).

TABLE 3 | Net photosynthesis (Pn), stomatal conductance (Cond), transpiration rate (Tr), and intercellular CO_2 concentration (Ci) data subjected to the zoom lens lighting-emitting diode (Z-LED) and conventional non-lens LED (C-LED).

Photosynthesis parameter	Z-LED	C-LED
Pn (μmol $CO_2m^{-2}s^{-1}$)	2.72 ± 0.46b	4.57 ± 0.43a
Cond (mol $H_2Om^{-2}s^{-1}$)	0.04 ± 0.01b	0.07 ± 0.02a
Tr (mmol $H_2Om^{-2}s^{-1}$)	0.30 ± 0.08b	0.48 ± 0.09a
Ci (μmol CO_2mol^{-1})	265.43 ± 11.96b	297.70 ± 24.54a

Data were analyzed by analysis of variance, and different letters within the column indicate significant differences at $P \leq 0.05$ according to the least significant difference test.

TABLE 4 | Concentrations of sucrose, nitrate, protein, chlorophyll a (Chl a), and chlorophyll b (Chl b) of lettuce under Z-LED and C-LED.

Physiological parameter	Z-LED	C-LED
Sucrose (mg/g)	34.08 ± 10.48a	12.55 ± 8.59b
Nitrate (μg/g)	177.81 ± 68.06b	233.73 ± 53.38a
Protein (mg/g)	0.26 ± 0.01a	0.26 ± 0.01a
Chl a (mg/g)	0.40 ± 0.01a	0.43 ± 0.05a
Chl b (mg/g)	0.10 ± 0.01a	0.10 ± 0.02a

Data were analyzed by analysis of variance, and different letters within the column indicate significant differences at $P \leq 0.05$ according to the least significant difference test.

The focused lighting in the Z-LED revealed a tremendous enhancement effect on the accumulation of soluble sucrose, leading to a remarkable increase of 171.55% in its concentration compared with that of the C-LED, while the nitrate content in the Z-LED treatment was decreased by 23.92%. The different illumination modes seemed to have little influence on the production capacity of the photochemical products, as similar contents of protein, Chl a, and Chl b were observed in both treatments.

DISCUSSION

Performance Characteristics and Electric Energy Consumption of the Lighting Systems

The tangency of the contiguous OSSs suggests that leaf overlapping was about to be observed, thereby reducing the energy efficiency of the system. Before that, a large number of reserved growing spaces were energy occupied without photosynthetic yield, representing considerable potential in improving energy efficiency. To provide the plant canopy with the designed light intensity (120 μmol·m^{-2}·s^{-1}) when the energy of single LED was dispersed with the OSS expansion, a higher single LED power was required to achieve an identical PPF to the C-LED. In this study, 9 W seemed to be the minimum power supply to meet the needs of the experiments, especially for the fully grown lettuce. Serving as one of the LCU components, convex lenses were used to gather light by narrowing the emission angle of the LEDs. The selected luminous angle (60°) ensured that all focused light fell on the Fresnel lenses, even though the distance between them was maximized to create a small-size OSS on the cultivation board for the seedlings. For the Fresnel lenses, the optical parameters described above were essential characteristics, with which the Fresnel lens array is capable of providing a continuously variable OSS size by adjusting the distance away from the LCUs.

For the electricity saving property, the photons dissipated due to the much wider luminous angle of the C-LEDs, especially of the LEDs that were located on the edge of the cultivation system, being focused onto the plant canopy in the Z-LED treatment. Furthermore, the improved light distribution technology eliminated the extraneous irradiation used to illuminate the non-canopy area. However, this technology, which had the best energy savings effect before the flourishing stage of the lettuce, subsequently declined along with the growth (**Table 5**).

The seedlings were transplanted at the density for fully grown lettuce. The application of this technology in practical production, in which the transplanting process would be done approximately three times, could achieve identical performance for conservation as described in this study as long as the two principles of transplanting described earlier are followed.

Influence of Temperature

The Z-LED significantly decreased the amount of energy entering the plant during growth by 52.06%, thereby having an obvious effect on the temperature of the growing environment. The 10th day was the key inflection point for both treatments at all inspection sites because of the elevation of the PPF from 70 to 120 μmol·m^{-2}·s^{-1} on the plant canopy according to the experiment design, which introduced more heat into both treatments. Due to the use of this technology, much less thermal energy was generated to achieve the PPF. Thus the temperatures of the C-LED were always higher than those of the Z-LED on the cultivation board and nutrient solution for the entire growth phase (**Figure 6**).

Figure 6B indicates that the cultivation boards of the Z-LED treatment were not completely exposed under the light sources, and accordingly, the temperature was stable at a low level for the whole period. The irradiation that was supposed to be distributed

TABLE 5 | Piecewise energy consumption under Z-LED and C-LED, recorded by an electricity meter every 5 days.

Piecewise energy consumption (kWh)	Z-LED	C-LED
1–5 days	0.66	3.84
5–10 days	0.78	3.84
10–15 days	2.21	5.52
15–25 days	8.32	11.04
Total	11.98	24.24

on the cultivation boards below the C-LED was blocked by the rapidly growing leaves, resulting in a decline of the temperature even though the PPF was higher than before.

As shown in **Figure 6A**, the solution of the C-LED treatment was warmed up by the significant excess energy from the cultivation board through the thermal transition effect. Along with the lowering of temperature on the cultivation board as described before, the solution temperature also showed a tendency to decrease. With the rising of the PPF after day 10, the temperature of the Z-LED went up under the heating effect.

An interesting phenomenon occurred during the temperature monitoring of the plant leaves (**Figure 6C**). The Z-LED treatment presented a higher temperature with much less energy intake. The reason might be the improvement of photosynthesis in the C-LED treatment due to the relatively higher temperature of the growth environment (Berry and Bjorkman, 1980). As described before, all photosynthetic parameters of the C-LED treatment were significantly higher than those of the Z-LED treatment (**Table 3**). More specifically, the transpiration rate was 60% higher in the C-LED treatment than in the Z-LED treatment, which led to a conspicuous reduction of the leaf epidermis temperature (Gates, 1964; Pallas et al., 1967).

Plant Growth

The lettuce growth was significantly affected by the photosynthesis (Nelson, 1988). Our study showed that the much higher photosynthesis in C-LED, benefitting from the excess irradiation, would result in a large increase in plant yield. The reason might be the light brought in by reflection from the cultivation board where the lettuce was grown (Poulet et al., 2014). However, the morphological parameters of the lettuce were more likely to be affected by the light quality and intensity (Tei et al., 1996; Kitaya et al., 1998; Dougher and Bugbee, 2001; Folta, 2004; Kim et al., 2004; Folta and Childers, 2008), which were set to be consistent within treatments. Contributions to the much higher yields in C-LED might be from the relatively lower root zone temperature (Challa et al., 1995), combined with the thicker leaves when grown at a cooler leaf temperature (Wolfe, 1991).

As one of the most important environmental factors, temperature plays a very important role in plant growth. Berry and Bjorkman (1980) have shown that raising the temperature would contribute to the improvement of photosynthesis in an appropriate range of 20–30°C. He et al. (2001) indicated that a higher temperature in the root zone could improve the photosynthesis and stomatal conductance, consistent with Gosselin and Trudel (1986). Agreeing with them, in our study, the relatively high temperature of the C-LED on the cultivation board and in the nutrient solution results in outstanding improvements in both photosynthesis and plant yield compared to Z-LED, even though the dissolved oxygen value would be lowered (Goto et al., 1996; Yoshida et al., 1997). Furthermore, a high transpiration rate had been reported to be helpful in the cooling of the leaf epidermis (Gates, 1964; Pallas et al., 1967). The higher transpiration rate in the C-LED treatment would decrease the leaf ambient temperature, which would be of great help to improve the yield in the C-LED treatment.

To provide a more complete system for applying this technology to practical applications, the photosynthetic and plant growth performance must be improved to overcome the described drawbacks while still maintaining the energy-saving and high-LUE features of Z-LED. The temperature of the growth environment, firstly, could be slightly increased through the reduced use of air conditioning in the facility, while achieving a further energy saving effect because most of the air conditioning was employed to lower the temperature. Moreover, a growth promotion spectrum such as far-red could be applied in the light sources to enhance the nutritional value and growth of the plants (Li and Kubota, 2009) in appropriate ways. In addition, a significantly higher PPF could be achieved to improve photosynthesis and plant growth, not only by shortening the distance between the light sources and plant canopies (Li et al., 2014) but also by consuming more energy at the expense of the reduction in LUE.

Phytochemical Accumulation

The phytochemical concentrations in the leaves were also affected by photosynthesis. On account of the increased leaf temperature in the Z-LED, the respiration rate increased considerably (Bolstad et al., 2003), while accelerating the transformation of carbohydrates into sucrose (Williams and Farrar, 1990). To compensate for the shortage of carbohydrates, as was reported by Blom-Zandstra and Lampe (1985), nitrate may serve as the osmoticum instead of sugars in suboptimal photosynthesis, which is the probable cause of the decreased concentration of nitrate in Z-LED. The higher intercellular CO_2 concentration of the C-LED also played a positive role in the accumulation of nitrate in the C-LED (Kaiser and Förster, 1989; Kaiser and Brendle-Behnisch, 1991). Photosynthetic pigments such as Chl a and Chl b might be much more sensitive to light parameters (Senger, 1982; Kurilčik et al., 2008; Poudel et al., 2008; Li and Kubota, 2009; Li et al., 2012). In this research, we demonstrated that when the parameters are at the same level, Chl a and Chl b have no significant difference from each other, although the photosynthesis has much difference.

CONCLUSION

The irradiation on a reserved growing space occupied a large amount of energy, which could be cut off by employing precise illumination before and after transplanting. Precise illumination could reduce electricity use by 52.06% and achieve a 55.64% increase in LUE, while bringing considerable economic benefits. Interestingly, the lower temperature in the growth environment induced by the energy reduction imposed adverse effects on the photosynthesis, reducing the yield significantly. Several countermeasures have been presented and remain to be tested. During the practical production process, technology could be employed combining ordinary multiple planting density adjustment cultivation to achieve the identical performance of energy savings. This took place

in the circumstance that the seedlings were transplanted in the density of fully grown plants with no more transplant processing, as long as the two principles during transplanting were followed.

AUTHOR CONTRIBUTIONS

KL brought up the idea, designed the system and experiments, modified the manuscript and discussed with reviewers and editor. ZL manufactured the illuminating system, conducted the experiments, analyzed the experiment data and initially formed the manuscript. QY made recommendations, suggestions and modified the manuscript.

FUNDING

This project was funded by the National High Technology Research and Development Plan of China (863 Project, grant No. 2013AA103001) and Key Program for International S&T Cooperation Projects of China (grant No. 2014DFG32110).

ACKNOWLEDGMENTS

We thank Guodong Wu and Qiang Wei for their mechanical design; Sheng Zhou and Bo Zhou for providing help to build the system; and Ping Xiao for the technical support.

REFERENCES

Andersen, A. (1986). Comparison of fluorescent lamps as an energy source for production of tomato plants in a controlled environment. *Sci. Hort.* 28, 11–18. doi: 10.1016/0304-4238(86)90119-6

Austin, R. B. (1965). The effectiveness of light from two artificial sources for promoting plant growth. *J. Agric. Eng. Res.* 10, 15–18. doi: 10.1016/0021-8634(65)90104-6

Beck, D. J., and Bibby, B. G. (1961). A modified anthrone colorimetric technique for use in investigations related to the cariogenicity of foodstuffs. *J. Dent. Res.* 40, 161–170. doi: 10.1177/00220345610400010801

Berry, J., and Bjorkman, O. (1980). Photosynthetic response and adaptation to temperature in higher plants. *Ann. Rev. Plant Physiol.* 31, 491–543. doi: 10.1146/annurev.pp.31.060180.002423

Blom-Zandstra, M., and Lampe, J. E. M. (1985). The role of nitrate in the osmoregulation of lettuce (*Lactuca sativa* L.) grown at different light intensities. *J. Exp. Bot.* 36, 1043–1052. doi: 10.1093/jxb/36.7.1043

Bolstad, P. V., Reich, P., and Lee, T. (2003). Rapid temperature acclimation of leaf respiration rates in *Quercus alba* and *Quercus rubra*. *Tree Physiol.* 23, 969–976. doi: 10.1093/treephys/23.14.969

Bradford, M. M. (1976). A rapid and sensitive method for the quantitation of microgram quantities of protein utilizing the principle of protein-dye binding. *Anal. Biochem.* 72, 248–254. doi: 10.1016/0003-2697(76)90527-3

Bülow-Hübe, H. (2008). Daylight in glazed office buildings: a comparative study of daylight availability, luminance and illumince distribution for an office room with three different glass areas. *Rep. EBD* 43, 291–307.

Cataldo, D. A., Maroon, M., Schrader, L. E., and Youngs, V. L. (1975). Rapid colorimetric determination of nitrate in plant tissue by nitration of salicylic acid. *Commun. Soil. Sci. Plant. Anal.* 6, 71–80. doi: 10.1080/00103627509366547

Challa, H., Heuvelink, E., and Meeteren, U. (1995). "Crop growth and development," in *The Greenhouse Climate Control*, eds J. C. Bakker, G. P. A. Bot, H. Challa, and N. J. V. D. Braak (Wageningen: Wageningen Press), 62–84.

Christou, P. (2013). From medicinal plants to medicines in plants: plant factories for the production of valuable pharmaceuticals. *Curr. Pharm. Des.* 19, 5469–5470. doi: 10.2174/1381612811319310001

Dougher, T. A. O., and Bugbee, B. (2001). Differences in the response of wheat, soy bean and lettuce to reduced blue radiation. *Photochem. Photobiol.* 73, 199–207. doi: 10.1562/0031-8655(2001)0730199DITROW2.0.CO2

Folta, K. M. (2004). Green light stimulates early stem elongation, antagonizing light mediated growth inhibition. *Plant Physiol.* 135, 1407–1416. doi: 10.1104/pp.104.038893

Folta, K. M., and Childers, K. S. (2008). Light as a growth regulator: controlling plant biology with narrow-bandwidth solid-state lighting systems. *HortScience* 43, 1957–1964.

Gates, D. M. (1964). Leaf temperature and transpiration. *J. Agron.* 56, 273–277. doi: 10.2134/agronj1964.00021962005600030007x

Gosselin, A., and Trudel, M. (1986). Root-zone temperature effects on pepper. *J. Am. Soc. Hort. Sci.* 111, 220–224.

Goto, E., Both, A. J., Albright, L. D., Langhans, R. W., and Leed, A. R. (1996). Effect of dissolved oxygen concentration on lettuce growth in floating hydroponics. *Acta. Hort.* 440, 205–210. doi: 10.17660/ActaHortic.1996.440.36

Hashimoto, Y. (1991). Computer integrated plant growth factory for agriculture and horticulture. *Math. Control Appl. Agric. Hort.* 63, 105–110. doi: 10.1016/B978-0-08-041273-3.50023-9

He, J., Lee, S. K., and Dodd, I. C. (2001). Limitations to photosynthesis of lettuce grown under tropical conditions: alleviation by root - zone cooling. *J. Exp. Bot.* 52, 1323–1330. doi: 10.1093/jexbot/52.359.1323

Hogewoning, S. W., Trouwborst, G., Maljaars, H., Poorter, H., Leperen, W. V., and Harbinson, J. (2010). Blue light does–responses of leaf photosynthesis, morphology, and chemical composition of *Cucumis sativus* grown under different combinations ofred and blue light. *J. Exp. Bot.* 61, 3107–3117. doi: 10.1093/jxb/erq132

Holst Centre (2012). Flexible organic LED (OLED) lighting reaches high energy efficiency thanks to shared research effort. *Optik Photonik* 7, 28. doi: 10.1002/opph.201290058

Hu, M. H., Ao, Y. S., Yang, X. E., and Li, T. Q. (2008). Treating eutrophic water for nutrient reduction using an aquatic macrophyte (Ipomoea aquatica Forsskal) in a deep flow technique system. *Agric. Water Manage.* 95, 607–615. doi: 10.1016/j.agwat.2008.01.001

Hyun, I. T., Lee, J. H., Yoon, Y. B., Lee, K. H., and Nam, Y. (2014). The potential and utilization of unused energy sources for large-scale horticulture facility applications under korean climatic conditions. *Energies* 7, 4781–4801. doi: 10.3390/en7084781

Ijaz, F., Siddiqui, A., Im, B. K., and Lee, C. (2012). "Remote management and control system for LED based plant factory using ZigBee and Internet," in *Advanced Communication Technology*, ed. S.-T. Kim (PyeongChang: IEEE), 942–946.

Ikeda, A., Tanimura, Y., Ezaki, K., Kawai, Y., Nakayama, S., Iwao, K., et al. (1992). Environmental control and operation monitoring in a plant factory using artificial light. *Acta Hort.* 151–158. doi: 10.17660/ActaHortic.1992.304.16

Johkan, M., Shoji, K., Goto, F., Hahida, S., and Yoshihara, T. (2012). Effect of green light wavelength and intensity on photomorphogenesis and photosynthesis in *Lactuca sativa*. *Environ. Exp. Bot.* 75, 128–133. doi: 10.1016/j.envexpbot.2011.08.010

Kaiser, W. M., and Brendle-Behnisch, E. (1991). Rapid modulation of spinach leaf nitrate reductase activity by photosynthesis I. Modulation in vivo by CO_2 availability. *Plant Physiol.* 96, 363–367. doi: 10.1104/pp.96.2.363

Kaiser, W. M., and Förster, J. (1989). Low CO_2 prevents nitrate reduction in leaves. *Plant Physiol.* 91, 970–974. doi: 10.1104/pp.91.3.970

Kato, K., Maruyama, S., Hirai, T., Hiwasa-Tanase, K., Mizoguchi, T., Goto, E., et al. (2011). A trial of production of the plant-derived high-value protein in a plant factory: photosynthetic photon fluxes affect the accumulation of recombinant miraculin in transgenic tomato fruits. *Plant Signal. Behav.* 6, 1172–1179. doi: 10.4161/psb.6.8.16373

Kato, K., Yoshida, R., Kikuzaki, A., Hirai, T., Kuroda, H., Hiwasa-Tanase, K., et al. (2010). Molecular breeding of tomato lines for mass production of miraculin in a plant factory. *J. Agric. Food. Chem.* 58, 9505–9510. doi: 10.1021/jf101874b

Kim, H. H., Goins, G. D., Wheeler, R. M., and Sager, J. C. (2004). Green-light supplementation for enhanced lettuce growth under red- and blue-light-emitting diodes. *HortScience* 39, 1617–1622.

Kitaya, Y., Niu, G., Kozai, T., and Ohashi, M. (1998). Photosynthetic photon flux, photoperiod, and CO_2 concentration affect growth and morphology of lettuce plug transplants. *HortScience* 33, 988–991.

Kurilčik, A., Miklušytė-Čanova, R., Dapkūnienė, S., Žilinskaitė, S., Kurilčik, G., Tamulaitis, G., et al. (2008). In vitro culture of chrysanthemum plantlets using light-emitting diodes. *Central Euro. J. Biol.* 3, 161–167. doi: 10.2478/s11535-008-0006-9

Kwon, S., Ryu, S., and Lim, J. (2014). Design and implementation of an integrated management system in a plant factory to save energy. *Cluster Comput.* 17, 727–740. doi: 10.1007/s10586-013-0295-2

Li, H. M., Tang, C. M., Xu, Z. G., Liu, X. Y., and Han, X. L. (2012). Effects of different light sources on the growth of non-heading Chinese cabbage (*Brassica campestris* L.). *J. Agric. Sci.* 4, 262–273. doi: 10.5539/jas.v4n4p262

Li, H. M., Xu, Z. G., and Tang, C. M. (2010). Effect of light emitting diodes on growth and morphogenesis of upland cotton (*Gossypium hirsutum* L.) plantlets in vitro. *Plant Cell Tissue Organ. Cult.* 103, 155–163. doi: 10.1007/s11240-010-9763-z

Li, K., Yang, Q., Tong, Y., and Cheng, R. (2014). Using movable light-emitting diodes for electricity savings in a plant factory growing lettuce. *Horttechnology* 24, 546–553.

Li, Q., and Kubota, C. (2009). Effects of supplemental light quality on growth and phytochemicals of baby leaf lettuce. *Environ. Exp. Bot.* 67, 59–64. doi: 10.1016/j.envexpbot.2009.06.011

Lichtentaler, H. K., and Wellburn, A. R. (1983). Determinations of carotenoids and chlorophylls a and b of leaf extracts in different solvents. *Biochem. Soc. Trans.* 11, 591–592. doi: 10.1007/978-94-017-6368-4_3

Luján, R., Lledías, F., Martínez, L. M., Barreto, R., Cassab, G. I., and Nieto-Sotelo, J. (2009). Small heat-shock proteins and leaf cooling capacity account for the unusual heat tolerance of the central spike leaves in *Agave tequilana* var. *Weber. Plant. Cell Environ.* 32, 1791–1803. doi: 10.1111/j.1365-3040.2009.02035.x

Minaxi, and Saxena, J. (2010). Disease suppression and crop improvement in moong beans (*Vigna radiata*) through *Pseudomonas* and Burkholderia strains isolated from semi arid region of Rajasthan, India. *Biocontrology* 55, 799–810. doi: 10.1007/s10526-010-9292-z

Murase, H. (2000). Development of Micro-precision agriculture by plant factory. *J. Soc. High Technol. Agric.* 12, 99–104. doi: 10.2525/jshita.12.99

Nelson, C. J. (1988). Genetic associations between photosynthetic characteristics and yield: review of the evidence. *Plant Physiol. Biochem.* 26, 543–554.

Nishimura, M., Kozai, T., Kubota, C., and Chun, C. (2001). Analysis of electric energy consumption and its cost for a closed-type transplant production system. *SHITA J.* 13, 204–209.

Ohyama, K., Fujiwara, M., Kozai, T., and Chun, C. (2001). Consumption of electric energy and water for eggplant plug transplant production in a closed-type transplant production system. *J. Soc. High Technol. Agric.* 13, 1–6. doi: 10.2525/jshita.13.1

Pallas, J. E., Michel, B. E., and Harris, D. G. (1967). Photosynthesis, transpiration, leaf temperature, and stomatal activity of cotton plants under varying water potentials. *Plant Physiol.* 42, 76–88. doi: 10.1104/pp.42.1.76

Pamungkas, A. P., Hatou, K., and Morimoto, T. (2014). Evapotranspiration model analysis of crop water use in plant factory system. *Environ. Control Biol.* 52, 183–188. doi: 10.2525/ecb.52.183

Poudel, P. R., Kataoka, I., and Mochioka, R. (2008). Effect of red-and blue-light-emitting diodes on growth and morphogenesis of grapes. *Plant Cell Tissue Organ. Cult.* 92, 147–153. doi: 10.1007/s11240-007-9317-1

Poulet, L., Massa, G. D., Morrow, R. C., Bourget, C. M., Wheeler, R. M., and Mitchell, C. A. (2014). Significant reduction in energy for plant-growth lighting in space using targeted LED lighting and spectral manipulation. *Life Sci. Space Res.* 2, 43–53. doi: 10.1016/j.lssr.2014.06.002

Sager, J. C., Smith, W. O., Edwards, J. L., and Cyr, K. L. (1982). Photosynthetic efficiency and phytochrome photoequilibria determination using spectral data. *Trans. Am. Soc. Agric. Eng.* 31, 1882–1889. doi: 10.13031/2013.30952

Samuolienė, G., Sirtautas, R., Brazaitytė, A., and Duchovskis, P. (2012). LED lighting and seasonality effects antioxidant properties of baby leaf lettuce. *Food Chem.* 134, 1494–1499. doi: 10.1016/j.foodchem.2012.03.061

Senger, H. (1982). The effect of blue light on plants and microorganisms. *Photochem. Photobiol.* 35, 911–920. doi: 10.1111/j.1751-1097.1982.tb02668.x

Seo, K. K., and Choi, D. Y. (2011). Efficiency analysis of construction firms using a combined AHP and DEA model. *J. Korea Contents Assoc.* 11, 302–310. doi: 10.5392/JKCA.2011.11.6.302

Shimizu, H., Saito, Y., Nakashima, H., Miyasaka, J., and Ohdoi, K. (2011). "Light environment optimization for lettuce growth in plant factory," in *Proceedings of the 18th IFAC World Congress. International Federation of Automatic Control*, Vol. 18, eds B. Sergio, C. Angelo, and Z. Sandro (Kyoto: International Federation of Automatic Control), 605–609. doi: 10.3182/20110828-6-IT-1002.02683

Tei, F., Scaife, A., and Aikman, D. P. (1996). Growth of lettuce, onion, and red beet. 1. Growth analysis, light interception, and radiation use efficiency. *Ann. Bot.* 78, 633–643. doi: 10.1006/anbo.1996.0171

Tibbitts, T. W., Morgan, D. C., and Warrington, I. J. (1983). Growth of lettuce, spinach, mustard, and wheat plants under four combinations of high-pressure sodium, metal halide, and tungsten halogen lamps at equal PPFD. *J. Am. Soc. Hort. Sci.* 108, 622–630.

Ting, K. C., Giacomelli, G. A., and Fang, W. (1993). "Decision support system for single truss tomato production," in *Proceedings of XXV CIOSTA-CIGR V Congress*, (Wageningen), 70–76.

Togawa, T., Fujita, T., Dong, L., Fujii, M., and Ooba, M. (2014). Feasibility assessment of the use of power plant-sourced waste heat for plant factory heating considering spatial configuration. *J. Cleaner Prod.* 81, 60–69. doi: 10.1016/j.jclepro.2014.06.010

Watanabe, H. (2009). Light-controlled plant cultivation system in Japan-development of a vegetable factory using LEDs as a light source for plants. *Acta Hort.* 907, 37–44. doi: 10.17660/ActaHortic.2011.907.2

Wen, J. (2009). *Influence of Wave Crest and R/B of Red and Blue LED on Crop Growing in the Closed Plant Factory (in Chinese)*, Master's thesis, Chinese Academy of Agricultural Sciences MS Dissertation Abstract, Beijing, 16–19.

Williams, J. H. H., and Farrar, J. F. (1990). Control of barley root respiration. *Physiol. Plant.* 79, 259–266. doi: 10.1111/j.1399-3054.1990.tb06740.x

Wolfe, D. W. (1991). Low temperature effects on early vegetative growth, leaf gas exchange and water potential of chilling-sensitive and chilling-tolerant crop species. *Ann. Bot.* 67, 205–212.

Wu, M. C., Hou, C. Y., Jiang, C. M., Wang, Y. T., Wang, C. Y., Chen, H. H., et al. (2007). A novel approach of LED light radiation improves the antioxidant activity of pea seedlings. *Food Chem.* 101, 1753–1758. doi: 10.1016/j.foodchem.2006.02.010

Wu, M. Y., Lin, Y. H., and Ke, C. K. (2012). WSN-based automatic monitoring management platform for plant factory. *Int. J. Digital Content Technol. Appl.* 6, 303–311. doi: 10.4156/jdcta.vol6.issue6.35

Yamada, C., Ohyama, K., and Kozai, T. (2000). Photosynthetic photon flux control for reducing electric energy consumption in a closed-type transplant production system. *Envrion. Control Biol.* 38, 255–261. doi: 10.2525/ecb1963.38.255

Yoshida, S., Kitano, M., and Eguchi, H. (1997). Growth of lettuce plants (*Lactuca sativa* L.) under control of dissolved O_2 concentration in hydroponics. *Biotronics* 26, 39–45.

Conflict of Interest Statement: The authors declare that the research was conducted in the absence of any commercial or financial relationships that could be construed as a potential conflict of interest.

frontiers in Plant Science

ORIGINAL RESEARCH
published: 07 April 2016
doi: 10.3389/fpls.2016.00448

Nighttime Supplemental LED Inter-lighting Improves Growth and Yield of Single-Truss Tomatoes by Enhancing Photosynthesis in Both Winter and Summer

*Fasil T. Tewolde[1,2], Na Lu[2], Kouta Shiina[3], Toru Maruo[1], Michiko Takagaki[1,2], Toyoki Kozai[4] and Wataru Yamori[2,5]**

[1] Graduate School of Horticulture, Chiba University, Matsudo, Japan, [2] Center for Environment, Health and Field Sciences, Chiba University, Kashiwa, Japan, [3] JA-Zen-Noh, Kashiwa, Japan, [4] Japan Plant Factory Association, Kashiwa, Japan, [5] Department of Biological Sciences, Faculty of Science, The University of Tokyo, Tokyo, Japan

Greenhouses with sophisticated environmental control systems, or so-called plant factories with solar light, enable growers to achieve high yields of produce with desirable qualities. In a greenhouse crop with high planting density, low photosynthetic photon flux density (PPFD) at the lower leaves tends to limit plant growth, especially in the winter when the solar altitude and PPFD at the canopy are low and day length is shorter than in summer. Therefore, providing supplemental lighting to the lower canopy can increase year-round productivity. However, supplemental lighting can be expensive. In some places, the cost of electricity is lower at night, but the effect of using supplemental light at night has not yet been examined. In this study, we examined the effects of supplemental LED inter-lighting (LED inter-lighting hereafter) during the daytime or nighttime on photosynthesis, growth, and yield of single-truss tomato plants both in winter and summer. We used LED inter-lighting modules with combined red and blue light to illuminate lower leaves right after the first anthesis. The PPFD of this light was 165 μmol m^{-2} s^{-1} measured at 10 cm from the LED module. LED inter-lighting was provided from 4:00 am to 4:00 pm for the daytime treatments and from 10:00 pm to 10:00 am for the nighttime treatments. Plants exposed only to solar light were used as controls. Daytime LED inter-lighting increased the photosynthetic capacity of middle and lower canopy leaves, which significantly increased yield by 27% in winter; however, photosynthetic capacity and yield were not significantly increased during summer. Nighttime LED inter-lighting increased photosynthetic capacity in both winter and summer, and yield increased by 24% in winter and 12% in summer. In addition, nighttime LED inter-lighting in winter significantly increased the total soluble solids and ascorbic acid content of the tomato fruits, by 20 and 25%, respectively. Use of nighttime LED inter-lighting was also more cost-effective than daytime inter-lighting. Thus, nighttime LED inter-lighting can effectively improve tomato plant growth and yield with lower energy cost compared with daytime both in summer and winter.

Keywords: LED, supplemental lighting, lighting period, single-truss tomato, photosynthesis, yield, fruit quality, plant factory

OPEN ACCESS

Edited by:
Alejandro Isabel Luna-Maldonado, Universidad Autónoma de Nuevo León, Mexico

Reviewed by:
Zhihui Cheng, Northwest A&F University, China
Hao Peng, Washington State University, USA

****Correspondence:***
Wataru Yamori
wataru.yamori@bs.s.u-tokyo.ac.jp

Specialty section:
This article was submitted to Crop Science and Horticulture, a section of the journal Frontiers in Plant Science

Received: *30 January 2016*
Accepted: *22 March 2016*
Published: *07 April 2016*

Citation:
Tewolde FT, Lu N, Shiina K, Maruo T, Takagaki M, Kozai T and Yamori W (2016) Nighttime Supplemental LED Inter-lighting Improves Growth and Yield of Single-Truss Tomatoes by Enhancing Photosynthesis in Both Winter and Summer. Front. Plant Sci. 7:448. doi: 10.3389/fpls.2016.00448

INTRODUCTION

"Plant factory" refers to an environmentally controlled, plant production facility that can be divided into two types in terms of light source: plant factories with artificial light and plant factory with solar light. The former is a thermally insulated and nearly airtight warehouse-like structure in which the environment for plant growth can be controlled as precisely as desired and used for commercial production of leafy greens (e.g., lettuce etc.), herbs (e.g., perilla, mint, basil, etc.) and transplants (e.g., tomato, cucumber, paprika etc.) (Kozai, 2013; Merrill et al., 2016). The latter refers to greenhouses with sophisticated environmental control systems, or so-called plant factories with solar light, enable growers to achieve a high yield of produce with desirable qualities (Janes and McAvoy, 1991; Heuvelink et al., 2006; Yamori et al., 2014). However, predictable and consistent yields are difficult to accomplish (Cooper, 1961). In traditional multi-truss (high wire) cultivation, tomato plants have an indeterminate growth pattern and the cultural management is labor intensive (Fisher et al., 1990). Even tomato plants with 4 or 5 truss using hydroponic system combined with about 0.5 m height of benches/gutters, ladders would be needed for plant management. Single-truss tomato cultivation can drastically reduce labor requirements for training, pruning, and harvesting, and workplace ergonomics can be considerably improved by the use of high benches but demand more labor for frequent replanting and pinching (Okano et al., 2001). Moreover, single-truss tomato cultivation systems are superior to multi-truss tomato cultivation systems because they allow multiple cropping, predictable and consistent harvests, and use of moveable benches, and they have the potential for automation (Giniger et al., 1988; McAvoy and Janes, 1988; McAvoy et al., 1989; Fisher et al., 1990; Janes and McAvoy, 1991; Giacomelli et al., 1994; Logendra and Janes, 1999; Okano et al., 2001; Wada et al., 2006). Most importantly, growers using this system can capitalize on the premium paid for dependability and consistency of supply, especially for winter-produced tomatoes, which command a higher price (Janes and McAvoy, 1991).

However, light is a limiting environmental factor in the winter (Hao and Papadopoulos, 1999) and it affects photosynthesis and thus yield, since plant growth and yield depend largely on photosynthesis (Yamori, 2013; Yamori and Shikanai, 2016; Yamori et al., 2016). Because single-truss cultivation uses high plant density, light is a major limiting factor for the lower canopy leaves (Lu et al., 2012a). In winter solar light interception is limited in both top and lower canopy leaves, whereas during summer the lower canopy leaves continue to receive limited light due to the high plant density (Gunnlaugsson and Adalsteinsson, 2006), even though there is abundant light at the top of the foliar canopy (Ackerly and Bazzaz, 1995). In general, it is considered that a decrease of 1% in cumulative daily light throughout the growing season leads to a loss of 1% yield under greenhouse cultivation (Cockshull et al., 1992).

High planting density reduces light distribution along the plant profile, which is associated with mutual shading (Zhang et al., 2015). The understory leaves of tomato plants have a very low net photosynthetic rate due to both lower incident light and leaf senescence (Acock et al., 1978; Xu et al., 1997), but compared with uppermost leaves, the poor light distribution which leads to senescence had a larger effect on the photosynthetic rate of understory leaves (Acock et al., 1978). Frantz et al. (2000) suggested that supplemental light within a cowpea canopy significantly delayed senescence of the interior leaves. Supplying upward lighting from underneath also retarded the senescence of outer leaves and increased the photosynthetic rate, leading to improvement of total plant growth in lettuce (Zhang et al., 2015).

Inter-lighting can be more effective than traditional top-mounted supplemental lighting (Adams et al., 2002) and improves the net photosynthesis contribution of the lower canopy and thus yield (Hovi et al., 2004; Pettersen et al., 2010). In most cases, inter-lighting improved yield up to 50% in various crops (Hovi et al., 2004; Hovi and Tahvonen, 2008; Pettersen et al., 2010; Lu et al., 2012a,b), although some studies using different strategies and locations showed no increase in yield (Gunnlaugsson and Adalsteinsson, 2006; Heuvelink et al., 2006; Trouwborst et al., 2010). Moreover, in single-truss tomato cultivation, inter-lighting increased yield by 20% in winter and 14% in autumn (Lu et al., 2012a,b). Therefore, lighting the lower part of the canopy can be beneficial.

LEDs are considered a suitable light source for inter-lighting (Hao et al., 2012) because they produce less heat and therefore are less likely to burn leaves as compared with high-pressure sodium (HPS) lamps. In the past two decades, development of LEDs as an alternative light source has enabled not only researchers but also farmers to control spectral qualities by combining various light sources with different waveband emissions (Goto, 2003; Merrill et al., 2016). Economically efficient use of light based on the desired photosynthetic photon flux density (PPFD), lighting period (day/night cycle), and the plant growth stage when LED inter-lighting is used are key to the feasibility of the cultivation systems. The efficient plant growth stages and light qualities of inter-lighting application have been discussed (Lu et al., 2012a,b); however, no study on optimizing the lighting period with supplemental inter-lighting in winter and summer has been reported.

In addition, energy efficient use of lighting can be achieved by adjusting the LED inter-lighting schedule so that more is used at night, because the price per unit kilowatt can be lower with off-peak time-of-use (TOU), which is mostly at night. Other industries have rescheduled their operations to take advantage of discounted off-peak rates to reduce their electricity bills (Ashok and Banerjee, 2000; Ashok, 2006; Middelberg et al., 2009). In greenhouse crop production, growers are interested in alternative lighting strategies that can increase yield while reducing operating expenses. However, no study on the effect of nighttime supplemental inter-lighting on photosynthesis, growth and yield has been reported. In this study, we examined the effects of daytime and nighttime LED inter-lighting on photosynthesis, growth, and yield in a single-truss tomato cultivation system in both winter and summer.

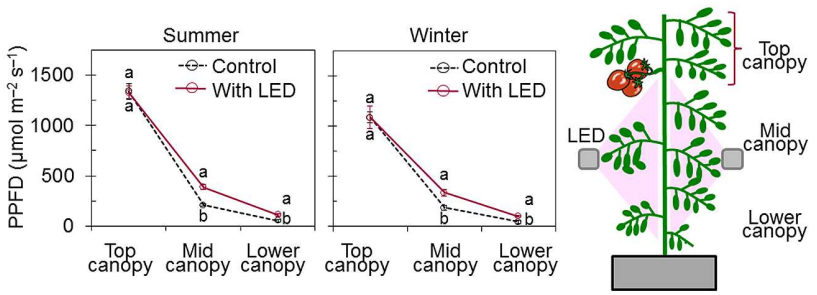

FIGURE 1 | Effect of LED inter-lighting on photosynthetic photon flux density (PPFD) along the profile of tomato plant canopy (top, middle, and lower canopy). PPFD was measured by using a quantum sensor positioned at the inclination angle of representative canopy leaves near the point of measurement. Data represent means ± SE ($n = 10$). For each canopy level, different letters indicate statistically significant differences (t-test at $P < 0.05$).

MATERIALS AND METHODS

Plant Material and Growth Conditions

Tomato (*Solanum lycopersicum* L., cv. Sanbi) seeds were sown in 128-cell plug trays filled with vermiculite. After 2 days in a dark room at a temperature of 26°C for germination, the trays were transferred to a walk-in type environment-controlled growth chamber (Nae Terrace, Mitsubishi Plastics Agri Dream Co., Ltd., Tokyo, Japan). Seedlings were cultivated using Otsuka nutrient solution with 2.0 ± 0.2 EC and 5.5 ∼ 6.0 pH supplied only once a day using ebb and flow system. In the growth chamber, temperature was 20/16°C day/night during the winter and 22/18°C day/night temperature in the summer, under cool white fluorescent lamps with 360 μmol m^{-2} s^{-1} PPFD and 1200 ppm CO_2 concentration.

After 3 weeks in the growth chamber, the seedlings were transplanted in a greenhouse at a plant density of 10 plants per square meter (on 7 December 2013 and 1 August 2014 for winter and summer, respectively). The greenhouse was equipped with heat pumps to keep the day/night temperature of 22/17°C in winter, and pad and fan system were used to keep the day/night temperature at 26/20°C during the summer. The irrigation system was a modified nutrient film technique (NFT) designed to distribute nutrient solution evenly to each plant through longitudinal flow of the nutrient solution, rather than flowing from the start to the end of the growing bed (Zen-Noh Co., Ltd., Tokyo, Japan). Otsuka nutrient solution (Otsuka Chemical Co., Ltd., Osaka) was used for fertigation with an application schedule of 10 min with a subsequent 30 min break during the day and an hour break during the night. The pH was maintained at 6.0 at all times. Electrical conductivity was set at 2.5 dS m^{-1} at the time of transplanting and was increased progressively up to 12 dS m^{-1} until the harvest date in order to increase the total soluble solids content of the tomato fruits for commercial production. The tomato cultivation method was a high-plant-density single truss tomato production system in which each plant was allowed to develop only a single truss of fruit (Giacomelli et al., 1994). To achieve this, the apical meristem of each plant was pinched after the first anthesis, leaving two leaves above the first flowering truss and all flowers that set fruits were kept intact. To improve fruit setting, fully blooming flowers were sprayed once using 4-chlorophenoxy acetic acid with 15 mg L^{-1} and 7.5 mg L^{-1} concertation in summer and winter, respectively as described (Yoshida et al., 2014).

LED Inter-lighting

LED inter-lighting (Philips Green Power LED inter-lighting module DR/B, Philips, Eindhoven, the Netherlands) was used to illuminate the understory leaves. The lamp spectrum was red and blue combined (Supplementary Figure S1) with a PPFD of 165 μmol m^{-2} s^{-1} measured at 10 cm from the LED module. LED modules were positioned on both sides of the aisle at a distance of 50 cm from the stem (10 cm away from the mid-canopy leaves, on average), and at a height of 40 cm from the Styrofoam panel under which the root system was established (**Figure 1**).

Previous studies reported that yield is positively correlated with the total incident light during the period from anthesis to harvest for single-truss tomato plants (McAvoy et al., 1989; Lu et al., 2012a). Therefore, we applied LED inter-lighting from the time of the very first anthesis until harvest in order to maximize yield while keeping energy cost low (from 4 September to 2 October in summer and from 16 January to 13 March in winter). To compare the electric energy use efficiency of between the daytime and nighttime LED inter-lighting schedules, we used Tokyo Electric Power Corporation's "Otokuna night 10" as an example; this plan gives a discount rate for using power during specific off-peak periods. Plants were subjected to one of the following lighting schedules: (1) Control: solar light without LED inter-lighting, (2) daytime LED inter-lighting from 4:00 am to 4:00 pm, or (3) nighttime LED inter-lighting from 10:00 pm to 10:00 am.

Measurements

Plant Growth

Internode length and stem diameter under the fruit truss, leaf chlorophyll content, leaf area, leaf mass per unit area (LMA), and shoot dry weight were measured. Chlorophyll content was determined using a spectrophotometer, as described previously (Yamori et al., 2005; Zhang et al., 2015). Leaf area was measured using an LI-3000C portable leaf area meter (Li-Cor, Lincoln, NE, USA). In addition to the growth parameters, we measured

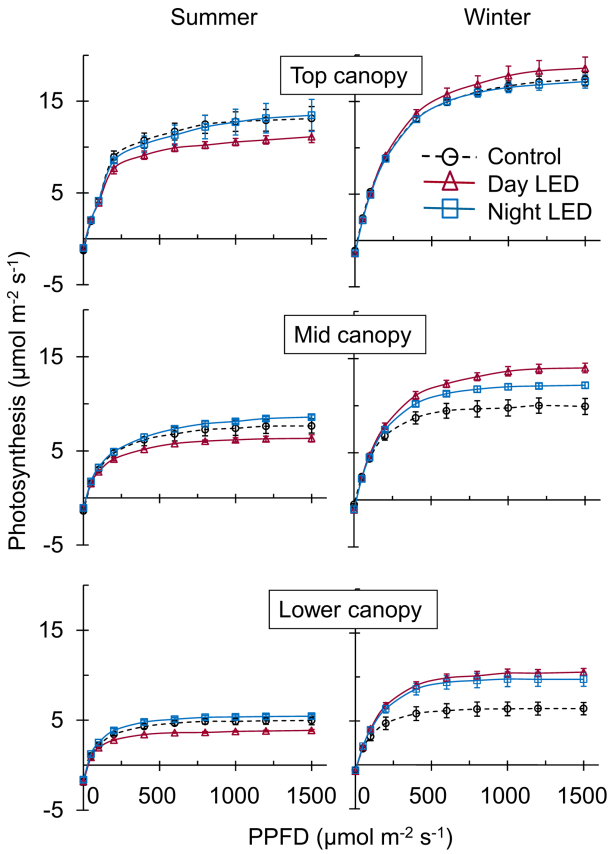

FIGURE 2 | Effect of LED inter-lighting on single-truss tomato leaf photosynthetic capacity. Measurements were taken in representative leaves from each canopy section (top, middle, and lower) of control and LED inter-lighted plants. We measured the light–response curve of the photosynthetic rate, from 10:00 am to 2:00 pm under growth condition. Data represent means ± SE ($n = 5$).

temperature and relative humidity in the microenvironment around mid-canopy by using a Thermo-hygro-CO_2 meter (TR-76Ui; T&D Corporation, Nagano, Japan).

Light Distribution Along the Plant Profile

Light distribution along the plant profile was measured at each canopy level (top, middle, and lower) with a quantum sensor (LI-190SA; Li-Cor). The sensor was positioned such that the angle of inclination was the same as that of the representative canopy leaves. For LED inter-lighting measurement was made while LED inter-lighting was in use. Solar irradiance alone was used as a control and was measured similarly but in the absence of LED inter-lighting.

Leaf Gas Exchange

Photosynthetic rate was measured with a portable gas exchange system (LI-6400; Li-Cor) as described previously (Yamori et al., 2009, 2010). We measured the light–response curve of the photosynthetic rate, from 10:00 am to 2:00 pm under growth condition. Photosynthetic rate was measured in representative leaves from three layers of the canopy (top, middle, and lower).

Diurnal photosynthetic rate and PPFD were also measured under growth conditions using three LI-6400 gas exchange systems at the same time, one each for the control plants and plants treated with daytime and nighttime LED inter-lighting. Measurements were made using representative leaves from mid-canopy. Although the leaves were originally positioned at different distances from the LED module, the leaf cuvettes were set at a representative distance of 10 cm from the LED module. Leaves were inserted into the leaf cuvettes positioned at their original inclination angle. Diurnal PPFD was recorded by positioning quantum sensors next to each leaf subjected to diurnal photosynthetic rate measurement.

Yield and Fruit Quality

The fresh weight of each fruit was recorded, and two quality parameters were measured as described in Lu et al. (2015): ascorbic acid content using an RQ Flex plus (Merck Co., Ltd., Darmstadt, Germany) and total soluble solids content using a refractometer (Atago Co., Ltd., Tokyo, Japan).

Use of Electricity and Cost Performance

Electric energy consumption of the LED modules was measured with a multimeter and a clamp ammeter (Hioki 3169-01; Hioki E.E. Corporation, Nagano, Japan) as described previously in Zhang et al. (2015). Electric energy use efficiency was calculated as:

Electric energy use efficiency ((kg kWh^{-1}) = [increase in yield with LED treatment (kg m^{-2})]/[electric energy consumption (kWh m^{-2})].

Light use efficiency (g MJ^{-1}) = Electric use efficiency (kg kWh^{-1})/the conversion coefficient from electrical energy to photosynthetically active radiation energy (Kozai and Niu, 2016), which is around 0.4 for recently developed LEDs (Mitchell et al., 2012).

Cost performance of LED inter-lighting was calculated as:

Cost performance (return/cost) = [price of tomato (Yen kg^{-1}) × increase in yield (kg m^{-2})]/[electricity used for LED lighting per crop season (kWh m^{-2}) × price of electricity (Yen kWh^{-1}) + LED depreciation cost per crop season (Yen m^{-2})].

Statistical Analysis

Data were examined using the statistical software SPSS version 21.0 (SPSS, Chicago, IL, USA); the significance of mean differences was analyzed either with Tukey's HSD test (for more than two means) or with *t*-test (for two means).

RESULTS

Without LED inter-lighting, light distribution along middle and lower canopy leaves were highly deteriorated (**Figure 1**). Estimated diurnal changes in PPFD at three different canopy levels (top, middle, and lower) indicated that only 33 and 18% of the daily light reached the middle and lower foliar canopy, respectively, compared with the total incident light at the top of the foliar canopy. Introducing LED inter-lighting significantly improved the light distribution to the middle and lower canopy

TABLE 1 | Effect of LED inter-lighting on leaf photosynthetic rate of single-truss tomato plants.

		Mid canopy photosynthetic rate (μmol $m^{-2}s^{-1}$)		
		Light saturation (1500 μmol m^{-2} s^{-1})	**With LED (400 μmol m^{-2} s^{-1})**	**Without LED (200 μmol m^{-2} s^{-1})**
Summer	Control	7.0 ± 0.4^{b}	5.6 ± 0.3^{ab}	4.3 ± 0.2^{a}
	Day LED	6.3 ± 0.4^{b}	5.2 ± 0.1^{b}	4.1 ± 0.1^{a}
	Night LED	8.6 ± 0.2^{a}	6.4 ± 0.3^{a}	4.9 ± 0.4^{a}
Winter	Control	10.0 ± 0.9^{b}	8.7 ± 0.7^{b}	6.8 ± 0.4^{a}
	Day LED	14.0 ± 0.5^{a}	11.1 ± 0.4^{a}	7.8 ± 0.3^{a}
	Night LED	13.1 ± 0.5^{a}	10.8 ± 0.4^{a}	7.8 ± 0.3^{a}

The photosynthetic rate was measured from mid-canopy leaves at 1500, 400, and 200 μmol m^{-2} s^{-1} to represent light saturation, growth conditions with LED inter-lighting, and growth conditions without LED inter-lighting, respectively, at the ambient CO_2 concentration of 400 ppm. Data represent means ± SE ($n = 5$). Different letters indicate statistically significant differences by Tukey's HSD ($P < 0.05$).

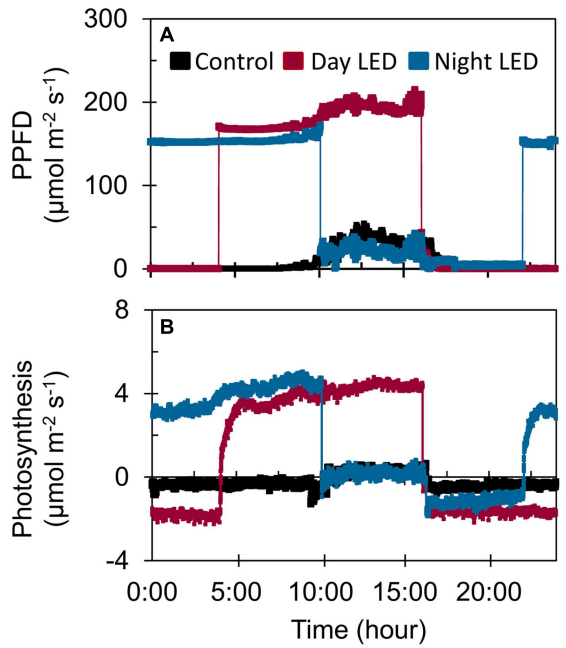

FIGURE 3 | The effect of LED inter-lighting on (A) diurnal photosynthetic photon flux density (PPFD) and (B) photosynthetic rate. Measurements were made on 14 February using fully expanded mid-canopy leaves from control plants and plants exposed to daytime or nighttime LED inter-lighting treatments. Daytime LED inter-lighting was provided from 4:00 am to 4:00 pm and nighttime from 10:00 pm to 10:00 am.

leaves (**Figure 1**). The light distribution within mid-canopy leaves was twice as high in plants that had direct irradiance from LED inter-lighting than in controls that were only exposed to solar light.

LED inter-lighting also altered micro-environments around the mid-canopy where there was direct irradiance. Daytime LED inter-lighting significantly increased average daytime temperature by 5.3 and 6.7% in summer and winter, respectively (Supplementary Table S1). Similarly, the nighttime LED inter-lighting significantly increased average nighttime temperatures, by 7.1 and 6.8% in summer and winter, respectively. In contrast, the relative humidity was significantly higher in the controls than in plants receiving nighttime LED inter-lighting treatments, in both seasons (Supplementary Table S1).

The overall change in plant micro-environment due to nighttime LED inter-lighting was accompanied by a higher photosynthetic capacity of middle and lower canopy leaves in both summer and winter. In contrast, daytime LED inter-lighting had a positive effect on leaf photosynthetic capacity in the winter but not in the summer (**Figure 2**). The photosynthetic rates in response to growth condition PPFD were measured in mid-canopy leaves from control and both daytime and nighttime LED inter-lighting plants (**Table 1**). The mid-canopy leaf photosynthetic rate under plant growth conditions for controls at 200 μmol m^{-2} s^{-1} PPFD (without LED inter-lighting) was 4.3, and the rate for LED inter-lighting at 400 μmol m^{-2} s^{-1} PPFD was 5.2 for daytime inter-lighting and 6.4 μmol m^{-2} s^{-1} for nighttime inter-lighting (**Table 1**). The photosynthetic rate was higher in plants exposed to daytime LED inter-lighting than in controls. However, leaves treated with daytime LED inter-lighting had lower leaf photosynthetic capacity than control leaves (**Figure 2**), which offset the net photosynthetic rate under growth conditions (**Table 1**).

The increased light distribution along mid-canopy leaves due to daytime or nighttime LED inter-lighting (Supplementary Figure S2) increased the diurnal photosynthetic rate in mid-canopy leaves by 5 μmol m^{-2} s^{-1} on average, as compared with a rate of about −0.4 μmol m^{-2} s^{-1} in control plants (**Figure 3**). When both daytime and nighttime LED inter-lighting were turned off, between 4:00 pm and 10:00 pm, the leaf respiration rate was higher for leaves from plants exposed to daytime or nighttime inter-lighting than for control leaves (**Figure 3**). In addition, LED inter-lighting significantly increased chlorophyll content in both middle and lower canopy leaves, but not in top canopy leaves, (**Figure 4**), to which LED inter-lighting did not contribute PPFD (**Figure 1**). LED inter-lighting had no significant effect on leaf area index (LAI) (**Table 2**), but a significant increase in stem diameter and LMA with short internode length under the fruit truss was observed (**Table 2**).

Most importantly, we found that daytime LED inter-lighting increased yield by 27% in winter, but had no effect in summer. However, nighttime LED inter-lighting increased yield in both

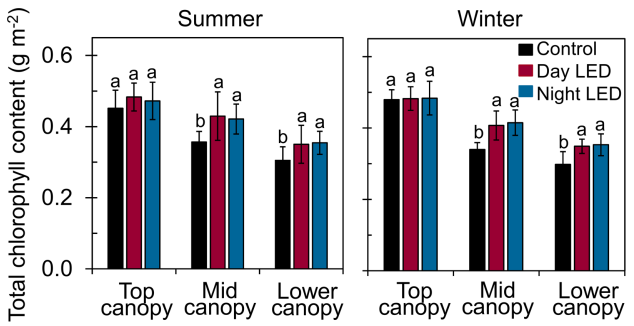

FIGURE 4 | Total chlorophyll content of single-truss tomato leaves. Chlorophyll was measured from leaves at each level of the canopy (top, middle, and lower canopy) in plants grown under daytime or nighttime LED inter-lighting and controls, during both summer and winter. Data represent means ± SE ($n = 15$). Different letters indicate statistically significant differences (Tukey's HSD at $P < 0.05$).

winter and summer by 24 and 12%, respectively (**Figure 5**). Fruit quality also significantly improved as a result of LED inter-lighting. Daytime LED inter-lighting increased total soluble solids by 8.2% in summer and 24% in winter. Nighttime LED inter-lighting significantly increased total soluble solids by 20% in winter, but the increase in summer was not significant (**Figure 6**). Winter LED inter-lighting significantly increased ascorbic acid content, by 24% for daytime inter-lighting and 25% for nighttime inter-lighting. However, neither treatment altered the ascorbic acid content during the summer (**Figure 6**).

Because we used LED inter-lighting for the same duration (12 h) for the daytime and nighttime treatments, the total electric energy used was similar, 72 kWh m^{-2} for 2 months of LED inter-lighting in winter and 36 kWh m^{-2} for 1 month of LED inter-lighting during summer. The increase in yield from LED inter-lighting during the winter was statistically equivalent for daytime (0.9 kg m^{-2}) and nighttime (0.8 kg m^{-2}) LED inter-lighting (Supplementary Table S2). In summer, nighttime LED inter-lighting increased the yield by 0.3 kg m^{-2}, but daytime LED inter-lighting was deleterious, decreasing yield by 0.3 kg m^{-2} (Supplementary Table S2). Light use efficiency during winter for both daytime and nighttime LED lighting was 8.6 and 7.7 g MJ^{-1}, respectively. In summer nighttime LED lighting had 3.9 g MJ^{-1} light use efficiency, but daytime LED light had negative effect. The cost-performance analysis for LED inter-lighting shows that only winter nighttime LED lighting can effectively improve tomato yield with high cost performance (Supplementary Figure S3), whereas summer nighttime and winter daytime LED lightings improved yield but the economic returns from the lighting were smaller than the running cost of electricity.

DISCUSSION

Development of plant factories in Japan brought single-truss tomato cultivation method for more improvement as an alternative system for its merits over multi-truss cultivation. However, at high planting density with a LAI higher than 3, light becomes a limiting factor for plant growth, because the leaf architecture and mutual shading prevent the light from penetrating to the lower canopy and thereby suppress photosynthetic activity (Okano et al., 2001). High planting density and canopy architecture plays a pivotal role for canopy light interception (Falster and Westoby, 2003; Sarlikioti et al., 2011). Therefore, providing inter-lighting to the lower leaves can be viable for year-round greenhouse crop production (Adams et al., 2002; Hovi et al., 2004; Pettersen et al., 2010). Generally, inter-lighting is based on three principles: increased light absorption in lower leaves, more efficient use of light by providing more homogeneous vertical light distribution, and preserving photosynthetic capacity of lower leaves (Giniger et al., 1988). However, it is also important to consider in which growth stage and with which lighting schedule (daytime or nighttime) inter-lighting can enhance crop yield with higher energy and cost efficiency. Previous studies showed that the yield of tomato plants increased with the increase in the total amount of PPFD received from anthesis to harvest (McAvoy et al., 1989; Lu et al., 2012a,b). However, the lighting schedule (daytime or nighttime) was not considered in previous studies.

Application of supplemental lighting when there is low light interception could improve canopy light interception, leaf chlorophyll content, and leaf photosynthetic capacity, as well as the assimilate supply to the fruit, resulting in enhanced crop yield (McAvoy and Janes, 1988; Hovi et al., 2004; Pettersen et al., 2010; Trouwborst et al., 2010). Our study clearly showed that LED inter-lighting significantly improved light distribution in the middle and lower canopy (**Figure 1**), leading to a significantly higher photosynthetic rate compared to control leaves that were grown under only solar light (**Figure 2**). This was also supported by the data that LED inter-lighting enhanced the diurnal photosynthetic rate due to better vertical light distribution (**Figure 3**). Most importantly, nighttime LED inter-lighting significantly increased tomato yield during both winter and summer, although daytime LED inter-lighting increased tomato yield only in winter (**Figure 5**). Supplemental light is expected to increase leaf photosynthesis (McAvoy and Janes, 1988; Dorias et al., 1991; Pettersen et al., 2010) and thus yield; however, in our study daytime LED inter-lighting in summer had a negative effect on leaf photosynthetic capacity which offset the net photosynthetic rate at growth condition (**Table 1**) and led to no improvement in yield (**Figure 5**). Other studies has been reported that inter-lighting did not increase yield significantly (Gunnlaugsson and Adalsteinsson, 2006; Heuvelink et al., 2006; Trouwborst et al., 2010). Trouwborst et al. (2010) explained that, the reason could be partly due to significantly reduced vertical and horizontal light interception caused by extreme leaf curling, the LED-light spectrum used, or the relatively low irradiances from above. In addition, some tomato cultivars grow equally well whether they are lit by top-lighting only or partially by inter-lighting (Gunnlaugsson and Adalsteinsson, 2006). It has also been reported that temperatures above 33°C must be avoided with most tomato cultivars when aiming to produce fruit (Adams et al., 2001; Domínguez et al., 2005). Usually supplemental lighting should be turned off when solar irradiation exceeds a desired set point, which is about 1300 μmol m^{-2} s^{-1} in

TABLE 2 | The effect of LED inter-lighting on growth of single-truss tomato plants.

		Growth parameters			
		Stem diameter (mm)	**Internode length (cm)**	**LAI**	**LMA (g m^{-2})**
Summer	Control	10.2 ± 0.6^{b}	9.6 ± 0.7^{a}	4.7 ± 0.4^{a}	38.3 ± 5.3^{b}
	Day LED	11.1 ± 0.9^{a}	8.2 ± 0.7^{b}	5.1 ± 0.5^{a}	46.0 ± 1.6^{a}
	Night LED	11.8 ± 0.8^{a}	8.7 ± 0.9^{b}	5.0 ± 0.6^{a}	46.9 ± 5.3^{a}
Winter	Control	11.1 ± 0.7^{b}	10.6 ± 1.0^{a}	3.6 ± 0.7^{a}	43.1 ± 6.3^{b}
	Day LED	12.2 ± 1.1^{a}	9.1 ± 0.9^{b}	3.7 ± 0.9^{a}	47.1 ± 6.2^{a}
	Night LED	11.8 ± 0.8^{a}	9.3 ± 0.9^{b}	3.7 ± 1.0^{a}	51.5 ± 3.2^{a}

Stem diameter and internode length were measured just under the fruit truss. Both leaf area index (LAI) and leaf mass per unit area (LMA) were measured from individual leaves, and the cumulative value for a plant was used for the analysis. Data represent means ± SE (n = 15 for stem diameter and internode length, n = 5 for LAI and LMA). Different letters indicate statistically significant differences by Tukey's HSD (P < 0.05).

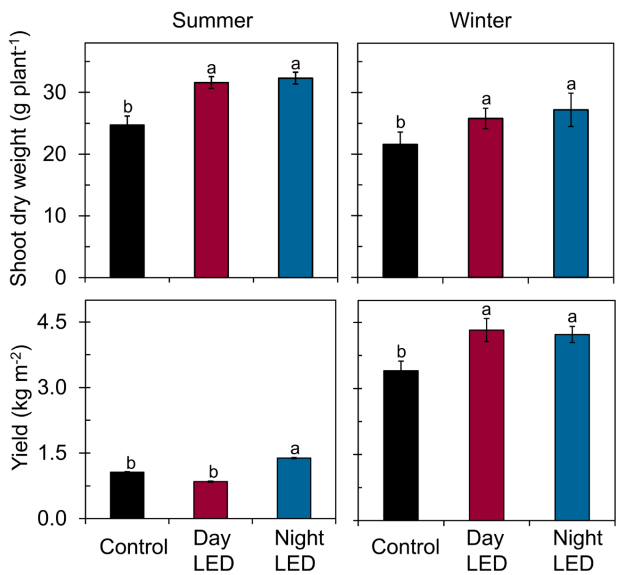

FIGURE 5 | Shoot dry weight and fruit yield of single-truss tomato plants. Measurements were made in plants grown under daytime or nighttime LED inter-lighting or control. Data represent means ± SE (n = 5 and 15 for dry weight and fruit yield, respectively). Different letters indicate statistically significant differences (Tukey's HSD at $P < 0.05$).

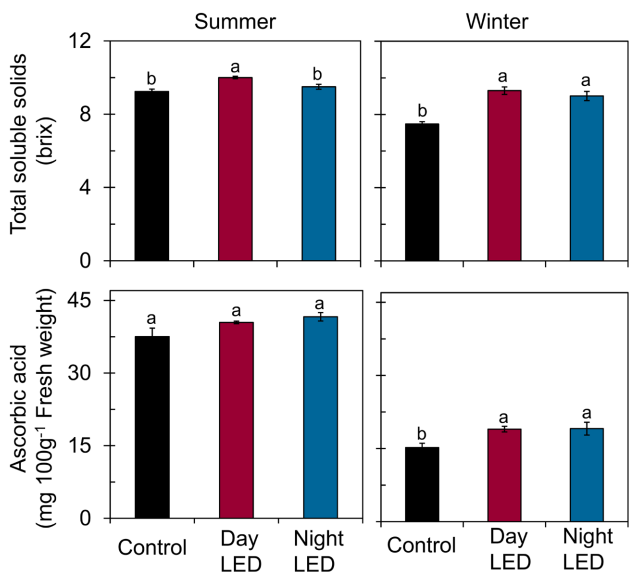

FIGURE 6 | Total soluble solids and ascorbic acid content of tomato fruits. Measurements were made from single-truss tomato fruits grown under daytime or nighttime LED inter-lighting or control. Data represent means ± SE (n = 10). Different letters indicate statistically significant differences (Tukey's HSD at $P < 0.05$).

a greenhouse (Dorias, 2003; Gunnlaugsson and Adalsteinsson, 2006). In our study, the average light irradiation during the middle of the day was above 1300 μmol m^{-2} s^{-1} and the temperature exceeded 33°C during the middle of the day in the summer (Supplementary Table S1). In addition, daytime LED inter-lighting increased light distribution and temperature significantly around mid-canopy (**Figure 1**; Supplemental Table S1). Therefore, it is possible that the high temperature and high solar irradiation during mid-day in summer exceeded the optimal range for tomato production and thus reduced yield.

Low light environment decreases the total soluble solids content of tomato fruit (Mc Collum, 1944; Yanagi et al., 1995). Previous studies showed that introducing inter-lighting has positive effects on fruit quality (Hovi et al., 2004), and tomato fruits exposed to high light had 35% more ascorbic acid than fruits exposed to low light (Mc Collum, 1944). In our study, daytime LED inter-lighting enhanced the total soluble solids content of single-truss tomato fruit both in winter and summer, whereas nighttime inter-lighting produced significantly higher total soluble solids than control in winter. Moreover, tomato fruit ascorbic acid content increased significantly for both daytime and nighttime inter-lighting in winter but not in summer (**Figure 6**). Among environmental factors light intensity and temperature are the most important in determining the final ascorbic acid content (Lee and Kader, 2000). In tomato, based on the promoter analysis of the genes studied by Ioannidi et al. (2009), light plays an important role in the expression of ascorbate-related genes and its gene expression was light induced with high expression during fruit development and ripening. However, summer ascorbic acid content would

have been probably due to high ascorbic acid degradation in fruit at elevated temperatures with increased light exposure (Torres et al., 2006; Gautier et al., 2008).

Energy is second only to labor as the highest expense in greenhouse production (Frantz et al., 2010), and supplemental lighting may not be economically feasible (Heuvelink et al., 2006). Therefore, greenhouse crop production systems need energy-efficient lighting strategies. As a result of the increasing cost of electricity, lighting plants at night to take advantage of off-peak discounted electricity tariffs could be an alternative strategy to increase yield and decrease the cost of production. The interruption of the daily rhythm of the light-to-dark cycle might change or reset circadian rhythms in plants influencing photosynthesis (Dodd et al., 2005), but study of the canopy photosynthesis were not able to detect any disadvantage with light interrupting the night (Markvart et al., 2009). Moreover, tomatoes are day-neutral plants and photoperiod-insensitive perennials (Lifschitz and Eshed, 2006). In our study we found that nighttime LED inter-lighting increased yield and decreased energy costs in winter and summer (**Figure 5**; Supplementary Table S2). Nighttime LED inter-lighting had also higher light use efficiency. Previous study reported light use efficiency of tomato cultivation between 2.8 and 4.0 g MJ^{-1} (Heuvelink and Dorais, 2005). In our result, nighttime LED lighting had up to 8.6 g MJ^{-1} in winter. By taking advantage of lower off-peak electricity rates, LED inter-lighting at night could become a viable approach to increase yield and decrease cost of electricity. In our study, only winter nighttime LED lighting could be economically viable (Supplementary Figure S3). This suggests that whether or not to invest on supplemental LED lighting critically depends on reliable yield expectations and cost of LED for a specific condition. Fortunately, historical and projected evolution of LED is rapid and cost is decreasing; each decade, LED prices have fallen by a factor of 10 while performance has grown by a factor of 20 (Morrow, 2008).

CONCLUSION

Daytime LED inter-lighting to enhance light distribution of the lower canopy leaves did not lead to higher photosynthetic capacity and yield in summer. However, photosynthesis, growth, and yield of single-truss tomatoes were improved when LED inter-lighting was provided during the daytime in winter. Nighttime LED inter-lighting had a positive effect on photosynthesis, growth, and yield in both seasons. Our results suggest that nighttime LED inter-lighting can be used cost efficiently to increase yields by taking advantage of off-peak electricity pricing, both in summer and winter. This is the first report that provides an evidence on LED inter-lighting at nighttime to take advantage of off-peak electricity discount rate.

AUTHOR CONTRIBUTIONS

FT, NL, and WY conceived and designed the experiments. FT performed the experiments. FT analyzed the data. FT, NL, and WY prepared the manuscript, and FT, NL, KS, TM, MT, TK, and WY contributed extensively to its finalization.

ACKNOWLEDGMENTS

We would like to thank Mr. Takakazu Iijima for his help during plant cultivation and Ms. Geng Zhang and Prof. Masao Kikuchi for their comments on the manuscript. We would like to thank Philips Lighting for providing LED modules.

SUPPLEMENTARY MATERIAL

The Supplementary Material for this article can be found online at: http://journal.frontiersin.org/article/10.3389/fpls.2016.00448

REFERENCES

Ackerly, D. D., and Bazzaz, F. A. (1995). Leaf dynamics, self-shading and carbon gain in seedlings of a tropical pioneer tree. *Oecologia* 101, 289–298. doi: 10.1007/BF00328814

Acock, B., Charles-Edwards, D. A., Fitter, D. J., Hand, D. W., Ludwig, L. J., Warren Wilson, J., et al. (1978). The contribution of leaves from different levels within a tomato crop to canopy net photosynthesis: an experimental examination of two canopy models. *J. Exp. Bot.* 111, 815–827. doi: 10.1093/jxb/29.4.815

Adams, S. R., Cockshull, K. E., and Cave, C. R. J. (2001). Effect of temperature on the growth and development of tomato fruits. *Ann. Bot.* 88, 869–877. doi: 10.1006/anbo.2001.1524

Adams, S. R., Woodward, G. C., and Valdés, V. M. (2002). The effects of leaf removal and of modifying temperature set-points with solar radiation on tomato yields. *J. Hortic. Sci. Biotechnol.* 77, 733–738. doi: 10.1080/14620316.2002.11511565

Ashok, S. (2006). Peak-load management in steel plants. *Appl. Energy* 83, 413–424. doi: 10.1016/j.apenergy.2005.05.002

Ashok, S., and Banerjee, R. (2000). Load-management applications for the industrial sector. *Appl. Energy* 66, 105–111. doi: 10.1016/S0306-2619(99)00125-7

Cockshull, K. E., Graves, C. J., and Cave, C. R. J. (1992). The influence of shading on yield of greenhouse tomatoes. *J. Hortic. Sci. Biotechnol.* 67, 11–24. doi: 10.1080/00221589.1992.11516215

Cooper, A. J. (1961). Observations on the seasonal trends in the growth of the leaves and fruit of glasshouse tomato plants, considered in relation to light duration and plant age. *J. Hortic. Sci.* 36, 55–69. doi: 10.1080/00221589.1961.11514000

Dodd, A. N., Salathia, N., Hall, A., Kevei, E., Toth, R., Nagy, F., et al. (2005). Plant circadian clocks increase photosynthesis, growth, survival, and competitive advantage. *Science* 309, 630–633. doi: 10.1126/science.1115581

Domínguez, E., Cuartero, J., and Fernandez-Munoz, R. (2005). Breeding tomato for pollen tolerance to low temperatures by gametophytic selection. *Euphytica* 142, 253–263. doi: 10.1007/s10681-005-2042-0

Dorias, M. (2003). "The use of supplemental lighting for vegetable crop production: light intensity, crop response, nutrition, crop management, cultural practices," in *Proceeding of the Canadian Greenhouse Conference*, October 9, 2003, Nutrition.

Dorias, M., Gosselin, A., and Trudel, M. J. (1991). Annual greenhouse tomato production under a sequential intercropping system using supplemental light. *Sci. Hortic.* 45, 225–234. doi: 10.1016/0304-4238(91)90067-9

Falster, D. S., and Westoby, M. (2003). Leaf size and angle vary widely across species: what consequences for light absorption? *New Phytol.* 158, 509–525. doi: 10.1046/j.1469-8137.2003.00765.x

Fisher, D. F., Giacomelli, G. A., and Janes, H. W. (1990). A system of intensive tomato production using ebb-flood benches. *Prof. Hortic.* 4, 99–106.

Frantz, J. M., Hand, B., Buckingham, L., and Ghos, S. (2010). Virtual grower: software to calculate heating costs of greenhouse production in the United States. *Horttechnology* 20, 778–785.

Frantz, J. M., Joly, R. J., and Mitchell, C. A. (2000). Intra-canopy lighting influences radiation capture, productivity, and leaf senescence in cowpea canopies. *J. Am. Soc. Hortic. Sci.* 125, 694–701.

Gautier, H., Diakou-Verdin, V., Benard, C., Reich, M., Buret, M., Bourgaud, F., et al. (2008). How does tomato quality (sugar, acid and nutritional quality) vary with ripening stage, temperature and irradiation. *J. Agric. Food Chem.* 56, 1241–1250. doi: 10.1021/jf072196t

Giacomelli, G. A., Ting, K. C., and Mears, D. R. (1994). "Design of a single truss tomato production system (STTPS)," in *Proceedings of the International Symposium on New Cultivation Systems in Greenhouse 361*, eds Acta Horticulturae (Cagliari: Acta Horticulturae), 77–84. doi: 10.17660/ActaHortic.1994.361.6

Giniger, M. S., McAvoy, R. J., Giacomelli, G. A., and Janes, H. W. (1988). Computer simulation of a single truss tomato cropping system. *Am. Soc. Agric. Eng.* 31, 1176–1179. doi: 10.13031/2013.30840

Goto, E. (2003). Effect of light quality on growth of crop plants under artificial lighting. *Environ. Control Biol.* 41, 121–132. doi: 10.2525/ecb1963.41.121

Gunnlaugsson, E., and Adalsteinsson, S. (2006). "Inter-lighting and plant density in year-round production of tomato at northern latitudes," in *Proceeding of the V International Symposium on Artificial Lighting in Horticulture 711*, eds Acta Horticulturae (Cagliari: Acta Horticulturae), 71–75. doi: 10.17660/ActaHortic.2006.711.6

Hao, X., and Papadopoulos, A. P. (1999). Effects of supplemental lighting and cover materials on growth, photosynthesis, biomass partitioning, early yield and quality of greenhouse cucumber. *Sci. Hortic.* 80, 1–18. doi: 10.1016/S0304-4238(98)00217-9

Hao, X., Zheng, J. M., Little, C., and Khosla, S. (2012). "LED inter-lighting in year-round greenhouse mini-cucumber production," in *Proceeding of the VII International Symposium on Light in Horticultural Systems 956*, eds Acta Horticulturae (Cagliari: Acta Horticulturae), 335–340. doi: 10.17660/ActaHortic.2012.956.38

Heuvelink, E., Bakker, M. J., Hogendonk, L., Janse, J., Kaarsemaker, R., and Maaswinkel, R. (2006). "Horticultural lighting in the Netherlands: new developments," in *Proceedings of the V International Symposium on Artificial Lighting in Horticulture 711*, eds Acta Horticulturae (Cagliari: Acta Horticulturae), 25–33. doi: 10.17660/ActaHortic.2006.711.1

Heuvelink, E., and Dorais, M. (2005). "Crop growth and yield," in *Tomatoes,* ed. E. Heuvelink (Oxon: CAB international).

Hovi, T., Nakkila, J., and Tahvonen, R. (2004). Intra-canopy lighting improves production of year-round cucumber. *Sci. Hortic.* 102, 283–294. doi: 10.1016/j.scienta.2004.04.003

Hovi, T., and Tahvonen, R. (2008). Effect of inter-lighting on yield and external fruit quality in year-round cultivated cucumber. *Sci. Hortic.* 116, 152–161. doi: 10.1016/j.scienta.2007.11.010

Ioannidi, E., Kalamaki, M., Engineer, C., Pateraki, I., Alexandrou, D., Mellidou, I., et al. (2009). Expression profiling of ascorbic acid-related genes during tomato fruit development and ripening and in response to stress conditions. *J. Exp. Bot.* 60, 663–678.

Janes, H. W., and McAvoy, R. J. (1991). Environmental control of a single-cluster greenhouse tomato crop. *Horttechnology* 1, 110–114.

Kozai, T. (2013). Plant factory in Japan: current situation and perspectives. *Chron. Hortic.* 53, 8–11.

Kozai, T., and Niu, G. (2016). "Plant factory as a resource-efficient closed plant production system," in *Plant Factory: An Indoor Vertical Farming System for Efficient Quality Food Production*, eds T. Kozai, G. Niu, and M. Takagaki (Amsterdam: Elsevier), 69–90.

Lee, S. K., and Kader, A. A. (2000). Preharvest and postharvest factors influencing vitamin C content of horticultural crops. *Postharvest Biol. Technol.* 20, 207–220. doi: 10.1016/S0925-5214(00)00133-2

Lifschitz, E., and Eshed, Y. (2006). Universal florigenic signals triggered by FT homologues regulate growth and flowering cycles in perennial day-neutral tomato. *J. Exp. Bot.* 57, 3405–3414. doi: 10.1093/jxb/erl106

Logendra, L. S., and Janes, H. W. (1999). "Hydroponics tomato production: growing media requirements," in *Proceeding of the V International Symposium on Growing Media and Hydroponics 481*, eds Acta Horticulturae (Cagliari: Acta Horticulturae), 483–486. doi: 10.17660/ActaHortic.1999.481.56

Lu, N., Maruo, T., Johkan, M., Hohjo, M., Tsukagoshi, S., Ito, Y., et al. (2012a). Effects of supplemental lighting within the canopy at different developing stages on tomato yield and quality of single-truss tomato plants grown at high density. *Environ. Control Biol.* 50, 1–11. doi: 10.2525/ecb.50.63

Lu, N., Maruo, T., Johkan, M., Hohjo, M., Tsukagoshi, S., Ito, Y., et al. (2012b). Effects of supplemental lighting with light-emitting diodes (LEDs) on tomato yield and quality of single-truss tomato plants grown at high planting density. *Environ. Control Biol.* 50, 63–74. doi: 10.2525/ecb.50.63

Lu, N., Nukaya, T., Kamimura, T., Zhang, D., Kurimoto, I., Takagaki, M., et al. (2015). Control of vapor pressure deficit (VPD) in greenhouse enhanced tomato growth and productivity during the winter season. *Sci. Hortic.* 197, 17–23. doi: 10.1016/j.scienta.2015.11.001

Markvart, J., Rosenqvist, E., Sorensen, H., Ottosen, C. O., and Aaslyng, J. M. (2009). Canopy photosynthesis and time-of-day application of supplemental light. *HortScience* 44, 1284–1290.

Mc Collum, J. P. (1944). Some factors affecting the ascorbic acid content of tomatoes. *Am. Soc. Hortic. Sci.* 45, 382–386.

McAvoy, R. J., and Janes, H. W. (1988). Alternative production strategies for greenhouse tomato using supplemental lighting. *Sci. Hortic.* 35, 161–166. doi: 10.1016/0304-4238(88)90109-4

McAvoy, R. J., Janes, H. W., Godfriaux, B. L., Secks, M., Duchai, D., and Wittman, W. K. (1989). The effect of total available photosynthetic photon flux on single truss tomato growth and production. *J. Hortic. Sci.* 64, 331–338. doi: 10.1080/14620316.1989.11515961

Merrill, B. F., Lu, N., Yamaguchi, T., Takagaki, M., Maruo, T., Kozai, T., et al. (2016). "The next revolution of agriculture: a review of innovations in Plant factories," in *Handbook of Photosynthesis*, 3rd Edn, ed. M.Pessarakli (Boca Raton, FL: CRC Press), 952.

Middelberg, A., Zhang, J., and Xia, X. (2009). An optimal control model for load shifting – With application in the energy management of a colliery. *Appl. Energy* 86, 1266–1273. doi: 10.1016/j.apenergy.2008.09.011

Mitchell, C. A., Both, A. J., Bourget, C. M., Burr, J. F., Kubota, C., Lopez, R. G., et al. (2012). LEDs: the future of greenhouse lighting! *Chron. Hortic.* 52, 6–11.

Morrow, R. C. (2008). LED lighting in horticulture. *HortScience* 43, 1947–1950.

Okano, K., Nakano, Y., and Watanabe, S. (2001). Single-truss tomato system- a labor-saving management system for tomato production. *Jpn. Agric. Res. Q.* 35, 177–184.

Pettersen, R. I., Torre, S., and Gislerod, H. R. (2010). Effects of intera-canopy lighting on photosynthesis characteristics in cucumber. *Sci. Hortic.* 125, 77–81. doi: 10.1016/j.scienta.2010.02.006

Sarlikioti, V., De Visser, P. H. B., and Marcelis, L. F. M. (2011). Exploring the spatial distribution of light absorption and photosynthesis of canopies by means of a functional–structural plant model. *Ann. Bot.* 107, 875–883. doi: 10.1093/aob/mcr006

Torres, C. A., Andrews, P. K., and Davies, N. M. (2006). Physiological and biological response of fruit exocarp of tomato (*Lycopersicon esculentum* Mill.) mutants to natural photo-oxidative conditions. *J. Exp. Bot.* 57, 1933–1947. doi: 10.1093/jxb/erj136

Trouwborst, G., Oosterkamp, J., Hogewoning, S. W., Harbinson, J., and Ieperen, W. V. (2010). The response of light interception, photosynthesis and fruit yield of cucumber to LED-lighting within the canopy. *Physiol. Plant.* 138, 289–300. doi: 10.1111/j.1399-3054.2009.01333.x

Wada, T., Ikeda, H., Matsushita, K., Kambara, A., Hirai, H., and Abe, K. (2006). Effect of shading in summer on yield and quality of tomatoes grown on a single-truss system. *J. Jpn. Soc. Hortic. Sci.* 75, 51–58. doi: 10.2503/jjshs.75.51

Xu, H. L., Gauthier, L., Desjardins, Y., and Gosselin, A. (1997). Photosynthesis in leaves, fruits, stem and petioles of greenhouse-grown tomato plants. *Photosynthetica* 33, 113–112. doi: 10.1023/A:1022135507700

Yamori, W. (2013). Improving photosynthesis to increase food and fuel production by biotechnological strategies in crops. *J. Plant Biochem. Physiol.* 1:113. doi: 10.4172/2329-9029.1000113

Yamori, W., Kondo, E., Sugiura, D., Terashima, I., Suzuki, Y., and Makino, A. (2016). Enhanced leaf photosynthesis as a target to increase grain yield: insights from transgenic rice lines with variable Rieske FeS protein content in the cytochrome b6/f complex. *Plant Cell Environ.* 39, 80–87. doi: 10.1111/pce.12594

Yamori, W., Noguchi, K., Hikosaka, K., and Terashima, I. (2009). Cold-tolerant crop species have greater temperature homeostasis of leaf respiration and photosynthesis than cold-sensitive species. *Plant Cell Physiol.* 50, 203–215. doi: 10.1093/pcp/pcn189

Yamori, W., Noguchi, K., Hikosaka, K., and Terashima, I. (2010). Phenotypic plasticity in photosynthetic temperature acclimation among crop species with different cold tolerances. *Plant Physiol.* 152, 388–399. doi: 10.1104/pp.109.145862

Yamori, W., Noguchi, K., and Terashima, I. (2005). Temperature acclimation of photosynthesis in spinach leaves: analyses of photosynthetic components and temperature dependencies of photosynthetic partial reactions. *Plant Cell Environ.* 28, 536–547. doi: 10.1111/j.1365-3040.2004.01299.x

Yamori, W., and Shikanai, T. (2016). Physiological functions of cyclic electron transport around photosystem I in sustaining photosynthesis and plant growth. *Annu. Rev. Plant Biol.* 67. doi: 10.1146/annurev-arplant-043015-112002

Yamori, W., Zhang, G., Takagaki, M., and Maruo, T. (2014). Feasibility study of rice growth in plant factories. *Rice Res.* 2:119. doi: 10.4172/jrr.1000119

Yanagi, T., Ueda, E., Sato, H., Hirai, H., and Oda, Y. (1995). Effects of shading and fruit set order on fruit quality in single-truss tomato (in Japanese with English summary). *J. Jpn. Soc. Hortic. Sci.* 64, 291–297. doi: 10.2503/jjshs.64.291

Yoshida, Y., Irie, N., Vinh, T. D., Ooyama, M., Tanaka, Y., Yasuba, K., et al. (2014). Incidence of blossom-end rot in relation to the water-soluble calcium concentration in tomato fruits as affected by calcium nutrition and cropping season. *J. Jpn. Soc. Hortic. Sci.* 83, 282–289. doi: 10.2503/jjshs1.CH-107

Zhang, G., Shen, S., Takagaki, M., Kozai, T., and Yamori, W. (2015). Supplemental upward lighting from underneath to obtain higher marketable lettuce (*Lactuca sativa*) leaf fresh weight by retarding senescence of outer leaves. *Front. Plant Sci.* 6:1110. doi: 10.3389/fpls.2015.01110

Conflict of Interest Statement: The authors declare that the research was conducted in the absence of any commercial or financial relationships that could be construed as a potential conflict of interest.

frontiers in Plant Science

ORIGINAL RESEARCH
published: 10 March 2016
doi: 10.3389/fpls.2016.00250

Leaf Morphology, Photosynthetic Performance, Chlorophyll Fluorescence, Stomatal Development of Lettuce (*Lactuca sativa* L.) Exposed to Different Ratios of Red Light to Blue Light

Jun Wang[1,2], Wei Lu[1,2], Yuxin Tong[1,2] and Qichang Yang[1,2]**

[1] *Institute of Environment and Sustainable Development in Agriculture, Chinese Academy of Agricultural Sciences, Beijing, China,* [2] *Key Laboratory of Energy Conservation and Waste Management of Agricultural Structures, Ministry of Agriculture, Beijing, China*

OPEN ACCESS

Edited by:
Alejandro Isabel Luna-Maldonado, Universidad Autónoma de Nuevo León, Mexico

Reviewed by:
Xuming Huang, South China Agricultural University, China
Fulai Liu, University of Copenhagen, Denmark

***Correspondence:**
Yuxin Tong
tongyuxin@caas.cn;
Qichang Yang
yangqichang@caas.cn

Specialty section:
This article was submitted to Crop Science and Horticulture, a section of the journal Frontiers in Plant Science

Received: *09 November 2015*
Accepted: *15 February 2016*
Published: *10 March 2016*

Citation:
Wang J, Lu W, Tong Y and Yang Q (2016) Leaf Morphology, Photosynthetic Performance, Chlorophyll Fluorescence, Stomatal Development of Lettuce (Lactuca sativa L.) Exposed to Different Ratios of Red Light to Blue Light. Front. Plant Sci. 7:250. doi: 10.3389/fpls.2016.00250

Red and blue light are both vital factors for plant growth and development. We examined how different ratios of red light to blue light (R/B) provided by light-emitting diodes affected photosynthetic performance by investigating parameters related to photosynthesis, including leaf morphology, photosynthetic rate, chlorophyll fluorescence, stomatal development, light response curve, and nitrogen content. In this study, lettuce plants (*Lactuca sativa* L.) were exposed to 200 $\mu mol \cdot m^{-2} \cdot s^{-1}$ irradiance for a 16 $h \cdot d^{-1}$ photoperiod under the following six treatments: monochromatic red light (R), monochromatic blue light (B) and the mixture of R and B with different R/B ratios of 12, 8, 4, and 1. Leaf photosynthetic capacity (A_{max}) and photosynthetic rate (P_n) increased with decreasing R/B ratio until 1, associated with increased stomatal conductance, along with significant increase in stomatal density and slight decrease in stomatal size. P_n and A_{max} under B treatment had 7.6 and 11.8% reduction in comparison with those under R/B = 1 treatment, respectively. The effective quantum yield of PSII and the efficiency of excitation captured by open PSII center were also significantly lower under B treatment than those under the other treatments. However, shoot dry weight increased with increasing R/B ratio with the greatest value under R/B = 12 treatment. The increase of shoot dry weight was mainly caused by increasing leaf area and leaf number, but no significant difference was observed between R and R/B = 12 treatments. Based on the above results, we conclude that quantitative B could promote photosynthetic performance or growth by stimulating morphological and physiological responses, yet there was no positive correlation between P_n and shoot dry weight accumulation.

Keywords: R/B ratio, photosynthetic performance, chlorophyll fluorescence, stomata, dry weight, *Lactuca sativa* L.

INTRODUCTION

As a signal and energy source, light is one of the most important environment factors for plant growth and development. Compared with light intensity and photoperiod, light quality shows much more complex effects on plant morphology and physiology. Specific spectrum stimulates different morphological and physiological responses. Red light (R) and blue light (B) absorbed by photosynthetic pigments are more effective than other wavelengths (Pfündel and Baake, 1990). It is well known that R influences stem elongation, root to shoot ratio, chlorophyll content, photosynthetic apparatus (Appelgren, 1991; Aksenova et al., 1994; Sæbø et al., 1995). B causes physiological responses via phototropins, including phototropism, hypocotyl elongation, leaf expansion, stomatal opening, leaf anatomy, enzyme synthesis, chloroplast movements, and genes expression (Christie, 2007; Inoue et al., 2008; Wang et al., 2009).

However, monochromatic R or B could not meet the requirement of plant growth. Plants under R alone displayed abnormal leaf morphology and reduced photosynthetic rate (P_n) compared with white light or R supplemented with B (Goins et al., 1998; Wang et al., 2009, 2015; Hogewoning et al., 2010b). Hogewoning et al. (2010b) reported that leaf photosynthetic machinery dysfunction appeared under R alone, only 7% B was sufficient to prevent any overt dysfunctional photosynthesis. In addition, B alone could also reduce P_n in many species, such as chrysanthemum plantlets (Kim et al., 2004), *Withania Somnifera* (L.) plantlets (Lee et al., 2007). B involves inhibition of cell expansion or division (Appelgren, 1991; Folta et al., 2003; Dougher and Bugbee, 2004), therefore a reduction in B could increase leaf area (LA; Dougher and Bugbee, 2001; Hogewoning et al., 2010a; Hernández and Kubota, 2014), which promotes light interception and dry weight accumulation.

It has been reported that P_n and shoot dry weight could be increased by mixture of R and B compared with monochromatic light (Brown et al., 1995; Goins et al., 1997; Ohashi-Kaneko et al., 2006; Hogewoning et al., 2010b; Nanya et al., 2012; Li et al., 2013). However, there are discrepancies for different plants in response to B dose in the background R. It has been reported that the optimal R/B ratio for fresh and dry weight accumulation in strawberry plantlet, rapeseed (*Brassica napus* L.) plantlets *in vitro*, and cucumber seedlings was 7/3 (Nhut et al., 2003), 1/3 (Li et al., 2013), and 9 (Hernández and Kubota, 2016), respectively.

Lettuce as a fresh salad food is an important vegetable throughout the world because of its fast growth and commercial value, and it is known to be sensitive to light quality as a model crop (Dougher and Bugbee, 2001; Lin et al., 2013). For lettuce, addition of B under R could inhibit hypocotyl extension and cotyledon elongation (Hoenecke et al., 1992), increase dry weight, LA, and leaf number (Yorio et al., 1998, 2001; Johkan et al., 2010; Wojciechowska et al., 2015). In contrast, it also been reported that greater dry weight and LA under R treatment were observed than those under mixture of R and B treatments (Ohashi-Kaneko et al., 2007; Son and Oh, 2013; Wollaeger and Runkle, 2014). Therefore, the optimal R/B ratio under a combination of red and blue light-emitting diodes (LEDs) is not yet determined. And few studies have been reported about the effects of different R/B ratios on leaf photosynthetic performance of lettuce.

The objective of the present study was to determine the effects of different R/B ratios on morphology and photosynthetic performance of lettuce by investigating photosynthetic rate, chlorophyll fluorescence, stomatal development, light response curve, and nitrogen content. The results of this study would be used to give guidance on light sources design for lettuce cultivation in a controlled environment.

MATERIALS AND METHODS

Plant Material and Experimental Setup

Lettuce (*Lactuca sativa* L.) seeds were sown in substrate containing a mixture of vermiculite and peat (3:1, V/V), and geminated under 150 $\mu mol \cdot m^{-2} \cdot s^{-1}$ irradiance provided by fluorescent lamps (TL-D 36W, Philips) in a controlled environment. After the second leaf was fully expanded, the seedlings were randomly divided into six groups and transferred to six separate hydroponic (Yamasaki lettuce nutrient solution; pH≈5.8; EC≈1.5 $mS \cdot cm^{-1}$) systems in a controlled environment. Air temperature was 24°C during photoperiod and 20°C during dark period. Photoperiod, relative humidity and CO_2 concentration were 16 $h \cdot d^{-1}$, 60%, and 400 $\mu mol \cdot mol^{-1}$, respectively. LEDs were equipped with light plates (Dongguan Bio-lighting Sciences and Technology Co. Ltd, China) and power DC supply (PKU-MS605D). Irradiance of R and B was individually controlled by adjusting electric current of power DC supply for each treatment. LEDs provided R with peak wavelength of 657 nm and B with peak wavelength of 450 nm. All plants were subjected to 200 $\mu mol \cdot m^{-2} \cdot s^{-1}$ irradiance measured by spectrometer (AvaSpec-2048-USB2, the Netherland) at the top of the canopy. Six light quality treatments based on different R/B ratios, were created and labeled as R, R/B = 12, R/B = 8, R/B = 4, R/B = 1, and B. Lettuce plants were grown for 30 days after transplanting before harvest. All the treatments were repeated twice.

Chlorophyll Concentration

Samples were excised from the leaves of 10 plants at a similar position for each treatment. Leaves were weighed out in 0.1–0.2 g (fresh weight, FW). The extractions were performed using 10 ml (V) of 80% acetone until the leaf turned white. The optical density was measured with UV-1800 spectrophotometer (Shimadzu, Japan) at 663nm (OD663) and at 645 nm (OD645) for chlorophyll a (Chl a) and chlorophyll b (Chl b). The chlorophyll concentrations (Chl) were determined using (Lichtenthaler and

Abbreviations: A_{max}, photosynthetic capacity; Ab, abaxial surfaces of lettuce; Ad, adaxial surfaces of lettuce; B, blue light; C_i, intercellular carbon dioxide concentration; Chl, chlorophyll content; Chl/LA, chlorophyll content per leaf area; F_s, the light-adapted steady state fluorescence; FW, fresh weight; F_v'/F_m', the efficiency of excitation capture by open PSII center; g_m, apparent mesophyll conductance; g_s, stomatal conductance; L_s, stomatal limitation value; LA, leaf area; LED, light-emitting diode; LMA, leaf mass area; N, nitrogen content per unit dry weight; N/LA, nitrogen content per unit LA; NUE, A_{max} per unit N/LA; P_n, photosynthetic rate; R, red light; R/B ratio, the ratio of R to B; VPD, vapor pressure difference; α, photochemical efficiency at low light; ΦPSII, the effective quantum yield of PSII.

Wellburn, 1983):

$$Chl\,a(mg \cdot g^{-1}) = \frac{(12.72 \times OD_{663} - 2.59 \times OD_{645}) \cdot V}{1000 \times W} \quad (1)$$

$$Chl\,b(mg \cdot g^{-1}) = \frac{(22.88 \times OD_{645} - 4.67 \times OD_{663}) \cdot V}{1000 \times W} \quad (2)$$

Where V is the total volume of acetone extract (ml) and W is FW (g) of sample.

Photosynthetic Characteristics and Chlorophyll Fluorescence

Photosynthetic light response curves and photosynthetic characteristics were measured on fully expanded second leaves of four plants from each treatment using the method of Li et al. (2014) with slight modification. The light response curve was measured by using 10 light intensities in the range from 0 to 1200 $\mu mol \cdot m^{-2} \cdot s^{-1}$. The starting light intensity was 200 $\mu mol \cdot m^{-2} \cdot s^{-1}$, followed by 100, 50, 25, 0, 400, 600, 800, 1000, and 1200 $\mu mol \cdot m^{-2} \cdot s^{-1}$. Measurements of photosynthetic light response curves and photosynthetic characteristics were all performed on a single leaf exposed to light source (10% B, 90% R) provided by a portable photosynthesis system (Li-6400, Li-Cor Inc., Lincoln, NE, USA). Leaf temperature and CO_2 concentration in the leaf chamber were 24°C and 400 $\mu mol \cdot mol^{-1}$, respectively. The VPD in the leaf chamber was maintained at 1.1 kPa. Data were taken when P_n reached steady state at each light intensity level. Samples from each treatment were measured in the order of R, R/B = 12, R/B = 8, R/B = 4, R/B = 1, and B; hereafter the same measurements were repeated three times. When light response curves were measured, data obtained at light intensity of 200 $\mu mol \cdot m^{-2} \cdot s^{-1}$ were considered as photosynthetic characteristics.

Chlorophyll fluorescence was also measured on the fully expanded second leaves of four plants from each treatment by a portable photosynthesis system (Li-6400, Li-Cor Inc., Lincoln, NE, USA). Saturating flashes (8000 $\mu mol \cdot m^{-2} \cdot s^{-1}$) were applied to determine the maximum fluorescence yield during actinic light (F_m'). The effective quantum yield of PSII (ΦPSII) was calculated: $\Phi PSII = (F_m' - F_s)/F_m'$ (Genty et al., 1989). F_s is the light-adapted steady state fluorescence.

Stomata Characteristic and Leaf Gas Exchange

Samples were excised from the fully expanded second leaves of four plants at a similar position for each treatment. To observe the stomata, transparent nail polish was smeared on the surface of the leaves. The slides made by the leaf epidermal fingerprint with the transplant nail polish method (Zeng et al., 2008) were observed by optical microscope (Olympus DP71, Olympus Inc., Japan). The length, width and density of stomata were measured with Image-Pro Express software (Olympus Inc., Japan).

Stomatal limitation value (L_s) was calculated as $1\text{-}C_i/C_a$ (Farquhar and Sharkey, 1982), C_a was CO_2 concentration in leaf chamber. Apparent mesophyll conductance (g_m) was calculated as P_n/C_i (Fischer et al., 1998). C_i was intercellular CO_2 concentration.

LMA, Sucrose, Starch, Carbon, and Nitrogen Content

The leaf mass area (LMA) was calculated using (Hernández and Kubota, 2016):

$$LMA\ (g \cdot cm^{-2}) = \frac{leaf\ dry\ weight}{leaf\ area} \quad (3)$$

Samples were excised from the leaves of four plants for each treatment before the end of dark period. Total sugar was extracted using the method of Li et al. (2013). The sucrose concentration was determined using the resorcinol method and measured at 480 nm. Extraction of starch was obtained by the method of Takahashi et al. (1995). Starch content was calculated by converting glucose to starch equivalents using a factor of 0.9 (Li et al., 2010). The glucose concentration was determined by using the sulfuric acid anthrone method and measured at 620 nm. Leaf nitrogen content was determined with element analyzer (Isoprime GC5, Italy).

Statistical Analysis

The fitting parameters of light response curve, including photosynthetic capacity (A_{max}), dark respiration rate (R_d) and photochemical efficiency at low light (α), were fitted with a non-rectangular hyperbola (Thornley, 1976) using the non-linear fitting procedure ARSIN in SAS (SAS Institute Inc. 9.1, Cary, NC, USA).

All measurements were based on four replicate plants. Statistical analysis was subjected to one-way analysis of using variance ANOVA, and significant differences between the means were tested using Duncan's multiple range test at 95% confidence.

RESULTS

Leaf Photosynthesis and L_s

The same trend was observed on results of the repeated experiments. Thus, one dataset of the repeated experiments was shown in this study. P_n differed significantly under different R/B ratios treatments (**Figure 1A**). Decreased R/B ratio led to increasing P_n, except B. Similar trends were observed in C_i, g_m and stomatal conductance (g_s) in the change of R/B ratio (**Figures 1B,D** and **4**). P_n under B treatment did not follow the trend of P_n increasing with decreasing R/B ratio, which was 7.6% lower compared to that under R/B = 1 treatment. P_n under B and R/B = 1 treatments was 53.2 and 74.0% higher than that under R treatment, respectively. However, L_s had the opposite trend with decreasing R/B ratio (**Figure 1C**). P_n correlated positively with g_m and g_s and inversely with L_s (**Figure 2**).

Growth and Morphology

Growth and morphology in lettuce showed significant difference under different R/B ratios treatments (**Table 1**). Shoot dry weight gradually increased with increasing R/B ratio with the greatest

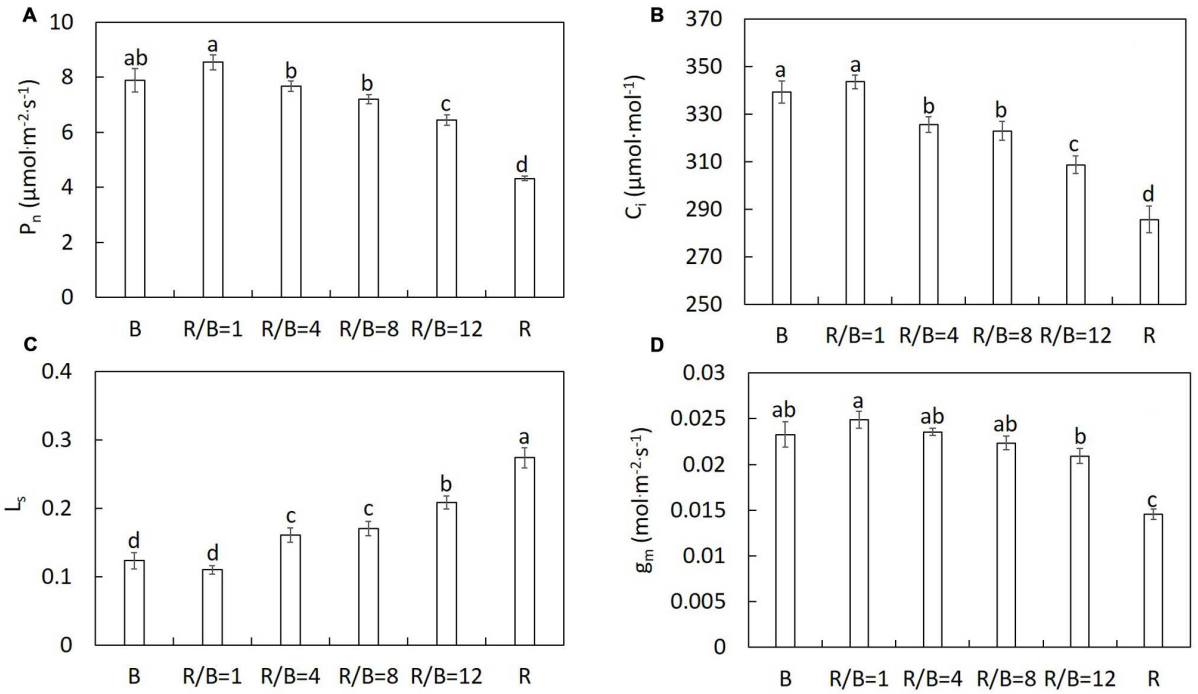

FIGURE 1 | The effect of different R/B ratios on P_n (A), C_i (B), L_s (C), and g_m (D) at the growth irradiance of lettuce. Values were the means of four replicates with standard errors shown by vertical bars. Different letters indicate significant differences using the Duncan's Multiple Range Test ($p < 0.05$; $n = 4$).

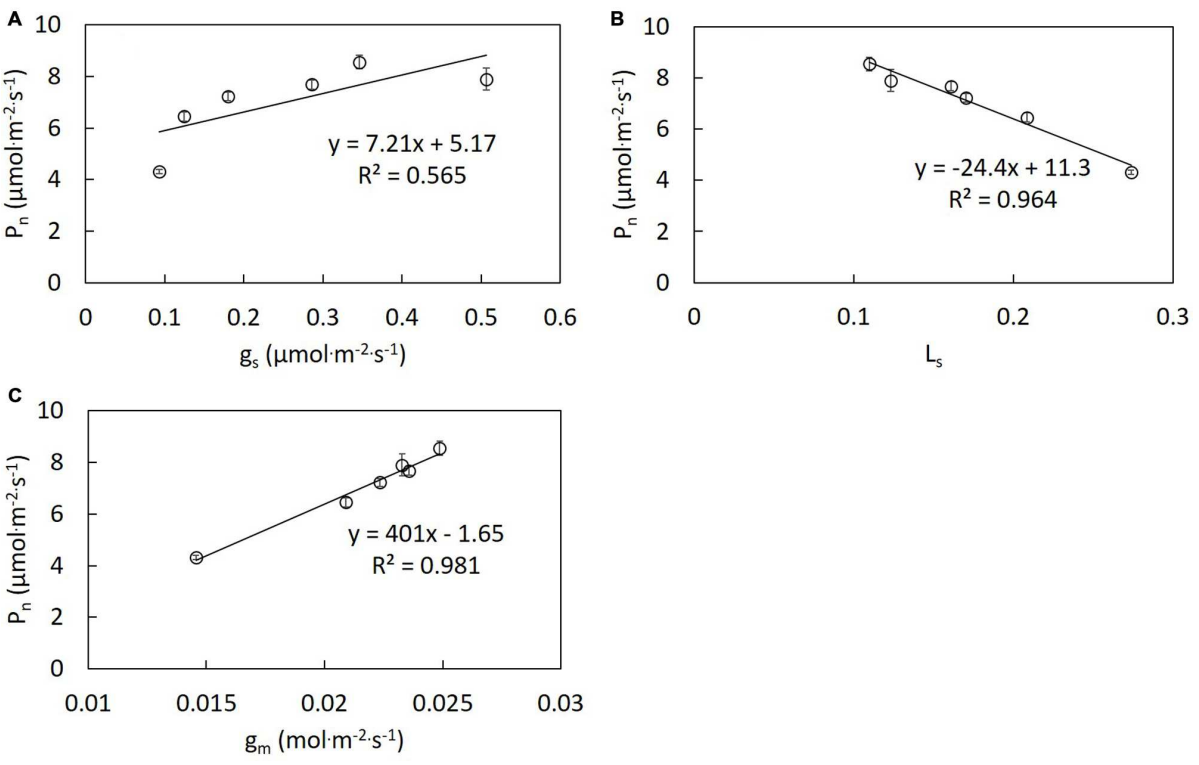

FIGURE 2 | Correlation analysis between P_n and g_s (A), L_s (B), and g_m (C) of lettuce grown under different R/B ratios treatments. Values were the means of four replicates with standard errors shown by vertical bars. Different letters indicate significant differences using the Duncan's Multiple Range Test ($p < 0.05$; $n = 4$).

TABLE 1 | Effects of different R/B ratios on shoot dry weight, leaf number, Chl, Chl a/b, LA, Chl per leaf area (Chl/LA) and LMA.

R/B ratio	B	R/B = 1	R/B = 4	R/B = 8	R/B = 12	R
Shoot dry weight (g)	0.95^{c}	1.04^{c}	1.37^{b}	1.67^{a}	1.83^{a}	1.80^{a}
Leaf number	20^{c}	22^{c}	25^{b}	30^{a}	28^{ab}	26^{b}
Chl (mg·g^{-1} FW)	0.85^{a}	0.77^{ab}	0.81^{a}	0.74^{ab}	0.69^{bc}	0.60^{c}
Chl a/b	3.20^{ab}	3.15^{ab}	3.28^{a}	3.18^{ab}	3.00^{bc}	2.83^{c}
LA (cm^2)	545^{c}	597^{c}	771^{b}	898^{a}	956^{a}	950^{a}
Chl/LA (g·m^{-2})	0.27^{bc}	0.30^{ab}	0.32^{a}	0.32^{a}	0.30^{ab}	0.24^{c}
LMA (g·m^{-2})	17.3^{a}	17.4^{a}	$17.\ 8^{a}$	18.7^{a}	18.8^{a}	19.0^{a}

Different letters indicate significant differences using the Duncan's Multiple Range Test ($p < 0.05$; $n = 4$).

value under R/B = 12 treatment, and no significant difference was observed between R/B = 12 and R treatments. Shoot dry weight under B treatment was 48.1 and 47.2% lower in comparison with those under R/B = 12 and R treatments, respectively. Similar trends were observed for plants in leaf number, LA and LMA. For LMA, there was no significant difference among plants cultured under the six treatments. Chl increased with decreasing R/B ratio. Addition of B increased Chl a/b of lettuce leaves compared to that of R-grown leaves with the lowest value. Chlorophyll content per leaf area (Chl/LA) under mixture of R and B treatments was higher than those grown under monochromatic R or B treatment.

Photosynthetic Light Response Curves and Fluorescence Characteristics

Different R/B ratios significantly affected P_n in the change of irradiance. The differences in P_n between R and other treatments became increasingly greater with the increase of irradiance. The enhanced effect of decreasing R/B ratio on P_n was similar with that caused by increasing irradiance (**Figure 3**). For the fitting parameters of photosynthetic light response curve, a reduction in R/B ratio led to increasing A_{max}, except for B treatment (**Table 2**). A_{max} under B and R/B = 1 treatments was 82.7 and 97.8% higher than that under R treatment, respectively. R_d was the highest under R/B = 8 treatment and the lowest under B treatment. Compared with monochromatic light treatments, α was higher under mixture of R and B treatments, with the maximum value under R/B = 12 treatment.

Plants grown under B treatment had a lower efficiency of excitation capture by open PSII center (F_v'/F_m') compared to the other treatments. Similar result was observed in ΦPSII (**Table 3**).

Stomatal Characteristics

g_s of lettuce leaves had been significantly altered after being exposed to different R/B ratios in the change of irradiance ranging from 0 to 200 μmol·m^{-2}·s^{-1}. g_s increased with increasing irradiance under B, R/B = 1, R/B = 4, R/B = 8, and R/B = 12 treatments, except for R treatment. g_s under R treatment was almost unresponsive to increasing irradiance. The highest g_s was observed under B treatments, followed by R/B = 1, R/B = 4, R/B = 8, and R/B = 12, with the lowest value under R treatment at the same measured irradiance (**Figure 4**). The effect of decreasing R/B ratio on g_s was similar with that caused by increasing irradiance.

As shown in **Table 4**, stomatal development differed greatly under different R/B ratios treatments at the growth irradiance. Decreased R/B ratio gradually caused higher stomatal density on the abaxial and adaxial surfaces. Leaves under B treatment did not follow the trend of stomatal density increasing with

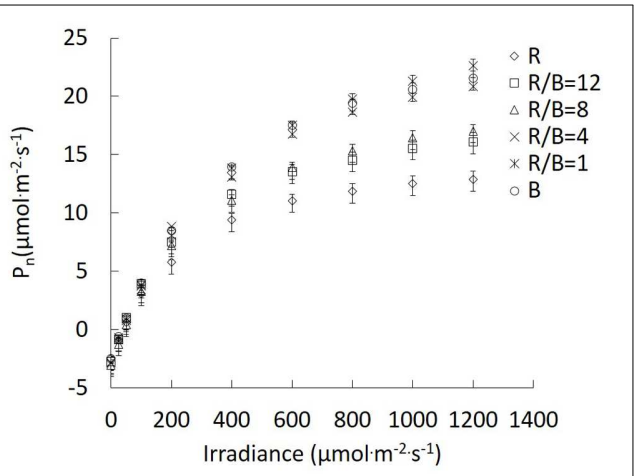

FIGURE 3 | Response of P_n to irradiance for lettuce leaves grown under different R/B ratios treatments. Values were the means of four replicates with standard errors shown by vertical bars ($n = 4$).

TABLE 2 | Effects of different R/B ratios on the fitting parameters of photosynthetic light response curve, including A_{max}, R_d and α.

R/B ratio	B	R/B = 1	R/B = 4	R/B = 8	R/B = 12	R
A_{max} (μmol CO_2·m^{-2}·s^{-1})	27.6^{b}	31.3^{a}	29.7^{ab}	23.8^{c}	20.7^{d}	18.0^{e}
R_d (μmol CO_2·m^{-2}·s^{-1})	2.3^{c}	2.7^{b}	2.8^{b}	3.3^{a}	2.7^{b}	2.6^{bc}
α (μmol photons·m^{-2}·s^{-1})	0.082^{b}	0.086^{ab}	0.114^{ab}	0.108^{ab}	0.117^{a}	0.084^{b}

Different letters indicate significant difference using the Duncan's Multiple Range Test ($p < 0.05$; $n = 4$).

TABLE 3 | Effects of different R/B ratios on the efficiency of excitation capture by open PSII center (F_v'/F_m'), and ΦPSII.

R/B ratio	B	R/B = 1	R/B = 4	R/B = 8	R/B = 12	R
F_v'/F_m'	0.69^b	0.76^a	0.76^a	0.76^a	0.77^a	0.77^a
ΦPSII	0.62^b	0.67^a	0.67^a	0.67^a	0.68^a	0.68^a

Different letters indicate significant difference using the Duncan's Multiple Range Test ($p < 0.05$; $n = 4$).

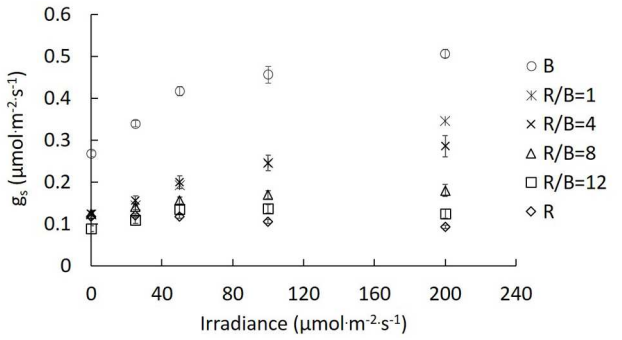

FIGURE 4 | Response of g_s to irradiance for lettuce leaves grown under different R/B ratios. Values were the means of four replicates with standard errors shown by vertical bars ($n = 4$).

decreasing R/B ratio, which were 26 and 42% lower than R/B = 1 treatment on the abaxial and adaxial surfaces, respectively. Stomatal length on the abaxial and adaxial surfaces increased with increasing R/B ratio under mixture of R and B treatments but with no significant differences, which were significantly higher than those under monochromatic R or B treatment. There were no significant differences among stomatal widths on the abaxial and adaxial surfaces of plants cultured under the six treatments. Stomatal pore length and pore width on the abaxial surface under R and B treatments were lower than those under the other treatments. Stomatal pore length and pore width on the adaxial surface increased with increasing R/B ratio under mixture of R and B treatments, but were slightly lower under R treatment. These results indicated that an addition of B under background R could increase stomatal density and stomatal aperture compared with R.

NUE, Nitrogen and Carbohydrate Content

The ratio of A_{max} to nitrogen content per LA (NUE) increased with decreasing R/B ratio with the highest value under R/B = 1 treatment, but was significantly lower under B treatment (**Figure 5**). NUE under B and R/B = 1 treatments was 57 and 76% higher than that under R treatment, respectively. The accumulation of sucrose under R and R/B = 12 treatments were higher than those under R/B = 8, R/B = 4, R/B = 1, and B treatments. The accumulation of starch was the highest under R treatment and the lowest under B treatment (**Table 5**).

DISCUSSION

Additional B had a Greater Impact on P_n and A_{max} by Combination of R

Combination of R and B has been proved to be effective in driving photosynthesis. As shown in **Figure 1A** and **Table 2**, increasing P_n and A_{max} with decreasing R/B ratio until 1 has been observed in the present study. This result indicated that photosynthetic performance of lettuce plant could be efficiently improved by increasing B fraction. The same trends have been reported in rice (Matsuda et al., 2004), and cucumber seedling (Hogewoning et al., 2010b; Hernández and Kubota, 2016). For example, Matsuda et al. (2004) reported that P_n in rice plants grown under R/B = 4 treatment increased 88 and 53% than those grown under R treatment at the measured irradiance of 1600 and 200 μmol·m^{-2}·s^{-1}, respectively. Hogewoning et al. (2010b) tested the effect of different B fractions on leaf photosynthesis of cucumber seedlings. They found that P_n and A_{max} increased with increasing B fraction up to 50% (irradiance: 100 μmol·m^{-2}·s^{-1}; photoperiod: 16 h·d^{-1}). This result was supported by analyzing

TABLE 4 | Effects of different R/B ratios on leaf stomata development. Ab and Ad represented abaxial and adaxial surfaces of lettuce leaves.

R/B ratio	Stomatal length (μm)		Stomatal width (μm)		Pore length (μm)		Pore width (μm)		Stomatal density (stomata mm^{-2})	
	Ab	Ad	Ab	Ad	Ab	Ad	Ab	Ad	Ab	Ad
B	28.0^b	29.6^b	20.8^a	21.2^a	8.6^{ab}	6.4^c	3.1^b	2.4^b	269^b	253^{cd}
R/B = 1	29.4^{ab}	29.8^b	21.8^a	21.9^a	9.8^{ab}	7.0^{bc}	3.8^a	2.4^b	363^a	434^a
R/B = 4	29.8^{ab}	30.9^{ab}	21.9^a	22.0^a	10.0^{ab}	7.1^{bc}	4.1^a	3.1^{ab}	283^b	320^b
R/B = 8	30.0^{ab}	31.2^{ab}	22.1^a	22.1^a	10.6^a	8.4^{ab}	3.9^a	3.2^a	257^{bc}	278^{bc}
R/B = 12	31.1^a	32.6^a	21.9^a	22.2^a	10.2^{ab}	9.2^a	3.7^a	3.0^{ab}	223^{bc}	230^d
R	27.9^b	28.6^b	20.9^a	20.6^a	8.5^b	7.7^{abc}	3.1^b	2.9^{ab}	200^d	224^d

Data were means of 40 fields of view for four samples from each treatment. Different letters indicate significant difference using the Duncan's Multiple Range Test ($p < 0.05$; $n = 4$).

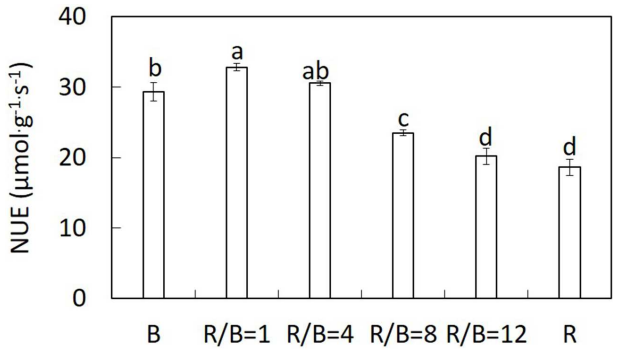

FIGURE 5 | Effect of different R/B ratios on the ratio of leaf A_{max} to nitrogen content per LA (NUE). Values were the means of four replicates with standard errors shown by vertical bars. Different letters indicate significant difference using the Duncan's Multiple Range Test ($p < 0.05$; $n = 4$).

the effects of different R/B ratios on Chl, stomatal characteristics, chlorophyll fluorescence, nitrogen content and carbohydrate content.

Chlorophyll is the pigment used for absorbing red and blue light, and Chl a is the molecule that makes photosynthesis possible (Johkan et al., 2010). An increase in Chl with decreasing R/B ratio was shown in **Table 1**. A higher Chl could increase light absorption, which was beneficial for P_n. Earlier studies have shown that B-deficiency was adverse to chlorophyll biosynthesis in wheat seedling (Tripathy and Brown, 1995), spinach (Matsuda et al., 2008), Rosa × hybrida (Terfa et al., 2013), and cucumber seedling (Hogewoning et al., 2010b; Hernández and Kubota, 2016). Plants grown under mixture of R and B or B treatments had a higher Chl a/b compared with R treatment (**Table 1**). A higher Chl a/b indicates a high light-adapted photosynthetic apparatus with less Chl b containing light-harvesting antennae, and thereby a higher capacity for electron transport and more Calvin cycle enzymes on a Chl basis (Evans, 1988). Therefore, plants grown under mixture of R and B or B treatments had higher P_n on a Chl basis in the current study.

B is perceived directly by phototropins and activates a signaling cascade that results in fast stomatal opening under background R (Shimazaki et al., 2007). Leaves exhibited higher g_s with decreasing R/B ratio. The lowest P_n and A_{max} under R treatment were attributed to unresponsive g_s to increasing irradiance (**Figure 4**) and stomatal limitation. This was confirmed by the highest L_s under R treatment (**Figure 1C**). Similar result was found by Hogewoning et al. (2010b), who reported that R alone resulted in a more restricted diffusion into leaf and lower $C_i \cdot C_a^{-1}$ in cucumber seedlings compared with R supplemented with B. Correlation analysis between P_n and g_s, g_m and L_s indicated that an increase in P_n with decreasing R/B ratio was mainly due to increased g_m and g_s and decreased stomatal limitation by decreasing R/B ratio (**Figure 2**). Although single stomatal size and stomatal pore area at the growth irradiation had a slight decrease with decreasing R/B ratio, stomatal density appeared to significantly increase (**Table 4**), resulting in an increase in g_s. These results suggested that there was a direct effect of B fraction on stomatal development, further affecting photosynthesis.

R is considered as the most efficient wavelength for photosynthesis. McCree (1972) reported that the relative quantum efficiency of R (600–700 nm) was higher than that of B (400–500 nm), because fractional B was absorbed by flavonoids in vacuoles and/or pigments (anthocyanins) without function for photosynthesis in chloroplasts or less efficient in transferring energy to the reaction centers. However, it should be noted that plants grown under R treatment had the lowest P_n and A_{max} from all the treatments (**Figure 1A** and **Table 2**). A lower α under R treatment indicated that there were problems in photosystem. Similar result was also reported by Hogewoning et al. (2010b), who found that in cucumber seedlings B-deficiency led to leaf photosynthetic machinery dysfunction, resulting in lower P_n and A_{max}. Miao et al. (2016) also reported that R alone could induce suboptimal activity of photosystems and inhibit electron transport from PSII donor side to PSI. Plants grown under B treatment also had a slight decrease in P_n in comparison with plants grown under R/B = 1 treatment. For B-grown leaves, higher g_s and C_i could not be limiting factors for slight decrease in P_n. The possible explanation was imbalance of energy allocation between two photosystems (Tennessen et al., 1994). This was verified by lower F_v'/F_m' and ΦPSII in plants subjected to monochromatic B (**Table 3**).

NUE increased with decreasing R/B ratio until 1(**Figure 5**), indicating that N availability didn't limit the exertion of photosynthetic capacity (Hogewoning et al., 2010b). However, accumulation of carbohydrate in leaves should be an impact factor for P_n. Higher starch content, along with a lower P_n under R treatment was shown than other treatments (**Table 5**). This result was similar with previous studies showed that the increase of sucrose and starch content under R treatment resulting from restriction of export of photosynthetic products out of the leaves (Sæbø et al., 1995; Li et al., 2013), which was not conducive to photosynthesis (Bondada and Syvertsen, 2003). Down-regulated P_n by carbohydrate accumulation in source leaves was a response to limited sink demand (Franck et al., 2006).

TABLE 5 | Effects of different R/B ratios on sucrose and starch content.

R/B ratios	B	R/B = 1	R/B = 4	R/B = 8	R/B = 12	R
Sucrose (mg·g^{-1})	0.37^{b}	0.34^{b}	0.38^{b}	0.36^{b}	0.53^{a}	0.50^{a}
Starch (mg·g^{-1})	0.10^{d}	0.10^{d}	0.13^{c}	0.16^{ab}	0.14^{bc}	0.17^{a}

Different letters indicate significant difference by the Duncan's Multiple Range Test ($p < 0.05$; $n = 4$).

Conflicting Effects on Growth and P_n Under Different R/B Ratios

As shown in **Table 1** and **Figure 1A**, an increase in shoot dry weight, LA and leaf number with increasing R/B ratio was observed, while opposite trend was shown in P_n. Similar results has been reported in previous studies in cucumber seedlings (Hernández and Kubota, 2014, 2016). Hernández and Kubota (2016) found that shoot dry weight decreased with increasing B fraction ranging from 10 to 75%, along with decreased LA and increased P_n. Hernández and Kubota (2014) reported that cucumber seedlings showed a reduction in shoot dry weight, leaf number, and LA with an increase of B fraction and no significant difference for P_n in a greenhouse with supplemental LED lighting (5.2 ± 1.2 mmol·m^{-2}·s^{-1}). One of the possible explanations for this result was that shoot dry weight accumulation of lettuce plant was determined not only by P_n, but also other related factors, such as LA, leaf number. Furthermore, P_n measured for single leaf cannot represent P_n of entire canopy and/or whole plant (Yorio et al., 2001). Instead, variation in LA was much more efficient in determinant of variation for plant growth rate than variation in P_n before the canopy achieves full light interception (Gifford and Jenkins, 1981). Hence, compared with R/B = 12 treatment, although P_n under B, R/B = 1, R/B = 4, and R/B = 8 treatments was 12–32% higher, 6–43% (except for higher leaf number under R/B = 8 treatment) reduction in LA and 11–29% decline in leaf number under B, R/B = 1, R/B = 4, and R/B = 8 treatments resulted in decreasing shoot dry weight accumulation with decreasing R/B ratio. Another possible explanation for increasing shoot dry weight with increasing R/B ratio was due to the fact that plant exhibited greater puffiness with loose plant structure, induced by elongation of stem and leaf petiole with increasing R, leading to much more photosynthetic active radiation to be captured for growth.

Decreasing LA with decreasing R/B ratio was similar to leaf response to high irradiance (Poorter et al., 2009; Hogewoning et al., 2010b). Decreased R/B ratio might provoke high irradiance response of decreasing LA (Hernández and Kubota, 2014), which was associated with restriction of cell expansion or division induced by B (Appelgren, 1991; Folta et al., 2003; Dougher and Bugbee, 2004). Leaf extension in the vertical and horizontal directions is controlled by different genes. Blue light causes an imbalance in expression of these genes, resulting in inhibition of leaf expansion (Tsukaya, 1998). However, the effect of B dose on LA was species and cultivars specific. For example, Dougher and Bugbee (2001) tested the effect of B fraction on LA under high pressure sodium (HPS) and metal halide lamps (MH), creating five B fractions. They found LA of lettuce increased with increasing B fraction from 0 to 6% at 200 μmol·m^{-2}·s^{-1}and from 0 to 2% at 500 μmol·m^{-2}·s^{-1} under HPS treatments; yet there was little response to different B fraction under MH treatments (6, 12, and 26%, B fraction). In this study, LA under R and R/B = 12 treatments had no significant difference. The differences in these results suggested that other wavelengths except R and B in HPS or MH have promoting or inhibiting effects on leaf extension. In addition, increasing leaf number with increasing R/B ratio up to 12 was due to shorter growth stage induced by increasing R (Ohashi-Kaneko et al., 2007).

Although P_n under R treatment was significantly lower than those under R/B = 12 treatment, no significant difference was found in shoot dry weights under R and R/B = 12 treatments, which were higher than other mixture of R and B treatments or B treatment. Similar results were also found in tomato, salvia, and petunia (Wollaeger and Runkle, 2014), and in lettuce, tomato, and komatsuna (Ohashi-Kaneko et al., 2007). For example, Wollaeger and Runkle (2014) reported that shoot dry weight of tomato, salvia, and petunia under R treatment increased by 48–112% compared to those under R supplemented with 25% or greater B treatments, along with increasing 47–130% greater LA. Ohashi-Kaneko et al. (2007) also reported that shoot dry weight of lettuce, tomato, and komatsuna under R treatment were 14–29, 10–16, and 44–52% higher than those under mixture of R and B treatments and B treatment, respectively. In this study, this result was partly because R promoted petiole and stem elongation (Kim et al., 2004), resulting in loose leaf structure to capture much more light for growth. On the other hand, plants grown under R treatment had no reduction in LMA, LA and leaf number compared to plants grown R/B = 12 treatment, not affecting light interception. Similarly, for the above parameters, there were no significant differences between R/B = 12 and R/B = 8 treatments. However, compared with R/B = 12 treatment, a slight reduction in dry weight under R/B = 8 treatment was due to higher R_d (**Table 2**). Based on above results, there might be a maximum threshold value of B for optimal lettuce growth under R-based light source.

CONCLUSION

In this study, our results showed that compared with monochromic R or B, a combination of R and B was much more efficient in facilitating lettuce growth and photosynthesis. Lettuce plants under R/B = 1 treatment exhibited the highest P_n and A_{max}. An increase of P_n and A_{max} with decreasing R/B ratio was mainly associated with stomatal characteristics. However, the highest shoot dry weight was observed under R/B = 12 treatment with the greatest leaf number and LA. There was no positive relationship between P_n of single leaf and shoot dry weight accumulation. Therefore further studies should be constructed to investigate the relationship between P_n of entire plant and dry weight accumulation.

AUTHOR CONTRIBUTIONS

JW carried out the measurements, data analysis and drafted the manuscript. WL participated in part of measurements and data analysis. YT and QY made substantial guide about experiment design, and critically revised the manuscript.

ACKNOWLEDGMENT

This work was financially supported from the National High Technology Research and Development Plan of China (863 Project, grant No. 2013AA103007).

REFERENCES

Aksenova, N. P., Konstantinova, T. N., Sergeeva, L. I., Macháčková, I., and Golyanovskaya, S. A. (1994). Morphogenesis of potato plants in vitro. I. Effect of light quality and hormones. *J. Plant Growth Regul.* 13, 143–146. doi: 10.1007/BF00196378

Appelgren, M. (1991). Effects of light quality on stem elongation of *Pelargonium* in vitro. *Sci. Hortic.* 45, 345–351. doi: 10.1016/0304-4238(91)90081-9

Bondada, B. R., and Syvertsen, J. P. (2003). Leaf chlorophyll, net gas exchange and chloroplast ultrastructure in citrus leaves of different nitrogen status. *Tree Physiol.* 23, 553–559. doi: 10.1093/treephys/23.8.553

Brown, C. S., Schuerger, A. C., and Sager, J. C. (1995). Growth and photomorphogenesis of pepper plants under red light-emitting diodes with supplemental blue or far-red lighting. *J. Am. Soc. Hortic. Sci.* 120, 808–813.

Christie, J. M. (2007). Phototropin blue-light receptors. *Annu. Rev. Plant Biol.* 58, 21–45. doi: 10.1146/annurev.arplant.58.032806.103951

Dougher, T. A., and Bugbee, B. (2001). Differences in the response of wheat, soybean and lettuce to reduced blue radiation. *Photochem. Photobiol.* 73, 199–207.

Dougher, T. A., and Bugbee, B. G. (2004). Long-term blue light effects on the histology of lettuce and soybean leaves and stems. *J. Am. Soc. Hortic. Sci.* 129, 467–472.

Evans, J. R. (1988). Acclimation by the thylakoid membranes to growth irradiance and the partitioning of nitrogen between soluble and thylakoid proteins. *Aust. J. Plant Physiol.* 15, 93–106. doi: 10.1071/PP9880093

Farquhar, G. D., and Sharkey, T. D. (1982). Stomatal conductance and photosynthesis. *Annu. Rev. Plant Physiol.* 33, 317–345. doi: 10.1146/annurev.pp.33.060182.001533

Fischer, R. A., Rees, D., and Sayre, K. D. (1998). Wheat yield progress associated with higher stomatal conductance and photosynthetic rates, and cooler canopies. *Crop Sci.* 38, 1467–1475. doi: 10.2135/cropsci1998.0011183X003800060011x

Folta, K. M., Lieg, E. J., Durham, T., and Spalding, E. P. (2003). Primary inhibition of hypocotyl growth and phototropism depend differently on phototropin-mediated increases in cytoplasmic calcium induced by blue light. *Plant Physiol.* 133, 1464–1470. doi: 10.1104/pp.103.024372

Franck, N., Vaast, P., Génard, M., and Dauzat, J. (2006). Soluble sugars mediate sink feedback down-regulation of leaf photosynthesis in field-grown *Coffea arabica*. *Tree Physiol.* 26, 517–525. doi: 10.1093/treephys/26.4.517

Genty, B., Briantais, J. M., and Baker, N. R. (1989). The relationship between the quantum yield of photosynthetic electron transport and quenching of chlorophyll fluorescence. *Biochim. Biophys. Acta* 990, 87–92. doi: 10.1016/S0304-4165(89)80016-9

Gifford, R. M., and Jenkins, C. L. (1981). "Prospects of applying knowledge of photosynthesis toward improving crop production," in *Photosynthesis: CO2 Assimilation and Plant Productivity*, Vol. 2, ed. Govindjee (New York, NY: Academic Press).

Goins, G. D., Yorio, N. C., Sanwo, M. M., and Brown, C. S. (1997). Photomorphogenesis, photosynthesis, and seed yield of wheat plants grown under red light-emitting diodes (LEDs) with and without supplemental blue lighting. *J. Exp. Bot.* 48, 1407–1413. doi: 10.1093/jxb/48.7.1407

Goins, G. D., Yorio, N. C., Sanwo-Lewandowski, M. M., and Brown, C. S. (1998). Life cycle experiments with *Arabidopsis* under red light-emitting diodes (LEDs). *Life Support Biosph. Sci.* 5, 143–149.

Hernández, R., and Kubota, C. (2014). Growth and morphological response of cucumber seedlings to supplemental red and blue photon flux ratios under varied solar daily light integrals. *Sci. Hortic.* 173, 92–99. doi: 10.1016/j.scienta.2014.04.035

Hernández, R., and Kubota, C. (2016). Physiological responses of cucumber seedlings under different blue and red photon flux ratios using LEDs. *Environ. Exp. Bot.* 121, 66–74. doi: 10.1016/j.envexpbot.2015.04.001

Hoenecke, M. E., Bula, R. J., and Tibbitts, T. W. (1992). Importance of 'blue' photon levels for lettuce seedlings grown under red-light-emitting diodes. *HortScience* 27, 427–430.

Hogewoning, S. W., Douwstra, P., Trouwborst, G., van Ieperen, W., and Harbinson, J. (2010a). An artificial solar spectrumsubstantially alters plant development compared with usual climate room irradiance spectra. *J. Exp. Bot.* 61, 1267–1276. doi: 10.1093/jxb/erq005

Hogewoning, S. W., Trouwborst, G., Maljaars, H., Poorter, H., van Ieperen, W., and Harbinson, J. (2010b). Blue light dose-responses of leaf photosynthesis, morphology, and chemical composition of *Cucumis sativus* grown under different combinations of red and blue light. *J. Exp. Bot.* 61, 3107–3117. doi: 10.1093/jxb/erq132

Inoue, S. I., Kinoshita, T., Matsumoto, M., Nakayama, K. I., Doi, M., and Shimazaki, K. I. (2008). Blue light-induced autophosphorylation of phototropin is a primary step for signaling. *Proc. Natl. Acad. Sci. U.S.A.* 105, 5626–5631. doi: 10.1073/pnas.0709189105

Johkan, M., Shoji, K., Goto, F., Hashida, S. N., and Yoshihara, T. (2010). Blue light-emitting diode light irradiation of seedlings improves seedling quality and growth after transplanting in red leaf lettuce. *HortScience* 45, 1809–1814.

Kim, S. J., Hahn, E. J., Heo, J. W., and Paek, K. Y. (2004). Effects of LEDs on net photosynthetic rate, growth and leaf stomata of chrysanthemum plantlets in vitro. *Sci. Hortic.* 101, 143–151. doi: 10.1016/j.scienta.2003.10.003

Lee, S. H., Tewari, R. K., Hahn, E. J., and Paek, K. Y. (2007). Photon flux density and light quality induce changes in growth, stomatal development, photosynthesis and transpiration of *Withania somnifera* (L.) Dunal. plantlets. *Plant Cell Tissue Organ Cult.* 90, 141–151. doi: 10.1007/s11240-006-9191-2

Li, H., Tang, C., and Xu, Z. (2013). The effects of different light qualities on rapeseed (*Brassica napus* L.) plantlet growth and morphogenesis in vitro. *Sci. Hortic.* 150, 117–124. doi: 10.1016/j.scienta.2012.10.009

Li, H., Xu, Z., and Tang, C. (2010). Effect of light-emitting diodes on growth and morphogenesis of upland cotton (*Gossypium hirsutum* L.) plantlets in vitro. *Plant Cell Tissue Organ Cult.* 103, 155–163. doi: 10.1007/s11240-010-9763-z

Li, T., Heuvelink, E., Dueck, T. A., Janse, J., Gort, G., and Marcelis, L. F. M. (2014). Enhancement of crop photosynthesis by diffuse light: quantifying the contributing factors. *Ann. Bot.* 114, 145–156. doi: 10.1093/aob/mcu071

Lichtenthaler, H. K., and Wellburn, A. R. (1983). Determination of total carotenoids and chlorophylls a and b of leaf extracts in different solvents. *Biochem. Soc. Trans.* 603, 591–592. doi: 10.1042/bst0110591

Lin, K. H., Huang, M. Y., Huang, W. D., Hsu, M. H., Yang, Z. W., and Yang, C. M. (2013). The effects of red, blue, and white light-emitting diodes on the growth, development, and edible quality of hydroponically grown lettuce (*Lactuca sativa* L. var. capitata). *Sci. Hortic.* 150, 86–91. doi: 10.1016/j.scienta.2012.10.002

Matsuda, R., Ohashi-Kaneko, K., Fujiwara, K., Goto, E., and Kurata, K. (2004). Photosynthetic characteristics of rice leaves grown under red light with or without supplemental blue light. *Plant Cell Physiol.* 45, 1870–1874. doi: 10.1093/pcp/pch203

Matsuda, R., Ohashi-Kaneko, K., Fujiwara, K., and Kurata, K. (2008). Effects of blue light deficiency on acclimation of light energy partitioning in PSII and CO2 assimilation capacity to high irradiance in spinach leaves. *Plant Cell Physiol.* 49, 664–670. doi: 10.1093/pcp/pcn041

McCree, K. J. (1972). The action spectrum, absorptance and quantum yield of photosynthesis in crop plants. *Agric. Meteorol.* 9, 191–216. doi: 10.1016/0002-1571(71)90022-7

Miao, Y. X., Wang, X. Z., Gao, L. H., Chen, Q. Y., and Qu, M. (2016). Blue light is more essential than red light for maintaining the activities of photosystem II and I and photosynthetic electron transport capacity in cucumber leaves. *J. Integr. Agric.* 15, 87–100. doi: 10.1016/S2095-3119(15)61202-3

Nanya, K., Ishigami, Y., Hikosaka, S., and Goto, E. (2012). Effects of blue and red light on stem elongation and flowering of tomato seedlings. *Acta Hortic.* 956, 261–266. doi: 10.17660/ActaHortic.2012.956.29

Nhut, D. T., Takamura, T., Watanabe, H., Okamoto, K., and Tanaka, M. (2003). Responses of strawberry plantlets cultured in vitro under superbright red and blue light-emitting diodes (LEDs). *Plant Cell Tissue Organ Cult.* 73, 43–52. doi: 10.1023/A:1022638508007

Ohashi-Kaneko, K., Matsuda, R., Goto, E., Fujiwara, K., and Kurata, K. (2006). Growth of rice plants under red light with or without supplemental blue light. *Soil Sci. Plant Nutr.* 52, 444–452. doi: 10.1111/j.1747-0765.2006.00063.x

Ohashi-Kaneko, K., Takase, M., Kon, N., Fujiwara, K., and Kurata, K. (2007). Effect of light quality on growth and vegetable quality in leaf lettuce, spinach and komatsuna. *Environ. Control Biol.* 45, 189–198. doi: 10.2525/ecb.45.189

Pfündel, E., and Baake, E. (1990). A quantitative description of fluorescence excitation spectra in intact bean leaves greened under intermittent light. *Photosynth. Res.* 26, 19–28. doi: 10.1007/BF00048973

Poorter, H., Niinemets, U., Pooter, L., Wright, I. J., and Villar, R. (2009). Causes and consequences of vibration in leaf mass per area (LMA): a meta-analysis. *New Phytol.* 182, 565–588. doi: 10.1111/j.1469-8137.2009.02830.x

Shimazaki, K. I., Doi, M., Assmann, S. M., and Kinoshita, T. (2007). Light regulation of stomatal movement. *Annu. Rev. Plant Biol.* 58, 219–247. doi: 10.1146/annurev.arplant.57.032905.105434

Son, K. H., and Oh, M. M. (2013). Leaf shape, growth, and antioxidant phenolic compounds of two lettuce cultivars grown under various combinations of blue and red light-emitting diodes. *HortScience* 48, 988–995.

Sæbø, A., Krekling, T., and Appelgren, M. (1995). Light quality affects photosynthesis and leaf anatomy of birch plantlets in vitro. *Plant Cell Tissue Organ Cult.* 41, 177–185. doi: 10.1007/BF00051588

Takahashi, K., Fujino, K., Kikuta, Y., and Koda, Y. (1995). Involvement of the accumulation of sucrose and the synthesis of cell wall polysaccharides in the expansion of potato cells in response to jasmonic acid. *Plant Sci.* 111, 11–18. doi: 10.1016/0168-9452(95)04222-G

Tennessen, D. J., Singsaas, E. L., and Sharkey, T. D. (1994). Light-emitting diodes as a light source for photosynthesis research. *Photosynth. Res.* 39, 85–92. doi: 10.1007/BF00027146

Terfa, M. T., Solhaug, K. A., Gislerød, H. R., Olsen, J. E., and Torre, S. (2013). A high proportion of blue light increases the photosynthesis capacity and leaf formation rate of *Rosa* × *hybrida* but does not affect time to flower opening. *Physiol. Plant.* 148, 146–159. doi: 10.1111/j.1399-3054.2012.01698.x

Thornley, J. H. M. (1976). *Mathematical Models in Plant Physiology: A Quantitative Approach to Problems in Plant and Crop Physiology*. London: Academic Press.

Tripathy, B. C., and Brown, C. S. (1995). Root-shoot interaction in the greening of wheat seedlings grown under red light. *Plant Physiol.* 107, 407–411.

Tsukaya, H. (1998). Genetic evidence for polarities that regulate leaf morphogenesis. *J. Plant Res.* 111, 113–119. doi: 10.1007/BF02507157

Wang, H., Gu, M., Cui, J., Shi, K., Zhou, Y., and Yu, J. (2009). Effects of light quality on CO2 assimilation, chlorophyll-fluorescence quenching, expression of Calvin cycle genes and carbohydrate accumulation in *Cucumis sativus*. *J. Photochem. Photobiol. B Biol.* 96, 30–37. doi: 10.1016/j.jphotobiol.2009.03.010

Wang, X. Y., Xu, X. M., and Cui, J. (2015). The importance of blue light for leaf area expansion, development of photosynthetic apparatus, and chloroplast ultrastructure of *Cucumis sativus* grown under weak light. *Photosynthetica* 53, 213–222. doi: 10.1007/s11099-015-0083-8

Wojciechowska, R., Długosz-Grochowska, O., Kołton, A., and Żupnik, M. (2015). Effects of LED supplemental lighting on yield and some quality parameters of lamb's lettuce grown in two winter cycles. *Sci. Hortic.* 187, 80–86. doi: 10.1016/j.scienta.2015.03.006

Wollaeger, H. M., and Runkle, E. S. (2014). Growth of impatiens, petunia, salvia, and tomato seedlings under blue, green, and red light-emitting diodes. *HortScience* 49, 734–740.

Yorio, N. C., Goins, G. D., Kagie, H. R., Wheeler, R. M., and Sager, J. C. (2001). Improving spinach, radish, and lettuce growth under red light-emitting diodes (LEDs) with blue light supplementation. *HortScience* 36, 380–383.

Yorio, N. C., Wheeler, R. M., Goins, G. D., Sanwo-Lewandowski, M. M., Mackowiak, C. L., Brown, C. S., et al. (1998). Blue light requirements for crop plants used in bioregenerative life support systems. *Life Support Biosph. Sci.* 5, 119–128.

Zeng, B., Wang, Q. Y., and Tang, C. M. (2008). Anatomic analysis on heterosis in three transgenic bt pest-resistant hybrid cotton (*G. hirsutum* L.). *Acta Agron. Sin.* 34, 496–505. doi: 10.3724/SP.J.1006.2008.00496

Conflict of Interest Statement: The authors declare that the research was conducted in the absence of any commercial or financial relationships that could be construed as a potential conflict of interest.

frontiers in Plant Science

ORIGINAL RESEARCH
published: 14 December 2015
doi: 10.3389/fpls.2015.01110

Supplemental Upward Lighting from Underneath to Obtain Higher Marketable Lettuce (*Lactuca sativa*) Leaf Fresh Weight by Retarding Senescence of Outer Leaves

*Geng Zhang[1,2], Shanqi Shen[2], Michiko Takagaki[1,2], Toyoki Kozai[3] and Wataru Yamori[2,4]**

[1] Graduate School of Horticulture, Chiba University, Matsudo, Japan, [2] Center for Environment, Health and Field Sciences, Chiba University, Kashiwa, Japan, [3] Japan Plant Factory Association, Kashiwa, Japan, [4] Precursory Research for Embryonic Science and Technology, Japan Science and Technology Agency, Kawaguchi, Japan

Recently, the so-called "plant factory with artificial lighting" (PFAL) approach has been developed to provide safe and steady food production. Although PFALs can produce high-yielding and high-quality plants, the high plant density in these systems accelerates leaf senescence in the bottom (or outer) leaves owing to shading by the upper (or inner) leaves and by neighboring plants. This decreases yield and increases labor costs for trimming. Thus, the establishment of cultivation methods to retard senescence of outer leaves is an important research goal to improve PFAL yield and profitability. In the present study, we developed an LED lighting apparatus that would optimize light conditions for PFAL cultivation of a leafy vegetable. Lettuce (*Lactuca sativa* L.) was hydroponically grown under white, red, or blue LEDs, with light provided from above (downward), with or without supplemental upward lighting from underneath the plant. White LEDs proved more appropriate for lettuce growth than red or blue LEDs, and the supplemental lighting retarded the senescence of outer leaves and decreased waste (i.e., dead or low-quality senescent leaves), leading to an improvement of the marketable leaf fresh weight.

Keywords: LED, light color, supplemental upward lighting, photosynthesis, plant factory, supplemental lighting

OPEN ACCESS

Edited by:
Alejandro Isabel Luna Maldonado, Universidad Autónoma de Nuevo León, Mexico

Reviewed by:
Chenglin Chai, Louisiana State University, USA
Andreas Savvides, Cyprus University of Technology, Cyprus

***Correspondence:**
Wataru Yamori
wataru.yamori@chiba-u.jp

Specialty section:
This article was submitted to Crop Science and Horticulture, a section of the journal Frontiers in Plant Science

Received: *21 October 2015*
Accepted: *23 November 2015*
Published: *14 December 2015*

Citation:
Zhang G, Shen S, Takagaki M, Kozai T and Yamori W (2015) Supplemental Upward Lighting from Underneath to Obtain Higher Marketable Lettuce (Lactuca sativa) Leaf Fresh Weight by Retarding Senescence of Outer Leaves. Front. Plant Sci. 6:1110. doi: 10.3389/fpls.2015.01110

INTRODUCTION

Population growth has led to a steady increase in the demand for food, and now poses a threat to food security. In recent years, air pollution, rapid population growth, and resource shortages have focused increasing attention on food security. An emerging industry with the potential to alleviate some of these problems takes advantage of what have been called "plant factories", which can produce high-yield and high-quality plants using less water, nutrients, land, and labor than is possible with conventional agriculture (Kozai, 2013a; Hu et al., 2014; Yamori et al., 2014). Plant factories with artificial lighting (PFALs) create an enclosed cultivation system that allows control of environmental factors such as lighting, temperature, humidity, and CO_2 concentration. Moreover, PFALs can overcome adverse conditions such as heavy rain, heavy snow, strong winds, and temperature extremes. PFALs have been already commercially used for the production of leafy vegetables in Japan, China, and Taiwan (Kozai, 2013b).

Light sources such as fluorescent lamps, metal-halide lamps, and high-pressure sodium lamps are generally used for plant cultivation. They are used to increase the photosynthetic photon flux density (PPFD), but they also provide wavelengths that are not used efficiently or at all to support photosynthesis and plant growth (McCree, 1972; Björkman, 1981). In comparison, LED lighting systems have several advantages, including greater wavelength specificity (i.e., a narrow bandwidth), long operating lifetimes, and less heating. However, the optimal light wavelengths for plant cultivation remain unclear. Numerous studies have suggested that red and blue light are the most useful wavelength bands to drive photosynthesis, since chlorophyll has its maximum absorption in those bands (e.g., McCree, 1972; Okamoto et al., 1996), but blue light also plays an important photomorphogenic role (e.g., suppresses hypocotyl elongation; Goins et al., 1997; Massa et al., 2008) in plants. However, it has been shown that the optimal light color for plant growth differs among plant species (Kim et al., 2006). For example, lettuce (*Lactuca sativa* L.) grown under red LEDs developed more leaves than lettuce grown under blue LEDs (Yanagi et al., 1996), but for spinach (*Spinacia oleracea* L.) or radish (*Raphanus sativus* L.) growth, the use of only red LEDs was unsuitable (Yorio et al., 2001). Other studies have found that light sources that contain blue light improved dry matter production and the photosynthetic capacity in pepper (*Capsicum annuum* L.; Brown et al., 1995), wheat (*Triticum aestivum* L.; Goins et al., 1997), and spinach (*Spinacia oleracea* L.; Matsuda et al., 2007). Thus, it remains unclear what light source would be most suitable for plant cultivation in a PFAL system. It is therefore necessary to identify the optimal light sources for various species to maximize plant yields.

On the other hand, although PFALs can produce high yields, the high plant density creates suboptimal conditions, because the outer or lower leaves are shaded and therefore senesce faster. Owing to shading by upper or outer leaves and by neighboring plants, leaves beneath the plant canopy suffer from low light conditions (Terashima et al., 2005). The leaf senescence that occurs at low light intensity is accompanied by chlorophyll loss, degradation of photosynthetic proteins, a decline in photosynthetic activity, and the remobilization of nutrients to younger tissues (Gan and Amasino, 1997; Weaver and Amasino, 2001; Brouwer et al., 2012). The senescent leaves become visibly yellow (chlorotic) and wilted (McCabe et al., 2001), leading to a reduction of the market price. Thus, these leaves must be removed, which can significantly decrease plant yield and increase labor costs. Therefore, establishing cultivation methods that retard senescence of outer leaves is an important goal to improve yield and profitability.

Since the main problem is the low light conditions experienced by shaded leaves, improving the light conditions of these leaves could delay senescence. Previous studies have shown that irradiation of both the adaxial and abaxial sides of a leaf can increase photosynthesis (Terashima, 1986; Soares et al., 2008), and different light colors have different effects on leaf senescence (Causin et al., 2006). However, no studies have examined the effects of supplemental upward lighting of the abaxial sides of leaves from underneath the plant to delay senescence of shaded leaves and improve plant growth. The present study therefore had two purposes: to study the effect of light color on photosynthesis and plant growth of romaine lettuce, and to analyze the effect of supplemental upward lighting from underneath the plant on leaf senescence in the outer leaves. We also analyzed the economic benefits of this technique. We found that white LEDs were more appropriate for romaine lettuce than red or blue LEDs, and that the supplemental upward lighting retarded senescence of the outer leaves and reduced waste, leading to an improvement in marketable leaf fresh weight; it also improved the nutrient quality of the plants.

MATERIALS AND METHODS

Plant Materials and Growth Conditions

The experiment was conducted in a commercial plant factory, which has two cultivating compartments: one is a nursery room and the other is a cultivation room. Romaine lettuce (*Lactuca sativa* L. var. Romana; Takii Seed Co., Kyoto, Japan) seeds were sown in sponge blocks (W 2.3 cm × D 2.3 cm × H 2.7 cm), and the seedlings were grown in the nursery room at 20/17°C (day/night) under a PPFD of 350 ± 10 μmol m^{-2} s^{-1} for 12 h provided by cool white fluorescent lamps. At 22 days after sowing, the seedlings were transplanted into the cultivation room equipped with 200 μmol m^{-2} s^{-1} PPFD of downward-facing white LEDs, red LEDs (peak wavelength 660 nm), or blue LEDs (peak wavelength 450 nm; Supplementary Figure S1A; red and blue LEDs were provided by Shibasaki Inc., Saitama, Japan; white LEDs were provided by ODC Co., Ltd., Kanagawa, Japan). Plants were grown in a deep-flow hydroponic system (37 plants m^{-2}) in Enshi formula nutrient solution with an electrical conductivity of 1.7 ± 0.1 dS m^{-1} and a pH of 6.8 ± 0.2. The air temperature was maintained at 25/20°C (day/night), the relative humidity at 60%, the photoperiod at 16 h, and the CO_2 concentration at 1000 ppm. We chose 1000 ppm CO_2 because this is the most common concentration used in Japanese PFALs (Kozai, 2013a). The supplemental upward lighting treatments were performed from 15 days (when all outer leaves became shaded) or 22 days (when visible senescence of outer leaves began) after transplanting, with illumination at 40 μmol m^{-2} s^{-1} PPFD at the height of the outer leaves (4.0 ± 0.5 cm). The illumination was provided by supplemental LEDs placed on cultivation panels in order to direct the light upward from underneath the plants (**Figure 1**). The light colors of these supplemental LEDs were same to those of the LEDs used for downward lighting from above (Supplementary Figure S1B).

Measurements of Gas Exchange and Chlorophyll Fluorescence

Gas exchange was measured with a portable gas exchange system (LI-6400; Li-Cor Inc., Lincoln, NE, USA) as described previously (Yamori et al., 2009, 2010). Plants were divided into six layers of leaves. Counting from the lowest leaf, the first to third layers of leaves (white light, 10–11 leaves per plant; red light, 10–11 leaves per plant; blue light, 5–6 leaves per plant) were the outer leaves, and the fourth to sixth layers of leaves (white light, 9–10 leaves

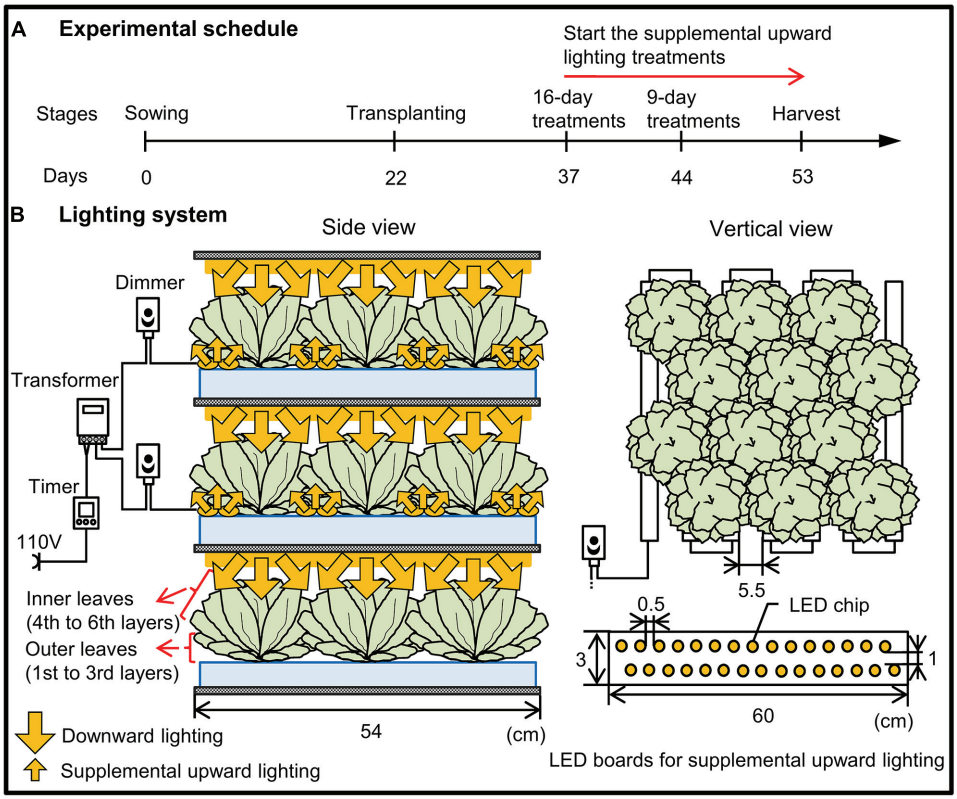

FIGURE 1 | Schematic diagram of the experimental schedule (A) and the lighting system (B) used in the present study. (A) At 22 days after sowing, the seedlings were transplanted into growth chambers equipped with 200 μmol m^{-2} s^{-1} PPFD of downward-facing white, red, or blue LEDs and with light provided for 16 h per day. The supplemental upward lighting treatments were performed from 15 or 22 days after transplanting until harvest. **(B)** There were three vertically arranged cultivation beds for each light color. Lettuce grown in the top and middle layers received light from above (downward lighting), with supplemental upward lighting for 9 and 16 days, respectively. Lettuce grown in the bottom layer received light only from above, without any supplemental upward lighting. The treatment arrangement was the same for each LED color: lettuce was grown at 37 plants m^{-2}, with 22 LED boards (each board containing two rows of LED chips) m^{-2} used for supplemental upward lighting. A digital timer, dimmer, and transformer were used to maintain the light period (16 h, the same as the downward lighting) and light intensity (40 μmol m^{-2} s^{-1} PPFD).

per plant; red light, 8–9 leaves per plant; blue light, 6–7 leaves per plant) were the inner leaves. After 30 min of illumination to obtain steady-state photosynthesis, the net photosynthetic rate of the inner leaves (sixth layer) and outer leaves (third layer) were measured.

To evaluate the degree of leaf senescence, we measured the maximum potential photochemical efficiency (the ratio of variable to maximum fluorescence, F_v/F_m) using an Imaging-PAM fluorometer (Walz, Effeltrich, Germany). Leaf disks (1.3 cm in diameter) were taken from the outer and inner leaves of each treatment (from the first to sixth layers), and were then vacuum-infiltrated in deionized water that included 0.005% Tween 20 (Shao et al., 2013). F_v/F_m was measured after 30 min of incubation in darkness.

Determinations of Chlorophyll, Carbon, and Nitrogen Contents

Right after the gas exchange and chlorophyll fluorescence measurements, leaf disks (0.85 cm in diameter) were taken from the outer and inner leaves (same leaves with the measurements of F_v/F_m) of each treatment. Chlorophyll was extracted in *N,N*-dimethylformamide and its content was determined using a spectrophotometer, according to the procedure of Porra et al. (1989). Leaf carbon and nitrogen contents were measured with a Vario EL III elemental analyzer (Elementar, Hanau, Germany) as described by Yamori et al. (2005).

Plant Growth and Nutritional Quality of the Romaine Lettuce

At 53 days after sowing, plants were harvested, and the leaf angle, leaf number, total leaf area, root length, leaf and root fresh weights, and leaf and root dry weights were measured. Total leaf area was determined using a leaf area meter (LI-300; Li-Cor Inc., Lincoln, NE, USA), and the dry weights of leaf and root were measured after oven-drying at 80°C for more than 72 h.

As a measure of the nutrient quality, the ascorbic acid and nitrate contents in the outer and inner leaves (all leaves in each group of layers were cut into pieces, and the 1 g fresh samples were used for measurements) of plants in each treatment were quantified by using an RQ Flex plus reflectometer (Merck,

Darmstadt, Germany), following the method of Pantelidis et al. (2007).

Electricity Consumption Measurements

The consumption of electrical energy by each LED panel was measured with a multimeter and a clamp ammeter (Hioki 3169-01, Hioki E.E. Corporation, Nagano, Japan), and were used to evaluate the economics of the supplemental lighting.

Statistical Analysis

Values were compared between illumination treatments by Tukey's multiple-comparison test (for photosynthetic rates without supplemental lighting, fresh weights, and wastage rates) or Student's *t*-test (for photosynthetic rates with supplemental lighting and nutrient contents) in SPSS statistical software v. 21.0 (SPSS, Chicago, IL, USA). Differences were considered significant at $P < 0.05$.

RESULTS

Leaf Characteristics

In plants grown under downward lighting but without upward lighting, the total chlorophyll content (**Figure 2A**, Supplementary Table S1) and maximum potential photochemical efficiency (F_v/F_m; **Figure 2E**, Supplementary Table S1) were highest in the most newly expanded leaves (sixth layer), but gradually decreased from the inner leaves (fourth to sixth layers) to the outer leaves (first to third layers).

However, supplemental upward lighting maintained significantly higher total chlorophyll content and F_v/F_m values in the outer leaves of plants grown under white LEDs (**Figures 2B,F**, Supplementary Table S1) and red LEDs (**Figures 2C,G**, Supplementary Table S1), but not under blue LEDs (**Figures 2D,H**, Supplementary Table S1), than in plants grown without upward lighting (**Figures 2A,E**, Supplementary Table S1). The 9-day supplemental lighting treatments maintained high total chlorophyll content and F_v/F_m in the outer leaves to some extent, but the 16-day treatments showed a more pronounced effect in retarding senescence of the outer leaves. White or red supplemental lighting also maintained the leaf nitrogen content in the outer leaves (Supplementary Table S2). However, blue supplemental lighting (but not red or white) allowed a significant decrease in the leaf nitrogen content in the inner leaves.

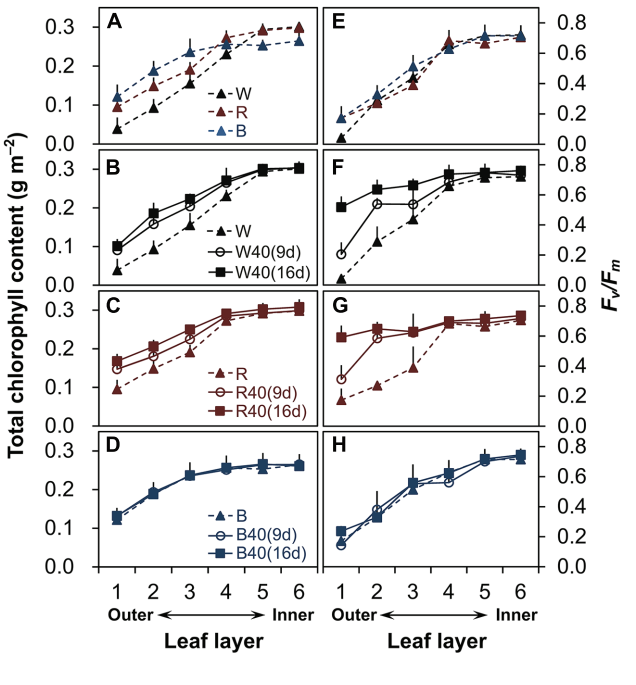

FIGURE 2 | Total chlorophyll content (A–D) and maximum quantum yield (F_v/F_m) (E–H) in lettuce leaves from the six layers of leaves in plants grown under downward lighting by white (W), red (R), or blue (B) LEDs, without or with supplemental upward lighting for 9 days ("9d") or 16 days ("16d") at 40 μmol m^{-2} s^{-1} PPFD. Data represent means ± SD ($n = 3$ to 5). **(A,E)** No supplemental upward lighting. **(B–D,F–H)** Same downward lighting as in **(A)**, but with supplemental **(B,F)** white, **(C,G)** red, or **(D,H)** blue upward lighting.

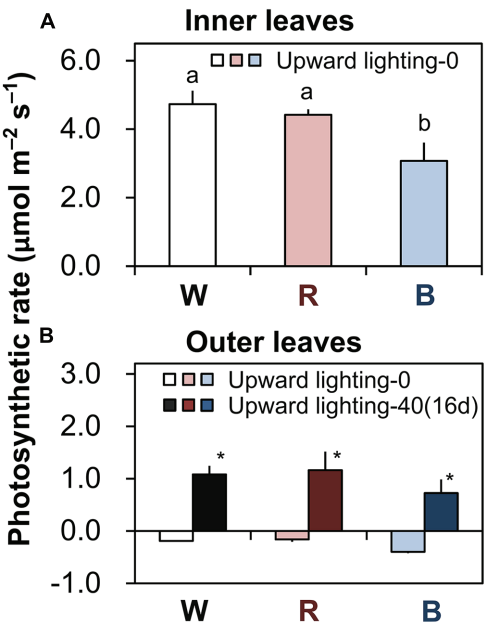

FIGURE 3 | Photosynthetic rates of plants grown under downward lighting by white, red, or blue LEDs, with or without supplemental upward lighting. Data represent means ± SD ($n = 3$). **(A)** Photosynthetic rates were measured under ambient light conditions in the most newly expanded leaves (in the sixth layer) in plants grown without upward lighting. Bars labeled with different letters differ significantly (Tukey's HSD test, $P < 0.05$) among the three light colors. **(B)** Photosynthetic rates were measured under ambient light conditions in the outer leaves (in the third layer) in plants grown under downward lighting by white, red, or blue LEDs, with or without supplemental upward lighting for 16 days. Bars labeled with "*" differ significantly for a given light color (Student's *t*-test, $P < 0.05$). "Upward lighting-0" denotes plants grown without supplemantal upward lighting; "Upward lighting-40 (16d)" denotes plants grown with 16 days of supplemental upward lighting at 40 μmol m^{-2} s^{-1} PPFD.

Photosynthesis

In plants grown under downward lighting but without upward lighting, the photosynthetic rates of the most newly expanded leaves (in the sixth layer) were highest in plants grown under white or red LEDs, which did not differ significantly, and were significantly lower under blue LEDs (**Figure 3A**).

With supplemental upward lighting, the outer leaves showed positive net photosynthetic rates. In contrast, without upward lighting, plants had negative net photosynthetic rates in the outer leaves (**Figure 3B**). These results show that supplemental upward lighting could shift the carbon balance from negative to positive (i.e., it improved photosynthesis in the outer leaves).

Plant Growth

Romaine lettuce showed distinct growth responses to the different light colors (Supplementary Figures S2–S4). In plants grown under downward lighting without upward lighting, the white LEDs yielded the highest total leaf fresh weights, and the blue LEDs produced the lowest total fresh weight (**Figure 4A**); this corresponded to the results for photosynthetic rate in the most newly expanded leaves of lettuce grown only with downward lighting (**Figure 3A**). Moreover, marketable leaf biomass, which represents the remaining leaves after removal of the outer senesced leaves, showed the same trend as total fresh weight (**Figure 4A**). Root mass generally varied little between treatments, although it was significantly greater with white LEDs than with red or blue LEDs in the absence of supplemental lighting. Other growth parameters, including leaf number, total leaf area, and root fresh and dry weights, were also greatest in plants grown under white LEDs (Supplementary Table S3). The wastage rate, which equaled the difference between the total and marketable leaf fresh weights, was higher in plants grown under white LEDs than in plants grown under red or blue LEDs without supplemental lighting (**Figure 5A**).

White or red upward lighting increased the total leaf fresh weight compared with plants grown without upward lighting, and the difference was significant with 16 days of supplemental lighting (**Figures 4B,C**). Moreover, the white and red supplemental lighting significantly increased marketable leaf fresh weight, leading to significantly lower wastage rates, especially in the 16-day treatments (**Figures 5B,C**). However, blue supplemental lighting made no significant difference (**Figures 4D** and **5D**).

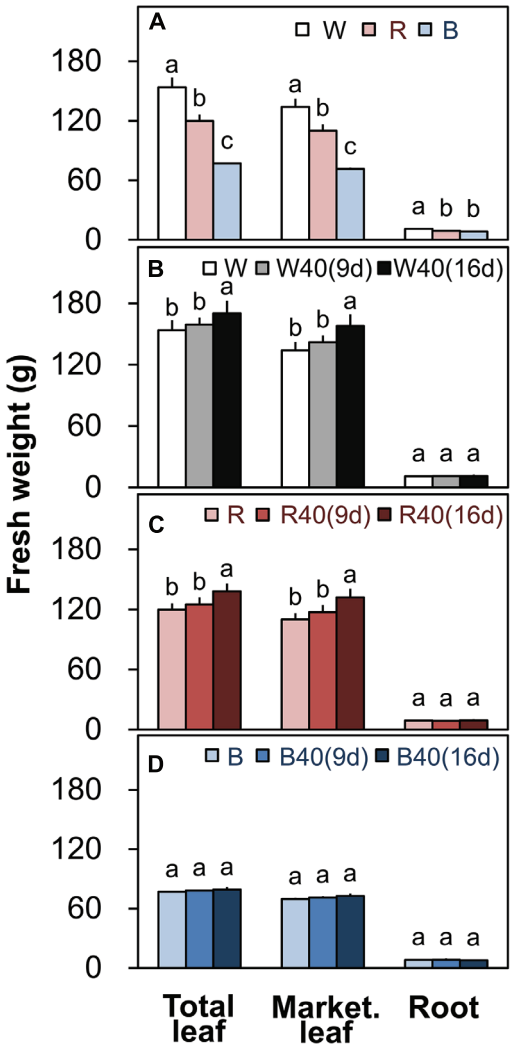

FIGURE 4 | Total leaf fresh weights, marketable leaf fresh weights, and root fresh weights of plants grown under (A) white (W), red (R), and blue (B) LEDs without supplemental upward lighting, or under the same downward lighting from above with supplemental upward lighting from (B) white, (C) red, or (D) blue LEDs. Data represent means ± SD ($n = 3$ to 5). Supplemental upward lighting was provided for 9 days ("9d") or 16 days ("16d") at 40 μmol m^{-2} s^{-1} PPFD. Bars labeled with different letters differ significantly (Tukey's HSD test, $P < 0.05$).

Ascorbic Acid and Nitrate Contents of the Romaine Lettuce

The ascorbic acid and nitrate contents were greatly influenced by the different light colors without upward lighting. The ascorbic acid content was generally highest under red LEDs, followed by blue and then white LEDs (**Figure 6A**). Conversely, the nitrate content of lettuce was significantly lower in leaves grown under red LEDs than in leaves grown under white or blue LEDs (**Figure 6E**).

Supplemental lighting significantly increased the ascorbic acid content in the outer leaves with white LEDs and in the outer and total leaves with red LEDs (**Figures 6B,C**), but did not significantly affect the nitrate content (**Figures 6F,G**). Supplemental lighting with blue LEDs did not significantly affect either (**Figures 6D,H**).

DISCUSSION

White LEDs had a Greater Effect on Plant Biomass Production than Red or Blue LEDs

Romaine lettuces grown under white LEDs had significantly greater total and marketable leaf biomass than those grown under

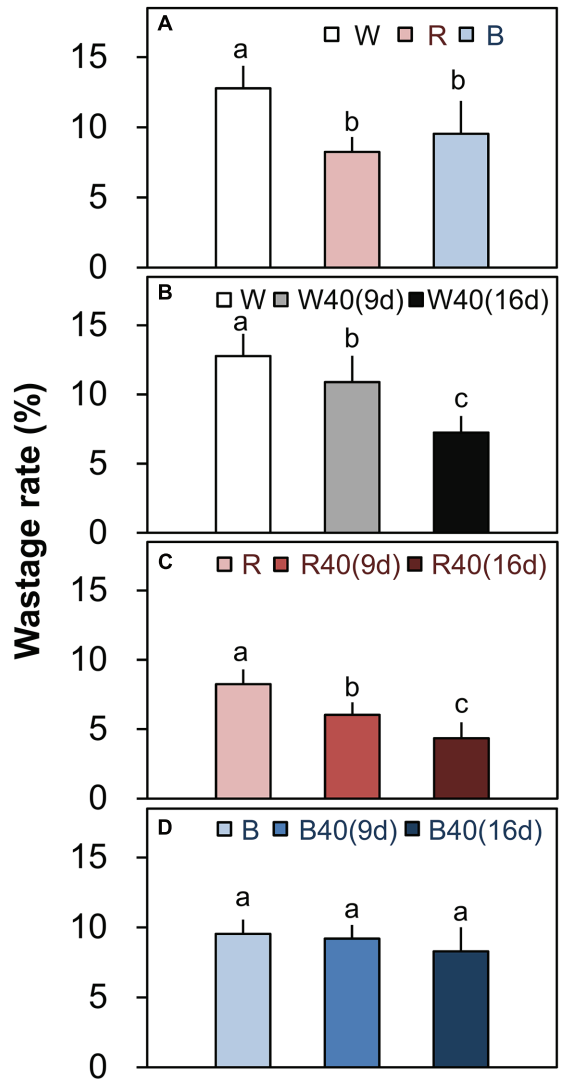

FIGURE 5 | Wastage rates (total leaf fresh weight minus marketable leaf fresh weight; Figure 4) of outer senesced leaves of plants grown under downward lighting by white, red, or blue LEDs (A) without and (B–D) with supplemental upward lighting. Data represent means ± SD ($n = 3$ to 5). Supplemental upward lighting was provided for 9 days ("9d") or 16 days ("16d") at 40 μmol m^{-2} s^{-1} PPFD. Bars labeled with different letters differ significantly between treatments (Tukey's HSD test, $P < 0.05$).

red or blue LEDs (**Figure 4A**), indicating that white light was a superior light source for the production of romaine lettuce in PFALs. Generally, there are two methods to generate white light: single-chip and multi-chip LEDs. Single-chip white LEDs include (1) a blue LED + a yellow phosphor (the most common type), (2) a blue LED + red and green phosphors, and (3) a near-ultraviolet LED + red, green, and blue phosphors. Multi-chip white LEDs include (1) red + green + blue LEDs and (2) blue + green + orange LEDs (Damilano et al., 2001; Taguchi, 2003). The white LEDs used in the present study combined a blue LED with a yellow phosphor (Supplementary Figure S1A). The results with the white LEDs in the present study suggest that combining light wavelengths could have a greater impact on plant production than the use of red and/or blue LEDs, which have been believed to be useful for plant cultivation in PFALs (e.g., Lee et al., 2010; Son and Oh, 2013). This hypothesis is supported by previous studies which showed that the dry mass of lettuce and spinach grown under only red light was significantly lower than that under white light, which provided both red and blue wavelengths (Yorio et al., 2001), and leaf fresh weight of lettuce grown under combined red and blue LEDs was significantly lower than under a combination of red, blue, and white LEDs (Lin et al., 2013). An increasing number of white LEDs are being manufactured for use in home lighting, resulting in reduced prices, and thus white LEDs might offer a good compromise between cost and optimal spectral characteristics as a light source for commercial plant productions in PFALs.

The different light colors influenced the ascorbic acid and nitrate contents in romaine lettuce (**Figures 6A,E**). Plants grown under red LEDs had the highest ascorbic acid content and the lowest nitrate content. If growers demand a higher ascorbic acid content or a lower nitrate content, red light could therefore help them meet their requirements. In PFALs, it is possible to match the light source to the production target. The levels of functional nutritional components such as ascorbic acid, alpha-carotene, and phenolic compounds can be increased by treatment with UV light (Xie et al., 2015) or red light (Bliznikas et al., 2012) during the late stages of cultivation. Therefore, in the future, it may be possible to achieve high plant yields with a high content of ascorbic acid or other nutrients by growing plants under white light and supplying red light during the late cultivation stage (e.g., 1 week before harvest) or directly under white light with supplemental red light.

Supplemental Upward Lighting can Improve Plant Growth by Retarding Senescence of the Outer Leaves as Well as by Increasing Photosynthesis Rate

Plant cultivation at the high density used inside PFALs increases the annual production capacity per unit area (Kozai, 2013b). However, the outer leaves of plants grown at this high plant density cannot receive sufficient light from above and thus senesce faster. Our results confirm this hypothesis: the chlorophyll content and the maximum potential photochemical efficiency (F_v/F_m) both decreased drastically in the outer leaves without supplemental upward lighting (**Figures 2A,E**), which are typical phenomena when leaves senesce (Thimann and Satler, 1979; Wingler et al., 2004). However, our results clearly show that the upward lighting maintained a higher chlorophyll content (**Figures 2B,C**) and higher F_v/F_m (**Figures 2F,G**) in the outer leaves, indicating retardation of senescence. Moreover, it was apparent that the supplemental lighting promoted photosynthesis in the outer leaves, whereas the plants without supplemental lighting had a negative carbon balance (**Figure 3B**). This interpretation is supported by the higher nitrogen content in the outer leaves of plants with supplemental lighting (Supplementary Table S2). Nitrogen is a major component

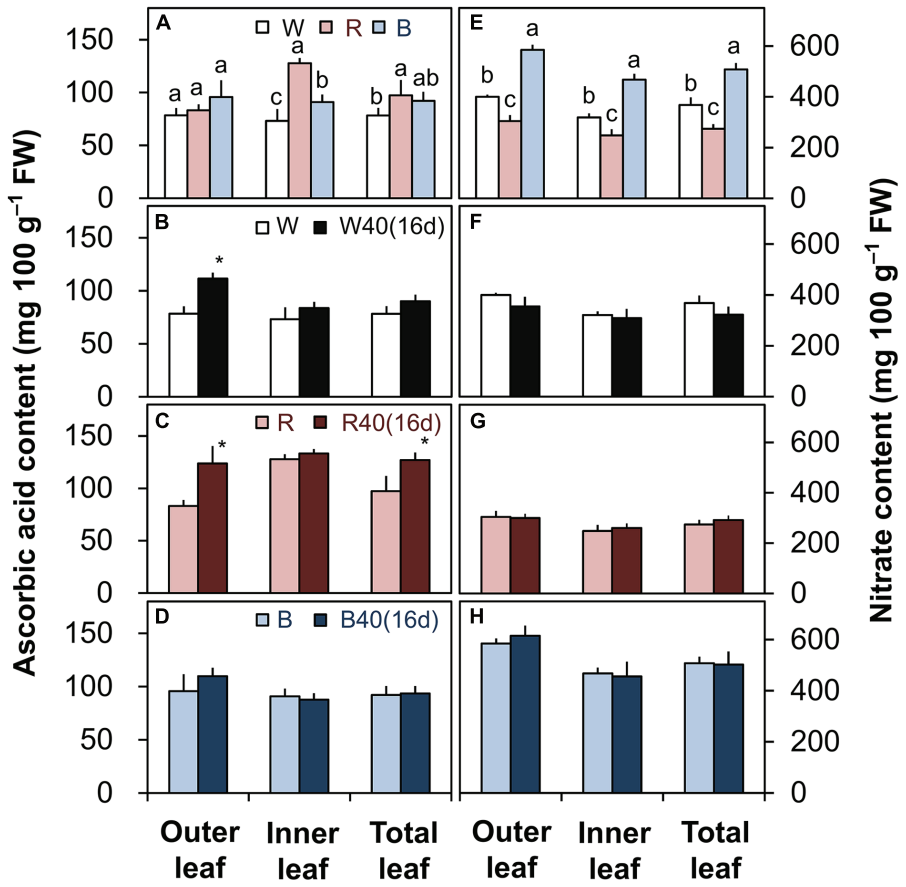

FIGURE 6 | Ascorbic acid (A–D) and nitrate contents (E–H) in the outer leaves, inner leaves, and total leaves of lettuce plants grown under downward lighting by white (W), red (R), or blue (B) LEDs: (A,E) without or (B–D,F–H) with supplemental upward lighting at 40 μmol m^{-2} s^{-1} PPFD for 16 days ("16d"). Data represent means ± SD ($n = 3$ to 5). **(A,E)** Bars labeled with different letters differ significantly among the same plant parts (Tukey's HSD test, $P < 0.05$). **(B–D,F–H)** Bars labeled with "*" differ significantly between treatments (Student's *t*-test, $P < 0.05$).

of stromal enzymes and thylakoid proteins, so its availability strongly affects the plant's photosynthetic capacity (Evans, 1989; Yamori et al., 2011). These results demonstrate that supplemental upward lighting both retarded leaf senescence and improved photosynthesis in the outer leaves, and that this increased plant yields (**Figures 4B,C**). Given the higher plant production, we propose that a novel cultivation system should be developed that includes supplemental upward lighting from below the plants to optimize the light conditions in PFALs. However, it will be necessary to perform additional research to determine whether the best results can be obtained with a single light color or a combination of colors.

It should also be noted that the effect of supplemental upward lighting could differ among plant species and light colors, as well as being a function of the plant qualities (e.g., total biomass, nutrient content) the breeder prioritizes. In the present study, the plants grown under blue LEDs grew more erect (Supplementary Figure S4, Supplementary Table S4) and therefore could not efficiently absorb the upward lighting (**Figures 2D,H** and **4D**). Thus, it is necessary to select suitable plant species and light sources for this cultivation method. Further research will be needed to optimize the cultivation system using supplemental upward lighting.

Economic Benefit Analysis of Supplemental Upward Lighting

Because of the vertical cultivation pattern (**Figure 1**), a PFAL with 10 tiers of plants can have an annual production capacity of leafy vegetables that is 90–117 times the values that can be achieved in an open field (Kozai, 2013b). The largest PFAL in Japan (Spread Inc., Kyoto, Japan) can produce 21,000 lettuce heads per day, and the largest one in Taiwan (Yasai Corp., Taiwan) can produce 40,000 per day. Although these production rates are extremely high, yield losses caused by outer leaf senescence are also large. Based on total and marketable leaf fresh weights of 153.7 and 134.0 g, respectively, under white downward lighting from above with no supplemental upward lighting (Supplementary Table S3), senescence of the outer leaves in these operations could cause losses of 413.7 kg FW/day in the Japanese PFAL and 788.0 kg FW/day in the Taiwanese PFAL. The present results clearly show that the wastage rate can be significantly decreased by the use of supplemental upward lighting (**Figures 5B,C**). Thus,

supplemental upward lighting to delay senescence of outer leaves could be an attractive way to solve this problem while also decreasing labor requirements to remove the senesced leaves.

To analyze the economic benefits of the supplemental upward lighting, it is necessary to account for the energy cost of the lighting. Supplementary Table S5 provides this comparison based on an electricity cost of 17.49 JPY/kW h, and the difference between the net retail price of the lettuce plants with and without supplemental upward lighting (i.e., the net income of the supplemental upward lighting). In the 9-day treatments, white LEDs (11.5 JPY/plant) produced a higher net income than red LEDs (1.62 JPY/plant), and blue LEDs (−2.27 JPY/plant). The results were similar for the 16-day treatment: the highest net income was again obtained with white LEDs (40.3 JPY/plant) followed by red LEDs (20.9 JPY/plant) and blue LEDs (−3.56 JPY/plant). White LEDs with 16 days of supplemental upward white lighting yielded the highest biomass (158.0 g/plant) and the highest net income (40.3 JPY/plant). The net incomes calculated in this analysis don't include the savings that result from decreasing the labor cost for trimming of senesced leaves during packing, and thus the net benefit would be greater than our estimates. Although the 9-day supplemental treatments would reduce the electricity costs, plant biomass and net income increased less than in the 16-day treatments (Supplementary Table S5). Thus, in order to increase production and net income, it is better to provide supplemental upward lighting for 16 days or even longer (e.g., from transplanting to harvest). However, determining the optimal duration and spectral characteristics of the supplemental light remains a challenge for future research.

AUTHOR CONTRIBUTIONS

GZ and WY conceived and designed the experiments. GZ performed the experiments. GZ and WY prepared the manuscript, and WY, GZ, SS, TK, and MT contributed extensively to its finalization.

ACKNOWLEDGMENT

We would like to thank Dr. L. Irving and Dr. N. Lu for valuable comments on the manuscript.

SUPPLEMENTARY MATERIAL

The Supplementary Material for this article can be found online at: http://journal.frontiersin.org/article/10.3389/fpls.2015.01110

REFERENCES

Björkman, O. (1981). "Responses to different quantum flux densities," in *Physiological Plant Ecology I*, eds O. L. Lange, P. S. Nobel, C. B. Osmond, and H. Ziegler (Berlin: Springer-Verlag), 57–107. doi: 10.1007/978-3-642-68090-8_4

Bliznikas, Z., Žukauskas, A., Samuoliene, G., Viršile, A., Brazaityte, A., Jankauskiene, J., et al. (2012). Effect of supplementary pre-harvest LED lighting on the antioxidant and nutritional properties of green vegetables. *Acta Hortic.* 939, 85–91. doi: 10.17660/ActaHortic.2012.939.10

Brouwer, B., Ziolkowska, A., Bagard, M., Keech, O., and Gardeström, P. (2012). The impact of light intensity on shade-induced leaf senescence. *Plant Cell Environ.* 35, 1084–1098. doi: 10.1111/j.1365-3040.2011.02474.x

Brown, C. S., Schuerger, A. C., and Sager, J. C. (1995). Growth and photomorphogenesis of pepper plants under red light-emitting diodes with supplemental blue or far-red lighting. *J. Am. Soc. Hortic. Sci.* 120, 808–813.

Causin, H. F., Jauregui, R. N., and Barneix, A. J. (2006). The effect of light spectral quality on leaf senescence and oxidative stress in wheat. *Plant Sci.* 171, 24–33. doi: 10.1016/j.plantsci.2006.02.009

Damilano, B., Grandjean, N., Pernot, C., and Massies, J. (2001). Monolithic white light emitting diodes based on InGaN/GaN multiple-quantum wells. *Jpn. J. Appl. Phys.* 40:L918. doi: 10.1143/JJAP.40.L918

Evans, J. R. (1989). Photosynthesis and nitrogen relationships in leaves of C3 plants. *Oecologia* 78, 9–19. doi: 10.1007/BF00377192

Gan, S., and Amasino, R. M. (1997). Making sense of senescence (molecular genetic regulation and manipulation of leaf senescence). *Plant Physiol.* 113, 313–319.

Goins, G. D., Yorio, N. C., Sanwo, M. M., and Brown, C. S. (1997). Photomorphogenesis, photosynthesis, and seed yield of wheat plants grown under red light-emitting diodes (LEDs) with and without supplemental blue lighting. *J. Exp. Bot.* 48, 1407–1413. doi: 10.1093/jxb/48.7.1407

Hu, M. C., Chen, Y. H., and Huang, L. C. (2014). A sustainable vegetable supply chain using plant factories in Taiwanese markets: a Nash-Cournot model. *Int. J. Prod. Econ.* 152, 49–56. doi: 10.1016/j.ijpe.2014.01.026

Kim, H. H., Wheeler, R. M., Sager, J. C., Goins, G. D., and Norikane, J. H. (2006). Evaluation of lettuce growth using supplemental green light with red and blue light-emitting diodes in a controlled environment-a review of research at Kennedy Space Center. *Acta Hortic.* 711, 111–119. doi: 10.17660/ActaHortic.2006.711.11

Kozai, T. (2013a). Resource use efficiency of closed plant production system with artificial light: concept, estimation and application to plant factory. *Proc. Jpn. Acad. Ser. B Phys. Biol. Sci.* 89, 447–461. doi: 10.2183/pjab.89.447

Kozai, T. (2013b). Plant factory in Japan - current situation and perspectives. *Chron. Hortic.* 53, 8–11.

Lee, J. G., Oh, S. S., Cha, S. H., Jang, Y. A., Kim, S. Y., Um, Y. C., et al. (2010). Effects of red/blue light ratio and short-term light quality conversion on growth and anthocyanin contents of baby leaf lettuce. *J. Bio-Environ. Control* 19, 351–359.

Lin, K. H., Huang, M. Y., Huang, W. D., Hsu, M. H., Yang, Z. W., and Yang, C. M. (2013). The effects of red, blue, and white light-emitting diodes on the growth, development, and edible quality of hydroponically grown lettuce (*Lactuca sativa* L. var. *capitata*). *Sci. Hortic.* 150, 86–91. doi: 10.1016/j.scienta.2012.10.002

Massa, G. D., Kim, H. H., Wheeler, R. M., and Mitchell, C. A. (2008). Plant productivity in response to LED lighting. *HortScience* 43, 1951–1956.

Matsuda, R., Ohashi-Kaneko, K., Fujiwara, K., and Kurata, K. (2007). Analysis of the relationship between blue-light photon flux density and the photosynthetic properties of spinach (*Spinacia oleracea* L.) leaves with regard to the acclimation of photosynthesis to growth irradiance. *Soil Sci. Plant Nutr.* 53, 459–465. doi: 10.1111/j.1747-0765.2007.00150.x

McCabe, M. S., Garratt, L. C., Schepers, F., Jordi, W. J., Stoopen, G. M., Davelaar, E., et al. (2001). Effects of PSAG12-IPT gene expression on development and senescence in transgenic lettuce. *Plant Physiol.* 127, 505–516. doi: 10.1104/pp.010244

McCree, K. J. (1972). The action spectrum, absorptance and quantum yield of photosynthesis in crop plants. *Agric. Meteorol.* 9, 191–216. doi: 10.1016/0002-1571(71)90022-7

Okamoto, K., Yanagi, T., Takita, S., Tanaka, M., Higuchi, T., Ushida, Y., et al. (1996). Development of plant growth apparatus using blue and red LED as artificial light source. *Acta Hortic.* 440, 111–116. doi: 10.17660/ActaHortic.1996.440.20

Pantelidis, G. E., Vasilakakis, M., Manganaris, G. A., and Diamantidis, G. (2007). Antioxidant capacity, phenol, anthocyanin and ascorbic acid contents in raspberries, blackberries, red currants, gooseberries and Cornelian cherries. *Food Chem.* 102, 777–783. doi: 10.1016/j.foodchem.2006.06.021

Porra, R. J., Thompson, W. A., and Kriedemann, P. E. (1989). Determination of accurate extinction coefficients and simultaneous equations for assaying chlorophylls a and b extracted with four different solvents: verification of the concentration of chlorophyll standards by atomic absorption spectroscopy. *Biochim. Biophys. Acta (BBA)-Bioenergetics* 975, 384–394. doi: 10.1016/S0005-2728(89)80347-0

Shao, L., Chen, X. W., Chen, Y. J., Sun, B. Y., Chow, W., and Peng, C. (2013). Differential responses of photosystem II activity to photooxidation in red and green tissues of *Amaranthus tricolor* leaves. *Pakistan J. Bot.* 45, 1905–1912.

Soares, A. S., Driscoll, S. P., Olmos, E., Harbinson, J., Arrabaça, M. C., and Foyer, C. H. (2008). Adaxial/abaxial specification in the regulation of photosynthesis and stomatal opening with respect to light orientation and growth with CO_2 enrichment in the C4 species *Paspalum dilatatum*. *New Phytol.* 177, 186–198. doi: 10.1111/j.1469-8137.2007.02218.x

Son, K. H., and Oh, M. M. (2013). Leaf shape, growth, and antioxidant phenolic compounds of two lettuce cultivars grown under various combinations of blue and red light-emitting diodes. *HortScience* 48, 988–995.

Taguchi, T. (2003). Present status of white LED lighting technologies in Japan. *J. Light Vis. Environ.* 27, 131–139. doi: 10.2150/jlve.27.131

Terashima, I. (1986). Dorsiventrality in photosynthetic light response curves of a leaf. *J. Exp. Bot.* 37, 399–405. doi: 10.1093/jxb/37.3.399

Terashima, I., Araya, T., Miyazawa, S. I., Sone, K., and Yano, S. (2005). Construction and maintenance of the optimal photosynthetic systems of the leaf, herbaceous plant and tree: an eco-developmental treatise. *Ann. Bot.* 95, 507–519. doi: 10.1093/aob/mci049

Thimann, K. V., and Satler, S. O. (1979). Relation between leaf senescence and stomatal closure: senescence in light. *Proc. Natl. Acad. Sci. U.S.A.* 76, 2295–2298. doi: 10.1073/pnas.76.6.2770

Weaver, L. M., and Amasino, R. M. (2001). Senescence is induced in individually darkened *Arabidopsis* leaves, but inhibited in whole darkened plants. *Plant Physiol.* 127, 876–886. doi: 10.1104/pp.010312

Wingler, A., Marès, M., and Pourtau, N. (2004). Spatial patterns and metabolic regulation of photosynthetic parameters during leaf senescence. *New Phytol.* 161, 781–789. doi: 10.1111/j.1469-8137.2004.00996.x

Xie, Z., Charles, M. T., Charlebois, D., Rolland, D., Roussel, D., Deschênes, M., et al. (2015). Preharvest exposure to UV-C radiation: impact on strawberry fruit quality. *Acta Hortic.* 1079, 589–592. doi: 10.17660/ActaHortic.2015.1079.79

Yamori, W., Nagai, T., and Makino, A. (2011). The rate-limiting step for CO_2 assimilation at different temperatures is influenced by the leaf nitrogen content in several C3 crop species. *Plant Cell Environ.* 34, 764–777. doi: 10.1111/j.1365-3040.2011.02280.x

Yamori, W., Noguchi, K., Hikosaka, K., and Terashima, I. (2009). Cold-tolerant crop species have greater temperature homeostasis of leaf respiration and photosynthesis than cold-sensitive species. *Plant Cell Physiol.* 50, 203–215. doi: 10.1093/pcp/pcn189

Yamori, W., Noguchi, K., Hikosaka, K., and Terashima, I. (2010). Phenotypic plasticity in photosynthetic temperature acclimation among crop species with different cold tolerances. *Plant Physiol.* 152, 388–399. doi: 10.1104/pp.109.145862

Yamori, W., Noguchi, K., and Terashima, I. (2005). Temperature acclimation of photosynthesis in spinach leaves: analyses of photosynthetic components and temperature dependencies of photosynthetic partial reactions. *Plant Cell Environ.* 28, 536–547. doi: 10.1111/j.1365-3040.2004.01299.x

Yamori, W., Zhang, G., Takagaki, M., and Maruo, T. (2014). Feasibility study of rice growth in plant factories. *Rice Res. Open Access* 2, 119. doi: 10.4172/jrr.1000119

Yanagi, T., Okamoto, K., and Takita, S. (1996). Effects of blue, red, and blue/red lights of two different PPF levels on growth and morphogenesis of lettuce plants. *Acta Hortic.* 440, 117–122. doi: 10.17660/ActaHortic.1996.440.21

Yorio, N. C., Goins, G. D., Kagie, H. R., Wheeler, R. M., and Sager, J. C. (2001). Improving spinach, radish, and lettuce growth under red light-emitting diodes (LEDs) with blue light supplementation. *HortScience* 36, 380–383.

Conflict of Interest Statement: The authors declare that the research was conducted in the absence of any commercial or financial relationships that could be construed as a potential conflict of interest.

frontiers in Plant Science

ORIGINAL RESEARCH
published: 27 July 2016
doi: 10.3389/fpls.2016.01114

Circadian Oscillation of the Lettuce Transcriptome under Constant Light and Light–Dark Conditions

*Takanobu Higashi[1], Koh Aoki[1], Atsushi J. Nagano[2,3,4], Mie N. Honjo[4] and Hirokazu Fukuda[5,6]**

[1] Graduate School of Life and Environmental Sciences, Osaka Prefecture University, Sakai, Japan, [2] Faculty of Agriculture, Ryukoku University, Otsu, Japan, [3] Core Research for Evolutional Science and Technology – Japan Science and Technology Agency, Kawaguchi, Japan, [4] Center for Ecological Research, Kyoto University, Otsu, Japan, [5] Graduate School of Engineering, Osaka Prefecture University, Sakai, Japan, [6] Precursory Research for Embryonic Science and Technology, Japan Science and Technology Agency, Kawaguchi, Japan

Although, the circadian clock is a universal biological system in plants and it orchestrates important role of plant production such as photosynthesis, floral induction and growth, there are few such studies on cultivated species. Lettuce is one major cultivated species for both open culture and plant factories and there is little information concerning its circadian clock system. In addition, most of the relevant genes have not been identified. In this study, we detected circadian oscillation in the lettuce transcriptome using time-course RNA sequencing (RNA-Seq) data. Constant light (LL) and light–dark (LD) conditions were used to detect circadian oscillation because the circadian clock has some basic properties: one is self-sustaining oscillation under constant light and another is entrainment to environmental cycles such as light and temperature. In the results, 215 contigs were detected as common oscillating contigs under both LL and LD conditions. The 215 common oscillating contigs included clock gene-like contigs *CCA1* (*CIRCADIAN CLOCK ASSOCIATED 1*)-like, *TOC1* (*TIMING OF CAB EXPRESSION 1*)-like and *LHY* (*LATE ELONGATED HYPOCOTYL*)-like, and their expression patterns were similar to those of *Arabidopsis*. Functional enrichment analysis by GO (gene ontology) Slim and GO Fat showed that the GO terms of response to light stimulus, response to stress, photosynthesis and circadian rhythms were enriched in the 215 common oscillating contigs and these terms were actually regulated by circadian clocks in plants. The 215 common oscillating contigs can be used to evaluate whether the gene expression pattern related to photosynthesis and optical response performs normally in lettuce.

Keywords: circadian clocks, enrichment, lettuce, oscillations, plant factories, transcriptome

OPEN ACCESS

Edited by:
Alejandro Isabel Luna-Maldonado, Universidad Autónoma de Nuevo León, Mexico

Reviewed by:
Biswapriya Biswavas Misra, University of Florida, USA
Hao Peng, Washington State University, USA

****Correspondence:***
Hirokazu Fukuda
fukuda@me.osakafu-u.ac.jp

Specialty section:
This article was submitted to Crop Science and Horticulture, a section of the journal Frontiers in Plant Science

Received: *12 May 2016*
Accepted: *13 July 2016*
Published: *27 July 2016*

Citation:
Higashi T, Aoki K, Nagano AJ, Honjo MN and Fukuda H (2016) Circadian Oscillation of the Lettuce Transcriptome under Constant Light and Light–Dark Conditions. Front. Plant Sci. 7:1114. doi: 10.3389/fpls.2016.01114

INTRODUCTION

The circadian clock is a universal biological system in plants that has been well-studied in *Arabidopsis* (Harmer et al., 2000; Haydon et al., 2011; Farré and Weise, 2012). The circadian clock consists of three components: input, central oscillator and output pathways. Each component involves a number of genes. *PHY*s (*PHYTOCHROME*s), *CRY*s (*CRYPTOCHROME*s), and *PHOT*s

(*PHOTOTROPIN*s) are the best-known light receptor genes of input pathways and transmit external light stimuli to the central oscillator (Christie, 2007; Pruneda-Paz and Kay, 2010). *CCA1* (*CIRCADIAN CLOCK ASSOCIATED 1*), *LHY* (*LATE ELONGATED HYPOCOTYL*), *TOC1* (*TIMING OF CAB EXPRESSION 1*) and *PRR*s (*PSEUDO-RESPONSE REGULATORs*) are central oscillator genes – they are known as clock genes and are important in generating the circadian rhythm (Gardner et al., 2006; Nakamichi et al., 2010, 2012). *CO* (*CONSTANS*) and *FT* (*FLOWERING LOCUS T*) are downstream genes of circadian clocks in the output pathways and regulate flowering (Suárez-López et al., 2001; Corbesier et al., 2007). Recent study indicated that circadian clocks control several physiological events such as photosynthesis and stress response (Dodd et al., 2005, 2014; Covington et al., 2008; Lai et al., 2012). In addition, controlling circadian clocks has potential to enhance productivity of cultivated species such as broccoli, petunia and lettuce by effects on growth, floral induction and pest resistance (Goodspeed et al., 2013; Fenske et al., 2015; Higashi et al., 2015; Tanigaki et al., 2015; Thiruvengadam et al., 2015; Zhai et al., 2015). These results show that controlling circadian clocks has potential to achieve high efficiency in plant production. Because circadian clocks are readily controlled by external stimuli, especially light and temperature, one target among plant production systems is closed-type plant factories as environmental parameters are readily tightly controlled (Rensing and Ruoff, 2002; Fukuda et al., 2013).

Lettuce is a typical crop in closed-type plant factories because it is suitable for hydroponic culture and can be cultivated under a low-light conditions (Li et al., 2016; Moriyuki and Fukuda, 2016; Wang et al., 2016). Lettuce is a diploid ($2n = 18$) species with genome size of 2.7 Gb (Truco et al., 2007, 2013); however, many genes including clock genes have not have been identified. Therefore, there are few studies on the circadian clock in lettuce. One application suited to analyzing the behavior of circadian clocks without genome information is RNA sequencing (RNA-Seq), a revolutionary tool for omics studies (Wang et al., 2009). RNA-Seq can obtain transcriptome information and oscillating genes (or contigs) can be detected from time-course RNA-Seq data (Nagano et al., 2012; Matsuzaki et al., 2015; Schick et al., 2016). To detect the oscillating contigs generated by the circadian clock, time-course transcriptome data of lettuce cultivated under both constant light (LL) and 12 h light and 12 h dark (LD) conditions are needed. Circadian clocks have some basic properties: one is self-sustaining oscillation under constant light or dark conditions and the other is entrainment to environmental fluctuations such as light and temperature (Nakamichi et al., 2004). Thus, oscillating contigs generated by circadian clocks cannot correctly be detected using only one of the two light conditions.

In this study, we tried to detect the oscillating contigs generated by circadian clocks using time-course transcriptome data of lettuce, which is a typical crop in closed-type plant factories. We performed the experiments under LL and LD conditions and detected the oscillating contigs common to both. In addition, we also used homology and gene ontology (GO) analysis to estimate the function of the oscillating contigs in lettuce.

MATERIALS AND METHODS

Plant Materials and Growing Systems

Lettuce plants (*Lactuca sativa* L. cv. Frill Ice from Snow Brand Seed, Co. Ltd, Hokkaido, Japan) were grown in a closed cultivation system. Seeds were sown on a water-laden urethane sponge in a tray (400 mm × 280 mm × 70 mm) filled with water and incubated for a week under fluorescent light [photosynthetic photon flux density (PPFD) = 250–450 μmol m^{-2} s^{-1}]. The environmental parameters of germination and growing conditions were 22°C and 12-h light and 12-h darkness (12L:12D).

After 1 week, seedlings were transplanted to the multistage hydroponic system. The light sources used were red, green and blue LEDs (660, 520, and 450 nm, respectively; Shibasaki, Inc., Saitama, Japan). Cultivation was performed using a Deep Flow Technique hydroponic system. A submersible pump was placed in a tank containing the culture medium to maintain constant circulation at 10–15 L min^{-1}, and a total of three cultivation beds (2720 mm × 640 mm × 150 mm; Sanki Keiso, Co. Ltd, Saitama, Japan) were filled with the culture medium at a specified constant pH and electric conductivity (EC). In each bed, three cultivation panels (885 mm × 590 mm × 30 mm; M Hydroponic Research, Co. Ltd, Aichi, Japan) were installed with open planting holes and root zones at a water depth of 90 mm. The inter-hole distance was 70 mm across the length and 100 mm across the width. The cultivation medium was composed of tap water and fertilizer ($N:P_2O_5:K_2O:CaO:MgO$ = 10:8:27:0:4 and 11:0:0:23:0; Otsuka House No. 1 and 2, respectively; Otsuka Chemical, Co. Ltd, Osaka, Japan) at pH 6.0 and EC 2.0. The pH and EC settings were performed with reference to the Otsuka Chemical standard solution formulations. Transplanted seedlings were grown in the multistage hydroponic system for 15 days. The environmental parameters were 22°C, 50% relative humidity, 1000 μmol mol^{-1} CO_2 concentration and LL or LD, with R:G:B = 120:40:40; total PPFD = 180–220 μmol m^{-2} s^{-1}. In the LL experiment, light condition was set 12L:12D and switched to LL at 12 days after transplanting because the oscillating component disappears if cultivated continuously under LL condition for a long time (Nakamichi et al., 2004; Higashi et al., 2014).

We sampled the largest leaves every 2 h for 2 days, starting at 13 days and ending 15 days after transplanting. These leaves were immediately frozen in liquid nitrogen and stored at −80°C.

RNA-Seq Assay and Data Analysis

We applied DNase treatment to reduce DNA contamination and isolated total RNA using an RNeasy Plant Mini Kit (Qiagen). Its quality was checked using an Agilent 2100 Bioanalyzer (Agilent Technologies, Palo Alto, CA, USA). RNA quantity control was performed using a Qubit® 2.0 Fluorometer (Life Technologies, Carlsbad, CA, USA). We prepared a RNA-Seq library (Wang et al., 2011; Nagano et al., 2015). Then we obtained the sequence

read files using a HiSeq 2000 sequencer (single end, 50 bp; Illumina, San Diego, CA, USA). These sequence data are available in the DDBJ Sequenced Read Archive[1] under the accession numbers DRA004542 and DRA004561.

All reads of each sample were quality-checked by FastQC and mapped using RSEM (RNA-Seq by Expectation Maximization; Li and Dewey, 2011) with Bowtie2 software (Langmead and Salzberg, 2012) to the predicted transcriptome models in the NCBI database[2]. We confirmed about 90% of the bases were aligned to these models (Supplementary Table S1). By these processes, we obtained the data of expression levels of contig for each sample. Finally, we used the reads per kilobase per million mapped reads measure to normalize the expression for total read length and the number of sequencing reads.

Clock gene expression data of *Arabidopsis thaliana* were obtained from the Diurnal database[3]. We obtained time-course clock gene expression data at 4-h intervals using LLHC [LL combined with temperature of hot and cool (HC) at 12-h intervals] and LDHC (LD combined with HC) conditions. We normalized each expression level using their averages and standard deviations. The normalized expression level was calculated as the value of expression level minus average expression level, divided by the standard deviation.

Detection of Oscillating Contigs

We utilized the molecular timetable method (Ueda et al., 2004; Higashi et al., 2016) to detect oscillating contigs for LL and LD conditions. This method can detect some genes with high amplitude and periodicity from the time-course transcriptome data. Furthermore, it can detect collective behavior of oscillating genes by developing expression profiles.

First we selected contigs whose expression indicated high amplitude and periodicity. The amplitude value (a) was calculated as the standard deviation divided by the average of expression level. To analyze periodicity, we prepared 1440 test cosine curves. These curves had different peaks (0–24 h) measured at 1-min increments. We fitted test cosine curves to data from each time-course transcriptome generated via RNA-Seq and calculated the correlation value (r) to identify the best-fitting cosine curve. The peak time of the best-fitting curve was estimated as the peak time for each contig. This estimated peak time was defined as the molecular peak time. We set the cut-off values of $a = 0.15$ and $r = 0.8$, according to values from Ueda et al. (2004). Then we normalized expression level of oscillating contigs using their averages and standard deviations. The normalized expression level was calculated as the value of expression level minus average expression level, divided by the standard deviation.

Second, we selected common contigs detected as oscillating contigs by the molecular timetable method under both LL and LD conditions. Hereby, we detected oscillating contigs independent of light conditions.

Finally, the oscillating contigs were submitted to the BLAST program to undertake GO analysis and improve reliability as the subsistent genes. The cut-off values were minimal E-value of 10^{-20} and minimal query cover and identity of 60% for BLASTn and BLASTx between oscillating contigs and the NCBI database. Oscillating contigs were initially submitted to BLASTn and then non-hit contigs were submitted to BLASTx.

Calculation of Measurement Noise

We calculated the measurement noise for the expression profiles of common oscillating contigs, using a previous molecular timetable method (Ueda et al., 2004; Higashi et al., 2016). We calculated the measurement noise from the standard deviation of the difference between a real and an estimated expression of all selected oscillating contigs.

Functional Categorization by GO Slim and GO Fat

Functional categorization by GO Slim was performed using the TAIR10 database[4]. Corresponding *Arabidopsis* orthologs for detected oscillating contigs were determined by KEGG database[5] using several plant gene identifications obtained by BLAST result.

Functional categorization by GO Fat was performed using the DAVID database[6]. The GO Fat database contains more specific terms than the GO database (Dennis et al., 2003). We used *Arabidopsis* TAIR ID as input information for the oscillating contigs and used GO Fat with default status.

Functional Enrichment Analysis

Functional enrichment analysis for oscillating contigs was performed using the Biological Networks Gene Ontology (BiNGO) software (Maere et al., 2005). BiNGO is an open-source Java tool and can be used as a Cytoscape plugin[7] (Shannon et al., 2003). We also used *Arabidopsis* TAIR ID as the input information for the oscillating contigs and performed functional enrichment analysis with default status.

RESULTS

Detection of Oscillating Contigs under Both LL and LD Conditions

First, we determined oscillating contigs for LL and LD conditions using the molecular timetable method. Under LL conditions, 1255 contigs were detected as oscillating (**Figure 1A**); under LD conditions, only 423 contigs were detected as oscillating. Next, we determined 279 common oscillating contigs for both LL and LD conditions; we used the BLAST program for functional analysis and to confirm identity of the subsistent genes. This resulted in 215 common oscillating contigs under both LL and

[1]http://trace.ddbj.nig.ac.jp/DRASearch

[2]http://www.ncbi.nlm.nih.gov/

[3]http://diurnal.mocklerlab.org/diurnal_data_finders/new

[4]https://www.arabidopsis.org

[5]http://www.genome.jp/kegg/

[6]https://david.ncifcrf.gov/home.jsp

[7]http://www.cytoscape.org

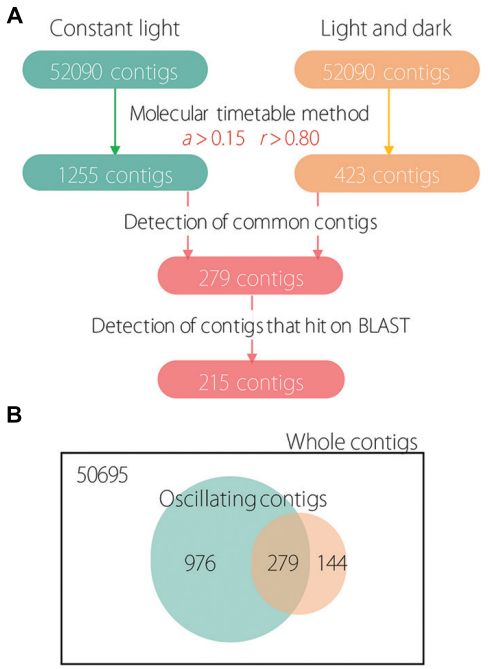

FIGURE 1 | Scheme of oscillating analysis and the number of detected contigs. (A) Numbers in colored boxes indicate the detected number of contigs. **(B)** Venn diagram showing unique and shared contigs under LL and LD conditions.

LD conditions (Supplementary Table S2). As a result, 972 and 144 contigs were detected as unique contigs that oscillated only under LL or LD conditions, respectively; and 279 contigs were detected as shared contigs that oscillated under both LL and LD conditions (**Figure 1B**).

The expression profiles of the 215 common oscillating contigs for each time point are shown in **Figure 2**. We confirmed that the collective behavior of the 215 contigs showed stable periodicity, hence each common oscillating contig was expressed periodically under both LL and LD conditions. Measurement noise of expression profiles under LL conditions was in the range of 30–61% [mean ± standard deviation of 40 ± 6%], and under LD conditions was 39–57% (49 ± 5%). Thus, measurement noise tended to be larger under LD than LL conditions.

Comparison of Expression Pattern between Lettuce Clock Gene-Like Contigs and *Arabidopsis* Clock Genes

Some clock gene-like contigs existed in 215 common oscillating contigs. *CCA1*, *LHY*, and *TOC1* are central oscillator genes in the circadian clock. *GI* (*GIGANTEA*) and *FKF1* (*FLAVIN-BINDING, KELCH REPEAT, F-BOX 1*) regulate flowering through regulation of transcription of *CO* gene. *CO* encodes the transcriptional regulator of *FT* and triggers floral induction. Every clock gene-like contig indicated periodic expression and these expression patterns were similar to those of *Arabidopsis* for LL and LD conditions (**Figure 3**).

Functional Categorization and Enrichment Analysis

We analyzed functional categorization of 215 common oscillating contigs using *Arabidopsis* orthologs by GO Slim. In the biological process (BP), 215 common oscillating contigs were especially enriched for the term of response to abiotic or biotic stimulus and response to stress except for other cellular and metabolic processes (**Figure 4A**). Contigs related to response to external stimulus accounted for a substantial fraction of the 215 common oscillating contigs. In the cellular component (CC), 215 common oscillating contigs were especially enriched for the terms of chloroplast and plastid related to photosynthesis (**Figure 4B**). In the molecular component (MC), 215 common oscillating contigs were especially enriched for terms of protein binding and hydrolase activity (**Figure 4C**). Furthermore, we analyzed more specific functional categorization using GO Fat. In each category, 215 common oscillating contigs were enriched for the terms related to light stimuli and photosynthesis, such as response to light stimulus, photosynthesis/light reaction, chloroplast part, photosystem, chlorophyll binding, and photoreceptor activity (Supplementary Table S3).

We performed BP-specific enrichment analysis using BiNGO software to visualize the result of BP concerning which category was linked to application for plant production. In the terms related to response to stimulus, contigs were enriched describing response to stress, abiotic stimulus and external stimulus (**Figure 5A**). In particular, response to blue light was significantly enriched compared to red or far red light. In the terms related to biological regulation, contigs describing regulation of cell size, circadian rhythm, flowering and anion channel activity in response to blue light were enriched (**Figure 5B**); overall, this category showed low enrichment compared to other categories. In the terms related to metabolic process, contigs were enriched describing photosynthesis and chlorophyll metabolic process (**Figure 5C**). In addition, thiamin biosynthesis process – a major nutrient for lettuce and related to stress response – was also enriched. Of other functions, contigs were enriched describing circadian rhythm, transport and chloroplast and plastid localization (**Figure 5D**). In particular, rhythmic process and circadian rhythm were significantly enriched.

DISCUSSION

The molecular timetable method clearly showed fewer detected oscillating contigs under LD than LL conditions (**Figure 1**). This indicated that the expression pattern of contigs under LD conditions approximated cosine curves (as fitted using the molecular timetable method) in time-course expression data to detect periodicity. This is likely due to the 'square wave' in the application of the light cycle, in which plants receive an instantaneous change in light stimulus at the time of light-on and light-off. These instantaneous light stimuli can be considered to affect gene expression as some noise. In fact, *CCA1* expression was not stable for the LD cycle with the square wave; however, it was stable under the LD cycle with a cosine curve in lettuce (Higashi et al., 2014). The effect of the square wave was also

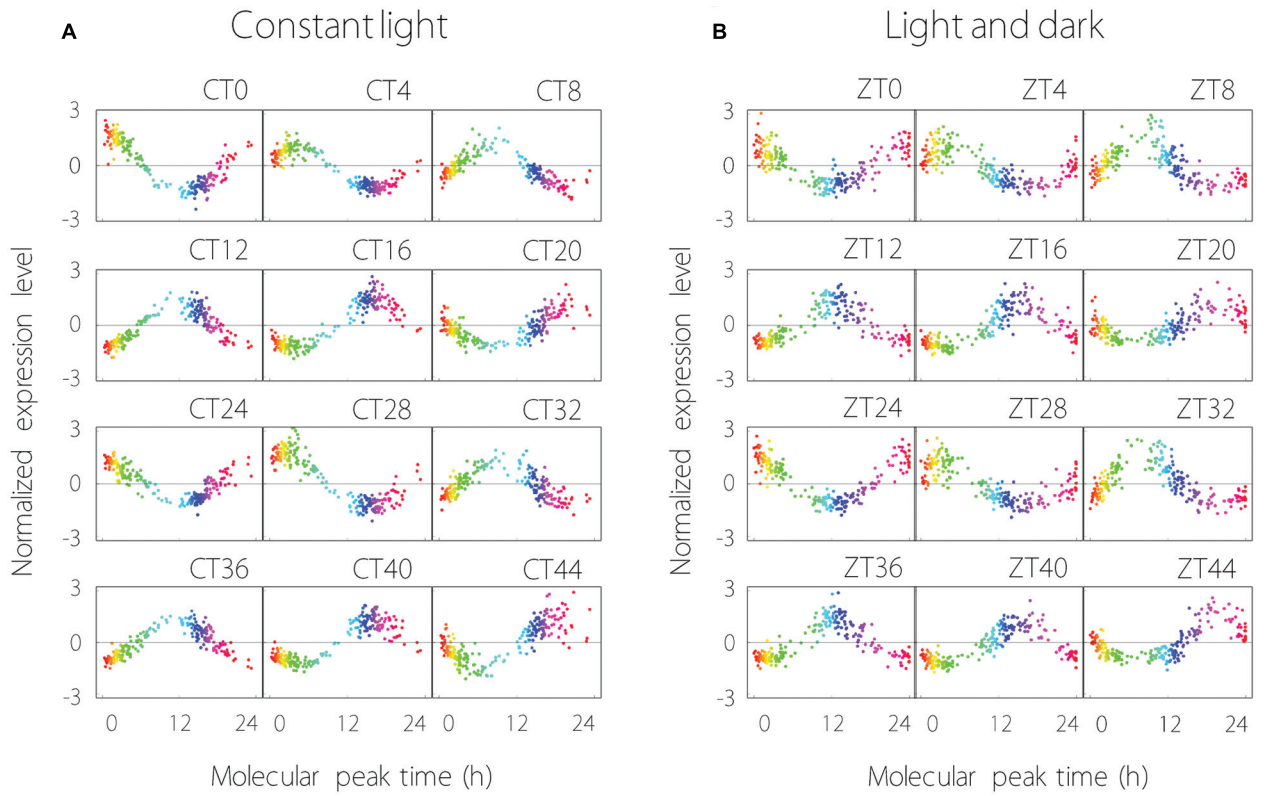

FIGURE 2 | Global analysis of 215 oscillating contigs using the molecular timetable method under LL (A) and LD (B) conditions. (A) The time at the top right of the plot area indicates sampling time. CT0 (Circadian Time 0) is the time at the first sampling point. The range from blue to pink represents subjective night-time. Each plot indicates individual contig expression. **(B)** ZT0 (Zeitgeber Time 0) is the time at the first sampling point. The range from blue to pink represents night-time. Each plot indicates individual contig expression.

evident in expression profiles of 215 common oscillating contigs. Although, expression profiles indicated periodicity for each light condition, measurement noise tended to be larger under LD than LL conditions. This suggests that the light cycle with a square wave caused some noise for gene expression in plants. The light cycle with a square wave may negatively affect plants because it is not present under natural conditions. In contrast, previous studies indicated that periodic gene expression was stable under fluctuating field conditions (Nagano et al., 2012; Matsuzaki et al., 2015; Higashi et al., 2016). In the present study, 144 contigs oscillated under LD but not under LL conditions (**Figure 1B**). This is not surprising, given that the periodicity of gene expression depends on light conditions and there was a clear difference between LL and LD conditions. In *Arabidopsis*, some CCA1 target genes indicated different expression patterns between LL and LD conditions (Nagel et al., 2015). In cyanobacteria, some genes whose expression exhibits periodicity under LL and LD conditions were detected by time-course transcriptional analysis (Toepel et al., 2008). The present study revealed that some periodic genes showed a differential expression pattern between LL and LD conditions. Furthermore, from the aspect of omics analysis, it was not always true that protein abundance indicated periodicity even though gene expression showed periodicity under LD condition in cyanobacteria (Waldbauer et al., 2012); however, they used only a light–dark specific analysis and did not consider a circadian clock system. In fact, coordination of transcriptome and metabolome by circadian clock system was revealed in mice and *Arabidopsis* (Fukushima et al., 2009; Eckel-Mahan et al., 2012). These omics studies suggest that the 215 common oscillating contigs detected in the lettuce transcriptome were probably coordinated by a circadian clock because they showed the self-sustaining oscillation characteristic of circadian clocks (Nakamichi et al., 2004; Higashi et al., 2014) and presumably the metabolome was coordinated on a periodic basis.

Clock gene-like contigs of lettuce existed in 215 common oscillating contigs and were expressed similarly to *Arabidopsis* under both LL and LD conditions. Although the expression period and peak phase had slight differences between lettuce and *Arabidopsis* under LL conditions, they seemed to depend on light quality. In a previous study, the period of circadian rhythm was altered by qualities such as red and blue light (Higashi et al., 2014). The differences in light quality might be shown in expression patterns. Furthermore, the expression pattern under LD conditions was noisy and did not clearly conform to a cosine curve compared to LL conditions. This supports that a light cycle with a square wave caused some noise and made it difficult to detect periodicity. The similarity

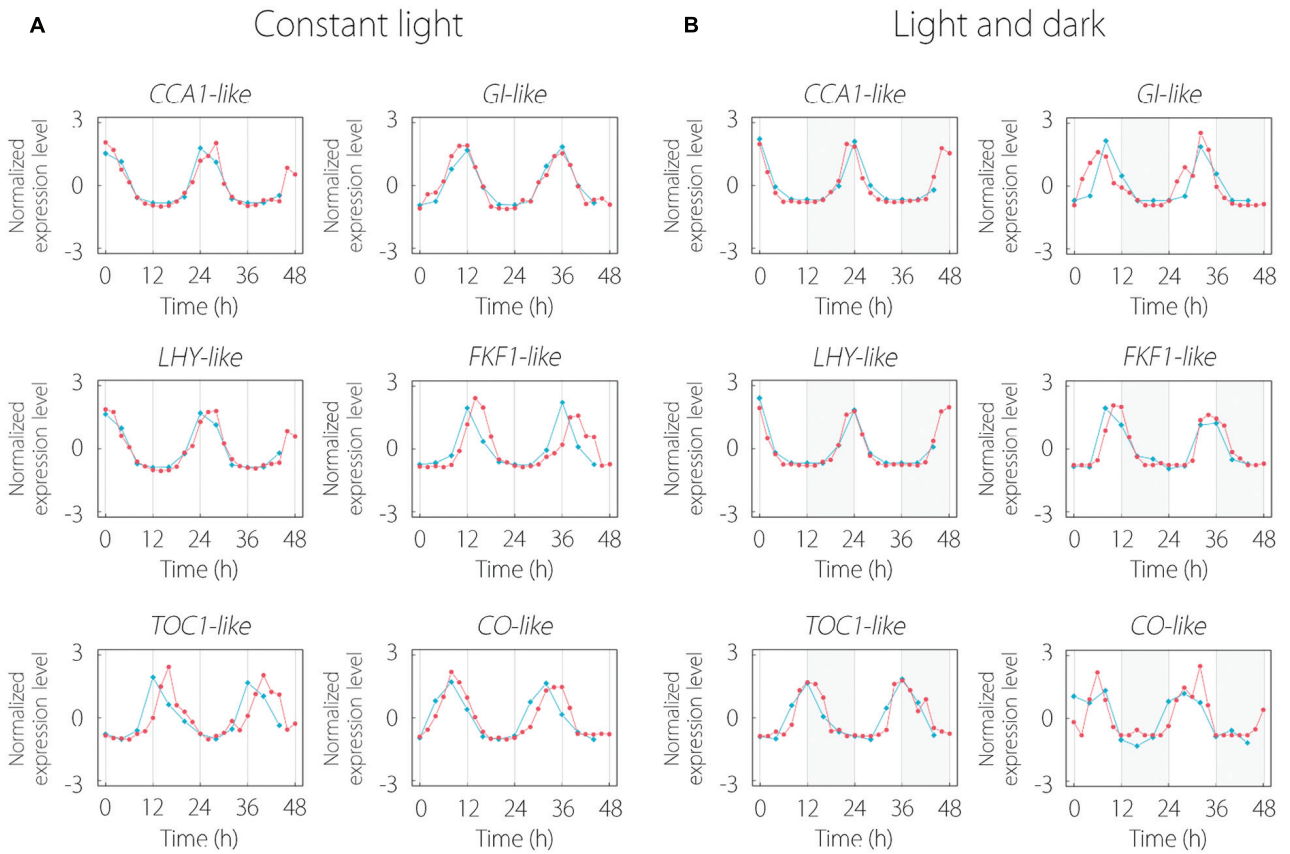

FIGURE 3 | Expression pattern of clock gene-like contigs under LL (A) and LD (B) conditions. The red and blue lines indicate the expression patterns in lettuce and *Arabidopsis*, respectively. Clock gene expression data of *Arabidopsis thaliana* were obtained from the Diurnal database. Gray area in **(B)** represents the dark period.

of expression pattern of clock gene-like contigs between lettuce and *Arabidopsis* seem to improve the reliability of determination of the subsistent genes because they had similar homology of alignment as well as expression pattern. In addition, the results suggest that detection of periodic contigs under both LL and LD conditions could reliably determine clock comprising genes by their periodic expression.

The functional categorization showed that the contigs related to the function of response to abiotic and biotic stimulus, response to stress and photosynthesis were the main part of the 215 common oscillating contigs (**Figure 4**). These results were particularly clarified by functional enrichment analysis (**Figure 5**). It is unsurprising that contigs related to the function of response to light stimulus were enriched because light stimulus is one effective external factor for circadian clocks (Barak et al., 2000; Alabadí et al., 2001; Fukuda et al., 2013). It is likely that response to blue light was significantly enriched. One likely reason is that *PHOT*s tended to express clear periodicity compared to *PHY*s and *CRY*s. The present study showed that 215 common oscillating contigs included both *PHOT1* and *PHOT2*. Actually, a previous study demonstrated that lettuce plants could receive low-intensity blue light and their circadian clock entrained to the weak blue light stimuli (Higashi et al., 2014) and both *PHOT1* and *PHOT2* also had clear periodic expression in tomato (Higashi et al., 2016). In contrast, *PHY*s and *CRY*s were not found to oscillate in either lettuce or tomato. Another reason is that some genes related to photosynthesis were also assigned the GO term for response to blue light. In rice, it was reported that stomatal opening, chloroplast movement and photosynthesis were activated by blue light signal (Lakshmanan et al., 2015), and these are major functions orchestrated by the circadian clock (Barak et al., 2000). Furthermore, recent studies indicated that the circadian clock regulates stress response (Harmer, 2009; Goodspeed et al., 2012; Lai et al., 2012; Marcolino-Gomes et al., 2014; Grundy et al., 2015). In the present study, oscillating contigs in lettuce showed similar results in that contigs related to the function of response to stress were significantly enriched. The enriched functions of the 215 common oscillating contigs such as response to light stimulus, response to stress and photosynthesis are important factors for plant production. This suggests that the 215 common oscillating contigs can be used as molecular markers for lettuce production. The valuable capabilities of molecular timetable methods can detect rhythm disorders and estimate the phase of the circadian clock from the expression profile of collective genes (Ueda et al., 2004). Therefore, it is possible to evaluate whether

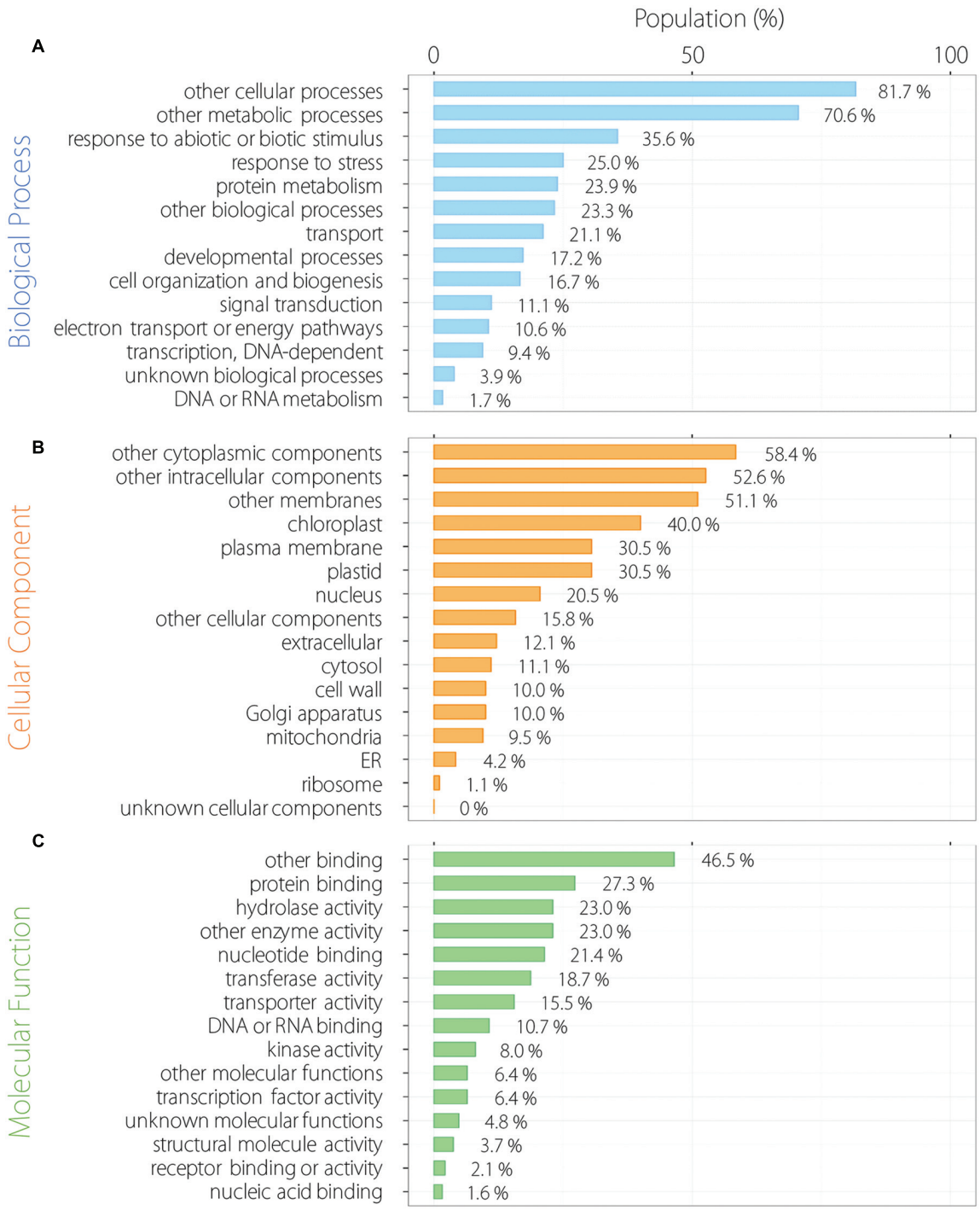

FIGURE 4 | Functional categorization of 215 oscillating contigs. Biological process **(A)**, cellular component **(B)** and molecular function **(C)**.

the gene expression pattern related to photosynthesis and optical response performs normally by analyzing periodicity of the 215 common oscillating contigs in lettuce. Moreover, a previous study showed that rhythm disorders and mismatching the phase of the circadian clock with the phase of environmental cycles caused poor growth in *Arabidopsis* (Dodd et al., 2005). Hence, the 215 common oscillating contigs may become molecular markers for determining optimal environmental cycles such as the LD ratio and temperature control in closed-type plant factories. This original approach has potential to be adapted to other cultivated plant with few genome resources and for application in closed-type plant factories.

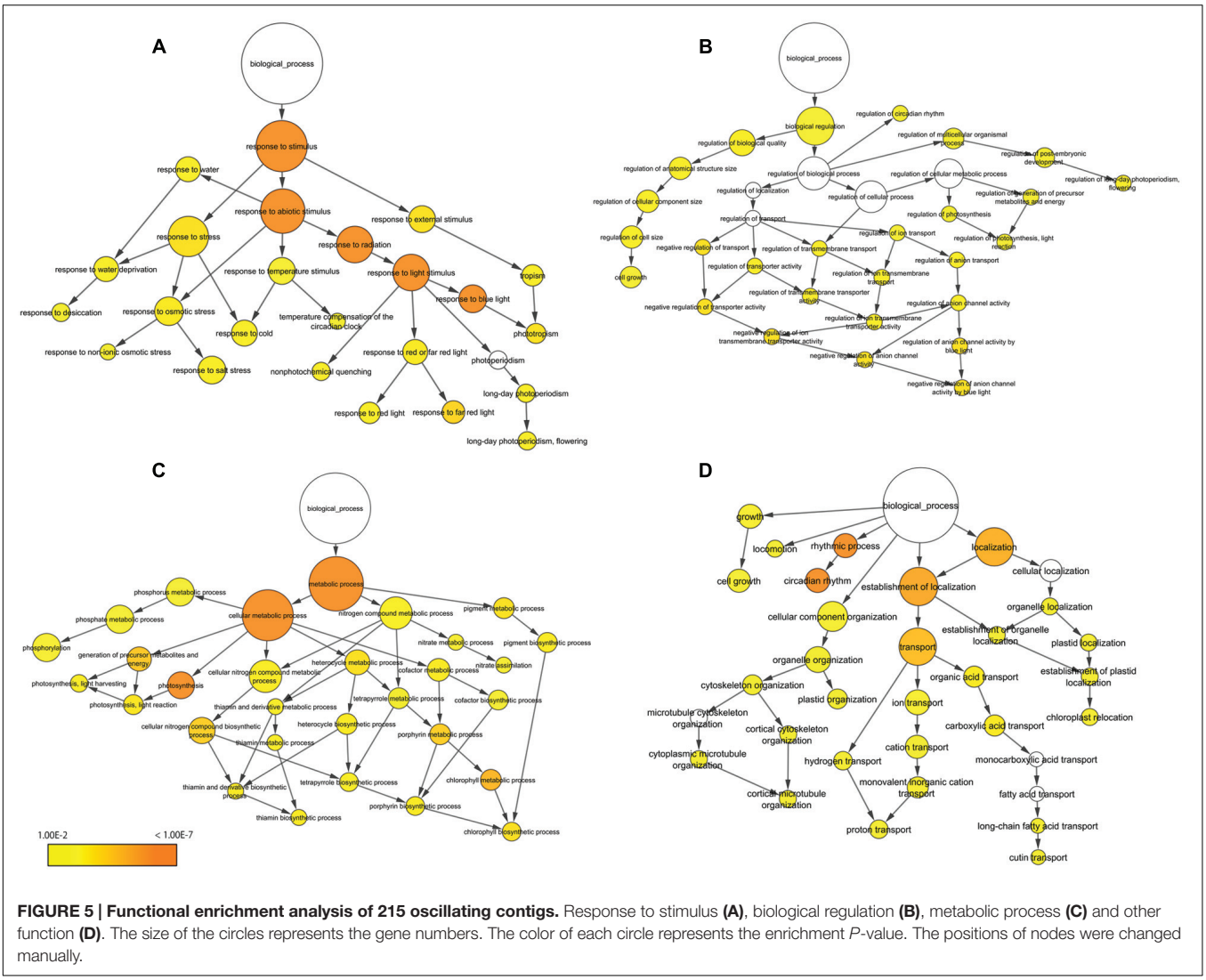

FIGURE 5 | Functional enrichment analysis of 215 oscillating contigs. Response to stimulus **(A)**, biological regulation **(B)**, metabolic process **(C)** and other function **(D)**. The size of the circles represents the gene numbers. The color of each circle represents the enrichment *P*-value. The positions of nodes were changed manually.

We detected 976 contigs as LL-specific oscillating contigs and 144 as LD-specific oscillating contigs. There were 279 contigs detected as LL–LD common oscillating contigs, which were generated by circadian clocks in lettuce and BLAST results conclusively showed that 215 common oscillating contigs were targeted. These 215 oscillating contigs included clock gene-like contigs such as *CCA1* and *TOC1*, which showed similar expression patterns to those of *Arabidopsis* under both LL and LD conditions, and are assumed to have important roles in the circadian clock system. The GO Slim and GO Fat analyses showed that the GO terms of response to light stimulus, response to stress, photosynthesis and circadian rhythms were enriched in the 215 oscillating contigs and these terms were actually regulated by circadian clocks in several plants.

AUTHOR CONTRIBUTIONS

HF and TH designed this research. KA revised this article critically. AN and MH prepared a RNA-Seq library. TH performed data analysis. TH and HF wrote the manuscript. All authors discussed the results and implications and commented on the manuscript.

ACKNOWLEDGMENT

We are grateful to Professor Hiroshi Kudoh for RNA-Seq and Dr. Yusuke Tanigaki for discussion. The present study was supported by the Joint Usage/Research Program of the Center for Ecological Research, Kyoto University. This study was partially supported by Grants-in-Aid for JSPS Fellows (No. 15J12133 to TH), Grants-in-Aid for Scientific Research (Nos. 25712029 and 25119721 to HF), PRESTO JST and the Canon Foundation.

SUPPLEMENTARY MATERIAL

The Supplementary Material for this article can be found online at: http://journal.frontiersin.org/article/10.3389/fpls.2016.01114

REFERENCES

Alabadí, D., Oyama, T., Yanovsky, M. J., Harmon, F. G., Más, P., and Kay, S. A. (2001). Reciprocal regulation between TOC1 and LHY/CCA1 within the *Arabidopsis* circadian clock. *Science* 293, 880–883. doi: 10.1126/science.1061320

Barak, S., Tobin, E. M., Andronis, C., Sugano, S., and Green, R. M. (2000). All in good time: the *Arabidopsis* circadian clock. *Trends Plant Sci.* 5, 517–522. doi: 10.1016/S1360-1385(00)01785-4

Christie, J. M. (2007). Phototropin blue-light receptors. *Annu. Rev. Plant Biol.* 58, 21–45. doi: 10.1146/annurev.arplant.58.032806.103951

Corbesier, L., Vincent, C., Jang, S., Fornara, F., Fan, Q., Searle, I., et al. (2007). FT protein movement contributes to long-distance signaling in floral induction of *Arabidopsis*. *Science* 316, 1030–1033. doi: 10.1126/science.1140035

Covington, M. F., Maloof, J. N., Straume, M., Kay, S. A., and Harmer, S. L. (2008). Global transcriptome analysis reveals circadian regulation of key pathways in plant growth and development. *Genome Biol.* 9, R130. doi: 10.1186/gb-2008-9-8-r130

Dennis, G., Sherman, B., Hosack, D., Yang, J., Gao, W., Lane, H., et al. (2003). DAVID: Database for annotation, visualization, and integrated discovery. *Genome Biol.* 4, R60. doi: 10.1186/gb-2003-4-9-r60

Dodd, A. N., Kusakina, J., Hall, A., Gould, P. D., and Hanaoka, M. (2014). The circadian regulation of photosynthesis. *Photosynth. Res.* 119, 181–190. doi: 10.1007/s11120-013-9811-8

Dodd, A. N., Salathia, N., Hall, A., Kévei, E., Tóth, R., Nagy, F., et al. (2005). Plant circadian clocks increase photosynthesis, growth, survival, and competitive advantage. *Science* 309, 630–633. doi: 10.1126/science.1115581

Eckel-Mahan, K. L., Patel, V. R., Mohney, R. P., Vignola, K. S., Baldi, P., and Sassone-Corsi, P. (2012). Coordination of the transcriptome and metabolome by the circadian clock. *Proc. Natl. Acad. Sci. U.S.A.* 109, 5541–5546. doi: 10.1073/pnas.1118726109

Farré, E. M., and Weise, S. E. (2012). The interactions between the circadian clock and primary metabolism. *Plant Biol.* 15, 293–300. doi: 10.1016/j.pbi.2012.01.013

Fenske, M. P., Hewett Hazelton, K. D., Hempton, A. K., Shim, J. S., Yamamoto, B. M., Riffell, J. A., et al. (2015). Circadian clock gene LATE ELONGATED HYPOCOTYL directly regulates the timing of floral scent emission in *Petunia*. *Proc. Natl. Acad. Sci. U.S.A.* 112, 9775–9780. doi: 10.1073/pnas.1422875112

Fukuda, H., Murase, H., and Tokuda, I. T. (2013). Controlling circadian rhythms by dark-pulse perturbations in *Arabidopsis thaliana*. *Sci. Rep.* 3, 1533. doi: 10.1038/srep01533

Fukushima, A., Kusano, M., Nakamichi, N., Kobayashi, M., Hayashi, N., Sakakibara, H., et al. (2009). Impact of clock-associated *Arabidopsis* pseudo-response regulators in metabolic coordination. *Proc. Natl. Acad. Sci. U.S.A.* 106, 7251–7256. doi: 10.1073/pnas.0900952106

Gardner, M. J., Hubbard, K. E., Hotta, C. T., Dodd, A. N., and Webb, A. A. R. (2006). How plants tell the time. *Biochem. J.* 397, 15–24. doi: 10.1042/BJ20060484

Goodspeed, D., Chehab, E. W., Min-Venditti, A., Braam, J., and Covington, M. F. (2012). *Arabidopsis* synchronizes jasmonate-mediated defense with insect circadian behavior. *Proc. Natl. Acad. Sci. U.S.A.* 109, 4674–4677. doi: 10.1073/pnas.1116368109

Goodspeed, D., Liu, J. D., Chehab, E. W., Sheng, Z., Francisco, M., Kliebenstein, D. J., et al. (2013). Postharvest circadian entrainment enhances crop pest resistance and phytochemical cycling. *Curr. Biol.* 23, 1235–1241. doi: 10.1016/j.cub.2013.05.034

Grundy, J., Stoker, C., and Carré, I. A. (2015). Circadian regulation of abiotic stress tolerance in plants. *Front. Plant Sci.* 6:648. doi: 10.3389/fpls.2015.00648

Harmer, S. L. (2009). The circadian system in higher plants. *Annu. Rev. Plant Biol.* 60, 357–377. doi: 10.1146/annurev.arplant.043008.092054

Harmer, S. L., Hogenesch, J. B., Strume, M., Chang, H. S., Han, B., Zhu, T., et al. (2000). Orchestrated transcription of key pathways in *Arabidopsis* by the circadian clock. *Science* 290, 2110–2113. doi: 10.1126/science.290.5499.2110

Haydon, M. J., Bell, L. J., and Webb, A. A. R. (2011). Interactions between plant circadian clocks and solute transport. *J. Exp. Bot.* 62, 2333–2348. doi: 10.1093/jxb/err040

Higashi, T., Kamitamari, A., Okamura, N., Ukai, K., Okamura, K., Tezuka, T., et al. (2014). Characterization of circadian rhythms through a bioluminescence reporter assay in *Lactuca sativa* L. *Environ. Control Biol.* 52, 21–27. doi: 10.2525/ecb.52.21

Higashi, T., Nishikawa, S., Okamura, N., and Fukuda, H. (2015). Evaluation of growth under non-24 h period lighting conditions in *Lactuca sativa* L. *Environ. Control Biol.* 53, 7–12. doi: 10.2525/ecb.53.7

Higashi, T., Tanigaki, Y., Takayama, K., Nagano, A. J., Honjo, M. N., and Fukuda, H. (2016). Detection of diurnal variation of tomato transcriptome through the molecular timetable method in a sunlight-type plant factory. *Front. Plant Sci.* 7:87. doi: 10.3389/fpls.2016.00087

Lai, A. G., Doherty, C. J., Mueller-Roeber, B., Kay, S. A., Schippers, J. H. M., and Dijkwel, P. P. (2012). CIRCADIAN CLOCK-ASSOCIATED 1 regulates ROS homeostasis and oxidative stress responses. *Proc. Natl. Acad. Sci. U.S.A.* 109, 17129–17134. doi: 10.1073/pnas.1209148109

Lakshmanan, M., Lim, S. H., Mohanty, B., Kim, J. K., Ha, S. H., and Lee, D. Y. (2015). Unraveling the light-specific metabolic and regulatory signatures of rice through combined in silico modeling and multiomics analysis. *Plant Physiol.* 169, 3002–3020. doi: 10.1104/pp.15.01379

Langmead, B., and Salzberg, S. L. (2012). Fast gapped-read alignment with Bowtie2. *Nat. Methods* 9, 357–359. doi: 10.1038/nmeth.1923

Li, B., and Dewey, C. N. (2011). RSEM: accurate transcript quantification from RNA-Seq data with or without a reference genome. *BMC Bioinformatics* 12:323. doi: 10.1186/1471-2105-12-323

Li, K., Li, Z., and Yang, Q. (2016). Improving light distribution by zoom lens for electricity savings in a plant factory with light-emitting diodes. *Front. Plant Sci.* 7:92. doi: 10.3389/fpls.2016.00092

Maere, S., Heymans, K., and Kuiper, M. (2005). BiNGO: a cytoscape plugin to assess overrepresentation of gene ontology categories in biological networks. *Bioinformatics* 21, 3448–3449. doi: 10.1093/bioinformatics/bti551

Marcolino-Gomes, J., Rodrigues, F. A., Fuganti-Pagliarini, R., Bendix, C., Nakayama, T. J., Celaya, B., et al. (2014). Diurnal oscillations of soybean circadian clock and drought responsive genes. *PLoS ONE* 9:e86402. doi: 10.1371/journal.pone.0086402

Matsuzaki, J., Kawahara, Y., and Izawa, T. (2015). Punctual transcriptional regulation by the rice circadian clock under fluctuating conditions. *Plant Cell* 27, 633–648. doi: 10.1105/tpc.114.135582

Moriyuki, S., and Fukuda, H. (2016). High-throughput growth prediction for *Lactuca sativa* L. seedlings using chlorophyll fluorescence in a plant factory with artificial lighting. *Front. Plant Sci.* 7:394. doi: 10.3389/fpls.2016.00394

Nagano, A. J., Honjo, M. N., Mihara, M., Sato, M., and Kudoh, H. (2015). Detection of plant viruses in natural environments by using RNA-Seq. *Methods Mol. Biol.* 1236, 89–98. doi: 10.1007/978-1-4939-1743-3_8

Nagano, A. J., Sato, Y., Mihara, M., Antonio, B. A., Motoyama, R., Itoh, H., et al. (2012). Deciphering and prediction of transcriptome dynamics under fluctuating field conditions. *Cell* 151, 1358–1369. doi: 10.1016/j.cell.2012.10.048

Nagel, D. H., Doherty, C. J., Pruneda-Paz, J. L., Schmitz, R. J., Ecker, J. R., and Kay, S. A. (2015). Genome-wide identification of CCA1 targets uncovers an expanded clock network in *Arabidopsis*. *Proc. Natl. Acad. Sci. U.S.A.* 112, E4802–E4810. doi: 10.1073/pnas.1513609112

Nakamichi, N., Ito, S., Oyama, T., Yamashino, T., Kondo, T., and Mizuno, T. (2004). Characterization of plant circadian rhythms by employing *Arabidopsis* cultured cells with bioluminescence reporters. *Plant Cell Physiol.* 45, 57–67. doi: 10.1093/pcp/pch003

Nakamichi, N., Kiba, T., Henriques, R., Mizuno, T., Chua, N. H., and Sakakibara, H. (2010). PSEUDO-RESPONSE REGULATORS 9, 7, and 5 are transcriptional repressors in the *Arabidopsis* circadian clock. *Plant Cell* 22, 594–605. doi: 10.1105/tpc.109.072892

Nakamichi, N., Kiba, T., Kamioka, M., Suzuki, T., Yamashino, T., Higashiyama, T., et al. (2012). Transcriptional repressor PRR5 directly regulates clock-output pathways. *Proc. Natl. Acad. Sci. U.S.A.* 109, 17123–17128. doi: 10.1073/pnas.1205156109

Pruneda-Paz, J. L., and Kay, S. A. (2010). An expanding universe of circadian networks in higher plants. *Trends Plant Sci.* 15, 259–265. doi: 10.1016/j.tplants.2010.03.003

Rensing, L., and Ruoff, P. (2002). Temperature effect on entrainment, phase shifting, and amplitude of circadian clocks and its molecular bases. *Chronobiol. Int.* 19, 807–864. doi: 10.1081/CBI-120014569

Schick, S., Becker, K., Thakurela, S., Fournier, D., Hampel, M. H., Legewie, S., et al. (2016). Identifying novel transcriptional regulators with circadian expression. *Mol. Cell Biol.* 36, 545–558. doi: 10.1128/MCB.00701-15

Shannon, P., Markiel, A., Ozier, O., Baliga, N. S., Wang, J. T., Ramage, D., et al. (2003). Cytoscape: a software environment for integrated models of biomolecular interaction networks. *Genome Res.* 13, 2498–2504. doi: 10.1101/gr.1239303

Suárez-López, P., Wheatley, K., Robson, F., Onouchi, H., Valverde, F., and Coupland, G. (2001). CONSTANS mediates between the circadian clock and the control of flowering in *Arabidopsis*. *Nature* 410, 1116–1119. doi: 10.1038/35074138

Tanigaki, Y., Higashi, T., Takayama, K., Nagano, A. J., Honjo, M. N., and Fukuda, H. (2015). Transcriptome analysis of plant hormone-related tomato (*Solanum lycopersicum*) genes in a sunlight-type plant factory. *PLoS ONE* 10:e0143412. doi: 10.1371/journal.pone.0143412

Thiruvengadam, M., Shih, C. F., and Yang, C. H. (2015). Expression of an antisense *Brassica oleracea* GIGANTEA (BoGI) gene in transgenic broccoli causes delayed flowering, leaf senescence, and post-harvest yellowing retardation. *Plant Mol. Biol. Rep.* 33, 1499–1509. doi: 10.1007/s11105-015-0852-3

Toepel, J., Welsh, E., Summerfield, T. C., Pakrasi, H. B., and Sherman, L. A. (2008). Differential transcriptional analysis of the cyanobacterium *Cyanothece* sp. Stain ATCC 51142 during light-dark and continuous-light growth. *J. Bacteriol.* 190, 3904–3913. doi: 10.1128/JB.00206-08

Truco, M. J., Antonise, R., Lavelle, D., Ochoa, O., Kozik, A., Witsenboer, H., et al. (2007). A high-density, integrated genetic linkage map of lettuce (*Lactuca* spp.). *Theor. Appl. Genet.* 115, 735–746. doi: 10.1007/s00122-007-0599-9

Truco, M. J., Ashrafi, H., Kozik, A., van Leeuwen, H., Bowers, J., Wo, S. R. C., et al. (2013). An ultra-high-density, transcript-based, genetic map of lettuce. *G3 (Bethesda)* 3, 617–631. doi: 10.1534/g3.112.004929

Ueda, H. R., Chen, W., Minami, Y., Honma, S., Honma, K., Iino, M., et al. (2004). Molecular-timetable methods for detection of body time and rhythm disorders from single-time-point genome-wide expression profiles. *Proc. Natl. Acad. Sci. U.S.A.* 101, 11227–11232. doi: 10.1073/pnas.0401882101

Waldbauer, J. R., Rodrigue, S., Coleman, M. L., and Chisholm, S. W. (2012). Transcriptome and proteome dynamics of a light-dark synchronized bacterial cell cycle. *PLoS ONE* 7:e43432. doi: 10.1371/journal.pone.0043432

Wang, J., Tong, Y., Yang, Q., and Xin, M. (2016). Performance of introducing outdoor cold air for cooling a plant production system with artificial light. *Front. Plant Sci.* 7:270. doi: 10.3389/fpls.2016.00270

Wang, L., Si, Y., Dedow, L. K., Shao, Y., Liu, P., and Brutnell, T. P. (2011). A low-cost library construction protocol and data analysis pipeline for illumina-based strand-specific multiplex RNA-Seq. *PLoS ONE* 6:e26426. doi: 10.1371/journal.pone.0026426

Wang, Z., Gerstein, M., and Snyder, M. (2009). RNA-Seq: a revolutionary tool for transcriptomics. *Nat. Rev. Genet.* 10, 57–63. doi: 10.1038/nrg2484

Zhai, H., Lü, S., Wu, H., Zhang, Y., Zhang, X., Yang, J., et al. (2015). Diurnal expression pattern, allelic variation, and association analysis reveal functional features of the E1 gene in control of photoperiodic flowering in soybean. *PLoS ONE* 10:e0135909. doi: 10.1371/journal.pone.0135909

Conflict of Interest Statement: The authors declare that the research was conducted in the absence of any commercial or financial relationships that could be construed as a potential conflict of interest.

frontiers in Plant Science

REVIEW
published: 03 June 2016
doi: 10.3389/fpls.2016.00763

Exploiting Phenylpropanoid Derivatives to Enhance the Nutraceutical Values of Cereals and Legumes

Sangam L. Dwivedi[1], Hari D. Upadhyaya[1, 2, 3], Ill-Min Chung[4], Pasquale De Vita[5], Silverio García-Lara[6], Daniel Guajardo-Flores[6], Janet A. Gutiérrez-Uribe[6], Sergio O. Serna-Saldívar[6], Govindasamy Rajakumar[4], Kanwar L. Sahrawat[1], Jagdish Kumar[7] and Rodomiro Ortiz[8]*

[1] International Crops Research Institute for the Semi-Arid Tropics, Patancheru, India, [2] Department of Agronomy, Kansas State University, Manhattan, KS, USA, [3] UWA Institute of Agriculture, University of Western Australia, Crawley, WA, Australia, [4] Department of Applied Life Science, College of Life and Environmental Science, Konkuk University, Seoul, Korea, [5] Consiglio per la Ricerca in Agricoltura e l'Analisi dell'Economia Agraria, Centro di Ricerca per la Cerealicoltura, Foggia, Italy, [6] Tecnológico de Monterrey, Centro de Biotecnología-FEMSA, Escuela de Ingeniería y Ciencias, Monterrey, Mexico, [7] Sevita International, Inkerman, ON, Canada, [8] Swedish University of Agricultural Sciences, Alnarp, Sweden

OPEN ACCESS

Edited by:
Alejandro Isabel Luna-Maldonado, Universidad Autónoma de Nuevo León, Mexico

Reviewed by:
Biswapriya Biswavas Misra, University of Florida, USA
Georg Langenkämper, Max Rubner Institut, Germany

***Correspondence:**
Hari D. Upadhyaya
h.upadhyaya@cgiar.org

Specialty section:
This article was submitted to Crop Science and Horticulture, a section of the journal Frontiers in Plant Science

Received: *27 January 2016*
Accepted: *17 May 2016*
Published: *03 June 2016*

Citation:
Dwivedi SL, Upadhyaya HD, Chung I-M, De Vita P, García-Lara S, Guajardo-Flores D, Gutiérrez-Uribe JA, Serna-Saldívar SO, Rajakumar G, Sahrawat KL, Kumar J and Ortiz R (2016) Exploiting Phenylpropanoid Derivatives to Enhance the Nutraceutical Values of Cereals and Legumes. Front. Plant Sci. 7:763. doi: 10.3389/fpls.2016.00763

Phenylpropanoids are a diverse chemical class with immense health benefits that are biosynthesized from the aromatic amino acid L-phenylalanine. This article reviews the progress for accessing variation in phenylpropanoids in germplasm collections, the genetic and molecular basis of phenylpropanoid biosynthesis, and the development of cultivars dense in seed-phenylpropanoids. Progress is also reviewed on high-throughput assays, factors that influence phenylpropanoids, the site of phenylpropanoids accumulation in seed, *Genotype* × *Environment* interactions, and on consumer attitudes for the acceptance of staple foods rich in phenylpropanoids. A paradigm shift was noted in barley, maize, rice, sorghum, soybean, and wheat, wherein cultivars rich in phenylpropanoids are grown in Europe and North and Central America. Studies have highlighted some biological constraints that need to be addressed for development of high-yielding cultivars that are rich in phenylpropanoids. Genomics-assisted breeding is expected to facilitate rapid introgression into improved genetic backgrounds by minimizing linkage drag. More research is needed to systematically characterize germplasm pools for assessing variation to support crop genetic enhancement, and assess consumer attitudes to foods rich in phenylpropanoids.

Keywords: anthocyanins, cereals, flavonoids, *Genotype* × *Environment* interaction, genetics and biosynthesis, germplasm, legumes, phenolics

INTRODUCTION

Polyphenols are secondary metabolites that are synthesized by plants from the amino acid phenylalanine. They are derived from the C_6-C_3 (phenyl-propane) skeleton. Plant biosynthesis produces various phenols that can be grouped generally as flavonoids and phenolics. Flavones, flavonols, flavanones, flavan-3-ols, anthocyanidins, isoflavones, coumarins, stilbenes, and lignans are the main flavonoids (Pereira et al., 2009). These are structurally distinct because of their

specific hydroxylation, methylation, and conjugation patterns, with various monosaccharides and disaccharides (Graf et al., 2005; He and Giusti, 2010; Ignat et al., 2011; de Oliveira et al., 2014). Some flavonoids are exclusively synthesized by specific plants, such as phlobaphenes in maize (Sharma et al., 2012) and isoflavonoids in legumes (Mazur et al., 1998). Phenolic acids exist primarily as benzoic-acid and cinnamic-acid derivatives, and can occur in the free or conjugated forms. Gallic, *p*-benzoic, protocatechuic, syringic, and vanillic acids are benzoic-acid derivatives, while caffeic, ferulic, *p*-coumaric, and sinapic acids are cinnamic-acid derivatives (Razzaghi-As et al., 2013; de Oliveira et al., 2014).

Polyphenols are involved in various plant functions. They provide shades of color to flowers (color attracts pollinators), fruit, vegetables, and grains. Their bitter or astringent taste attributes can repel birds and other animals. Polyphenols protect plants from UV radiation and provide defense against environmental stress, as well as against pathogens and pests, and they act as signaling molecules to facilitate symbiotic nitrogen fixation and confer seed dormancy (Subramanian et al., 2007; Yang et al., 2008; Gu et al., 2011; Soares et al., 2013; de Oliveira et al., 2014). The phenylpropanoids have received considerable attention owing to their potential benefits for human health.

This article reviews the phenylpropanoid constituents, with emphasis on the mining of germplasm variation for flavonoids (excluding lignans and stilbenes) and phenolics, the site and factors that influence phenylpropanoid accumulation in seed, the *Environment*, *Genotype*, and *Genotype* × *Environment* interactions, the genetic and molecular basis of phenylpropanoid biosynthesis, and the development of seed-phenylpropanoid dense cultivars. Updates on flavonoids as promoters of micronutrient bioavailability and human health, high-throughput assays for estimation of phenylpropanoids, and consumer attitudes to accepting phenylpropanoid-dense foods are also included here.

HUMAN HEALTH AND MICRONUTRIENT BIOAVAILABILITY

As a dietary component, phenylpropanoids have health-promoting properties due to their high antioxidant capacity that has been shown in both *in-vivo* and *in-vitro* systems (Cook and Samman, 1996). The antioxidant capacity of flavonoids is conferred by the high number of hydroxyl substitutions in each flavonoid molecule, which has a direct effect on the donating ability of hydrogen atoms to scavenge free radicals (Pietta, 2000). The food matrix and its processing conditions have strong effects on the retention of these compounds and their use as a functional food ingredient (Chavez-Santoscoy et al., 2016). Unfortunately, the availability of micronutrients and phytochemicals has been studied through reductionist and pharmacological approaches to date, while the beneficial effects of health-promoting compounds should in addition be analyzed holistically as food is not a drug. Furthermore, a compound that has been shown to be bioactive might have different effects when tested in a complex matrix (Fardet and Rock, 2014). Hence, it is important to identify and validate the stability of bioactive compounds both in isolation as well as once they have been incorporated into functional foods.

Combining cereals and legumes improves not only the nutritional content of these foods, but also their health-promoting effects. Anton et al. (2008) investigated the effects of red, black, and pinto or navy common bean (*Phaseolus vulgaris* L.) flour in wheat tortilla, and noted that tortillas with black beans had higher levels of crude protein, total phenols, and *in-vitro* antioxidant activity than those solely made with wheat flour. Black bean flavonoids, such as quercetin-3-*O*-glucoside, can have strong effects on down-regulation of expression of lipogenic proteins (Chavez-Santoscoy et al., 2014; Ramírez-Jiménez et al., 2015). Anthocyanin consumption from the original food matrix or once extracted inhibits tumorigenesis of esophageal cancer and changes inflammatory markers in rats (Peiffer et al., 2016). For example, 3-*O*-glucosylated anthocyanins (i.e., delphinidin, petunidin, malvidin) in the seed-coat extract of black violet beans is associated with antioxidant and anti-inflammatory activities (Oomah et al., 2010; Mojica et al., 2015). Furthermore, black-seeded common bean cultivars are superior to other food crops as nutraceutical supplements (Chavez-Santoscoy et al., 2013; Guajardo-Flores et al., 2015; Rosales-Serna et al., 2015).

Non-communicable diseases such as cancer, diabetes, heart disease, and stroke are some of the major challenges to global health, and they are often associated with the negative effects of globalization, rapid urbanization, diet, and increasingly sedentary lifestyles (Wagner and Brath, 2012). Flavonoids are implicated in the prevention of cardiovascular diseases (Mink et al., 2007; Curtis et al., 2009; Weseler et al., 2011). Soluble vascular adhesion molecule-1 (sVCAM-1) is an important biomarker that is used to predict the risk of death from coronary heart diseases (Blankenberg et al., 2001). Phenolic metabolites have stronger effects on reducing the sVCAM-1 levels than the corresponding flavonoids (Warner et al., 2016). Thus, the metabolism of flavonoids is critical to increases in their vascular efficacy, and this explains the differences among individuals when phenolic compounds are tested *in-vivo*. Colon cancer is a major public health burden in both developed and developing countries (Torre et al., 2015). Adoption of a Western diet is the major cause of colon cancer (Center et al., 2009). Sorghum [*Sorghum bicolor* (L.) Conrad Moench] flavonoids contribute to colon cancer prevention at concentrations that are achievable through the diet (Yang et al., 2014). They also noted that the composition of phenolic compounds, not content, has a major effect on estrogenic activity and on the protective efficacy of sorghum in preventing colon cancer.

Another global challenge to human health is being overweight or obese (Ng et al., 2014). Increased consumption of flavonoid-rich fruit and vegetables can help with weight management. Higher intake of foods rich in flavonols, flavan-3-ols, anthocyanins, and flavonoid polymers has been associated with less weight gain among men and women aged 27–65 years who were followed for up to 24 years (Bertoia et al., 2015). This association remained statistically significant for anthocyanins after further adjustment for fiber intake, which indicated that food sources with a high contents of anthocyanin and flavonoid

polymers can be associated with less weight gain through mechanisms other than fiber content.

Phytic acid is the major contributor to reduced bioavailability of micronutrients in cereals and legumes, while polyphenols are major inhibitors of iron (Fe) absorption and act in a manner similar to phytate, by complexing Fe (Dwivedi et al., 2012). The metal-chelating characteristics of flavonoids are an important factor in antioxidant activities (Bonina et al., 1996; Boyle et al., 2000). Studies have demonstrated high binding capacities of polyphenols for Fe (Teucher et al., 2004; Perron and Brumaghim, 2009; Cercamondi et al., 2014). Flavonoids can bind nonheme iron and inhibit intestinal absorption of Fe from food (Mladenka et al., 2011; Corcoran et al., 2012). Nonheme iron is the principal form of Fe in plant foods, dairy products, and iron supplements. Flavonoids in colored bean seed coats strongly inhibit Fe bioavailability in bean digests (Hu et al., 2006). The chelation of metal ions by flavonoids can render the ions inactive in the generation of radicals, or alternately, flavonoids can themselves intercept radicals that are generated (Tako et al., 2015). Some polyphenols can reduce Fe(III) to Fe(II) (Perron and Brumaghim, 2009), thus promoting iron bioavailability. Catechin, 3,4-dihydroxybenzoic acid, kaempferol, and kaempferol 3-glucoside have been shown to promote Fe uptake, while myricetin, myricetin 3-glucoside, quercetin, and quercetin 3-glucoside inhibit Fe uptake (Hart et al., 2015). These inhibitors are, however, found in greater amounts than the promoters, which is consistent with the net inhibitory effects observed for black bean seed coats. The promotion of Fe uptake by some polyphenols and the identification of specific polyphenols that inhibit Fe uptake suggest the potential for breeding beans with improved Fe nutritional quality (Grieger et al., 2008; Tako and Glahn, 2010; Tako et al., 2015).

Flavonoids enhance the function of vitamin C, thus improving its absorption and protecting it from oxidation (Pietta, 2000). Vitamin C is a multi-functional micronutrient that is required in its reduced form (L-ascorbic acid) for many enzymatic reactions, and as a scavenger of free radicals generated from numerous physiological and biochemical processes (Evans and Halliwell, 2001). Flavonoids might also regenerate other antioxidants, such as tocopherols, by donating a hydrogen atom to the tocopheroxyl radical in a way that is reminiscent of their action on vitamin C (Boyle et al., 2000).

ANALYTICAL DETERMINATION OF PHENYLPROPANOIDS

Various assays for determining phenolic compounds have been developed (Bravo, 1998; Khoddami et al., 2013). These can be classified as those that quantify the total phenolics content, or those that quantify or identify a specific group or class of phenolics. Colorimetric methods are used to determine the total phenolics levels, and high performance liquid chromatography (HPLC) is used to identify and quantify specific phenolic compounds. The colorimetric methods include Folin-Ciocalteu assays (Singleton et al., 1999), Prussian blue tests (Graham, 1992), ferric ammonium citrate tests (International Organization for Standardization), and vanillin-HCl and butanol-HCl tests (Price et al., 1978; Watterson and Butler, 1983; Porter et al., 1986). These methods have been used for total phenol determination in barley (*Hordeum vulgare* L.), common bean (Hart et al., 2015), rice (*Oryza sativa* L.; Begum et al., 2015), sorghum (Beta et al., 1999; Waniska and Rooney, 2000; Dykes et al., 2005; Dlamini et al., 2007; Chiremba et al., 2012), soybean [*Glycine max* (L.) Merr.; Nikolova et al., 2014; Phommalath et al., 2014], einkorn wheat (*Triticum monococcum* L.), and bread wheat (*Triticum aestivum* L.; Fogarasi et al., 2015). HPLC techniques coupled with photodiode array, fluorescence, or mass spectroscopy detectors have been used to identify and quantify specific phenolics in rice (Zhou et al., 2004), sorghum (Svensson et al., 2010; Chiremba et al., 2012), soybean (Kim et al., 2014; Kumar et al., 2015), and wheat (Ficco et al., 2014). Sriseadka et al. (2012) identified and quantified 11 flavonoids in black rice using liquid chromatography electrospray ionization tandem mass spectrometry, six of which were reported for the first time. Due to their chemical nature, the extraction method used, the standards used, and the presence of interfering substances, the various methods available for the analysis of phenylpropanoids remain too complex, time consuming, and labor intensive for routine screening. These limitations represent a bottleneck for modern studies of functional genomics and modern plant breeding (Furbank and Tester, 2011).

Near infrared (NIR) spectroscopy appears to be an appropriate technique to achieve these goals. It is faster than chromatographic or wet-chemical methods, and it can provide correct identification in less than 2 min without destroying the sample. NIR spectroscopy simultaneously measures several quality traits that are routinely tested in cereals (Bao et al., 2001, 2007; Wu et al., 2002; Wu and Shi, 2004, 2007; Osborne, 2006). It has been applied for the determination of phenolic compounds, flavonoid content, and antioxidant capacity in food derived from rice, sorghum, cocoa (*Theobroma cacao* L.), wine, grapes (*Vitis vinifera* L.), apples (*Malus domestica* Borkh., 1803), and tea [*Camellia sinensis* (L.) Kuntze; Whitacre et al., 2003; Cozzolino et al., 2004, 2008; Janik et al., 2007; Chen et al., 2008; Zhang et al., 2008; Pissard et al., 2013; Dykes et al., 2014; Hassan et al., 2015]. NIR spectroscopy has a high degree of precision when applied to the analysis of nutraceutical and antioxidant compounds in terms of their concentrations and antioxidant activities in foods (Ignat et al., 2011; Bunaciu et al., 2012; Lu and Rasco, 2012; Bittner et al., 2013; Cozzolino, 2015). Hence, NIR spectroscopy can provide very useful qualitative and quantitative information on different antioxidants, combined with its simplicity and low cost. Calibration development is critical to establishing a successful method based on NIR spectroscopy. Although the polyphenol quantification method is well established, a modified Folin-Cioalteu method incorporates the convenience of spectrometric measurements using 96-well microplates (Zhang et al., 2006). Automation of the workflow using 384-well microplates, as optimized for robotics, automated readers, and liquid handling systems, makes it possible to use much smaller quantities of reagents and solvents, and to significantly

increase the throughput of the analysis of the compounds tested.

A 96-well microtiter assay that has been used for decades in the pharmaceutical industry has been standardized for screening total phenolic, flavonoid, and tannin contents, and for 2,2-diphenyl-1-picrylhydrazyl free radical (DPPH)-scavenging activity in grape, sorghum (Herald et al., 2012, 2014; Bobo-García et al., 2015) and wheat (Cheng et al., 2006) extracts. This assay is thus as robust and reproducible as the conventional method for determining phenolic compounds. Most commonly used assays for measuring antioxidant activity, including those with DPPH, have both conceptual and technical limitations (Apak et al., 2013; Tian and Schaich, 2013; Xie and Schaich, 2014; Schaich et al., 2015), especially when comparing different food matrices. Although, it is necessary to continue investigating antioxidant efficacy using fundamental chemistry (Schaich et al., 2015), high-throughput assays remain a strategic asset to monitor variations in antioxidant activity in large germplasm collections. Laus et al. (2015) proposed the $QUENCHER_{ABTS}$ for determination of antioxidant capacity, which is quick, easy, new, cheap, and reproducible. This method can also be used to accurately discriminate antioxidant capacity associated with the insoluble-bound phenolics of wheat grain without any preliminary sample extraction. Thus, it allows good discrimination among wheat genotypes, with better physiological significance than the classical Trolox equivalent antioxidant capacity and 2,2′-azinobis-(3-ethylbenzothiazoline-6-sulfonic acid) measurements. In addition, high-throughput oxygen-radical absorbance capacity assays conducted with more detailed and revised protocols might be a valuable alternative to the common testing methods for antioxidants (Huang et al., 2002).

Imaging systems working in the UV, visible, NIR, and Raman spectral ranges of the electromagnetic spectrum can be used to obtain information on composition and distribution of phenylpropanoids. As the hyperspectral imaging techniques combine spectroscopic and imaging systems, they can be used for detecting very low levels of chemical constituents in cereal and legume grain along with spatial distributions (Budevska, 2002; Kezhu et al., 2014; Mahajan et al., 2015). The hyperspectral microspectroscopic imaging techniques have been used to study the endosperm/aleurone/pericarp area of mature kernels of maize (*Zea mays* L.; Budevska, 2002). Hyperspectral imaging systems have also been used to develop single kernel methods to determine the physical and biochemical traits of cereals (Codgill et al., 2002, 2004; Fox and Manley, 2014). These methods focus on the calibration of the hyperspectral imaging instrument to predict the constituent concentrations in single kernels using NIR hyperspectral images.

ENVIRONMENT AND GENOTYPE EFFECTS ON PHENYLPROPANOIDS

The flavonoid content is dominantly influenced by both genotype and environment. Better understanding of genotype and environment effects is a prerequisite to selecting food crops with enhanced flavonoids, so that cultivars high in flavonoids can be targeted to suitable environments.

Most studies on legumes as a source of functional foods has focused on soybean. For example, field research on six non-transgenic soybean genotypes grown in 23 environments (E) was carried out in Argentina to study seed nutraceutical composition. This showed that although *Environment* was the most important source, *Genotype* and *Genotype* × *Environment* interactions also had significant effects on grain nutraceutical composition (Carrera et al., 2014). These results agreed with those reported earlier by Lee et al. (2003), who showed that in South Korea, the main effects of *Year*, *Site*, *Genotype*, and all possible interactions between these were significant for all of the isoflavones. Murphy et al. (2009a) reported that breeding for relative isoflavone content was possible in two soybean populations in Ontario, Canada. Nonetheless, they cautioned that breeding for absolute stability is a challenge, because of the very strong effects of the environment on isoflavone accumulation in soybean. Temperature, precipitation, and soil moisture in the field conditions are the most important factors that influence flavonoid contents in soybean genotypes (Kim et al., 2012a), while temperature and soil moisture status change the isoflavone and anthocyanin contents of soybean under controlled conditions (Caldwell et al., 2005; Lozovaya et al., 2005; Chennupati et al., 2011).

Variable effects of genotype and environment on phenylpropanoid compounds were reported in wheat. Mpofu et al. (2006) and Fernandez-Orozco et al. (2010) showed greater contribution of environment than genotypes on flavonoid and phenolic content, while others reported greater genotypic effects than environment on polyphenols (Martini et al., 2015; Rascio et al., 2015). Variation in sowing date is also reported to cause significant differences in polyphenol content; i.e., polyphenols were increased in spring-sown compared to winter-sown wheats (Rascio et al., 2015). This variation depended on genotypes. A negative effect of spring sowing on grain yield was observed, but positive effects on 1000-kernel weight suggested that high temperatures can lead to a net accumulation of healthy substances in grain, but not a relative increase due to grain shriveling. There is a need to confirm these data in multiple environments, because such an approach facilitates the specific enrichment of cereal-based foods as per consumer requirements (Rascio et al., 2015). Total phenolics and phenolic acids were mostly affected by the environment in a 3-year field evaluation of durum wheat in Italy (Martini et al., 2015).

Changes in anthocyanin content of wheat cultivars were associated with sink-source (i.e., availability of carbohydrate for anthocyanin production) transition, grain position (i.e., the anthocyanin content decreased when grain position was more distal), and physiological stage of the crop. Magnesium fertilization and early harvest (at physiological maturity) increased anthocyanin content and concentrations by 65 and 39%, respectively (Bustos et al., 2012). Heat stress can adversely affect compounds that are beneficial or detrimental to human health (Dias and Lidon, 2010; Laino et al., 2010). More recently, de Leonardis et al. (2015) reported that in addition to affecting

seed nutritional composition, 5-day heat stress (37°C) after flowering impacted on the antioxidant capacities and metabolic profiles of durum wheats. This response to heat stress was genotype-dependent, with most analyzed metabolites increasing in "Primadur" (high in seed carotenoids), but decreasing in "T1303" (high in seed anthocyanin).

Goufo and Trindade (2014) indicated that among four types of rice that were ranked by color, black rice cultivars were the highest in flavonoids, followed by the purple, red, and brown cultivars. These results were influenced by both the genotype and the environment. For example, elevated carbon dioxide reduced total phenolics, total flavonoids, and individual flavonoids (flavone, and some unidentified flavonoids) in rice kernels and all of the rice milling fractions. These results emphasize the importance of future atmospheric scenarios in breeding rice cultivars with increased antioxidant content (Goufo and Trindade, 2014; Goufo et al., 2014). The distribution of flavonoids in rice cultivars was not significantly affected by agronomic practices, but flavonoid content was significantly affected by the season, and the genotype, and by their interactions (de Mira et al., 2009; Liu et al., 2013).

Taleon et al. (2012) investigated the effects of both the genotype and environment on flavonoid concentrations in black sorghum grain in Texas. Significant variation due to the genotype, the environment, and their interactions was observed. Most of the variation was, however, associated with *Genotype* or *Environment*. The genotypic variation was greater than that for environment variation for flavones, while for flavanones, the environment variation was greater. Hence, the identification of both the best genotype and environment will provide the highest yields of total flavonoid content, and sorghum breeders need to evaluate these traits in multiple environments to select the genotypes with stable and high content of flavonoids of interest (Taleon et al., 2012). Similar results were reported and conclusions drawn for flavonoid content in red and lemon-yellow sorghum grain. The evaluation of genotypes in multiple environments was emphasized to obtain the best data related to the flavonoid content (Taleon et al., 2014).

Functional components including starch, protein, dietary fiber, and phenolic antioxidants were considerably influenced by the environment, genotype, type (i.e., hull-less, with hulls) and their interactions for barley grown in 23 different environments in eastern Canada (Abdel-Aal and Choo, 2014). The starch, which is the main available carbohydrate in barley, varied according to year, barley type and individual cultivars or lines. The absence of hulls tended to enhance the protein and total antioxidant capacity (Abdel-Aal and Choo, 2014).

Clearly, *Environment*, *Genotype,* and *Genotype* × *Environment* interactions have significant impact on phenylpropanoid constituents, which emphasizes the need for multi-environment testing to identify seed with phenylpropanoid-dense germplasm for use in plant breeding. Multi-environment testing across diverse agro-ecologies will also reveal which of the environments are more favorable for the production of phenylpropanoid-rich staple grain crops.

FACTORS INFLUENCING ACCUMULATION OF PHENYLPROPANOIDS

Crops can produce a large number of phenolic secondary metabolites that are not essential in the primary process of growth and development, but are of vital significance for their interactions with the environment and for their defense mechanisms (Cheynier et al., 2013). Flavonoids have relevant roles during the establishment of plants in the growing environment (Agati et al., 2013). The production of flavonoids is a response to developmental signals during seed development and to environmental signals, for protection. Thus, flavonoids are involved in protecting crops against major biotic and abiotic stresses (Liu et al., 2013). For some specific flavonoids, there is good understanding of the signals and activation of the phenolic biosynthetic genes (Cheynier et al., 2013). There are various biotic and abiotic stresses that influence the accumulation of specific flavonoids in crops (Supplementary Table 1).

Abiotic Factors

Legumes

Drought stress decreased polyphenols in common bean seeds (Ovando-Martínez et al., 2014). Carbon dioxide and water stress increased the isoflavone content of soybean seed, but elevated temperature decreased total isoflavone content by about 65% (Caldwell et al., 2005). Water stress, elevated temperature, and solar radiation led to significant reductions in the specific and total content of isoflavones in soybean (Carrera and Dardanelli, 2015). Likewise, soil drought reduced the total phenolic content in the seeds of pea (*Pisum sativum* L.) and yellow lupin (*Lupinus luteus* L.; Juzoń et al., 2013). In mung bean [*Vigna radiata* (L.) R. Wilczek], water deficit reduced the total phenolics content (Afzal et al., 2014), while elevated UV-B radiation significantly reduced the concentrations of isoflavones and phenolic compounds in soybean seed (Kim et al., 2011). Genotypic differences in response to elevated ozone were noted across mung-bean cultivars, i.e., some cultivars were more sensitive to ozone (O_3) stress (as measured by differences in antioxidants, metabolites, growth, total biomass, and yield) than others, suggesting the possibility of selection of suitable O_3 resistant cultivars with improved phenylpropanoids in seeds for areas experiencing high concentation of O_3 (Chaudhary and Agrawal, 2015).

Cereals

In maize, grain flavonoid increased considerably due to water stress, but the accumulation of phenolic compounds and carotenoids decreased (Ali et al., 2010). A marked increase in the total phenolics accumulation was observed in response to drought and salinity, and to a combination of these factors in barley kernels (Ahmed et al., 2013a). Salt increased the nutraceutical quality of mature grains in rice, as measured by total phenolics content, and anthocyanins and proanthocyanins (Chunthaburee et al., 2015), whereas drought led to increased total phenolic acids and carotenoids in wheat grain (Chakraborty and Pradhan, 2012). Stress as a result of

nitrogen fertilization increased total free phenolic acids, but decreased conjugated soluble phenolic acids in wheat grain (Stumpf et al., 2015). Rice exposure to high CO_2 resulted in decreased seed total phenolics content, with the highest reduction in sinapic and *p*-hydroxybenzoic acids. The total flavonoids content also decreased, with apigenin highly affected (Goufo et al., 2014). In whole rice kernels, γ-irradiation led to the accumulation of the main phenolic compounds (e.g., *p*-coumaric acid, ferulic acid), but it decreased anthocyanins (e.g., cyanidin-3-glucoside, peonidin-3-glucoside; Zhu et al., 2010). Wheat exposed to higher levels of solar UV radiation resulted in the production of red kernels and increased the concentrations of phenolic acids, flavonoids, and lutein (Lukow et al., 2012).

Biotic Factors

Legumes

Seed flavonoids contribute to a constitutive defense mechanism, and they might accumulate after recurrent infection and as a result of several types of stress (Treutte, 2006). Seed concentrations of flavonoids, alkaloids, and terpenoids define the levels of effectiveness in the control of pathogens and insect pests in most legumes, and especially in common beans (Ndakidemi and Dakora, 2003). Seed accumulation of high amounts of phenolic compounds is toxic to bruchid [*Callosobruchus maculatus* (Fabricius 1775)] and provides resistance to storage pests in cowpea [*Vigna unguiculata* (L.) Walp], chickpea (*Cicer arietinum* L.), and soybean (Sharma and Thakur, 2014). Furthermore, flavonoids and isoflavonoids are considered to have major roles in host plant defense in the Fabaceae family (Mapope and Dakora, 2013). For example, the specific isoflavone content in legumes is strongly related to resistance to pathogens (Treutte, 2006). Rubiales et al. (2015) suggested a prominent role for flavonoid-related compounds in the specific defense against fungi, bacteria, and insects.

Cereals

Cell-wall phenolic acids in cereal grains are known to be associated with innate grain resistance to pests and pathogens (Santiago et al., 2013). For instance, the phenolic acids that are accumulated during wheat-kernel development contributed positively to *Fusarium* resistance (McKeehen et al., 1999). Analogous effects of *Fusarium* infection in barley showed that inoculation significantly reduced the ferulic acid content and increased the catechin content in the grain (Eggert et al., 2010). Increased accumulation of phenolic acids in maize pericarp is also associated with weevil [*Sitophilus zeamais* (Motschulsky, 1855)] resistance in tropical genotypes (García-Lara and Bergvinson, 2014). Similar findings in maize were reported for the effects of phenolic compounds against Angoumois grain moths [*Sitotroga cerealella* (Olivier, 1789); Ahmed et al., 2013b]. In contrast, phenolic acids, chlorogenic acids, and tannins were not involved in the infestation and damage caused by rice weevils [*Sitophilus oryzae* (Linnaeus, 1763); Bamisile et al., 2014].

PHENYLPROPANOID ACCUMULATION IN SEED

Cereal bran is rich in polyphenols, but these are usually removed from the grain before it is consumed as food. Most of the phytochemicals are lost following milling; thus, there is a trend to increase whole-grain consumption (Schaffer-Lequart et al., 2015). Wheat grain bran and germ contain up to 83% total phenolics, which is 15–18-fold higher on a μmol of gallic acid equiv 100 g^{-1} basis than in the endosperm fraction. Total phenolics progressively decreased during the progress in de-branning from the aleurone layer to the internal portions of the kernel (Adom et al., 2006).

The concentration, type and distribution of flavonoids differs among rice phenotypes. For example, proanthocyanidins are found in red kernels, anthocyanins in black grain, and phenolics in the non-pigmented counterparts (Abdel-Aal et al., 2006; Finocchiaro et al., 2007), whereas anthocyanins are found in the aleurone layer and the pericarp of purple, blue, and red wheat kernels (Havrlentová et al., 2014). Maize with red/ blue and blue kernels often contains a higher proportion of acylated anthocyanins than maize with red and purple kernels. Magenta-colored anthocyanins are concentrated in both the pericarp and aleurone layers, whereas blue maize grains accumulate pigments only in the aleurone layer (Žilić et al., 2012).

Matrix-assisted laser desorption/ionization coupled to imaging mass spectrometry allows simultaneous investigation of the content and spatial distribution of a wide range of biomolecules. Yoshimura et al. (2012) used this mass spectrometry technique to study the distribution of flavonoids in black-pigmented rice seeds, and they identified seven species of anthocyanin monoglycosides and two species of anthocyanin diglycosides. Anthocyanins composed of a pentose moiety (e.g., cyanidin-3-*O*-pentoside, petunidin-3-*O*-pentoside) were found throughout the pericarp, whereas anthocyanins composed of a hexose moiety (e.g., cyanidin-3-*O*-hexoside, peonidin-3-*O*-hexoside) were found only in the dorsal pericarp. Thus, anthocyanin species composed of different sugar moieties have different localization patterns in the pericarp of black rice. Galland et al. (2014) studied the localization, nature, and relative abundance of flavonoids in mature and germinated non-pigmented rice seeds of "Nipponbare" (a *japonica* cultivar) using a combination of confocal microscopy, mass spectrometry and gene expression analysis. They showed that matured rice seed exclusively accumulates flavones mostly in the embryo and to a lesser extent in the pericarp/testa. They detected 21 different flavones. Schaftoside and its two isomers were the major flavones in the embryo (54% of flavonoid compounds, as rhamnetin equivalents $seed^{-1}$). Tricin and its conjugated derivatives accounted for 24% of the flavonoid signal distribution, making these the second largest contributor to the total flavone content of the embryo. In contrast, the pericarp/testa fraction accumulated exclusively schaftoside and two schaftoside isomers. The embryo has both *O*- and *C*-glycosylated flavones, while the pericarp/testa fraction accumulated only *C*-glycosylated flavones. The embryo flavone content is therefore very high

when compared with that of the pericarp/testa in "Nipponbare" seeds.

GENETICS AND BIOSYNTHESIS PATHWAYS

Genetics

Flavonoids in Legumes

The concentration of isoflavones in soybean is a complex multigenic trait. There are at least 50 quantitative trait loci (QTL) related to this trait (Meksem et al., 2001; Primomo et al., 2005; Gutierrez-Gonzalez et al., 2009, 2011; Zeng et al., 2009; Meng et al., 2011; Yang et al., 2011). Of these, two QTL with main effects that are located in Gm05 (LGA1) and GM08 (LGA2) consistently affected isoflavone content across environments (Gutierrez-Gonzalez et al., 2011). Isoflavone content in soybean is also affected significantly by additive genetic variance (Bi et al., 2015). Gutierrez-Gonzalez et al. (2010) found 35 main-effect genomic regions and many epistatic interactions that control genistein, daidzein, glycitein, and total isoflavone accumulation in soybean seeds. These findings suggest that a complex network of multiple minor-effect loci interconnected by epistatic interactions control isoflavone accumulation in soybean. The magnitude and significance of the effects of many of the nodes and connections in this network varied, however, according to the environment. This study made it possible to identify putative candidate genes for several main-effect and epistatic QTL and for known QTL (Gutierrez-Gonzalez et al., 2010). Wang et al. (2015) noted 34 QTL, of which 23 were new, for both individual and total seed isoflavone contents in soybean; while 6, 7, 10, and 11 QTL were associated with daidzein, glycitein, genistein and total isoflavone, respectively, in multi-generation soybean recombinant inbred lines (RILs; $F_{5:6}$, $F_{5:7}$, $F_{5:8}$). Several DNA markers linked to QTL were identified across environments, thereby indicating that they can be used in the selection of segregants for higher isoflavone content, and also in map-based gene cloning.

Gutierrez-Gonzalez et al. (2010) showed that many enzymes in the phenylpropanoid pathway underlie QTL and modification of genes encoding for enzymes involved in this pathway might promote the biosynthesis of isoflavone in soybean seeds (Hao et al., 2008). Wang et al. (2014) found 33 expression QTL (eQTL) underlying the transcript abundance for the four gene families (*PAL*, *CHS*, *IFS*, *F3H*) on 15 chromosomes. Furthermore, the eQTL between Satt 278-Sat-134, Sat-134-Sct-010, and Satt 149-Sat-234 underlie the expression of both the *IFS* and *CHS* genes. More importantly, they identified five eQTL intervals that overlapped with phenotype QTL (pQTL), and a total of 11 candidate genes within the overlapped eQTL and pQTL.

Flavonoids in Cereals

Polyphenol compounds that impart red pigment to wheat grain are synthesized through the flavonoid biosynthetic pathways. Himi and Noda (2005) showed that the expression of *CHS*, *CHI*, *F3H,* and *DFR* in the flavonoid pathway is completely suppressed indeveloping white grain, but not in red grain, in wheat. All four genes were highly up-regulated in the grain coat tissue of the red lines, whereas there was no significant expression in the white- colored lines, thus indicating that the *R* gene (Myb-type transcription factor) is involved in the activation of early flavonoid biosynthesis genes in wheat (Himi et al., 2005). Flavanone 3-hydroxylase (F3H) is a key enzyme at a divergence point of the flavonoid pathway that leads to the production of different pigments, proanthocyanidin, and anthocyanin. Himi et al. (2011) isolated *F3H-A1*, *F3H-B1*, and *F3H-D1* on chromosomes 2A, 2B, and 2D of wheat. These genes were highly expressed in red grain and coleoptiles, and they appeared to be controlled by flavonoid regulators in each tissue. Moreover, the telomeric regions of the long arms of the chromosomes of homoeologous group 2 of wheat showed a syntenic relationship to the telomeric region of the long arm of rice chromosome 4, where the rice *F3H* gene is located. To date, a number of structural [*Pal*, *Chs*, *Chi*, *F3h*, *F3′5′h*, *Dfr* (*TaDfr*), *Ans*, *Mt* (*Fmt*), and *Rt* (*3Rt*)] and regulatory [Myc (*TaMyc*), Myb10 (*Tamyb 10),* and *Mpc1*] genes are known to be involved in flavonoid biosynthesis in wheat. In most cases, the information on the number of loci involved, chromosomal/intra-chromosomal localization, and sequences (complete or partial) of the gene copies are known (Khlestkina et al., 2015).

Jin et al. (2009) reported two QTL on chromosome 2, as *qPH-2* for phenolic and *qFL-2-1* for flavonoid content, which are flanked by CT87 and G1234, and which show large additive effects that account for 17 and 13%, respectively, of the phenotypic variation in rice. High narrow-sense heritability was estimated using 84 hybrids from an 11-parent diallel mating design, thus showing the importance of additive genetic variance for total phenols in maize (Mahan et al., 2013). A genome-wide association study that involved a global sorghum diversity panel ($n = 381$) and 404,628 SNP markers (Rhodes et al., 2014) identified novel QTL associated with polyphenols in sorghum. Some of these were co-localized with homolog of flavonoid pathway genes from other plants, including an ortholog of maize *Pr1* and a homolog of *Arabidopsis TT16*. General linear models (GLMs) did not precisely map a loss-of-function allele of the *Tannin 1* gene (*tan 1*), while either a GLM accounting for population structure or a standard linear model considering kinship did identify it (Morris et al., 2013). Furthermore, *tan 1* was accurately mapped using a simple loss-of-function genome scan for the genotype-phenotype co-variation only in the putative loss-of-function allele.

Anthocyanins in Cereals

The deposition of proanthocyanidins in the seed testa results in red grain whereas anthocyanins in the pericarp and aleurone layer give rise to purple and blue colored wheat kernels, respectively (Zeven, 1991). *Ba1* (Keppenne and Baenziger, 1990) and *Ba2* (Dubcovsky et al., 1996) were found to control blue grain in a tall wheat grass [*Thinopyrum ponticum* (hereonward referred as *Th. ponticum*) = *Agropyron elongatum*] and in *Triticum monococcum*, respectively. These two genes were physically mapped: *Ba1* at FL0.71-0.80 on chromosome 4Ag (Zheng et al., 2006), and *Ba2* near the centromere on chromosome 4AL (Dubcovsky et al., 1996). The wild relative *Th. bessarabicum*

bears the gene *BaThb,* which produced blue grain and has been physically mapped between the centromere and FL0.52 on chromosome arm 4JL. *BaThb* differs from *Ba1* and *Ba2*, and has a strong dose effect, thus confirming *Th. bessarabicum* as another source of blue aleurone grain in wheat (Shen et al., 2013). To date, several blue wheat elite lines have been developed. These lines carry *Th. ponticum* or *T. monococcum* introgressed chromosomes. Burešováet et al. (2015) found that 17 of 26 such lines have introgression from *Th. ponticum*, while the remaining bear *T. monococcum* chromatin. This finding suggests that these blue aleurone wheat lines show major differences in chromatin composition. Introgression activates the blue aleurone trait, which is inactivated in bread wheat germplasm lacking the *Th. ponticum* chromosome segment.

The genes *Pp1* and *Pp3* mapped on the short chromosome arms of the homeologous group 7 and on chromosome arm 2AL, respectively, control purple grain color in wheat (Dobrovolskaya et al., 2006; Khlestkina et al., 2010; Tereshchenko et al., 2012). Furthermore, the *Pp1* genes are orthologs to both maize *C1* and rice *OsC1*, and encode MYB-like transcription factors that activate structural genes related to enzymes associated with anthocyanin biosynthesis (Khlestkina, 2013). *Pp3* is orthologous to *Ra* in rice (Wang and Shu, 2007) and *Lc* in maize (Ludwig et al., 1989). It encodes *TaMYC1*, which is strongly expressed in the pericarp (Shoeva et al., 2014). *Pp1* and *Pp3* upregulate the transcript abundance of structural genes *Chi* (Chalcone-flavone isomerase) and *F3h* (flavanone 3-hydroxylase) in the pericarp of near isogenic lines carrying various combinations of *Pp* alleles (Gordeeva et al., 2015).

The pericarp of red rice grains accumulates proanthocyanidin (Sweeney et al., 2006), while purple rice grain accumulate anthocyanin (Rahman et al., 2013). Maeda et al. (2014) confirmed that *Pp* on chromosome 1 and *Pb* on chromosome 4 acted together to influence grain color (Wang and Shu, 2007; Rahman et al., 2013). They also indicated that *Kala1*, *Kala3*, and *Kala4* are essential for black pigmentation. Their loci were mapped between RM7405 and RM7419 on chromosome 1, between RM15008 and RM 3400 on chromosome 3, and between RM1354 and RM7210 on chromosome 4, respectively. Ectopic expression of the *Kala4 bHLH* gene leads to expression of anthocyanin biosynthesis genes in the pericarp, and produces black rice grains, while a DNA duplication event at the 5′-end of the gene that correlated with *kala4* expression also controls black grain (Oikawa et al., 2015).

Wei et al. (2013) showed that in barley a dominant gene *Blp* mapped on chromosome 1HL controls black grain, while the complementary dominant genes *Pre1* and *Pre2* mapped on chromosome 2HL determine the purple color. They also indicated that the complementary dominant genes *Blx1*, *Blx3*, and *Blx4* mapped on chromosome 4H, plus *Blx2* and *Blx5* mapped on chromosome 7HL, are responsible for blue colored barley kernels.

Anthocyanin biosynthesis in maize is regulated by interactions between two sets of transcription factors that are encoded by *c1/pl1* and *r1/b1*; *c1* and *r1* regulate pigmentation in the kernel aleurone, and *pl1* and *b1* regulate it in the plant body (Chandler et al., 1989). The *pr1* gene has a role in the *cl*- and *rl*-regulated anthocyanin biosynthesis pathway (Sharma et al., 2011). The *pr1* locus accumulates red (pelargonidin) and the *Pr1* accumulates purple (cyanidin) anthocyanins in the aleurone cells of seeds. The putative F3′H encoding gene (*Zmf3′h1*) was mapped on chromosome 5L, while purple and red anthocyanins accumulated in *Pr1* and *pr1* lines, respectively. Furthermore, *pr1* has four alleles, which are characterized by insertion or deletion polymorphisms that co-segregated with the red aleurone phenotype in the F_2 population containing *Pr1* and *pr1* alleles. This gene is under the regulatory control of anthocyanin transcription factors *red1* and *colorless1*. Moreover, Sharma et al. (2012) showed that *Zmf3′h1* also participates in biosynthesis of phlobaphenes and 3-deoxyflavonoid compounds, which accumulate in maize pericarp and cob glumes and silks, and are under regulatory control by *P1*. Thus, *Zmf3′h1* has a significant role in generation of diversity for anthocyanin, phlobaphenes, 3-deoxyanthocyanidin and C-glycosyl flavone compounds; the latter two of these compounds impart maize plant resistant to pests and pathogens (Nicholson and Hammerschmidt, 1992; Byrne et al., 1996).

PERICARP COLOR 1 (*P1*) is an R2R3-MYB type transcription factor that controls the accumulation of brick red phlobaphenes pigments in grain pericarp in maize. Phlobaphenes are polymers of the flavan-4-ols apiforol and luteoforol, and are generated from naringenin or eriodictyol by dehydroflavonol reductase (DFR), which is encoded by maize *A1*. *P1* alleles specify different pericarp and cob glume colors. For example, *P1-ww* results in white pericarps and white cob glumes, whereas *P1-rr* produces red pericarps and red cob glumes. *A1* mutants in a *P1-rr* background (*P1-rr; a1*) display an unidentified brown pigment that contrasts with the white *P1-ww* pericarp, thereby suggesting metabolic shunting toward a different branch of the flavonoid pathway (Casas et al., 2014). Most of the elite lines used in the production of hybrid maize lack flavones. Casas et al. (2014) showed that maize lines harboring the *P1-rr* allele in combination with recessive *a1* accumulate flavones to the same levels as flavone-rich vegetables. These results suggest that nutritionally beneficial flavones can be re-introduced into elite lines to increase the dietary benefits of maize.

Clearly, over the years a greater understanding of phenylpropanoid genetics has been achieved, and this knowledge-based inheritance can now facilitate the enriching of staple grain crops with health-promoting compounds.

Biosynthesis Pathways

Flavonoid biosynthesis (**Figure 1**) begins with the phenylpropanoid pathway, in which phenylalanine is converted into p-coumaroyl CoA. This pathway is mediated by the flavonoid metabolon, which is attached to the cytoplasmic face of the endoplasmic reticulum. Metabolons are multienzyme complexes. They represent highly organized assemblies of sequential enzymes in a metabolic pathway, and they provide increased metabolic efficiency and higher substrate selectivity (Kaur-Sawhney et al., 2003). The basic carbon structure of flavonoids is generated by a two-step condensation process that is mediated by chalcone synthase (CHS) and chalcone isomerase (CHI). The resulting colorless naringenin is then oxidized by F3H to dihydrokaempferol. Naringenin can

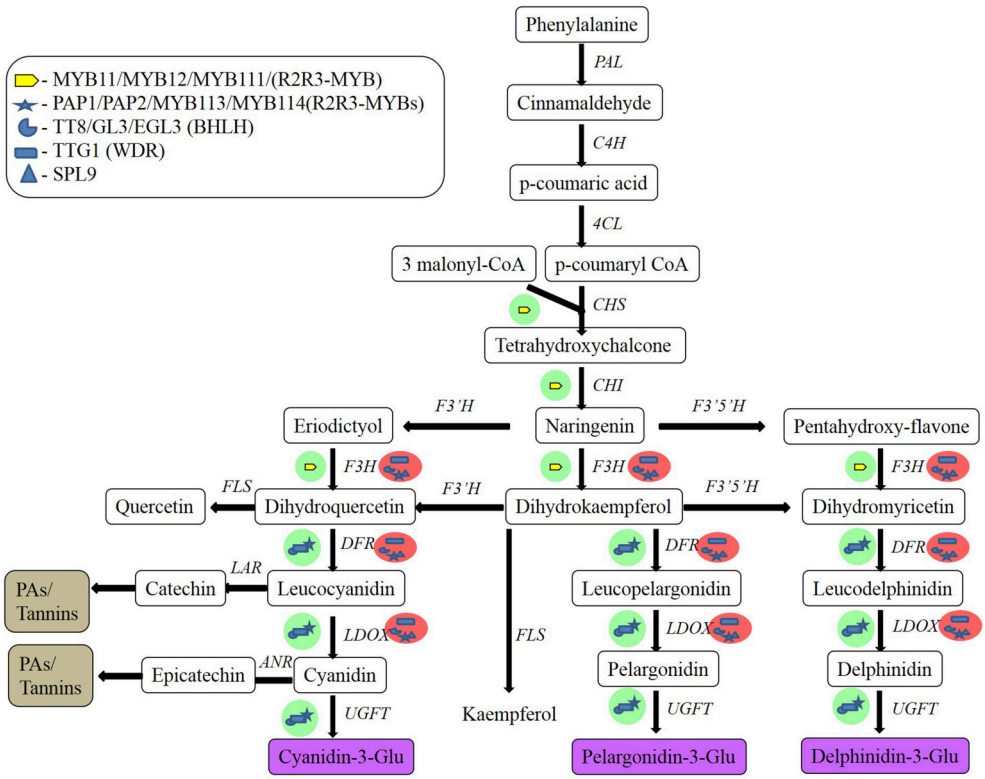

FIGURE 1 | Flavonoid biosynthetic pathway in plant cells and regulatory gene regulation of this pathway in *Arabidopsis*. Green and red circles indicate activation and repression, respectively. MYB, myeloblast; PAP, production of anthocyanin pigment; TT8, transparent testa A8; bHLHs, basic helix-loop-helix proteins; TTG1, transparent testa glabrous1; SPL9, squamosa promoter binding protein-like 9; PAL, phenyalanine ammonia-lyase; C4H, cinnamic acid 4-hydroxylase; 4CL, 4-coumarate CoA ligase; CHS, chalcone synthase; CHI, chalcone isomerase; F3H, flavanone 3′-hydroxylase; F3′H, flavonoid 3′-hydroxylase; F3′5′H, flavonoid 3′5′-hydroxylase; DFR, dihydroflavonol reductase; LDOX, leucoanthocyanidin oxidase; UGFT, UDP-glucose flavonoid 3-O-glucosyl transferase; FLS, flavonol synthase; LAR, leucoanthocyanidin reductase; ANR, anthocyanidin reductase (After Pandey et al., 2014).

also be directly hydroxylated to yield dihydroflavonols, and then later converted into anthocyanidins. Despite the central biosynthetic pathway being conserved in plants, various enzymes can modify the basic flavonoid skeletal structure including reductases, isomerases, hydroxylases, and dioxygenases, to form different subclasses of flavonoids in different species. Transferases add groups like sugars, methyl, or acyl groups to the backbone structure. The synthesis of proanthocyanidins branches off from the anthocyanin pathway subsequent to the reduction of dihydroquercetin to leucocyanidin. The two major enzymes involved in the formation of proanthocyanidins are leucoanthocyanidin reductase (LAR) and anthocyanidin reductase (ANR) (Bogs et al., 2005).

The flavonoid biosynthesis pathway is extensively regulated by transcription factors, such as the MYB proteins, basic helix-loop-helix (bHLH) factors, and WD-repeat-containing proteins. Transcriptional regulation has been extensively investigated in maize and *Arabidopsis*. This has facilitated the identification of differences in regulation between monocots and dicots (Ferreyra et al., 2012). The MYB domain is made up of one (MYBR1), two (R2R3-MYB), or three (MYB3) repeats of about 52 amino acids, with R2R3-MYB being the most predominant. Specific motifs and conserved residues mean that these proteins can regulate single branches of the flavonoid pathway (Hichri et al., 2010; Lin-Wang et al., 2010). The overexpression of VlMYBA-1 in the hair roots of grapevine induces the expression of only the genes involved in anthocyanin biosynthesis and transport, whereas the overexpression of VvMYBPA1 and VvMYBPA2 selectively activates genes involved in the synthesis of proanthocyanidins. Albert (2015) isolated *Tr-MYB133* and *Tr-MYB134* in white clover (*Trifolium repens* L.), which encode R2R3-MYBs that antagonize the activity of MBW activation complexes. These two genes are also conserved in other legume species, and form two subclades within the larger anthocyanin/proanthocyanidin clade of MYB repressors. However, unlike petunia (*Petunia* sps.) and *Arabidopsis,* these R2RS-MYB repressors do not prevent ectopic accumulation of anthocyanins or proanthocyanidins. Instead, they are expressed when anthocyanins or proanthocyanidins are synthesized, and provide feedback regulation to MBW complexes. This feedback occurs because *Tr-MYB133* and *Tr-MYB134* are themselves regulated by MBW complexes. *Tr-MYB133* is regulated by MBW complexes that contain

anthocyanin-related R2R3-MYB proteins (Tr-RED LEAF), while *Tr-MYB134* is regulated by complexes containing the proanthocyanidin R2RS-MYBs (Tr-MYB14). Thus, regulation of *Tr-MYB133* and *Tr-MYB134* by pathway-specific MBW complexes results in anthocyanin or proanthocyanidin synthesis (Albert, 2015).

The bHLH proteins are ubiquitous transcription factors that are found across eukaryotes, from yeast to human. They are widely distributed in plants and are characterized by the presence of a critical region, called the bHLH domain. The basic region of the bHLH domain consists of 15–17 amino acids, and this is responsible for DNA binding and activation. The bHLH proteins form heterodimers and function as repressors in the absence of the basic region (Toledo-Ortiz et al., 2003). The first 200 amino acids of the protein on the N'-terminal are referred to as MIR (MYB–interacting region), and the next 200 amino acids are known as the WD-40/AD domain, which facilitates the formation of ternary complexes known as MBW complexes in plant species. The bHLH proteins can bind DNA as a single molecule or as a dimer, with MYB proteins based on the promoter target (Hichri et al., 2011). Unlike MYB proteins, some bHLH proteins can influence more than one branch of the flavonoid pathway. The TT8 (transparent testa 8) factor of *Arabidopsis* is an example of the regulation of both the anthocyanin and proanthocyanidins pathways.

Ternary complexes that comprise the above-mentioned transcription factors that are referred to as MBW complexes have been comprehensively identified in model plants and crops (Supplementary Table 2). In *Arabidopsis*, the MYB protein controls the target-gene specificity of the ternary complex. The presence of PAP1/PAP2 (production of anthocyanin pigment), TT2 (transparent testa 2), GL1 (glabrous 1), WER (werewolf), and AtMYB61 regulate anthocyanin accumulation in seedlings, proanthocyanidins biosynthesis in seed integuments, trichome formation, root-hair initiation, and mucilage production in seed integuments, respectively (Baudry et al., 2004). Flavonoid biosynthesis is also regulated by environmental factors, such as light and external stresses in grape (*Vitis vinifera* L.; Li et al., 2014), and the intensity of light and sucrose conditions in *Arabidopsis* (Das et al., 2012), which is mediated by the MYBL2 factor. In mulberry (*Morus* spp.), transcriptional levels of regulatory genes involved in the biosynthesis of anthocyanins are directly related to the degree of ripening and the coloration intensity of the fruits (Qi et al., 2014).

In summary here, elucidating the intricate regulatory patterns of the flavonoid biosynthesis pathway will pave the way for genetic enhancement. Understanding how biosynthetic enzymes are regulated and their spatio-temporal organization will enable modification of the patterns of flavonoid expression and accumulation. Manipulation of the pathways can generate fruit and vegetables enriched in antioxidant and nutritional compounds, as well as provide other medicinal benefits. Future research should be aimed at delineation of the factors that control the expression of the regulatory genes, and also at understanding the allelic variability between cultivars of the same species to identify useful DNA markers as aids for indirect selection in breeding.

GERMPLASM MINING FOR VARIATIONS IN PHENYLPROPANOIDS

Flavonoids in Legumes

A systematic search reveals that there have been limited germplasm accessions evaluated for flavonoids among grain legume crops (**Table 1**). Up to two-fold variations in flavonoid content were noted in cowpea, groundnut (*Arachis hypogaea* L.), guar [*Cyamopsis tetragonoloba* (L.) Taub.], mung bean, and soybean germplasm. The differences in chickpea and lima bean (*Phaseolus lunatus* L.) germplasm were 76- and 86-fold, respectively. In common bean, 2–13-fold differences were reported among landraces and wild and weedy types, with the latter showing maximum fold differences in flavonoid content. Kaempferol and quercetin were the main flavonoid compounds in common bean (Espinosa-Alonso et al., 2006; Mishra et al., 2012). Four-fold differences were found in cowpea and 6–76-fold in common bean germplasm. In cowpea, seed color and content of flavonol were correlated, with red-seeded accessions containing greater flavonol than white-seeded cowpeas. Other seed color types had limited variations, except for light-brown-seeded accession IAR 48, which showed exceptionally high flavonol content [0.796 mg g^{-1} dry weight (DW)] among light-brown-seeded cowpeas (Ojwang et al., 2012). Quercetin was the most abundant flavonol in cowpea (Ojwang et al., 2012), while kaempferol and quercetin flavonol were the most abundant flavonols in common bean (Doria et al., 2012).

Multi-fold differences were noted in isoflavone content among common bean germplasm, with black-, ivory-, and brown-yellow-seeded accessions showing the highest isoflavones (Doria et al., 2012; de Lima et al., 2014). There were 2–14-fold differences in isoflavone content in soybean. Daizin, genistin, glycitin, malonyldaidzin, malonylglycitin, and malonylgenistin were the major moieties (Kim et al., 2012a; Zhang et al., 2014). Maturity groups (MG) had significant differences in isoflavone content in soybean. For example, MG V and VI had significantly higher total isoflavones compared to MG 0 to IV. Differences among MG 0 to IV or between MG V and VI were, however, not statistically significant (Zhang et al., 2014). Seed size influenced mean isoflavone content among geographically different soybean accessions. For example, small-seeded accessions from North America and Korea had similar isoflavone (2.53, 2.56 mg g^{-1}, respectively), the medium-seeded accessions from North America and Korea had higher isoflavone (2.24, 2.48 mg g^{-1}, respectively) than those from China (1.38 mg g^{-1}), while large-seeded Korean accessions had higher isoflavone (1.83 mg g^{-1}) levels than those from North America and China accessions (1.20, 1.34 mg g^{-1}, respectively; Kim et al., 2012b).

Flavonoids in Cereals

Barley, rice, sorghum, and wheat germplasm/cultivars have been studied for variations in flavonoids (**Table 2**). About 2-fold variation among barley and up to 21-fold variation among rice germplasm were noted. Black-grained and red-grained rice accessions had greater flavonoids than white-grained types (Shen et al., 2009; Shao et al., 2014a). Wheat germplasm that differed in grain color had relatively narrow genetic differences for

TABLE 1 | Germplasm-wide variations in total phenylpropanoid constituents in food legumes.

Germplasm (no.)	Variation for flavonoids	References
FLAVONOID		
Common bean (*Phaseolus vulgaris* L.)		
Landraces (20)	0.05–0.41 mg quercetin (QUE) equivalent (QUAE) g^{-1} DW	Mishra et al., 2012
Wild and weedy types (64)	0.008–0.106 mg g^{-1} FW, G 12896-B and G 11025B being highest	Espinosa-Alonso et al., 2006
Zolfino landraces (4)	0.302–0.711 mg g^{-1} FW	Romani et al., 2004
Chickpea (*Cicer arietinum* L.)		
Landraces (20)	0.05–0.41 mg quercetin equivalent (QUAE) g^{-1} DW	Mishra et al., 2012
Cowpea (*Vigna unguiculata* (L.) Walp.)		
Black, red, tan, and white grains (8)	0.253–0.442 mg g^{-1} DW, quercetin being highest (0.214–0.279 mg)	Wang et al., 2008
Groundnut (*Arachis hypogaea* L.)		
Black, pink, red, tan, and white grains (8)	0.138–0.336 μg g^{-1} DW, quercetin being highest (0.133–0.288 mg)	Wang et al., 2008
Guar (*Cyamopsis tetragonoloba* (L.) Taub.)		
Accession (36)	13–23 mg 100 g^{-1} DW; Kaempferol, the major component (10.7–19.8 mg)	Wang and Morris, 2007
Lima bean (*Phaseolus lunatus* L.)		
Black, brown, pink, red, and white-grains (50)	0.2–17.3 mg rutin equiv. (RUE) g^{-1} DW	Agostini-Costa et al., 2015
Mung bean (*Vigna radiata* (L.) R. Wilczek)		
Accession (50)	1.204–2.932 mg g^{-1} DW	Kim et al., 2013
Soybean (*Glycine max* (L.) Merr.)		
Black, brown, green, red, and yellow grains (8)	0.892–0.916 mg g^{-1} DW; genistein (0.438–0.458 mg) and daidzein (0.315–0.354 mg) greater than Kaempferol (0.038–0.068 mg)	Wang et al., 2008
FLAVONOL		
Common bean		
Gene pools differing in seed color (16)	0.002–0.125 mg g^{-1} DW	de Lima et al., 2014
Landrace-based populations (10)	0.011–0.081 mg g^{-1} DW	Doria et al., 2012
Zolfino landraces (4)	1.18–7.09 mg g^{-1} FW	Romani et al., 2004
Cowpea (*Vigna unguiculata* (L.) Walp.)		
Black, brown, green, golden, and white grains (10)	0.27–1.06 mg g^{-1} DW, red-seeded had greater (mean 0.97 mg) than white-seeded (0.27 mg)	Ojwang et al., 2012
ISOFLAVONE		
Common bean		
Gene pools differing in seed color (16)	0.0008–0.14 mg g^{-1} DW	de Lima et al., 2014
Landrace-based populations (10)	0.009–0.113 mg g^{-1} DW	Doria et al., 2012
Zolfino landraces (4)	0.002–0.015 mg g^{-1} FW	Romani et al., 2004
Soybean		
Indian and exotic accessions (46)	0.234–2.092 mg g^{-1} DW	Kumar et al., 2015
0 to VI maturity groups (40)	0.551–7.584 mg g^{-1} DW	Zhang et al., 2014
Cultivars (44)	0.276–1.709 mg g^{-1} DW	Kim et al., 2014
Seed size variations (204)	0.682–4.778 mg g^{-1} DW	Kim et al., 2012b
0 to II maturity groups (210)	1.161–2.743 mg g^{-1} DW	Wang et al., 2000

Original data on phenylpropanoid constituents given in papers cited here were converted and presented into mg g^{-1} dry weight.

flavonoids. Up to 12-fold difference in flavone and up to 6-fold difference in flavanone content were observed among sorghum open-pollinated and hybrid cultivars.

Anthocyanin in Legumes

Nine-fold differences in anthocyanin levels were noted among common bean germplasm lines differing in seed color and weight. Accessions with brown, red, or black seed color had higher levels of anthocyanins (0.003–0.005 mg g^{-1} DW; Akond et al., 2011). Kidney-bean germplasm showed large range variations in total anthocyanins (0.07–2.78 mg g^{-1} DW), black-seeded types being richer sources of anthocyanins than red- or brown-seeded types (Choung et al., 2003). About 2-fold differences in total anthocyanin were recorded among cowpea lines. Black-seeded cultivars had higher levels of anthocyanins than the green-seeded type. The predominant anthocyanin compounds include delphidin-3-*O*-glucoside, cyanidin-*O*-glucoside, petunidin-*O*-glucoside, and malvidin-*O*-glucoside (Ojwang et al., 2012). In soybean, several-fold differences (30–213 times) were noted among Chinese and Japanese cultivars and landraces, with cyanidin-3-glucoside being the most abundant (Zhang et al., 2011; Phommalath et al., 2014).

TABLE 2 | Germplasm-wide variations in total phenylpropanoid constituents in staple cereals.

Germplasm (no.)	Variation for flavonoids	References
FLAVONOID		
Barley (*Hordeum vulgare* L.)		
Landraces (37)	0.47–1.23 mg catechin equival. (CE) mg g^{-1} dry weight (DW)	Abidi et al., 2015
Hulled and hull-less (11)	27–66 mg quercetin equiv. (QUE) g^{-1} extract	Mahmoudi et al., 2015
Rice (*Oryza sativa* L.)		
Diverse accessions (20)	0.19–3.28 and 0.20–3.54 mg CE g^{-1} DW in two seasons	Shao et al., 2014a
Cultivars with pigmented and non-pigmented grains (11)	0.0012–0.0258 mg QE g^{-1} bran; higher flavonoid in pigmented than non-pigmented; greater flavanol in black-colored *indica* than black-colored *japonica*	Huang and Ng, 2012
Black, red, and white grains (481)	0.89–2.86 mg Rutin equiv. (RE) g^{-1} DW, average values greater in black (0.24 mg) than red (0.15 mg) and white (0.13 mg) grains	Shen et al., 2009
Wheat (*Triticum aestivum* L.)		
Black, purple, and white grains (4)	0.236–0.319 mg RE g^{-1} DW, with black grains being highest in flavonoid	Li et al., 2015
FLAVONE AND FLAVANONE		
Sorghum (*Sorghum bicolor* (L.) Conrad Moench)		
Colored grains (12)	Flavone: 0.008–0.1 mg g^{-1} DW; flavanone: 0.008–0.048 mg g^{-1} DW	Dykes et al., 2009
Black grained lines and hybrids (8)	Flavone: 0.018–0.056 mg g^{-1} DW; flavanone: 0.089–0.119 mg g^{-1} DW	Dykes et al., 2013

Original data on phenylpropanoid constituents given in papers cited here were converted and presented into mg g^{-1} dry weight.

Anthocyanins in Cereals

Variations in anthocyanin levels in germplasm/cultivars have been reported for barley, maize, rice, sorghum, and wheat (**Table 3**). Two-fold to eighty-fold variation in anthocyanin concentration was noted among barley germplasm. Purple-grain and blue-grain barley groups had significantly greater mean anthocyanin levels (0.32 mg g^{-1}) than black barley (0.04 mg g^{-1}). The most common anthocyanins in purple barley were cyanidin-3-glucoside, peonidin-3-glucoside, and pelargonidin-3-glucoside, whereas delphinidin-3-glucoside was the most abundant anthocyanin in blue and black barley groups (Kim et al., 2007). The predominant anthocyanins were delphidin-3-malonylglucoside and cyanidin-3-malonylglucoside, followed by delphidin-3-glucoside and cyanidin-3-glucoside in blue barley (Diczházi and Kursinszki, 2014). In maize, multi-fold differences in total anthocyanins, with most reporting 15–36-fold were observed among colored-grain accessions. Cyanidin-glucoside was the major anthocyanin (Lopez-Martinez et al., 2009; Kuhnen et al., 2011; Mendoza-Díaz et al., 2012; Žilić et al., 2012). Maize with dark-red, blue, or purple grain colors holds immense promise for the development of functional foods and natural colorants. Several-fold differences, which ranged from 4 to 121 times, were noted among pigmented rice germplasm. Cyanidin-3-glucoside, peonidin-3-glucoside, cyanidin diglucoside, and malvidin were the major anthocyanins in black-rice and red-rice kernels (Ryu et al., 1998; Abdel-Aal et al., 2006; Lee, 2010; Zhang et al., 2010; Chen et al., 2012). Red-grained and black-grained sorghum cultivars showed up to 21-fold differences in anthocyanins.

Wheat germplasm lines and cultivars showed up to 30-fold difference in anthocyanin content. Blue and purple grain accessions had higher levels of anthocyanins (Abdel-Aal et al., 2006; Eticha et al., 2011; Žofajova et al., 2012; Ficco et al., 2014). Five to eight anthocyanin compounds were noticed in blue grain wheat extracts, compared to three anthocyanin compounds in purple and red wheat (Ficco et al., 2014). Delphinidin-3-*O*-rutinoside, delphinidin 3-*O*-glucoside, and malvidin-3-*O*-glucoside were the predominant anthocyanins in blue wheat, while cyanidin-3-*O*-glucoside, peonidin-3-*O*-glucoside, and malvidin-3-*O*-glucoside were found in purple wheat (Abdel-Aal et al., 2006; Ficco et al., 2014). Zeven (1991) gave details on the origin and history of wheat with blue and purple grains.

Phenolics in Legumes

Table 4 gives the variations reported for phenolics in grain legumes. Among lima bean germplasm, there was 2–4-fold variation for phenols, except for one study that indicated a very high level (97-fold; Agostini-Costa et al., 2015). Ferulic acid was the most abundant, followed by p-coumaric and sinapic acids (Espinosa-Alonso et al., 2006; Luthria and Pastor-Corrales, 2006). Black, brown and red common beans had higher phenols than white grain types (Akond et al., 2011; Agostini-Costa et al., 2015). Up to 13-fold differences in total phenols were noted among chickpea germplasm with colored grains. *Desi* types had higher levels of phenols compared to *Kabuli* types. Among the anatomical parts, the seed coat was the major source of variation for total phenols. Cowpea germplasm and cultivars showed 3–11-fold differences in total phenols. Protocatechuic acid was the major phenolic, while p-hydroxybenzoic, caffeic, p-coumaric, ferulic, 2,4-dimethoxybenzoic, and cinnamic acids were also reported (Cai et al., 2003). Valencia groundnut (var. *fastiggiata*) differing in seed color showed 34-fold differences in total phenols. Seeds with pink color had significantly higher levels of phenols than those with gray and yellow color. The major phenolic compounds in the testae of nearly all genotypes were

TABLE 3 | Germplasm-wide variations in total phenylpropanoid constituents in staple cereals.

Germplasm (no.)	Variation in total anthocyanin content	References
Barley (*Hordeum vulgare* L.)		
Colored grains (4)	0.047–0.084 mg g^{-1} dry weight (DW)$	Diczházi and Kursinszki, 2014
Hulled and unhulled colored grains (127)	0.013–1.038 mg catechin equiv. g^{-1} DW	Kim et al., 2007
Maize (*Zea mays* L.)		
Blue-grain hybrids/varieties (7)	0.65–1.05 mg cyaniding 3-glucoside (Cy3Glu) equiv. g^{-1} DW	Urias-Lugo et al., 2015
Waxy maize (49)	0.07–1.06 mg Cy3Glu equiv. g^{-1} DW	Harakotr et al., 2015
Colored grains (4)	1.74–9.63 mg Cy3Glu equiv. g^{-1} DW	Mendoza-Díaz et al., 2012
Colored grains (10)	0.002–0.696 mg Cy3Glu equiv. g^{-1} DW	Žilić et al., 2012
Red and blue grains (9)	0.02–0.72 mg Cy3Glu equiv. g^{-1} DW	Montilla et al., 2011
Waxy colored and normal yellow grains (3)	0.001–2.761 mg Cy3Glu equiv. g^{-1} DW	Hu and Xu, 2011
Colored grains (18)	0.30–8.50 mg Cy3Glu equiv. g^{-1}; purple, 0.93 to8.50 mg; black, 0.76-1.20 mg; Red, 0.85–1.54 mg	Lopez-Martinez et al., 2009
Colored grains (9)	0.051–1.277 mg g^{-1} DW$	Abdel-Aal et al., 2006
Rice (*Oryza sativa* L.)		
Colored grains (9)	0.21–2.98 mg g^{-1} DW$	Chen et al., 2012
Black and red grains (13)	Black grains: 1.09–2.56 mg Cy3Glu equiv. 100 g^{-1} DW; Red grains: 0.003–0.014 mg Cy3Glu equiv. g^{-1} DW	Sompong et al., 2011
Black grains (12)	12.31–51.01 mg Cy3Glu equiv. g^{-1} DW	Zhang et al., 2010
Black grains (10)	0.052–1.684 mg Cy3Glu equiv. g^{-1} DW	Lee, 2010
Wild rice with colored grains (3)	0.027–3.276 mg g^{-1} DW$	Abdel-Aal et al., 2006
Sorghum (*Sorghum bicolor* (L.) Conrad Moench)		
Colored grains (12)	0.032–0.68 mg g^{-1} DW$	Dykes et al., 2009
Black grained lines and hybrids (8)	0.33–1.05 mg g^{-1} DW$	Dykes et al., 2013
Wheat (*Triticum* species)		
Durum and bread wheat colored grains (76)	Blue colored bread wheat, 0.082–0.174 mg g^{-1} DW, mean 0.118 mg; purple and red colored durum wheat, 0.008–0.05 (mean, 0.023), and 0.001–0.025 mg (mean, 0.01), respectively$	Ficco et al., 2014
Colored grains (4)	0.007–0.12 mg g^{-1} DW$	Žofajova et al., 2012
Pigmented grains (13)	0.0034–0.0752 cyanidin glucoside equiv. mg g^{-1} DW	Eticha et al., 2011
Colored grains (7)	0.007–0.212 mg g^{-1} DW$	Abdel-Aal et al., 2006

Original data on phenylpropanoid constituents given in papers cited here were converted and presented into mg g^{-1} dry weight. $total anthocyanin (not the anthocyanin compounds) value was given in the original literature.

p-coumaric and vanillic acids. Korean mung bean germplasm had 5-fold differences in total phenols. Kim et al. (2013) detected a total of 25 phenolic compounds in mung bean germplasm, with rutin being predominant, and its concentration among these germplasm varied from 1.09 to 2.72 mg g^{-1}.

Soybean germplasm from landraces and cultivars from China, Korea, and the USA showed 8–12-fold variations in total phenols. US soybean germplasm had higher mean total seed phenols (2.73 mg GAE g^{-1}) than those from Korea (1.98 mg g^{-1}) and China (1.680 mg g^{-1}) (Kim et al., 2012b), as for black-grain Chinese germplasm (23.57 mg g^{-1}; Zhang et al., 2011). Furthermore, the total phenols varied from 0.93 to 5.56 mg g^{-1} in North American soybean, 0.72 to 4.21 mg g^{-1} in Chinese soybean, 0.65 to 5.07 mg g^{-1} in Korean soybean (Kim et al., 2012b), 53 to 384 mg GAE g^{-1} in Japanese soybean (Phommalath et al., 2014) and 5.12 to 6.06 mg g^{-1} in black-grain Chinese germplasm (Zhang et al., 2011). Grain-size variations had significant effects on phenols, with higher mean total phenols in small- (2.24 mg g^{-1}) as compared to medium- (1.93 mg g^{-1}) and large- (1.95 mg g^{-1}) grain types (Kim et al., 2012b). This suggests that phenolic compounds are condensed in small-grain soybean, whereas they appear diffused at lower densities in large-grain soybean (Kim et al., 2012b).

Phenolics in Cereals

Cereal germplasm and cultivars have been the most extensively studied for variations in phenolics (**Table 5**). Two-fold to three-fold variations were noted for total phenols in barley. Catechine, *p*-coumaric, and ferulic acids were the most abundant (Dvořáková et al., 2008; Abdel-Aal et al., 2012; Gamel and Abdel-Aal, 2012). Genotypic differences for specific groups were also observed. For example, protocatechuic and caffeic acids were found in Egyptian hulled cultivars, but not in Canadian hulled cultivars (Gamel and Abdel-Aal, 2012). Blue-grain accessions had higher mean phenolics (7.73 mg g^{-1} DW) than white (6.69 mg g^{-1}), purple (6.14 mg g^{-1}), and black (5.61 mg g^{-1})-grain barley types (Siebenhandl-Ehn et al., 2011). Kim et al. (2007) also reported higher mean phenolics (0.27 mg g^{-1} DW) in blue

TABLE 4 | Germplasm-wide variations in phenylpropanoid constituents in food legumes.

Germplasm (no.)	Variation in total phenols	References
Common bean (*Phaseolus vulgaris*)		
Black, brown, pink, red, and white-grains (50)	0.1–9.7 mg GAE g^{-1} DW	Agostini-Costa et al., 2015
Landrace-based populations (10)	0.007–0.032 mg GAE g^{-1} DW	Doria et al., 2012
Varying in seed color and weight (29)	6–14 mg g^{-1} GAE DW	Akond et al., 2011
Wild and weedy types (64)	50–131 mg kg^{-1} GAE fresh weight	Espinosa-Alonso et al., 2006
Market types (15)	0.19–0.48 mg g^{-1} GAE DW	Luthria and Pastor-Corrales, 2006
Chickpea (*Cicer arietinum* L.)		
Colored grains (17)	0.2–32.6 mg catechin equiv. (CAE) g^{-1} DW; seed coat the major source of phenolics	Segev et al., 2010
Cowpea (*Vigna unguiculata* (L.) Walp.)		
Brown and white-grained (7)	0.85–2.95 mg GAE g^{-1} DW	Noubissié et al., 2012
Cultivars (17)	0.35–3.77 mg g^{-1} DW	Cai et al., 2003
Groundnut (*Arachis hypogaea* L.)		
Gray, pink, purple, red, yellow, and variegated colored Valencia's (15)	Seed testa: 2.5–84.5 mg GAE g^{-1} DW; significantly greater phenols among accessions with pink grain color	Khaopha et al., 2012
Mung bean (*Vigna radiata* (L.) R. Wilczek)		
Germplasm (56)	0.12–0.59 mg g^{-1} DW	Kim et al., 2013
Soybean (*Gylcine max* (L.) Merr)		
Black grains Japanese cultivars and landraces (227)	75–380 and 19–389 mg GAE g^{-1} DW in two seasons; more phenols in purple flowers than white flowers producing cultivars	Phommalath et al., 2014
Seed size variation (204)	0.65–5.22 mg g^{-1} DW	Kim et al., 2012b
Black grains (60)	5.12–60.58 mg GAE g^{-1} DW	Zhang et al., 2011

Original data on phenylpropanoid constituents given in papers cited here were converted and presented into mg g^{-1} dry weight.

and purple barley than in black-grained barley (0.21 mg g^{-1}). Furthermore, a large range for total phenolics was noted within each group, which suggested that there are accessions with high phenolics in each color group (Siebenhandl-Ehn et al., 2011; Abdel-Aal et al., 2012).

Maize germplasm showed about 2-fold variation in total phenolics, except studies by Lopez-Martinez et al. (2009) and Hu and Xu (2011), who noted 16–20-fold variations. High phenolic content was found among Mexican landrace germplasm and in waxy corn germplasm from China. Black and purple grain showed higher levels of phenolics compared to red grain, while white kernels contained the lowest levels of phenolics (Lopez-Martinez et al., 2009; Hu and Xu, 2011; Montilla et al., 2011; González-Muñoz et al., 2013). Ferulic acid was the major phenolic, whereas *p*-coumaric, *o*-coumaric, vanillic, vanillin, and protocatechuic acids were found in significant quantities (Lopez-Martinez et al., 2009; Hu and Xu, 2011; Montilla et al., 2011; Žilić et al., 2012; González-Muñoz et al., 2013).

Total phenolics in rice germplasm showed up to 15-fold variation. One study involved 20 diverse rice accessions containing red and white grain types (Shao et al., 2014a) and another study had 481 accessions with black, red and white grain types (Shen et al., 2009); these showed large variability in total phenolics. Black rice germplasm contained higher levels of phenolics than red and white grain types, while white grain germplasm had the lowest levels of phenolics. Red grain types had higher levels of phenolics than white grain types, but lower levels than black grain types (Shen et al., 2009; Huang and Ng, 2012; Park et al., 2012; Shao et al., 2014a,b). Ferulic, p-coumaric, and salicylic acids were the major phenolic compounds (de Mira et al., 2009; Huang and Ng, 2012; Park et al., 2012), with pigmented rice grain containing greater soluble phenolic compounds than non-pigmented rice grain.

Wide range variations (7–38-fold) for total phenols were noted among sorghum germplasm (668 accessions) differing in grain color, while eight lines and hybrids showed 4-fold differences in phenols. High levels of total phenols were observed in pigmented genotypes (Dykes et al., 2014). Grain color had a significant effect on phenolic compounds. For example, red grain contained higher amounts of 3-deoxyanthocyanidins than brown or white grain, while brown grain contained significantly greater mean proanthocyanidins than red, white, or yellow grain (Rhodes et al., 2014). The grouping of sorghum germplasm based on biological and geographical origin also significantly affected total phenols and phenolic compounds. For example, *bicolor* and *caudatum* germplasm as a group had higher mean total phenols than *durra* and *guinea*, while *bicolor* and *guinea-caudatum* had higher mean proanthocyanidins and *bicolor-durra* and *guinea-caudatum* contained higher mean 3-deoxyanthocyanidins (Rhodes et al., 2014).

Wheat landraces and cultivars showed narrow variations (1.3–2.5-fold) for mean total phenols. Ferulic and *p*-coumaric acids were the major phenolics, while other compounds such as vanillic, syringic, 2,4-dihydroxybenzoic, and sinapic acids were also reported (Siebenhandl-Ehn et al., 2007; Li et al., 2008; Gawlik-Dziki et al., 2012; Ragaee et al., 2012). Some cultivar

TABLE 5 | Germplasm-wide variations in total phenylpropanoid constituents in staple cereals.

Germplasm (no.)	Variation in total phenols	References
Barley (*Hordeum vulgare* L.)		
Landraces (37)	0.70–1.95 mg gallic acid equivalents (GAE) g^{-1} dry weight (DW)	Abidi et al., 2015
Hulled and hull-less (11)	0.06–0.14 mg GAE g^{-1} extract	Mahmoudi et al., 2015
Colored grains (18)	5.04–13.94; 7.97–14.12; 4.15–14.33; 8.20–8.94 mg g^{-1} GAE DW in black, blue, yellow, and mixed grain color, respectively	Abdel-Aal et al., 2012
Two- and six-rows, hulled and hulless normal and waxy grains (6)	171–554 mg g^{-1} DW	Gamel and Abdel-Aal, 2012
Hulled and hulless cultivars (12)	4.81–6.76 mg GAE g^{-1} DW	Holtekjølen et al., 2011
Hulled and hulless cultivars (10)	0.25–0.67 mg g^{-1} DW[$]	Andersson et al., 2008
Cultivars (10)	0.25–0.49 mg GAE g^{-1} DW	Dvořáková et al., 2008
Black, blue, purple grains (127)	0.19–0.40 mg GAE g^{-1} DW; unhulled (0.27 g^{-1}) > hulled (0.21 mg g^{-1}); blue and purple (0.27 mg g^{-1})> black (0.21 mg g^{-1})	Kim et al., 2007
Maize (*Zea mays* L.)		
Blue-grain (7)	10.10–13.47 mg GAE g^{-1} DW	Urias-Lugo et al., 2015
Waxy (49)	0.005–0.012 mg GAE g^{-1} DW	Harakotr et al., 2015
Landrace populations (33)	1.32–2.62 mg of GAE g^{-1} DW	González-Muñoz et al., 2013
Inbred and landraces (10)	5.23–10.53mg GAE g^{-1} DW	Žilić et al., 2012
Red and blue colored grains (9)	3.11–8.18 mg GAE g^{-1} DW	Montilla et al., 2011
Waxy and normal yellow grains (4)	0.23–3.88 mg GAE g^{-1} DW	Hu and Xu, 2011
Colored and white grains (18)	1.70–3.40 mg GAE g^{-1} DW	Lopez-Martinez et al., 2009
Rice (*Oryza sativa* L.)		
Diverse accessions (20)	0.40–5.62 and 0.44–6.62 mg GAE g^{-1} DW in two seasons	Shao et al., 2014a
Black, red, and white grains (3)	0.31–1.57 mg GAE g^{-1} DW	Shao et al., 2014b
Black and white grains (15)	0.15–0.37 mg g^{-1} DW; greater variation in total soluble phenolics in black (0.17–0.37 mg g^{-1}) than white (0.15–0.17 mg g^{-1}) grains	Park et al., 2012
Black, red, and white grains (6)	1.40–11.87 mg GAE g^{-1} DW	Bordiga et al., 2014
Cultivars with pigmented and non-pigmented grains (11)	0.001–0.014 mg GAE g^{-1} bran; higher phenols in pigmented than non-pigmented; greater phenols in black-colored *indica* than black-colored *japonica*	Huang and Ng, 2012
Black and red grains (13)	Black grains: 3.37–6.65 mg g^{-1} FAE DW; Red grains: 0.79–6.91 mg g^{-1} FAE DW	Sompong et al., 2011
Black grains (12)	23.65–73.67 mg GAE g^{-1} DW	Zhang et al., 2010
Colored and white grains (21)	1.07–4.25 mg FAE g^{-1} DW	de Mira et al., 2009
Wild (11)	2.47–4.07 mg FAE g^{-1} DW	Qiu et al., 2009
White, red and black grains (481)	1.08–1.24 mg GAE g^{-1} DW; black grains (10.56 mg) > red (4.70 mg) > white (1.52 mg)	Shen et al., 2009
Rye (*Secale cereale L.*)		
Cultivars (10)	0.49–1.08 mg g^{-1} DW[$]	Nyström et al., 2008
Sorghum (*Sorghum bicolor* (L.) Conrad Moench)		
Colored and white grains (381)	2–14 mg GAE g^{-1} DW; proanthocyanidins high in brown while 3-deoxyanthocyanidins in red grains	Rhodes et al., 2014
Colored and white grains (287)	1–38 mg GAE g^{-1} DW; accessions with pigmented seeds had higher phenols	Dykes et al., 2014
Lines and hybrids with black grains (8)	5–20 mg GAE g^{-1} DW	Dykes et al., 2013
Wheat (*Triticum aestivum* L.)		
Black, purple, and white grains (4)	0.51–0.66 mg GAE g^{-1} DW	Li et al., 2015
Cultivars (23)	2.90–5.65 mg GAE g^{-1} bran DW	Narwal et al., 2014
Spelt (6)	0.51–1.26 mg GAE g^{-1} DW	Gawlik-Dziki et al., 2012
Hard and soft Canadian wheat cultivars (21)	Soluble and bound phenols, respectively, ranged from 0.11–0.15 and 0.80–1.07 mg g^{-1} DW	Ragaee et al., 2012
Colored grains (13)	120–177 mg FAE 100 g^{-1} DW; purple and blue grains had greater phenolic than red-grains	Eticha et al., 2011
Market class (51)	3.41–6.70 mg g^{-1} GAE DW	Verma et al., 2008
Spring and winter wheat, spelt, durum, einkorn, emmer (175)	durum, spring, and winter wheat (0.61–0.70 mg FAE g^{-1}); emmer (0.78 mg g^{-1})>einkorn (0.61 mg g^{-1})>Spelt (0.57 mg g^{-1}); 2–3.6-fold variation within each group; winter wheat had greater variability (0.33–1.17 mg g^{-1})	Li et al., 2008

Original data on phenylpropanoid constituents given in papers cited here were converted and presented into mg g^{-1} dry weight. [$]total anthocyanin (not the anthocyanin compounds) value was given in the original literature.

groups showed larger variability than others. For example, Li et al. (2008) showed greater range variations in winter wheat (3.6-fold; 0.33–1.17 mg g^{-1}) than other cultivar groups (1.8–2.3-fold; spring: 0.46–0.89 mg g^{-1}; durum: 0.54–1.08 mg g^{-1}; spelt: 0.38–0.73 mg g^{-1}; einkorn: 0.45–0.82 mg g^{-1}; emmer: 0.51–1.16 mg g^{-1}). Canadian "Western Red" spring wheat cultivars also showed greater variability in total phenols, with 4.62–6.70 mg g^{-1} in bran (Verma et al., 2008). Ancient cultivars showed significantly more phenolic compounds and isomer forms than modern wheat cultivars (Dinelli et al., 2009). However, ancient cultivars differed only slightly from modern wheats for most of the bioactive compounds (Laus et al., 2015; Shewry and Hey, 2015).

The key to successful crop improvement is a continued supply of genetic diversity that includes new or improved variability for target traits. Research toward the identification of health-promoting germplasm (i.e., containing more phenylpropanoids) is still in its infancy. Between 2009 and 2015, only a set of 4214 germplasm accessions of cereals and legumes were evaluated (**Tables 1**–**5**). Clearly, more investment is needed to identify germplasm that is rich in phenylpropanoids; screening of representative sets, such as core (Frankel, 1984) and mini core (Upadhyaya and Ortiz, 2001) subsets, will facilitate this task.

DEVELOPING ELITE GERMPLASM/CULTIVARS HIGH IN PHENYLPROPANOIDS

Variation in seed color is associated with significant differences in phytochemicals. An indirect screening method that includes color parameters (i.e., L^*, lightness; b^*, yellowness; a^*, redness; H^*, hue angle) with an automatic color difference meter can be used for selecting phenylpropanoid-rich crops (Shen et al., 2009; Jaafar et al., 2013; Sharma et al., 2014).

Legumes

Soybean seeds are highly nutritious because they are rich in protein (>40%), oil (>18%), soluble carbohydrates (15%), and dietary fiber (15%). These seeds are exceptionally rich in isoflavones, such as genestein, daidzein, and glycetein, which are among the major components. High isoflavone cultivars are available in most soybean growing areas. The *tofu* (large-seeded) and the *natto* types (small-seeded, eaten as whole seeds) are grown in the USA and Canada (Anderson and Wolf, 1995). Soybean mutants modify seed chemistry based on single gene traits or by showing strong additive effects (Boerma and Specht, 2004). Combining genes to achieve the desired genotypes and capitalize on epistatic effects is being undertaken to improve this crop, both as food and feed (Wilson, 2012). Mutants enable genetic flexibility in tailoring soybean seed composition. The negative correlation between grain protein and isoflavone concentration might impose some biological constraint on the selection for these two beneficial traits (Murphy et al., 2009b). In contrast, similar relationships between isoflavone and linolenic (18:3) will be beneficial to the development of cultivars with high isoflavone and lower linolenic acid, the most undesirable trait (Wilson, 2012). The investment for crossbreeding soybean is smaller than that for transgenic breeding of this crop (Kumar and Ablett, 2010). Crossbred soybean is used for the improvement of transgenic soybean, because the gene base for crossbreeding is much wider than for transgenic breeding (Carter et al., 2004; Cui et al., 2004; Kumar and Ablett, 2010). It will be a challenge to maintain grain yield competitive soybean cultivars in a conventional background, as compared to transgenic soybean. This is likely to remain as a novel food until other traits are added to the trait profile of new cultivars. Despite these challenges, new cultivars with dramatic improvements in food and nutraceutical traits will emerge from global breeding programs. Soybean genomics will improve its breeding, which will greatly benefit human diets (Schmutz et al., 2010).

Cereals

Crossbreeding has led to cultivars and breeding populations rich in phenylpropanoids. For example, blue landraces in maize are a rich source of anthocyanins (Mendoza-Díaz et al., 2012). Highly productive blue maize hybrids adapted to subtropical environments or to Mexican highlands were bred with similar nutraceutical profiles to that of blue maize landraces (Urias-Peraldí et al., 2013; Urias-Lugo et al., 2015).

Some people prefer pigmented (red or black) rice grains due to their taste, texture, aroma, and ceremonial or medicinal value (Sweeney et al., 2006). Wickert et al. (2014) bred the cultivars "SCS119 Rubi" and "SCS120 Onix," with red and black grains, respectively, for specialty rice markets in Brazil. These cultivars had the same protein, lipid, carbohydrate, mineral, and fiber content as white rice, but contained higher levels of anthocyanins and phenolics than their ancestor cultivars. The mean grain yields of these cultivars were only 78% of the best white grain control (9.8 t ha^{-1}), which suggests that greater efforts are needed to raise the yield potential of such rice cultivars.

Red pericarp introgression lines (ILs) that originated from interspecific crosses showed several-fold differences in total phenolics, flavonoids, proanthocyanidins, and tannins in brown and milled rice fractions (Sharma et al., 2014). Furthermore, their yield and physiological grain traits were comparable to those of their respective recurrent parents. More recently, advanced breeding lines were evaluated for yield and phenylpropanoids in China. Several lines combined high phenolic, anthocyanin, and antioxidant capacities with high grain yield potential (Zhang et al., 2015).

Sorghum lines "Tx3362," "ATx3363," and "BTx3363" with black seed pericarp have been registered as elite lines that have very high levels of 3-deoxyanthocyanins. These lines can be used as seed parents to produce hybrids rich in 3-deoxyanthocyanins or as breeding lines to produce additional lines with these unique characteristics (Rooney et al., 2013a,b). The black-grained sorghum hybrid "ATx3363 × RTx3362" yielded 70–76% of red grain hybrids, but it contained exceptionally high levels of total phenols, tannins, and 3-deoxyanthocyanins (Rooney et al., 2013a). Although a set of six black-grained sorghum hybrids contained significantly higher concentrations of phenols, tannins and 3-deoxyanthocyanins across environments, the grain yield of the best hybrid ("A05029 × Tx3362") was only

78% of the commercial white-grained hybrid ("ATx631×RT-x- 436"; Hayes and Rooney, 2015). This low yield of black-grained hybrids showed that black grain is associated with some unknown factors that have a negative influence on grain yield.

The HEALTHGRAIN project in Europe clearly demonstrated substantial variations for bioactive compounds (e.g., alkylresorcinols, β-glucan, carotenoids, folates, phenolics, sterols, tocols), which are genetically determined, although environmental effects were also conspicuous (Ward et al., 2008; Shewry, 2009; Van der Kamp, 2012). Nevertheless it appears feasible to select for high levels of bioactive compounds, which will lead to a new generation of healthy cereals. Various genebank accessions, and advanced breeding lines and cultivars with blue or purple grain characteristics (e.g., "Amethyst," "Indigo," "Capo," "Saturnus," "Skorpion") have been identified or crossbred in wheat (Zeven, 1991; Qualset et al., 2005; Zheng et al., 2009; Eticha et al., 2011; Guo et al., 2011; Jaafar et al., 2013; Martinek et al., 2014). There has been increased use of wheat genetic resources with different grain colors to develop blue- or purple-grain wheat cultivars (Martinek et al., 2014). Genetic research suggests that it is possible to increase the anthocyanin content using different genetic backgrounds for purple pericarp and blue-aleurone germplasm in wheat. The total anthocyanin content among breeding lines ranged from 0.018 to 0.298 mg g^{-1} (mean 0.13 mg g^{-1}), and many lines contained anthocyanins in amounts $\geq$0.1 mg g^{-1} (Jaafar et al., 2013). The Crop Development Center at the University of Saskatchewan, Canada, bred the purple wheat cultivar "AnthoGrain™" that contained twice the anthocyanin content of earlier cultivars (http://www.agwest.sk.ca/blog/posts/wheat-of-the-future-might-be-purple.html). More recently, Gordeeva et al. (2015) bred near isogenic wheat lines (NILs) carrying various combinations of purple pericarp (*Pp*) alleles, using marker-aided back-crossing. These NILs represent a useful resource for studying the effects of grain pigmentation on other wheat traits.

A marker-aided recurrent backcrossing scheme using a high anthocyanin tropical maize line carrying regulatory genes (i.e., *B1*, *Pl1*) that are associated with anthocyanin production successfully converted traditional yellow popcorn into anthocyanin-rich popcorn (Lago et al., 2013, 2014). The popping ability, the expansion capacity of the kernel, the flake volume, and the taste preference of the bred cultivar were similar to the commercial yellow popcorn line.

ACCESSING CONSUMER BEHAVIOR TO EATING FOODS HIGH IN PHENYLPROPANOIDS

Consumer acceptance of phytochemicals (such a flavonoids and phenols) in foods is widely recognized as a key factor for market orientation of new products. Bornkessel et al. (2011) noted that acceptance is mainly influenced by three factors: consumer characteristics, their purchasing power, and the product characteristics. Consumer characteristics concern personal health status and consumer awareness of phytochemicals as a special ingredient associated with certain additional benefits. The three main focus areas include consumer acceptance in general, health aspects and ingredients. The acceptance is determined by various factors such as primary health concerns, consumer familiarity with the new food concept and with the functional ingredients, nature of the product carrier, and communication and publicity of the health benefits. New product acceptance could be hindered because of the taste even though consumers perceive the benefits (Saba et al., 2010). Consumer knowledge of the health benefits of newly developed functional ingredients from phytochemicals appears to be relatively limited. Recent studies have shown that consumers of today are genuinely interested in products that are beneficial to their health. Middle-aged and elderly consumers tend to be substantially more health conscious than the younger generations. This is because they or members of their immediate social environment are much more likely to be diagnosed with a lifestyle-related disease (Nocella and Kennedy, 2012; Lähteenmäki, 2013).

The regulation of policies on health claims receives much attention worldwide because this helps consumers make informed healthy choices. Dean et al. (2007) researched public perceptions relating to different healthy grain-based foods (i.e., bread, pasta, biscuits) in Europe and how gender, nationality, type of food, health claims, and perceptions of the manufacturing processes influenced them. The results confirmed that perception of phytochemicals supplied by foods varies with gender, country, and differences in consumer perception of benefits relating to functional grain products. Men perceived more benefit in products with specific health claims than women did for products with general health claims. At the individual level, male level of perceived benefit in products with general health claims was, however, equally high as that of the women. Furthermore, modification of staple foods was perceived as being more beneficial than fun foods, and people preferred processes such as fortification and traditional cross-breeding to genetic modification. Lampila et al. (2009) investigated consumer perceptions of flavonoids using focus-group discussions in Europe. They noted that the average consumer was not familiar with the term "flavonoid." However, consumer showed positive attitudes once informed about the beneficial effects of flavonoids on human health.

Consumer knowledge on the health effects of flavonoids is limited. Hence, there is need to improve marketing programs by including reliable nutritional information in food labels. The rising demand for such foods can be explained by the increasing cost of healthcare, the steady increase in life expectancy, and because older people wish to lead improved life quality during their "golden years" (Roberfroid, 2002; Siro et al., 2008). It should be noted that many industry-designed marketed nutritional supplements do not have beneficial effects for arresting the development of chronic diseases (such as cancer, cardiovascular diseases, diabetes, hypertension, inflammation, and obesity). This is partially due to the health effects resulting from a complex synergetic action of numerous phytochemicals supplied by foods

or diets at nutritional doses and considering that a food is not a drug (Fardet and Rock, 2014).

OUTLOOK

Consumers worldwide are becoming aware of the benefits of nutraceutical foods. A paradigm shift is gradually emerging for the development of nutritionally dense cultivars in addition to integrating genes for productivity and stress tolerance. As a result, nutrient-dense cultivars are being bred in cereals and legumes. Breeding for staple crops rich in phenylpropanoids is just beginning. A positive development is the search for phenylpropanoid-rich germplasm both in cereals and legumes that show broad variations in genebank germplasm. Many breeding programs are transferring this variation into the cultigen pool. As expected some yield penalty has been noted, which should be further investigated to assess cause-effect relationships to overcome the negative trade-off using cross-breeding or biotechnology facilitated genetic betterment. A systematic evaluation of germplasm using representative subsets is the ideal approach to discover new sources of variations for these compounds. An approach combining high throughput assays and wet chemistry should be integrated to support such breeding programs. The sensory attributes and consumer acceptance of flavonoid-rich staple foods should be further investigated for their wide acceptance. A food matrix-based approach instead of a reductionist approach is suggested with investigations into the effects of these compounds on human health.

AUTHOR CONTRIBUTIONS

SD and RO conceptualized the idea and finalized the outlines together with coauthors who contributed equally in manuscript writing and reading the full draft. RO, SD, and KS edited, while SD organized the paper.

ACKNOWLEDGMENTS

SD acknowledges the contribution of Ramesh Kotnana of Knowledge Sharing and Innovation Program of ICRISAT for arranging reprints on phytochemicals in cereals and legumes as a resource for drafting this manuscript. RO thanks the funding to SLU from PlantePigment—a project led by Chr. Hansen A/S with a grant from GUDP (Green Development and Demonstration Program, Denmark), while IC acknowledges funding from Basic Science Research Program through the National Research Foundation of Korea (NRF) funded by the Ministry of Science, ICT and Future Planning (2014R1A2A2A01002202). SG acknowledges the funding to Research Nutriomics Chair (CAT-005) from Tecnologico de Monterrey, Escuela de Ingeniería y Ciencias. We are grateful to the two anonymous reviewer's for making useful suggestions on improving the manuscript.

SUPPLEMENTARY MATERIAL

The Supplementary Material for this article can be found online at: http://journal.frontiersin.org/article/10.3389/fpls.2016.00763

REFERENCES

Abdel-Aal, E. S. M., and Choo, T. M. (2014). Differences in compositional properties of a hulless barley cultivar grown in 23 environments in eastern Canada. *Can. J. Plant Sci.* 94, 807–815. doi: 10.4141/cjps2013-301

Abdel-Aal, E. M., Choo, T.-M., Dhillon, S., and Rabalski, I. (2012). Free and bound phenolic acids and total phenolics in black, blue, and yellow barley and their contribution to free radical scavenging capacity. *Cereal Chem.* 89, 198–204. doi: 10.1094/CCHEM-10-11-0116

Abdel-Aal, E. M., Young, J. C., and Rabalski, I. (2006). Anthocyanin composition in black, blue, pink, purple, and red cereal grains. *J. Agric. Food Chem.* 54, 4696–4704. doi: 10.1021/jf0606609

Abidi, I., Mansouri, S., Radhouane, L., Ksouri, R., Felah, M. E., and Bouzid, S. (2015). Phenolic, flavonoid and tannin contents of Tunisian barley landraces. *Int. J. Agric. Innov. Res.* 3, 1317–1323.

Adom, K. K., Sorrells, M. E., and Liu, R. H. (2006). Phytochemicals and antioxidant activity of milled fractions of different wheat varieties. *J. Agric. Food Chem.* 53, 2297–2306. doi: 10.1021/jf048456d

Afzal, A., Gulzar, I., Shahbaz, M., and Ashraf, M. (2014). Water deficit-induced regulation ofgrowth, gas exchange, chlorophyll fluorescence, inorganic nutrient accumulation and antioxidative defense mechanism in mungbean (*Vigna radiata* (L.) Wilczek). *J. Appl. Bot. Food Qual.* 87, 147–156. doi:10.5073/JABFQ.2014.087.022

Agati, G., Brunetti, C., Di Ferdinando, M., Ferrini, F., Pollastri, S., and Tattini, M. (2013). Functional roles of flavonoids in photoprotection: new evidence, lessons from the past. *Plant Physiol. Biochem.* 72, 35–45. doi: 10.1016/j.plaphy.2013.03.014

Agostini-Costa, T. S., Teodoro, A. F. P., Alves, R. B. N., Braga, L. R., Ribeiro, I. F., Silva, J. P., et al. (2015). Total phenolics, flavonoids, tannins and antioxidant activity of lima beans conserved in a Brazilian genebank. *Ciência Rural Santa Maria* 45, 335–341. doi: 10.1590/0103-8478cr20140030

Ahmed, I. M., Cao, F., Han, Y., Nadira, U. A., Zhang, G., and Wu, F. (2013a). Differential changes in grain ultrastructure, amylase, protein and amino acid profiles between Tibetan wild and cultivated barleys under drought and salinity alone and combined stress. *Food Chem.* 141, 2743–2750. doi: 10.1016/j.foodchem.2013.05.101

Ahmed, S., Faridi, U., Shahid, M., and Nisar, M. (2013b). Effect of phenolics in maize grains of different varieties on biology of Angoumois grain moth, *Sitotroga cerealella* (Oliv.) (Lepidoptera: Gelechiidae). *Cereal Res. Commun.* 41, 636–646. doi: 10.1556/CRC.2013.0026

Akond, A. S. M. G. M., Khandaker, L., Berthold, J., Gates, L., Peters, K., Delong, H., et al. (2011). Anthocyanin, total polyphenols and antioxidant activity of common bean. *Am. J. Food Technol.* 6, 385–394. doi: 10.3923/ajft.2011.385.394

Albert, N. W. (2015). Subspecialization of R2R3-MYB repressors for anthocyanin and proanthocyanidin reduction in forage legumes. *Front. Plant Sci.* 6:1165. doi: 10.3389/fpls.2015.01165

Albert, N. W., Lewis, D. H., Zhang, H., Schwinn, K. E., Jameson, P. E., and Davies, K. M. (2011). Members of an R2R3-MYB transcription factor family in *Petunia* are developmentally and environmentally regulated to control complex floral and vegetative pigmentation patterning. *Plant J.* 65, 771–784. doi: 10.1111/j.1365-313X.2010.04465.x

Ali, Q., Ashraf, M., and Anwar, F. (2010). Seed composition and seed oil antioxidant activity of maize under water stress. *J. Am. Oil Chem. Soc.* 87, 1179–1187. doi: 10.1007/s11746-010-1599-5

Andersson, A. A. M., Lampi, A.-M., Nyström, L., Piironen, V., Li, L., Ward, J. L., et al. (2008). Phytochemical and dietary fiber components in barley varieties in the health grain diversity screen. *J. Agric. Food Chem.* 56, 9767–9776. doi: 10.1021/jf802037f

Anderson, R. L., and Wolf, W. J. (1995). Compositional changes in trypsin inhibitors, phytic acid, and isoflavones related to soybean processing. *J. Nutr.* 125, 581S–588S.

Anton, A. A., Lukow, O. M., Fulcher, R. G., and Arntflied, S. D. (2008). Influence of added bean flour (*Phaseolus vugaris* L.) and some physical and nutritional properties of wheat flour tortillas. *Food Chem.* 109, 33–41. doi: 10.1016/j.foodchem.2007.12.005

Apak, R., Gorinstein, S., Böhm, V., Schaich, K. M., Özyürek, M., and Güçlü, K. (2013). Methods of measurement and evaluation of natural antioxidant capacity activity (IUPAC Technical Report). *Pure Appl. Chem.* 85, 957–998. doi: 10.1351/PAC-REP-12-07-15

Bai, Y., Pattanaik, S., Patra, B., Werkman, J. R., Xie, C. H., and Yuan, L. (2011). Flavonoid-related basic helix–loop–helix regulators, NtAn1a and NtAn1b, of tobacco have originated from two ancestors and are functionally active. *Planta* 234, 363–375. doi: 10.1007/s00425-011-1407-y

Bamisile, B. S., Adesina, J. M., and Ofuya, T. I. (2014). Relative susceptibility and proximate composition of some imported and local rice varieties to infestation and damage by *Sitophilus oryzae* L. (Coleoptera: Curculionidae). *Mol. Entomol.* 5, 18–29. doi: 10.5376/me.2014.05.0003

Ban, Y., Honda, C., Hatsuyama, Y., Igarashi, M., Bessho, H., and Moriguchi, T. (2007). Isolation and functional analysis of a MYB transcription factor gene that is a key regulator for the development of red coloration in apple skin. *Plant Cell Physiol.* 48, 958–970. doi: 10.1093/pcp/pcm066

Bao, J. S., Cai, Y. Z., and Corke, H. (2001). Prediction of rice starch quality parameters by near infrared reflectance spectroscopy. *J. Food Sci.* 66, 936–939. doi: 10.1111/j.1365-2621.2001.tb08215.x

Bao, J. S., Wang, Y. F., and Shen, Y. (2007). Determination of apparent amylose content, pasting properties and gel texture of rice starch by near infrared spectroscopy. *J. Sci. Food Agric.* 87, 2040–2048. doi: 10.1002/jsfa.2960

Baudry, A., Heim, M. A., Dubreucq, B., Caboche, M., Weisshaar, B., and Lepiniec, L. (2004). TT2, TT8, and TTG1 synergistically specify the expression of BANYULS and proanthocyanidin biosynthesis in *Arabidopsis thaliana*. *Plant J.* 39, 366–380. doi: 10.1111/j.1365-313X.2004.02138.x

Begum, A., Goswami, A., and Chowdhury, P. (2015). A comparative study on free and bound phenolic acid content and their antioxidant activity in bran of rice (*Oryza sativa* L.) cultivars of Eastern Himalayan range. *Int. J. Food Sci. Technol.* 50, 2529–2536. doi: 10.1111/ijfs.12920

Bertoia, M. L., Rimm, E. B., Mukamal, K. J., Hu, F. B., Willett, W. C., and Cassidy, A. (2015). Dietary flavonoid intake and weight maintenance: three prospective cohorts of 124 086 US men and women followed for up to 24 years. *Br. Med. J.* 352, i17. doi: 10.1136/bmj.i17

Beta, T., Rooney, L. W., Marovatsanga, L. T., and Taylor, J. R. N. (1999). Phenolic compounds and kernel characteristics of Zimbabwean sorghums. *J. Sci. Food Agric.* 79, 1003–1010.

Bi, Y., Li, W., Xiao, J., Lin, H., Liu, M., Luan, X., et al. (2015). Heterosis and combining ability estimates in isoflavone content using different parental soybean accessions: wild soybean, a valuable germplasm for soybean breeding. *PLoS ONE* 10:e0114827. doi: 10.1371/journal.pone.0114827

Bittner, L. K., Schoenbichler, S. A., Bonn, G. K., and Huck, C. W. (2013). Near infrared spectroscopy (NIRS) as a tool to analyze phenolic compounds in plants. *Curr. Anal. Chem.* 9, 417–423. doi: 10.2174/15734110113090 30010

Blankenberg, S., Rupprecht, H. J., Bickel, C., Peetz, D., Hafner, G., Tiret, L., et al. (2001). Circulating cell adhesion molecules and death in patients with coronary artery disease. *Circulation* 104, 1336–1342. doi: 10.1161/hc3701.095949

Bobo-García, G., Davidov-Pardo, G., Arroqui, C., Vírseda, P., Marín-Arroyo, M. R., and Navarro, M. (2015). Intra-laboratory validation of microplate methods for total phenolic content and antioxidant activity on polyphenolic extracts, and comparison with conventional spectrophotometric methods. *J. Sci. Food Agric.* 95, 204–209. doi: 10.1002/jsfa.6706

Boerma, H. R., and Specht, J. E. (eds.). (2004). *Soybeans: Improvement, Production and Uses. 3rd Edn. Agron. Monogr. Vo.l 16*. Madison, WI: ASA, CSSA, and SSSA.

Bogs, J., Downey, M. O., Harvey, J. S., Ashton, A. R., Tanner, G. J., and Robinson, S. P. (2005). Proanthocyanidin synthesis and expression of genes encoding leucoanthocyanidin reductase and anthocyanidin reductase in developing grape berries and grapevine leaves. *Plant Physiol. Biochem.* 139, 652–663. doi: 10.1104/pp.105.064238

Bonina, F., Lanza, M., Montenegro, L., Puglisi, C., Tomaino, A., Trombetta, D., et al. (1996). Flavonoids as potential protective agents against photo-oxidative skin damage. *Int. J. Pharm.* 145, 87–94. doi: 10.1016/S0378-5173(96)04728-X

Bordiga, M., Gomez-Alonso, S., Locatelli, M., Travaglia, F., Coïsson, J. D., Hermosin-Guiterrez, I., et al. (2014). Phenolics characterization and antioxidant activity of six different pigmented *Oryza sativa* cultivars grown in Piedmong (Italy). *Food Res. Int.* 65, 282–290. doi: 10.1016/j.foodres.2014.03.007

Bornkessel, S., Bröring, S., and Omta, S. W. F. (2011). "Consumer acceptance of functional foods and their ingredients-positioning options for innovations on the borderline between foods and drugs," in *International Food and Agribusiness Management Association. 21st Annual World Symposium* (Frankfurt).

Boyle, S. P., Dobson, V. L., Duthie, S. J., Hinselwood, D. C., Kyle, J. A. M., and Collins, A. R. (2000). Bioavailability and efficiency of rutin as an antioxidant: a human supplementation study. *Eur. J. Clin. Nutr.* 54, 774–782. doi: 10.1038/sj.ejcn.1601090

Bravo, L. (1998). Polyphenols: chemistry, dietary sources, metabolism, and nutritional significance. *Nutr. Rev.* 56, 317–333. doi: 10.1111/j.1753-4887.1998.tb01670.x

Budevska, B. O. (2002). *Vibrational Spectroscopy Imaging of Agricultural Products*. New York, NY: John Wiley and Sons, Ltd.

Bunaciu, A. A., Aboul-Enein, H. Y., and Fleschin, S. (2012). FTIR spectrophotometric methods used for antioxidant activity assay in medicinal plants. *Appl. Spectrosc. Rev.* 47, 245–255. doi: 10.1080/05704928.2011.645260

Burešováet, V., Kopecký, D., Bartoš, J., Martinek, P., Watanabe, N., Vyhnánek, T., et al. (2015). Variation in genome composition of blue-aleurone wheat. *Theor. Appl. Genet.* 128, 273–282. doi: 10.1007/s00122-014-2427-3

Bustos, D. V., Riegel, R., and Calderini, D. F. (2012). Anthocyanin content of grains in purple wheat is affected by grain position, assimilate availability and agronomic management. *J. Cereal Sci.* 55, 257–264. doi: 10.1016/j.jcs.2011.12.001

Byrne, P. F., McMullen, M. D., Snook, M. E., Musket, T. A., Theuri, J. M., Windstrom, N. W., et al. (1996). Quantitative trait loci and metabolic pathways: genetic control of the concentration of maysin, a corn earworm resistance factor, in maize silks. *Proc. Natl. Acad. Sci. U.S.A.* 93, 8820–8825. doi: 10.1073/pnas.93.17.8820

Cai, R., Hettiarachchy, N. S., and Jalaluddin, M. (2003). High performance of liquid chromatography determination of phenolic constituents in 17 varieties of cowpeas. *J. Agric. Food Chem.* 51, 1623–1627. doi: 10.1021/jf020867b

Caldwell, C. R., Britz, S. J., and Mirecki, R. M. (2005). Effect of temperature, elevated carbon dioxide, and drought during seed development on the isoflavone content of dwarf soybean [*Glycine max* (L.) Merrill] grown in controlled environments. *J. Agric. Food Chem.* 53, 1125–1129. doi: 10.1021/jf0355351

Carey, C. C., Strahle, J. T., Selinger, D. A., and Chandler, V. L. (2004). Mutations in the *pale aleurone color1* regulatory gene of the *Zea mays* anthocyanin pathway have distinct phenotypes relative to the functionally similar *TRANSPARENT TESTA GLABRA1* gene in *Arabidopsis thaliana*. *Plant Cell* 16, 450–464. doi: 10.1105/tpc.018796

Carrera, C. S., and Dardanelli, J. L. (2015). Changes in the relationship between temperature during the seed-filling period and soybean seed isoflavones under water-deficit conditions. *J. Agron. Crop Sci*. doi: 10.1111/jac.12147

Carrera, C. S., Dardanelli, J. L., and Soldini, D. O. (2014). Genotypic and environmental variation in seed nutraceutical and industrial composition of non-transgenic soybean (*Glycine max*) genotypes. *Crop Pasture Sci.* 65, 1311–1322. doi: 10.1071/cp14114

Carter, T. E. Jr., Nelson, R. L., Sneller, C. H., and Cui, Z. (2004). "Genetic diversity in soybeans" in *The Soybeans: Improvement, Production and Uses*, *Agron. Monogr. Vol. 16, 3rd Edn*., eds H. R. Boerma and J. E. Specht (Madison, WI: ASA, CSSA, and SSSA), 303–416.

Casas, M. I., Duarte, S., Doseff, A. I., and Grotewold, E. (2014). Flavone-rich maize: an opportunity to improve the nutritional value of an important commodity crop. *Front. Plant Sci.* 5:440. doi: 10.3389/fpls.2014.00440

Center, M. M., Jemal, A., and Ward, E. (2009). International trends in colorectal cancer incidence rates. *Cancer Epidemiol. Biomark. Prev.* 18, 1688–1694. doi: 10.1158/1055-9965.EPI-09-0090

Cercamondi, C. I., Egli, I. M., Zeder, C., and Hurrell, R. F. (2014). Sodium iron edta and ascorbic acid, but not polyphenol oxidase treatment, counteract the strong inhibitory effect of polyphenols from brown sorghum on the

absorption of fortification iron in young women. *Br. J. Nutr.* 111, 481–489. doi: 10.1017/S0007114513002705

Chakraborty, U., and Pradhan, B. (2012). Drought stress-induced oxidative stress and antioxidative responses in four wheat (*Triticum aestivum* L.) varieties. *Arch. Agron. Soil Sci.* 58, 617–630. doi: 10.1080/03650340.2010.533660

Chandler, V. L., Radicella, J. P., Robbins, T. P., Chen, J., and Turks, D. (1989). Two regulatory genes of the maize anthocyanin pathway are homologous: isolation of B utilizing R genomic sequences. *Plant Cell* 1, 1175–1183. doi: 10.1105/tpc.1.12.1175

Chaudhary, N., and Agrawal, S. B. (2015). The role of elevated ozone on growth, yield and seed quality amongst six cultivars of mung bean. *Ecotoxicol. Environ. Safety* 111, 286–294. doi: 10.1016/j.ecoenv.2014.09.018

Chavez-Santoscoy, R. A., Gutierrez-Uribe, J. A., Granados, O., Torre-Villalvazo, I., Tovar, A. R., Serna-Saldivar, S. O., et al. (2014). Flavonoids and saponins extracted from black bean (*Phaseolus vulgaris* L.) seed coats modulate lipid metabolism and biliary cholesterol secretion in C57BL/6 mice. *Br. J. Nutr.* 112, 886–899. doi: 10.1017/S0007114514001536

Chavez-Santoscoy, R. A., Gutierrez-Uribe, J. A., and Serna-Saldívar, S. O. (2013). Effect of flavonoids and saponins extracted from black bean (*Phaseolus vulgaris* L.) seed coats as cholesterol micelle disruptors. *Plant Foods Hum. Nutr.* 68, 416–423. doi: 10.1007/s11130-013-0384-7

Chavez-Santoscoy, R. A., Gutierrez-Uribe, J. A., Serna-Saldívar, S. O., and Perez-Carrilo, E. (2016). Production of maize tortillas and cookies from nixtamalized flour enriched with anthocyanins, flavonoids and saponins extracted from black bean (*Phaseolus vulgaris*) seed coat. *Food Chem.* 192, 90–97. doi: 10.1016/j.foodchem.2015.06.113

Chen, X. Q., Nagao, N., Itani, T., and Irifune, K. (2012). Anti-oxidative analysis, and identification and quantification of anthocyanin pigments in different colored rice. *Food Chem.* 135, 2783–2788. doi: 10.1016/j.foodchem.2012.06.098

Chen, Q., Zhao, J., Liu, M., Cai, J., and Liu, J. (2008). Determination of total phenols content in green tea using FT-NIR spectroscopy and different PLS algorithms. *J. Pharm. Biomed. Anal.* 46, 568–573. doi: 10.1016/j.jpba.2007.10.031

Cheng, Z., Moore, J., and Yu, L. (2006). High-throughput relative DPPH radical scavenging capacity assay. *J. Agric. Food Chem.* 54, 7429–7436. doi: 10.1021/jf0611668

Chennupati, P., Seguin, P., and Liu, W. (2011). Effects of high temperature stress at different stages on soybean isoflavone and tocopherol concentrations. *J. Food Agric. Chem.* 59, 13081–13088. doi: 10.1021/jf2037714

Cheynier, V., Comte, G., Davies, K. M., Lattanzio, V., and Martens, S. (2013). Plant phenolics: recent advances on their biosynthesis, genetics, and ecophysiology. *Plant Physiol. Biochem.* 72, 1–20. doi: 10.1016/j.plaphy.2013.05.009

Chiremba, C., Taylor, J. R. N., Rooney, L. W., and Beta, T. (2012). Phenolic acid content of sorghum and maize cultivars varying in hardness. *Food Chem.* 134, 81–88. doi: 10.1016/j.foodchem.2012.02.067

Choung, M.-G., Choi, B.-R., An, Y.-N., Chu, Y.-C., and Cho, Y.-S. (2003). Anthocyanin profiles of Korean cultivated kidney bean (*Phaseolus vulgaris* L.). *J. Agric. Food Chem.* 51, 7040–7043. doi: 10.1021/jf0304021

Chunthaburee, S., Sanitchon, J., Pattanagul, W., and Theerakulpisut, P. (2015). Effects of salt stress after late booting stage on yield and antioxidant capacity in pigmented rice grains and alleviation of the salt-induced yield reduction by exogenous spermidine. *Plant Prod. Sci.* 18, 32–42. doi: 10.1626/pps.18.32

Codgill, R. P., Hurburgh, C. R. Jr., Jensen, T. C., and Jones, R. W. (2002). "Single kernel maize analysis by near-infrared hyperspectral imaging," in *Proc. 10th Int. Conf. on Near-infrared Spectroscopy*, eds A. M. C. Davies and R. K. Cho (Chichester: NIR publications), 243–247.

Codgill, R. P., Hurburgh, C. R. Jr., and Rippke, G. R. (2004). Single kernel maize analysis by near-infrared hyperspectral imaging. *T. ASABE* 47, 311–320.

Cook, N. C., and Samman, S. (1996). Flavonoid chemistry, metabolism, cardioprotective effects and dietary sources. *J. Nutr. Biochem.* 7, 66–76. doi: 10.1016/0955-2863(95)00168-9

Corcoran, M. P., McKay, D. L., and Blumberg, J. B. (2012). Flavonoid basics: chemistry, sources, mechanisms of action, and safety. *J. Nutr. Gerontol. Geriatr.* 31, 176–189. doi: 10.1080/21551197.2012.698219

Cozzolino, D. (2015). The role of visible and infrared spectroscopy combined with chemometrics to measure phenolic compounds in grape and wine samples. *Molecules* 20, 726–735. doi: 10.3390/molecules20010726

Cozzolino, D., Cynkar, W. U., Dambergs, R. G., Mercurio, M. D., and Smith, P. A. (2008). Measurement of condensed tannins and dry matter in red grape homogenates using near infrared spectroscopy and partial least squares. *J. Agric. Food Chem.* 56, 7631–7636. doi: 10.1021/jf801563z

Cozzolino, D., Kwiatkowski, M. J., Parker, M., Cynkar, W. U., Dambers, R. G., Gishen, M., et al. (2004). Prediction of phenolic compounds in red wine fermentations by visible and near infrared spectroscopy. *Anal. Chim. Acta* 513, 73–80. doi: 10.1016/j.aca.2003.08.066

Cui, Z., James, A. T., Miyazaki, S., Wilson, R. F., and Carter, T. E. Jr. (2004). "Breeding specialty soybeans for traditional and new soy foods" in *The Soybeans as Functional Foods and Ingredients*, ed K. S. Liu (Champaign, IL: Am. Oil Chem. Soc. Press), 264–322.

Curtis, P. J., Kroon, P. A., Hoollands, W. J., Walls, R., Jenkins, G., Kay, C., D., et al. (2009). Cardiovascular disease risk biomarkers and liver and kidney function are not altered in postmenopausal women after ingesting in elderberry extract rich in anthocyanins for 12 weeks. *J. Nutr.* 139, 2266–2671. doi: 10.3945/jn.109.113126

Das, P. K., Shin, D. H., Choi, S. B., Yoo, S. D., Choi, G., and Park, Y. I. (2012). Cytokinins enhance sugar-induced anthocyanin biosynthesis in *Arabidopsis*. *Mol. Cells.* 34, 93–101. doi: 10.1007/s10059-012-0114-2

Dean, M., Shepherd, R., Aryola, A., Vassallo, M., Winkelmann, M., Claupein, E., et al. (2007). Consumer perceptions of healthy cereal products and production methods. *J. Cereal Sci.* 46, 188–196. doi: 10.1016/j.jcs.2007.06.007

de Lima, P. F., Colombo, C. A., Chiorato, A. F., Yamaguchi, L. F., Kato, M. J., and Carbonell, S. A. M. (2014). Occurrence of flavonoids in Brazilian common bean germplasm (*Phaseolus vulgaris* L.). *J. Agric. Food Chem.* 62, 9699–9704. doi: 10.1021/jf5033312

de Leonardis, A. M., Fragasso, M., Beleggia, R., Ficco, D. B. M., de Vita, P., and Mastrangelo, A. M. (2015). Effect of heat stress on metabolite accumulation and composition, and nutritional properties of durum wheat grain. *Int. J. Mol. Sci.* 16, 30382–30404. doi: 10.3390/ijms161226241

de Oliveira, L. L., de Carvalho, M. V., and Melo, L. (2014). Health promoting and sensory properties of phenolic compounds in food. *Rev. Ceres Viçosa* 61, 764–779. doi: 10.1590/0034-737x201461000002

Deluc, L., Barrieu, F., Marchive, C., Lauvergeat, V., Decendit, A., Richard, T., et al. (2006). Characterization of a grapevine R2R3-MYB transcription factor that regulates the phenylpropanoid pathway. *Plant Physiol.* 140, 499–511. doi: 10.1104/pp.105.067231

de Mira, N. V. M., Massaretto, I. L., Pascual, C. M. C. I., and Marquez, U. M. L. (2009). Comparative study of phenolic compounds in different Brazilian rice (*Oryza sativa* L.) genotypes. *J. Food Comp. Anal.* 22, 405–409. doi: 10.1016/j.jfca.2008.06.012

Dias, A. S., and Lidon, F. C. (2010). Bread and durum wheat tolerance under heat stress: a synoptical overview. *J. Food Agric.* 22, 412–436. doi: 10.9755/ejfa.v22i6.4660

Diczházi, I., and Kursinszki, L. (2014). Anthocyanin content and composition in winter blue barley cultivars and lines. *Cereal Chem.* 91, 195–200. doi: 10.1094/CCHEM-05-13-0091-R

Dinelli, G., Carretero, A. S., Di Silvestro, R., Marotti, I., Fu, S., Benedettelli, S., et al. (2009). Determination of phenolic compounds in modern and old varieties of durum wheat using liquid chromatography coupled with time-of-flight mass spectrometry. *J. Chromatogr. A* 1216, 7229–7240. doi: 10.1016/j.chroma.2009.08.041

Dlamini, N. R., Taylor, J. R. N., and Rooney, L. W. (2007). The effect of sorghum type and processing on the antioxidant properties of African sorghum-based foods. *Food Chem.* 105, 1412–1419. doi: 10.1016/j.foodchem.2007.05.017

Dobrovolskaya, O., Arbuzova, V. S., Lohwasser, U., Röder, M. S., and Börner, A. (2006). Microsatellite mapping of complementary genes for purple grain color in bread wheat (*Triticum aestivum* L.). *Euphytica* 150, 355–364. doi: 10.1007/s10681-006-9122-7

Doria, E., Campion, B., Sparvooli, F., Tava, A., and Nielsen, E. (2012). Anti-nutrient components and metabolites with health implications in seeds of 10 common bean (*Phaseolus vulgaris* L. and *P. lunatus L.)* landraces cultivated in southern Italy. *J. Food Comp. Anal.* 26, 72–80. doi: 10.1016/j.jfca.2012.03.005

Dubcovsky, J., Luo, M. C., Zhong, G. Y., Bransteitter, R., Desai, A., Kilian, A., et al. (1996). Genetic map of diploid wheat, *Triticum monococcum* L., and its comparison with maps of *Hordeum vulgare* L. *Genetics* 143, 983–999.

Dubos, C., Le Gourrierec, J., Baudry, A., Huep, G., Lanet, E., Debeaujon, I., et al. (2008). MYBL2 is a new regulator of flavonoid biosynthesis in *Arabidopsis thaliana*. *Plant J.* 55, 940–953. doi: 10.1111/j.1365-313X.2008.03564.x

Dvořáková, M., Guido, L. F., Dostálek, P., Skulilová, Z., Moreira, M. M., and Barros, A. A. (2008). Antioxidant properties of free, soluble ester and insoluble-bound phenolic compounds in different barley varieties and corresponding malts. *J. Inst. Brew.* 114, 27–33. doi: 10.1002/j.2050-0416.2008.tb00302.x

Dwivedi, S., Sahrawat, K. L., Rai, K. N., Blair, M. W., Anderson, M. S., and Pfeiffer, W. (2012). Nutritionally enhanced staple food crops. *Plant Breed. Rev.* 36, 169–291. doi: 10.1002/9781118358566.ch3

Dykes, L., Hoffmann, L., Portillo-Rodriguez, O., Rooney, W. L., and Rooney, L. W. (2014). Prediction of total phenols, condensed tannins, and 3-deoxyanthocyanidins in sorghum grain using near-infrared (NIR) spectroscopy. *J. Cereal Sci.* 60, 138–142. doi: 10.1016/j.jcs.2014.02.002

Dykes, L., Rooney, W. L., and Rooney, L. W. (2013). Evaluation of phenolics and antioxidant activity of black sorghum. *J. Cereal Sci.* 58, 278–283. doi: 10.1016/j.jcs.2013.06.006

Dykes, L., Rooney, L. W., Waniska, R. D., and Rooney, W. L. (2005). Phenolic compounds and antioxidant activity of sorghum grains of varying genotypes. *J. Agric. Food Chem.* 53, 6813–6818. doi: 10.1021/jf050419e

Dykes, L., Seitz, L. M., Rooney, W. L., and Rooney, L. W. (2009). Flavonoid composition of red sorghum genotypes. *Food Chem.* 116, 313–317. doi: 10.1016/j.foodchem.2009.02.052

Eggert, K., Hollmann, J., Hiller, B., Kruse, H. P., Rawel, H. M., and Pawelzik, E. (2010). Effects of fusarium infection on the phenolics in emmer and naked barley. *J. Agric. Food Chem.* 58, 3043–3049. doi: 10.1021/jf903545j

Espinosa-Alonso, L. G., Lygin, A., Widholm, J. M., Valverde, M. E., and Paredes-Lopez, O. (2006). Polyphenols in wild and weedy Mexican common beans (*Phaseolus vulgaris* L.). *J. Agric. Food Chem.* 54, 4436–4444. doi: 10.1021/jf060185e

Espley, R. V., Hellens, R. P., Putterill, J., Stevenson, D. E., Kutty-Amma, S., and Allan, A. C. (2007). Red coloration in apple fruit is due to the activity of the MYB transcription factor, MdMYB10. *Plant J.* 49, 414–427. doi: 10.1111/j.1365-313X.2006.02964.x

Eticha, F., Grausgruber, H., Siebenhandl-Ehn, S., and Berghofer, E. (2011). Some agronomic and chemical traits of blue aleurone and purple pericarp wheat (*Triticum* L.). *J. Agric. Sci. Technol. B* 1, 48–58.

Evans, P., and Halliwell, B. (2001). Micronutrients: oxidant/antioxidant status. *Br. J. Nutr.* 85, S67–S74. doi: 10.1079/bjn2000296

Fardet, A., and Rock, E. (2014). The search for a new paradigm to study micronutrient and phytochemical bioavailability: from reductionism to holism. *Med. Hypoth.* 82, 181–186. doi: 10.1016/j.mehy.2013.11.035

Fernandez-Orozco, R., Li, L., Harflett, C., Shewry, P. R., and Ward, J. L. (2010). Effects of environment and genotype on phenolic acids in wheat in the healthgrain diversity screen. *J. Agric. Food Chem.* 58, 9341–9352. doi: 10.1021/jf102017s

Ferreyra, M. L. F., Rius, S. P., and Casati, P. (2012). Flavonoids: biosynthesis, biological functions, and biotechnological applications. *Front. Plant Sci.* 3:222. doi: 10.3389/fpls.2012.00222

Ficco, D. B. M., de Simone, V., Colecchia, S. A., Pecorella, I., Platani, C., Nigro, F., et al. (2014). Genetic variability in anthocyanin composition and nutritional properties of blue, purple, and red bread (*Triticum aestivum* L.) and durum (*T. turgidum L. ssp.* turgidum convar. durum) wheats. *J. Agric. Food Chem.* 62, 8686–8695. doi: 10.1021/jf5003683

Finocchiaro, F., Ferrari, B., Gianinetti, A., Dall'Asta, C., Galaverna, G., Scazzina, F., et al. (2007). Characterization of antioxidant compounds of red and white rice and changes in total antioxidant capacity during processing. *Mol. Nutr. Food Res.* 51, 1006–1019. doi: 10.1002/mnfr.200700011

Fogarasi, A. L., Kun, S., Tankó, G., Stefanovits-Bányai, É., and Hegyesné-Vecseri, B. (2015). A comparative assessment of antioxidant properties, total phenolic content of einkorn, wheat, barley and their malts. *Food Chem.* 167, 1–6. doi: 10.1016/j.foodchem.2014.06.084

Fox, G., and Manley, M. (2014). Applications of single kernel conventional and hyperspectral imaging near infrared spectroscopy in cereals. *J. Sci. Food Agric.* 94, 174–179. doi: 10.1002/jsfa.6367

Frankel, O. H. (1984). "Genetic perspective of germplasm collection" in *The Genetic Manipulations: Impact on Man and Society*, eds W. Arber, K. Limensee, W. J. Peacock, and P. Stralinger (Cambridge: Cambridge University Press), 161–170.

Furbank, R. T., and Tester, M. (2011). Phenomics technologies to relieve the phenotyping bottleneck. *Trends Plant Sci.* 16, 635–644. doi: 10.1016/j.tplants.2011.09.005

Galland, M., Boutet-Mercey, S., Lounifi, I., Godin, B., Belzergue, S., Grandjean, O., et al. (2014). Compartmentation and dynamics of flavone metabolism in dry and germinated rice seeds. *Plant Cell Physiol.* 55, 1646–1659. doi: 10.1093/pcp/pcu095

Gamel, T. H., and Abdel-Aal, E. M. (2012). Phenolic acids and antioxidant properties of barley whole grain and pearling fractions. *Agric. Food Sci.* 21, 118–131.

García-Lara, S., and Bergvinson, D. J. (2014). Phytochemical changes during recurrent selection for storage pest resistance in tropical maize. *Crop Sci.* 54, 2423–2432. doi: 10.2135/cropsci2014.03.0223

Gawlik-Dziki, U., Świeca, M., and Dziki, D. (2012). Comparison of phenolic acids profile and antioxidant potential of six varieties of Spelt (*Triticum spelta* L.). *J. Agric. Food Chem.* 60, 4603–4612. doi: 10.1021/jf3011239

González-Muñoz, A., Quesille-Villalobos, A. M., Fuentealba, C., Shetty, K., and Ranilla, L. G. (2013). Potential of Chilean native corn (*Zea mays* L.) accessions as natural sources of phenolic antioxidants and in vitro bioactivity for hyperglycemia and hypertension management. *J. Agric. Food Chem.* 61, 10995–11007. doi: 10.1021/jf403237p

Gonzalez, A., Zhao, M., Leavitt, J. M., and Lloyd, A. M. (2008). Regulation of the anthocyanin biosynthetic pathway by the TTG1/bHLH/Myb transcriptional complex in *Arabidopsis* seedlings. *Plant J.* 53, 814–827. doi: 10.1111/j.1365-313X.2007.03373.x

Gordeeva, E. I., Shoeva, O. Y., and Khlestkina, E. K. (2015). Marker-assisted development of bread wheat near-isogenic lines carrying various combinations of purple pericarp (*Pp*) alleles. *Euphytica* 203, 469–476. doi: 10.1007/s10681-014-1317-8

Gou, J. Y., Felippes, F. F., Liu, C. J., Weigel, D., and Wang, J. W. (2011). Negative regulation of anthocyanin biosynthesis in *Arabidopsis* by a miR156-targeted SPL transcription factor. *Plant Cell* 23, 1512–1522. doi: 10.1105/tpc.111.084525

Goufo, P., Pereira, J., Figueiredo, N., Oliveira, M. B. P. P., Carranca, C., Rosa, E. A. S., et al. (2014). Effect of elevated carbon dioxide (CO_2) on phenolic acids, flavonoids, tocopherols, tocotrienols, γ-oryzanol and antioxidant capacities of rice (*Oryza sativa* L.). *J. Cereal Sci.* 59, 15–24. doi: 10.1016/j.jcs.2013.10.013

Goufo, P., and Trindade, H. (2014). Rice antioxidants: phenolic acids, flavonoids, anthocyanins, proanthocyanidins, tocopherols, tocotrienols, γ oryzanol and phytic acid. *Food Sci. Nutr.* 2, 75–104. doi: 10.1002/fsn3.86

Graf, B., Milbury, P., and Blumberg, J. (2005). Flavonols, flavones, flavanones, and human health: epidemiological evidence. *J. Med. Food*, 8, 281–290. doi: 10.1089/jmf.2005.8.281

Graham, H. D. (1992). Stabilization of the Prussian blue color in the determination of polyphenols. *J. Agric. Food chem.* 40, 801–805. doi: 10.1021/jf00017a018

Grieger, J. A., Haas, J. D., Murray-Kolb, L. E., Kris-Etherton, P., and Beard, J. L. (2008). Nutrient adequacy and food group consumption of Filipino novices and religious sisters over a nine month period. *Asia Pac. J. Clin. Nutr.* 17, 566–572.

Grotewold, E., Sainz, M. B., Tagliani, L., Hernandez, J. M., Bowen, B., and Chandler, V. L. (2000). Identification of the residues in the Myb domain of maize C1 that specify the interaction with the bHLH cofactor R. *Proc. Natl. Acad. Sci. U.S.A.* 97, 13579–13584. doi: 10.1073/pnas.250379897

Gu, X. Y., Foley, M. E., Horvath, D. P., Anderson, J. V., Feng, J., Zhang, L., et al. (2011). Association between seed dormancy and pericarp color is controlled by a pleiotropic gene that regulates abscisic acid and flavonoid synthesis in weedy red rice. *Genetics* 189, 1515–1524. doi: 10.1534/genetics.111.131169

Guajardo-Flores, D., Rempel, C., Gutiérrez-Uribe, J. A., and Serna-Saldívar, S. O. (2015). Influence of excipients and spray drying on the physical and chemical properties of nutraceutical capsules containing phytochemicals from black bean extract. *Molecules* 20, 21626–21635. doi: 10.3390/molecules201219792

Guo, Z., Xu, P., Zhang, Z., Wang, D., Jin, M., and Teng, A. (2011). Segregation ratio of coloured grains in crossed wheat. *Australian J. Crop Sci.* 5, 589–594.

Gutierrez-Gonzalez, J. J., Vuong, T. D., Zhong, R., Yu, O., Lee, J. D., Shannon, G., et al. (2011). Major locus and other novel additive and epistatic loci involved in modulation of isoflavone concentration in soybean seeds. *Theor. Appl. Genet.* 123, 1375–1385. doi: 10.1007/s00122-011-1673-x

Gutierrez-Gonzalez, J. J., Wu, X., Gillman, J. D., Lee, J.-D., Yu, O., Shannon, G., et al. (2010). Intricate environment-modulated genetic networks control

isoflavone accumulation in soybean seeds. *BMC Plant Biol.* 10:105. doi: 10.1186/1471-2229-10-105

Gutierrez-Gonzalez, J. J., Wu, X., Zhang, J., Lee, J. D., Ellersieck, M., Shannon, J. G., et al. (2009). Genetic control of soybean seed isoflavone content: importance of statistical model and epistasis in complex traits. *Theor. Appl. Genet.* 119, 1069–1083. doi: 10.1007/s00122-009-1109-z

Hao, C., Oliver, Y., and Deyue, Y. (2008). Polymorphisms of *IFS1* and *IFS2* gene are associated with isoflavone concentrations in soybean seeds. *Plant Sci.* 175, 505–512. doi: 10.1016/j.plantsci.2008.05.020

Harakotr, B., Suriharn, B., Scott, M. P., and Lertrot, K. (2015). Genotypic variability in anthocyanins, total phenolics, and antioxidant activity among diverse waxy corn germplasm. *Euphytica* 203, 237–248. doi: 10.1007/s10681-014-1240-z

Hart, J. J., Tako, E., Kochian, L. V., and Glahn, R. P. (2015). Identification of black bean (*Phaseolus vulgaris* L.) polyphenols that inhibit and promote iron uptake by Caco-2 cells. *J. Agric. Food Chem.* 63, 5950–5956. doi: 10.1021/acs.jafc.5b00531

Hassan, H., Fan, M., Zhang, T., and Yang, K. (2015). Prediction of total phenolics and flavonoids contents in Chinese wild rice (*Zizania latifolia*) using FT-NIR spectroscopy. *Am. J. Food Technol.* 10, 109–117. doi: 10.3923/ajft.2015.109.117

Havrlentová, M., Pšenáková, I., Žofajová, A., Rückschloss, Ľ., and Kraic, J. (2014). Anthocyanins in wheat seed–A mini review. *Nova Biotechnol. Chim.* 13, 1–12. doi: 10.2478/nbec-2014-0001

Hayes, C. M., and Rooney, W. L. (2015). Agronomic performance and heterosis of specialty grain sorghum hybrids with a black pericarp. *Euphytica* 196, 459–466. doi: 10.1007/s10681-013-1047-3

He, J., and Giusti, M. (2010). Anthocyanins: natural colorants with health promoting properties. *Ann. Rev. Food Sci. Technol.* 1, 163–187. doi: 10.1146/annurev.food.080708.100754

Herald, T. J., Gadgil, P., Perumal, R., Bean, S. R., and Wilson, J. D. (2014). High-throughput micro-plate HCl–vanillin assay for screening tannin content in sorghum grain. *J. Sci. Food Agric.* 94, 2133–2136. doi: 10.1002/jsfa.6538

Herald, T. J., Gadgil, P., and Tilley, M. (2012). High-throughput micro plate assays for screening flavonoid content and DPPH-scavenging activity in sorghum bran and flour. *J. Sci. Food Agric.* 92, 2326–2331. doi: 10.1002/jsfa.5633

Hichri, I., Barrieu, F., Bogs, J., Kappel, C., Delrot, S., and Lauvergeat, V. (2011). Recent advances in the transcriptional regulation of the flavonoid biosynthetic pathway. *J. Exp. Bot.* 62, 2465–2483. doi: 10.1093/jxb/erq442

Hichri, I., Heppel, S. C., Pillet, J., Leon, C., Czemmel, S., Delrot, S., et al. (2010). The basic helix-loop-helix transcription factor myc1 is involved in the regulation of the flavonoid biosynthesis pathway in grapevine. *Mol. Plant* 3, 509–523. doi: 10.1093/mp/ssp118

Himi, E., Maekawa, M., and Noda, K. (2011). Differential expression of three flavanone 3-hydroxylase genes in grains and coleoptiles of wheat. *Int. J. Plant Genom.* 2011:369460. doi: 10.1155/2011/369460

Himi, E., Nisar, A., and Noda, K. (2005). Colour genes (*R* and *Rc*) for grain and coleoptile upregulate flavonoid biosynthesis genes in wheat. *Genome* 48, 747754. doi: 10.1139/g05-026

Himi, E., and Noda, K. (2005). Red grain colour gene (*R*) of wheat is a Myb-type transcription factor. *Euphytica* 143, 239–242. doi: 10.1007/s10681-005-7854-4

Himi, E., and Taketa, S. (2015). Isolation of candidate genes for the barley *Ant1* and wheat *Rc* genes controlling anthocyanin pigmentation in different vegetative tissues. *Mol. Genet. Genom.* 290, 1287–1298. doi: 10.1007/s00438-015-0991-0

Holtekjølen, A. K., Sahlstrø, S., and Knutsen, S. H. (2011). Phenolic contents and antioxidant activities in covered whole grain flours of Norwegian barley varieties and fractions obtained after pearling. *Acta Agric. Scand. Sect. B Soil Plant Sci.* 61, 67–74. doi: 10.1080/09064710903496527

Hu, Y., Cheng, Z., Heller, L. I., Krasnoff, S. B., Glahn, R. P., and Welch, R. M. (2006). Kaempferol in red and pinto bean seed (*Phaseolus vulgaris* L.) coats inhibits iron bioavailability using an *in vitro* digestion/human Caco-2 cell model. *J. Agric. Food Chem.* 54, 9254–9261. doi: 10.1021/jf0612981

Hu, Q.-P., and Xu, J.-G. (2011). Profiles of carotenoids, anthocyanins, phenolics, and antioxidant activity of selected color waxy corn grains during maturation. *J. Agric. Food Chem.* 59, 2026–2033. doi: 10.1021/jf104149q

Huang, S.-H., and Ng, L.-T. (2012). Quantification of polyphenolic content and bioactive constituents of some commercial rice varieties in Taiwan. *J. Food Comp. Anal.* 26, 122–127. doi: 10.1016/j.jfca.2012.03.009

Huang, D., Ou, B., Hampsch-Woodill, M., Flanagan, J., and Prior, R. (2002). Using a multichannel liquid handling system coupled with a microplate fluorescence reader in 96-well format. *J. Agric. Food Chem*, 50, 4427–4444. doi: 10.1021/jf0201529

Ignat, I., Volf, I., and Popa, V. (2011). A critical review of methods for characterization of polyphenolic compounds in fruits and vegetables. *Food Chem.* 126, 1821–1835. doi: 10.1016/j.foodchem.2010.12.026

Jaafar, S. N. S., Baron, J., Siebenhandl-Ehn, S., Rosenau, T., Böhmdorfer, S., and Grausgruber, H. (2013). Increased anthocyanin content in purple × blue aleurone wheat crosses. *Plant Breed.* 132, 546–552. doi: 10.1111/pbr.12090

Janik, L. J., Cozzolino, D., Dambergs, R., Cynkar, W., and Gishen, M. (2007). The prediction of total anthocyanin concentration in red grape homogenates using visible-near-infrared spectroscopy and artificial neural networks. *Anal. Chim. Acta* 594, 107–118. doi: 10.1016/j.aca.2007.05.019

Jin, L., Xiao, P., Lu, Y., Shao, Y., Shen, Y., and Bao, J. (2009). Quantitative trait loci for brown rice color, phenolics, flavonoid content, and antioxidant capacity in rice grain. *Cereal Chem.* 86, 609–615. doi: 10.1094/CCHEM-86-6-0609

Juzoń, K., Skrzypek, E., Czyczlo-Mysza, I., and Marcińska, I. (2013). Effect of soil drought on the yield structure, protein and phenolics content in *Pisum sativum* and *Lupinus luteus*. *Acta Agronom. Hungarica* 61, 267–278. doi: 10.1556/AAgr.61.2013.4.3

Kaur-Sawhney, R., Tiburcio, A. F., Altabella, T., and Galston, A. W. (2003). Polyamines in plants: an overview. *J. Cell Mol. Biol.* 2, 1–12.

Keppenne, V. D., and Baenziger, S. (1990). Inheritance of the blue aleurone trait in diverse wheat crosses. *Genome* 33, 525–529. doi: 10.1139/g90-078

Kezhu, T., Yuhua, C., Weixian, S., and Xiaoda, C. (2014). Detection of isoflavones content in soybean based on Hyperspectral Imaging Technology. *Sensors Transducers* 169, 55–60.

Khaopha, S., Senawong, T., Jogloy, S., and Patanothai, A. (2012). Comparison of total phenolic content and composition of individual phenolic acids in testae and testae-removed kernels of 15 Valencia-type peanut (*Arachis hypogaea* L.) genotypes. *Afr. J. Biotechnol.* 11, 15923–15930. doi: 10.5897/AJB12.1389

Khlestkina, E. K. (2013). Genes determining coloration of different organs in wheat. *Russ. J. Genet. Appl. Res.* 3, 54–65. doi: 10.1134/S2079059713010085

Khlestkina, E. K., Röder, M. S., and Börner, A. (2010). Mapping genes controlling anthocyanin pigmentation on the glume and pericarp in tetraploid wheat (*Triticum durum* L.). *Euphytica* 171, 65–69. doi: 10.1007/s10681-009-9994-4

Khlestkina, E. K., Shoeva, O. Y., and Gordeeva, E. I. (2015). Flavonoid biosynthesis genes in wheat. *Russ. J. Genet. Appl. Res.* 5, 268–278. doi: 10.1134/S2079059715030077

Khoddami, A., Wilkes, M. A., and Roberts, T. H. (2013). Techniques for analysis of plant phenolic compounds. *Molecules* 18, 2328–2375. doi: 10.3390/molecules18022328

Kim, M.-J., Hyun, J.-N., Kim, J.-A., Park, J.-C., Kim, M.-Y., Kim, J.-G., et al. (2007). Relationship between phenolic compounds, anthocyanins content and antioxidant activity in colored barley germplasm. *J. Agric. Food Chem.* 55, 4802–4809. doi: 10.1021/jf0701943

Kim, E. H., Kim, S. L., Kim, S. H., and Chung, I. M. (2012a). Comparison of isoflavones and anthocyanins in soybean [*Glycine max* (L.) Merrill] seeds of different planting dates. *J. Agric. Food Chem.* 60, 10196–10202. doi: 10.1021/jf3031259

Kim, J.-K., Kim, E.-H., Lee, O.-K., Park, S.-Y., Lee, B., Kim, S.-H., et al. (2013). Variation and correlation analysis of phenolic compounds in mung bean (*Vigna radiata* L.) varieties. *Food Chem.* 141, 2988–2997. doi: 10.1016/j.foodchem.2013.05.060

Kim, J.-K., Kim, E.-H., Park, I., Yu, B.-R., Lim, J. D., Lee, Y.-S., et al. (2014). Isoflavones profiling of soybean [*Glycine max* (L.) Merrill] germplasm and their correlations with metabolic pathways. *Food Chem.* 153, 258–264. doi: 10.1016/j.foodchem.2013.12.066

Kim, E.-H., Ro, H.-M., Kim, S.-L., Kim, H.-S., and Chung, I. M. (2012b). Analysis of isoflavones, phenolic, soyasapogenol, and tocopherol compounds in soybean [*Glycine max* (L.) Merrill] germplasms of different seed weights and origins. *J. Agric. Food Chem.* 60, 6045–6055. doi: 10.1021/jf300463f

Kim, E. H., Seguin, P., Lee, J. E., Yoon, C. G., Song, H. K., Ahn, J. K., et al. (2011). Elevated ultraviolet-B radiation reduces concentrations of isoflavones and phenolic compounds in soybean seeds. *J. Agron. Crop Sci.* 197, 75–80. doi: 10.1111/j.1439-037X.2010.00444.x

Kuhnen, S., Lemos, P. M. M., Campestrini, L. H., Ogliari, J. B., Dias, P. F., and Maraschin, M. (2011). Carotenoid and anthocyanin contents of grains of Brazilian maize landraces. *J. Sci. Food Agric.* 91, 1548–1553. doi: 10.1002/jsfa.4346

Kumar, J., and Ablett, G. R. (2010). The soybean improvement in North America," in *All About Soybeans in Japanese,* ed K. Kitamura (Tokyo: Science Forum), 24–33.

Kumar, V., Rani, A., Rawal, R., Mourya, V., Putrevu, J., Jhawar, J., et al. (2015). Genetic diversity of soybean genotypes differing in isoflavones content as revealed by HPLC and SSR markers. *Australian J. Crop Sci.* 9, 844–852.

Lago, C., Cassani, E., Zanzi, C., Landoni, M., Trovato, R., and Pilu, R. (2014). Development and study of a maize cultivar rich in anthocyanins: colored polenta, a new functional food. *Plant Breed.* 133, 210–217. doi: 10.1111/pbr.12153

Lago, C., Landoni, M., Cassani, C., Doria, E., Nielsen, E., and Pilu, R. (2013). Study and characterization of a novel functional food: purple corn. *Mol. Breed.* 31, 575–585. doi: 10.1007/s11032-012-9816-6

Lähteenmäki, L. (2013). Claiming health in food products. *Food Qual. Pref.* 27, 196–201. doi: 10.1016/j.foodqual.2012.03.006

Laino, P., Shelton, D., Finnie, C., De Leonardis, A. M., Mastrangelo, A. M., Svensson, B., et al. (2010). Comparative proteome analysis of metabolic proteins from seeds of durum wheat (cv. Svevo) subjected to heat stress. *Proteomics* 10, 2359–2368. doi: 10.1002/pmic.200900803

Lampila, P., Van Lieshout, M., Gremmen, B., and Lähteenmäki, L. (2009). Consumer attitudes towards enhanced flavonoid content in fruit. *Food Res. Int.* 42, 122–129. doi: 10.1016/j.foodres.2008.09.002

Laus, M. N., Benedetto, N. A., Caporizzi, R., Tozzi, D., Soccio, M., Giuzio, L., et al. (2015). Evaluation of phenolic antioxidant activity in grains of modern and old durum wheat genotypes by the Novel QUENCHER$_{ABTS}$ approach. *Plant Foods Hum. Nutr.* 70, 207–214. doi: 10.1007/s11130-015-0483-8

Lee, J. H. (2010). Identification and quantification of anthocyanins from the grains of black rice (*Oryza sativa* L.) varieties. *Food Sci. Biotechnol.* 19, 391–397. doi: 10.1007/s10068-010-0055-5

Li, Q., He, F., Zhu, B., Liu, B., Sun, R., Duan, C., et al. (2014). Comparison of distinct transcriptional expression patterns of flavonoid biosynthesis in Cabernet Sauvignon grapes from east and west China. *Plant Physiol. Bioch.* 84, 45–56. doi: 10.1016/j.plaphy.2014.08.026

Li, Y., Ma, D., Sun, D., Wang, C., Zhang, J., Xie, Y., et al. (2015). Total phenolics, flavonoid content, and antioxidant activity of flour, noodles, and steamed bread made from different colored wheat grains by three milling methods. *The Crop J.* 3, 328–334. doi: 10.1016/j.cj.2015.04.004

Li, L., Shewry, P. R., and Ward, J. L. (2008). Phenolic acids in wheat varieties in the HEALTHGRAIN diversity screen. *J. Agric. Food Chem.* 56, 9732–9739. doi: 10.1021/jf801069s

Lee, S. J., Yan, W., Ahn, J. K., and Chung, I. M. (2003). Effects of year, site, genotype and their interactions on various soybean isoflavones. *Field Crops Res.* 81, 181–192. doi: 10.1016/S0378-4290(02)00220-4

Lin-Wang, K., Bolitho, K., Grafton, K., Kortstee, A., Karunairetnam, A., McGhie, T. K., et al. (2010). An R2R3 MYB transcription factor associated with regulation of the anthocyanin biosynthetic pathway in *Rosaceae*. *BMC Plant Biol.* 10:50. doi: 10.1186/1471-2229-10-50

Liu, Z., Liu, Y., Pu, Z., Wang, J., Zheng, Y., Li, Y., et al. (2013). Regulation, evolution, and functionality of flavonoids in cereal crops. *Biotechnol. Letts.* 35, 1765–1780. doi: 10.1007/s10529-013-1277-4

Lopez-Martinez, L., Oliart-Ros, R. M., Valerio-Alfaro, G., Lee, C.-H., Parkin, K. L., and Garcia, H. S. (2009). Antioxidant activity, phenolic compounds and anthocyanins content of eighteen strains of Mexican maize. *LWT Food Sci. Technol.* 42, 1187–1192. doi: 10.1016/j.lwt.2008.10.010

Lozovaya, V. V., Lygin, A. V., Ulanov, A. V., Nelson, R. L., Daide, J., and Widholm, J. M. (2005). Effect of temperature and soil moisture status during seed development on soybean seed isoflavone concentration and composition. *Crop Sci.* 45, 1934–1940. doi: 10.2135/cropsci2004.0567

Lu, X., and Rasco, B. A. (2012). Determination of antioxidant content and antioxidant activity in foods using infrared spectroscopy and chemometrics: a review. *Crit. Rev. Food Sci. Nutr.* 52, 853–875. doi: 10.1080/10408398.2010.511322

Ludwig, S. R., Habera, L. F., Dellaporta, S. L., and Wessler, S. R. (1989). *Lc*, a member of the maize *R* gene family responsible for tissue-specific anthocyanin production, encodes a protein similar to transcription activators and contain the *myc*-homology region. *Proc. Natl. Acad. Sci. U.S.A.* 86, 7092–7096. doi: 10.1073/pnas.86.18.7092

Lukow, O., Suchy, J., Adams, K., Brown, D., Depauw, R., Fox, S., et al. (2012). Effect of solar radiation, plant maturity and post-harvest treatment on the color and phenolic and carotenoid contents in seed of red and white Canadian wheat. *J. Plant Cell Sci.* 3, 1–13.

Luthria, D. L., and Pastor-Corrales, M. A. (2006). Phenolic acid content of fifteen dry edible bean (*Phaseolus vulgaris* L.) varieties. *J. Food Comp. Anal.* 19, 205–211. doi: 10.1016/j.jfca.2005.09.003

Maeda, H., Yamaguchi, T., Omoteno, M., Takarada, T., Fujita, K., Murata, K., et al. (2014). Genetic dissection of black grain rice by the development of a near isogenic line. *Breed. Sci.* 64, 134–141. doi: 10.1270/jsbbs.64.134

Mahajan, S., Das, A., and Sardana, H. K. (2015). Image acquisition techniques for assessment of legume quality. *Trends Food Sci. Tech.* 42, 116–133. doi: 10.1016/j.tifs.2015.01.001

Mahan, A. L., Murray, S. C., Rooney, L. W., and Crosby, K. M. (2013). Combining ability for total phenols and secondary traits in a diverse set of colored (red, blue, and purple) maize. *Crop Sci.* 53, 1248–1255. doi: 10.2135/cropsci2012.06.0385

Mapope, N., and Dakora, F. D. (2013). "Role of flavonoid and isoflavonoid molecules in symbiotic functioning and host-plant defense in the leguminosae," in *The Chemistry for Sustainable Development in Africa,* eds A. Gurib-Fakim and J. N. Eloff (Berlin; Heidelberg: Springer), 33–48.

Mahmoudi, T., Oveisi, M. R., Jannat, B., Behzad, M., Hajimahmoodi, M., and Sadeghi, N. (2015). Antioxidant activity of Iranian barley grain cultivars and their malts. *Afr. J. Food Sci.* 9, 534–539. doi: 10.5897/AJFS2014.1210

Martinek, P., Jirsa, O., Veculová, K., Chrpova, J., Watanabe, N., Burešová, V., et al. (2014). Use of wheat gene resources with different grain colour in breeding. *64 Tagung der Vereinigung der Pflanzenzüchter und Saatgutkaufleute Österreichs* 2013, 75–78.

Martini, D., Taddei, F., Ciccoritti, R., Pasquini, M., Nicoletti, I., Corradini, D., et al. (2015). Variation of total antioxidant activity and of phenolic acid, total phenolics and yellow coloured pigments in durum wheat (*Triticum turgidum* L. var. *durum*) as a function of genotype, crop year and growing area. *J. Cereal Sci.* 65, 175–185. doi: 10.1016/j.jcs.2015.06.012

Matsui, K., Umemura, Y., and Ohme-Takagi, M. (2008). AtMYBL2, a protein with a single MYB domain, acts as a negative regulator of anthocyanin biosynthesis in *Arabidopsis*. *Plant J.* 55, 954–967. doi: 10.1111/j.1365-313X.2008.03565.x

Matus, J. T., Poupin, M. J., Canon, P., Bordeu, E., Alcalde, J. A., and Arce-Johnson, P. (2010). Isolation of WDR and bHLH genes related to flavonoid synthesis in grapevine (*Vitis vinifera* L.). *Plant Mol. Biol.* 72, 607–620. doi: 10.1007/s11103-010-9597-4

Mazur, W. M., Duke, J. A., Wähälä, K., Rasku, S., and Adlecreutz, H. (1998). Isoflavonoids and lignans in legumes: nutritional and health aspects in humans. *J. Nutr. Biochem.* 9, 193–200. doi: 10.1016/S0955-2863(97)00184-8

McKeehen, J. D., Busch, R. H., and Fulcher, R. G. (1999). Evaluation of wheat (*Triticum aestivum* L.) phenolic acids during grain development and their contribution to Fusarium resistance. *J. Agric. Food Chem.* 47, 1476–1482. doi: 10.1021/jf980896f

Meksem, K., Njiti, V. N., Banz, W. J., Iqbal, M. J., Kassem, M. M., Hyten, D. L., et al. (2001). Genomic regions that underlie soybean seed isoflavone content. *J. Biomed. Biotechnol.* 1, 38–44. doi: 10.1155/S1110724301000110

Mendoza-Díaz, S., del Carmen Ortiz-Valerio, M., Castaño-Tostado, E., de Dios Figueroa-Cárdennas, J., Reynoso-Camacho, R., Ramos-Gómez, M., et al. (2012). Antioxidant capacity and antimutagenic activity of anthocyanin and carotenoid extracts from nixtamalized pigmented Creole maize races (*Zea mays* L.). *Plant Foods Hum. Nutr.* 67, 442–449. doi: 10.1007/s11130-012-0326-9

Meng, F. L., Han, Y. P., Teng, W. L., Li, Y. G., and Li, W. B. (2011). QTL underlying resistance to soybean aphid (*Aphis glycines* Matsumura) through isoflavone-mediated antibiosis in soybean cultivar Zhongdou 27. *Theor. Appl. Genet.* 123, 1459–1465. doi: 10.1007/s00122-011-1680-y

Mink, P. J., Scraffold, C. G., Barraj, L. M., Harnack, L., Hong, C. P., Nettleton, J. A., et al. (2007). Flavonoid intake and cardiovascular disease mortality: a prospective study in postmenopausal women. *Am. J. Clin. Nutr.* 85, 895–909.

Mishra, J., Singh, R. D., Jadoon, V. S., Gusain, M. P., and Aradhana. (2012). HPTLC profile of quercetin content of common bean (Uttarakhand) landraces growing in Uttarakhand. *Am. J. Food Technol.* 7, 96–100. doi: 10.3923/ajft.2012.96.100

Mladenka, P., Macakova, K., Filipsky, T., Zatloukalova, L., Jahodar, L., Bovicelli, P., et al. (2011). *In vitro* analysis of iron chelating activity of flavonoids. *J. Inorg. Biochem.* 105, 693–701. doi: 10.1016/j.jinorgbio.2011.02.003

Mojica, L., Meyer, A., Berhow, M. A., and Gonzalez de Mejía, E. (2015). Bean cultivars (*Phaseolus vulgaris* L.) have similar high antioxidant capacity, *in vitro* inhibition of α - amylase and α -glucosidase while diverse phenolic composition and concentration. *Food Res. Int.* 69, 38–48. doi: 10.1016/j.foodres.2014.12.007

Montilla, E. C., Hillebrand, S., Antezana, A., and Winterhalter, P. (2011). Soluble and bound phenolic compounds in different Bolivian purple corn (*Zea mays* L.) cultivars. *J. Agric. Food Chem.* 59, 7068–7074. doi: 10.1021/jf201061x

Morris, G. P., Rhodes, D. H., Brenton, Z., Ramu, P., Thayil, S. D., Hash, C. T., et al. (2013). Dissecting genome-wide association signals for loss-of-function phenotypes in sorghum flavonoid pigmentation traits. G3 3, 2085–2094. doi: 10.1534/g3.113.008417

Mpofu, A., Sapirstein, H. D., and Beta, T. (2006). Genotype and environmental variation in phenolic content, phenolic acid composition, and antioxidant activity of hard spring wheat. *J. Agric. Food Chem.* 54, 1265–1270. doi: 10.1021/jf052683d

Murphy, S. E., Lee, E. A., Woodrow, L., Seguin, P., Kumar, J., Rajcan, I., et al. (2009a). Genotype × Environment interaction for isoflavone content in soybean. *Crop Sci.* 49, 1313–1321. doi: 10.2135/cropsci2008.09.0533

Murphy, S. E., Lee, E. A., Woodrow, L., Seguin, P., Kumar, J., Rajcan, I., et al. (2009b). Association of seed and agronomic traits with isoflavone levels in soybean. *Canadian J. Plant Sci.* 89, 477–484. doi: 10.4141/CJPS08148

Narwal, S., Thakur, V., Sheoran, S., Dahiya, S., Jaswal, S., and Gupta, R. K. (2014). Antioxidant activity and phenolic content of the Indian wheat varieties. *J. Plant Biochem. Biotechnol.* 23, 11–17. doi: 10.1007/s13562-012-0179-1

Ndakidemi, P. A., and Dakora, F. D. (2003). Legume seed flavonoids and nitrogenous metabolites as signals and protectants in early seedling development. *Funct. Plant Biol.* 30, 729–745. doi: 10.1071/FP03042

Ng, M., Fleming, T., Robinson, M., Thomson, B., Graetz, N., Margono, C., et al. (2014). Global, regional, and national prevalence of overweight and obesity in children and adults during 1980–2013: a systematic analysis for the global burden of disease study. *Lancet* 384, 766–781. doi: 10.1016/S0140-6736(14)60460-8

Nicholson, R. L., and Hammerschmidt, R. (1992). Phenolic compounds and their role in disease resistance. *Ann. Rev. Phytopathol.* 30, 369–389. doi: 10.1146/annurev.py.30.090192.002101

Nikolova, M., Dimitrova, M., Tasheva, K., Todorova, R., Dimitrova, M., Ravishankar, G., et al. (2014). Comparison of antiradical activity and total phenolic content in seeds of five soybean cultivars by applying different extraction solvents. *Genet. Plant Physiol.* 4, 110–116.

Nocella, G., and Kennedy, O. (2012). Food health claims: what consumers understand. *Food Policy* 37, 571–580. doi: 10.1016/j.foodpol.2012.06.001

Noubissié, J. B. T., Youmbi, E., Njintang, N. Y., Abatchoua, M. A., Nguimboou, R. M., and Bell, J. M. (2012). Inheritance of phenolic contents and antioxidant capacity of dehulled seeds in cowpea (*Vigna unguiculata* L. *Walp.). Int. J. Agr. Agric. Res.* 2, 7–18.

Nyström, L., Lampi, A.-M., Andersson, A. A. M., Kamal-Eldin, A., Gebruers, K., Courtin, C. M., et al. (2008). Phytochemicals and dietary fiber components in rye varieties in the health grain diversity screens. *J. Agric. Food Chem.* 56, 9758–9766. doi: 10.1021/jf801065r

Oikawa, T., Maeda, H., Oguchi, T., Yamaguchi, T., Tanabe, N., Ebana, K., et al. (2015). The birth of a black rice gene and its local spread by introgression. *Plant Cell* 27, 2401–2014. doi: 10.1105/tpc.15.00310

Ojwang, L. O., Dykes, L., and Awika, J. M. (2012). Ultra-performance of liquid chromatography tandem quadrupole mass spectrometry profiling of anthocyanins and flavonols in cowpea (*Vigna unguiculata*) of varying genotypes. *J. Agric. Food Chem.* 60, 3735–3744. doi: 10.1021/jf2052948

Oomah, B. D., Corbè, A., and Balasubramanian, P. (2010). Antioxidant and anti-inflammatory activities of bean (*Phaseolus vulgaris* L.) hulls. *J. Agric. Food Chem.* 58, 8225–8230. doi: 10.1021/jf1011193

Osborne, B. G. (2006). Applications of near infrared spectroscopy in quality screening of early-generation materials in cereal breeding programmes. *J. Near Infrared Spec.* 14, 93–101. doi: 10.1255/jnirs.595

Ovando-Martínez, M., Guzmán-Maldonado, S. H., Simsek, S., Bello-Pérez, L. A., and Osorio-Díaz, P. (2014). Effect of water regimes on dietary fiber, polyphenols and antioxidant capacity of black and pinto beans. *Agric. Sci.* 5, 342–352 doi: 10.4236/as.2014.54036

Pandey, A., Misra, P., Bhambhani, S., Bhatia, C., and Trivedi, P. K. (2014). Expression of *Arabidopsis* MYB transcription factor, *AtMYB111*, in tobacco requires light to modulate flavonol content. *Sci. Rep.* 4:5018. doi: 10.1038/srep05018

Park, S.-Y., Hua, S.-H., Lim, S.-H., Jung, J. Y., Lee, S. M., Yeo, Y., et al. (2012). Determination of phenolic acids in Korean rice (*Oryza sativa* L.) cultivars using Gas Chromatography-Time-of-Flight Mass. *Food Sci. Biotechnol.* 21, 1141–1148. doi: 10.1007/s10068-012-0149-3

Pattanaik, S., Kong, Q., Zaitlin, D., Werkman, J. R., Xie, C. H., Patra, B., et al. (2010). Isolation and functional characterization of a floral tissue-specific R2R3 MYB regulator from tobacco. *Planta* 231, 1061–1076. doi: 10.1007/s00425-010-1108-y

Peiffer, D. S., Wang, L., Zimmerman, N. P., Carmella, S. G., Kuo, C., Chen, J., et al. (2016). Dietary consumption of black raspberries or their anthocyanin constituents alters innate immune cell trafficking in esophageal cancer. *Cancer Immunol. Res.* 4, 72–82. doi: 10.1158/2326-6066.CIR-15-0091

Pereira, D. M., Valentão, P., Pereira, J. A., and Andrade, P. B. (2009). Phenolics: from chemistry to biology. *Molecules* 14, 2202–2211. doi: 10.3390/molecules14062202

Perron, N. R., and Brumaghim, J. L. (2009). A review of the antioxidant mechanisms of polyphenol compounds related to iron binding. *Cell Biochem. Biophys.* 53, 75–100. doi: 10.1007/s12013-009-9043-x

Phommalath, S., Teraishi, M., Yoshikawa, T., Saito, H., Tsukiyama, T., Nakazaki, T., et al. (2014). Wide genetic variation in phenolic compound content of seed coats among black soybean cultivars. *Breed. Sci.* 64, 409–415. doi: 10.1270/jsbbs.64.409

Pietta, P. G. (2000). Flavonoids as antioxidants. *J. Nat. Prod.* 63, 1035–1042. doi: 10.1021/np9904509

Pissard, A., Pierna, J. A. F., Baeten, V., Sinnaeve, G., Lognay, G., Mouteau, A., et al. (2013). Non-destructive measurement of vitamin C, total polyphenol and sugar content in apples using near-infrared spectroscopy. *J. Sci. Food Agric.* 93, 238–244. doi: 10.1002/jsfa.5779

Porter, L. J., Hrstich, L. N., and Chan, B. G. (1986). The conversion of procyanidins and prodelphinidins to cyanidin and delphinidin. *Phytochemistry* 25, 223–230. doi: 10.1016/S0031-9422(00)94533-3

Price, M. L., Van Scoyoc, S., and Butler, L. G. (1978). A critical evaluation of the vanillin reaction as an assay for tannin in sorghum grain. *J. Agric. Food Chem.* 26, 1214–1218. doi: 10.1021/jf60219a031

Primomo, V. S., Poysa, V., Ablett, G. R., Jackson, C. J., Gijzen, M., and Rajcan, I. (2005). Mapping QTL for individual and total isoflavone content in soybean seeds. *Crop Sci.* 45, 2454–2462. doi: 10.2135/cropsci2004.0672

Qi, X., Shuai, Q., Chen, H., Fan, L., Zeng, Q., and He, N. (2014). Cloning and expression analysis of anthocyanin biosynthetic genes in mulberry plants. *Mol. Genet. Genom.* 289, 783–793. doi: 10.1007/s00438-014-0851-3

Qiu, Y., Liu, Q., and Beta, T. (2009). Antioxidant activity of commercial wild rice and identification of flavonoid compounds in active fractions. *J. Agric. Food Chem.* 57, 7543–7551. doi: 10.1021/jf901074b

Qualset, C. O., Soliman, K. M., Jan, C. C., Dvorak, J., Mcguire, P. E., and Vogt, H. E. (2005). Registration of UC 66049 *Triticum aestivum* blue aleurone genetic stock. *Crop Sci.* 45, 432. doi: 10.2135/cropsci2005.0432

Ragaee, S., Guzar, I., Abdel-Aal, E.-S. M., and Seetharaman, K. (2012). Bioactive components and antioxidant capacity of Ontario hard and soft wheat varieties. *Can. J. Plant Sci.* 92, 9–30. doi: 10.4141/cjps2011-100

Rahman, M. M., Lee, K. E., Lee, E. S., Matin, M. N., Lee, D. S., Yun, J. S., et al. (2013). The genetic constitution of complementary genes *Pp* and *Pb* determine the purple color variation in pericarps with cyanidin-3-O-glucoside depositions in black rice. *J. Plant Biol.* 56, 24–31. doi: 10.1007/s12374-012-0043-9

Ramírez-Jiménez, A. K., Reynoso-Camacho, R., Tejero, M. E., León-Galván, F., and Loarca- Piña, G. (2015). Potential role of bioactive compounds of *Phaseolus vulgaris* L. on lipid-lowering mechanisms. *Food Res. Int.* 76, 92–104. doi: 10.1016/j.foodres.2015.01.002

Rascio, A., Picchi, V., Naldi, J. P., Colecchia, S., De Santis, G., Gallo, A., et al. (2015). Effects of temperature increase, through spring sowing, on antioxidant power and health-beneficial substances of old and new wheat. *J. Cereal Sci.* 61, 11–118. doi: 10.1016/j.jcs.2014.09.010

Razzaghi-As, N., Garrido, J., Khazraei, H., Borges, F., and Firuzi, F. (2013). Antioxidant properties of hydroxycinnamic acids: a review of structure-activity relationships. *Curr. Med. Chem.* 20, 123–135.

Rhodes, D. H., Hoffmann, L. Jr., Rooney, W. L., Ramu, P., Morris, G. P., and Kresovich, S. (2014). Genome-wide association study of grain polyphenol concentrations in global sorghum [*Sorghum bicolor* (L.) Moench] germplasm. *J. Agric. Food Chem.* 62, 10916–10927. doi: 10.1021/jf503651t

Roberfroid, M. B. (2002). Global view on functional foods: European perspectives. *Br. J. Nutr.* 88, S133–S138. doi: 10.1079/bjn20 02677

Romani, A., Vignolini, P., Galardi, C., Mulinacci, N., Benedettelli, S., and Heimler, D. (2004). Germplasm characterization of Zolfino landraces (*Phaseolus vulgaris* L.) by flavonoid content. *J. Agric. Food Chem.* 52, 3838–3842. doi: 10.1021/jf0307402

Rooney, W. L., Portillo, O., and Hayes, C. (2013a). Registration of ATx3363 and BTx3363 black sorghum germplasm. *J. Plant Reg.* 7, 342–346. doi: 10.3198/jpr2013.01.0006crg

Rooney, W. L., Rooney, L. W., Awika, J., and Dykes, L. (2013b). Registration of Tx3362 sorghum germplasm. *J. Plant Reg.* 7, 104–107. doi: 10.3198/jpr2012.04.0262crg

Rosales-Serna, R., Gutiérrez-Uribe, J. A., Reyes-Barraza, E., Mayek-Pérez, N., and Saldivar-Serna, S. R. O. (2015). Genetic relationship among common bean cultivars with enhanced accumulation of bioactive compounds. *J. Agric. Sci.* 7, 106–116. doi: 10.5539/jas.v7n9p106

Rubiales, D., Fondevilla, S., Chen, W., Gentzbittel, L., Higgins, T. J. V., Castillejo, M. A., et al. (2015). Achievements and challenges in legume breeding for pest and disease resistance. *Crit. Rev. Plant Sci.* 34, 195–236. doi: 10.1080/07352689.2014.898445

Ryu, S. N., Park, S. Z., and Ho, C.-T. (1998). High performance liquid chromatographic determination of anthocyanin pigments in some varieties of black rice. *J. Food Drug Anal.* 6, 729–736.

Saba, A., Vassallo, M., Shepherd, R., Lampila, P., Arvola, A., Dean, M., et al. (2010). Country-wise differences in perception of health-related messages in cereal-based food products. *Food Qual. Pref.* 21, 385–393. doi: 10.1016/j.foodqual.2009.09.007

Santiago, R., Barros-Rios, J., and Malvar, R. A. (2013). Impact of cell wall composition on maize resistance to pests and diseases. *Int. J. Mol. Sci.* 14, 6960–6980. doi: 10.3390/ijms14046960

Schaffer-Lequart, C., Lehmann, U., Ross, A. B., Roger, O., Eldridge, A. L., Ananta, E., et al. (2015). Whole grain in manufactured foods: current use, challenges and the way forward. *Crit. Rev. Food Sci. Nutr.* doi: 10.1080/10408398.2013.781012. [Epub ahead of print].

Schaich, K. M., Tian, X., and Xie, J. (2015). Hurdles and pitfalls in measuring antioxidant efficacy: a critical evaluation of ABTS, DDPH, and ORAC assays. *J. Funct. Foods* 14, 111–125. doi: 10.1016/j.jff.2015.01.043

Schmutz, J., Cannon, S. B., Schlueter, J., Ma, J., Mitros, T., Nelson, W., et al. (2010). Genome sequence of the palaeopolyploid soybean. *Nature* 463, 178–183. doi: 10.1038/nature08670

Schwinn, K., Venail, J., Shang, Y., Mackay, S., Alm, V., Butelli, E., et al. (2006). A small family of MYB-regulatory genes controls floral pigmentation intensity and patterning in the genus *Antirrhinum*. *Plant Cell* 18, 831–851. doi: 10.1105/tpc.105.039255

Segev, A., Badani, H., Kapulnik, Y., Shomer, I., Oren-Shamir, M., and Galili, S. (2010). Determination of polyphenols, flavonoids, and antioxidant capacity in colored chickpea (*Cicer arietinum* L.). *J. Food Sci.* 75, S115–S119. doi: 10.1111/j.1750-3841.2009.01477.x

Shao, Y., Tang, F., Huang, Y., Xu, F., Chen, Y., Tong, C., et al. (2014a). Analysis of Genotype × Environment interactions for polyphenols and antioxidant capacity of rice by association mapping. *J. Agric. Food Chem.* 62, 5361–5368. doi: 10.1021/jf500951e

Shao, Y., Xu, F., Sun, X., Bao, J., and Beta, T. (2014b). Phenolic acids, anthocyanins, and antioxidant capacity in rice (*Oryza sativa* L.) grains at four stages of development after flowering. *Food Chem.* 143, 90–96. doi: 10.1016/j.foodchem.2013.07.042

Sharma, M., Chai, C., Morohashi, K., Grotewold, E., Snook, M. E., and Chopra, S. (2012). Expression of flavonoid 3′-hydroxylase is controlled by *P1*, the regulator of 3-deoxyflavonoid biosynthesis in maize. *BMC Plant Biol.* 12:196. doi: 10.1186/1471-2229-12-196

Sharma, M., Cortes-Cruz, M., Ahern, K. R., McMullen, M., Brutnell, T. P., and Chopra, S. (2011). Identification of the *Pr1* gene product completes the anthocyanin biosynthesis pathway of maize. *Genetics* 188, 69–79. doi: 10.1534/genetics.110.126136

Sharma, N., Kaur, R., Mangat, G. S., and Singh, K. (2014). Red pericarp introgression lines derived from interspecific crosses of rice: physiochemical characteristics, antioxidative properties and phenolic content. *J. Sci. Food Agric.* 94, 2912–2920. doi: 10.1002/jsfa.6632

Sharma, S., and Thakur, D. R. (2014). Biochemical basis for bruchid resistance in cowpea, chickpea and soybean genotypes. *Am. J. Food Technol.* 9, 318–324. doi: 10.3923/ajft.2014.318.324

Shen, Y., Jin, L., Xiao, P., Lu, Y., and Bao, J. (2009). Total phenolics, flavonoids, antioxidant capacity in rice grain and their relations to grain color, size and weight. *J. Cereal Sci.* 49, 106–111. doi: 10.1016/j.jcs.2008.07.010

Shen, Y., Shen, J., Dawadondup, Zhuang, L., Wang, Y., Pu, J., et al. (2013). Physical localization of a novel blue-grained gene derived from *Thinopyrum bessarabicum*. *Mol. Breed.* 31, 195–204. doi: 10.1007/s11032-012-9783-y

Shewry, P. R. (2009). The HEALTHGRAIN programme opens new opportunities for improving wheat for nutrition and health. *Nutr. Bull.* 34, 225–231. doi: 10.1111/j.1467-3010.2009.01747.x

Shewry, P. R., and Hey, S. (2015). Do ancient wheat species differ from modern bread wheat in their contents of bioactive components? *J. Cereal Sci.* 65, 236–243. doi: 10.1016/j.jcs.2015.07.014

Shoeva, O. Y., Gordeeva, E. L., and Khlestkina, E. K. (2014). The regulation of anthocyanin synthesis in the wheat pericarp. *Molecules* 19, 20266–20279. doi: 10.3390/molecules191220266

Siebenhandl-Ehn, S., Grausgruber, H., Pellegrini, N., Del Rio, D., Fogliano, V., Pernice, R., et al. (2007). Phytochemical profile of main antioxidants in different fractions of purple and blue wheat, and black barley. *J. Agric. Food Chem.* 55, 8541–8547. doi: 10.1021/jf072021j

Siebenhandl-Ehn, S., Kinner, M., Leopold, L. F., Poppernitsch, M. B., Prückler, M., Wurbs, P., et al. (2011). *Hulless Barley—A Rediscovered source for Functional Foods Phytochemical Profile and Soluble Dietary Fiber Content in Naked Barley Varieties and their Antioxidant Properties.* Available online at: http://cdn.intechopen.com/pdfs-wm/25502.pdf

Singleton, V. L., Orthofer, R., and Lamuela-Raventos, R. M. (1999). Analysis of total phenols and other oxidation substrates and antioxidants by means of Folin-Ciocalteu reagent. *Method Enzymol.* 299, 152−178. doi: 10.1016/S0076-6879(99)99017-1

Siro, I., Kapolna, E., Kapolna, B., and Lugasi, A. (2008). Functional food. Product development, marketing and consumer acceptance: a review. *Appetite* 51, 456–467. doi: 10.1016/j.appet.2008.05.060

Soares, S., Kohl, S., Thalmann, S., Mateus, N., Meyerhof, W., and de Freitas, V. (2013). Different phenolic compounds activate distinct human bitter taste receptors. *J. Agric. Food Chem.* 61, 1525–1533. doi: 10.1021/jf304198k

Sompong, R., Siebenhandl-Ehn, S., Linsberger-Martin, G., and Berghofer, E. (2011). Physicochemical and antioxidative properties of red and black rice varieties from Thailand, China, and Sri Lanka. *Food Chem.* 124, 132–140. doi: 10.1016/j.foodchem.2010.05.115

Spelt, C., Quattrocchio, F., Mol, J. N., and Koes, R. (2000). *Anthocyanin1* of petunia encodes a basic helix–loop–helix protein that directly activates transcription of structural anthocyanin genes. *Plant Cell* 12, 1619–1632. doi: 10.1105/tpc.12.9.1619

Sriseadka, T., Wongpornchai, S., and Rayanakorn, M. (2012). Quantification of flavonoids in black rice by liquid chromatography-negative electrospray ionization tandem mass spectrometry. *J. Agric. Food Chem.* 60, 11723–11732. doi: 10.1021/jf303204s

Stracke, R., Ishihara, H., Huep, G., Barsch, A., Mehrtens, F., Niehaus, K., et al. (2007). Differential regulation of closely related R2R3-MYB transcription factors controls flavonol accumulation in different parts of the *Arabidopsis thaliana* seedling. *Plant J.* 50, 660–677. doi: 10.1111/j.1365-313X.2007.03078.x

Stumpf, B., Yan, F., and Honermeier, B. (2015). Nitrogen fertilization and maturity influence the phenolic concentration of wheat grain (*Triticum aestivum*). *J. Plant Nutr. Soil Sci.* 178, 118–125. doi: 10.1002/jpln.201400139

Subramanian, S., Stacey, G., and Yu, O. (2007). Distinct, crucial roles of flavonoids during legume nodulation. *Trends Plant Sci.* 12, 82–85. doi: 10.1016/j.tplants.2007.06.006

Svensson, L., Sekwati-Monang, B., Lutz, D. L., Schieber, A., and Gänzle, M. G. (2010). Phenolic acids and flavonoids in nonfermented and fermented red sorghum (*Sorghum bicolor* (L.) Moench). *J. Agric. Food Chem.* 58, 9214–9220. doi: 10.1021/jf101504v

Sweeney, M. T., Thomsoon, M. J., Pfeil, B. E., and McCouch, S. (2006). Caught red-handed: *Rc* encodes a basic helix-loop-helix protein conditioning red pericarp in rice. *Plant Cell* 18, 283–294. doi: 10.1105/tpc.105.038430

Tako, E., and Glahn, R. P. (2010). White beans provide more bioavailable iron than red beans: studies in poultry (*Gallus gallus*) and an *in vitro* digestion/Caco-2 model. *Int. J. Vitam. Nutr. Res.* 80, 416–429. doi: 10.1024/0300-9831/a000028

Tako, E., Reed, S. M., Budiman, J., Hart, J. J., and Glahn, R. P. (2015). Higher iron pearl millet (*Pennisetum glaucum* L.) provides more absorbable iron that is limited by increased polyphenolic content. *Nutr. J.* 14, 1–11. doi: 10.1186/1475-2891-14-11

Taleon, V., Dykes, L., Rooney, W. L., and Rooney, L. W. (2012). Effect of genotype and environment on flavonoid concentration and profile of black sorghum grains. *J. Cereal Chem.* 56, 470–475. doi: 10.1016/j.jcs.2012.05.001

Taleon, V., Dykes, L., Rooney, W. L., and Rooney, L. W. (2014). Environmental effect on flavonoid concentrations and profiles of red and lemon-yellow sorghum grains. *J. Food Compos. Anal.* 34, 178–185. doi: 10.1016/j.jfca.2014.03.003

Tereshchenko, O. Y., Gordeeva, E. I., Arbuzova, V. S., Börner, A., and Khlestkina, E. K. (2012). The D genome carries a gene determining purple grain colour in wheat. *Cereal Res. Commun.* 40, 334–341. doi: 10.1556/CRC.40.2012.3.2

Teucher, B., Olivares, M., and Cori, H. (2004). Enhancers of iron absorption: ascorbic acid and other organic acids. *Int. J. Vit. Nutr. Res.* 74, 403–419. doi: 10.1024/0300-9831.74.6.403

Tian, X., and Schaich, K. M. (2013). Effects of molecular structure on kinetics and dynamics of the trolox equivalent antioxidant capacity assay with ABTS. *J. Agric. Food Chem.* 61, 5511–5519. doi: 10.1021/jf4010725

Toledo-Ortiz, G., Huq, E., and Quail, P. H. (2003). The *Arabidopsis* basic/helix–loop–helix transcription factor family. *Plant Cell* 15, 1749–1770. doi: 10.1105/tpc.013839

Torre, L. A., Bray, F., Siegel, R. L., Ferlay, J., Lortet-Tieulent, J., and Jemal, A. (2015). Global cancer statistics. *CA-Cancer J. Clin.* 65, 87–108. doi: 10.3322/caac.21262

Treutte, D. (2006). Significance of flavonoids in plant resistance: a review. *Environ. Chem. Letts.* 4, 147–157. doi: 10.1007/s10311-006-0068-8

Upadhyaya, H. D., and Ortiz, R. (2001). A mini core subset for capturing diversity and promoting utilization of chickpea genetic resources in crop improvement. *Theor. Appl. Genet.* 102, 1292–1298. doi: 10.1007/s00122-001-0556-y

Urias-Lugo, D. A., Heredia, J. B., Serna-Saldivar, S. O., Muy-Rangel, M. D., and Valdez-Torres, J. B. (2015). Total phenolics, total anthocyanins and antioxidant capacity of native and elite blue maize hybrids (*Zea mays* l.). *CyTA J. Food* 13, 336–339. doi: 10.1080/19476337.2014.980324

Urias-Peraldí, M., Gutiérrez-Uribe, J. A., Perciado-Ortiz, R. E., Cruz-Morales, A. S., Serna-Saldívar, S. O., and García-Lara, S. (2013). Nutraceutical profiles improved blue maize (*Zea mays* L.) hybrids for subtropical regions. *Field Crops Res.* 141, 69–76. doi: 10.1016/j.fcr.2012.11.008

Van der Kamp, J. W. (2012). Paving the way for innovation in enhancing the intake of whole grain. *Trends Food Sci. Technol.* 25, 101–107. doi: 10.1016/j.tifs.2011.12.005

Verma, B., Hucl, P., and Chibbar, R. N. (2008). Phenolic content and antioxidant properties of grain in 51 wheat cultivars. *Cereal Chem.* 85, 544–549. doi: 10.1094/CCHEM-85-4-0544

Wagner, K.-H., and Brath, H. (2012). A global view on the development of non communicable diseases. *Prev. Med.* 54, S38–S48. doi: 10.1016/j.ypmed.2011.11.012

Wang, Y., and Frei, M. (2011). Stressed food - The impact of abiotic environmental stresses on crop quality. *Agric. Ecosyst. Environ.* 141, 271–286. doi: 10.1016/j.agee.2011.03.017

Wang, M. L., Gillaspie, A. G., Morris, J. B., Davis, J., and Pederson, G. A. (2008). Flavonoid content in different legume germplasm seeds quantified by HPLC. *Plant Genet. Resour.* 6, 62–69. doi: 10.1017/S1479262108923807

Wang, Y., Han, Y., Teng, W., Zhao, X., Li, Y., Wu, L., et al. (2014). Expression quantitative trait loci infer the regulation of isoflavone accumulation in soybean (*Glycine max* L. *Merr.*) seed. *BMC Genom.* 15:680. doi: 10.1186/1471-2164-15-680

Wang, Y., Han, Y., Zhao, X., Li, Y., Teng, W., Li, D., et al. (2015). Mapping isoflavone QTL with main, epistatic and QTL × environment effects in recombinant inbred lines of soybean. *PLoS ONE* 10:e0118447. doi: 10.1371/journal.pone.0118447

Wang, M. L., and Morris, J. B. (2007). Flavonoid content in seeds of guar germplasm using HPLC. *Plant Genet. Resour.* 5, 96–99. doi: 10.1017/S1479262107672335

Wang, C., Sherrard, M., Pagadala, S., Wixon, R., and Scott, R. A. (2000). Isoflavone content among maturity group 0 to II soybeans. *J. Am. Oil Chem. Soc.* 77, 483–487. doi: 10.1007/s11746-000-0077-6

Wang, C., and Shu, Q. (2007). Fine mapping and candidate gene analysis of purple pericarp gene *Pb* in rice (*Oryza sativa* L.). *Chin. Sci. Bull.* 52, 3097–3104. doi: 10.1007/s11434-007-0472-x

Waniska, R. D., and Rooney, L. W. (2000). "Structure and chemistry of the sorghum caryopsis," in *The Sorghum: Origin, History, Technology, and Production*, eds C. W. Smith, and R. A. Frederiksen (New York, NY: John Wiley and Sons, Inc,), 649–687.

Ward, J. L., Poutanen, K., Gebruers, K., Piironsen, V., Lampi, A.-M., Nyström, L., et al. (2008). The HEALTHGRAIN cereal diversity screen: concept, results, and prospects. *J. Agric. Food Chem.* 56, 9699–9709. doi: 10.1021/jf8009574

Warner, E. F., Zhang, Q., Raheem, K. S., O'Hagan, D., O'Connell, M. A., and Kay, C. D. (2016). Common phenolic metabolites of flavonoids, but not their un-metabolized precursors, reduce the secretion of vascular cellular adhesion molecules by human endothelial cells. *J. Nutr.* 146, 465–473. doi: 10.3945/jn.115.217943

Watterson, J. J., and Butler, L. G. (1983). Occurrence of an unusual leucoanthocyanidin and absence of proanthocyanidins in sorghum leaves. *J. Agric. Food Chem.* 31, 41–45. doi: 10.1021/jf00115a011

Wei, H., Zhu, J.-H., Shang, Y., Jia, Q.-J., Wang, J.-M., and Yang, J.-M. (2013). Research advanced in colored barley. *J. Plant Genet. Resour.* 14, 1020–1024.

Weseler, A. R., Ruijters, E. J., Drittij-Reijnders, M. J., Reesink, K. D., Haenen, G. R., and Bast, A. (2011). Pleiotropic benefit of monomeric and oligomeric flavanols on vascular health – a randomized controlled clinical study. *PLoS ONE* 6:e28460. doi: 10.1371/journal.pone.0028460

Whitacre, E., Oliver, J., van den Broek, R., van Engelen, P., Kremers, B., van der Horst, B., et al. (2003). Predictive analysis of cocoa procyanidins using near-infrared spectroscopy techniques. *J. Food Sci.* 68, 2618–2622. doi: 10.1111/j.1365-2621.2003.tb05779.x

Wickert, E., Schiocchet, M. A., Noldin, J. A., Raimondi, J. A., de Andrade, A., Scheuermann, K. K., et al. (2014). Exploring variability: New Brazilian varieties SCS119 Rubi and SCS120 Onix for the specialty rices market. *Open J. Genet.* 4, 157–165. doi: 10.4236/ojgen.2014.42016

Wilson, R. F. (ed.). (2012). *Designing Soybeans for 21st Century Markets.* Urbana, IL: AOCS Press.

Wu, J. G., and Shi, C. H. (2004). Prediction of grain weight, brown rice weight and amylose content in single rice grains using near-infrared reflectance spectroscopy. *Field Crop Res.* 87, 13–21. doi: 10.1016/j.fcr.2003.09.005

Wu, J. G., and Shi, C. H. (2007). Calibration model optimization for rice cooking characteristics by near infrared reflectance spectroscopy (NIRS). *Food Chem.* 103, 1054–1061. doi: 10.1016/j.foodchem.2006.07.063

Wu, J. G., Shi, C. H., and Zhang, X. M. (2002). Estimating the amino acid composition in the milled rice powder by near-infrared reflectance spectroscopy. *Field Crop Res.* 75, 1–7. doi: 10.1016/S0378-4290(02)00006-0

Xie, J., and Schaich, K. M. (2014). Re-evaluation of the 2,2-diphenyl-1-picrylhydrazyl free radical (DPPH) assay for antioxidant activity. *J. Agric. Food Chem.* 62, 4251–4260. doi: 10.1021/jf500180u

Yang, L., Allred, C. D., and Awika, J. M. (2014). Emerging evidence on the role of estrogenic sorghum flavonoids in colon cancer prevention. *Cereal Foods World* 59, 244–251. doi: 10.1094/CFW-59-5-0244

Yang, R.-Y., Lin, S., and Kuo, G. (2008). Content and distribution of flavonoids among 91 edible plant species. *Asia Pac. J. Clin. Nutr.* 17, 275–279.

Yang, K., Moon, J. K., Jeong, N., Chun, H. K., Kang, S. T., Back, K., et al. (2011). Novel major quantitative trait loci regulating the content of isoflavone in soybean seeds. *Genes Genom.* 33, 685–692. doi: 10.1007/s13258-011-0043-z

Yoshimura, Y., Zaima, N., Moriyama, T., and Kawamura, Y. (2012). Different localization patterns of anthocyanin species in the pericarp of black rice revealed by imaging mass spectrometry. *PLoS ONE* 7:e31285. doi: 10.1371/journal.pone.0031285

Zeng, G., Li, D., Han, Y., Teng, W., Wang, J., Qiu, L., et al. (2009). Identification of QTL underlying isoflavone contents in soybean seeds among multiple environments. *Theor. Appl. Genet.* 118, 1455–1463. doi: 10.1007/s00122-009-0994-5

Zeven, A. C. (1991). Wheats with purple and blue grains: a review. *Euphytica* 56, 243–258. doi: 10.1007/BF00042371

Zhang, J., Ge, Y., Han, F., Li, B., Yan, S., Sun, J., et al. (2014). Isoflavone content of soybean cultivars from maturity group 0 to VI grown in northern and southern China. *J. Am. Oil Chem. Soc.* 91, 1019–1028. doi: 10.1007/s11746-014-2440-3

Zhang, H., Shao, Y., Bao, J., and Beta, T. (2015). Phenolic compounds and antioxidant properties of breeding lines between the white and black rice. *Food Chem.* 172, 630–639. doi: 10.1016/j.foodchem.2014.09.118

Zhang, C., Shen, Y., Chen, J., Xiao, P., and Bao, J. (2008). Nondestructive prediction of total phenolics, flavonoid contents, and antioxidant capacity of rice grain using near-infrared spectroscopy. *J. Agric. Food Chem.* 56, 8268–8272. doi: 10.1021/jf801830z

Zhang, Q., Zhang, J., Shen, J., Silva, A., Dennis, D. A., and Barrow, C. J. (2006). A simple 96-well microplate method for estimation of total polyphenol content in seaweeds. *J. Appl. Phycol.* 18, 445–450. doi: 10.1007/s10811-006-9048-4

Zhang, M. W., Zhang, R. F., Zhang, F. X., and Liu, R. H. (2010). Phenolic profiles and antioxidant activity of black rice bran of different commercially available varieties. *J. Agric. Food Chem.* 58, 7580–7587. doi: 10.1021/jf1007665

Zhang, R. F., Zhang, F. X., Zhang, M. W., Zhen, C. W., Yang, C. Y., Zhang, Y., et al. (2011). Phenolic composition and antioxidant activity in seed coats of 60 Chinese black soybean (*Glycine max* L. *Merr.) varieties. J. Agric. Food Chem.* 59, 5935–5944. doi: 10.1021/jf201593n

Zheng, Q., Li, B., Li, H., and Li, Z. (2009). Utilization of blue-grained character in wheat breeding derived from *Thinopyrum poticum*. *J. Genet. Genom.* 36, 575–580. doi: 10.1016/S1673-8527(08)60149-6

Zheng, Q., Li, B., Mu, S., Zhou, H., and Li, Z. (2006). Physical mapping of the blue-grained gene(s) from *Thinopyrum ponticum* by GISH and FISH in a set of translocation lines with different seed colors in wheat. *Genome* 49, 1109–1114. doi: 10.1139/g06-073

Zhou, Z., Robards, K., Helliwell, S., and Blanchard, C. (2004). The distribution of phenolic acids in rice. *Food Chem.* 87, 401–406. doi: 10.1016/j.foodchem.2003.12.015

Zhu, F., Cai, Y. Z., Bao, J., and Corke, H. (2010). Effect of γ-irradiation on phenolic compounds in rice grain. *Food Chem.* 120, 74–77. doi: 10.1016/j.foodchem.2009.09.072

Zhu, H. F., Fitzsimmons, K., Khandelwal, A., and Kranz, R. G. (2009). CPC, a single-repeat R3MYB, is a negative regulator of anthocyanin biosynthesis in *Arabidopsis*. *Mol. Plant* 2, 790–802. doi: 10.1093/mp/ssp030

Žilić, S., Serpen, A., Akıllıoğlu, G., Gökmen, V., and Vančetović, J. (2012). Phenolic compounds, carotenoids, anthocyanins, and antioxidant capacity of colored maize (*Zea mays* L.) kernels. *J. Agric. Food Chem.* 60, 1224–1231. doi: 10.1021/jf204367z

Žofajova, A., Pšenáková, I., Havrlentová, M., and Piliarová, M. (2012). Accumulation of total anthocyanins in wheat grain. *Agriculture* 58, 50–56.

Conflict of Interest Statement: The authors declare that the research was conducted in the absence of any commercial or financial relationships that could be construed as a potential conflict of interest.

frontiers in Plant Science

ORIGINAL RESEARCH
published: 08 February 2016
doi: 10.3389/fpls.2016.00087

Detection of Diurnal Variation of Tomato Transcriptome through the Molecular Timetable Method in a Sunlight-Type Plant Factory

Takanobu Higashi[1], *Yusuke Tanigaki*[2], *Kotaro Takayama*[3], *Atsushi J. Nagano*[4, 5, 6], *Mie N. Honjo*[5] *and Hirokazu Fukuda*[2, 6*]

[1] *Graduate School of Life and Environmental Sciences, Osaka Prefecture University, Sakai, Japan,* [2] *Graduate School of Engineering, Osaka Prefecture University, Sakai, Japan,* [3] *Faculty of Agriculture, Ehime University, Matsuyama, Japan,* [4] *Faculty of Agriculture, Ryukoku University, Otsu, Japan,* [5] *Center for Ecological Research, Kyoto University, Otsu, Japan,* [6] *Precursory Research for Embryonic Science and Technology, Japan Science and Technology Agency, Kawaguchi, Japan*

OPEN ACCESS

Edited by:
Alejandro Isabel Luna Maldonado, Universidad Autónoma de Nuevo León, Mexico

Reviewed by:
Hao Peng, Washington State University, USA
Michael H. Walter, Leibniz Institute of Plant Biochemistry, Germany

****Correspondence:***
Hirokazu Fukuda
fukuda@me.osakafu-u.ac.jp

Specialty section:
This article was submitted to Crop Science and Horticulture, a section of the journal Frontiers in Plant Science

Received: *06 November 2015*
Accepted: *17 January 2016*
Published: *08 February 2016*

Citation:
Higashi T, Tanigaki Y, Takayama K, Nagano AJ, Honjo MN and Fukuda H (2016) Detection of Diurnal Variation of Tomato Transcriptome through the Molecular Timetable Method in a Sunlight-Type Plant Factory. Front. Plant Sci. 7:87. doi: 10.3389/fpls.2016.00087

The timing of measurement during plant growth is important because many genes are expressed periodically and orchestrate physiological events. Their periodicity is generated by environmental fluctuations as external factors and the circadian clock as the internal factor. The circadian clock orchestrates physiological events such as photosynthesis or flowering and it enables enhanced growth and herbivory resistance. These characteristics have possible applications for agriculture. In this study, we demonstrated the diurnal variation of the transcriptome in tomato (*Solanum lycopersicum*) leaves through molecular timetable method in a sunlight-type plant factory. Molecular timetable methods have been developed to detect periodic genes and estimate individual internal body time from these expression profiles in mammals. We sampled tomato leaves every 2 h for 2 days and acquired time-course transcriptome data by RNA-Seq. Many genes were expressed periodically and these expressions were stable across the 1st and 2nd days of measurement. We selected 143 time-indicating genes whose expression indicated periodically, and estimated internal time in the plant from these expression profiles. The estimated internal time was generally the same as the external environment time; however, there was a difference of more than 1 h between the two for some sampling points. Furthermore, the stress-responsive genes also showed weakly periodic expression, implying that they were usually expressed periodically, regulated by light–dark cycles as an external factor or the circadian clock as the internal factor, and could be particularly expressed when the plant experiences some specific stress under agricultural situations. This study suggests that circadian clock mediate the optimization for fluctuating environments in the field and it has possibilities to enhance resistibility to stress and floral induction by controlling circadian clock through light supplement and temperature control.

Keywords: circadian clocks, molecular timetable method, stress-responsive genes, plant factory, tomato, transcriptome

INTRODUCTION

Recently agricultural technologies have been rapidly developing, for example, application of information and communication technology, automation, and cultivation in closed systems with controlled temperature, humidity, and light conditions. In particular, plant factories are the more recent and highly regarded. These are of two types, closed-type, and sunlight-type. Both types have abilities of mass production, stable supply, and safe products. Furthermore, both types can control the cultivation environment artificially compared with open culture. Accordingly, there has been increased expectation of the ability to create cultivation control technologies for several cultivars according to various internal factors, which could be a key for high productivity or high quality. There is a real need for an exhaustive understanding of gene expression or metabolism to determine what these internal factors are, for example stress responses (Mittler and Blumwald, 2010). With this background, there have been great advances in technologies to analyze the genome, transcriptome, proteome, and metabolome. These analyses are increasingly user-friendly and their use in studies has increased rapidly. These molecular biological approaches have potential to solve several agricultural problems. In the case of fruit vegetables, there is a need to clarify some of the internal factors responsible for such physiological disorders as fruit cracking, blossom-end rot (Cuartero and Fernández-Muñoz, 1999; Guichard et al., 2001), and floral induction (Lifschitz et al., 2006; Corbesier et al., 2007). These are also critical issues for yield improvements.

Searching of these internal factors through biological statistical analysis has shown the usefulness of biological models (Takahashi et al., 2012; Guanter et al., 2014). However, because many genes are expressed periodically, diurnal variation must be considered when choosing a time for measurement (Harmer et al., 2000). These periodic expressions are generated by the day–night environment as the external factor and the circadian clock as the internal factor. Most living organisms have a circadian clock system and that of plants orchestrates physiological events such as gene expression, protein phosphorylation, chloroplast movement, stomatal opening, and flowering (Barak et al., 2000). The circadian clock system has three components (Farré and Weise, 2012): input pathways receive the external stimuli such as light and temperature fluctuations; the oscillator generates the endogenous circadian rhythms; and output pathways regulate general metabolism (e.g., of nitrogen and sugars). Endogenous circadian rhythms are generated by a number of genes; for example, *CCA1* (*CIRCADIAN CLOCK ASSOCIATED 1*), *TOC1* (*TIMING OF CAB EXPRESSION 1*), *LHY* (*LATE ELONGATED HYPOCOTYL*), and *PRRs* (*PSEUDO-RESPONSE REGULATORs*), which create feedback loops in each cell (Alabadí et al., 2001; Nakamichi et al., 2010, 2012; Haydon et al., 2011). These genes—including *PHYs*, which are the far-red light receptors; and *CRYs*, which are the blue light receptors (Pruneda-Paz and Kay, 2010)—receive signals from the input pathway and are expressed periodically with control of their own amplitude, period, and phase. It is well known that controlling the circadian rhythm enhances growth and herbivory resistance (Dodd et al., 2005; Goodspeed et al., 2012, 2013; Higashi et al., 2015), and the circadian clock can be controlled by external stimuli that change the light–dark cycle and by temperature fluctuation, because the circadian clock has characteristics of entrainment to the environment (Rensing and Ruoff, 2002; James et al., 2012; Fukuda et al., 2013). The circadian clock regulates hundreds of genes in Arabidopsis (*Arabidopsis thaliana*). Photosynthesis or phenylpropanoid biosynthesis genes are expressed periodically, with these genes peaking at different times such as subjective day and dawn under constant light (Harmer et al., 2000). These studies have shown that many genes generate circadian fluctuations without external stimuli. One recent study indicated that the day–night environment as the external oscillator and the circadian clock as the internal molecular oscillator activated transcription factors and mediated the circadian outputs (Haydon et al., 2011). The output adapts the circadian gene expression and entrains it to the external environment. This study suggests that the day–night environment as the external oscillator is a fast pathway and that the circadian clock as the internal molecular oscillator is a slow pathway for activation of transcriptome factors. Furthermore, hundreds of genes oscillate with circadian and circannual rhythms in rice (*Oryza sativa*) under field conditions (Nagano et al., 2012). They can generate comparatively stable rhythms under greatly variable conditions through the internal molecular oscillator. This indicates that in many cases we should consider the plant's internal rhythm and take care choosing a measurement time. Thus, very accurate analysis of diurnal variation will have application in development of biological models for yield improvements.

In this study, we tried to develop a highly accurate analysis of diurnal variation in tomato leaves in a sunlight-type plant factory as a basis for exhaustive study of the transcriptome and metabolome. We obtained time-course transcriptome data and used the molecular timetable method (Ueda et al., 2004) to analyze diurnal variation. Using these methods, we selected some periodic genes and estimated the phase of the circadian clock in tomato (internal time) from these periodic gene expression profiles.

MATERIALS AND METHODS

Plant Materials and Growing Systems

Experiments were carried out using tomato (*Solanum lycopersicum* cv. Taiankichijitsu, Nanto Seed Co. Ltd., Nara, Japan) cultivated in a sunlight-type plant factory (4480 cm [W] × 2300 cm [D] × 500 cm [H]) in the Faculty of Agriculture, Ehime University, Japan. Individual plants are usually cultivated for a year; in this experiment, tomato seedlings were grown by Berg Earth Co. Ltd. (Ehime, Japan) and transplanted into rockwool cubes (10 cm [W] × 10 cm [D] × 6.5 cm [H], Grodan Delta, GRODAN, Roermond, The Netherlands) in August 2013. Rockwool cubes were placed on rockwool slabs (100 cm [W] × 20 cm [D] × 7.5 cm [H], Grotop Expert, GRODAN) at four per slab. The four rockwool cubes were placed at 25 cm

intervals and watered using nutrient solution (Sonneveld, 1985). There were 20 slabs set in a line, with 28 lines per greenhouse. We sampled their leaves in January 2014. The light condition, relative humidity, and carbon dioxide concentration were ambient. Air temperature was maintained at 14°C during 18:00–8:00.

We sampled the fifth leaves every 2 h for 2 days, starting at 14:00 on 6 January 2014 and ending at 14:00 on 8 January 2014. We sliced leaf segments and stored them at 0°C with RNA-later solution (Qiagen, Valencia, CA, USA), an aqueous nontoxic tissue storage reagent that rapidly permeates tissue to stabilize and protect the integrity of RNA.

RNA-Seq Assay and Data Analysis

We isolated total RNA using an RNeasy Plant Mini Kit (Qiagen). RNA quality was checked using an Agilent 2100 Bioanalyzer (Agilent Technologies, Palo Alto, CA, USA) and RNA quantity control was performed using a Qubit® 2.0 Fluorometer (Life Technologies, Carlsbad, CA, USA). We prepared a RNA-Seq library (Wang et al., 2011; Nagano et al., 2015) and sequencing was performed by BGI (Yantian District, Shenzhen, China). Then we obtained the sequence read files using a HiSeq 2000 sequencer (single end, 50 bp; Illumina, San Diego, CA, USA). These sequence data are available in the DDBJ Sequenced Read Archive (http://trace.ddbj.nig.ac.jp/DRASearch) under the accession number DRA003529 and DRA 003530.

All reads of each sample were quality checked by FastQC and mapped using RSEM (RNA-Seq by Expectation Maximization) (Li and Dewey, 2011) with Bowtie2 software (Langmead and Salzberg, 2012) to the reference sequence. RSEM is a user-friendly software package able to accurately quantify transcript abundances. By these processes, we obtained the data of gene expression levels for each sample. Finally, we used the reads per kilobase per million mapped reads measure to normalize the gene expression for total read length and the number of sequencing reads. In this study, we calculated the average expression level of each sampling time for each genes. Then we cut off some genes whose average expression level is less than 5% of average expression level of whole genes and we identified 18,332 genes were significantly expressed.

Molecular Timetable Method

Molecular timetable methods have been developed for administration of medicine to animals, with the objective to detect internal body time from periodic gene expression profiles (Ueda et al., 2004). As an outline of this methods, they selected "time-indicating genes," which expressed periodically and represented internal body time from every 2 h for 2 days microarray data in the mouse liver. Then they developed gene expression profiles from time-indicating genes and estimated internal body time at each sampling time. To verify the performance of this methods, they calculated the sensitivity and specificity in the presence of different measurement noise and different number of time-indicating genes. We adapted this methods to use RNA-Seq data processing with cultivated plants.

First, we selected genes whose expression indicated periodicity and high amplitude from the time-course transcriptome data—these were time-indicating genes. To analyze periodicity, we prepared 1440 test cosine curves. These curves had different peaks (0–24 h) measured at increments of 1 min. We fitted test cosine curves to data from each time-course gene expression generated via RNA-Seq and calculated the correlation value (r) to identify the best-fitting cosine curve. The peak time of the best-fitting curve was estimated as the peak time for each gene. This estimated peak time defined as the molecular peak time. Thus, molecular peak time was estimated from a single gene, and all genes were estimated it individually. Then, to analyze amplitude, we calculated the average and standard deviation for every gene expression level. The amplitude value (a) was calculated as the standard deviation divided by the average of gene expression level.

Second, we plotted expression profiles of time-indicating genes. The number of time-indicating genes was determined by the cut-off values of r and a. We normalized the expression level of each time-indicating gene using its average and standard deviation. Normalized expression level was defined as the value of expression level minus average expression level, divided by the standard deviation. We then plotted expression profiles composed of the molecular peak time and normalized expression level for every sampling time. The horizontal axis indicated the molecular peak time and the vertical axis indicated normalized expression level.

Finally, the internal time was estimated by the plotted expression profile. We prepared 1440 test cosine curves with 1-min differences from each other and fitted them to the expression profiles. We identified the best-fitting cosine curve, and its peak time indicated the estimated internal time. Thus, the internal time was estimated from a number of periodic genes.

In this study, we selected 143 time-indicating genes by setting the cut-off values of $r = 0.915$ and $a = 0.15$ in whole genes and 150 time-indicating genes by setting the cut-off values of $r = 0.635$ and $a = 0.15$ in stress-responsive genes. In the previous study, they indicated that 150 time-indicating genes with 100% measurement noise could estimate internal time with high accuracy. Table S1 shows the measurement noise with 143 time-indicating genes in whole genes and 150 time-indicating genes in stress-responsive genes for each sampling time (see Supplementary Material). We calculated the standard deviation of the difference between a real and an estimated expression of all time-indicating genes as the measurement noise. Each measurement noise represent less than 100%. Thus, 143 and 150 time-indicating genes are enough to estimate the internal time with high accuracy.

Mapman Analysis

We used MapMan to categorize stress-responsive genes in tomato (Thimm et al., 2004). MapMan BINs were generated by Mercator (http://mapman.gabipd.org/web/guest/app/mercator) based on TAIR10 in Arabidopsis. MapMan software can be downloaded from http://mapman.gabipd.org/web/guest/mapman.

RESULTS

Environmental Conditions in a Sunlight-Type Plant Factory

We sampled tomato leaves every 2 h during 6–8 January 2014 in a sunlight-type plant factory in the Faculty of Agriculture, Ehime University, Japan (Takayama et al., 2012). Because it was winter during the experiments, the air temperature, relative humidity, and illuminance were comparatively low and day–night cycle had short days (day of 10 h and night of 14 h) (**Figure 1A**). As it rained on 8 January, this caused decreases in air temperature and illuminance, and increased relative humidity. Air temperature was relatively stable over the 1st and 2nd days of the experiment (**Figure 1B**); in contrast, relative humidity, and illuminance were relatively unstable on each day (**Figures 1C,D**). These results show that relative humidity and illuminance were strongly influenced by the rainy day.

Selection of Time-Indicating Genes and Development of these Expression Profiles

Then we analyzed the diurnal oscillation in gene expressions using the molecular timetable method. To select time-indicating genes that were definitely expressed periodically, we calculated the correlation value (r) which indicates periodicity, and amplitude value (a) for 18,332 genes (see Materials and Methods). The histograms showed that neither r nor a values were normally distributed (**Figures 2A,B**) and more than half of all genes had $r < 0.5$. About 5% of all genes exhibited clear periodic expression. In contrast, the histogram of a values showed that a values were distributed around 0.5 and spread widely around high value. About 70% of all genes had a

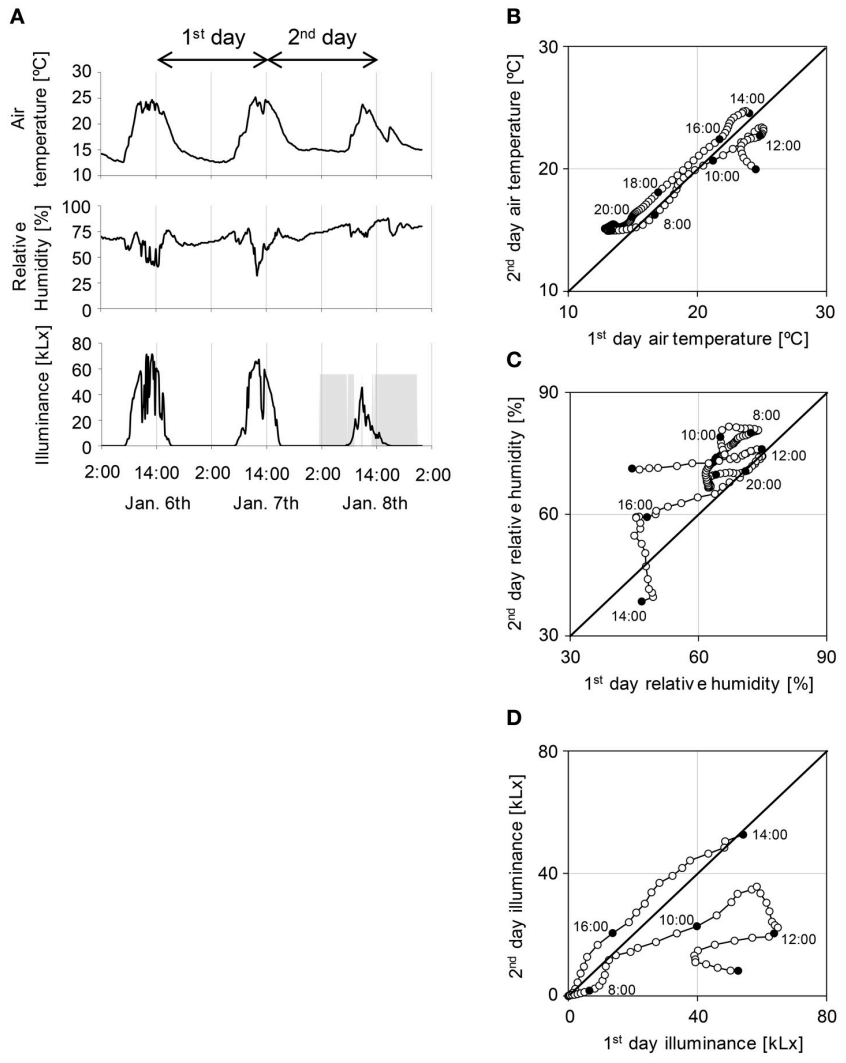

FIGURE 1 | Environmental conditions in a sunlight-type plant factory in Ehime University (A) and comparison of the 1st with the 2nd day for each environmental condition (B–D). (A) Air temperature, relative humidity, and illuminance in a sunlight-type plant factory. Gray area of illuminance indicates precipitation. **(B–D)** Open circles indicate each values for every 10 min and filled circles indicate the sampling point. Sampling started at 14:00.

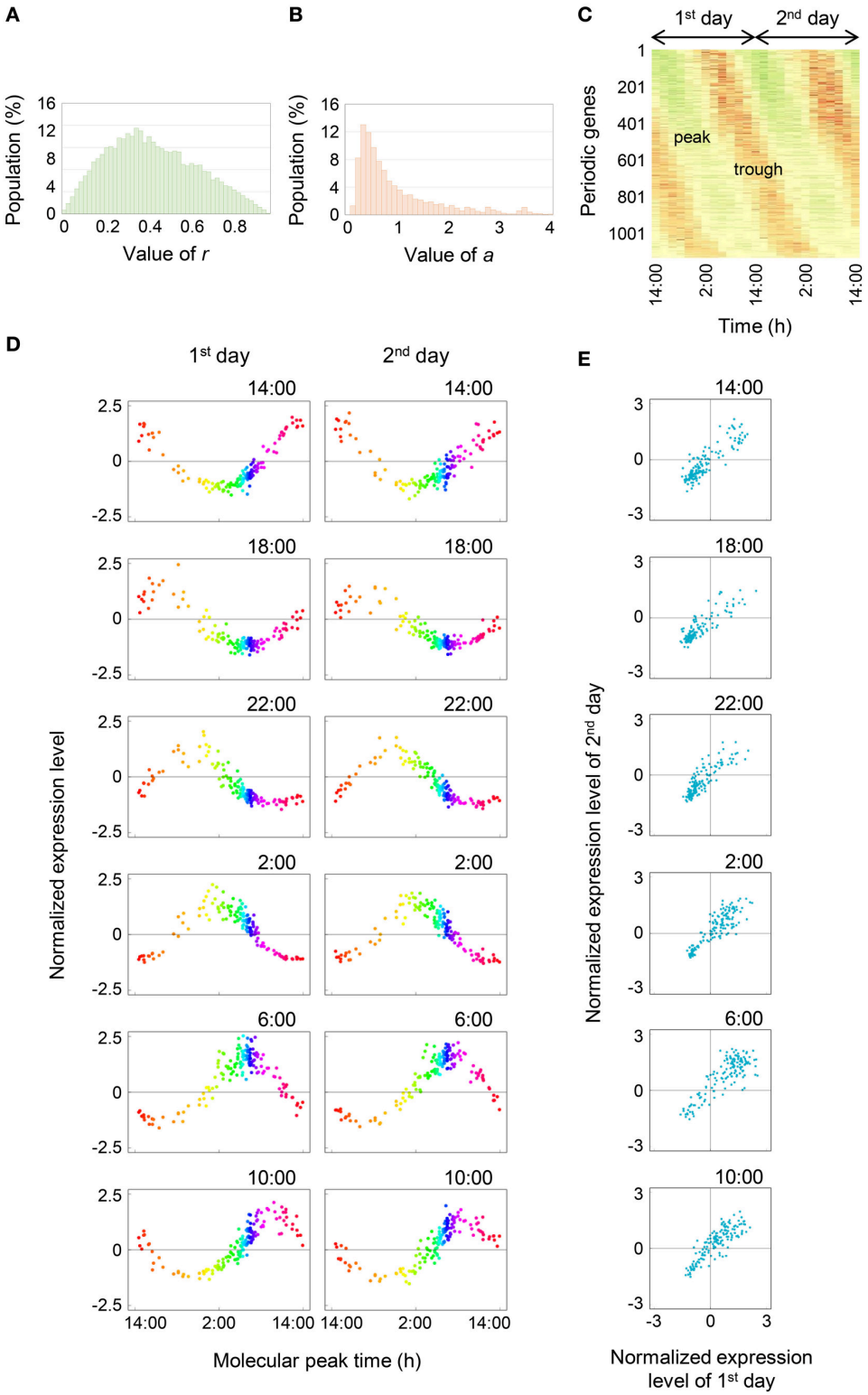

FIGURE 2 | Comprehensive analysis of diurnal oscillation in gene expressions. (A,B) Histograms of the *r* and *a* values, respectively. **(C)** Oscillation behavior of time-indicating genes. Green area indicates the peak and red area indicates the trough. **(D)** Expression profiles of 143 time-indicating genes for the 1st and 2nd days. The time at the top right of the plot area indicates the sampling time. The range from orange to purple represents night-time and other colored areas represent day-time. **(E)** Correlations between normalized expression levels for the 1st and 2nd days. The time at the top right of the plot area indicates the sampling time.

values within 0–1. The heat map of 1132 periodic genes, which indicated periodicity and high amplitude through setting of cut-off values of $r = 0.80$ and $a = 0.15$, clearly showed a diagonal striped pattern, indicating that we could correctly select the periodic genes (**Figure 2C**). We showed the expression profiles of 143 time-indicating genes through setting the cut-off values of $r = 0.915$ and $a = 0.15$ for each time point on the 1st and 2nd days (**Figure 2D**). The vertical axis represents the normalized expression level and the horizontal axis represents the molecular peak time. Thus, **Figure 2D** shows the overall behavior of 143 time-indicating genes at each sampling time. Genes related to photosynthesis, translocation of sugar and photoreceptor were pooled in 143 time-indicating genes and the timing of their expression was consistent with their physiological function (Table S2). As time proceeded, the peak position shifted at regular intervals. Furthermore, the expression profiles on the 1st and 2nd days were similar in most respects. This indicates that these 143 genes showed stable periodic expression at daily intervals under fluctuating field conditions. We plotted normalized expression levels for the 1st and 2nd days to verify stability (**Figure 2E**). All genes were plotted in a linear fashion despite the 2nd day being rainy. The determination coefficient (R^2) between them was high ($R^2 \approx 0.7$; **Figure 3B**). Thus, this supports the claim that time-indicating genes were stably expressed under fluctuating field conditions.

Validation of the Internal Time Estimation

We estimated the internal time from the expression profiles of 143 time-indicating genes for each time and calculated the difference between time and estimated internal time (**Figure 3A**). Internal time showed much the same time as the sampling time; however, there was a difference of more than 1 h between the two for some sampling points. As an additional indication of stability, we showed the transition of R^2 between normalized expression levels of the 1st and 2nd days (**Figure 3B**). There was a high correlation indicated by high R^2 values (>0.65) at all times.

Diurnal Gene Expression Profiles of Stress-Responsive Genes

We focused on the stress-responsive genes, which are important to increase sweetness in tomato fruit and to defend against disease. Furthermore, stress-responsive genes are possible markers of the internal factors because these genes show sensitivity to external stimuli and affect several physiological events (Wang et al., 2003; Chinnusamy et al., 2005; Umezawa et al., 2006; Cattivelli et al., 2008). We extracted 1048 stress-responsive genes from all genes using the MapMan and analyzed them by the molecular timetable method. The heat map of the 1048 stress-responsive genes indicated that they were expressed periodically under fluctuating field conditions without the addition of external stress such as heat or drought during the experiment (**Figure 4A**). Then we separated the stress-responsive genes into three types—day-time (434 genes), night-time (786 genes), and low-expression (47 genes)—according to the molecular peak times, and categorized them using the MapMan (**Figure 4B**). Day-time was 7:00–17:00 (10 h) and night-time was 17:00–7:00 (14 h). More than half of the stress-responsive genes had expression peaks at night in tomato leaves. Genes related to cold, heat, and drought stress had expression peaks equally during day and night. Then we showed the expression profiles of 150 time-indicating genes, which indicated periodicity and high amplitude, through setting the cut-off values of $r = 0.635$ and $a = 0.15$ in the stress-responsive genes (**Figure 4C**). These expression profiles were clearly noisy compared with expression profiles of the 143 most-periodic time-indicating genes (**Figure 2D**); however, there was certainly periodicity without stress being applied.

DISCUSSION

At least 1000 genes, included some clock-related genes (Presentation S1), indicated periodic expression clearly in tomato leaves under agricultural situations in winter. In addition, 143 time-indicating genes indicated stable periodic expression even though the alterations in the environment had a possibility to affect such aspects of plant physiology as photosynthesis and sucrose metabolism (Feugier and Satake, 2013; McCormick and Kruger, 2015), and so the expression of relevant genes would likely be influenced by external stimuli (Nagano et al., 2012). This mediation system seemed to be generated by the

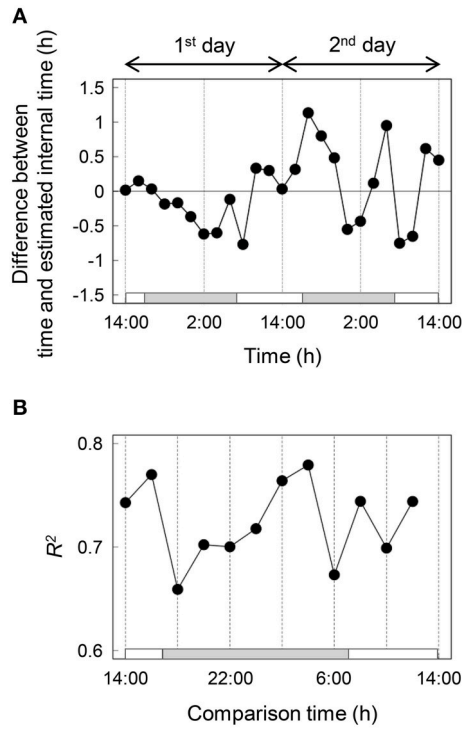

FIGURE 3 | Validation of the internal time estimation (A) and transition of the determination coefficient between normalized expression levels for the 1st and 2nd days (B). White and gray bars represent light and dark, respectively.

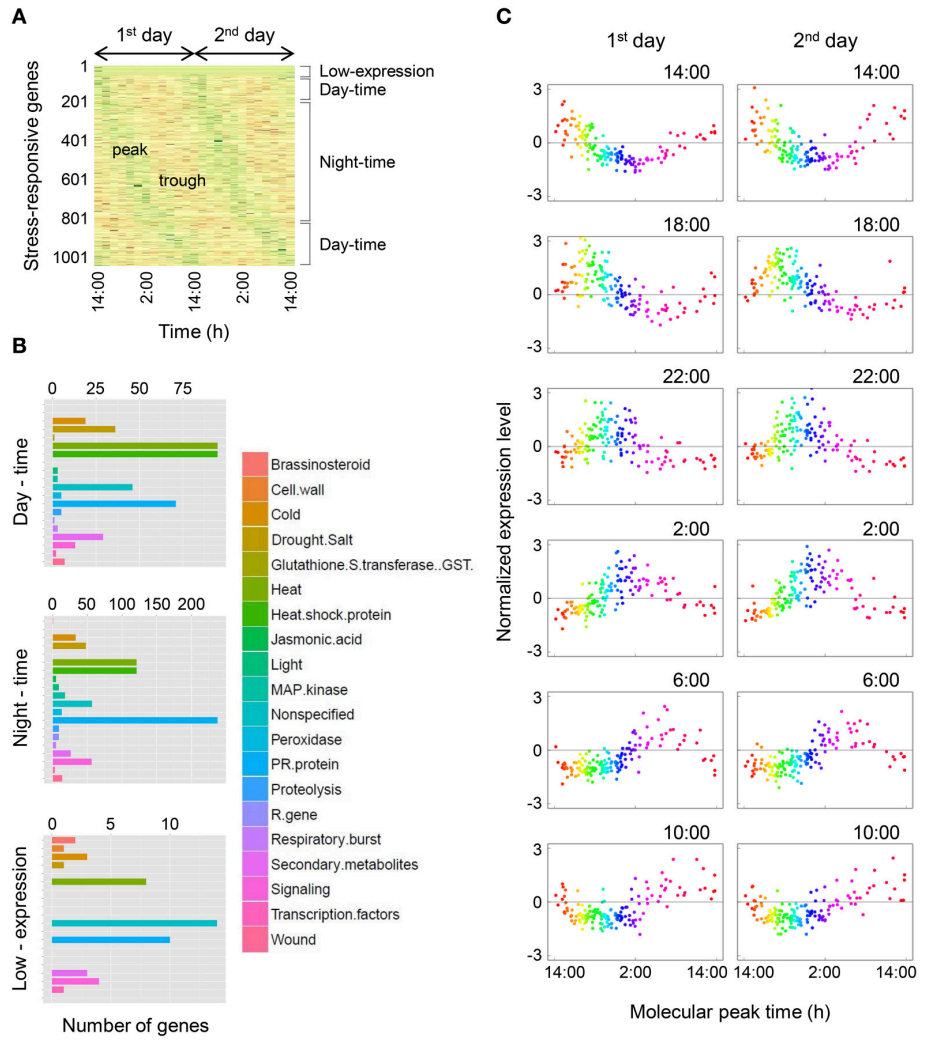

FIGURE 4 | Diurnal gene expression profiles of stress-responsive genes. (A) Oscillation behavior of stress-responsive genes. Green areas indicate the peak and red areas indicate the trough. **(B)** Categorization of stress-responsive genes using MapMan. Day-time was 7:00–17:00 (10 h) and night-time was 17:00–7:00 (14 h). **(C)** Expression profiles of 150 time-indicating genes for the 1st and 2nd days in stress-responsive genes. The time at the top right of the plot area indicates the sampling time. The range from orange to purple represents night-time and other colored areas represent day-time.

internal oscillator of the circadian clock. Although 143 time-indicating genes indicated stable periodic expression, some estimated internal time showed little difference between the sampling times. It suggested that the phase of periodic genes, or of genes downstream, had their circadian clock precisely regulated to adjust to a non-constant environment and so kept their periodicity (Presentation S1). Thus, the periodicity of these genes was sufficiently stable, although there were some differences in expression level. Circadian stability was reported in rice leaves under fluctuating field conditions (Matsuzaki et al., 2015). In the case of rice, the difference between sampling times and estimated internal times was $\leq$ 22 min and gene expression was not affected by external factors. These differences between tomato and rice may be due to species differences. Circadian clocks exist in almost all living organisms and characteristics of plant circadian rhythms have been studied in Arabidopsis (Nakamichi et al., 2004); however, characteristics of circadian rhythm in *Lactuca sativa* differed from Arabidopsis (Higashi et al., 2014). Furthermore, tomato leaves may have an unusual circadian clock system because they develop a detrimental leaf injury when grown under constant light (Cushman and Tibbitts, 1998; Velez-Ramirez et al., 2011). One characteristic of circadian clocks is that they generate circadian rhythm under continuous conditions. This suggest that an unusual circadian clock system in tomato affected expression of the clock genes or downstream genes and resulted in the difference of estimated internal time. Recently, the inclusive CCA1 target genes in Arabidopsis were reported (Nagel et al., 2015). Then we located orthologs of the time-indicating genes using the KEGG database and identified how many orthologs of the CCA1 target genes were present

in the time-indicating gene pool of tomato. We identified 23 CCA1 target genes among the time-indicating genes, accounting for about 16% of 143 time-indicating genes. This suggests that a number of time-indicating genes were expressed periodically depending on the day–night environment or influence of other clock genes, at least in this experiment. This low proportion of CCA1 target genes to time-indicating genes in tomato might affect the difference in estimated internal time. On the other hand, to detect the accurate internal time is important because plant circadian rhythms can be controlled by external stimuli (Barak et al., 2000; Covington et al., 2008; Fukuda et al., 2013). Thus, the timing of environmental control such as light supplement and temperature control affect the circadian rhythms and therefore the dimension of physiological events. It has possibilities to enhance growth and floral induction.

Stress-responsive genes were also indicated for periodic expression. Thus the stress-responsive genes were normally expressed periodically as regulated by light–dark cycle as the external factor or the circadian clock as the internal factor, and they could be specifically expressed when some stresses were experienced by the plant. Similar events were also reported for soybean, barley, and Arabidopsis (Covington et al., 2008; Habte et al., 2014; Marcolino-Gomes et al., 2014). It suggests that circadian regulation of stress-responsive genes expression may be widely-conserved systems and it provides some advantage that plant survive under fluctuating field conditions (Goodspeed et al., 2012, 2013; Grundy et al., 2015). Furthermore, this result suggests that stress-responsive genes may be competent markers for agriculture because they are simple to apply although normally expressed periodically and especially transiently.

In conclusion, we demonstrated that many genes were expressed periodically and that gene expression was stable in a sunlight-type plant factory. Furthermore, internal time could be estimated from time-course gene expression data in tomato leaves through molecular timetable method. The results also showed that stress-responsive genes were expressed periodically under non-stressed conditions. This study suggests that circadian clock mediate the optimization for fluctuating environments and environmental control tailored to internal time may enhance resistibility to stress and floral induction, eventually the yieldability.

AUTHOR CONTRIBUTIONS

HF and TH designed the experiments. YT did the MapMan analysis and constructed the heat map. KT supported the sampling in a sunlight-type plant factory. AN and MH prepared a RNA-Seq library. TH performed RNA-Seq data analysis and the molecular timetable method. TH and HF wrote the manuscript. All authors discussed the results and implications and commented on the manuscript.

ACKNOWLEDGMENTS

We are grateful to Dr. Noriko Takahashi for the plant cultivation, Professor Hiroshi Kudoh for RNA-Seq and Professor Koh Aoki for discussion. The present study was supported by the Joint Usage/Research Program of the Center for Ecological Research, Kyoto University. This study was partially supported by Grants-in-Aid for JSPS Fellows (No. 15J12133 to TH), Grants-in-Aid for Scientific Research (No. 25712029 and 25119721 to HF), PRESTO JST, and the Canon Foundation.

SUPPLEMENTARY MATERIAL

The Supplementary Material for this article can be found online at: http://journal.frontiersin.org/article/10.3389/fpls.2016.00087

REFERENCES

Alabadí, D., Oyama, T., Yanovsky, M. J., Harmon, F. G., Más, P., and Kay, S. A. (2001). Reciprocal regulation between TOC1 and LHY/CCA1 within the Arabidopsis circadian clock. *Science* 293, 880–883. doi: 10.1126/science.1061320

Barak, S., Tobin, E. M., Andronis, C., Sugano, S., and Green, R. M. (2000). All in good time: the Arabidopsis circadian clock. *Trends Plant Sci.* 5, 517–522. doi: 10.1016/S1360-1385(00)01785-4

Cattivelli, L., Rizza, F., Badeck, F. W., Mazzucotelli, E., Mastrangelo, A. M., Francia, E., et al. (2008). Drought tolerance improvement in crop plants: an integrated view from breeding to genomics. *Field Crops Res.* 105, 1–14. doi: 10.1016/j.fcr.2007.07.004

Chinnusamy, V., Jagendorf, A., and Zhu, J. K. (2005). Understanding and improving salt tolerance in plants. *Crop Sci.* 45, 437–448. doi: 10.2135/cropsci2005.0437

Corbesier, L., Vincent, C., Jang, S., Fornara, F., Fan, Q., Searle, I., et al. (2007). FT protein movement contributes to long-distance signaling in floral induction of Arabidopsis. *Science* 316, 1030–1033. doi: 10.1126/science.1141752

Covington, M. F., Maloof, J. N., Straume, M., Kay, S. A., and Harmer, S. L. (2008). Global transcriptome analysis reveals circadian regulation of key pathways in plant growth and development. *Genome Biol.* 9:R130. doi: 10.1186/gb-2008-9-8-r130

Cuartero, J., and Fernández-Muñoz, R. (1999). Tomato and salinity. *Sci. Hortic.* 78, 83–125.

Cushman, K. E., and Tibbitts, T. W. (1998). The role of ethylene in the development of constant-light injury of potato and tomato. *J. Am. Soc. Hort. Sci.* 123, 239–245.

Dodd, A. N., Salathia, N., Hall, A., Kévei, E., Tóth, R., Nagy, F., et al. (2005). Plant circadian clocks increase photosynthesis, growth, survival, and competitive advantage. *Science* 309, 630–633. doi: 10.1126/science.1115581

Farré, E. M., and Weise, S. E. (2012). The interactions between the circadian clock and primary metabolism. *Plant Biol.* 15, 293–300. doi: 10.1016/j.pbi.2012.01.013

Feugier, F. G., and Satake, A. (2013). Dynamical feedback between circadian clock and sucrose availability explains adaptive response of starch metabolism to various photoperiods. *Front. Plant Sci.* 3:305. doi: 10.3389/fpls.2012.00305

Fukuda, H., Murase, H., and Tokuda, I. T. (2013). Controlling circadian rhythms by dark-pulse perturbations in *Arabidopsis thaliana*. *Sci. Rep.* 3:1533. doi: 10.1038/srep01533

Goodspeed, D., Chehab, E. W., Min-Venditti, A., Braam, J., and Covington, M. F. (2012). Arabidopsis synchronizes jasmonate-mediated defense with insect circadian behavior. *Proc. Natl. Acad. Sci. U.S.A.* 109, 4674–4677. doi: 10.1073/pnas.1116368109

Goodspeed, D., Liu, J. D., Chehab, E. W., Sheng, Z., Francisco, M., Kliebenstein, D. J., et al. (2013). Postharvest circadian entrainment enhances crop

pest resistance and phytochemical cycling. *Curr. Biol.* 23, 1235–1241. doi: 10.1016/j.cub.2013.05.034

Grundy, J., Stoker, C., and Carré, I. A. (2015). Circadian regulation of abiotic stress tolerance in plants. *Front. Plant Sci.* 6:648. doi: 10.3389/fpls.2015.00648

Guanter, L., Zhang, Y., Jung, M., Joiner, J., Voigt, M., Berry, J. A., et al. (2014). Global and time-resolved monitoring of crop photosynthesis with chlorophyll fluorescence. *Proc. Natl. Acad. Sci. U.S.A.* 111, E1327–E1333. doi: 10.1073/pnas.1320008111

Guichard, S., Bertin, N., Leonardi, C., and Gary, C. (2001). Tomato fruit quality in relation to water and carbon fluxes. *Agronomie* 21, 385–392. doi: 10.1051/agro:2001131

Habte, E., Müller, L. M., Shtaya, M., Davis, S. J., and VonKorff, M. (2014). Osmotic stress at the barley root affects expression of circadian clock genes in the shoot. *Plant Cell Environ.* 37, 1321–1327. doi: 10.1111/pce.12242

Harmer, S. L., Hogenesch, J. B., Strume, M., Chang, H. S., Han, B., Zhu, T., et al. (2000). Orchestrated transcription of key pathways in Arabidopsis by the circadian clock. *Science* 290, 2110–2113. doi: 10.1126/science.290.5499.2110

Haydon, M. J., Bell, L. J., and Webb, A. A. R. (2011). Interactions between plant circadian clocks and solute transport. *J. Exp. Bot.* 62, 2333–2348. doi: 10.1093/jxb/err040

Higashi, T., Kamitamari, A., Okamura, N., Ukai, K., Okamura, K., Tezuka, T., et al. (2014). Characterization of circadian rhythms through a bioluminescence reporter assay in *Lactuca sativa* L. *Environ. Control Biol.* 52, 21–27. doi: 10.2525/ecb.52.21

Higashi, T., Nishikawa, S., Okamura, N., and Fukuda, H. (2015). Evaluation of growth under Non-24 h period lighting conditions in *Lactuca sativa* L. *Environ. Control Biol.* 53, 7–12. doi: 10.2525/ecb.53.7

James, A. B., Syed, N. H., Bordage, S., Marshall, J., Nimmo, G. A., Jenkins, G. I., et al. (2012). Alternative splicing mediates responses of the Arabidopsis circadian clock to temperature changes. *Plant Cell* 24, 961–981. doi: 10.1105/tpc.111.093948

Langmead, B., and Salzberg, S. L. (2012). Fast gapped-read alignment with Bowtie2. *Nat. Methods* 9, 357–359. doi: 10.1038/nmeth.1923

Li, B., and Dewey, C. N. (2011). RSEM: accurate transcript quantification from RNA-Seq data with or without a reference genome. *BMC Bioinformatics* 12:323. doi: 10.1186/1471-2105-12-323

Lifschitz, E., Eviatar, T., Rozman, A., Shalit, A., Goldshmidt, A., Amsellem, Z., et al. (2006). The tomato FT ortholog triggers systemic signals that regulate growth and flowering and substitute for diverse environmental stimuli. *Proc. Natl. Acad. Sci. U.S.A.* 103, 6398–6403. doi: 10.1073/pnas.0601620103

Marcolino-Gomes, J., Rodrigues, F. A., Fuganti-Pagliarini, R., Bendix, C., Nakayama, T. J., Celaya, B., et al. (2014). Diurnal oscillations of soybean circadian clock and drought responsive genes. *PLoS ONE* 9:e86402. doi: 10.1371/journal.pone.0086402

Matsuzaki, J., Kawahara, Y., and Izawa, T. (2015). Punctual transcriptional regulation by the rice circadian clock under fluctuating conditions. *Plant Cell* 27, 633–648. doi: 10.1105/tpc.114.135582

McCormick, A. J., and Kruger, N. J. (2015). Lack of fructose 2, 6-bisphosphate compromises photosynthesis and growth in Arabidopsis in fluctuating environments. *Plant J.* 81, 670–683. doi: 10.1111/tpj.12765

Mittler, R., and Blumwald, E. (2010). Genetic engineering for modern agriculture: challenges and perspectives. *Annu. Rev. Plant Biol.* 61, 443–462. doi: 10.1146/annurev-arplant-042809-112116

Nagano, A. J., Honjo, M. N., Mihara, M., Sato, M., and Kudoh, H. (2015). Detection of plant viruses in natural environments by using RNA-Seq. *Methods Mol. Biol.* 1236, 89–98. doi: 10.1007/978-1-4939-1743-3_8

Nagano, A. J., Sato, Y., Mihara, M., Antonio, B. A., Motoyama, R., Itoh, H., et al. (2012). Deciphering and prediction of transcriptome dynamics under fluctuating field conditions. *Cell* 151, 1358–1369. doi: 10.1016/j.cell.2012.10.048

Nagel, D. H., Doherty, C. J., Pruneda-Paz, J. L., Schmitz, R. J., Ecker, J. R., and Kay, S. A. (2015). Genome-wide identification of CCA1 targets uncovers an expanded clock network in Arabidopsis. *Proc. Natl. Acad. Sci. U.S.A.* 112, E4802–E4810. doi: 10.1073/pnas.1513609112

Nakamichi, N., Ito, S., Oyama, T., Yamashino, T., Kondo, T., and Mizuno, T. (2004). Characterization of plant circadian rhythms by employing Arabidopsis cultured cells with bioluminescence reporters. *Plant Cell Physiol.* 45, 57–67. doi: 10.1093/pcp/pch003

Nakamichi, N., Kiba, T., Henriques, R., Mizuno, T., Chua, N. H., and Sakakibara, H. (2010). PSEUDO-RESPONSE REGULATORS 9, 7, and 5 are transcriptional repressors in the Arabidopsis circadian clock. *Plant Cell* 22, 594–605. doi: 10.1105/tpc.109.072892

Nakamichi, N., Kiba, T., Kamioka, M., Suzuki, T., Yamashino, T., Higashiyama, T., et al. (2012). Transcriptional repressor PRR5 directly regulates clock-output pathways. *Proc. Natl. Acad. Sci. U.S.A.* 109, 17123–17128. doi: 10.1073/pnas.1205156109

Pruneda-Paz, J. L., and Kay, S. A. (2010). An expanding universe of circadian networks in higher plants. *Trends Plant Sci.* 15, 259–265. doi: 10.1016/j.tplants.2010.03.003

Rensing, L., and Ruoff, P. (2002). Temperature effect on entrainment, phase shifting, and amplitude of circadian clocks and its molecular bases. *Chronobiol. Int.* 19, 807–864. doi: 10.1081/CBI-120014569

Sonneveld, C. (1985). *A Method for Calculating the Composition of Nutrient Solutions for Soilless Cultures*, *2nd Edn*. Naaldwijk: Glasshouse Crops.

Takahashi, T., Ishigami, Y., Goto, E., Niibori, K., and Goto, K. (2012). Modeling the growth and yield of tomatoes cultivated with a low node-order pinching system at high plant density. *Environ. Control Biol.* 50, 53–61. doi: 10.2525/ecb.50.53

Takayama, K., Miguchi, Y., Manabe, Y., Takahashi, N., and Nishina, H. (2012). Analysis of ΦPS II and NPQ during the slow phase of the chlorophyll fluorescence induction phenomenon in tomato leaves. *Environ. Control Biol.* 50, 181–187. doi: 10.2525/ecb.50.181

Thimm, O., Bläsing, O., Gibon, Y., Nagel, A., Meyer, S., Krüger, P., et al. (2004). MAPMAN: a user-driven tool to display genomics data sets onto diagrams of metabolic pathways and other biological processes. *Plant J.* 37, 914–939. doi: 10.1111/j.1365-313X.2004.02016.x

Ueda, H. R., Chen, W., Minami, Y., Honma, S., Honma, K., Iino, M., et al. (2004). Molecular-timetable methods for detection of body time and rhythm disorders from single-time-point genome-wide expression profiles. *Proc. Natl. Acad. Sci. U.S.A.* 101, 11227–11232. doi: 10.1073/pnas.0401882101

Umezawa, T., Fujita, M., Fujita, Y., Yamaguchi-Shinozaki, K., and Shinozaki, K. (2006). Engineering drought tolerance in plants: discovering and tailoring genes to unlock the future. *Curr. Opin. Biotechnol.* 17, 113–122. doi: 10.1016/j.copbio.2006.02.002

Velez-Ramirez, A. I., Ieperen, W. V., Vreugdenhil, D., and Millenaar, F. F. (2011). Plants under continuous light. *Trends Plant Sci.* 16, 310–318. doi: 10.1016/j.tplants.2011.02.003

Wang, L., Si, Y., Dedow, L. K., Shao, Y., Liu, P., and Brutnell, T. P. (2011). A low-cost library construction protocol and data analysis pipeline for illumina-based strand-specific multiplex RNA-Seq. *PLoS ONE* 6:e26426. doi: 10.1371/journal.pone.0026426

Wang, W., Vinocur, B., and Altman, A. (2003). Plant responses to drought, salinity and extreme temperatures: towards genetic engineering for stress tolerance. *Planta* 218, 1–14. doi: 10.1007/s00425-003-1105-5

Conflict of Interest Statement: The authors declare that the research was conducted in the absence of any commercial or financial relationships that could be construed as a potential conflict of interest.

frontiers in Plant Science

ORIGINAL RESEARCH
published: 27 June 2016
doi: 10.3389/fpls.2016.00908

Genome-Wide Sequence Variation Identification and Floral-Associated Trait Comparisons Based on the Re-sequencing of the 'Nagafu No. 2' and 'Qinguan' Varieties of Apple (*Malus domestica* Borkh.)

Libo Xing†, Dong Zhang†, Xiaomin Song†, Kai Weng, Yawen Shen, Youmei Li, Caiping Zhao, Juanjuan Ma, Na An and Mingyu Han*

College of Horticulture, Northwest Agriculture and Forestry University, Yangling, China

OPEN ACCESS

Edited by:
Juan Antonio Vidales, Universidad Autónoma de Nuevo León, Mexico

Reviewed by:
Thomas Dandekar, University of Würzburg, Germany
Andrea Mazzucato, University of Tuscia, Italy

***Correspondence:**
Mingyu Han
hanmy@nwsuaf.edu.cn

†Co-first authors

Specialty section:
This article was submitted to Crop Science and Horticulture, a section of the journal Frontiers in Plant Science

Received: *07 December 2015*
Accepted: *08 June 2016*
Published: *27 June 2016*

Citation:
Xing L, Zhang D, Song X, Weng K, Shen Y, Li Y, Zhao C, Ma J, An N and Han M (2016) Genome-Wide Sequence Variation Identification and Floral-Associated Trait Comparisons Based on the Re-sequencing of the 'Nagafu No. 2' and 'Qinguan' Varieties of Apple (Malus domestica Borkh.). Front. Plant Sci. 7:908. doi: 10.3389/fpls.2016.00908

Apple (*Malus domestica* Borkh.) is a commercially important fruit worldwide. Detailed information on genomic DNA polymorphisms, which are important for understanding phenotypic traits, is lacking for the apple. We re-sequenced two elite apple varieties, 'Nagafu No. 2' and 'Qinguan,' which have different characteristics. We identified many genomic variations, including 2,771,129 single nucleotide polymorphisms (SNPs), 82,663 structural variations (SVs), and 1,572,803 insertion/deletions (INDELs) in 'Nagafu No. 2' and 2,262,888 SNPs, 63,764 SVs, and 1,294,060 INDELs in 'Qinguan.' The 'SNP,' 'INDEL,' and 'SV' distributions were non-random, with variation-rich or -poor regions throughout the genomes. In 'Nagafu No. 2' and 'Qinguan' there were 171,520 and 147,090 non-synonymous SNPs spanning 23,111 and 21,400 genes, respectively; 3,963 and 3,196 SVs in 3,431 and 2,815 genes, respectively; and 1,834 and 1,451 INDELs in 1,681 and 1,345 genes, respectively. Genetic linkage maps of 190 flowering genes associated with multiple flowering pathways in 'Nagafu No. 2,' 'Qinguan,' and 'Golden Delicious,' identified complex regulatory mechanisms involved in floral induction, flower bud formation, and flowering characteristics, which might reflect the genetic variation of the flowering genes. Expression profiling of key flowering genes in buds and leaves suggested that the photoperiod and autonomous flowering pathways are major contributors to the different floral-associated traits between 'Nagafu No. 2' and 'Qinguan.' The genome variation data provided a foundation for the further exploration of apple diversity and gene–phenotype relationships, and for future research on molecular breeding to improve apple and related species.

Keywords: genome variation, INDELs, re-sequencing, flowering genes, apple (*Malus domestica* Borkh.)

INTRODUCTION

The domesticated apple (*Malus domestica* Borkh.) is one of the most commercially important fruit worldwide, with over 60 million tons produced each year (Food and Agriculture Organization of the United Nations, 2013[1]). There are more than 10,000 documented cultivars of apples (Hummer and Janick, 2009), resulting in a range of desired characteristics. China is the leading apple-producing country, with a planting area of 3.1 million hectares and production of 33 million tons annually[1]. 'Nagafu No. 2,' which accounts for more than 65% of the total cultivated area, is the dominant cultivar in China. However, 'Nagafu No. 2' apples have difficulty forming flower buds and have an alternate bearing problem, which results in unstable and low fruit production. 'Qinguan' is an elite variety bred in China with strong disease resistance, easy flowering, high yield, and easy management. 'Nagafu No. 2' and 'Qinguan' are important materials for apple breeding and genetic research in China because of their different flowering and drought resistance characteristics. However, the genetic basis underlying these differences and the associated genomic information for these two varieties are poorly understood.

Genomic sequences of perennial fruit crops, such as grape (Jaillon et al., 2007), apple (Velasco et al., 2010), peach (Verde et al., 2013), pear (Wu et al., 2013), and sweet orange (Xu et al., 2013), have been determined over the past 10 years. The first physical map of the apple genome was constructed from bacterial artificial chromosome clones by (Han et al., 2007) and covered ∼927 Mb. Numerous expressed sequence tags (ESTs) were collected in apple from libraries covering a variety of genotypes and tissues, under different experimental conditions (Gasic et al., 2009)[2], and have allowed the efficient development of DNA-based markers (Park et al., 2006), gene discovery (Chagné et al., 2008), and comparative genomics (Gasic et al., 2009). However, compared with other model plants, the study of the apple genome is still in its infancy.

Next-generation sequencing (NGS) technologies have enabled the identification of genome-wide patterns of genetic variation in perennial fruit crops in a rapid, efficient, relatively low cost, and high-throughput manner (Chagné et al., 2012; Montanari et al., 2013; Cao et al., 2014). Genetic variation comprises structural alterations and sequence variations. Sequence variations are categorized into single nucleotide polymorphisms (SNPs), short sequence insertions and deletions (INDELs), microsatellites (simple sequence repeats), and transposable elements (Zheng et al., 2011). To date, whole-genome INDELs and SNPs have been developed for evolutionary and functional studies in many plants, including apple (Velasco et al., 2010), pear (Montanari et al., 2013), and peach (Cao et al., 2014). NGS was used to detect SNPs covering the apple genome and the Illumina InfiniumH II system was developed as a medium- to high-throughput SNP screening tool to identify allelic variation in apple (Chagné et al., 2012). Additionally, NGS was used to detect SNPs in the pear genome and a medium-throughput SNP assay was designed (Montanari et al., 2013). Incorporation of the new pear SNPs into the apple 8 K array enabled the study of SNP transferability not only within the genus *Pyrus*, but also between the genera *Malus* and *Pyrus*. In addition, 10 wild and 74 cultivated peach varieties were resequenced on a large scale and 4.6 million SNPs were identified (Cao et al., 2014). Structural alterations are generally described as copy number variations and presence/absence variations, which include large-scale duplications, insertions, deletions, translocations, and inversions (Zheng et al., 2011). Multiple repeats of a promoter segment cause transcription factor autoregulation in red apples (Espley et al., 2009).

Molecular mechanisms regulating the flowering process have been extensively studied. Four major flowering promotion pathways (photoperiodic, autonomous, vernalization-response, and gibberellin) have been established in model annual plants (Andres and Coupland, 2012). In perennials, however, the molecular mechanisms controlling flowering are poorly understood. In apple, many of the homeotic genes of floral development have been isolated and their expression patterns examined (Koutinas and Pepelyankov, 2010). Recently, some genes have been functionally characterized, for example, the overexpression of an FT-homologous gene in apple induced early flowering in annual and perennial plants (Traenkner et al., 2010). *MdFT1* and/or *MdFT2* might also be associated with flowering and fruiting by interacting with proteins of the *TCP* and *VOZ* families of transcription factors in apple (Mimida et al., 2011). To date, however, there have been no studies on the genetic control of floral initiation and development in apple using high-throughput re-sequencing technology.

We used Solexa sequencing technology and the Illumina HiSeq^{TM} 2000 to re-sequence the genomes of 'Nagafu No. 2' and 'Qinguan,' and to analyze their genetic structures. We developed effective DNA markers to explore agronomic traits-related genes by comparing the 'Nagafu No. 2' and 'Qinguan' sequences with the published reference genome. A comparison of the variation data defined potential genomic regions and metabolic pathways related to floral-associated traits. The genomic resources provided here are useful for comparative genomics and molecular breeding in apple and related species.

MATERIALS AND METHODS

Plant Material and Sample Collection

The materials used in this study were collected from the Apple Demonstration Nursery of Yangling Modern Agriculture Technology Park (Northwest Agriculture and Forestry University) in the Shaanxi Province of China (34°52′ N, 108°7′ E). Young leaves of apple varieties (*Malus domestica* Borkh.) 'Nagafu No. 2' and 'Qinguan' were used as materials for re-sequencing. Physiological differentiation stage of apple flower bud was from May 5th, 2014 (ES, early stage) to June 25th, 2014 (LS, late stage). And bud growth including length, width, and fresh weight during the flower bud physiological stage (ES, MS, and LS) can be seen in our published paper (Xing et al., 2015). Leaf and bud samples of 'Nagafu No. 2' and 'Qinguan' were collected for gene expression analysis on June 5th, 2014,

[1]http://faostat.fao.org/

[2]http://www.rosaceae.org/

45 days after full bloom (MS, the middle stage of flower bud physiological differentiation). Each reaction was performed with three replicates.

DNA Sequencing and Mapping

Genomic DNA was extracted from young leaves of 'Nagafu No. 2' and 'Qinguan' using a modified CTAB method (Zhang et al., 2011). The DNA was then randomly sheared and then purified using a QIAquick PCR Purification Kit 28104 (Qiagen, Beijing, China). Adaptor ligation and DNA cluster preparation were performed, followed by Solexa sequencing using an Illumina HiSeq^{TM} 2000. Low-quality reads (<20), reads with adaptor sequences, and duplicated reads were eliminated. The remaining high-quality data were used for mapping.

We used the published genome of 'Golden Delicious' as a reference (Velasco et al., 2010). We mapped the reads of each accession to the scaffold of the reference genome using BWA software[3] under default parameters, with a small modification: allowing no more than three mismatches in the sequence and not allowing gaps (−o 0). Reads that aligned to more than one position of the reference genome were filtered and used to determine reads mapping to multiple positions in the reference and unmapped reads. After mapping, the reads were sorted by their scaffold coordinates. The mapping result was used to detect DNA polymorphisms, such as SNPs, INDELs, and SVs.

Detection of SNP, INDEL, and SV Polymorphisms

SAMtools software[4] was used to detect SNPs using the following parameters: u -fa -C 50 – bcftools view -I -N- b-v -c -g. The detected SNPs were screened using the following criteria: coverage depth ≥2×, heterozygous locus ≥3×, average depth ≤3×, no less than 20 for the quality value of the genomic type, and discarding SNPs detected in repeat regions.

Structural variations (SVs) were detected using Pindel[5] and Breakdancer[6] software, with their default parameters. To obtain reliable SVs, the detected SVs were returned to the pair-end reads alignments between samples and the reference, and were validated under the following criteria: 2× to 100× for coverage depth and more than 20 for SV quality. We detected insertion (INS), deletion (DEL), deletion including insertion (IDE), inversion (INV), intra-chromosomal translocation (ITX), and inter-chromosomal translocation (CTX) SVs. INDELs were defined as the insertion or deletion of 1–5 bp.

Annotation of SNPs, INDELs, and SVs

The locations of SNPs, INDELs, and SVs were based on the annotation of gene models from the reference genome database[7]. Polymorphisms in the gene region and other genome regions were annotated as genic and intergenic, respectively. The genic SNPs and SVs were classified as exonic and intronic based on their location. SNPs in coding DNA sequences (CDSs) were further separated into synonymous and non-synonymous using Genewise[8].

Identifying Genes Associated with DNA Polymorphisms and Their Functional Analysis

Using the 'Golden Delicious' gene set as the reference, genes containing DNA polymorphism were identified in the 'Nagafu No. 2' and 'Qinguan' apple varieties. The genes associated with the DNA polymorphisms were annotated in databases, such as Swissprot, COG, Nr, and GO, for both 'Nagafu No. 2' and 'Qinguan' apples (Ashburner et al., 2000; Tatusov et al., 2000; Apweiler et al., 2004). In addition, the KEGG[9] analysis of genes with DNA polymorphisms identified those enriched in particular pathways, based on the hypergeometric distribution test (Kanehisa et al., 2004). The Fisher's exact test was used to identify pathways significantly enriched (P-value <0.1) with related genes.

Cloning of the *FT* Promoter Region

The primers used to amplify the *FT* promoter region were based on those described in a previous study on apples (Traenkner et al., 2010). Using the promoter sequence obtained for *FT*, primers were redesigned to compare sequences among different cultivars. PCR products were analyzed on 1.0% agarose gels, and for each reaction product, a single fragment was recovered from gels and purified using a DNA purification kit (Takara, Ohtsu, Japan). The fragment was then ligated into the plasmid pMD18-T vector, transformed into *Escherichia coli* DH5α competent cells (Takara, Ohtsu, Japan), and sequenced (Sangon Biotech, Shanghai, China). In addition, we predicted the transcription factor binding sites in the *FT* promoters of the two apple varieties using Plant CARE[10].

RNA Extraction, cDNA Synthesis, and qRT-PCR Validation of Flowering Genes

Total RNA was isolated from each sample using a modified CTAB method (Xing et al., 2014). The concentration of total RNA was measured using a Nanodrop 2000 after DNase I digestion of genomic DNA. First-strand cDNA was synthesized from 4 μg of DNA-free RNA using a Revert Aid^{TM} First-Strand cDNA Synthesis Kit (Fermentas, Glen Burnie, MD, USA). The cDNA was diluted 10-fold, and 2 μL was used as the template for qRT-PCR analyses. Each qRT-PCR reaction mixture contained 10.0 μL SYBR Premix Ex Taq^{TM} (Takara, Ohtsu, Japan), 0.4 μL each primer (10 μM), 2 μL cDNA, and 7.2 μL RNase-free water in a total volume of 20 μL. The reactions were incubated in an iCycler iQ5 (BIO-RAD) for 30 s at 95°C; followed by 40 cycles of 5 s at 95°C and 35 s at 60°C. Then, an additional 81 cycles were run for the melt curve. The qRT-PCR primers were designed using primer 3 software[11]. The primers used in the qRT-PCR

[3]http://bio-bwa.sourceforge.net/bwa.shtml

[4]http://samtools.sourceforge.net/samtools.shtml

[5]https://trac.nbic.nl/Pindel/

[6]http://BreakDancer.sourceforge.net/BreakDancermax.html

[7]http://www.rosaceae.org/species/malus/malus_x_domestica

[8]http://www.ebi.ac.uk/Tools/psa/genewise/

[9]http://www.genome.jp/kegg/

[10]http://bioinformatics.psb.ugent.be/webtools/plantcare/html/

[11]http://simgene.com/Primer3

experiments are listed in Supplementary Table S1. Each reaction was performed with three replicates.

Statistical Analysis

The expression levels of the flowering genes in the buds and leaves of 'Nagafu No. 2' and 'Qinguan' apple varieties were analyzed by one-way analyses of variance with Tukey–Kramer multiple comparison tests using DPS software, version 7.0 (Zhejiang University, Hangzhou, China).

RESULTS

Agronomic and Floral-Associated Traits of the Apple Varieties Used for Re-sequencing

'Nagafu No. 2' is a hybrid progeny of 'Red Delicious' and 'Ralls Genet' introduced to China in 1966. It has the good agronomic traits of fleshy fruit, delicate flavor, and great storability; however, it has difficulty flowering (The flowering rate in 6-year-old trees is just ∼20%), poor disease resistance, and environmental adaptation (**Table 1**). 'Qinguan' is a hybrid progeny of 'Golden Delicious' and 'Cockscomb' that shows high drought resistance during the whole growth period. 'Qinguan' flowers easily (The flowering rate in 6-year-old trees is ∼70%), has a high yield and is easy to manage (**Table 1**). These apple varieties differ in a number of floral-associated traits (**Table 1**). The two easy-flowering varieties ('Qinguan' and 'Golden Delicious') had higher proportions of spurs, budding rates, flower formation rates, and formed spurs and full blooms at earlier dates compared with 'Nagafu No. 2' (**Table 1**). The variation in the biological traits of these three varieties provides the basis to study gene-trait associations by examining the sequence polymorphisms and structural variations at the whole-genome level.

Mapping of Re-sequencing Reads to the Reference Apple Genome

Whole-genome sequencing produced 171,118,509 reads (91,406,980 reads for 'Nagafu No. 2' and 79,711,529 reads for 'Qinguan'; **Table 2**). For the clean reads, 80.22% from 'Nagafu No. 2' and 81.52% from 'Qinguan' were mapped successfully onto the reference genome of 'Golden Delicious' (**Table 2**). Details of the data quality, including base distribution, cycle average phred score, and quality distribution, of the two apple varieties are presented in Supplementary Figures S1 and S2, respectively. The sequencing depth distribution and the distribution on chromosomes are shown in Supplementary Figures S3 and S4, respectively. Compared with the reference genome, the identities of 'Nagafu No. 2' and 'Qinguan' were 98.62% and 98.7%, respectively (**Table 2**). The re-sequencing data have been deposited in NCBI Sequence Read Archive (SRA[12]). And accession number was SRP072330.

TABLE 1 | Agronomic and floral-associated traits of the apple varieties used for re-sequencing.

	Varieties		
Floral trait	**'Nagafu No.2'**	**'Qinguan'**	**'Golden delicious'**
Proportion of spur	19.5 ± 2.1% c	44.3 ± 2.5% a	37.9 ± 2.2% b
Budding rate	61.8 ± 2.7% b	66.7 ± 3.5 % a	64.3 ± 3.4% ab
Flower formation rate	19.3 ± 1.9% c	72.0 ± 2.6% a	65.3 ± 3.2% b
Date of forming spur	15th–20th May	8th–12th May	10th–14th May
Full-bloom stage	15th–21st April	10th–16th April	12th–16th April

The data are shown as means ± standard errors and were collected from plants grown in an experimental field in Yangling over three consecutive years (2011–2013). Different lowercase letters in the same row indicate significant differences at $P < 0.05$.

Detection and Characteristics of SNPs, SVs, and INDELs

Based on the alignment results between samples and the reference genome, 2,771,129 genome-wide SNPs (Supplementary Table S2), 82,663 SVs (Supplementary Table S2 and Additional file 1), and 1,572,803 INDELs were detected in 'Nagafu No. 2,' while 2,262,888 genome-wide SNPs, 63,764 SVs and 1,294,060 INDELs were detected in 'Qinguan' (Supplementary Table S2). The average densities of detected SNPs, SVs, and INDELs for 'Nagafu No. 2' and 'Qinguan,' when compared to samples the reference genome, were 4,546.9 and 3,746.0 SNPs per Mb, respectively, 135.9 and 105.3 SVs per Mb, respectively, and 2,584.1 and 2,145.4 INDELs per Mb, respectively (Supplementary Table S2).

Distribution of SNPs, SVs, and INDELs

Detailed distribution information for the SNPs, SVs, and INDELs in both 'Nagafu No. 2' and 'Qinguan' samples identified the landscape of genetic variation in the two apple varieties (**Figure 1**, Supplementary Table S2 and Additional file 2). Among the variations detected between the samples and reference genome 'Golden Delicious,' the highest numbers of SNPs, 231,577 in 'Nagafu No. 2,' and 193,484 in 'Qinguan,' were observed on chromosome 15, while the lowest numbers of SNPs, 104,010 in 'Nagafu No. 2' and 99,017 in 'Qinguan,' were observed on chromosome 16 (Supplementary Table S2). The highest numbers of SVs were observed on chromosome 15, 6,817 in 'Nagafu No. 2' and 5,475 in 'Qinguan,' while the lowest numbers of SVs, 3,448 in 'Nagafu No. 2' and 2,786 in 'Qinguan' were observed on chromosome 16 (Supplementary Table S2). The highest numbers of INDELs, 131,976 in 'Nagafu No. 2' and 109,667 in 'Qinguan,' were observed on chromosome 15, and the lowest numbers of INDELs, 60,055 in 'Nagafu No. 2' and 56,509 in 'Qinguan,' were observed on chromosome 16 (Supplementary Table S2).

Our result showed that the distribution of polymorphisms was uneven within chromosomes (**Figure 1**). The three peripheral circles represent the distribution of polymorphisms in 'Nagafu No. 2,' 'Qinguan,' and 'Golden Delicious,' respectively (**Figure 1**). These circles indicate the statistical information for total SNPs (blue line), non-synonymous SNPs (red line), and SNPs in structural domains (green line) on each chromosome. The promoter circles indicate the SNP numbers of 'Nagafu No. 2' (blue line), 'Qinguan' (red line), and Golden Delicious (green

[12]http://www.ncbi.nlm.nih.gov/Traces/sra_sub/sub.cgi

TABLE 2 | Summary of the original sequencing data of 'Nagafu No. 2' and 'Qinguan.'

	Index									
Variety	**Total reads**	**PE (%)**	**SE (%)**	**Total bases**	**GC (%)**	**Q30 (%)**	**Mapped (%)**	**Identity (%)**	**Depth**	**Coverage (%)**
'Nagafu No.2'	91,406,980	54.8	25.41	18,464,209,960	40.20	83.21	80.22	98.62	31.07	96.94
'Qinguan'	79,711,529	56.61	24.91	16,101,728,858	40.14	82.82	81.51	98.7	27.78	97.36

PE, pair-end reads; SE, single-end reads; Q30 (%) indicates the percentage of sequences with an error rate lower than 1%.

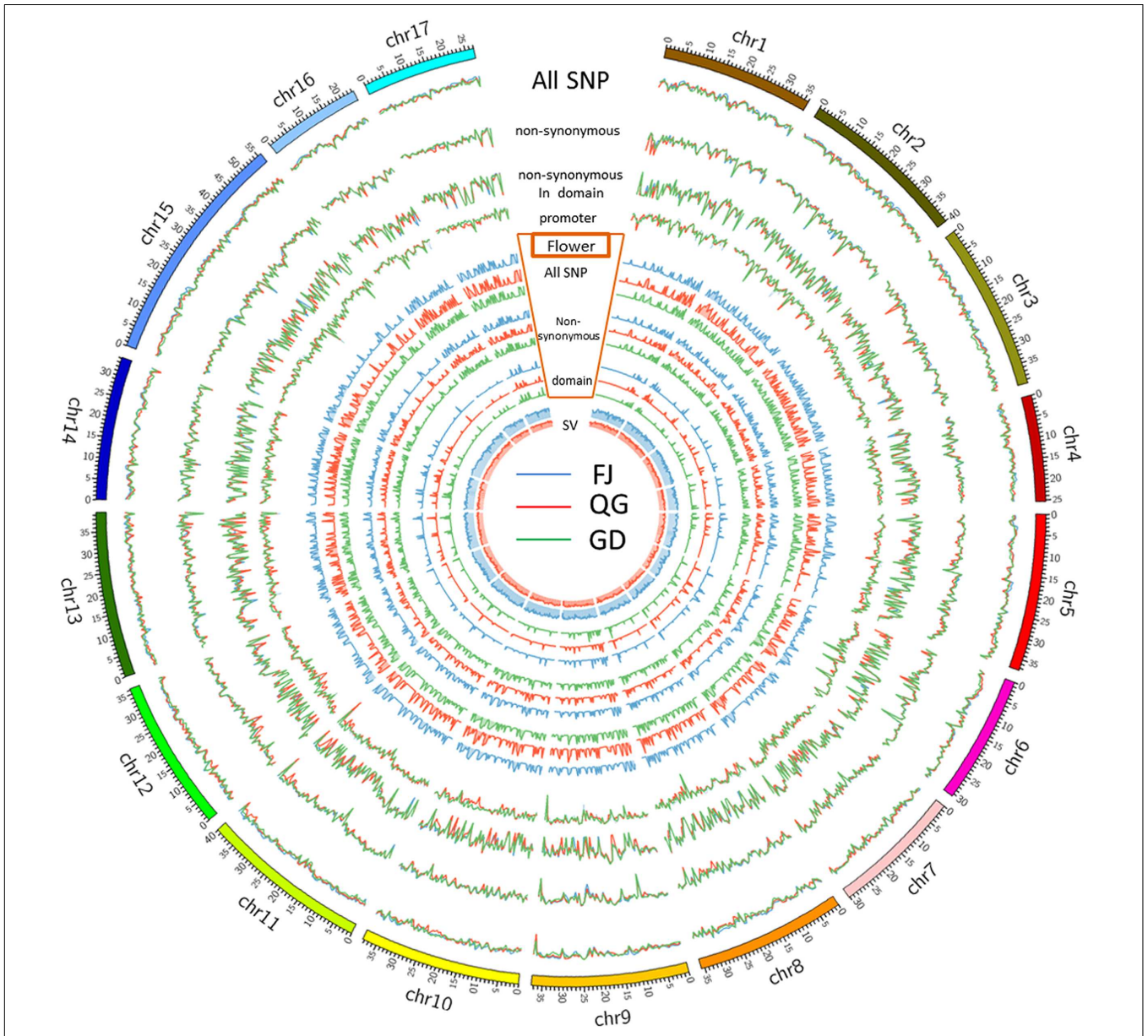

FIGURE 1 | Genetic variations and distributions of DNA polymorphisms (SNPs and SVs) and flowering genes in samples compared with the 'Golden Delicious' genome.

line), which are located in the 200 bp upstream of each coding region (**Figure 1**). Inside the promoter circles, there are three grouped circles, which represent the distribution of flowering genes on each chromosome of 'Nagafu No. 2,' 'Qinguan,' and 'Golden Delicious.' We chose flowering genes mainly based on previous research in the model plant *Arabidopsis thaliana*

(Blümel et al., 2015). The blue line indicates the total SNPs related to flowering, the red line indicates the sense mutation of SNPs related to flowering, and the green line indicates the SNPs related to flowering in structural domains (**Figure 1**). The inner circles represent the SV distribution on each chromosome of 'Nagafu No. 2' (blue line) and 'Qinguan' (red line).

In addition, detailed information on the distribution of SNPs and SVs detected between 'Nagafu No. 2' and 'Qinguan' on the 17 chromosomes is shown in Supplementary Figure S5. The distribution of polymorphisms was uneven within chromosomes, as well as between each chromosome of 'Nagafu No. 2' and 'Qinguan' (Supplementary Figure S5), and all of the chromosomes in both varieties were comprised of a mixture of SNP-dense and -sparse regions (Supplementary Figure S5). The number of SNPs (133,130) and SVs (4,016) in 'Nagafu No. 2' were significantly higher than in 'Qinguan' (115,431 SNPs and 3,245 SVs) for chromosome 1. Other chromosomes showed similar results (Supplementary Figure S5). Additionally, the distribution patterns of the two polymorphism types were similar in the two varieties (Supplementary Figure S5).

Characteristics of SNPs, SVs, and INDELs

The SNPs detected when comparing the two samples with the reference genome were classified as transitions (C/T and G/A) or transversions (C/G, T/A, A/C, and G/T) based on nucleotide substitutions (Supplementary Table S3). The proportions of transitions and transversions on individual chromosomes were very similar, but the proportions of transitions were significantly higher than the proportions of transversions in both samples (Supplementary Table S3). The proportions of heterozygosity were significantly higher than the proportions of homozygosity in the two samples, and the proportion of heterozygosity in 'Qinguan' was significantly higher than the proportion of heterozygosity in 'Nagafu No. 2' (Supplementary Table S3). The highest proportions of SNP heterozygosity, 89.66 and 93.67%, were observed on chromosome 7 of 'Nagafu No. 2' and 'Qinguan,' respectively, while the lowest proportions of SNP heterozygosity, 4.09 and 86.08%, were observed on chromosome 2 of 'Nagafu No. 2' and chromosome 8 of 'Qinguan,' respectively (Supplementary Table S3).

In addition, six types of SVs, INS, DEL, IDE, INV, ITX, and CTX, were identified in both cultivars, based on the annotation of 'Golden Delicious' genome (Supplementary Table S4). In 'Nagafu No. 2' and 'Qinguan,' 63,764 and 82,663 SVs, respectively, were detected (Supplementary Table S2). There was no significant difference in the percentage of each SV between 'Nagafu No. 2' and 'Qinguan.' Among them, DEL and INS were the major SVs, with 46,878 (56.71%) and 31,800 (38.47%), respectively, for 'Nagafu No. 2,' and 36,428 (57.13%) and 24,001 (37.64%), respectively, for 'Qinguan' (**Figure 2**). INX [314 (0.38%), and 274

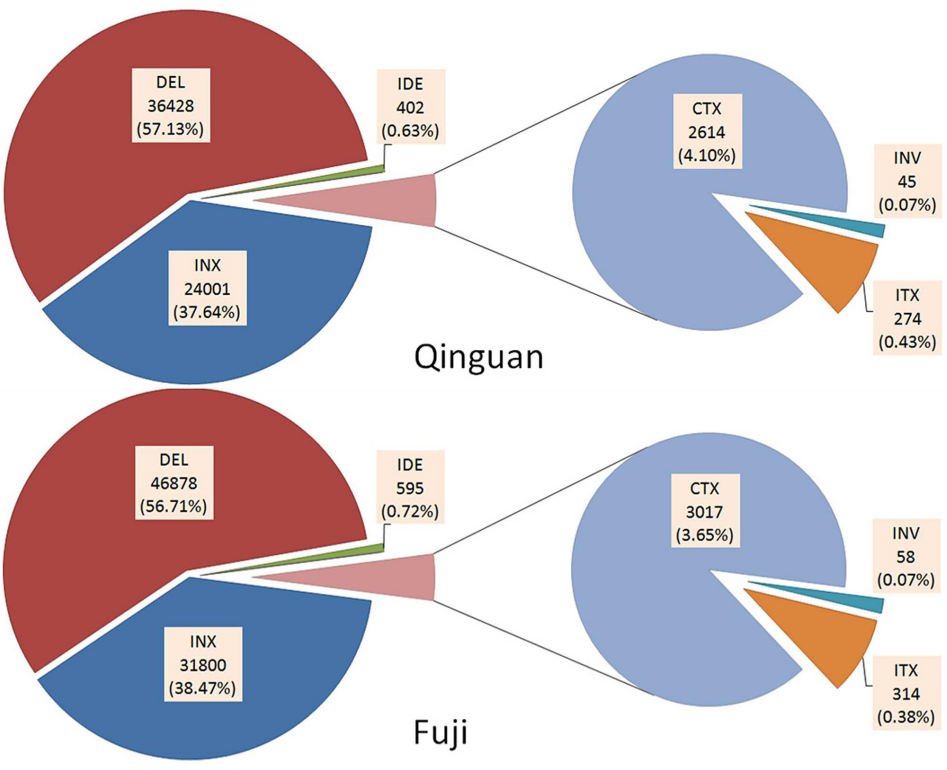

FIGURE 2 | Annotation of SVs identified in 'Nagafu No. 2' and 'Qinguan' apple varieties. Structural variations (SVs) were classified as INS (Insertion), DEL (Deletion), IDE (Deletion including insertion), INV (Inversion), ITX (Intra-chromosomal Translocation), or CTX (Inter-chromosomal Translocation) based on the annotation of the 'Golden Delicious' genome.

(0.43%) for 'Nagafu No. 2 and 'Qinguan,' respectively] and INV [314 (0.07%) and 45 (0.07%) for 'Nagafu No. 2 and 'Qinguan,' respectively] were the minor SVs in the two varieties (**Figure 2** and Supplementary Table S4). Among the variations detected between samples and 'Golden Delicious,' the highest densities of SVs were 162.97 per Mb, observed on chromosome 11 of 'Nagafu No. 2' and 114.42 per Mb on chromosome 17 of 'Qinguan.' The lowest densities of SVs were 111.31 per Mb and 89.94 per Mb observed on chromosome 1 in 'Nagafu No. 2' and 'Qinguan,' respectively (Supplementary Table S4).

Annotation of Genes with Genome Variations and Their Function Analysis

In the genomic regions of 'Nagafu No. 2' and 'Qinguan,' 4,827 and 3,719 INS, respectively, and 6,331 and 5,091 DEL, respectively, were identified from the 1-bp INDELs (**Figure 3**). In the CDS regions of 'Nagafu No. 2' and 'Qinguan,' 509 and 414 INS, respectively, and 841 and 678 DEL, respectively, were identified from the 1-bp INDELs (**Figure 3**). Detailed distribution information on INDELS of other sizes is shown in **Figure 3**. We identified 171,520 non-synonymous SNPs in 23,111 genes for 'Nagafu No. 2' and 147,090 non-synonymous SNPs in 21,400 genes for 'Qinguan' apple varieties, but there were relatively small numbers of frameshift INDELs within the genes of both apple varieties (Supplementary Table S5). We also analyzed the distribution of the SNPs in Pfam-containing genes, and the range of the ratio of non-synonymous-to-synonymous SNPs (ns/s SNPs) was 0.48 to 1.4 in these genes, indicating that the Pfam domains may have more amino acid substitutions in the genome (**Figure 4**).

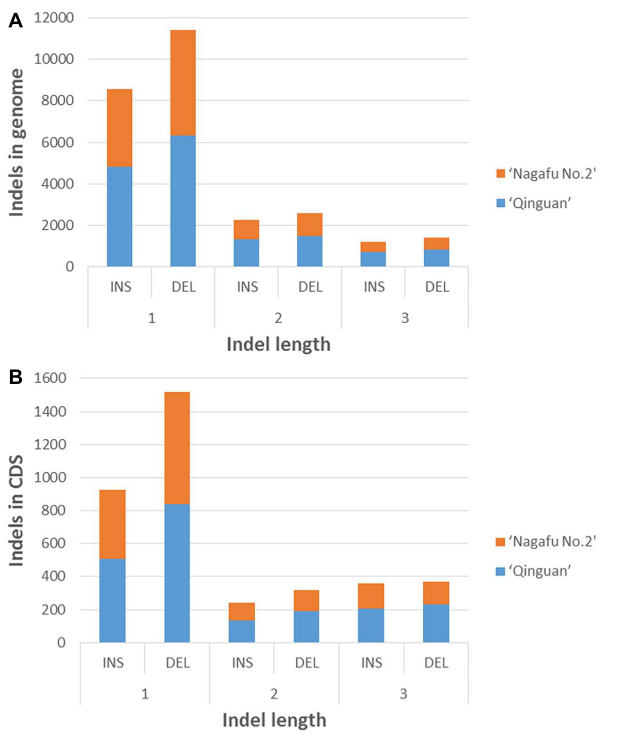

FIGURE 3 | Distribution of 1- to 3-bp INDELs in 'Nagafu No. 2' and 'Qinguan' apple varieties. (A) Number of INDELs of different lengtha in the genomic regions; **(B)** Number of INDELs of different lengths in the CDS regions.

The numbers of SNPs, non-synonymous SNPs, SVs, and frameshifts associated with the genes in both 'Nagafu No. 2' and 'Qinguan' apple varieties can be found in Additional file 2. Additionally, detailed information on the functional and annotation-related information from databases such as Swissprot, Nr, COG, GO, and KEGG for the SNPs, non-synonymous SNPs, SVs, and frameshifts in 'Nagafu No. 2' and 'Qinguan' apple varieties can be found in Additional file 3. The details of the GO function analysis for genes with SNPs, non-synonymous SNPs, SVs, and INDELs in the two varieties can be seen in Additional files 4, 5, 6, and 7. For example, the GO terms significantly enriched for genes with SNPs and non-synonymous SNPs in both 'Nagafu No. 2' and 'Qinguan' apple varieties were mainly involved in the defense response (GO:0006952), signal transduction (GO:0007165), arginine catabolic process (GO:0006527), protein targeting to membrane (GO:0006612), and ethylene biosynthetic process (GO:0009693) categories (P-value <0.01; Additional files 4 and 5). However, the genes with INDELs were mainly involved in sex determination (GO:0007530), succinate metabolic process (GO:0006105), regulation of ion transport (GO:0043269), response to herbivore (GO:0080027), positive regulation of flavonoid biosynthetic process (GO:0009963), and mitochondrial transport (GO:0006839; P-value <0.01; Additional file 6), suggesting that the biological functions of genes with different genome variations had significantly different effects on the phenotypes of these apple varieties.

Meanwhile, the KEGG analysis of the genes with DNA polymorphisms also identified particularly enriched pathways (Additional files 8, 9, 10 and 11). Among them, the different genes with SNPs were enriched in 104 KEGG pathways, and 11 pathways were significantly enriched, including plant hormone signal transduction (ko04075), circadian rhythm (ko04710), photosynthesis (ko00195), and glycerophospholipid metabolism (ko00564; P-value <0.1; Additional file 8). Genes with non-synonymous SNPs were significantly enriched in 12 pathways, including vitamin B6 metabolism (ko00750), plant hormone signal transduction (ko04075), and oxidative phosphorylation (ko00190; P-value <0.1; Additional file 9). The genes with INDELs were enriched in 72 KEGG pathways, but only four pathways were significantly enriched: ribosome (ko03010), vitamin B6 metabolism (ko00750), sulfur metabolism (ko00920), and mRNA surveillance pathway (ko03015; P-value <0.1; Additional file 10).

Genetic Variation between Easy-Flowering and Difficult-Flowering Apple Varieties

We speculated that some of the identified genetic variations might contribute to the phenotypic differences in floral-associated traits; therefore, we focused our analysis on SNPs, SVs,

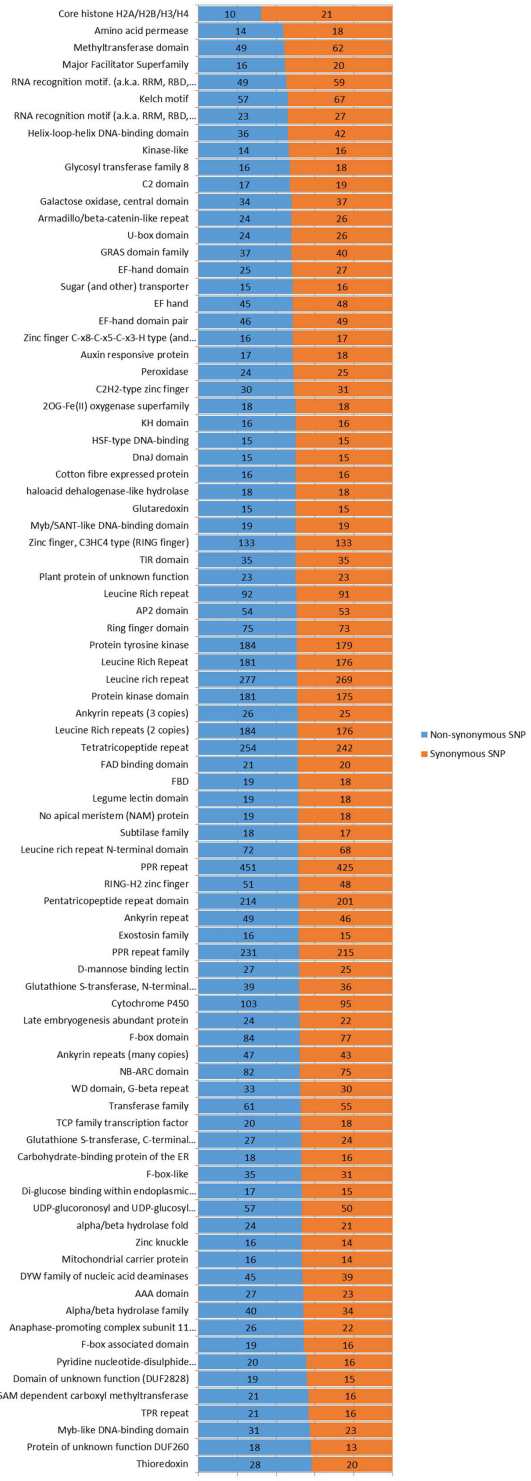

FIGURE 4 | Number and distribution of non-synonymous and synonymous SNPs in different Pfam genes in the apple genomes. Pfam gene families with 30 or more non-synonymous and synonymous SNPs were analyzed and listed. The Pfam genes are arranged based on the percentages of non-synonymous and synonymous SNP sites. The chi-square significance of the observed non-synonymous and synonymous SNP distributions for each Pfam group is shown: *P*-value <0.001.

and INDELs associated with flowering genes in genic regions. We used the gene set from the reference 'Golden delicious' genome as the control and identified all of the shared variations involved in flowering genes between the difficult-flowering 'Nagafu No. 2' and easy-flowering 'Qinguan' apple varieties. Genetic linkage maps of 'Nagafu No. 2,' 'Qinguan,' and 'Golden Delicious' were also constructed in association with the 190 flowering genes (**Figure 5**). The distribution of flowering genes was significantly different among the 17 chromosomes within each variety (**Figure 5**). For example, 18 flowering genes were found on chromosome 10, but there were just three on chromosome 9 (**Figure 5**). In addition, the locations and distributions of these flowering genes on each chromosome showed large differences among the varieties (for the details, see **Figure 5**).

Identification by qRT-PCR of Flowering Genes in Leaves and Buds

The expression profiles of 15 flowering genes, which were mainly involved in four major flowering promotion pathways, photoperiod, autonomous, vernalization, and gibberellin, were identified in leaves and buds of two apple varieties using RT-PCR (**Figures 6** and **7**). In this study, the *CO*, *FT*, *CRY*, and *FKF1* genes, which are related to photoperiod, showed higher expression levels in the leaves and buds of 'Qinguan' than of 'Nagafu No. 2' (**Figure 6**). The *FWA* expression level in the buds of 'Qinguan' was significantly higher than in 'Nagafu No. 2'; however, its expression level in the leaves of 'Qinguan' was significantly lower than in the leaves of 'Nagafu No. 2' (**Figure 6**). The vernalization pathway-related genes *VIN3* and *MSI1* were expressed significantly higher in the leaves and buds of 'Qinguan' than in those of 'Nagafu No. 2' (**Figure 6**). *FLC* plays a key role in the autonomous pathway, and its expression in the buds of 'Qinguan' was significantly higher than in 'Nagafu No. 2'; however, in leaves, its expression was significantly higher in 'Nagafu No. 2' (**Figure 6**). In the gibberellin pathway, the expression of *GAI* in 'Qinguan' was significantly higher than in 'Nagafu No. 2,' but the downstream gene, *AGL24*, showed the reverse expression pattern (**Figure 6**). In addition, a regulatory relationship diagram of these flowering genes in different pathways, as well as models of their expression profiles in leaves and buds between difficult-flowering apple variety 'Nagafu No. 2' and easy-flowering apple variety 'Qinguan,' are shown in **Figure 7**.

Isolation of the Upstream Regulatory Region of the Md*FT* Gene from 'Nagafu No. 2' and 'Qinguan'

We cloned and amplified the *FT* promoter region and obtained 1,622-bp and 1,624-bp sequences from 'Nagafu No. 2' and 'Qinguan' apple leaves, respectively. The two sequences of the *FT* promoter were very similar: 93.1% of the promoter sequence was identical; however, the remaining 6.9% of the sequence was significantly different and included deletions, conversions, and inversions (Supplementary Figure S6).

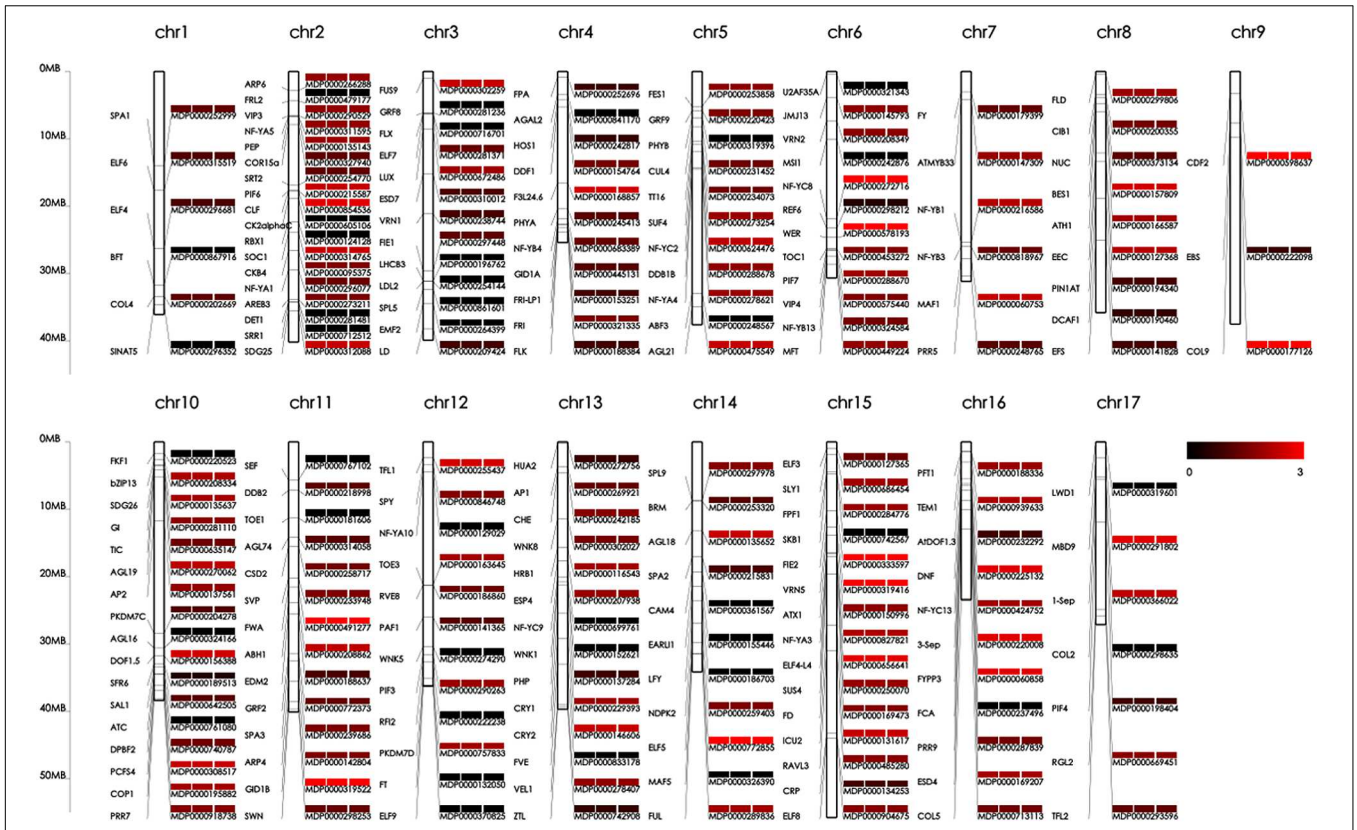

FIGURE 5 | Genetic linkage maps of 'Nagafu No. 2,' 'Qinguan,' and 'Golden Delicious' constructed using 190 flowering genes. The abbreviations for the flowering genes are shown on the left and the mutation indices of 'Nagafu No. 2,' 'Qinguan,' and 'Golden Delicious' are shown on the right. The mutation indices were obtained by SNP numbers in flowering genes at log10 among the three apple varieties. The corresponding values are shown as colors from black (0) to red (3).

DISCUSSION

Bioinformatics tools and the rapid development of sequencing technologies have made the complete genome sequencing of many perennial fruit crops possible, providing a starting point to unravel the genetic variation and diversity existing on the genome scale (Jaillon et al., 2007; Velasco et al., 2010; Verde et al., 2013; Wu et al., 2013; Xu et al., 2013). Genome-wide patterns of genetic variation were then captured by sampling a relatively small number of genomes. The whole-genome re-sequencing of two elite apple varieties 'Nagafu No. 2' and 'Qinguan,' and their comparisons with the reference 'Golden delicious' genome sequence (Velasco et al., 2010), allowed us to comprehensively survey SNPs and SVs. DNA polymorphisms on a genome-wide scale were identified, revealing a high level of genetic diversity between 'Nagafu No. 2' and 'Qinguan' Our results also showed how NGS technologies can be powerful tools for studying genome-wide DNA polymorphisms, querying genetic diversity, and enabling molecular-based improvements of apple breeding.

SNP markers have been employed widely to study evolutionary relationships, population structures, and association analyses in rice, peach, and pear (McNally et al., 2009; Parida et al., 2012; Bai H. et al., 2013; Lyu et al., 2013; Montanari et al., 2013; Cao et al., 2014). However, only a few studies have used genome-wide SNP markers to understand the structure and diversity in different genomes of Malus species (Chagné et al., 2008, 2012). In this study, 'Nagafu No. 2' had more SNPs than 'Qinguan,' which indicated that 'Qinguan' is more closely related to 'Golden Delicious' than 'Nagafu No. 2' (Supplementary Table S3). This is unsurprising because 'Qinguan' is a hybrid progeny of 'Golden Delicious' and 'Cockscomb.' A similar phenomenon was reported in rice (Bai S.L. et al., 2013). In addition, our results indicated that re-sequencing could be a good experimental tool to better understand evolutionary relationships in plant species. More genotypes are needed to produce a comprehensive understanding of the complex relationships and evolution in the Malus species.

The average proportions of genic SNPs, exons, introns, or intergenic, were similar in the 'Nagafu No. 2' and 'Qinguan' varieties (**Table 3**), and were similar to those in peach (Cao et al., 2014). Compared with *Arabidopsis* (Clark et al., 2007), rice (Feltus et al., 2004), and *Miscanthus sinensis* (Clark et al., 2014), the intergenic regions of apple genes harbor more SNPs, which might be related to the increased size of the intergenic regions in the apple genome (**Table 3**). The proportions of genic SVs were also similar between the two varieties (**Table 3**). The difference in genetic diversity between 'Nagafu No. 2' and 'Qinguan,' as well as the difference in the distribution of this diversity in

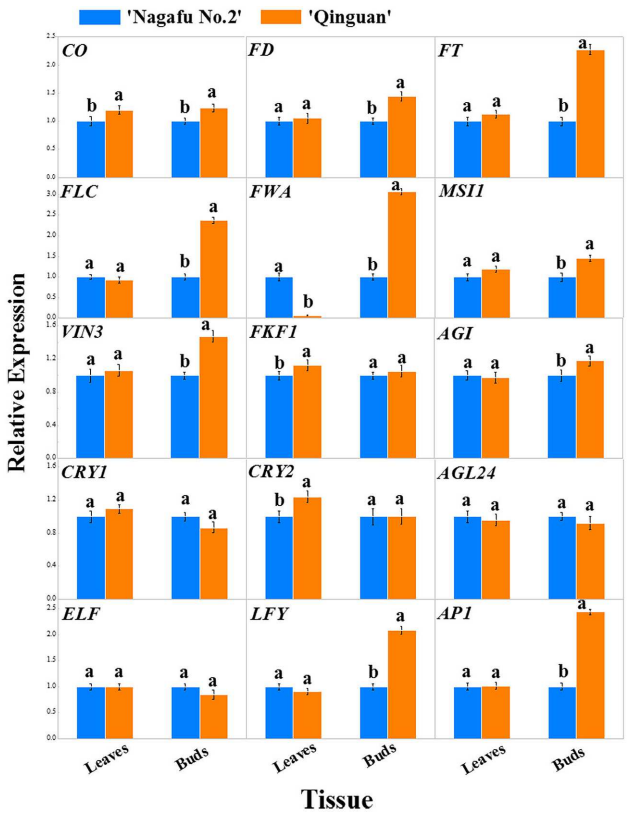

FIGURE 6 | Expression profiles of flowering genes associated with the multiple pathways in leaves and buds of 'Nagafu No. 2' and 'Qinguan' apples. Note: *CO, CONSTANS; FT, FLOWERING LOCUS T; FKF1, FLAVIN-BINDING KELCH REPEAT F BOX 1; ELF3, EARLY FLOWERING 3; CRY1, CRYPTOCHROME 1; CRY2, CRYPTOCHROME 2; AP1, APETALA1; VIN3, VERNALIZATION INSENSITIVE 3; FLC, FLOWERING LOCUS C; MSI1, MULTICOPY SUPRESSOR OF IRA1; FD; LFY; AGL24, AGAMOUS-LIKE 24; GAI, GIBBERELLIC ACID INSENSITIVE; FWA, FLOWERING WAGENINGEN.*

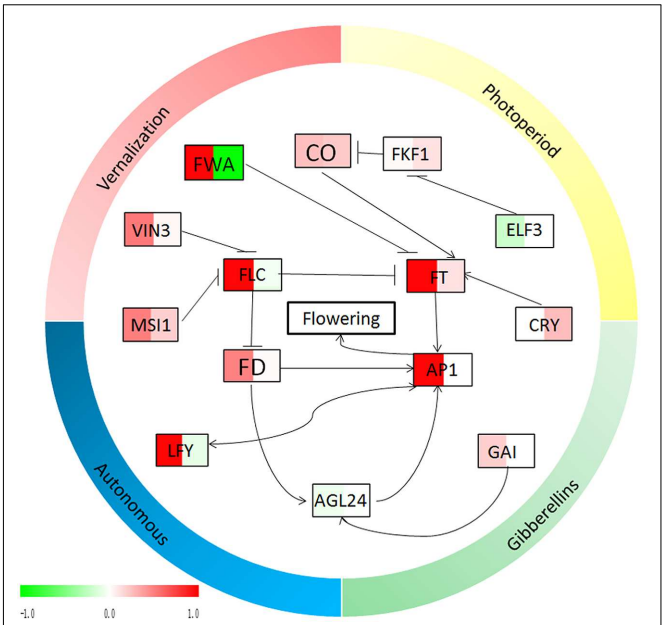

FIGURE 7 | Relationship diagram of the flowering genes from Figure 5. The expression profiles of the flowering genes, which were calculated by the relative expressions transformed by log 2 ('Qinguan'/'Nagafu No. 2'), are indicated by color, from green (-1) to red (1). In each frame, the left side indicates the relative expression levels in buds and the right side indicates the relative expression levels in leaves. Green indicates that the relative expression in 'Qinguan' is lower than in 'Nagafu No. 2,' and red indicates that the relative expression in 'Qinguan' is higher than in 'Nagafu No. 2.'

different genetic regions, may involve changes in agronomic and floral-associated traits between the two apple varieties.

In this study, we identified genetic variation, including large numbers of SNPs, SVs, and INDELs, in the two samples when compared with the 'Golden Delicious' reference genome. The distributions of these polymorphisms were uneven within the chromosomes. A similar study on peach (*Prunus persica*) showed multiple variation patterns and an uneven distribution of the variation across the genome (Cao et al., 2014), as did a study on *Sorghum bicolor* (Zheng et al., 2011). Indeed, many studies, for example, in rice (Caicedo et al., 2007; McNally et al., 2009; Subbaiyan et al., 2012), soybean (Kim et al., 2010), and peach (Cao et al., 2014), have shown that SNPs, SVs, and INDELs on each chromosome are unevenly distributed and are often concentrated in certain chromosomal regions. Meanwhile, in our results, chromosome 15 had the highest number of SNPs and chromosome 16 had the lowest number of SNPs in both cultivars. Moreover, for chromosome 1, 'Nagafu No. 2' had more SNPs and SVs than 'Qinguan,' which suggested that these different distribution types and features of variation may contribute to the differences in certain characteristics, such as flowering and resistance, between the two apple varieties. In addition, the distribution of SNPs within chromosomes is non-random; for example, a high SNP density was observed between 8.7 and 9.2 Mb on chromosome 8, but no SNPs were found in a longer interval of 200 kb, from 27.2 to 27.4 Mb, on chromosome 11 (Subbaiyan et al., 2012). A similar result was observed in our study (Supplementary Figure S5).

Our results showed that the number of INDELs of different lengths (1–3 bp) in the CDS regions and the whole genome were significantly different between 'Nagafu No. 2' and 'Qinguan,' and similar results have been seen in other plants (McNally et al., 2009; Subbaiyan et al., 2012). Compared with the high numbers of non-synonymous SNPs in 'Nagafu No. 2' and 'Qinguan,' relatively few frameshift INDELs within genes were observed, which was similar to studies in tomato (Hirakawa et al., 2013), rice (Parida et al., 2012), and apple (Chagné et al., 2012). Genome variations, such as SNPs (non-synonymous or synonymous), INDELs, and SVs, at the whole-genome level in the two apple varieties, which result in amino acid changes, were mainly caused by positive selection during adaptation to environmental changes during the evolutionary process.

The two varieties and 'Golden Delicious,' which is also easy to flower and the flowering rate in 6-year-old trees is ∼65%, have significant differences in floral characteristics; therefore, we constructed genetic linkage maps of flowering genes in the three

TABLE 3 | Annotation of SNPs identified between samples and the reference genome.

		Exon		Intron		Intergenic	
Variety	**Type**	**Number**	**percentage**	**Number**	**percentage**	**Number**	**percentage**
'Nagafu No.2'	SNP	280,835	10.13%	315,948	11.4%	2,174,946	78.47%
	SV	3,963	5.0%	19,659	24.75%	55,798	70.26%
'Qinguan'	SNP	242,328	10.71%	247,806	10.94%	1,773,297	78.35%
	SV	3,196	5.23%	15,072	24.64%	42,895	70.13%

SNPs and SVs were classified as genetic and intergenic, and locations within the gene models were annotated based on the annotations of the reference genome.

varieties and compared the genetic variation of these genes across the whole genome. The genome variation of these flowering genes showed significant differences among the three apple varieties (**Figure 5**), which may explain the differences in flowering-related traits among them. Additionally, genomic variation, such as large-effect SNPs, result in changes to biological characteristics, including growth characteristics, plant phenotypes, and the resistance responses (Zheng et al., 2011). Similar results have been reported in other plants (Parida et al., 2012; Clark et al., 2014). In addition, to determine the functions of genes with DNA polymorphisms between 'Nagafu No. 2' and 'Qinguan,' we performed GO and KEGG analyses of genes with SNPs, non-synonymous SNPs, SVs, and INDELs, in the two varieties (Additional files 4, 5, 6, 7, 8, 9, 10, and 11). This analysis focused on key genes with DNA polymorphisms in the two apple varieties, so that we can more accurately understand the relationships between these genes with DNA polymorphisms and the phenotypic traits.

Previous studies have shown that there are four major flowering pathways photoperiod, autonomous, vernalization, and gibberellin, which are associated with complex gene regulation process (Bernier and Périlleux, 2005; Amasino, 2010; Koutinas and Pepelyankov, 2010; Turnbull, 2011; Bernier, 2013). The photoperiod and vernalization pathways process environmental signals to the floral transition, whereas the autonomous and gibberellin pathways act independently of external signals (Mutasa-Gottgens and Hedden, 2009). The photoreceptor, circadian clock, and circadian clock-regulated genes constitute the photoperiod pathway and act in response to a long photoperiod (Searle and Coupland, 2004; Jung et al., 2007; Fornara and Coupland, 2009). In our study, the photoperiod genes *CO* and *FT* were significantly more highly expressed in the leaves and buds of 'Qinguan' compared with 'Nagafu No. 2.' The relatively higher expression levels of these flowering control genes associated with the photoperiod in plants can significantly promote flower bud formation (Gould et al., 2013; Fan et al., 2014). In addition, in the vernalization pathway, the *VIN3* and *MSI1* genes showed higher expression levels in 'Qinguan' and in buds. In addition, *FLC* plays a key role in the autonomous pathway (Liu et al., 2007; Porto et al., 2015). In the present study, *FLC* expression in the buds of 'Qinguan' was much higher than in those of 'Nagafu No. 2'; however, in leaves, its expression was lower than in 'Nagafu No. 2.' The expression profiles of these key flowering genes were significantly associated with bud growth, floral induction, and physiological phenotypic characteristics involved in flowering in plants (Jean Finnegan et al., 2011; Ream et al., 2014). Gibberellins play key roles in the regulation of flower induction as part of the complex floral regulatory networks (Mutasa-Gottgens and Hedden, 2009) and in multiple flowering pathways (Liu et al., 2008; Wilkie et al., 2008; Lee and Lee, 2010). Indeed, of the gibberellin pathway genes, the expression of *GAI* in 'Qinguan' buds was significantly higher than in 'Nagafu No. 2' buds; however, the downstream gene *AGL24* showed the reverse pattern, suggesting that differences in the expression levels of genes associated with multiple flowering pathways may contribute to differences in floral-associated traits between 'Nagafu No. 2' and 'Qinguan.' Meanwhile, the expression profiles of key flowering genes in apple buds and leaves in the four major flowering pathways suggested that the photoperiod and autonomous flowering pathways make a major contribution to the differences in the floral-associated traits of two apple varieties (**Figure 7**).

Sequence variation in promoter regions mediates a transcriptional regulation mechanism associated with anthocyanin biosynthesis genes in grape (Kobayashi et al., 2004) and apple (Espley et al., 2009). In our study, we speculated that some of the identified genetic variation might contribute to the phenotypic differentiation of floral-associated traits. We focused our analysis on SNPs, INDELs, and SVs in promoter regions between 'Nagafu No. 2' and 'Qinguan.' As a result, we amplified the *FT* promoter region from 'Nagafu No. 2' and 'Qinguan' to identify and compare the sequence variations between the two varieties. The sequences of the *FT* promoter regions were 93.1% identical, but 6.9%, including deletions, conversions, and inversions, was completely different (Supplementary Figure S6), and the expression of the *FT* gene in buds was significantly higher in 'Qinguan' than in 'Nagafu No. 2' (**Figure 6**). In addition, we predicted transcription factor-binding sites, including ARE, G-Box, GATA-motif, and Spl, in *FT* promoters between the two apple varieties (Supplementary Table S6). This suggested that the observed variation may result in different *FT* expression patterns between 'Nagafu No. 2' and 'Qinguan' apple varieties.

CONCLUSION

In the present study, we identified large-scale genomic variation, including SNPs, INDELS, and SVs, among two elite apple varieties 'Nagafu No 2,' 'Qinguan' and the reference variety 'Golden Delicious.' This can be used as a framework for future

comparative and functional genomic analyses in fruit trees, as well as providing information for molecular breeding, allele discovery, and agronomic trait screening in apple. 'Qinguan' is an elite variety with strong disease resistance and easy flowering, whereas the fruit quality of 'Nagafu No. 2' is better than that of other cultivars. Thus, genome-wide comparison studies of variations involved in floral-related traits and resistance responses will also provide a powerful resource to identify key genes and for function-related research. We also established genetic linkage maps of 'Nagafu No. 2,' 'Qinguan,' and 'Golden Delicious' using 190 flowering genes in multiple flowering pathways and compared the distribution characteristics of the genome variations in these genes, which may contribute to a deeper understanding of the differences among a variety of traits across the genome.

AUTHOR CONTRIBUTIONS

Conceived and designed the experiment: HM, XL, ZD, and ZC. Performed the experiments: XL, WK, and LY. Analyzed the data: XL, WK, JM, and NA. Developed the model: LX and KW. Wrote the paper: XL, ZD, and SX. Edited the manuscript: AN.

ACKNOWLEDGMENTS

This work was supported by the China Apple Research System (CARS-28), the National Science and Technology Supporting Project (2013BAD20B03), Special Financial Grant from the China Postdoctoral Science Foundation (No. 2014T70939), Shaanxi Fruit Industry Development of Collaborative Innovation Center Project, Yangling Subsidiary Center Project of National Apple Improvement Center, and the China Postdoctoral Science Foundation (No. 2014M56806).

SUPPLEMENTARY MATERIAL

The Supplementary Material for this article can be found online at: http://journal.frontiersin.org/article/10.3389/fpls.2016.00908

REFERENCES

Amasino, R. (2010). Seasonal and developmental timing of flowering. *Plant J.* 61, 1001–1013. doi: 10.1111/j.1365-313X.2010.04148.x

Andres, F., and Coupland, G. (2012). The genetic basis of flowering responses to seasonal cues. *Nat. Rev. Genet.* 13, 627–639. doi: 10.1038/nrg3291

Apweiler, R., Bairoch, A., Wu, C. H., Barker, W. C., Boeckmann, B., Ferro, S., et al. (2004). UniProt: the universal protein knowledgebase. *Nucleic Acids Res.* 32, D115–D119. doi: 10.1093/nar/gkh131

Ashburner, M., Ball, C. A., Blake, J. A., Botstein, D., Butler, H., Cherry, J. M., et al. (2000). Gene Ontology: tool for the unification of biology. *Nat. Genet.* 25, 25–29. doi: 10.1038/75556

Bai, H., Cao, Y., Quan, J., Dong, L., Li, Z., Zhu, Y., et al. (2013). Identifying the genome-wide sequence variations and developing new molecular markers for genetics research by re-sequencing a landrace cultivar of foxtail millet. *PLoS ONE* 8:e73514. doi: 10.1371/journal.pone.0073514

Bai, S. L., Saito, T., Sakamoto, D., Ito, A., Fujii, H., and Moriguchi, T. (2013). Transcriptome analysis of japanese pear (*Pyrus pyrifolia* Nakai) flower buds transitioning through endodormancy. *Plant Cell Physiol.* 54, 1132–1151. doi: 10.1093/pcp/pct067

Bernier, G. (2013). My favourite flowering image: the role of cytokinin as a flowering signal. *J. Exp. Bot.* 64, 5795–5799. doi: 10.1093/jxb/err114

Bernier, G., and Périlleux, C. (2005). A physiological overview of the genetics of flowering time control. *Plant Biotechnol. J.* 3, 3–16. doi: 10.1111/j.1467-7652.2004.00114.x

Blümel, M., Dally, N., and Jung, C. (2015). Flowering time regulation in crops—what did we learn from *Arabidopsis*? *Curr. Opin. Biotechnol.* 32, 121–129. doi: 10.1016/j.copbio.2014.11.023

Caicedo, A. L., Williamson, S. H., Hernandez, R. D., Boyko, A., Fledel-Alon, A., York, T. L., et al. (2007). Genome-wide patterns of nucleotide polymorphism in domesticated rice. *PLoS Genet.* 3:e163. doi: 10.1371/journal.pgen.0030163

Cao, K., Zheng, Z., Wang, L., Liu, X., Zhu, G., Fang, W., et al. (2014). Comparative population genomics reveals the domestication history of the peach, *Prunus persica*, and human influences on perennial fruit crops. *Genome Biol.* 15:415. doi: 10.1186/s13059-014-0415-1

Chagné, D., Crowhurst, R. N., Troggio, M., Davey, M. W., Gilmore, B., Lawley, C., et al. (2012). Genome-wide SNP detection, validation, and development of an 8K SNP array for apple. *PLoS ONE* 7:e31745. doi: 10.1371/journal.pone.0031745

Chagné, D., Gasic, K., Crowhurst, R. N., Han, Y., Bassett, H. C., Bowatte, D. R., et al. (2008). Development of a set of SNP markers present in expressed genes of the apple. *Genomics* 92, 353–358. doi: 10.1016/j.ygeno.2008.07.008

Clark, L. V., Brummer, J. E., Glowacka, K., Hall, M. C., Heo, K., Peng, J., et al. (2014). A footprint of past climate change on the diversity and population structure of *Miscanthus sinensis*. *Ann. Bot.* 114, 97–107. doi: 10.1093/aob/mcu084

Clark, R. M., Schweikert, G., Toomajian, C., Ossowski, S., Zeller, G., Shinn, P., et al. (2007). Common sequence polymorphisms shaping genetic diversity in *Arabidopsis thaliana*. *Science* 317, 338–342. doi: 10.1126/science.1138632

Espley, R. V., Brendolise, C., Chagne, D., Kutty-Amma, S., Green, S., Volz, R., et al. (2009). Multiple repeats of a promoter segment causes transcription factor autoregulation in red apples. *Plant Cell* 21, 168–183. doi: 10.1105/tpc.108.059329

Fan, C., Hu, R., Zhang, X., Wang, X., Zhang, W., Zhang, Q., et al. (2014). Conserved CO-FT regulons contribute to the photoperiod flowering control in soybean. *BMC Plant Biol.* 14:9. doi: 10.1186/1471-2229-14-9

Feltus, F. A., Wan, J., Schulze, S. R., Estill, J. C., Jiang, N., and Paterson, A. H. (2004). An SNP resource for rice genetics and breeding based on subspecies Indica and Japonica genome alignments. *Genome Res.* 14, 1812–1819. doi: 10.1101/gr.2479404

Fornara, F., and Coupland, G. (2009). Plant phase transitions make a SPLash. *Cell* 138, 625–627. doi: 10.1016/j.cell.2009.08.011

Gasic, K., Gonzalez, D. O., Thimmapuram, J., Liu, L., Malnoy, M., Gong, G., et al. (2009). Comparative analysis and functional annotation of a large expressed sequence tag collection of apple. *Plant Genome* 2, 23–38. doi: 10.3835/plantgenome2008.11.0014

Gould, P. D., Ugarte, N., Domijan, M., Costa, M., Foreman, J., Macgregor, D., et al. (2013). Network balance via CRY signalling controls the *Arabidopsis* circadian clock over ambient temperatures. *Mol. Syst. Biol.* 9:650. doi: 10.1038/msb.2013.7

Han, Y., Gasic, K., Marron, B., Beever, J. E., and Korban, S. S. (2007). A BAC-based physical map of the apple genome. *Genomics* 89, 630–637. doi: 10.1016/j.ygeno.2006.12.010

Hirakawa, H., Shirasawa, K., Ohyama, A., Fukuoka, H., Aoki, K., Rothan, C., et al. (2013). Genome-wide SNP genotyping to infer the effects on gene functions in tomato. *DNA Res.* 20, 221–233. doi: 10.1093/dnares/dst005

Hummer, K. E., and Janick, J. (2009). "Rosaceae: taxonomy, economic importance, genomics," in *Genetics and Genomics of Rosaceae*, eds K. M. Folta and S. E. Gardiner (New York, NY: Springer), 1–17.

Jaillon, O., Aury, J.-M., Noel, B., Policriti, A., Clepet, C., Casagrande, A., et al. (2007). The grapevine genome sequence suggests ancestral hexaploidization in major angiosperm phyla. *Nature* 449, 463–467. doi: 10.1038/nature06148

Jean Finnegan, E., Bond, D. M., Buzas, D. M., Goodrich, J., Helliwell, C. A., Tamada, Y., et al. (2011). Polycomb proteins regulate the quantitative induction of VERNALIZATION INSENSITIVE 3 in response to low temperatures. *Plant J.* 65, 382–391. doi: 10.1111/j.1365-313X.2010.04428.x

Jung, J.-H., Seo, Y.-H., Seo, P. J., Reyes, J. L., Yun, J., Chua, N.-H., et al. (2007). The GIGANTEA-regulated MicroRNA172 mediates photoperiodic flowering independent of CONSTANS in *Arabidopsis*. *Plant Cell Online* 19, 2736–2748. doi: 10.1105/tpc.107.054528

Kanehisa, M., Goto, S., Kawashima, S., Okuno, Y., and Hattori, M. (2004). The KEGG resource for deciphering the genome. *Nucleic Acids Res.* 32, D277–D280. doi: 10.1093/nar/gkh063

Kim, M. Y., Lee, S., Van, K., Kim, T.-H., Jeong, S.-C., Choi, I.-Y., et al. (2010). Whole-genome sequencing and intensive analysis of the undomesticated soybean (*Glycine soja* Sieb. and Zucc.) genome. *Proc. Natl. Acad. Sci. U.S.A.* 107, 22032–22037. doi: 10.1073/pnas.1009526107

Kobayashi, S., Goto-Yamamoto, N., and Hirochika, H. (2004). Retrotransposon-induced mutations in grape skin color. *Science* 304, 982–982. doi: 10.1126/science.1095011

Koutinas, N., and Pepelyankov, G. (2010). The transition to flowering in apple. *Biotechnol. Biotechnol. Equip.* 24, 1544–1548. doi: 10.2478/V10133-010-0002-X

Lee, J., and Lee, I. (2010). Regulation and function of SOC1, a flowering pathway integrator. *J. Exp. Bot.* 61, 2247–2254. doi: 10.1093/jxb/erq098

Liu, C., Chen, H., Er, H. L., Soo, H. M., Kumar, P. P., Han, J. H., et al. (2008). Direct interaction of AGL24 and SOC1 integrates flowering signals in *Arabidopsis*. *Development* 135, 1481–1491. doi: 10.1242/dev.020255

Liu, F. Q., Quesada, V., Crevillen, P., Baurle, I., Swiezewski, S., and Dean, C. (2007). The *Arabidopsis* RNA-binding protein FCA requires a lysine-specific demethylase 1 homolog to downregulate FLC. *Mol. Cell.* 28, 398–407. doi: 10.1016/j.molcel.2007.10.018

Lyu, J., Zhang, S., Dong, Y., He, W., Zhang, J., Deng, X., et al. (2013). Analysis of elite variety tag SNPs reveals an important allele in upland rice. *Nat. Commun.* 4:2138.

McNally, K. L., Childs, K. L., Bohnert, R., Davidson, R. M., Zhao, K., Ulat, V. J., et al. (2009). Genomewide SNP variation reveals relationships among landraces and modern varieties of rice. *Proc. Natl. Acad. Sci. U.S.A.* 106, 12273–12278. doi: 10.1073/pnas.0900992106

Mimida, N., Kidou, S.-I., Lwanami, H., Moriya, S., Abe, K., Voogd, C., et al. (2011). Apple FLOWERING LOCUS T proteins interact with transcription factors implicated in cell growth and organ development. *Tree Physiol.* 31, 555–566. doi: 10.1093/treephys/tpr028

Montanari, S., Saeed, M., Knaebel, M., Kim, Y., Troggio, M., Malnoy, M., et al. (2013). Identification of pyrus single nucleotide polymorphisms (SNPs) and evaluation for genetic mapping in European Pear and Interspecific Pyrus Hybrids. *PLoS ONE* 8:e77022. doi: 10.1371/journal.pone.0077022

Mutasa-Gottgens, E., and Hedden, P. (2009). Gibberellin as a factor in floral regulatory networks. *J. Exp. Bot.* 60, 1979–1989. doi: 10.1093/jxb/erp040

Parida, S. K., Mukerji, M., Singh, A. K., Singh, N. K., and Mohapatra, T. (2012). SNPs in stress-responsive rice genes: validation, genotyping, functional relevance and population structure. *BMC Genomics* 13:426. doi: 10.1186/1471-2164-13-426

Park, S., Sugimoto, N., Larson, M. D., Beaudry, R., and Van Nocker, S. (2006). Identification of genes with potential roles in apple fruit development and biochemistry through large-scale statistical analysis of expressed sequence tags. *Plant Physiol.* 141, 811–824. doi: 10.1104/pp.106.080994

Porto, D. D., Bruneau, M., Perini, P., Anzanello, R., Renou, J.-P., Santos, H. P. D., et al. (2015). Transcription profiling of the chilling requirement for bud break in apples: a putative role for FLC-like genes. *J. Exp. Bot.* 66, 2659–2672. doi: 10.1093/jxb/erv061

Ream, T. S., Woods, D. P., Schwartz, C. J., Sanabria, C. P., Mahoy, J. A., Walters, E. M., et al. (2014). Interaction of photoperiod and vernalization determines flowering time of *Brachypodium distachyon*1[C][W][OPEN]. *Plant Physiol.* 164, 694–709. doi: 10.1104/pp.113.232678

Searle, I., and Coupland, G. (2004). Induction of flowering by seasonal changes in photoperiod. *EMBO J.* 23, 1217–1222. doi: 10.1038/sj.emboj.7600117

Subbaiyan, G. K., Waters, D. L. E., Katiyar, S. K., Sadananda, A. R., Vaddadi, S., and Henry, R. J. (2012). Genome-wide DNA polymorphisms in elite indica rice inbreds discovered by whole-genome sequencing. *Plant Biotechnol. J.* 10, 623–634. doi: 10.1111/j.1467-7652.2011.00676.x

Tatusov, R. L., Galperin, M. Y., Natale, D. A., and Koonin, E. V. (2000). The COG database: a tool for genome-scale analysis of protein functions and evolution. *Nucleic Acids Res.* 28, 33–36. doi: 10.1093/nar/28.1.33

Traenkner, C., Lehmann, S., Hoenicka, H., Hanke, M.-V., Fladung, M., Lenhardt, D., et al. (2010). Over-expression of an FT-homologous gene of apple induces early flowering in annual and perennial plants. *Planta* 232, 1309–1324. doi: 10.1007/s00425-010-1254-2

Turnbull, C. (2011). Long-distance regulation of flowering time. *J. Exp. Bot.* 62, 4399–4413. doi: 10.1093/jxb/err191

Velasco, R., Zharkikh, A., Affourtit, J., Dhingra, A., Cestaro, A., Kalyanaraman, A., et al. (2010). The genome of the domesticated apple (*Malus* × *domestica* Borkh.). *Nat. Genet.* 42, 833–839. doi: 10.1038/ng.654

Verde, I., Abbott, A. G., Scalabrin, S., Jung, S., Shu, S., Marroni, F., et al. (2013). The high-quality draft genome of peach (*Prunus persica*) identifies unique patterns of genetic diversity, domestication and genome evolution. *Nat. Genet.* 45, 487–494. doi: 10.1038/ng.2586

Wilkie, J. D., Sedgley, M., and Olesen, T. (2008). Regulation of floral initiation in horticultural trees. *J. Exp. Bot.* 59, 3215–3228. doi: 10.1093/jxb/ern188

Wu, J., Wang, Z., Shi, Z., Zhang, S., Ming, R., Zhu, S., et al. (2013). The genome of the pear (*Pyrus bretschneideri* Rehd.). *Genome Res.* 23, 396–408. doi: 10.1101/gr.144311.112

Xing, L., Zhang, D., Li, Y., Zhao, C., Zhang, S., Shen, Y., et al. (2014). Genome-wide identification of vegetative phase transition-associated microRNAs and target predictions using degradome sequencing in *Malus hupehensis*. *BMC Genomics* 15:1125. doi: 10.1186/1471-2164-15-1125

Xing, L.-B., Zhang, D., Li, Y.-M., Shen, Y.-W., Zhao, C.-P., Ma, J.-J., et al. (2015). Transcription profiles reveal sugar and hormone signaling pathways mediating flower induction in apple (*Malus domestica* Borkh.). *Plant Cell Physiol.* 56, 2052–2068. doi: 10.1093/pcp/pcv124

Xu, Q., Chen, L.-L., Ruan, X., Chen, D., Zhu, A., Chen, C., et al. (2013). The draft genome of sweet orange (*Citrus sinensis*). *Nat. Genet.* 45, 59–66. doi: 10.1038/ng.2472

Zhang, D., Teng, Y., and Bo, L. (2011). Genetic diversity of red skinned chinese sand pear cultivars revealed by AFLP markers. *Acta hortic.* 918, 679–684.

Zheng, L.-Y., Guo, X.-S., He, B., Sun, L.-J., Peng, Y., Dong, S.-S., et al. (2011). Genome-wide patterns of genetic variation in sweet and grain sorghum (*Sorghum bicolor*). *Genome Biol.* 12:R114. doi: 10.1186/gb-2011-12-11-r114

Conflict of Interest Statement: The authors declare that the research was conducted in the absence of any commercial or financial relationships that could be construed as a potential conflict of interest.

frontiers in Plant Science

ORIGINAL RESEARCH
published: 30 August 2016
doi: 10.3389/fpls.2016.01291

Metabolism of Flavonoids in Novel Banana Germplasm during Fruit Development

*Chen Dong†, Huigang Hu†, Yulin Hu and Jianghui Xie**

Key Laboratory of Tropical Fruit Biology, Ministry of Agriculture, South Subtropical Crop Research Institute, Chinese Academy of Tropical Agricultural Science, Zhanjiang, China

Banana is a commercially important fruit, but its flavonoid composition and characteristics has not been well studied in detail. In the present study, the metabolism of flavonoids was investigated in banana pulp during the entire developmental period of fruit. 'Xiangfen 1,' a novel flavonoid-rich banana germplasm, was studied with 'Brazil' serving as a control. In both varieties, flavonoids were found to exist mainly in free soluble form and quercetin was the predominant flavonoid. The most abundant free soluble flavonoid was cyanidin-3-*O*-glucoside chloride, and quercetin was the major conjugated soluble and bound flavonoid. Higher content of soluble flavonoids was associated with stronger antioxidant activity compared with the bound flavonoids. Strong correlation was observed between antioxidant activity and cyanidin-3-*O*-glucoside chloride content, suggesting that cyanidin-3-*O*-glucoside chloride is one of the major antioxidants in banana. In addition, compared with 'Brazil,' 'Xiangfen 1' fruit exhibited higher antioxidant activity and had more total flavonoids. These results indicate that soluble flavonoids play a key role in the antioxidant activity of banana, and 'Xiangfen 1' banana can be a rich source of natural antioxidants in human diets.

Keywords: banana pulp, soluble flavonoids, bound flavonoids, fruit development, antioxidant activity

OPEN ACCESS

Edited by:
Humberto Rodríguez-Fuentes, Universidad Autónoma de Nuevo León, Mexico

Reviewed by:
Jianbo Xiao, University of Macau, Macau
Maria Carmen Gomez-Jimenez, University of Extremadura, Spain

****Correspondence:***
Jianghui Xie
313972374@qq.com

† These authors have contributed equally to this work.

Specialty section:
This article was submitted to Crop Science and Horticulture, a section of the journal Frontiers in Plant Science

Received: *28 January 2016*
Accepted: *12 August 2016*
Published: *30 August 2016*

Citation:
Dong C, Hu H, Hu Y and Xie J (2016) Metabolism of Flavonoids in Novel Banana Germplasm during Fruit Development. Front. Plant Sci. 7:1291. doi: 10.3389/fpls.2016.01291

INTRODUCTION

The general role of phenolic compounds in plant physiology and allelopathy has been known for several years (Treutter, 2001). Phenolics, including flavonoids, phenolic acids, tannins, stilbenes, and lignins, have been reported as beneficial components of functional food by nutritionists (Ross et al., 2009; Bataglion et al., 2015; Kraujalytė et al., 2015; Liu et al., 2015). The flavonoids are the most abundant polyphenols in human diets (Dai and Mumper, 2010; Tsamo et al., 2015), and the most common group of polyphenols in plants as well (Xi et al., 2014). They can be generally divided into different sub-classes: flavonols, flavones, flavanonols, flavanones, flavanols, isoflavones, chalcones, and anthocyanidins (Xiao et al., 2015, 2016). Previous reports showed that different solvents used for extraction can influence the compositions of flavonoids in extracts because the solubility of each flavonoid could differ in a given solvent (Lou et al., 2014). Flavonoids have also been found in the insoluble fraction and associated with dietary fiber in tomato peel and roselle tea (Wang et al., 2016). Flavonoids exhibit anti-inflammatory, anti-neoplastic, and hepatoprotective activities, as well as strong antioxidant capacity (Lewis et al., 1999; Xi et al., 2014; Sharma et al., 2015; Xie et al., 2015). The mechanism of antioxidant activity of flavonoids involves excited oxygen species or the direct scavenging of oxygen free radicals, as well as the inhibition

of oxidative enzymes that generate these reactive oxygen species (Kang et al., 2011). The health benefits of flavonoids are well recognized (Xiao et al., 2015, 2016; Yin et al., 2015), which arouses increasing interest in researchers for the development of agronomically important food crops with optimized flavonoid levels and composition (Rodrigues et al., 2011).

Banana is one of the most important fruit crops in the world (Yue-Lian and Qing-Fang, 2011), and serves as part of a well-balanced human diet and a staple food for more than 400 million people in many tropical and subtropical countries (Sun et al., 2013; Feng et al., 2016), and their utilization can be expected to increase in the future (Pereira and Maraschin, 2015; Tsamo et al., 2015). Banana fruits have pleasant flavor and offer excellent nutritional value (Santos et al., 2010). It has been reported as an important source of phenolic compounds, with the flavonoids being the major form (Schieber et al., 2001; Vijayakumar et al., 2008). However, few data have been reported regarding flavonoid metabolism in banana. To our knowledge, metabolism in banana pulp has not been reported and changes of different categories of flavonoids across development in banana have not been analyzed thus far. This study aimed to the change of flavonoid content in banana pulp by identifying and quantifying soluble and insoluble flavonoids in banana pulp at different stages of fruit development and to investigate the antioxidant activities of individual flavonoids and their potential health effects.

MATERIALS AND METHODS

Sample Preparation

Banana fruits (*Musa* spp. AAB cv. 'Xiangfen 1' and *Musa* spp. AAA cv. 'Brazil') were obtained from a banana plantation in China (Zhanjiang, China) (**Supplementary Figures S1** and **S2**). Three uniform fruits (each fruit was a replicate) were randomly sampled at different development stages according to the cut-off bud days (days 5, 25, 45, 65, 85, and 85 + 3). These fruits were transferred to the laboratory within half an hour of collection. The tissues were immediately frozen in liquid nitrogen after sampling and stored at −80°C until further use. All analyses were performed in triplicate.

Extraction of Soluble Phenolic Compounds

The levels of soluble phenolic compounds were determined using a modified method (Butsat et al., 2009). Soluble phenolic compounds refer to free and conjugated phenolic compounds in banana pulp. In brief, 2 g of each sample was extracted with 80% methanol (3 mL × 30 mL, 30 min each) through ultrasonication. Each extract was pooled and evaporated at 45°C to 10 mL under reduced pressure. The combined solution was extracted three times with the extraction solvent (ethyl acetate:diethyl ether = 1:1). The aqueous phase was collected for the conjugated phenolic compounds, whereas the organic phase was used to extract free phenolic compounds. For conjugated phenolic compounds, 0.9 mL of hydrochloric acid was added to the aqueous phase; the mixture was extracted three times with the extraction solvent (ethyl acetate:diethyl ether = 1:1) and was then lyophilized to dryness. The residue was dissolved in 2 mL of methanol and subjected to HPLC analysis. For free phenolic compounds, the organic phase was lyophilized to dryness, and the residue was dissolved in 2 mL of methanol and subjected to HPLC analysis.

Extraction of Bound Phenolic Compounds

The bound phenolics were extracted according to the method described previously by Adom and Liu (2002) with minor modifications. In brief, the residue from the soluble fractions described above was drained and hydrolyzed directly with 2.5 M sodium hydroxide at room temperature for 12 h with shaking under nitrogen gas. The resulting solution was neutralized with an appropriate amount of hydrochloric acid and extracted with hexane to remove the lipids. The final solution was extracted three times with the extract (ethyl acetate:diethyl ether = 1:1). The organic phase was evaporated to dryness. Phenolic compounds were dissolved with 2 mL of methanol and analyzed using HPLC.

HPLC Analysis of Flavonoids

Identification and quantification of banana flavonoids were done using the following method (Dykes et al., 2011). Flavonoids were separated using a SBC-18 (250 mm × 4 mm, 5 μm) column from Agilent (USA). The column temperature was maintained at 35°C. The injection volume was 20 μl. The mobile phase consisted of 4% formic acid in water (v/v) (Solvent A) and acetonitrile (Solvent B). The solvent flow rate was 1.0 ml/min. The 3-deoxyanthocyanidins were separated using the following gradients: 0–20 min, 12–20% B; 20–40 min, 20–50% B; 40–50 min, 50% B. Flavones and flavanones were separated using different gradient: 0–45 min, 15–41% B; 45–50 min, 41% B. The 3-deoxyanthocyanidins, flavones, and flavanones were detected at 485, 340, and 280 nm, respectively. Flavonoids were identified based on the retention times of commercial standards (**Supplementary Figure S3**), UV–Vis spectra, and data reported in the literature (Lewis et al., 1999). Quantification of each compound was accomplished by comparing the peak areas with that of a calibration curve of each standard.

Determination of Total Flavonoids

Total flavonoid level was tested with Folin–Ciocalteu's phenol reagent (Bouayed et al., 2011). One gram of each sample was extracted with 3 mL 95% methanol, and then the solution was added to a 25 mL volumetric flask containing 9 mL of water. Then, 1 mL of Folin–Ciocalteu'sphenol reagent was added to the mixture and shaken. After 5 min, 10 mL of 7% aqueous Na_2CO_3 solution was added. The solution was then immediately diluted to a final volume of 25 mL with water and mixed thoroughly. After incubation for 30 min at 40°C, the absorbance versus the prepared blanks was read at 760 nm. Total phenolic content in banana was defined as milligrams of gallic acid equivalents (GAE) 1 g of fresh weight of sample.

Antioxidant Capacity

Antioxidant capacity was detected according to a previous method (Boulekbache-Makhlouf et al., 2013), with modifications. About 1 mL of the sample extract was mixed with 1 mL of phosphate buffer (0.2 M, pH 6.6) and 1 mL of 1% potassium ferricyanide [$K_3Fe(CN)_6$]. The mixture was incubated at 50°C for 20 min. Trichloroacetic acid (1 mL, 10%) was added to the solution, which was then centrifuged at 3000 × *g* for 10 min. The supernatant was gathered and mixed with distilled water (1.5 mL) and $FeCl_3$ (150 μL, 0.1%), and the absorbance was measured at 700 nm. The mean of absorbance values was plotted against concentration, and a linear regression analysis was carried out. Ascorbic acid was used as the positive control.

Soluble Sugar Content and Fruit Weight

Soluble sugar content in the pulp extracts was determined using the anthrone method of Yemm and Willis (1954). Fruit weight was recorded using an electronic scale (METTLER TOLEDO, ME303).

Chemicals

All flavonoids standards (purity ≥ 98%, HPLC) were purchased from Sigma–Aldrich (St. Louis, MO, USA).

Statistical Analysis

Data were analyzed statistically by ANOVA, and differences in means were evaluated using Duncan's new multiple range test ($P < 0.05$) with SPSS version 16.0 (SPSS Inc., Chicago, IL, USA). Pearson's correlations were calculated to determine relationship among the measured variables.

RESULTS

Quercetin

The free soluble quercetin is relatively, whereas the conjugated soluble quercetin is abundant low in 'Brazil' banana (**Figure 1A**), with the highest level of free soluble quercetin observed on day 5. The lowest conjugated soluble quercetin level was observed on day 65, and the highest level was noted on day 85. Levels of bound quercetin increased during the early developmental period, reached its maximum level on day 45, and then decreased gradually afterward.

In 'Xiangfen 1' banana (**Figure 1B**), free soluble quercetin was undetected during the entire developmental period. It predominantly expressed the conjugated soluble quercetin.

In comparison, conjugated soluble quercetin and bound quercetin were the two main forms of quercetin and levels of conjugated soluble quercetin peaked on day 85 in both 'Brazil' and 'Xiangfen 1' banana. 'Xiangfen 1' exhibited twofold higher conjugated soluble quercetin content at the late developmental period compared with 'Brazil.' The total quercetin levels in 'Xiangfen 1' were higher than those in 'Brazil' at all stages, except for day 45. Collectively, these data suggested that conjugated soluble quercetin might be the main flavonoid in banana.

Cyanidin-3-*O*-Glucoside Chloride

As shown in **Figure 2A**, in 'Brazil' banana, the level of free soluble cyanidin-3-*O*-glucoside chloride were significantly higher than those of other forms of cyanidin-3-*O*-glucoside chloride ($P < 0.05$), and the level of bound cyanidin-3-*O*-glucoside chloride were the lowest. The level of free soluble cyanidin-3-*O*-glucoside chloride peaked on day 25, which was more than 10-fold higher than those on other days ($P < 0.05$). The highest level of conjugated soluble cyanidin-3-*O*-glucoside chloride was also observed on day 25. The bound cyanidin-3-*O*-glucoside chloride was not obtained till day 65, with its highest level shown on day 88 and the lowest level on day 85.

In 'Xiangfen 1' banana (**Figure 2B**), no free soluble cyanidin-3-*O*-glucoside chloride was detected on days 25, 45, and 88. The greatest level of free soluble cyanidin-3-*O*-glucoside chloride was found at the initial stage, and the lowest level was observed on day 85. The levels of both the conjugated soluble and bound cyanidin-3-*O*-glucoside chlorides were low during fruit development, with the conjugated soluble cyanidin-3-*O*-glucoside chloride increased gradually from day 25 to day 85 and the bound cyanidin-3-*O*-glucoside chloride peaked on day 88.

The level of cyanidin-3-*O*-glucoside chloride in 'Brazil' was significantly higher ($P < 0.05$) than those in 'Xiangfen 1' on days 25 and 45, but the level in 'Xiangfen 1' sharply increased by day 65 and were greater than those in 'Brazil' banana on days 65 and 85. Overall, the cyanidin-3-*O*-glucoside chloride mainly exists in free soluble form in banana fruits of both varieties, but its level is relatively higher in 'Brazil' than 'Xiangfen 1.'

Ellagic Acid

Figure 3A showed that free soluble ellagic acid was the main form of ellagic acid in 'Brazil' banana. The level of free soluble ellagic acid was very low during the initial period, but greatly increased after day 25, peaking on day 65.

For the 'Xiangfen 1' banana (**Figure 3B**), the free soluble ellagic acid was the sole form of ellagic acid. The free soluble ellagic acid content was lower at the early stage compared with those at the later stage. The greatest level of free soluble ellagic acid was found on day 65, after that it gradually decreased. The level of ellagic acid in 'Xiangfen 1' banana were higher than that in 'Brazil' banana at all stages.

Catechin

Free soluble catechin was the major type of catechin in 'Brazil' (**Figure 4A**). The highest level of free soluble catechin was observed on day 25 and then gradually decreased from day 25 to day 85. Conjugated soluble catechin was detected only on day 45.

The catechin in 'Xiangfen 1' was present mainly in free soluble form (**Figure 4B**), which gradually increased from day 5 to day 45 but after that it decreased quickly till day 65. Thus, the free soluble catechin level was significantly higher ($P < 0.05$) on day 45 than day 65. In fruits of both cultivars, high level of catechin was found on days 25 and 45, with the 'Brazil' showing a higher catechin level.

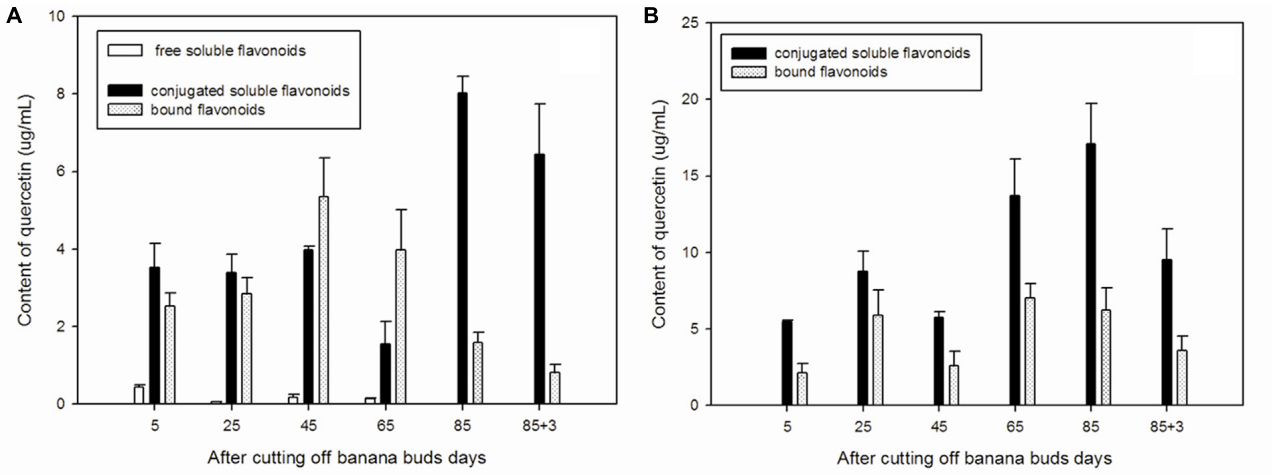

FIGURE 1 | Changes of quercetin levels in banana pulp during the development stage. (A) 'Brazil' banana, **(B)** 'Xiangfen 1' banana.

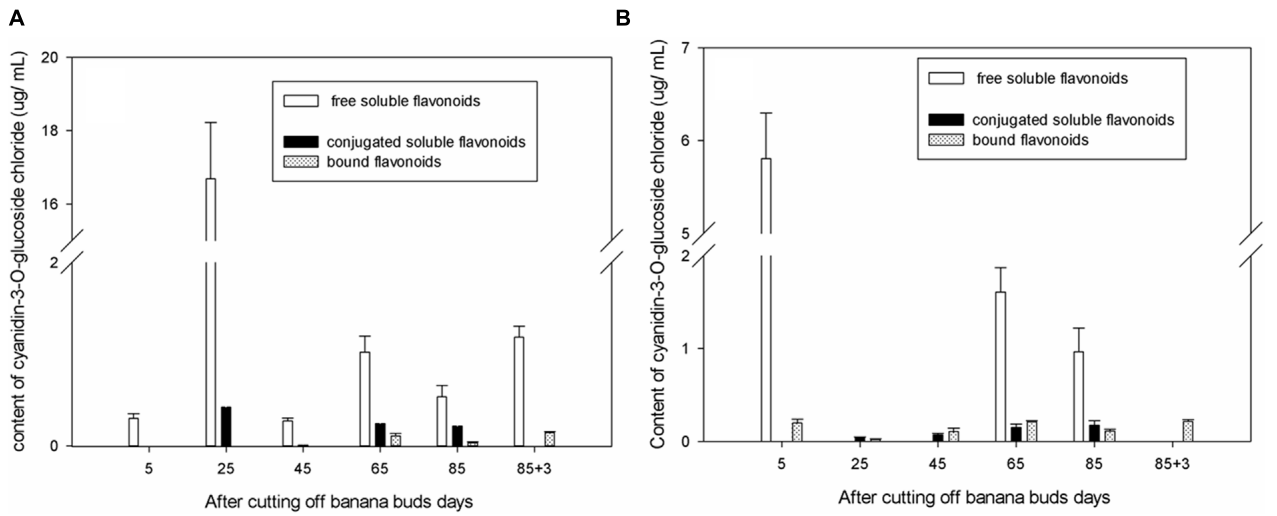

FIGURE 2 | Changes of cyanidin-3-*O*-glucoside chloride levels in banana pulp during the development stage. (A) 'Brazil' banana, **(B)** 'Xiangfen 1' banana.

Gallocatechin

Free and conjugated soluble gallocatechin were the main types of gallocatechin in 'Brazil' banana (**Figure 5A**), as no bound gallocatechin was observed at any stage. The free soluble gallocatechin in 'Brazil' banana was observed on days 5, 25, and 45, and its concentration was ninefold higher on day 25 than that on day 5. The conjugated soluble gallocatechin was detected from day 45 to day 88, with the highest level found on day 65.

The conjugated soluble form of gallocatechin was dominant in 'Xiangfen 1' (**Figure 5B**), with its highest level observed on day 45. Its level was significantly higher than the free soluble gallocatechin level on the same day ($P < 0.05$).

The highest level of gallocatechin in both types of banana was found on day 45. 'Xiangfen 1' showed a higher level of gallocatechin 'Brazil' at all stages except day 85. These observations reveal that the middle developmental period is an important stage for gallocatechin formation in banana.

Soluble and Bound Flavonoids

As shown in **Figure 6A**, the soluble flavonoid content in 'Brazil' peaked on day 25 (21.40 μg/mL) and then gradually decreased till day 65 to reach the lowest level (3.50 μg/mL). For bound flavonoids, the highest and lowest contents were observed on days 45 and 88, respectively. The soluble content was evidently higher than the bound content on days 25, 85, and 88 ($P < 0.05$).

In contrast, the content of soluble flavonoid in 'Xiangfen 1' (**Figure 6B**) peaked on day 85 (18.85 μg/mL), and the highest content of bound flavonoid was observed on day 65 (7.23 μg/mL). The content of soluble flavonoids were evidently greater than that of bound flavonoids in the entire developmental

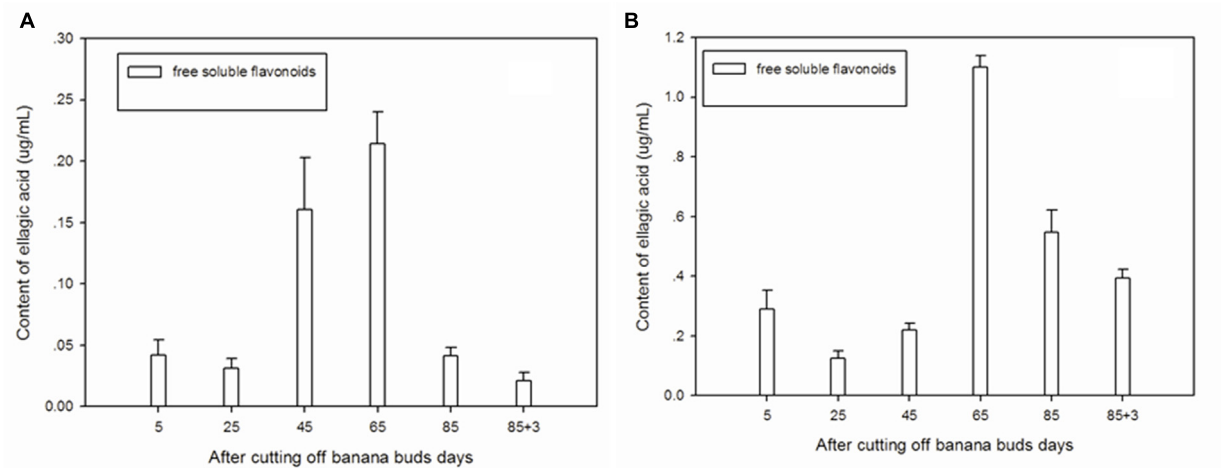

FIGURE 3 | Changes of ellagic acid levels in banana pulp during the development stage. (A) 'Brazil' banana, **(B)** 'Xiangfen 1' banana.

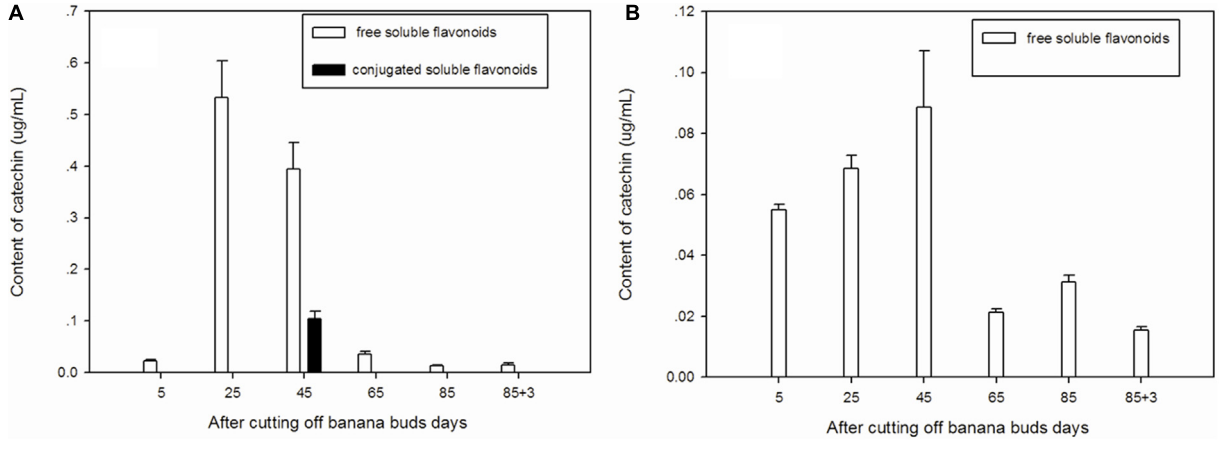

FIGURE 4 | Changes of catechin levels in banana pulp during the development stage. (A) 'Brazil' banana, **(B)** 'Xiangfen 1' banana.

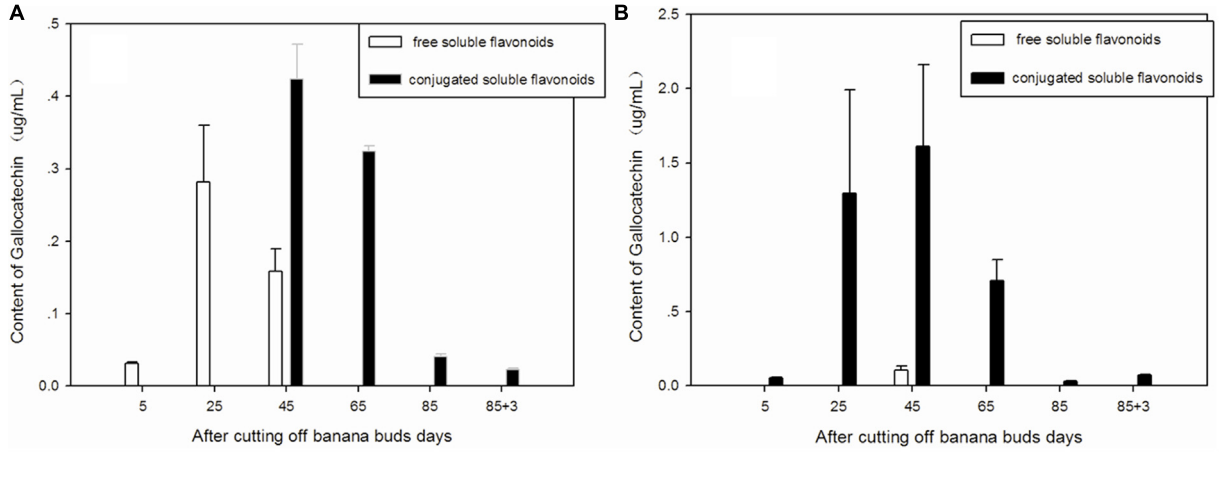

FIGURE 5 | Changes of gallocatechin levels in banana pulp during the development stage. (A) 'Brazil' banana, **(B)** 'Xiangfen 1' banana.

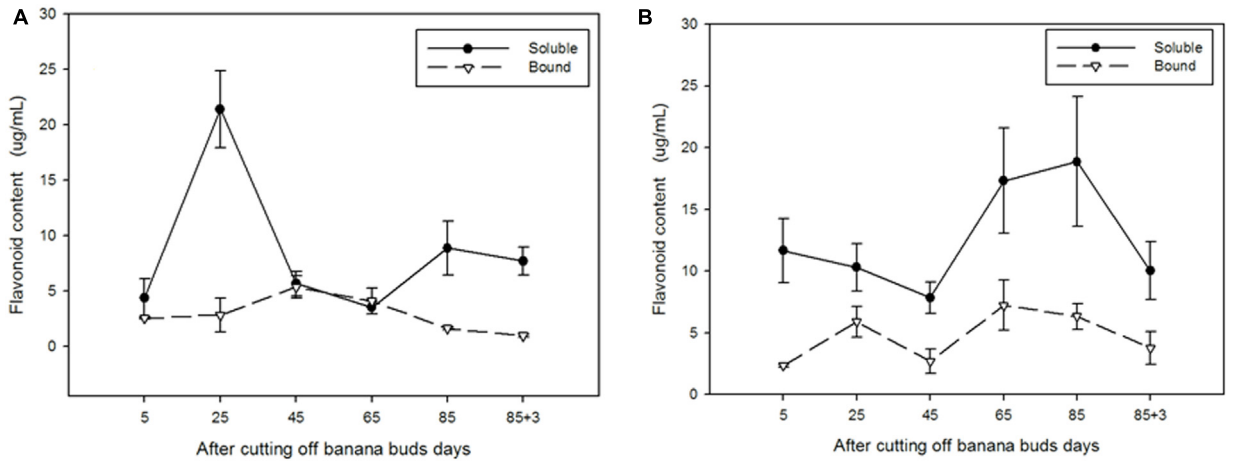

FIGURE 6 | The contents of soluble and bound flavonoids in 'Brazil' banana (A) and 'Xiangfen 1' banana (B).

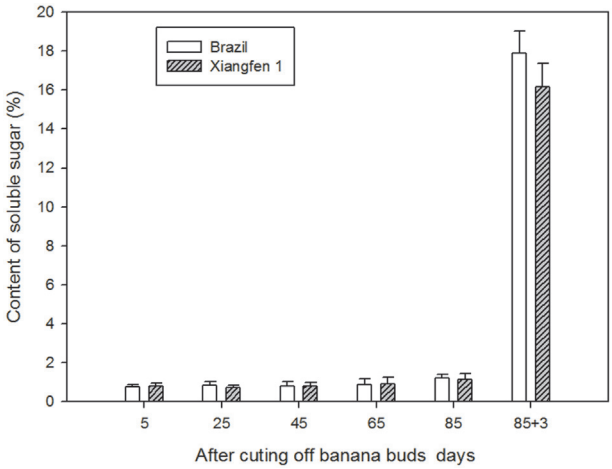

FIGURE 7 | Changes of soluble sugar levels in banana pulp during the development stage.

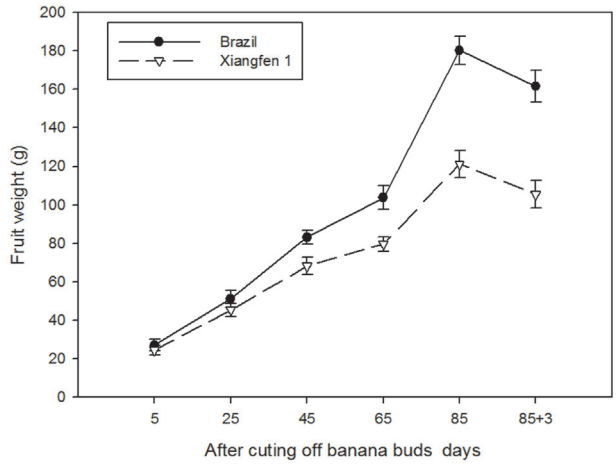

FIGURE 8 | Changes of fruit weight in banana pulp during the development stage.

period ($P < 0.05$). These results show that most of the flavonoids in banana pulp are soluble.

Soluble Sugar

The soluble sugar content was low in both types of fruits (before day 85, **Figure 7**), and there were no significant differences between them. However, the content increased sharply (from 1.2 to 17.9%) during the harvesting period (after day 85), with 'Brazil' showing a higher level than 'Xiangfen 1' on day 88, indicating the harvesting period is a crucial time for accumulation of soluble sugar content in banana.

Fruit Weight

As shown in **Figure 8**, the fruit weight in the two types of banana increased gradually with fruit development, and decreased after day 85. The fruit weight in 'Brazil' was significantly higher than that in 'Xiangfen 1' from day 45 to day 88 ($P < 0.05$). However, from day 5 to day 25, no significant difference was detected between the two types of banana. These findings reveal that difference in fruit weight among different types of banana is likely determined in the later developmental period.

Antioxidant Capacity of Soluble and Bound Flavonoids

For soluble flavonoids in 'Brazil', as shown in **Figure 9A**, the extracts on day 25 exhibited significantly higher antioxidant capacity than those on other days ($P < 0.05$), with the lowest antioxidant capacity showed on day 65 (0.72 $U \cdot g^{-1}$ FW). For bound flavonoids, the antioxidant capacity increased from day 5 to day 45 and then decreased till day 88. In comparison, the soluble flavonoids showed greater antioxidant capacity the bound ones at all stages except for days 45 and 65.

The antioxidant capacity of 'Xiangfen 1' fruit was evaluated as well (**Figure 9B**). For soluble flavonoids, the antioxidant capacity peaked and bottomed on day 85 (4.11 $U \cdot g^{-1}$ FW) and on day 45 (1.71 $U \cdot g^{-1}$ FW), respectively. For bound flavonoids, the strongest (1.68 $U \cdot g^{-1}$ FW) and lowest antioxidant capacities (0.56 $U \cdot g^{-1}$ FW) were observed on days 85 and 5, respectively. Similarly, the soluble flavonoids had higher antioxidant capacities compared with the bound extracts at all stages. These results indicate that soluble flavonoids are probably the major antioxidants in banana.

Total Flavonoid and Total Antioxidant Capacity (TAC)

As shown in **Figure 10A**, the level of total flavonoid gradually decreased with fruit development in 'Xiangfen 1.' The highest total flavonoid level was detected on day 5 and then decreased quickly till day 25. Consequently, a significantly lower total flavonoid level ($P < 0.05$) was observed on day 25 compared with that on day 5 in 'Xiangfen 1.' For the 'Brazil' fruits, the level of total flavonoid increased at the beginning and peaked on day 45, and gradually decreased thereafter. The total flavonoid level was significantly higher in 'Xiangfen 1' than that in 'Brazil' during the early developmental stage.

The TAC in 'Xiangfen 1' slowly increased at the beginning and then gradually decreased from day 25 to day 88 (**Figure 10B**). As a result, the highest TAC was detected on day 25, and the lowest TAC on day 88. The TAC fluctuated in the 'Brazil' fruits, with the highest TAC observed on day 25 and the lowest TAC on day 5.

The TAC in 'Xiangfen 1' was significantly higher than that in 'Brazil' in the first 65 days. No significant difference of TAC was found between them during the later period of development. These findings reveal that increase in flavonoids, both in soluble and bound forms, might contribute to increase in antioxidant activity in banana.

Correlation

Pearson correlations were calculated for the objective variables measured during banana development (**Tables 1** and **2**). The results showed statistically significant correlations ($r = 0.813$) between TAC and the level of cyanidin-3-*O*-glucoside chloride ($P < 0.05$; **Table 1**), which indicated that cyanidin-3-*O*-glucoside chloride likely plays a major role in the antioxidative activity in 'Brazil' banana. For 'Xiangfen 1' (**Table 2**), TAC was highly correlated with the flavonoid content ($r = 0.862$), which suggested that flavonoid was the main antioxidative component in the pulp. Significant correlations were also found between the flavonoid content and cyanidin-3-*O*-glucoside chloride level ($r = 0.834$). Taken together, these results illustrate that cyanidin-3-*O*-glucoside chloride, as a main type of flavonoids, is one of the major antioxidants in banana.

DISCUSSION

Flavonoids are the largest group of polyphenolic plant secondary metabolites (Rodrigues et al., 2011). Different subclasses of flavonoids exist in banana fruits (Tsamo et al., 2015), and flavonoids of different banana varieties share some characteristics (Bennett et al., 2010). In this study, five flavonoids (quercetin, cyanidin-3-*O*-glucoside chloride, ellagic acid, catechin, and gallocatechin) were detected in both banana varieties at all fruit developmental stages. This result is in agreement with a previous study (Someya et al., 2002), which also identified gallocatechin and anthocyanin in banana fruits. However, rutin and epicatechin were only found at some stages in both banana varieties, which is consistent with a previous study by Bennett et al. (2010) on banana fruit. It has been recognized that some fruits contain abundant quercetin (Kuti, 2004), which is one of the most commonly consumed flavonoids that has been studied for its potential health benefits (Kuti, 2004; Tsamo et al., 2015). In this study, quercetin was the predominant flavonoid at all stages in both types of banana. Moreover, the quercetin

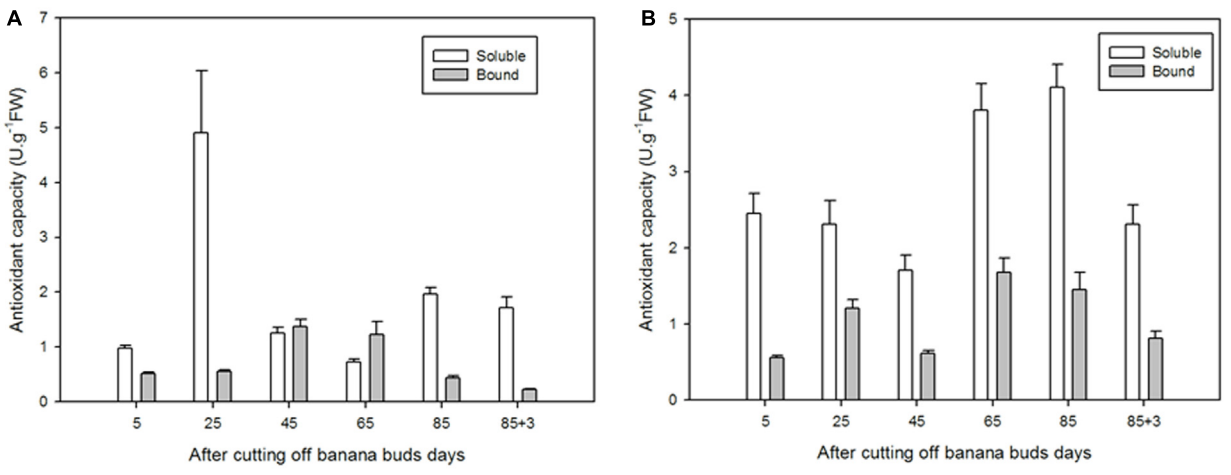

FIGURE 9 | The antioxidant capacities of soluble and bound flavonoids in 'Brazil' banana (A) and 'Xiangfen 1' banana (B).

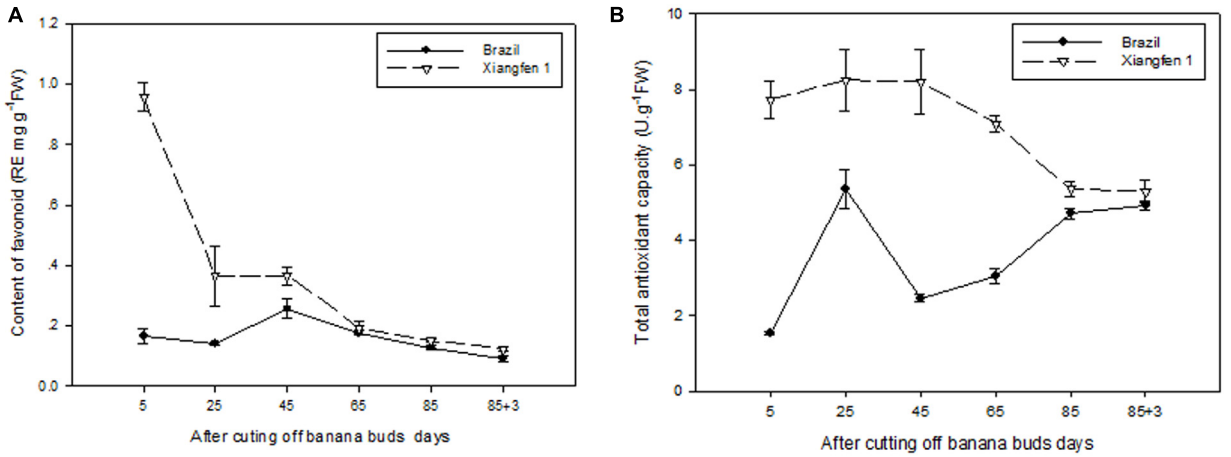

FIGURE 10 | Changes of total flavonoid level (A) and total antioxidant capacity (B) in banana pulp during the development stage.

TABLE 1 | Pearson correlations among total antioxidant capacity (TAC) and flavonoid of pulp during the development of 'Brazil' banana.

	TAC	Flavonoid	Quercetin	Cyanidin-3-*O*-glucoside chloride	Ellagic acid	Catechin	Gallocatechin
TAC	1	−0.665	0.058	0.813*	−0.481	0.386	−0.748
Flavonoid	−0.665	1	0.267	−0.189	0.695	0.167	0.987
Quercetin	0.058	0.267	1	−0.469	−0.085	0.580	0.958
Cyanidin-3-*O*-glucoside chloride	0.813*	−0.189	−0.469	1	−0.401	0.504	−0.655
Ellagic acid	−0.481	0.695	−0.085	−0.401	1	−0.768	0.358
Catechin	0.386	0.167	0.580	0.504	−0.768	1	0.323
Gallocatechin	−0.748	0.987	0.958	−0.655	0.358	0.323	1

**Significant difference at $P < 0.05$.*

TABLE 2 | Pearson correlations among TAC and flavonoid of pulp during the development of 'Xiangfen 1' banana.

	TAC	Flavonoid	Quercetin	Cyanidin-3-*O*-glucoside chloride	Ellagic acid	Catechin	Ggallocatechin
TAC	1	0.862*	−0.551	0.568	−0.339	0.754	0.897
Flavonoid	0.862*	1	−0.676	0.834*	−0.391	−0.802	0.914
Quercetin	−0.551	−0.676	1	−0.286	0.662	−0.019	−0.994
Cyanidin-3-*O*-glucoside chloride	0.568	0.834*	−0.286	1	0.101	−0.793	−0.888
Ellagic acid	−0.339	−0.391	0.662	0.101	1	−0.315	−0.871
Catechin	0.754	−0.802	−0.019	−0.793	−0.315	1	0.654
Gallocatechin	0.897	0.914	−0.994	−0.888	−0.871	0.654	1

**Significant difference at $P < 0.05$.*

content was the highest among conjugated soluble flavonoids and bound flavonoids. Free soluble flavonoids were the main types of flavonoids in 'Xiangfen 1' banana and 'Brazil' banana. This finding agreed with the results of Lou et al. (2014), who reported that the free soluble flavonoid content was significantly higher than that of other flavonoids in calamondin. Most of phenolic compounds with antioxidant activity in jujube existed as the free form (Wang et al., 2016).

Diverse flavonoid traits were found in different banana varieties (Bennett et al., 2010; Tsamo et al., 2015). In this study, the total quercetin, total ellagic acid, and gallocatechin contents of 'Xiangfen 1' banana during the entire developmental period were higher than those in 'Brazil' banana, whereas the cyanidin-3-*O*-glucoside chloride and catechin contents were lower in 'Xiangfen 1' banana than in 'Brazil' banana. A similar study report significant differences in total flavonols concentration of onion were observed between varieties (Rodrigues et al., 2011). Flavonoids have been shown to exhibit strong antioxidant capacities (Kang et al., 2011; Lou et al., 2015; Sait et al., 2015; Yang et al., 2015). In the present study, the total flavonoid content of 'Xiangfen 1' banana was higher than that of 'Brazil' banana during the first 45 days. During the same period, the

antioxidant capacity of 'Xiangfen 1' banana was also stronger than that of 'Brazil' banana. This result is in agreement with the study of Vijayakumar et al. (2008), who found that flavonoids from banana act as effective antioxidants. Another similar study showed that NO treatment significantly enhanced flavonoid contents in the mushrooms and the antioxidant activities in the NO-fumigated mushrooms were highly correlated with the contents of flavonoids (Dong et al., 2012). Study has shown that anthocyanins are the largest and most important group of water-soluble and vacuolar pigments in nature (Cavalcanti et al., 2011) and it have been identified in wild banana bracts (Kitdamrongsont et al., 2008). In the present study, the major free soluble flavonoid was cyanidin-3-*O*-glucoside chloride in banana pulp. Anthocyanins are pigments with a wide range of biological effects, including antioxidant activity (Cavalcanti et al., 2011; Li et al., 2014; Lee et al., 2015). The present results showed that cyanidin-3-*O*-glucoside chloride level was closely related to the antioxidant capacity of 'Brazil' banana, and the total flavonoid content was significantly correlated with the antioxidant capacity of 'Xiangfen 1' banana. Moreover, significant correlation was found between cyanidin-3-*O*-glucoside chloride content and total flavonoid content in 'Xiangfen 1' banana, suggesting that cyanidin-3-*O*-glucoside chloride is responsible for the antioxidant activity of banana. A similar result was also reported for 'dabai' fruits, which contain phenolic compounds (including flavonoids and anthocyanin) and exhibit strong antioxidant activity (Chew et al., 2011). However, further studies need to be performed to evaluate the role of these individual flavonoids that contribute to antioxidant activity.

CONCLUSION

In this study, the flavonoid profiles of banana pulp during the developmental period were monitored from the fruitlet stage to the fully ripe stage. Quercetin was the predominant flavonoid in the tested banana varieties and also the main conjugated soluble and bound flavonoid. The majority of the flavonoids were present in free soluble form, and cyanidin-3-*O*-glucoside chloride was the dominant free soluble flavonoid in all pulp extracts. High antioxidant activity was correlated to the levels of total flavonoid and cyanidin-3-*O*-glucoside chloride. The total flavonoid content was higher in 'Xiangfen 1' banana than that in the control variety, which is consistent with the antioxidant activity profile of 'Xiangfen 1' banana. Fruit weight and soluble sugar content in both varieties increased quickly during the later developmental period. Our results revealed that the levels and compositions of flavonoids vary considerably during the growth and development of banana. The observed levels of flavonoid, especially cyanidin-3-*O*-glucoside chloride, and the antioxidant properties of pulp extracts indicate that banana pulp can be a valuable source of antioxidant-rich nutraceuticals.

AUTHOR CONTRIBUTIONS

JX, HH, and CD conceived and designed the experiments. CD and YH performed the experiments and helped with the data analysis. HH and CD wrote the paper. All authors read and approved the final manuscript.

ACKNOWLEDGMENTS

This work was supported by the Public welfare research project (Project No.201503142-13), Modern Agro-industry Technology Research System (Project No.CARS-32-12), and the National Natural Science Foundation of China (Project No.31301756).

SUPPLEMENTARY MATERIAL

The Supplementary Material for this article can be found online at: http://journal.frontiersin.org/article/10.3389/fpls.2016.01291

FIGURE S1 | 'Brazil' banana and the orange pulp banana variety 'Xiangfen 1'.

FIGURE S2 | The banana in different developmental stages.

FIGURE S3 | HPLC chromatogram of standard flavonoids (A) and sample extract (B).

REFERENCES

Adom, K. K., and Liu, R. H. (2002). Antioxidant activity of grains. *J. Agric. Food Chem.* 50, 6182–6187. doi: 10.1021/jf0205099

Bataglion, G. A., da Silva, F. M., Eberlin, M. N., and Koolen, H. H. (2015). Determination of the phenolic composition from Brazilian tropical fruits by UHPLC–MS/MS. *Food chem.* 180, 280–287. doi: 10.1016/j.foodchem.2015.02.059

Bennett, R. N., Shiga, T. M., Hassimotto, N. M., Rosa, E. A., Lajolo, F. M., and Cordenunsi, B. R. (2010). Phenolics and antioxidant properties of fruit pulp and cell wall fractions of postharvest banana (*Musa acuminata* Juss.) cultivars. *J. Agric. Food Chem.* 58, 7991–8003. doi: 10.1021/jf1008692

Bouayed, J., Hoffmann, L., and Bohn, T. (2011). Total phenolics, flavonoids, anthocyanins and antioxidant activity following simulated gastro-intestinal digestion and dialysis of apple varieties: bioaccessibility and potential uptake. *Food chem.* 128, 14–21. doi: 10.1016/j.foodchem.2011.02.052

Boulekbache-Makhlouf, L., Slimani, S., and Madani, K. (2013). Total phenolic content, antioxidant and antibacterial activities of fruits of *Eucalyptus globulus* cultivated in Algeria. *Ind. Crops Prod.* 41, 85–89. doi: 10.1016/j.indcrop.2012.04.019

Butsat, S., Weerapreeyakul, N., and Siriamornpun, S. (2009). Changes in phenolic acids and antioxidant activity in Thai rice husk at five growth stages during grain development. *J. Agric. Food Chem.* 57, 4566–4571. doi: 10.1021/jf900549

Cavalcanti, R. N., Santos, D. T., and Meireles, M. A. A. (2011). Non-thermal stabilization mechanisms of anthocyanins in model and food systems—An overview. *Food Res. Int.* 44, 499–509. doi: 10.1016/j.foodres.2010.12.007

Chew, L. Y., Prasad, K. N., Amin, I., Azrina, A., and Lau, C. Y. (2011). Nutritional composition and antioxidant properties of *Canarium odontophyllum* Miq. (dabai) fruits. *J. Food Compost. Anal.* 24, 670–677. doi: 10.1016/j.jfca.2011.01.006

Dai, J., and Mumper, R. J. (2010). Plant phenolics: extraction, analysis and their antioxidant and anticancer properties. *Molecules* 15, 7313–7352. doi: 10.3390/molecules15107313

Dong, J., Zhang, M., Lu, L., Sun, L., and Xu, M. (2012). Nitric oxide fumigation stimulates flavonoid and phenolic accumulation and enhances antioxidant activity of mushroom. *Food Chem.* 135, 1220–1225. doi: 10.1016/j.foodchem.2012.05.055

Dykes, L., Peterson, G. C., Rooney, W. L., and Rooney, L. W. (2011). Flavonoid composition of lemon-yellow sorghum genotypes. *Food chem.* 128, 173–179. doi: 10.1016/j.foodchem.2011.03.020

Feng, B., Han, Y., Xiao, Y., Kuang, J., Fan, Z., Chen, J., et al. (2016). The banana fruit Dof transcription factor MaDof23 acts as a repressor and interacts with MaERF9 in regulating ripening-related genes. *J. Exp. Bot.* 67, 2263–2275. doi: 10.1093/jxb/erw032

Kang, J., Xie, C., Li, Z., Nagarajan, S., Schauss, A. G., Wu, T., et al. (2011). Flavonoids from acai (*Euterpe oleracea* Mart.) pulp and their antioxidant and anti-inflammatory activities. *Food chem.* 128, 152–157. doi: 10.1016/j.foodchem.2011.03.011

Kitdamrongsont, K., Pothavorn, P., Swangpol, S., Wongniam, S., Atawongsa, K., Svasti, J., et al. (2008). Anthocyanin composition of wild bananas in Thailand. *J. Agric. Food Chem.* 56, 10853–10857. doi: 10.1021/jf8018529

Kraujalytė, V., Venskutonis, P. R., Pukalskas, A., Česonienė, L., and Daubaras, R. (2015). Antioxidant properties, phenolic composition and potentiometric sensor array evaluation of commercial and new blueberry (*Vaccinium corymbosum*) and bog blueberry (*Vaccinium uliginosum*) genotypes. *Food chem.* 188, 583–590. doi: 10.1016/j.foodchem.2015.05.031

Kuti, J. O. (2004). Antioxidant compounds from four *Opuntia cactus* pear fruit varieties. *Food chem.* 85, 527–533. doi: 10.1016/S0308-8146(03)00184-5

Lee, E. J., Patil, B. S., and Yoo, K. S. (2015). Antioxidants of 15 onions with white, yellow, and red colors and their relationship with pungency, anthocyanin, and quercetin. *LWT-Food Sci. Technol.* 63, 108–114. doi: 10.1016/j.lwt.2015.03.028

Lewis, D. A., Fields, W. N., and Shaw, G. P. (1999). A natural flavonoid present in unripe plantain banana pulp (*Musa sapientum* L. var. paradisiaca) protects the gastric mucosa from aspirin-induced erosions. *J. Ethnopharmacol.* 65, 283–288. doi: 10.1016/S0378-8741(99)00005-7

Li, D., Luo, Z., Mou, W., Wang, Y., Ying, T., and Mao, L. (2014). ABA and UV-C effects on quality, antioxidant capacity and anthocyanin contents of strawberry fruit (*Fragaria ananassa* Duch.). *Postharvest Biol. Technol.* 90, 56–62. doi: 10.1016/j.postharvbio.2013.12.006

Liu, H., Cao, J., and Jiang, W. (2015). Evaluation and comparison of vitamin C, phenolic compounds, antioxidant properties and metal chelating activity of pulp and peel from selected peach cultivars. *LWT Food Sci. Technol.* 63, 1042–1048. doi: 10.1016/j.lwt.2015.04.052

Lou, S.-N., Lai, Y.-C., Huang, J.-D., Ho, C.-T., Ferng, L.-H. A., and Chang, Y.-C. (2015). Drying effect on flavonoid composition and antioxidant activity of immature kumquat. *Food chem.* 171, 356–363. doi: 10.1016/j.foodchem.2014.08.119

Lou, S.-N., Lin, Y.-S., Hsu, Y.-S., Chiu, E.-M., and Ho, C.-T. (2014). Soluble and insoluble phenolic compounds and antioxidant activity of immature calamondin affected by solvents and heat treatment. *Food Chem.* 161, 246–253. doi: 10.1016/j.foodchem.2014.04.009

Pereira, A., and Maraschin, M. (2015). Banana (*Musa* spp) from peel to pulp: ethnopharmacology, source of bioactive compounds and its relevance for human health. *J. Ethnopharmacol.* 160, 149–163. doi: 10.1016/j.jep.2014.11.008

Rodrigues, A., Pérez-Gregorio, M., García-Falcón, M., Simal-Gándara, J., and Almeida, D. (2011). Effect of meteorological conditions on antioxidant flavonoids in Portuguese cultivars of white and red onions. *Food chem.* 124, 303–308. doi: 10.1016/j.foodchem.2010.06.037

Ross, K., Beta, T., and Arntfield, S. (2009). A comparative study on the phenolic acids identified and quantified in dry beans using HPLC as affected by different extraction and hydrolysis methods. *Food chem.* 113, 336–344. doi: 10.1016/j.foodchem.2008.07.064

Sait, S., Hamri-Zeghichi, S., Boulekbache-Makhlouf, L., Madani, K., Rigou, P., Brighenti, V., et al. (2015). HPLC-UV/DAD and ESI-MSn analysis of flavonoids and antioxidant activity of an Algerian medicinal plant: *Paronychia argentea* Lam. *J. Pharm.Biomed. Anal.* 111, 231–240. doi: 10.1016/j.jpba.2015.03.027

Santos, J. U., Bakry, F., and Brillouet, J. (2010). A preliminary chemotaxonomic study on the condensed tannins of green banana flesh in the Musa genus. *Biochem. Syst. Ecol.* 38, 1010–1017. doi: 10.1016/j.bse.2010.10.001

Schieber, A., Stintzing, F. C., and Carle, R. (2001). By-products of plant food processing as a source of functional compounds—recent developments. *Trends Food Sci. Technol.* 12, 401–413. doi: 10.1016/S0924-2244(02)00012-2

Sharma, K., Ko, E. Y., Assefa, A. D., Ha, S., Nile, S. H., Lee, E. T., et al. (2015). Temperature-dependent studies on the total phenolics, flavonoids, antioxidant activities, and sugar content in six onion varieties. *J. Food Drug Anal.* 23, 243–252. doi: 10.1016/j.jfda.2014.10.005

Someya, S., Yoshiki, Y., and Okubo, K. (2002). Antioxidant compounds from bananas (*Musa* Cavendish). *Food chem.* 79, 351–354. doi: 10.1016/S0308-8146(02)00186-3

Sun, D., Lu, X., Hu, Y., Li, W., Hong, K., Mo, Y., et al. (2013). Methyl jasmonate induced defense responses increase resistance to *Fusarium oxysporum* f. sp. cubense race 4 in banana. *Sci. Hortic.* 164, 484–491. doi: 10.1016/j.scienta.2013.10.011

Treutter, D. (2001). Biosynthesis of phenolic compounds and its regulation in apple. *Plant Growth Regul.* 34, 71–89. doi: 10.1023/A:1013378702940

Tsamo, C. V. P., Herent, M.-F., Tomekpe, K., Emaga, T. H., Quetin-Leclercq, J., Rogez, H., et al. (2015). Phenolic profiling in the pulp and peel of nine plantain cultivars (*Musa* sp.). *Food chem.* 167, 197–204. doi: 10.1016/j.foodchem.2014.06.095

Vijayakumar, S., Presannakumar, G., and Vijayalakshmi, N. (2008). Antioxidant activity of banana flavonoids. *Fitoterapia* 79, 279–282. doi: 10.1016/j.fitote.2008.01.007

Wang, B., Huang, Q., Venkitasamy, C., Chai, H., Gao, H., Cheng, N., et al. (2016). Changes in phenolic compounds and their antioxidant capacities in jujube (*Ziziphus jujuba* Miller) during three edible maturity stages. *LWT Food Sci. Technol.* 66, 56–62. doi: 10.1016/j.lwt.2015.10.005

Xi, W., Fang, B., Zhao, Q., Jiao, B., and Zhou, Z. (2014). Flavonoid composition and antioxidant activities of Chinese local pummelo (*Citrus grandis* Osbeck.) varieties. *Food chem.* 161, 230–238. doi: 10.1016/j.foodchem.2014.04.001

Xiao, J., Capanoglu, E., Jassbi, A. R., and Miron, A. (2016). Advance on the Flavonoid C-glycosides and health benefits. *Crit. Rev. Food Sci. Nutr.* 56, 29–45. doi: 10.1080/10408398.2015.1067595

Xiao, J., Ni, X., Kai, G., and Chen, X. (2015). Advance in dietary polyphenols as aldose reductases inhibitors: structure-activity relationship aspect. *Crit. Rev. Food Sci. Nutr.* 55, 16–31. doi: 10.1080/10408398.2011.584252

Xie, Y., Zheng, Y., Dai, X., Wang, Q., Cao, J., and Xiao, J. (2015). Seasonal dynamics of total flavonoid contents and antioxidant activity of *Dryopteris erythrosora*. *Food chem.* 186, 113–118. doi: 10.1016/j.foodchem.2014.05.024

Yang, D., Xie, H., Jia, X., and Wei, X. (2015). Flavonoid C-glycosides from star fruit and their antioxidant activity. *J. Funct. Foods* 16, 204–210. doi: 10.1016/j.jff.2015.04.048

Yemm, E. W., and Willis, A. J. (1954). The estimation of carbohydrates in plant extracts by anthrone. *Biochem. J.* 57, 508. doi: 10.1042/bj0570508

Yin, D.-D., Yuan, R.-Y., Wu, Q., Li, S.-S., Shao, S., Xu, Y.-J., et al. (2015). Assessment of flavonoids and volatile compounds in tea infusions of water lily flowers and their antioxidant activities. *Food chem.* 187, 20–28. doi: 10.1016/j.foodchem.2015.04.032

Yue-Lian, L., and Qing-Fang, L. (2011). Identification and cultivation of a wild mushroom from banana pseudo-stem sheath. *Sci. Hortic.* 129, 922–925. doi: 10.1016/j.scienta.2011.06.002

Conflict of Interest Statement: The authors declare that the research was conducted in the absence of any commercial or financial relationships that could be construed as a potential conflict of interest.

frontiers in Plant Science

MINI REVIEW
published: 25 April 2016
doi: 10.3389/fpls.2016.00539

Molecular Breeding to Create Optimized Crops: From Genetic Manipulation to Potential Applications in Plant Factories

*Kyoko Hiwasa-Tanase and Hiroshi Ezura**

Graduate School of Life and Environmental Sciences, University of Tsukuba, Tsukuba, Japan

Crop cultivation in controlled environment plant factories offers great potential to stabilize the yield and quality of agricultural products. However, many crops are currently unsuited to these environments, particularly closed cultivation systems, due to space limitations, low light intensity, high implementation costs, and high energy requirements. A major barrier to closed system cultivation is the high running cost, which necessitates the use of high-margin crops for economic viability. High-value crops include those with enhanced nutritional value or containing additional functional components for pharmaceutical production or with the aim of providing health benefits. In addition, it is important to develop cultivars equipped with growth parameters that are suitable for closed cultivation. Small plant size is of particular importance due to the limited cultivation space. Other advantageous traits are short production cycle, the ability to grow under low light, and high nutriculture availability. Cost-effectiveness is improved from the use of cultivars that are specifically optimized for closed system cultivation. This review describes the features of closed cultivation systems and the potential application of molecular breeding to create crops that are optimized for cost-effectiveness and productivity in closed cultivation systems.

Keywords: plant factory, molecular breeding, agricultural crop trait, additional value, molecular farming, edible medicine

OPEN ACCESS

Edited by:
Alejandro Isabel Luna-Maldonado, Universidad Autónoma de Nuevo León, Mexico

Reviewed by:
Hao Peng, Washington State University, USA
Chong Zhang, University of Maryland Baltimore County, USA

****Correspondence:***
Hiroshi Ezura
ezura@gene.tsukuba.ac.jp

Specialty section:
This article was submitted to Crop Science and Horticulture, a section of the journal Frontiers in Plant Science

Received: *14 August 2015*
Accepted: *05 April 2016*
Published: *25 April 2016*

Citation:
Hiwasa-Tanase K and Ezura H (2016) Molecular Breeding to Create Optimized Crops: From Genetic Manipulation to Potential Applications in Plant Factories. Front. Plant Sci. 7:539. doi: 10.3389/fpls.2016.00539

INTRODUCTION

Plant factories consist of artificially controlled environments for the cultivation of plants within buildings. Agricultural commodities can be efficiently and continuously produced in plant factories regardless of season or external weather conditions. Optimal environmental conditions can be maintained by control of factors such as light intensity, light duration, CO_2 concentration, and nutrient levels. Plant factories are divided into the following three production types according to their light sources: (1) solar light, (2) combined solar and artificial light, and (3) perfection-artificial-light (Goto, 2011). Solar and combined-light factories are suitable for the cultivation of crops that need intense light. However, it is difficult to use multistage racking in these systems, and the management of pests and diseases is also challenging. Perfection-artificial-light systems, also known as closed cultivation systems, facilitate the maintenance of pest- and disease-free conditions and can therefore be used to produce pesticide-free cultivars. The use of closed cultivation systems to produce genetically modified crops helps prevent the spread of transgenic plants and pollen to the external environment. Closed cultivation systems can also be used to produce cultivars through the use of multistage-cultivation-racks,

which make efficient use of limited space, thereby contributing to increased cultivation number and yields per unit area (Kozai, 2013). However, due to the limited light intensity and limited space, such systems are not suitable for every crop. A further disadvantage is the high operating costs resulting from high energy requirements for artificial lighting and air-conditioning (Kozai, 2013).

Production cost is a major factor for plant factories. To be profitable, agricultural cultivation in plant factories is mostly limited to products such as leafy vegetables and flower and vegetable seedlings. Advantages of leafy vegetables, such as lettuce and arugula, include the large proportion of the plant that is edible, year-round demand, high productivity over a short life cycle, and short plant height. Additionally, the energy costs are relatively low because leafy vegetables can grow under low light intensities. High light intensities (photon flux density) can be achieved using high-pressure sodium lamps and metal halide lamps (Goto, 2011). If energy costs were not of concern, it would be possible to dramatically increase the number of crop species that could be cultivated in plant factories by using high-intensity lamps alongside air-conditioning.

In this review, molecular breeding of crops to enhance their suitability for cost-effectiveness in closed cultivation systems is discussed. Preferable crop traits for closed cultivation systems are also suggested in terms of the potential value.

INCREASING THE ADDED VALUE OF AGRICULTURAL PRODUCTS

Two major considerations of closed cultivation systems are the initial costs and the running costs, with high energy costs of particular concern (**Figure 1**). Profitability can be increased by producing crops with enhanced value.

Agricultural Crops with Health Benefits

Two of the main approaches to increasing the value of a food crop are (1) the accumulation of large quantities of a desirable intrinsic nutrient or reduction of undesirable compounds, and (2) accumulation of valuable compounds that are not normally produced in the crop (**Figure 1**).

Agricultural crops with added value, such as those with improved nutritional qualities, are under continuous development. Newell-McGloughlin (2008) reviewed improvements to various crops, including increased protein quantity and quality in maize, potato, rice, and soybean; increased vitamin content (vitamins C, E, or provitamin A) in maize, strawberry, and tomato; increased carotenoid levels (β-carotene, lycopene, or lutein) in rice, potato, and tomato; increased flavonoid levels in maize, rice, tomato, and soybean; increased iron content in rice and lettuce; and decreased glycoside and solanin levels in potato.

Other examples include improvements to the nutritional qualities of rice and tomato. Rice contains little natural β-carotene, a precursor of provitamin A. Golden rice was modified to accumulate β-carotene by the insertion of exogenous genes (Ye et al., 2000). In 2008, two transcription factors from snapdragons were expressed in tomato to enhance anthocyanin accumulation in tomato fruit to levels typically found in blackberries and blueberries (Butelli et al., 2008). These nutritionally and functionally enriched products may be valuable for human and animal health, particularly in situations where availability of nutrients is low. However, where nutritional compounds can be acquired from other foods naturally rich in those nutrients, the market value of nutritionally enhanced foods may not be high enough to justify the economic inputs required. Some economically valuable compounds can be produced that are not commonly found in a daily diet, such as therapeutic components of medicinal plants. The high value of such compounds may allow economically viable production.

Miraculin is a taste-modifying glycoprotein that is extracted from the miracle fruit (*Richadella dulcifica*). It has the unique ability to modify a sour taste into a sweet taste and has potential as a natural, safe, low-calorie alternative to artificial sweeteners for diabetics and people on restricted diets. However, despite its great potential, miracle fruit production is limited because it is a tropical plant that is difficult to cultivate (Kurihara and Nirasawa, 1997). Introduction of the miraculin gene into the tomato genome resulted in the production of tomato fruit that accumulated miraculin (Sun et al., 2007; Hirai et al., 2011a). One gram of miracle fruit pulp typically contains approximately 400 μg of miraculin glycoprotein. Genetically, modified tomatoes accumulated 100–1700 μg of miraculin per gram of fresh weight tomato fruit. Miraculin accumulation varied according to the promoter and terminator used for transgene expression, cultivation conditions, and host cultivar used (Hiwasa-Tanase et al., 2012). Furthermore, miraculin accumulation in modified tomato was more stable in a closed cultivation system than in a netted greenhouse (Hirai et al., 2010). In Japan, a single miracle fruit is worth more than $2. Miraculin-accumulating tomatoes and purified miraculin protein can be produced more cost-effectively than miracle fruit, and the high value of miraculin-producing tomatoes compared to normal tomatoes is sufficient to justify the use of plant factories.

Agricultural Crops as Edible Medicines

The production of therapeutic recombinant proteins using transgenic plants has been actively promoted due to the numerous potential advantages of this approach (Twyman et al., 2003; Obembe et al., 2011; Ahmad et al., 2012; Xu et al., 2012; Abiri et al., 2015). Compared to mammals and bacteria, plants act as cost-effective bioreactor systems that can be scaled up easily, lack prions, have no human viral pathogen or toxic contamination risks, and have high storage capacities when products accumulate in seeds. Furthermore, purifying and processing costs are limited and labor costs are minimized if the resultant plants can be directly consumed as medicines (Ahmad et al., 2012; Jacob et al., 2013). The commercial production of recombinant proteins using closed cultivation systems may allow more efficient and cost-effective production of feedstocks and bio-pharmaceutical products compared to other production systems. Several recent reviews highlighted the potential of plants for use in molecular farming of desirable compounds such as industrial enzymes and pharmaceutical vaccines and antibodies (Obembe et al., 2011; Ahmad et al., 2012;

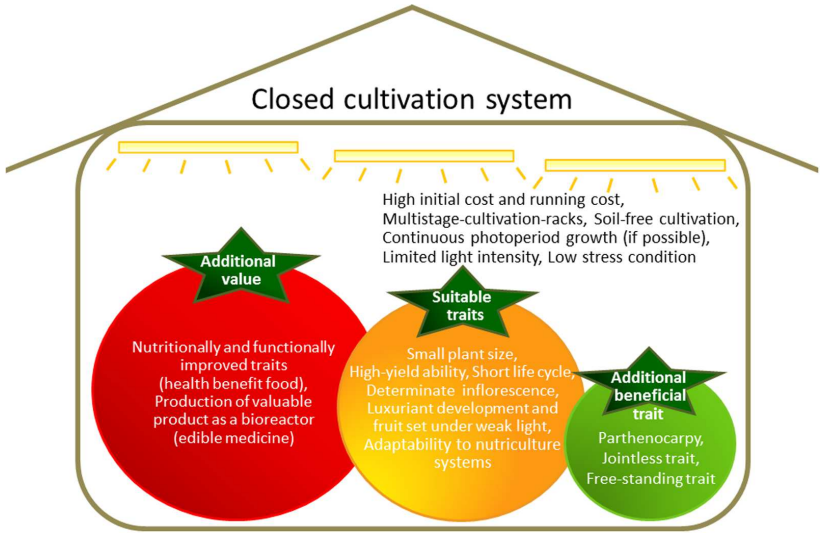

FIGURE 1 | Features of a closed cultivation system and ideal traits for cultivation in such a system.

Xu et al., 2012; Jacob et al., 2013; Abiri et al., 2015; Fahad et al., 2015).

Although the majority of vaccines are administered by injection, vaccines that can be delivered orally and absorbed through the mucosal immune system have practical advantages. Vaccines that are delivered via the mucosal immune system affect both local and systemic immunity, are easy to administer, and are less stressful for patients compared to painful injections. An "edible vaccine" is a crop that accumulates immunogenic antigens in the edible tissue for livestock or human use. There are numerous published studies regarding vaccine production in plants such as potato, lettuce, soybean, maize, tomato, banana, and rice (Obembe et al., 2011; Aswathi et al., 2014; Saxena and Rawat, 2014; Azegami et al., 2015; Fahad et al., 2015). Recently, soybeans that accumulated Alzheimer's disease vaccine peptides (Maruyama et al., 2014), carrots that produced HIV antigens (Lindh et al., 2014), and rice that accumulated peptide vaccines for pollen allergies (Takaiwa and Yang, 2014) were developed for human use.

In Japan, transgenic strawberries expressing dog interferon-α were commercialized and sold as an oral drug from March 2014. This is the first example of the use of a powdered transgenic plant as a medicine (Tabayashi and Matsumura, 2014). The powdered plant product was effective in the treatment of periodontal disease, and no extraction or purification of the active ingredients was needed. Patent applications were submitted and published in several countries (PTC number PTC/JP2007/050281). The transgenic strawberry is developed from cultivation to drug product in a completely closed cultivation system. Strawberry was selected as the host plant because it can be eaten without being cooked, which is an important advantage for the production of heat-sensitive interferon-α. In addition, strawberry can be readily reproduced by vegetative propagation, which decreases the risk of gene silencing (Stam et al., 1997; Sun et al., 2006; Hirai et al., 2011b), facilitates the development process, and aids production of consistent seed lots. Although, the strawberry plant is considerably less productive with respect to speed of growth and biomass accumulation compared to other plants, the advantages described above made strawberry an ideal subject for development of this medicine.

Overall, molecular farming is an excellent system for utilizing crop characteristics to produce edible medicines with low purification costs (**Figure 1**). Moreover, closed cultivation systems that allow stable and uniform production of a crop are extremely suitable for the consistent production of pharmaceutical and industrial compounds using transgenic plants.

CROP TRAITS TO ENHANCE CULTIVATION IN PLANT FACTORIES

Features of closed cultivation systems include basal multistage-rack cultivation, soil-free cultivation, optional continuous photoperiod growth, limited light intensity, and low-stress conditions (**Figure 1**). Therefore, many crops developed for cultivation in the field are unsuitable for closed cultivation system. If agricultural crops can be adapted for growth in closed cultivation systems, such as with lettuce, modification of growth patterns to allow high productivity will enhance cost-effectiveness. Furthermore, the specialized cultivars developed for use in closed cultivation systems can be used as host plants for genetic introduction of high-value traits.

There are several crucial factors that must be considered when developing crops for cultivation in enclosed and limited spaces, such as plant size, life-cycle duration, and yield (**Figure 1**). Plants need to be relatively small to suit the closed system, although the importance of this factor depends on the crop. Field rice and wheat cultivars acquired semi-dwarf traits during the "Green Revolution" (Hedden, 2003). Before plants with semi-dwarf traits

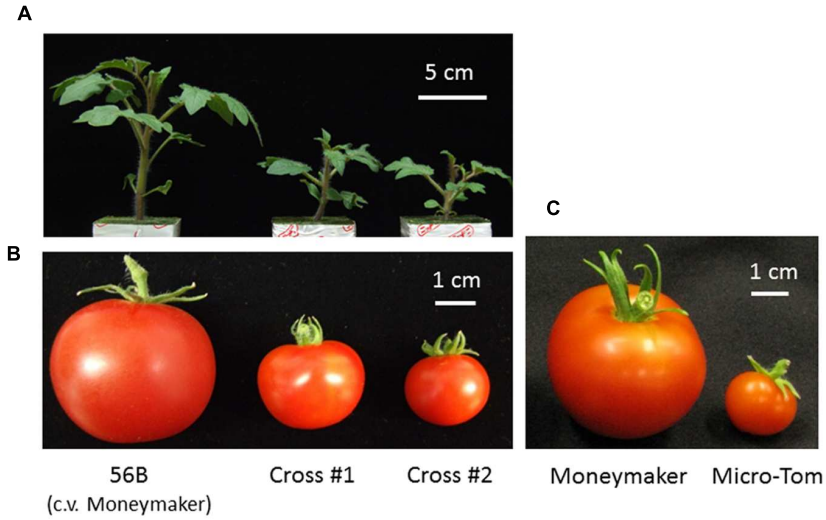

FIGURE 2 | A tomato developed for cultivation in a closed cultivation system. The tomato plant 56B (cv. Moneymaker), which accumulates miraculin, has a normal plant size and exhibits an indeterminate type; it was crossed with the dwarf, determinate-type tomato Micro-Tom with the aim of enhancing traits that would be beneficial for growth in a closed cultivation system. Hybrid lines were selected based on plant size, fruit size, determinate inflorescence and miraculin accumulation, and the lines were named cross #1 and cross #2 (Kato et al., 2010). **(A)** Seedlings at 22 days after germination. **(B,C)** Average size of red fruit. This figure was previously presented in Kato et al. (2010) and has been slightly modified.

became available, the stems of tall wheat and rice plants were not strong enough to support the heavy weight of the grain of high-yielding varieties. Therefore, large yield losses occurred as a result of plant lodging. The semi-dwarf trait confers lodging resistance under heavy manuring, and total biomass is increased. High yields can be attained by reducing production loss from lodging. The semi-dwarf genes in rice and wheat were identified from gibberellin (GA)-related mutations. The gene *Reduced height1* (*Rht1*), which is responsible for the semi-dwarf trait in wheat, encodes a negative regulator of the GA response (Peng et al., 1999). The gene *semi-dwarf1* (*sd1*), which is responsible for the semi-dwarf trait in rice, encodes the GA synthesis enzyme GA 20-oxidase (Sasaki et al., 2002; Sakamoto and Matsuoka, 2004). By contrast, the barley dwarfing gene *uzu* is GA-independent. Semi-dwarf barley does not respond to brassinosteroids (BRs), a type of plant steroid hormone. The uzu phenotype is caused by a missense mutation in the BR receptor protein, barley (*Hordeum vulgare*) HvBRI, a homolog of *Arabidopsis* BR-insensitive 1 (BRI1; Chono et al., 2003). The *BRI1* mutant homolog in rice, *OsBRI1*, shows not only the semi-dwarf phenotype but also an erect-leaf phenotype. Similar phenotypes were detected in rice by manipulating the C-22 hydroxylation step in the BR biosynthesis pathway (Sakamoto et al., 2006). The aboveground biomass of BR mutant rice plants was 1.4-fold higher than in WT plants. This increase was attributed to improved photosynthetic efficiency from the increased light penetration to lower leaves afforded by the erect-leaf phenotype (Sakamoto et al., 2006). Manipulation of BR levels and BR sensitivity via modification of other BR-related genes increased yields in rice, barley, cotton, and *Arabidopsis* (Divi and Krishna, 2009; Vriet et al., 2012).

In recent work, the expression of the chimeric repressor for *Arabidopsis* ILI1 binding bHLH (AtIBH1; *P35S:AtIBH1SRDX*), which has the plant-specific transcriptional repression domain SRDX fused to the C-terminus of AtIBH1, induced a dwarf phenotype in *Arabidopsis* and tobacco plants, with reduced cell size (Hiratsu et al., 2003; Ikeda et al., 2012; Nagatoshi et al., 2016). AtIBH1, which is a transcription factor, regulates cell elongation in response to brassinosteroid and gibberellin signaling (Ikeda et al., 2012). The *AtIBH1SRDX* tobacco plants produced four times more biomass per unit of cultivation volume, which means vertical farming that is stacking of multiple shelves for plant growth, compared with wild-type plants (Nagatoshi et al., 2016). When the genes for anti-hepatitis B virus antibodies were expressed in the *AtIBH1SRDX* tobacco plants, the dwarf plants produced about four times more antibody per unit of cultivation volume than in wild-type plants. They showed that *AtIBH1SRDX* is a useful tool for the manipulation of plant phenotype for cost-effective production of high-value products by transgenic plant in closed cultivation systems.

Shortening the life cycles of cultivated plants would increase annual production in a closed system. *Arabidopsis TERMINAL FLOWER 1* (*TFL1*) is a key gene that affects the developmental phases and architecture of *Arabidopsis* (Shannon and Meeks-Wagner, 1991; Alvarez et al., 1992; Ray et al., 1996). The recessive mutant *tfl1* exhibits a terminal flower phenotype and has a significantly shorter vegetative phase than wild-type plants due to its early transition to the reproductive phase (Shannon and Meeks-Wagner, 1991; Bradley et al., 1997). Conversely overexpression of *RCN1* and *RCN2*, rice *TFL1* homologs, revealed delay of phase change from the branch shoot to the floral meristem state (Nakagawa et al., 2002). In tomato, the *SELF-PRUNING* (*SP*) gene, which is a homolog of *TFL1,* regulates switching from vegetative to reproductive phase (Pnueli et al., 1998). The recessive *sp* mutant shows 'determinate' trait and the

trait confers the short plant height and the short life cycle in comparison with 'indeterminate' tomato. Numerous genes that regulate flowering time were previously identified and considered for plant breeding applications (Jung and Müller, 2009; Blümel et al., 2015).

The tomato (*Solanum lycopersicum*) cultivar Micro-Tom, which was bred for home gardening purposes, has a miniature growth phenotype. Although Micro-Tom fruits have poor flavor, the cultivar exhibits small features (height approximately 10–20 cm) and can be easily transformed, and it is therefore widely used as a tomato research model (Matsukura et al., 2008; Saito et al., 2011). The dwarf trait in Micro-Tom is attributed to at least two major recessive mutations: *dwarf* (*d*) in the gene encoding the BR biosynthetic enzyme, and *miniature* (*mmt*) in a GA signaling-related gene (Martí et al., 2006; Matsukura et al., 2008). Moreover, the Micro-Tom cultivar has a determinate phenotype derived from a mutation in the *SP*gene. Micro-Tom has a short life cycle (70–90 days from seed germination to fruit maturation) compared with most cultivated tomato varieties (90–110 days) (Saito et al., 2011), exhibits high fertility, and sets a large amount of fruit under normal fluorescent lamps. All of the traits exhibited by Micro-Tom are useful for breeding new plant varieties for use in closed cultivation systems. The genetically modified tomato cultivar "Moneymaker," which produces and accumulates miraculin as a result of an inserted exogenous gene, is indeterminate and has a normal size. Moneymaker was crossed with Micro-Tom to create a tomato suitable for a closed cultivation system (Kato et al., 2010). Selected hybrids were determinate and smaller than the Moneymaker parent. Hybrid fruits were larger than those of Micro-Tom, and the yield per area was also higher (**Figure 2**).

Luxuriant foliar development and fruit setting under weak light, as well as adaptability to nutriculture systems, contribute to balanced growth in closed environments; however, the factors that determine that these traits are not well-understood. Cultivars or mutants with desirable traits might be identified by screening genetic resources obtained from past breeding programs or from mutagenized populations developed using ethyl methane sulfonate (EMS) or gamma irradiation (TOMATOMA[1], Genes that Make Tomatoes[2], Tomato Genetics Resource Center[3]).

ADDITIONAL NOTES

This review highlights genetic targets that may be of use in molecular breeding programs to develop agricultural crops for profitable cultivation in closed cultivation systems. To create objective traits, a wide variety of genetic information and molecular breeding techniques are used, including marker-assisted selection, quantitative trait locus (QTL) analysis, genetic linkage maps, and transgenic techniques (Jiao et al., 2012; Lusser and Davies, 2013). Whole genomes have been completely sequenced for a variety of cultivated crops, including rice (2005), maize (2009), wheat (2014), soybean (2010), tomato (2012), melon (2012), watermelon (2012), potato (2008), cucumber (2009), and eggplant (2014). These rich sources of sequence information can be readily applied to breeding. Active accumulation of transgenic proteins for pharmaceutical and health purposes can be optimized using several approaches. These include selection of an appropriate host plant, codon optimization, choice of promoter and terminator, use of specific organs and tissues for protein secretion, and expression of the target gene from the nuclear or chloroplast genomes (Twyman et al., 2003; Xu et al., 2012; Abiri et al., 2015). These techniques and tools for molecular breeding make it possible to create agricultural crops with various useful and diverse traits.

In this review, breeding targets were discussed that are likely to be of greatest utility in optimizing plant growth in closed cultivation systems. Several additional traits could also be of use (**Figure 1**). For example, parthenocarpy, which is the production of fruit without fertilization, could reduce workloads and labor costs by reducing inputs needed for consistent pollination. Parthenocarpy is also valuable in the containment of transgenic plant materials. The jointless trait, where no abscission zones are formed on leaves, flowers, or fruit, would reduce product loss through dropping. The free-standing trait, which allows plants to grow without additional support structures, would be conducive to reducing time and material costs. The jointless and free-standing traits may be particularly useful for cultivation systems that employ moving shelves.

CONCLUSION

Since the beginning of agriculture, numerous plants have been developed through artificial selection for field cultivation. Modern closed cultivation systems allow environmental conditions to be tightly controlled and ensure the production. The systems offer great potential for production of specialized crops which have additional value. However, crop breeding specifically for closed cultivation systems had been limited to date despite its potential availability. Novel cultivars are required to sympathize with the challenges of agricultural technology. Breeding an indoor suitable cultivar can be accomplished through complex molecular techniques, which property benefits will familiarize closed cultivation systems.

AUTHOR CONTRIBUTIONS

All authors listed, have made substantial, direct and intellectual contribution to the work, and approved it for publication.

ACKNOWLEDGMENT

This study was supported by the project "Development of Fundamental Technologies for the Production of High-Value Materials Using Transgenic Plants" and by the Ministry of Economy, Trade, and Industry of Japan to HE.

[1]http://tomatoma.nbrp.jp/

[2]http://zamir.sgn.cornell.edu/mutants/

[3]http://tgrc.ucdavis.edu/index.aspx

REFERENCES

Abiri, R., Valdiani, A., Maziah, M., Shaharuddin, N. A., Sahebi, M., Yusof, Z. N. B., et al. (2015). A critical review of the concept of transgenic plants: insights into pharmaceutical biotechnology and molecular farming. *Curr. Issues Mol. Biol.* 18, 21–42.

Ahmad, P., Ashraf, M., Younis, M., Hu, X., Kumar, A., Akram, N. A., et al. (2012). Role of transgenic plants in agriculture and biopharming. *Biotechnol. Adv.* 30, 524–540. doi: 10.1016/j.biotechadv.2011.09.006

Alvarez, J., Guli, C. L., Yu, X.-H., and Smyth, D. R. (1992). TERMINAL FLOWER: a gene affecting inflorescence development in *Arabidopsis thaliana*. *Plant J.* 2, 103–116. doi: 10.1111/j.1365-313X.1992.00103.x

Aswathi, P. B., Bhanja, S. K., Yadav, A. S., Rekha, V., John, J. K., Gopinath, D., et al. (2014). Plant based edible vaccines against poultry diseases?: a review. *Adv. Anim. Vet. Sci.* 2, 305–311. doi: 10.14737/journal.aavs/2014/2.5.305.311

Azegami, T., Itoh, H., Kiyono, H., and Yuki, Y. (2015). Novel Transgenic Rice-Based Vaccines. *Arch. Immunol. Ther. Exp.* 63, 87–99. doi: 10.1007/s00005-014-0303-0

Blümel, M., Dally, N., and Jung, C. (2015). Flowering time regulation in crops—what did we learn from *Arabidopsis*? *Curr. Opin. Biotechnol.* 32, 121–129. doi: 10.1016/j.copbio.2014.11.023

Bradley, D., Ratcliffe, O., Vincent, C., Carpenter, R., and Coen, E. (1997). Inflorescence commitment and architecture in *Arabidopsis*. *Science* 275, 80–83. doi: 10.1126/science.275.5296.80

Butelli, E., Titta, L., Giorgio, M., Mock, H.-P., Matros, A., Peterek, S., et al. (2008). Enrichment of tomato fruit with health-promoting anthocyanins by expression of select transcription factors. *Nat. Biotechnol.* 26, 1301–1308. doi: 10.1038/nbt.1506

Chono, M., Honda, I., Zeniya, H., Yoneyama, K., Saisho, D., Takeda, K., et al. (2003). A semidwarf phenotype of barley uzu results from a nucleotide substitution in the gene encoding a putative brassinosteroid receptor. *Plant Physiol.* 133, 1209–1219. doi: 10.1104/pp.103.026195

Divi, U. K., and Krishna, P. (2009). Brassinosteroid: a biotechnological target for enhancing crop yield and stress tolerance. *New Biotechnol.* 26, 131–136. doi: 10.1016/j.nbt.2009.07.006

Fahad, S., Khan, F. A., Pandupuspitasari, N. S., Ahmed, M. M., Liao, Y. C., Waheed, M. T., et al. (2015). Recent developments in therapeutic protein expression technologies in plants. *Biotechnol. Lett.* 37, 265–279. doi: 10.1007/s10529-014-1699-7

Goto, E. (2011). Introduction and future prospects of plant factory with artificial light. *Japan. Soc. Agric. Machin* 73, 87–91.

Hedden, P. (2003). The genes of the Green Revolution. *Trends. Genet.* 19, 5–9. doi: 10.1016/S0168-9525(02)00009-4

Hirai, T., Fukukawa, G., Kakuta, H., Fukuda, N., and Ezura, H. (2010). Production of recombinant miraculin using transgenic tomatoes in a closed cultivation system. *J. Agric. Food Chem.* 58, 6096–6101. doi: 10.1021/jf100414v

Hirai, T., Kurokawa, N., Duhita, N., Hiwasa-Tanase, K., Kato, K., Kato, K., et al. (2011a). The HSP terminator of *Arabidopsis thaliana* induces a high level of miraculin accumulation in transgenic tomatoes. *J. Agric. Food Chem.* 59, 9942–9949. doi: 10.1021/jf202501e

Hirai, T., Shohael, A. M., Kim, Y. W., Yano, M., and Ezura, H. (2011b). Ubiquitin promoter-terminator cassette promotes genetically stable expression of the taste-modifying protein miraculin in transgenic lettuce. *Plant Cell Rep.* 30, 2255–2265. doi: 10.1007/s00299-011-1131-x

Hiratsu, K., Matsui, K., Koyama, T., and Ohme-Takagi, M. (2003). Dominant repression of target genes by chimeric repressors that include the EAR motif, a repression domain, in *Arabidopsis*. *Plant J.* 34, 733–739. doi: 10.1046/j.1365-313X.2003.01759.x

Hiwasa-Tanase, K., Hirai, T., Kato, K., Duhita, N., and Ezura, H. (2012). From miracle fruit to transgenic tomato: mass production of the taste-modifying protein miraculin in transgenic plants. *Plant Cell Rep.* 31, 513–525. doi: 10.1007/s00299-011-1197-5

Ikeda, M., Fujiwara, S., Mitsuda, N., and Ohme-takagi, M. (2012). A triantagonistic basic helix-loop-helix system regulates cell elongation in *Arabidopsis*. *Plant Cell* 24, 4483–4497. doi: 10.1105/tpc.112.105023

Jacob, S. S., Cherian, S., Sumithra, T. G., Raina, O. K., and Sankar, M. (2013). Edible vaccines against veterinary parasitic diseases-Current statu and future prospects. *Vaccine* 31, 1879–1885. doi: 10.1016/j.vaccine.2013.02.022

Jiao, Y., Zhao, H., Ren, L., Song, W., Zeng, B., Guo, J., et al. (2012). Genome-wide genetic changes during modern breeding of maize. *Nat. Genet.* 44, 812–815. doi: 10.1038/ng.2312

Jung, C., and Müller, A. E. (2009). Flowering time control and applications in plant breeding. *Trends Plant. Sci.* 14, 563–573. doi: 10.1016/j.tplants.2009.07.005

Kato, K., Yoshida, R., Kikuzaki, A., Hirai, T., Kuroda, H., Hiwasa-Tanase, K., et al. (2010). Molecular breeding of tomato lines for mass production of miraculin in a plant factory. *J. Agric. Food. Chem.* 58, 9505–9510. doi: 10.1021/jf101874b

Kozai, T. (2013). Resource use efficiency of closed plant production system with artificial light: concept, estimation and application to plant factoy. *Proc. Jpn. Acad. Ser. B* 89, 447–461. doi: 10.2183/pjab.89.447

Kurihara, Y., and Nirasawa, S. (1997). Structures and activities of sweetness-inducing substances (miraculin, curculin, strogin) and the heat- stable sweet protein, mabinlin. *F.F.I. J. Jpn.* 174, 67–74.

Lindh, I., Bråve, A., Hallengärd, D., Hadad, R., Kalbina, I., Strid, Å, et al. (2014). Oral delivery of plant-derived HIV-1 p24 antigen in low doses shows a superior priming effect in mice compared to high doses. *Vaccine* 32, 2288–2293. doi: 10.1016/j.vaccine.2014.02.073

Lusser, M., and Davies, H. V. (2013). Comparative regulatory approaches for groups of new plant breeding techniques. *New Biotechnol.* 30, 437–446. doi: 10.1016/j.nbt.2013.02.004

Martí, E., Gisbert, C., Bishop, G. J., Dixon, M. S., and García-Martínez, J. L. (2006). Genetic and physiological characterization of tomato cv. *Micro-Tom*. *J. Exp. Bot.* 57, 2037–2047. doi: 10.1093/jxb/erj154

Maruyama, N., Fujiwara, K., Yokoyama, K., Cabanos, C., Hasegawa, H., Takagi, K., et al. (2014). Stable accumulation of seed storage proteins containing vaccine peptides in transgenic soybean seeds. *J. Biosci. Bioeng.* 118, 441–447. doi: 10.1016/j.jbiosc.2014.04.004

Matsukura, C., Aoki, K., Fukuda, N., Mizoguchi, T., Asamizu, E., Saito, T., et al. (2008). Comprehensive resources for tomato functional genomics based on the miniature model tomato micro-tom. *Curr. Genomics* 9, 436–443. doi: 10.2174/138920208786241225

Nagatoshi, Y., Ikeda, M., Kishi, H., Hiratsu, K., Muraguchi, A., and Ohme-Takagi, M. (2016). Induction of a dwarf phenotype with IBH1 may enable increased production of plant-made pharmaceuticals in plant factory conditions. *Plant Biotechnol. J.* 14, 887–894. doi: 10.1111/pbi.12437

Nakagawa, M., Shimamoto, K., and Kyozuka, J. (2002). Overexpression of RCN1 and RCN2, rice TERMINAL FLOWER 1/CENTRORADIALIS homologs, confers delay of phase transition and altered panicle morphology in rice. *Plant J.* 29, 743–750. doi: 10.1046/j.1365-313X.2002.01255.x

Newell-McGloughlin, M. (2008). Nutritionally improved agricultural crops. *Plant Physiol.* 147, 939–953. doi: 10.1104/pp.108.121947

Obembe, O. O., Popoola, J. O., Leelavathi, S., and Reddy, S. V. (2011). Advances in plant molecular farming. *Biotechnol. Adv.* 29, 210–222. doi: 10.1016/j.biotechadv.2010.11.004

Peng, J., Richards, D. E., Hartley, N. M., Murphy, G. P., Devos, K. M., Flintham, J. E., et al. (1999). 'Green revolution' genes encode mutant gibberellin response modulators. *Nature* 400, 256–261. doi: 10.1038/22307

Pnueli, L., Carmel-Goren, L., Hareven, D., Gutfinger, T., Alvarez, J., Ganal, M., et al. (1998). The SELF-PRUNING gene of tomato regulates vegetative to reproductive switching of sympodial meristems and is the ortholog of CEN and TFL1. *Development* 125, 1979–1989.

Ray, A., Lang, J. D., Golden, T., and Ray, S. (1996). SHORT INTEGUMENT (SIN1), a gene required for ovule development in *Arabidopsis* also controls flowering time. *Development* 122, 2631–2638.

Saito, T., Ariizumi, T., Okabe, Y., Asamizu, E., Hiwasa-Tanase, K., Fukuda, N., et al. (2011). TOMATOMA: a novel tomato mutant database distributing micro-tom mutant collections. *Plant Cell Physiol.* 52, 283–296. doi: 10.1093/pcp/pcr004

Sakamoto, T., and Matsuoka, M. (2004). Generating high-yielding varieties by genetic manipulation of plant architecture. *Curr. Opin. Biotechnol.* 15, 144–147. doi: 10.1016/j.copbio.2004.02.003

Sakamoto, T., Morinaka, Y., Ohnishi, T., Sunohara, H., Fujioka, S., Ueguchi-Tanaka, M., et al. (2006). Erect leaves caused by brassinosteroid deficiency increase biomass production and grain yield in rice. *Nat. Biotechnol.* 24, 105–109. doi: 10.1038/nbt1173

Sasaki, A., Ashikari, M., Ueguchi-Tanaka, M., Itoh, H., Nishimura, A., Swapan, D., et al. (2002). Green revolution: a mutant gibberellin-synthesis gene in rice. *Nature* 416, 701–702. doi: 10.1038/416701a

Saxena, J., and Rawat, S. (2014). "Edible vaccines," in *Advances in Biotechnology*, eds I. Ravi, M. Baunthiyal, and J. Saxena (New Delhi: Springer), 207–226. doi: 10.1007/978-81-322-1554-7_12

Shannon, S., and Meeks-Wagner, D. R. (1991). A mutation in the *Arabidopsis* TFL1 gene affects inflorescence meristem development. *Plant Cell* 3, 877–892. doi: 10.2307/3869152

Stam, M., Mol, J. N. M., and Kooter, J. M. (1997). The silence of genes in transgenic plants. *Ann. Bot.* 79, 3–12. doi: 10.1006/anbo.1996.0295

Sun, H. J., Cui, M. L., Ma, B., and Ezura, H. (2006). Functional expression of the taste-modifying protein, miraculin, in transgenic lettuce. *FEBS Lett.* 580, 620–626. doi: 10.1016/j.febslet.2005.12.080

Sun, H. J., Kataoka, H., Yano, M., and Ezura, H. (2007). Genetically stable expression of functional miraculin, a new type of alternative sweetener, in transgenic tomato plants. *Plant Biotechnol. J.* 5, 768–777. doi: 10.1111/j.1467-7652.2007.00283.x

Tabayashi, N., and Matsumura, T. (2014). Forefront study of plant biotechnology for practical use: development of oral drug for animal derived from transgenic strawberry. *Soc. Biotechnol. J. Japn.* 92, 537–539.

Takaiwa, F., and Yang, L. (2014). Development of a rice-based peptide vaccine for Japanese cedar and cypress pollen allergies. *Transgenic Res.* 23, 573–584. doi: 10.1007/s11248-014-9790-3

Twyman, R. M., Stoger, E., Schillberg, S., Christou, P., and Fischer, R. (2003). Molecular farming in plants: host systems and expression technology. *Trends Biotechnol.* 21, 570–578. doi: 10.1016/j.tibtech.2003.10.002

Vriet, C., Russinova, E., and Reuzeau, C. (2012). Boosting crop yields with plant steroids. *Plant Cell* 24, 842–857. doi: 10.1105/tpc.111.094912

Xu, J., Dolan, M. C., Medrano, G., Cramer, C. L., and Weathers, P. J. (2012). Green factory: plants as bioproduction platforms for recombinant proteins. *Biotech. Adv.* 30, 1171–1184. doi: 10.1016/j.biotechadv.2011.08.020

Ye, X., Al-Babili, S., Klöti, A., Zhang, J., Lucca, P., Beyer, P., et al. (2000). Engineering the provitamin A (beta-carotene) biosynthetic pathway into (carotenoid-free) rice endosperm. *Science* 287, 303–305. doi: 10.1126/science.287.5451.303

Conflict of Interest Statement: The authors declare that the research was conducted in the absence of any commercial or financial relationships that could be construed as a potential conflict of interest.

frontiers in Plant Science

ORIGINAL RESEARCH
published: 05 February 2016
doi: 10.3389/fpls.2016.00005

Transcriptome Analysis of *Dendrobium officinale* and its Application to the Identification of Genes Associated with Polysaccharide Synthesis

Jianxia Zhang[1‡], Chunmei He[1‡], Kunlin Wu[1], Jaime A. Teixeira da Silva[2†], Songjun Zeng[1], Xinhua Zhang[1], Zhenming Yu[1], Haoqiang Xia[3] and Jun Duan[1]*

[1] Key Laboratory of South China Agricultural Plant Molecular Analysis and Gene Improvement, South China Botanical Garden, Chinese Academy of Sciences, Guangzhou, China, [2] Independent Researcher, Kagawa-ken, Japan, [3] Guangzhou Genedenovo Biotechnology Co., Ltd, Guangzhou, China

Dendrobium officinale is one of the most important Chinese medicinal herbs. Polysaccharides are one of the main active ingredients of *D. officinale*. To identify the genes that maybe related to polysaccharides synthesis, two cDNA libraries were prepared from juvenile and adult *D. officinale*, and were named Dendrobium-1 and Dendrobium-2, respectively. Illumina sequencing for Dendrobium-1 generated 102 million high quality reads that were assembled into 93,881 unigenes with an average sequence length of 790 base pairs. The sequencing for Dendrobium-2 generated 86 million reads that were assembled into 114,098 unigenes with an average sequence length of 695 base pairs. Two transcriptome databases were integrated and assembled into a total of 145,791 unigenes. Among them, 17,281 unigenes were assigned to 126 KEGG pathways while 135 unigenes were involved in fructose and mannose metabolism. Gene Ontology analysis revealed that the majority of genes were associated with metabolic and cellular processes. Furthermore, 430 glycosyltransferase and 89 cellulose synthase genes were identified. Comparative analysis of both transcriptome databases revealed a total of 32,794 differential expression genes (DEGs), including 22,051 up-regulated and 10,743 down-regulated genes in Dendrobium-2 compared to Dendrobium-1. Furthermore, a total of 1142 and 7918 unigenes showed unique expression in Dendrobium-1 and Dendrobium-2, respectively. These DEGs were mainly correlated with metabolic pathways and the biosynthesis of secondary metabolites. In addition, 170 DEGs belonged to glycosyltransferase genes, 37 DEGs were related to cellulose synthase genes and 627 DEGs encoded transcription factors. This study substantially expands the transcriptome information for *D. officinale* and provides valuable clues for identifying candidate genes involved in polysaccharide biosynthesis and elucidating the mechanism of polysaccharide biosynthesis.

Keywords: *D. officinale*, glycosyltransferase, secondary metabolism, polysaccharide synthesis, transcriptome

OPEN ACCESS

Edited by:
Humberto Rodríguez Fuentes, Universidad Autónoma de Nuevo León, Mexico

Reviewed by:
Shiqi Liu, Shandong Agricultural University, China
Hao Peng, Washington State University, USA

****Correspondence:***
Jun Duan
duanj@scbg.ac.cn

†Present Address:
Jaime A. Teixeira da Silva P.O. Box 7, Miki-cho post office, Ikenobe 3011-2, Kagawa-ken, 761-0799, Japan

‡These authors have contributed equally to this work.

Specialty section:
This article was submitted to Crop Science and Horticulture, a section of the journal Frontiers in Plant Science

Received: *08 August 2015*
Accepted: *06 January 2016*
Published: *05 February 2016*

Citation:
Zhang J, He C, Wu K, Teixeira da Silva JA, Zeng S, Zhang X, Yu Z, Xia H and Duan J (2016) Transcriptome Analysis of Dendrobium officinale and its Application to the Identification of Genes Associated with Polysaccharide Synthesis. Front. Plant Sci. 7:5. doi: 10.3389/fpls.2016.00005

INTRODUCTION

The *Orchidaceae* is one of the largest and most widespread families of flowering plants, with more than 250,000 species (Leitch et al., 2009). The genus *Dendrobium* is one of the largest genera of the *Orchidaceae* and has nearly 1100 species throughout the world and is spread widely in India across to Japan, south to Malaysia, and east to Australia, New Guinea, and the Pacific islands (Wu et al., 2009). *Dendrobium officinale*, a critically endangered orchid in the wild (http://www.iucnredlist.org/details/46665/0), has been one of the most important Chinese herbs in China for hundreds of years and is eaten or used as folk medicine for antipyretic, eye-benefitting and immune regulatory purposes (Yang et al., 2006).

The major active ingredients of *D. officinale* are polysaccharides, alkaloids, phenols, coumarins, terpenes, flavonoids, amino acids, benzyl compounds, and several trace mineral elements (Weng, 2003; Li et al., 2011). *D. officinale* has a thick water-soluble polysaccharide-rich stem. *Dendrobium* polysaccharides are mainly composed of glucose and mannose, as well as a small amount of rhamnose, xylose, and arabinose (Fan et al., 2009; Luo et al., 2010). Polysaccharides have been demonstrated in recent years to show prominent bioactivities, including antioxidant, immune stimulation, and anti-tumor (Hsieh et al., 2008; Fan et al., 2009; Luo et al., 2010; Wang et al., 2010; Liu et al., 2011; Xia et al., 2012). Soluble polysaccharides from *D. officinale* exerted stronger immune modulatory activity than *D. fimbriatum*, *D. nobile*, *D. chrysotoxum,* and *D. huoshanense* (Meng et al., 2013). *Dendrobium* polysaccharides have gained increasing attention in the biomedical and drug delivery fields. On the current market, the quality of *D. officinale* is mainly determined by the content of soluble polysaccharides. The component of polysaccharides from different *Dendrobium* species is different. For example, the polysaccharide fractions from *D. denneanum* are composed of glucose, mannose and galactose in the ratio of 227:59:17, as well as small amounts of xylose and arabinose (Fan et al., 2009). The polysaccharide fraction from *D. huoshanense* consists of glucose, mannose and galactose in the ratio of 31:10:8 (Zha et al., 2007). The polysaccharides from *D. officinale* were shown to be a 2-*O*-acetylglucomannan, composed of mannose, glucose, and arabinose in a 40.2:8.4:1 molar ratio (Hua et al., 2004). On the whole, mannose and glucose are the main monosaccharides in these *Dendrobium* species. Although the bioactivities, composition, structure, and physicochemical properties of polysaccharides from *Dendrobium* are well defined, the enzymes and encoding genes responsible for their synthesis and metabolic pathway remain poorly characterized. Therefore, an understanding of the molecular mechanisms underlying the synthesis of *Dendrobium* polysaccharides is essential.

So far, the transcriptome of only one *Dendrobium* species has been sequenced (Guo et al., 2013). It only revealed limited information related to genes in the stem in a certain stage, focusing on the putative alkaloid biosynthetic genes and genetic markers. The molecular mechanisms underlying polysaccharides synthesis and the related metabolic pathway for *D. officinale* remain unknown. In this study, we established two transcription databases for juvenile and adult *D. officinale* and identified 430 glycosyltransferase genes (GTs) and 89 cellulose synthase genes (CesA). Differentially expressed genes (DEGs) were analyzed. Differentially expressed GTs, CesA and transcription factors (TFs) are also reported. Such data for *D. officinale* could be used as an important resource to investigate GTs and the metabolic pathway of polysaccharides in *D. officinale*. Furthermore, this database will supply important clues to explore other biological mechanisms in this *Dendrobium* species and in other orchids.

Abbreviations: BLAST, Basic local alignment search tool; CBM, Carbohydrate-Binding Module; cDNA, Complementary DNA; CesA, Cellulose synthase; CE, Carbohydrate Esterase; *Csl*, Cellulose synthase-like; COG, Clusters of Orthologous Groups; DEG, Differential expression gene; DGE, Digital Gene Expression; EST, expressed sequence tag; gDNA, Genomic DNA; GH, Glycoside Hydrolase; GO, Gene Ontology; GT, Glycosyltransferase; FDR, False discovery rate; KEGG, Kyoto Encyclopedia of Genes and Genomes; NCBI, National Centre for Biotechnology Information; Nr, Non-redundant protein database; PL, Polysaccharide lyase; qRT-PCR, Quantitative real-time PCR; RPKM, Reads per kilobase of transcript per million reads mapped; SRA, Sequence Read Archive; TF, Transcription factor; TGICL, TGI Clustering Tool; UGT, UDP glycosyltransferase.

MATERIALS AND METHODS

Plant Materials and Growth Conditions

D. officinale was grown in the greenhouse of the South China Botanical Garden and used in this study. Seeds derived from selfing were germinated and cultured on half-strength Murashige and Skoog (MS) (Murashige and Skoog, 1962) medium containing 0.1% activated carbon, 2% sucrose, and 0.6% agar (pH = 5.4). The cultures were incubated at 26 ± 1°C with a 12 h photoperiod under cool white fluorescent lamps delivering a photosynthetic photon flux density (PPFD) of *ca.* 45 μmol $m^{-2}s^{-1}$. Material was collected from juvenile seedlings and adult plants. The juvenile seedlings were 10 months old after germinating *in vitro*. The adult plants were 18 months old after juvenile seedlings was transplanted into pots and placed in the greenhouse of the South China Botanical Garden at a day/night temperature of 28/25°C with a 12-h period. The materials used are shown in **Figure 1**. cDNA libraries were prepared from entire *D. officinale* plants at the juvenile and adult stages. Plants were collected in November 2013 at the vegetative stage.

Fresh samples were used to extract total RNA immediately.

cDNA Library Preparation and Illumina Sequencing for Transcriptome Analysis

Total RNA (25 μg) was extracted using Column Plant RNAout 2.0 (Tiandz Inc., Beijing, China) according to the manufacturer's protocol. Preparation of the cDNA library was described in detail in a previous study employed for another orchid, *Cymbidium sinense* (Zhang et al., 2013). Two cDNA libraries were constructed from juvenile seedlings and adult plants in which equal amounts of total RNA were pooled from three biological replicates. The library of the juvenile seedlings was named Dendrobium-1 while the library of the adult plants was named Dendrobium-2. The two libraries were used for comparative analysis of transcriptome sequencing. Finally, two libraries were sequenced using the Illumina HiSeq™ 2000 platform at the

Shenzhen Genome Institute (BGI, Shenzhen, China) and reads were generated in a 100 bp paired-end format according to the manufacturer's instructions (Illumina Inc. San Diego, CA). All raw transcriptome data were deposited in the GeneBank Short Read Archive. The accession numbers were SRR1904494 and SRR1909493for Dendrobium-1 and Dendrobium-2, respectively.

De novo Assembly and Functional Annotation Analysis of Illumina Sequencing

Raw reads from the sequencing machine were generated by base calling. After filtering raw reads by removing adaptor sequences, empty reads, reads with unknown nucleotides larger than 5% and low quality reads (with ambiguous sequences "N"), clean reads were obtained for *de novo* assembly. *De novo* assembly of the transcriptome was carried out with Trinity (*ver.* 2012-10-05) with the default parameters to form contigs (Grabherr et al., 2011). These contigs were then further processed with sequence clustering software, TGICL (Pertea et al., 2003), to form longer sequences defined as unigenes. The generated unigenes were used for BLASTX alignment ($E < 0.00001$) and annotation against protein databases, including non-redundant (nr), Swiss-Port, COG, and KEGG protein databases. With nr annotation, the Blast2GO program (Conesa et al., 2005) was used to obtain the Gene ontology (GO) annotation of unigenes, then WEGO software (Ye et al., 2006) was used to perform GO functional classification for all unigenes and to understand the distribution of gene functions. KEGG is a major public pathway-related database (Kanehisa et al., 2008) that is able to analyze a gene product during a metabolic process and related gene function in cellular processes. KEGG pathway annotation was performed using a BLAST search against the KEGG database (KEGG, http://www.genome.jp/kegg/).

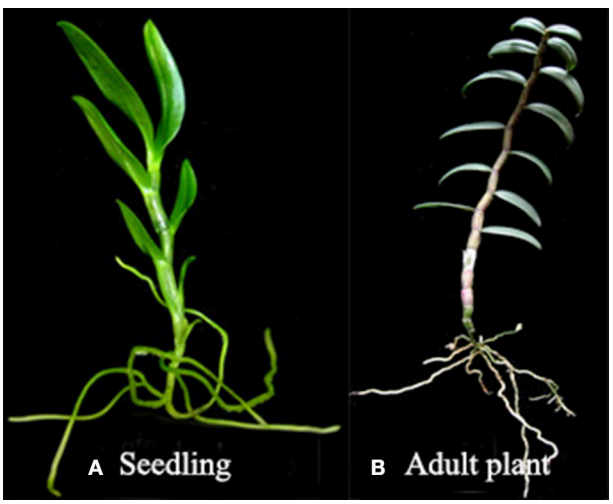

FIGURE 1 | Organs from *D. officinale* used to prepare cDNA libraries for Illumine sequencing. (A) Young seedling *of D. officinale* (Dendrobium-1); **(B)** Adult plant of *D. officinale* (Dendrobium-2).

TABLE 1 | Summary of Illumina sequencing and assembly of two *D. officinale* transcriptomes.

	Dendrobium-1	Dendrobium-2
Total number of raw reads	114,970,718	102,340,806
Total number of clean reads	102,982,138	86,515,904
Total clean nucleotides (nt)	10,298,213,800	8,651,590,400
Average read length	100	100
Total number of contigs	107086	129235
Mean length of contigs	824	728
Total number of unigenes	93881	114098
Mean length of unigenes	790	695

Identification of Differentially Expressed Genes (DEGs)

To compare the differences in gene expression at two developmental stages, the RPKM method (reads per kb per million reads) was used to calculate read density. By taking into account the variations in gene length and the total mapped number of sequencing reads, the RPKM measure provides normalized values of gene expression that enable transcript comparisons between samples. The false discovery rate (FDR) was used to determine the threshold *P*-value in multiple tests. We used an FDR < 0.001, $P \leq 0.05$ and

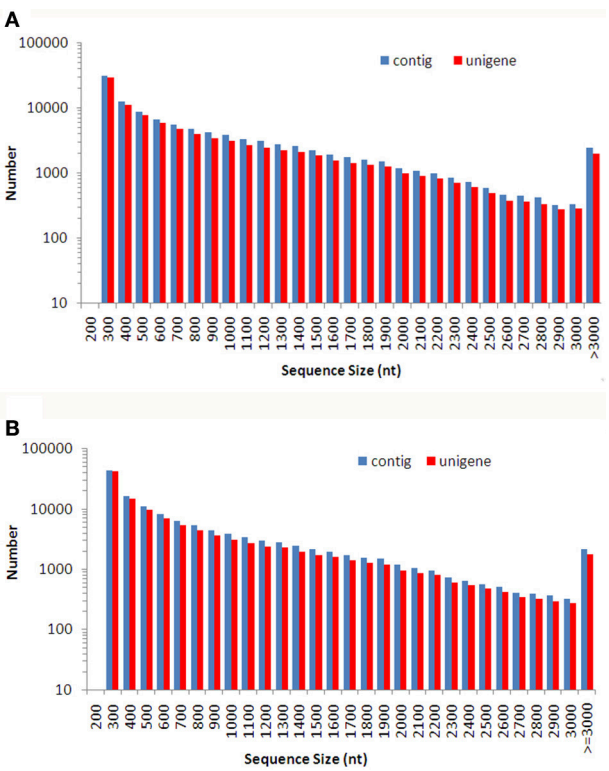

FIGURE 2 | The size distribution of *de novo* assembled contigs and unigenes for Dendrobium-1 (A) and Dendrobium-2 (B). A total of 107,086 contigs and 93,881 unigenes sizes were calculated for Dendrobium-1 **(A)**. A total of 129,235 contigs and 114,098 unigenes sizes were calculated for Dendrobium-2 **(B)**.

an absolute value of the $\log_2$ ratio >1 as the threshold to determine significant differences in gene expression. The DEGs were used for GO and KEGG enrichment analyses according to a method used for *Cymbidium sinense* (Zhang et al., 2013).

Quantitative Real-Time PCR Validation

Total RNA was extracted as indicated above. Each RNA sample was treated with RNase-free DNase (Promega, Madison, USA) following the manufacturer's protocol in an effort to remove any residual genomic DNA (gDNA). DNase-treated RNA (2 mg) was subjected to reverse transcriptase reactions using M-MLV reverse transcriptase (Promega, Madison, USA) according to the manufacturer's instructions. The sequences of the specific primer sets are listed in **Additional file 1**. The constitutively expressed gene, *D. officinale actin* (cloned by our laboratory; NCBI accession number: JX294908), was used as the internal control. qRT-PCR was performed according to our previously published study (He et al., 2015). The expression level was calculated as $2^{-\Delta\Delta Ct}$ and normalized to the Ct value of *D. officinale actin*. The qRT-PCR results were obtained from three biological replicates and three technical repeats for each gene and sample.

RESULTS

De novo Assembly and Sequence Annotation

A total of 102 million 100 bp reads were assembled into 107,086 contigs with a mean length of 824 bp in Dendrobium-1, and a total of 86 million 100 bp reads were assembled into 129,235 contigs with a mean length of 728 bp in Dendrobium-2 (**Table 1**). Using paired-end reads, the Dendrobium-1 contigs were further assembled into 93,881 unigenes by Trinity with a mean length of 790 bp. The size distribution of these contigs

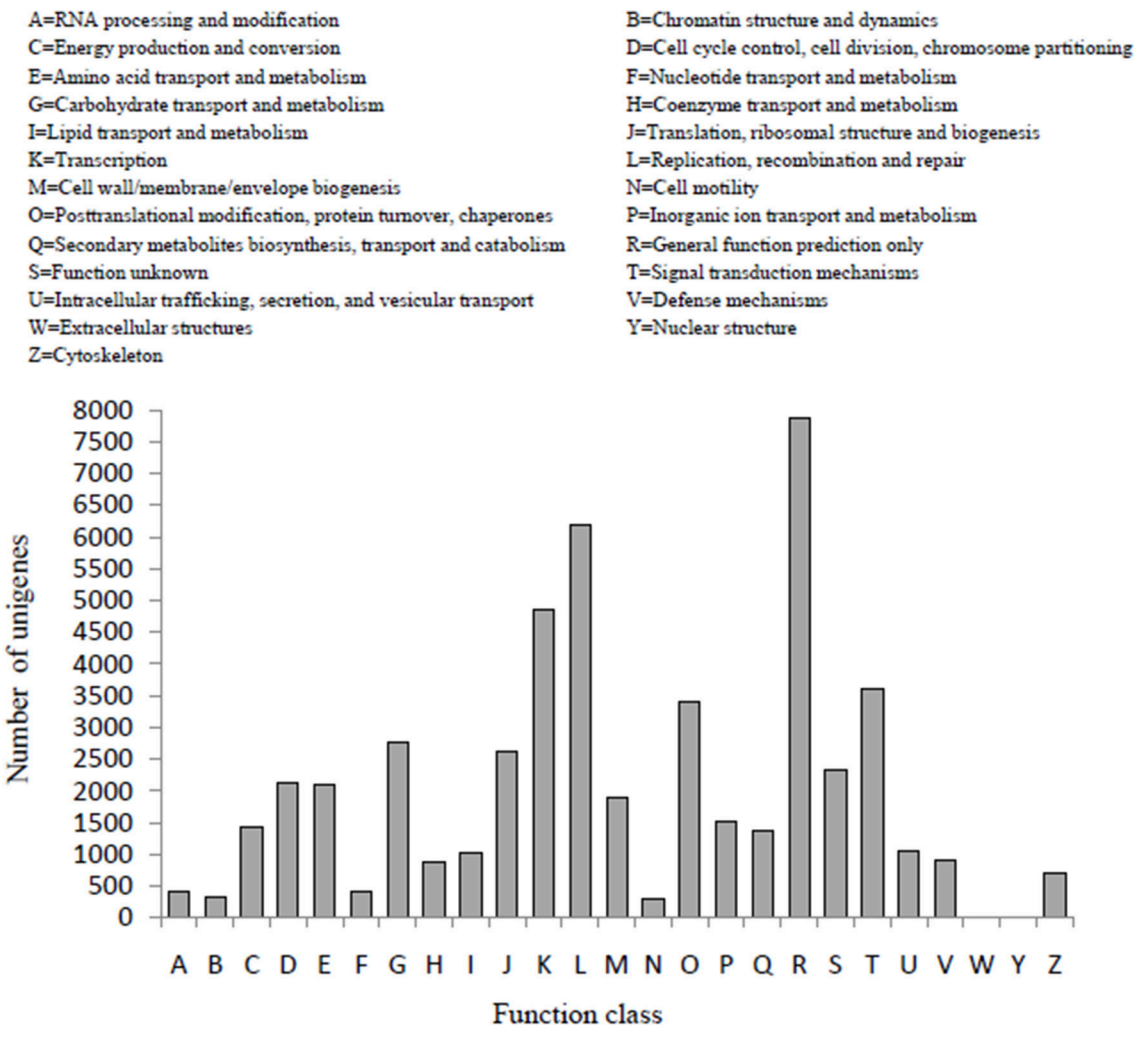

FIGURE 3 | COG function classification of *D. officinale* unigenes. A total of 25,982 unigenes were classified into 25 functional categories according to their predicted gene products using the COG database (cut-off *E*-value of 0.00001).

and unigenes in Dendrobium-1 are shown in **Figure 2A**. The assembly produced a substantial number of large contigs and unigenes: 34,113 contigs were >1000 bp in length and 27,968 unigenes were >1000 bp in length (**Figure 2A**). The contigs in Dendrobium-2 were further assembled into 114,098 unigenes by Trinity with a mean length of 695 bp. The size distribution of these contigs and unigenes are shown in **Figure 2B**. The assembly produced a substantial number of large contigs and unigenes: 33,624 contigs were >1000 bp in length and 27,229 unigenes were >1000 bp in length (**Figure 2B**).

The contigs in two transcriptome sequencing databases were integrated and assembled into a total of 145,791 unigenes. These unigenes were annotated using BLASTX searches against NCBI, Nr, Swiss-Prot, KEGG, and COG databases. In total, there were 67,396 annotated unigenes (46.23% of all unigenes), providing a significant BLAST result. Among them, 66,541 unigenes (98.73% of all annotated unigenes) showed significant similarity to known proteins in the Nr database and 25,982 unigenes (38.55%) were annotated in COG based on sequence homologies.

In the COG classification, 25,982 unigenes were classified into 25 functional classifications (**Figure 3**). The most dominant term was "General function prediction only" and 7861 unigenes (30%) matched it. "Translation," "replication, recombination, and repair" also shared a high percentage of genes among the categories, and only 4 and 19 unigenes matched the terms "nuclear structure" and "extracellular structures," respectively. In addition, 2754 unigenes were annotated as the "carbohydrate transport and metabolism" category and 1386 unigenes in the "secondary metabolites biosynthesis transport and catabolism" category, both of which may play an important role in the biosynthesis of polysaccharides and small molecules with proven bioactivity.

Gene Ontology Classification and Metabolic Pathway Assignment by KEGG

A total of 24,002 annotated unigenes were grouped into 41 functional groups by using GO assignments. Among these groups, 22 groups were involved in biological processes, 9 groups in cellular components and 10 groups in molecular functions. Metabolic processes and cellular processes were dominant in the biological process category. Within the molecular function category, a high percentage of genes were associated with

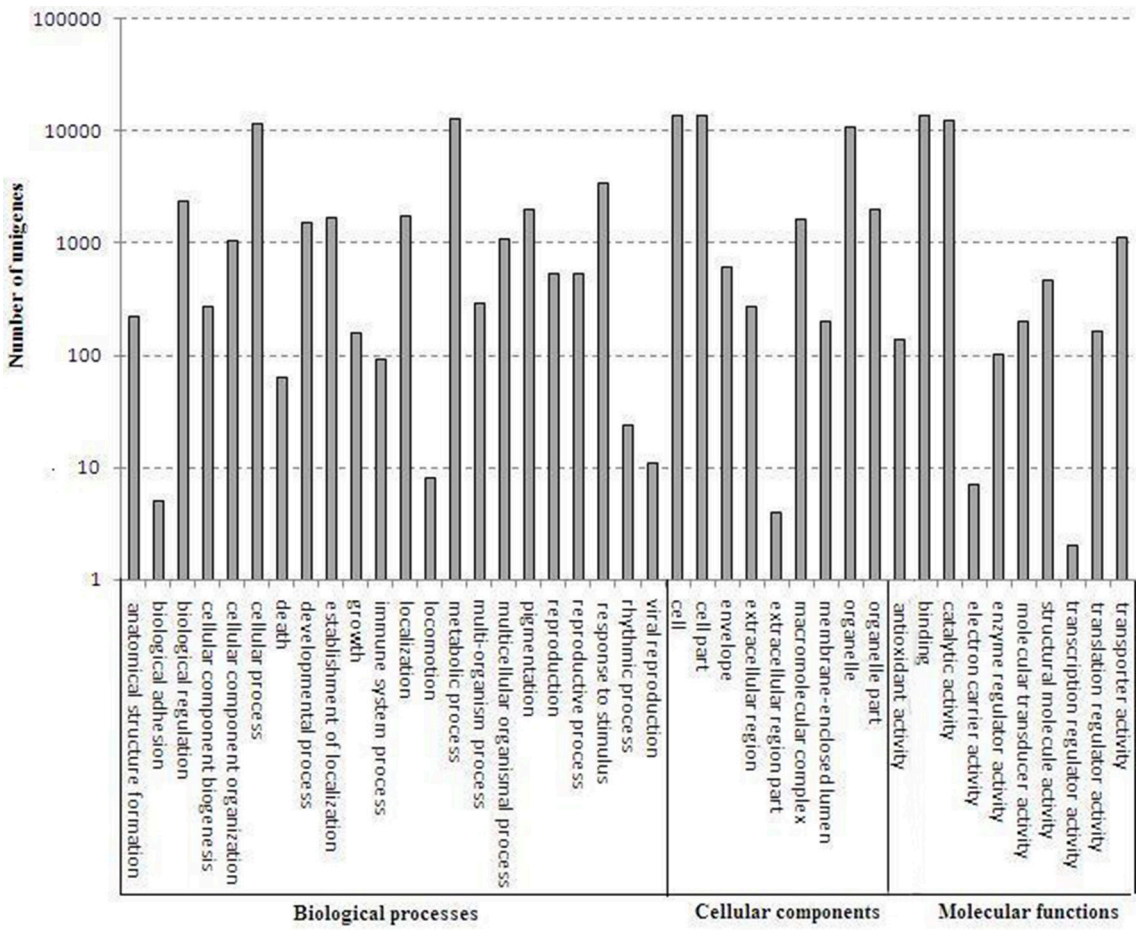

FIGURE 4 | Gene ontology categories of *D. officinale* unigenes. The results are summarized in mainly three categories: biological process, cellular component and molecular function.

catalytic activity and binding. Most assignments in cellular components were to cell components and cell membranes (**Figure 4**).

In this study, a total of 67,396 annotated sequences were mapped to reference canonical pathways in KEGG. In total, 17,281 sequences were assigned to 126 KEGG pathways (**Additional file 2**). The metabolic pathways represented the greatest group (4473 unigenes, or 25.88%), with most unigenes involved in starch and sucrose metabolism (320 unigenes), amino sugar and nucleotide sugar metabolism (288 unigenes), fructose and mannose metabolism (135 unigenes), and galactose metabolism (124 unigenes). A total of 2115 unigenes were involved in the biosynthesis of secondary metabolites, including phenylpropanoid biosynthesis, terpenoid backbone biosynthesis, cyanoamino acid metabolism, carotenoid biosynthesis, and others (**Table 2**). These pathways provide a valuable resource for investigating specific processes, functions and pathways during *D. officinale* development.

Mannose and glucose are the main monosaccharide building blocks in *D. officinale*. Fructose and mannose metabolism found in the KEGG pathway involved 135 unigenes. A detailed metabolic pathway for fructose and mannose metabolism is shown in **Figure 5**. Every gene in the pathway was associated with several unigenes. The pathway will be useful for further studies on the effect of the fructose and mannose metabolism pathway on the biosynthesis of active polysaccharides.

TABLE 2 | The pathways and number of unigenes related to secondary metabolites in *D. officinale*.

Biosynthesis of secondary metabolites pathway	All genes with pathway annotation (17281)	Pathway ID
Anthocyanin biosynthesis	1 (0.01%)	ko00942
Benzoxazinoid biosynthesis	1 (0.01%)	ko00402
Betalain biosynthesis	2 (0.01%)	ko00965
Brassinosteroid biosynthesis	19 (0.11%)	ko00905
Caffeine metabolism	6 (0.03%)	ko00232
Carotenoid biosynthesis	70 (0.41%)	ko00906
Cyanoamino acid metabolism	87 (0.5%)	ko00460
Diterpenoid biosynthesis	52 (0.3%)	ko00904
Flavone and flavonol biosynthesis	20 (0.12%)	ko00944
Flavonoid biosynthesis	57 (0.33%)	ko00941
Indole alkaloid biosynthesis	4 (0.02%)	ko00901
Isoquinoline alkaloid biosynthesis	34 (0.2%)	ko00950
Monoterpenoid biosynthesis	4 (0.02%)	ko00902
Nicotinate and nicotinamide metabolism	27 (0.16%)	ko00760
Phenylpropanoid biosynthesis	216 (1.25%)	ko00940
Sesquiterpenoid biosynthesis	13 (0.08%)	ko00909
Steroid biosynthesis	49 (0.28%)	ko00100
Stilbenoid, diarylheptanoid, and gingerol biosynthesis	48 (0.28%)	ko00945
Terpenoid backbone biosynthesis	104 (0.6%)	ko00900
Tropane, piperidine, and pyridine alkaloid biosynthesis	38 (0.22%)	ko00960

Identifying *D. officinale* Glycosyltransferase Genes and Cellulose Synthase Genes

A sequencing similarity search was conducted against the CAZy database by using BLASTX ($E < 0.00001$), identifying a total of 1081 carbohydrate-active related unigenes (**Additional file 3**), including 430 glycosyltransferase genes (GTs), 405 glycoside hydrolases, 150 carbohydrate esterases, 77 carbohydrate-binding modules, and 19 polysaccharide lyases (**Figure 6**).

GTs, which are enzymes that synthesize oligosaccharides, polysaccharides, and glycoconjugates, were dominant in carbohydrate-active related unigenes, and 430 GTs were divided into 35 GT families. A comparison of GTs families and numbers among *A. thaliana*, *O. sativa,* and *D. officinale* is shown in **Additional file 4**. *D. officinale* lacks several GT families, GT9, GT16, GT19, GT30, GT33, GT37, GT50, GT57, and GT58, which were present in *A. thaliana* and *O. sativa.* GT59 and GT76 were present in *A. thaliana* and *O. sativa*, but not in *D. officinale* while GT39 was present only in *D. officinale.*

The family of mannans is the most widespread group of polysaccharides in higher plants (Moreira and Filho, 2008). Cellulose synthase (CesA) superfamily genes were involved in the biosynthesis of mannan polysaccharides (Liepman et al., 2005). The CesA superfamily is classified into one CesA family and nine cellulose synthase-like (Csl) families, namely CslA/B/C/D/E/F/G/H/J. The CesA superfamily members of *A. thaliana* and *O. sativa* were used as bait for blasting the candidate unigenes from *D. officinale* protein libraries. A total of 89 candidate unigenes for CesA in *D. officinale* were identified and were listed in **Additional file 5**. A molecular phylogenetic tree (**Figure 7**) was constructed by using MEGA4 (Tamura et al., 2007), employing 19 unigenes that were translated into amino acid sequences, together with other CesA superfamily members from *A. thaliana* and *O. sativa*. The 19 unigenes were classified into six families, CesA, CslA, CslC, CslD, CslE, and CslH with 6 and 5 unigenes belonging to CesA and CslA families, respectively.

Screening and Identification of DEGs

To identify the DEGs during both developmental stages, the number of clean tags for each gene was calculated, and the genes that were differentially expressed between the two samples were identified according to the method described by Audic and Claverie (1997).

A total of 32,794 DEGs were obtained, including 22,051 up-regulated and 10,743 down-regulated genes in Dendrobium-2 compared to Dendrobium-1 (**Figure 8**). Furthermore, 1142 and 7918 unigenes expressed uniquely in Dendrobium-1 and Dendrobium-2, respectively, and 23,334 unigenes were expressed in both libraries, but at different levels (**Figure 9**). These specific DEGs in Dendrobium-1 and Dendrobium-2 are shown in **Additional files 6**, **7**, respectively.

Among 32,794 DEGs, a total of 18,517 (56.46% of all DEGs) unigenes provided a significant BLAST result. Approximately 4722 unigenes could be annotated in KEGG and 6356 unigenes could be annotated in GO based on sequence homologies,

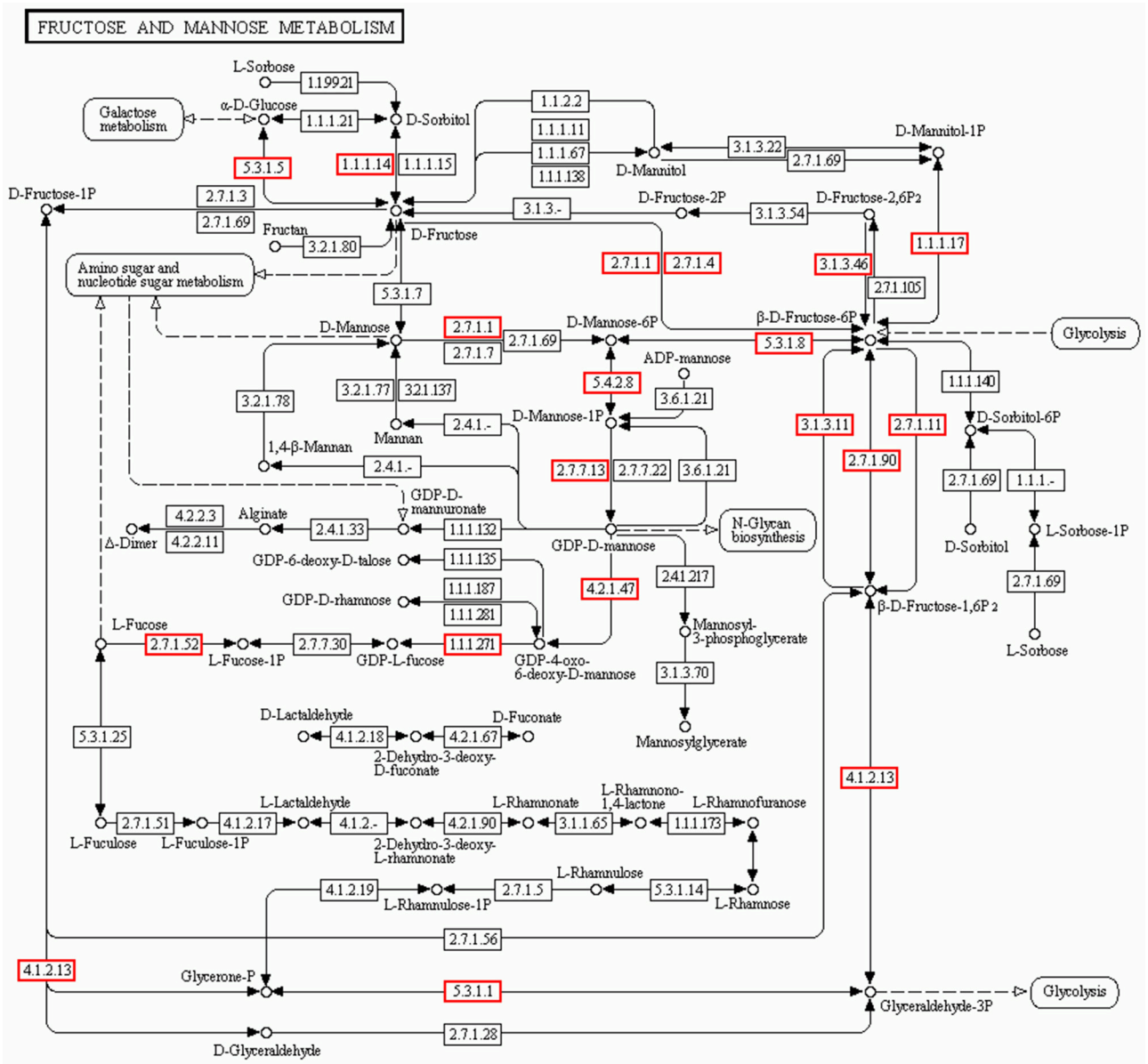

FIGURE 5 | Putative fructose and mannose metabolic pathway of *D.officinale*. Putative fructose and mannose metabolism of *D.officinale* was constructed based on KEGG annotation. A total of 135 unigenes were involved in the metabolic pathway. These unigenes were distributed in the rectangular boxes in the figure.

while 18046, 13790, and 7490 unigenes were annotated in Nr, SWISSprot, and COG, respectively.

In the KEGG classification, 4722 DEGs were significantly enriched in 42 pathways (**Additional file 8**). Most genes were correlated to metabolic pathways and biosynthesis of secondary metabolites. Gluconeogenesis was also significantly enriched. Furthermore, the number of up-regulated genes was more than the number of down-regulated genes in the three pathways.

The analysis of biological processes on these DEGs was performed based on GO functional classification. These genes, including specific unigenes in Dendrobium-1 and Dendrobium-2, as well as up-regulated and down-regulated unigenes in Dendrobium-1 vs. Dendrobium-2, were mainly correlated to metabolic and cellular processes and to responses to stimuli (**Additional file 9**). The main biological process for these DEGs was similar.

DEGs Related to Glycosyltransferases Genes, Cellulose Synthase Genes, and Transcription Factors

Among 1081 carbohydrate-related genes, only 235 DEGs were identified, including 94 up-regulated and 141 down-regulated genes. These carbohydrate-related DEGs included 170 GT, 28 mannnosyltransferase, 23 galactosylatransferase, 10

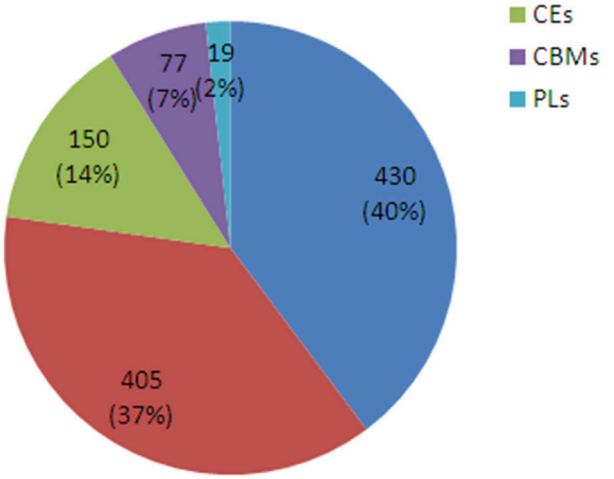

FIGURE 6 | The classification and number of carbohydrate-active enzyme families in *D. officinale* unigenes. GT, Glycosyltransferase; GH, Glycoside Hydrolase; CE, Carbohydrate Esterase; CBM, Carbohydrate-Binding Module; PL, Polysaccharide Lyase.

xylosyltransferase, and 4 fucosyltransferase DEGs (**Table 3**). 170 DEGs related to GT belonged to 28 GT families (list was shown in **Additional file 10**). Among them, GT1 and GT2 were the main families, including 38 and 33 DEGs, respectively. In the GT1 family, 10 DEGs were up-regulated and 28 DEGs were down-regulated. In contrast, in the GT2 family, 17 and 16 DEGs were up- and down-regulated, respectively (**Table 4**). Among 89 CesA-related genes, 37 genes showed differential expression, including seven up-regulated and 30 down-regulated genes. These were classified into five CslA families, CslA, CslD, CslE, CslF, and CslG, respectively (**Table 5**).

TFs have been implicated in a variety of developmental and physiological roles in plants. More TFs have also been isolated and characterized for several plant secondary metabolic pathways. In our *D. officinale* DEGs database, a total of 627 putative transcripts encoding TFs were identified, including 301 up-regulated unigenes and 326 down-regulated unigenes (**Table 6**). They belonged to known TF families, the most abundant being the MYB family, including 82 unigenes. In addition, 75 DEGs belonged to the bHLH family, 66 to the AP2/ERF family, 60 to the WRKY family, 33 to the Homeobox famlily, 30 to the MADS family, 24 to the NAC family, and 23 to the bZIP family. All these TFs have been identified as positive or negative regulators in the biosynthesis of secondary metabolites in other plants (Grotewold et al., 1998; van der Fits and Memelink, 2000).

Validation and Expression Analysis of Key Enzyme Genes

To validate changes in gene expression patterns, 18 key enzyme-encoding genes associated with GT biosynthesis, including GT1 (unigene0020469, unigene0022886, unigene0017200), GT2 (unigene0102284, unigene0157828, unigene0038137), GT8 (unigene0038402), GT28 (unigene0109540, unigene0134761), GT31 (unigene0127099), GT35 (unigene0104576), GT47 (unigene0112298), GT61 (unigene0150405, unigene0150401), and GT92 (unigene0157887), were randomly selected to examine gene expression using RT-qPCR. The two libraries exhibited differential expression and were identical to those obtained by sequencing (**Additional file 11**). Thus, the data generated in this study is sufficient to be used as a tool to investigate some genes related to polysaccharide synthesis and metabolism in *D. officinale*.

DISCUSSION

Illumina Sequencing and Sequence Annotation

D. officinale is a very important traditional Chinese herb within the *Orchidaceae*. Even though polysaccharides are one of the most important active constituents of *D. officinale*, little is known about the mechanisms responsible for polysaccharide synthesis and metabolism. The aims of this study were to generate a large amount of cDNA sequence data that would facilitate more detailed studies in *D. officinale*, and to identify the genes related to polysaccharide synthesis and metabolism. The availability of transcriptome data for *D. officinale* will meet the initial information needs for functional studies of this species and its relatives. In this study, two RNA-seq was performed using Illumina sequencing, which generated a total of 145,791 unigenes. A total of 67,396 (46.23%) unigenes provided a significant BLAST result. This information far exceeded that reported previously (Guo et al., 2013) and provides more adequate resources to study this *Dendrobium* species.

Glycosyltransferase Genes and their Differential Expression Patterns in *D. officinale*

D. officinale has a thick and soluble polysaccharide-rich stem. The biosynthesis of polysaccharides involves the action of hundreds of different GTs, which catalyze the transfer of sugar moieties from activated donor molecules to specific acceptor molecules to form glycosidic bonds. At the same time, the glycosylation reactions have a cascading effect, which affect many aspects of plant growth and development. The most recent update of CAZy (http://www.cazy.org/GlycosylTransferases.html) indicates that GTs from diverse species can be classified into 97 families. A total of 463 and 571 GT genes had been listed in *A. thaliana* and *O. sativa*, assigned to 42 and 43 families, respectively. We identified 430 possible GTs in the *D. officinale* transcriptome database that were divided into 35 GT families (**Additional file 4**).

The category and proportion of GT genes are different in different plants. The function of each GT family also shows differences. GT1 is a major GT family in plants and is commonly known as UDP glycosyltransferase (UGT) (Weis et al., 2008). GT1 plays an indispensable role in the biosynthesis and modification of plant natural products (Jones and Vogt, 2001).

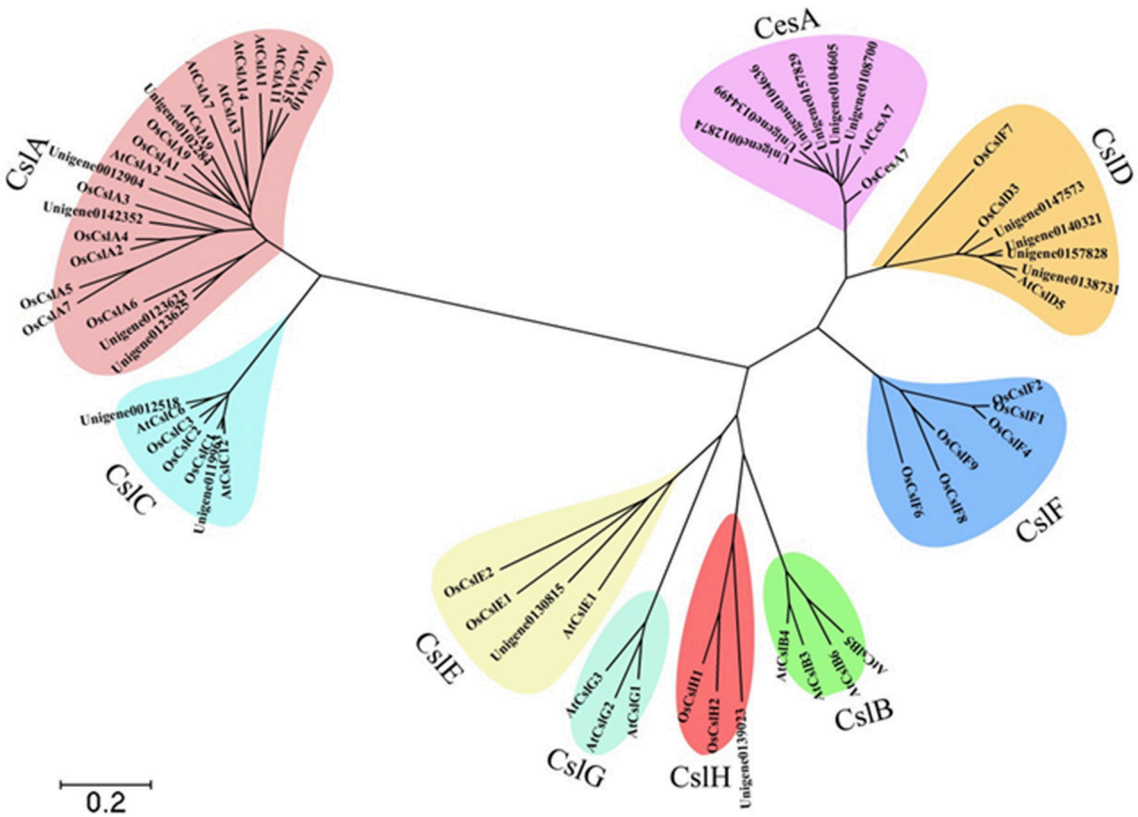

FIGURE 7 | Molecular phylogenetic tree of the amino acid sequences of the CesA superfamily of *D. officinale*, *A. thaliana,* and *O. sativa*. The tree was constructed using MEGA 4 by the neighbor-joining method. The tree was displayed as a phylogram in which branch lengths are proportional to distance. Bootstrap values for 1000 replicates were used to assess the robustness of the trees. The amino acid sequences of *A. thaliana* and *O. sativa* used for alignment are as follows: AtCesA7, gb|AAD32031.1|; AtCslA1, gb|AAO42230.1|; AtCslC12, gb|AAD15482.1|; AtCslG2, gbAAB63623.1|; AtCslA7, gb|AAL24081.1|; AtCslG3, gb|AAB63624.1|; AtCslG1, gb|AAB63622.1|; AtCslA15, gb|AEE83276.1; AtCslC6, gb|AAF02144.1|; AtCslD5, gb|AAF02892.1|; AtCslA3, gb|AAF79586.1|; AtCslB6, gb|AEE83584.1|; AtCslB5, gb|AAQ22621.1|; AtCslA9, gb|AAL31192.1|; AtCslA14, gb|AAO42815.1|; AtCslB4, gb|AAC25936.1|; AtCslB3, gb|AAC25935.1|; AtCslE1, gb|AAF79313.1|; AtCslA10, gb|AAF87149.1|; AtCslA2, gb|AAL24334.1|; AtCslA11, gb|AED92259.1|; OsCslA6, gb|AAL25127.1|; OsCslF1, gb|AAL25131.1|; OsCslE2, gb|AAL25130.1|; OsCslA9, gb|AAL25128.1|; OsCslA3, tpg|DAA01744.1|; OsCslD3, tpg|DAA01756.1|; OsCslC2, tpg|DAA01750.1|; OsCslF7, gb|AAK91320.1|; OsCslA2, gb|AAK98678.1|; OsCslF2, gb|AAL25132.1|; OsCslA5, gb|AAL82530.1|; OsCslA4, gb|AAL84294.1; OsCslH2, dbj|BAF14725.2|; OsCslC1, dbj|BAC10759.1|; OsCslH1, gb|AAN01252.1|; OsCslA7, gb|ABG34297.1|; OsCslF8, dbj|BAC65371.1|; OsCslF9, dbj|BAC80027.1|; OsCslF6, dbj|BAC66734.1|; OsCslD3, dbj|BAD01697.1|; OsCslF4, dbj|BAC83321.1|; OsCslC3, dbj|BAC98512.1|; OsCslA1, tpg|DAA01743.1|; OsCslE1, dbj|BAD46389.1|; OsCesA7, gb|AAK27814.1|.

In *A. thaliana* and *O. sativa*, GT1 is the major family (26 and 35%, respectively. The second group consists of GT2, GT8, GT31, and GT47 families, each accounting for approximately 6–9% of the genes. In *D. officinale*, the major GT families (GT1, GT2, and GT41) represent approximately 15–16% each of total GT genes. The third group consists of GT4 and GT8 (5 and 8%, respectively). The amount of GT41 in *D. officinale* exceeds that in *A. thaliana* and *O. sativa.* Moreover, GT51 and GT39 are specific to *D. officinale.* These specificities may reflect unique metabolic aspects of *D. officinale*.

In a previous study on *D. officinale*, polysaccharides were shown to be distributed in all organs, but mainly accumulated in stems while the soluble polysaccharide content changed in different developmental stages (He et al., 2015). The polysaccharide content in the stems of adult plants was higher than in seedlings but the content in the leaves and roots of adult plants was lower than in seedlings (He et al., 2015). In our present study, a total of 170 GTs showed differential expression in a comparison between adult plants and juvenile seedlings, including 70 up-regulated GTs and 100 down-regulated GTs (**Table 3**). The up-regulated GTs likely mainly accounted for the synthesis of soluble polysaccharides in adult plants while down-regulated GTs were probably used to build plant cell walls and other morphological structures in seedlings in the juvenile stage.

GT1 was the major gene among the down-regulated genes, and GT2 was the major gene among the up-regulated genes. The up-regulated and down-regulated GTs families contained 20 and 19 GT families, respectively. Furthermore, all DEGs, including up-regulated genes, down-regulated genes, as well as specific genes in adult plants or juvenile seedlings, showed similar metabolic pathways and biosynthesis of secondary metabolites (**Additional file 9**). All these results suggest that a variety of GTs together mediated the synthesis of soluble polysaccharides and the development of morphological structures. More studies

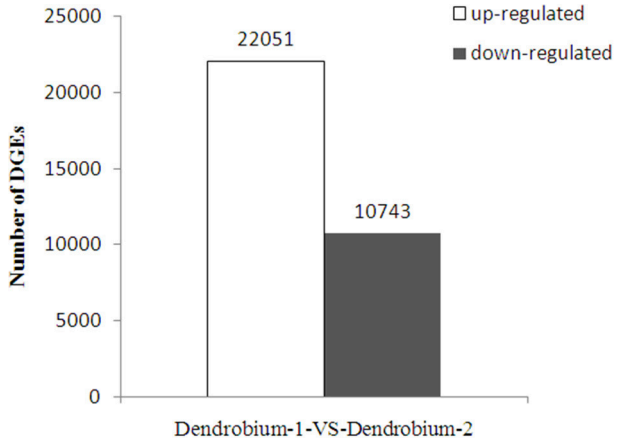

FIGURE 8 | Analysis of differentially expressed genes (DEGs) at two development stage. The y-axis indicates the number of DEGs with an absolute value of the $\log_2$ ratio >1 between Dendrobium-1 vs. Dendrobium-2. The number of up-regulated and down-regulated genes between Dendrobium-1 vs. Dendrobium-2 are summarized.

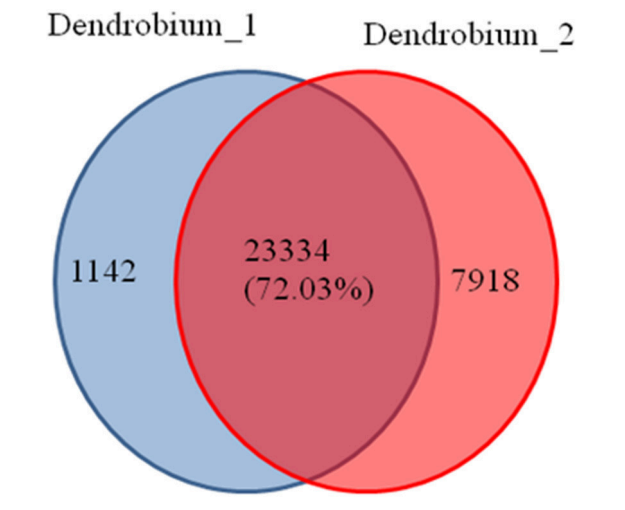

FIGURE 9 | Venn diagram of the unigenes at two development stage. The diagram shows the overlapping unigenes at the two development stage. A total of 23334 (72.03%) unigenes were expressed in the Dendrobium-1 and Dendrobium-2. While 1142 unigenes were expressed only in the Dendrobium-1 and 7918 unigenes were expressed only in the Dendrobium-2.

on their expression patterns and functions in the future could be used to elucidate the molecular mechanisms that regulate polysaccharide synthesis and secondary metabolism in *D. officinale*.

Cellulose Synthase Genes and their Differential Expression Patterns in *D. officinale*

Soluble polysaccharides are synthesized from monosaccharides such as mannose, glucose, galactose, arabinose, rhamnose, and others (Zha et al., 2007). Mannose is also the major component of polysaccharides from *Dendrobium* species such as *D. officinale*, *D. huoshanense*, *D. nobile*, *D. fimbriatum*, and *D. chrysotoxum* (Fan et al., 2009; Luo et al., 2010; Meng et al., 2013; He et al., 2015). Mannans are also promising bioactive polysaccharides for use in drugs (Alonso-Sande et al., 2009). Many studies have proven that CesA superfamily genes are involved in the biosynthesis of mannan polysaccharides (Liepman et al., 2005; Lerouxel et al., 2006).

TABLE 3 | The category and number of differentially expressed carbohydrate-related genes in DEGs database.

Category	Number of DEGs	Up-regulated	Down-regulated
Glycosyltransferase	170	70	100
Mannosyltransferase	28	15	13
Galactosylatransferase	23	8	15
Xylosyltransferase	10	1	9
Fucosyltransferase	4	1	3
Summary	235	94	141

The CesA superfamily is classified into one cellulose synthase (CesA) family and nine cellulose synthase-like (Csl) families, namely CslA/B/C/D/E/F/G/H/J. Among them, CslF, CslH, and CslJ are specific to monocotyledonous plants while CslB and CslG are found exclusively in dicotyledonous plants (Richmond and Somerville, 2000; Suzuki et al., 2006). Several studies have demonstrated that the Csl families are involved in the biosynthesis of mannan polysaccharides. For example, CslA subfamily members encode β-1,4-mannan synthase (Liepman et al., 2005; Yin et al., 2009), CslC subfamily members encode β-1,4-glucan synthase (Cocuron et al., 2007), while CslF and CslH subfamily members participate in the biosynthesis of β-(1,3;1,4)-D-glucan (Nemeth et al., 2010; Burton et al., 2011; Taketa et al., 2012). The function of the remaining subfamilies members is still unknown. We identified 89 CesA-related genes in the transcriptome database (**Additional file 5**), which were classified into one CseA family and nine Csl families, including CslB and CslG families. Among these CesA genes, 37 genes showed differential expression between adult plants with juvenile seedlings. These differentially expressed CesA genes only contained five CslA families (**Table 5**). Furthermore, the up-regulated genes were only found in CslE and CslG families while the down-regulated genes were found exclusively in CslA, CslD, and CslG families. The number of down-regulated genes exceeded that of up-regulated genes. We speculate that these up-regulated CslE and CslG family genes might encode some enzyme responsible for the synthesis of mannan polysaccharides in the stem of *D. officinale*. However, these down-regulated CslA, CslD, and CslG family genes might participate in the synthesis of the backbones of polysaccharides to build plant cell walls and other morphological structures in juvenile seedlings.

Transcription Factors Involved in Polysaccharide Biosynthesis and Other Secondary Metabolism

TFs play diverse roles in regulating the activity of polysaccharide biosynthesis and other secondary metabolism pathways. For

TABLE 4 | The category and number of GT families in the DEGs database.

Family	Number of DEGs	Up-regulated	Down-regulated
GT1	38	10	28
GT2	33	17	16
GT4	8	2	6
GT8	12	5	7
GT10	1	1	0
GT14	4	1	3
GT17	2	1	1
GT20	1	1	0
GT21	2	0	2
GT22	1	1	0
GT23	4	0	4
GT28	3	3	0
GT29	2	2	0
GT31	8	1	7
GT32	2	2	0
GT34	1	0	1
GT35	1	0	1
GT39	1	1	0
GT41	19	8	11
GT43	2	1	1
GT47	1	0	1
GT48	5	5	0
GT51	2	0	2
GT61	4	1	3
GT66	1	1	0
GT68	1	0	1
GT77	5	4	1
GT92	6	2	4
Summary	170	70	100

TABLE 5 | The category and number of Csl family in the DEGs database.

Family	Number of DEGs	Up-regulated	Down-regulated
CslA	13	0	13
CslD	9	0	9
CslE	4	4	0
CslF	8	0	8
CslG	3	3	0
Summary	37	7	30

example, *Arabidopsis* MYB58 and MYB63, as well as their ortholog PtrMYB28 from *Populus tricocarpa*, are transcriptional activators of the lignin biosynthetic pathway, whereas *Eucalyptus grandis* EgMYB2 and *Pinus taeda* PtMYB4 are involved in the regulation of the entire secondary wall biosynthetic program (Zhong and Ye, 2009). MYB75, which acts as a repressor of the lignin branch of the phenylpropanoid pathway, interacts with another secondary cell wall regulator, the KNOX TF, KNAT7. Together, they form functional complexes to regulate

TABLE 6 | The type and number of transcription factor families identified in the DEGs database of *D. officinale*.

Transcription factor factor	Number of unigenes	Up-regulated	Down-regulated
MYB	82	35	47
bHLH	75	37	38
AP2/ERF	66	21	45
WRKY	60	32	28
Homeobox	33	15	18
MADS	30	18	12
NAC	24	14	10
bZIP	23	13	10
GATA	15	4	11
NFY	11	7	4
LHW	7	3	4
TCP	6	1	5
IIIA	5	4	1
HEC4	5	1	4
ROC	5	1	4
MED	4	1	3
GRAS	4	1	3
PACC	4	1	3
CIGR2	3	2	1
MBF1	3	2	1
VIP-like	3	0	3
trihelix	3	1	2
RF2b-like	3	1	2
MYC	3	1	2
ABI3	3	1	2
ATF1	2	2	0
HY5-like	2	0	2
other	144	96	81
Total number	627	301	326

secondary cell wall deposition and to integrate the metabolic flux through the lignin, flavonoid, and polysaccharide pathways in *Arabidopsis* (Bhargava et al., 2010). Overexpression of PAP1, a MYB TF from *Arabidopsis*, resulted in strongly enhanced expression of phenylpropanoid biosynthesis genes as well as enhanced accumulation of lignin, hydroxycinnamic acid esters and flavonoids (Borevitz et al., 2000). In our study, 82 MYB TFs were found to be differential expression in both developmental stages, including 35 up-regulated TFs and 47 down-regulated TFs (**Table 6**). The up-regulated TFs were probably related with some aspect of secondary metabolism, including polysaccharide and alkaloid biosynthesis, and down-regulated TFs were likely related with morphogenesis, including cell wall formation. In recent years, many WRKY genes have been isolated from medicinal plants and have been shown to play an important role in secondary metabolism. *CjWRKY1* from *Coptis japonica* Makino was the first regulator identified in the biosynthesis of berberine, a benzylisoquinoline alkaloid, and transient expression of *CjWRKY1* in *C. japonica* protoplasts increased the level of

transcripts of berberine biosynthetic genes (Kato et al., 2007). *AaWRKY1* from *Artemisia annua* L. could activate Amorpha-4, 11-diene synthase to regulate artemisinin biosynthesis (Ma et al., 2009). *SUSIBA2*, a WRKY TF from *Hordeum vulgare* cv. "Pongo," was participated in sugar signaling by binding to the sugar-responsive elements of the iso1 promoter (Sun et al., 2003). In our study, 60 WARK TFs were discovered in the DEGs database (**Table 6**). There have been reports that AP2/ERF family TFs play an important role in plant secondary metabolism. For example, overexpression of the JA-inducible AP2/ERF-domain TF ORCA3 of *Catharanthus roseus*, led to increased expression of several metabolic biosynthetic genes and consequently increased the accumulation of terpenoid indole alkanoids in suspension cells (van der Fits and Memelink, 2000). The NIC2/ORCA3 ERF subfamily from *Nicotiana tabacum* was independently recruited to regulate jasmonate-inducible secondary metabolism in distinct plant lineages (Shoji et al., 2010). In our study, 66 AP2/ERF TFs were discovered in the DEGs database and differentially expressed in the two developmental stages: 21 were up-regulated and 45 were down-regulated (**Table 6**). In plants, bHLH and bZIP TFs were also isolated and confirmed to regulate secondary metabolism. CrMYC2 belongs to the bHLH TF family and regulates ORCA gene expression, and the AP2/ERF-domain TFs, ORCA2, and ORCA3, in turn regulate a subset of alkaloid biosynthesis genes in *C. roseus* (Zhang et al., 2011). In our work, 75 HLH TFs were discovered. All these TF types known to be involved in regulating secondary metabolism were found in our dataset. They may play important roles in *D. officinale* development, stress responses and secondary metabolism.

CONCLUSIONS

D. officinale is a very important Chinese medicinal herb. A total of 145,791 unigenes were obtained in two transcriptome databases of *D. officinale*, 135 of which were involved in fructose and mannose metabolism. In addition, 430 glycosyltransferase and 89 cellulose synthase genes were identified. Comparative analysis of the transcriptome in juvenile seedlings and adult plants revealed a total of 32,794 DEGs that were mainly correlated with metabolic pathways and the biosynthesis of secondary metabolites. A total of 170 glycosyltransferase genes, 37 cellulose synthase genes and 627 transcription factors showed differential expression. This data could be used to investigate pathways associated with polysaccharide biosynthesis and various secondary metabolites in *D. officinale*.

AUTHOR CONTRIBUTIONS

JZ performed the bioinformatics analyses and drafted the manuscript. CH carried out the experiments. KW and ZY cultured and provided the experimental material. JT critically evaluated the protocol and data, interpreted it, and revised the manuscript. SZ and XZ participated in the qRT-PCR experiment. HX performed the bioinformatics analyses. JD designed the study and revised the manuscript. All authors read and approved the final manuscript.

ACKNOWLEDGMENTS

This work was supported by the Forestry Science and Technology Innovation Fund Project of Guangdong province (Project number 2015KJCX040, 2013KJCX014-06), the Science and Technology Planning Project of Guangdong Province (Project number 2013B020302003), National Science Foundation of China Projects (Grant number 31370365), and the Guangxi Science and Technology Development Project (Project number 14125003-2-29).

SUPPLEMENTARY MATERIAL

The Supplementary Material for this article can be found online at: http://journal.frontiersin.org/article/10.3389/fpls.2016.00005

Additional file 1 | Primer sequences for qRT-PCR.

Additional file 2 | Metabolic pathway analysis result for unigenes by KEGG annotation.

Additional file 3 | The lists of carbohydrate-active related unigenes.

Additional file 4 | The category and number of GTs family in *D. officinale*, *A. thaliana,* and *O. sativa*.

Additional file 5 | The lists of CesA family related unigenes in *D. officinale*.

Additional file 6 | Specific expression of genes in Dendrobium-1.

Additional file 7 | Specific expression of genes in Dendrobium-2.

Additional file 8 | Gene set enrichment analysis in the comparison of Dendrobium-1 vs. Dendrobium-2 by KEGG.

Additional file 9 | The main biological process for specific unigenes in Dendrobium-1 (A), specific unigenes in Dendrobium-2 (B), up-regulated unigenes (C), down-regulated unigenes (D) in Dendrobium-1 vs. Dendrobium-2.

Additional file 10 | Lists of DEGs related to glycosyltransferases genes.

Additional file 11 | Differential expression genes related with GTs in *D. officinale* DEGs. (A) Heat map analysis of 18 GT-related genes in the comparison of Dendrobium-1 vs. Dendrobium-2. Each row represents a gene. Expression differences are shown in different colors. Red means high expression and green means low expression. **(B–D)** Validation of RNA-sequencing results by real-time PCR. The gene expression in Dendrobium-1 (blue bars), and Dendrobium-2 (red bars). The y-axis indicates relative normalized expression in the Dendrobium-1 and Dendrobium-2 samples. The relative normalized expression of 18 genes in Dendrobium-1 was calibrated as zero.

REFERENCES

Alonso-Sande, M., Teijeiro-Osorio, D., Remuñán-López, C., and Alonso, M. J. (2009). Glucomannan, a promising polysaccharide for biopharmaceutical purposes. *Eur. J. Pharm. Biopharm.* 72, 453–462. doi: 10.1016/j.ejpb.2008.02.005

Audic, S., and Claverie, J. M. (1997). The significance of digital gene expression profiles. *Genome Res.* 7, 986–995.

Bhargava, A., Mansfield, S. D., Hall, H. C., Douglas, C. J., and Ellis, B. E. (2010). MYB75 functions in regulation of secondary cell wall formation in the *Arabidopsis* inflorescence stem. *Plant Physiol.* 154, 1428–1438. doi: 10.1104/pp.110.162735

Borevitz, J. O., Xia, Y., Blount, J., Dixon, R. A., and Lamb, C. (2000). Activation tagging identifies a conserved MYB regulator of phenylpropanoid biosynthesis. *Plant Cell* 12, 2383–2394. doi: 10.1105/tpc.12.12.2383

Burton, R. A., Collins, H. M., Kibble, N. A., Smith, J. A., Shirley, N. J., Jobling, S. A., et al. (2011). Over-expression of specific HvCslF cellulose synthase-like genes in transgenic barley increases the levels of cell wall (1, 3; 1, 4)-β-d-glucans and alters their fine structure. *Plant Biotechnol. J.* 9, 117–135. doi: 10.1111/j.1467-7652.2010.00532.x

Cocuron, J. C., Lerouxel, O., Drakakaki, G., Alonso, A. P., Liepman, A. H., Keegstra, K., et al. (2007). A gene from the cellulose synthase-like C family encodes a β-1, 4 glucan synthase. *Proc. Natl. Acad. Sci. U.S.A.* 104, 8550–8555. doi: 10.1073/pnas.0703133104

Conesa, A., Götz, S., García-Gómez, J. M., Teról, J., Talon, M., and Robles, M. (2005). Blast2GO: a universal tool for annotation, visualization and analysis in functional genomics research. *Bioinformatics* 21, 3674–3676. doi: 10.1093/bioinformatics/bti610

Fan, Y. J., He, X. J., Zhou, S. D., Luo, A. X., He, T., and Chun, Z. (2009). Composition analysis and antioxidant activity of polysaccharide from *Dendrobium denneanum*. *Int. J. Biol. Macromol.* 45, 169–173. doi: 10.1016/j.ijbiomac.2009.04.019

Grabherr, M. G., Haas, B. J., Yassour, M., Levin, J. Z., Thompson, D. A., Amit, I., et al. (2011). Full-length transcriptome assembly from RNA-Seq data without a reference genome. *Nat Biotechnol.* 29, 644–652. doi: 10.1038/nbt.1883

Grotewold, E., Chamberlain, M., Snook, M., Siame, B., Butler, L., Swenson, J., et al. (1998). Engineering secondary metabolism in maize cells by ectopic expression of transcription factors. *Plant Cell* 10, 721–740. doi: 10.2307/3870660

Guo, X., Li, Y., Li, C., Luo, H., Wang, L., Qian, J., et al. (2013). Analysis of the *Dendrobium officinale* transcriptome reveals putative alkaloid biosynthetic genes and genetic markers. *Gene* 527, 131–138. doi: 10.1016/j.gene.2013.05.073

He, C., Zhang, J., Liu, X., Zeng, S., Wu, K., Yu, Z., et al. (2015). Identification of genes involved in biosynthesis of mannan polysaccharides in *Dendrobium officinale* by RNA-seq analysis. *Plant Mol. Biol.* 88, 219–231. doi: 10.1007/s11103-015-0316-z

Hsieh, Y. S., Chien, C., Liao, S. K., Liao, S. F., Hung, W. T., Yang, W. B., et al. (2008). Structure and bioactivity of the polysaccharides in medicinal plant *Dendrobium huoshanense*. *Bioorgan Med Chem.* 16, 6054–6068. doi: 10.1016/j.bmc.2008.04.042

Hua, Y. F., Zhang, M., Fu, C. X., Chen, Z. H., and Chan, G. Y. S. (2004). Structural characterization of a 2-*O*-acetylglucomannan from *Dendrobium officinale* stem. *Carbohyd Res.* 339, 2219–2224. doi: 10.1016/j.carres.2004.05.034

Jones, P., and Vogt, T. (2001). Glycosyltransferases in secondary plant metabolism: tranquilizers and stimulant controllers. *Planta* 213, 164–174. doi: 10.1007/s004250000492

Kanehisa, M., Araki, M., Goto, S., Hattori, M., Hirakawa, M., Itoh, M., et al. (2008). KEGG for linking genomes to life and the environment. *Nucleic Acids Res.* 36, D480–D484. doi: 10.1093/nar/gkm882

Kato, N., Dubouzet, E., Kokabu, Y., Yoshida, S., Taniguchi, Y., Dubouzet, J. G., et al. (2007). Identification of a WRKY protein as a transcriptional regulator of benzylisoquinoline alkaloid biosynthesis in *Coptis japonica*. *Plant Cell Physiol.* 48, 8–18. doi: 10.1093/pcp/pcl041

Leitch, I. J., Kahandawala, I., Suda, J., Hanson, L., Ingrouille, M. J., Chase, M. W., et al. (2009). Genome size diversity in orchids: consequences and evolution. *Ann. Bot.* 104, 469–481. doi: 10.1093/aob/mcp003

Lerouxel, O., Cavalier, D. M., Liepman, A. H., and Keegstra, K. (2006). Biosynthesis of plant cell wall polysaccharides-a complex process. *Curr. Opin. Plant Biol.* 9, 621–630. doi: 10.1016/j.pbi.2006.09.009

Li, J., Li, S., Huang, D., Zhao, X., and Cai, G. (2011). Advances in the of resources, constituents and pharmacological effects of *Dendrobium officinale*. *Sci. Technol. Rev.* 29, 74–79. doi: 10.3981/j.issn.1000-7857.2011.18.012

Liepman, A. H., Wilkerson, C. G., and Keegstra, K. (2005). Expression of cellulose synthase-like (Csl) genes in insect cells reveals that CslA family members encode mannan synthases. *Proc. Natl. Acad. Sci. U.S.A.* 102, 2221–2226. doi: 10.1073/pnas.0409179102

Liu, X. F., Zhu, J., Ge, S. Y., Xia, L. J., Yang, H. Y., Qian, Y. T., et al. (2011). Orally administered *Dendrobium officinale* and its polysaccharides enhance immune functions in BALB/c mice. *Nat. Prod. Commun.* 6, 867–870.

Luo, A. X., He, X. J., Zhou, S. D., Fan, Y. J., Luo, A. S., and Chun, Z. (2010). Purification, composition analysis and antioxidant activity of the polysaccharides from *Dendrobium nobile* Lindl. *Carbohyd. Polym.* 79, 1014–1019. doi: 10.1016/j.carbpol.2009.10.033

Ma, D., Pu, Q., Lei, C., Ma, L., Wang, H., Guo, Y., et al. (2009). Isolation and characterization of AaWRKYl, an *Artemisia annua* transcription factor that regulates the amorpha-4,ll-diene synthase gene, a key gene of artemisinin biosynthesis. *Plant Cell Physiol.* 50, 2146–2161. doi: 10.1093/pcp/pcp149

Meng, L. Z., Lv, G. P., Hu, D. J., Cheong, K. L., Xie, J., Zhao, J., et al. (2013). Effects of polysaccharides from different species of *Dendrobium* (Shihu) on macrophage function. *Molecules* 18, 5779–5791. doi: 10.3390/molecules18055779

Moreira, L. R., and Filho, E. X. (2008). An overview of mannan structure and mannan-degrading enzyme systems. *Appl. Microbiol. Biotechnol.* 79, 165–178. doi: 10.1007/s00253-008-1423-4

Murashige, T., and Skoog, F. (1962). A revised medium for rapid growth and bio assays with tobacco tissue cultures. *Physiol. Plant* 15, 473–497. doi: 10.1111/j.1399-3054.1962.tb08052.x

Nemeth, C., Freeman, J., Jones, H. D., Sparks, C., Pellny, T. K., Wilkinson, M. D., et al. (2010). Down-regulation of the CSLF6 gene results in decreased (1,3;1,4)-β-D-glucan in endosperm of wheat. *Plant Physiol.* 152, 1209–1218. doi: 10.1104/pp.109.151712

Pertea, G., Huang, X., Liang, F., Antonescu, V., Sultana, R., Karamycheva, S., et al. (2003). TIGR Gene Indices clustering tools (TGICL): a software system for fast clustering of large EST datasets. *Bioinformatics* 19, 651–652. doi: 10.1093/bioinformatics/btg034

Richmond, T. A., and Somerville, C. R. (2000). The cellulose synthase superfamily. *Plant Physiol.* 124, 495–498. doi: 10.1104/pp.124.2.495

Shoji, T., Kajikawa, M., and Hashimoto, T. (2010). Clustered transcription factor genes regulate nicotine biosynthesis in tobacco. *Plant Cell* 22, 3390–3409. doi: 10.1105/tpc.110.078543

Sun, C., Palmqvist, S., Olsson, H., Borén, M., Ahlandsberg, S., and Jansson, C. (2003). A novel WRKY transcription factor, SUSIBA2, participates in sugar signaling in barley by binding to the sugar-responsive elements of the iso1 promoter. *Plant Cell* 15, 2076–2092. doi: 10.1105/tpc.014597

Suzuki, S., Li, L. G., Sun, Y. H., and Chiang, V. L. (2006). The cellulose synthase gene superfamily and biochemical functions of xylem-specific cellulose synthase-like genes in *Populus trichocarpa*. *Plant Physiol.* 142, 1233–1245. doi: 10.1104/pp.106.086678

Taketa, S., You, T., Tonooka, T., Tsumuraya, Y., Inagaki, Y., Haruyama, N., et al. (2012). Functional characterization of barley betaglucanless mutants demonstrates a unique role for CslF6 in (1, 3; 1, 4)-β-D-glucan biosynthesis. *J. Exp. Bot.* 63, 381–392. doi: 10.1093/jxb/err285

Tamura, K., Dudley, J., Nei, M., and Kumar, S. (2007). MEGA4: molecular evolutionary genetics analysis (MEGA) software version 4.0. *Mol. Biol. Evol.* 24, 1596–1599. doi: 10.1093/molbev/msm092

van der Fits, L., and Memelink, J. (2000). ORCA3, a jasmonate responsive transcriptional regulator of plant primary and secondary metabolism. *Science* 289, 295–297. doi: 10.1126/science.289.5477.295

Wang, J. H., Luo, J. P., Zha, X. Q., and Feng, B. J. (2010). Comparison of antitumor activities of different polysaccharide fractions from the stems of *Dendrobium nobile* Lindl. *Carbohyd. Polym.* 79, 114–118. doi: 10.1016/j.carbpol.2009.07.032

Weis, M., Lim, E. K., Bruce, N. C., and Bowles, D. J. (2008). Engineering and kinetic characterisation of two glucosyltransferases from *Arabidopsis thaliana*. *Biochimie* 90, 830–834. doi: 10.1016/j.biochi.2008.01.013

Weng, D. (2003). FAAS determination of trace elements in *Dendrobium candidum* using suspension sampling with ultrasonic agitation. *Chin. Pharm. J.* 38, 704–706. doi: 10.3321/j.issn:1001-2494.2003.09.024

Wu, Z. Y., Raven, P. H., and Hong, D. Y. (2009). *Flora of China (Orchidaceae), Vol. 25*. Beijing; St.Louis, MO: Science Press; Missouri Botanical Garden Press.

Xia, L. J., Liu, X. F., Guo, H. Y., Zhang, H., Zhu, J., and Ren, F. Z. (2012). Partial characterization and immunomodulatory activity of polysaccharides from the stem of *Dendrobium officinale in vitro*. *J. Functional Foods* 4, 294–301. doi: 10.1016/j.jff.2011.12.006

Yang, L., Wang, Z., and Xu, L. (2006). Simultaneous determination of phenols (bibenzyl, phenanthrene, and fluorenone) in *Dendrobium* species by high-performance liquid chromatography with diode array detection. *J. Chromatogr. A*. 1104, 230–237. doi: 10.1016/j.chroma.2005.12.012

Ye, J., Fang, L., Zheng, H., Zhang, Y., Chen, J., Zhang, Z., et al. (2006). WEGO: a web tool for plotting GO annotations. *Nucleic Acids Res.* 34, W293–W297. doi: 10.1093/nar/gkl031

Yin, Y., Huang, J., and Xu, Y. (2009). The cellulose synthase superfamily in fully sequenced plants and algae. *BMC Plant Biology* 9:99. doi: 10.1186/1471-2229-9-99

Zha, X. Q., Luo, J. P., Luo, S. Z., and Jiang, S. T. (2007). Structure identification of a new immunostimulating polysaccharide from the stems of *Dendrobium huoshanense*. *Carbohyd. Polym*. 69, 86–93. doi: 10.1016/j.carbpol.2006.09.005

Zhang, H., Hedhili, S., Montiel, G., Zhang, Y., Chatel, G., Pré, M., et al. (2011). The basic helix–loop–helix transcription factor CrMYC2 controls the jasmonate-responsive expression of the ORCA genes that regulate alkaloid biosynthesis in *Catharanthus roseus*. *Plant J.* 67, 61–71. doi: 10.1111/j.1365-313X.2011.04575.x

Zhang, J., Wu, K., Zeng, S., Teixeira da Silva, J. A., Zhao, X., Tian, C. E., et al. (2013). Transcriptome analysis of *Cymbidium sinense* and its application to the identification of genes associated with floral development. *BMC Genomics* 14:279. doi: 10.1186/1471-2164-14-279

Zhong, R., and Ye, Z. H. (2009). Transcriptional regulation of lignin biosynthesis. *Plant Signal. Behav.* 4, 1028–1034. doi: 10.4161/psb.4.11.9875

Conflict of Interest Statement: The authors declare that the research was conducted in the absence of any commercial or financial relationships that could be construed as a potential conflict of interest.

frontiers in Plant Science

ORIGINAL RESEARCH
published: 18 February 2016
doi: 10.3389/fpls.2016.00166

Two *LcbHLH* Transcription Factors Interacting with *LcMYB1* in Regulating Late Structural Genes of Anthocyanin Biosynthesis in *Nicotiana* and *Litchi chinensis* During Anthocyanin Accumulation

Biao Lai[1,2], Li-Na Du[1], Rui Liu[1,2], Bing Hu[1,2], Wen-Bing Su[1,2], Yong-Hua Qin[1], Jie-Tang Zhao[1], Hui-Cong Wang[2] and Gui-Bing Hu[1,2]**

[1] State Key Laboratory for Conservation and Utilization of Subtropical Agro-Bioresources, College of Horticulture, South China Agricultural University, Guangzhou, China, [2] Physiological Laboratory for South China Fruits, College of Horticulture, South China Agricultural University, Guangzhou, China

OPEN ACCESS

Edited by:
Humberto Rodríguez Fuentes, Universidad Autónoma de Nuevo León, Mexico

Reviewed by:
Trine (Anne Kathrine) Hvoslef-Eide, Norwegian University of Life Sciences, Norway
Hao Peng, Washington State University, USA

***Correspondence:**
Gui-Bing Hu
guibing@scau.edu.cn;
Hui-Cong Wang
wanghc1972@263.net

Specialty section:
This article was submitted to Crop Science and Horticulture, a section of the journal Frontiers in Plant Science

Received: 18 September 2015
Accepted: 31 January 2016
Published: 18 February 2016

Citation:
Lai B, Du L-N, Liu R, Hu B, Su W-B, Qin Y-H, Zhao J-T, Wang H-C and Hu G-B (2016) Two LcbHLH Transcription Factors Interacting with LcMYB1 in Regulating Late Structural Genes of Anthocyanin Biosynthesis in Nicotiana and Litchi chinensis During Anthocyanin Accumulation. Front. Plant Sci. 7:166. doi: 10.3389/fpls.2016.00166

Anthocyanin biosynthesis requires the MYB-bHLH-WD40 protein complex to activate the late biosynthetic genes. *LcMYB1* was thought to act as key regulator in anthocyanin biosynthesis of litchi. However, basic helix-loop-helix proteins (bHLHs) as partners have not been identified yet. The present study describes the functional characterization of three litchi bHLH candidate anthocyanin regulators, *LcbHLH1*, *LcbHLH2,* and *LcbHLH3*. Although these three litchi bHLHs phylogenetically clustered with bHLH proteins involved in anthcoyanin biosynthesis in other plant, only LcbHLH1 and LcbHLH3 were found to localize in the nucleus and physically interact with *LcMYB1*. The transcription levels of all these bHLHs were not coordinated with anthocyanin accumulation in different tissues and during development. However, when co-infiltrated with *LcMYB1*, both *LcbHLH1* and *LcbHLH3* enhanced anthocyanin accumulation in tobacco leaves with *LcbHLH3* being the best inducer. Significant accumulation of anthocyanins in leaves transformed with the combination of LcMYB1 and LcbHLH3 were noticed, and this was associated with the up-regulation of two tobacco endogenous bHLH regulators, *NtAn1a* and *NtAn1b*, and late structural genes, like *NtDFR* and *NtANS*. Significant activity of the *ANS* promoter was observed in transient expression assays either with *LcMYB1-LcbHLH1* or *LcMYB1-LcbHLH3*, while only minute activity was detected after transformation with only *LcMYB1*. In contrast, no activity was measured after induction with the combination of *LcbHLH2* and *LcMYB1*. Higher DFR expression was also oberseved in paralleling with higher anthocyanins in co-transformed lines. LcbHLH1 and LcbHLH3 are essential partner of LcMYB1 in regulating the anthocyanin production in tobacco and probably also in litchi. The LcMYB1-LcbHLH complex enhanced anthocyanin accumulation may associate with activating the transcription of *DFR* and *ANS*.

Keywords: anthocyanins, MYB, bHLH, interaction, *Litchi chinensis*, tobacco

INTRODUCTION

Among the pigments that confer color to plants, anthocyanins are of particular interest because they are not only responsible for most of the red, blue, or black color in plants, but also for the beneficial effects on plant physiological processes and human health (Winkel, 2006). The biosynthetic pathway for anthocyanin biosynthesis has been well characterized and the corresponding genes have been isolated from various plant species (Hichri et al., 2011).

Research on model plants has shown that the expression of structural anthocyanin genes, particularly late genes, are orchestrated by a so-called MBW ternary complex, which is composed of MYB and bHLH transcription factors, together with WD40 repeat proteins (Broun, 2005; Koes et al., 2005; Hichri et al., 2011). In plants, R2R3 MYBs are considered to be key transcription factors known as the regulators of anthocyanin biosynthesis. MYBs in determining anthocyanin biosynthesis have been well characterized in model plants and fruit trees, such as *Arabidopsis* (Borevitz et al., 2000), antirrhinum (Schwinn et al., 2006), petunia (Quattrocchio et al., 1999), apple (Ban et al., 2007; Chagne et al., 2007, 2013), pear (Feng et al., 2010), grape (Kobayashi et al., 2002), litchi (Lai et al., 2014), mangosteen (Palapol et al., 2009), and Chinese bayberry (Niu et al., 2010). The R3 domain of MYBs suggests protein–protein interaction, especially with the bHLH co-factor, also known as MYC (Grotewold et al., 2000; Zimmermann et al., 2004).

The bHLH proteins are also a large class of transcription factors in plants, and have been divided into 26 subgroups (Pires and Dolan, 2010). bHLH transcription factors regulate many cellular processes such as fate of epidermal cells, hormonal response, metal homeostasis, photomorphogenesis, and development of floral organs (Hichri et al., 2011). Flavonoid related bHLHs have been grouped into subgroup IIIf. Maize regulatory gene (*R*) was the first isolated and characterized as a bHLH transcription factor which encodes a protein regulating anthocyanin accumulation (Ludwig et al., 1989, 1990). In *Arabidopsis*, bHLH proteins, TT8, GL3, and EGL3, are involved in production of different flavonoids (Shirley et al., 1995; Payne et al., 2000; Zhang et al., 2003). *NtAn1a* and *NtAn1b* originate from two ancestors of tobacco (*N. sylvestris* and *N. tomentosiformis*) and both enhance anthocyanin accumulation in tobacco flowers (Bai et al., 2011). G to A transition in the bHLH encoding *A* gene is the main reason for white flower color of pea in Mendel genetic research (Hellens et al., 2010). bHLH transcription factors are essential to anthocyanin biosynthesis in plants.

bHLH proteins function as anthocyanin regulator in cultivated fruit species had been reported so far for grape (Hichri et al., 2010), apple (Espley et al., 2007) and Chinese bayberry (Liu et al., 2013). The grape bHLH transcription factors *VvMYC1* and *MYCA1*, were found to be able to induce anthocyanin and proanthocyanidin production through physically interacts with MYBs and consequent activation of the promoters of genes involved in anthocyanin and/or proanthocyanidin synthesis (Hichri et al., 2010). Efficient induction of anthocyanin biosynthesis in transient assays by MdMYB10 was dependent on the co-expression of two distinct bHLH proteins from apple, MdbHLH3 and MdbHLH33 (Espley et al., 2007). Though MrbHLH1 and MrbHLH2 were clustered in IIIf group, only MrbHLH1 was the essential partner of MrMYB1 during anthocyanin biosynthesis regulation in bayberry, the function of MrbHLH2 still unknown (Liu et al., 2013). However, their role in anthocyanin regulation and how they work have not been fully uncovered and the effects of bHLH co-factors in anthocyanin regulation might differ among species (Montefiori et al., 2015; Xu et al., 2015).

The red pigment of litchi pericarp is due to the accumulation of anthocyanins (Lee and Wicker, 1991). *LcMYB1* was thought to act as key regulator in anthocyanin biosynthesis of litchi by activating the late structural genes *UFGT* in particular (Wei et al., 2011; Zhao et al., 2012; Lai et al., 2014). *LcMYB1* can strongly induce anthocyanin biosynthesis in tobacco leaves by its own, without requiring co-infiltration with a *bHLH* partner. However, the upregulation of *NtAn1b* in response to *LcMYB1* overexpression suggested the essential role of bHLH partner in regulating anthocyanin biosynthesis (Lai et al., 2014).

In this study, we isolated three putative litchi bHLH transcription factors, *LcbHLH1*, *LcbHLH2,* and *LcbHLH3*, and analyzed their expression profiles. Phylogenic analysis showed that these three bHLH transcription factors from litchi cluster with bHLH genes related to anthocyanin biosynthesis in other plants. However, expression patterns of these three genes in different litchi tissues and developmental stages do not correlate with anthocyanin contents. BiFC and Y2H assays show that LcbHLH1 and LcbHLH3 can interact *in vivo* with LcMYB1. Transient assays in tobacco leaves showed that both LcbHLH1 and LcbHLH3 enhanced the induction of anthocyanin accumulation by *LcMYB1* with the *LcbHLH3* being by far more efficient. Furthermore, dual LUC assays indicate that the high affinity of LcMYB1 for the promoter of *ANS* induced by LcbHLH3 may associate with enhanced anthocyanin accumulation in tobacco leaves.

RESULTS

Identification and Sequence Analysis of Three Candidate Anthocyanin Related bHLH Transcription Factors

Three putative members of the bHLH family of transcription factors were identified from the litchi pericarp transcriptomic (Lai et al., 2015) and genomic database[1], denominated as *LcbHLH1*, *LcbHLH2,* and *LcbHLH3.* The ORFs of *LcbHLH1*,

Abbreviations: AD, activation domain; ANS, anthocyanidin synthase; bHLH, basic helix-loop-helix; BiFC, bimolecular fluorescence complementation; CHI, chalcone isomerase; CHS, chalcone synthase; DAPI, 4′,6-diamidino-2-phenylindole; DBD, DNA-binding domain; DFR, dihydroflavonol 4-reductase; F3H, flavanone 3-hydroxylase; GFP, green fluorescent protein; LUC, luciferase; MBW, MYB-bHLH-WD40 protein complex; PAL, phenylalanine ammonia lyase; REN, renilla luciferase; UFGT, UDP-glucose:flavonoid 3-*O*-glucosyltransferase; Y2H, yeast two-hybrid assay; YFP, yellow fluorescent protein.

[1]http://litchidb.genomics.cn/page/species/index.jsp

LcbHLH2, and *LcbHLH3* encoded proteins with 657, 700, and 643 amino acids, respectively. Three conserved motifs are identified by sequence alignments of LcbHLH1, LcbHLH2, LcbHLH3, and other bHLH transcription factor proteins related to plant anthocyanin biosynthesis (**Figure 1**). The MYB interaction region presented in the N-terminal region of these proteins suggests for all of them protein-protein interaction with MYB transcription factors. A sequence rich in acidic amino acids, containing up to 30 acidic amino acids, is present at the C-terminal region of bHLH proteins (**Figure 1**). This domain was believed to be the transactivation (ACT) domain which interacts with the RNA polymerase II machinery and then initiates transcription (Pattanaik et al., 2008). All three litchi bHLH proteins contained such ACT-like domain, which has also been proven to be involved in the dimerization of plant basic-helix-loop-helix transcription factors (Feller et al., 2006).

A phylogenetic tree constructed with the neighbor-joining method using full-length amino acid sequences showed that the three litchi bHLHs belong to the group IIIf of *Arabidopsis* bHLH which contains bHLH factors involved in anthocyanin and other flavonoid biosynthesis (**Figure 2**) (Heim et al., 2003). The similarity of LcbHLH1 with CsMYC2 (ABR68793.1) and VvMYCA1 (ABM92332) at amino acid level were 67.4 and 60.1%, respectively. LcbHLH2 had 73.1 and 56.2% homology with MrbHLH1 (JX629461) and PhAN1 (AAG25927). LcbHLH3 showed relatively low similarity with AtEGL3 (NP_176552) and VvMYCA1 (NP_001267954.1), 49.9 and 47.7% homology, respectively. The identity between LcbHLH1 and LcbHLH2, LcbHLH1 and LcbHLH3, and LcbHLH2 and LcbHLH3 were 29.6, 47.9 and 28.2%, respectively.

Subcellular Localization of LcMYB1 and Three Litchi bHLH Proteins

Basic helix-loop-helix and MYB proteins are TFs and as such are expected to be localized to the nucleus. However, some bHLH proteins are also cytoplasm associated (Hichri et al., 2010). To analyze the subcellular localizations of LcMYB1 and LcbHLH proteins, their full-length coding sequences were fused in frame with the GFP gene. Transient expression of these constructs in epidermal cells of *N. benthamiana* and leaf protoplast showed that the fluorescence for LcMYB1-GFP and LcbHLH3-GFP was localized exclusively in the nucleus. By contrast, fluorescence was observed in the nucleus as well as in the cytoplasm for LcbHLH1-GFP, and LcbHLH2-GFP was mainly localized in the cytoplasm (**Figure 3** and Supplementary Figure S1).

Interaction of LcMYB1 with Different LcbHLH Partners

The Y2H was used to investigate the interactions between LcbHLHs and LcMYB1 (**Figure 4**). Expression of the full-length LcMYB1 fused with the DBD resulted in yeast in strong activation (autoactivation) of the reporters. We therefore produced four 3′-deletion fragments and among these, only LcMYB1D (1–402 bp of the LcMYB1 coding sequence) displayed no autoactivation in yeast (**Figures 4A,B**). LcMYB1D was then used in an assay with the three LcbHLHs. As shown in **Figure 4C**, yeast cells co-transformed the positive control (pGBKT7-53+pGADT7-T) and LcbHLH1 or LcbHLH3 with LcMYB1D could grow on selective medium (synthetic medium lacking tryptophan, leucine, histidine, and adenine) supplement with the toxic drug Aureobasidin A, and turned blue in the presence of the chromagenic substrate X-α-Gal. However, yeast cells harboring LcbHLH2 with LcMYB1 and the negative controls, could not grow on the selective medium and did not turn blue under the same conditions. These results suggested that LcMYB1 was able to form complex with either LcbHLH1 or LcbHLH3, but not with LcbHLH2.

Subsequently, interaction of LcMYB1 with LcbHLHs was further confirmed in BiFC assay (**Figure 5**). LcMYB1 tagged with split YFP N-terminal fragment (NYFP) and LcbHLH1 or LcbHLH3 tagged with split YFP C-terminal fragment (CYFP) were transiently co-infiltrated in epidermal cells of *N. benthamiana* leaves by *Agrobacterium*. As shown in **Figure 5** and Supplementary Figure S2, strong YFP fluorescent signal was detected in the nucleus of leaf protoplast and epidermal cells expressing LcMYB1-NYFP and LcbHLH1-CYFP fusion protein or LcMYB1-NYFP and LcbHLH3-CYFP, while no YFP fluorescent signal was observed either in the cells expressing the LcMYB1-NYFP with only CYFP, LcbHLH1-CYFP, or LcbHLH3-CYFP with only NYFP. No YFP signal was observed when transformed with both LcMYB1-NYFP and LcbHLH2-CYFP (data not shown). The BiFC assay not only demonstrated the *in vivo* interaction among the three proteins tested but also showed the localization of the interacting proteins, which was consistent with the subcellular localization of LcMYB1, LcbHLH1 and LcbHLH3.

Expression of Three Litchi *bHLH*s in Relation to Anthocyanin Accumulation

The transcription of three bHLHs was compared with the anthocyanin accumulation pattern in different tissues (**Figure 6A**). Anthocyanin content varies among different tissues in litchi. No anthocyanin is detectable in root, aril, stems and mature leaf of litchi, while mature pericarp and young leaf accumulated significant amount of anthocyanins. The expression patterns of *LcbHLH1*, *LcbHLH2,* and *LcbHLH3* were not parallel to the accumulation of anthocyanins in any of the analyzed tissues. The transcript amount for all three genes was actually lower in pigmented tissues than non-pigmented tissues.

The developmental patterns of transcript accumulation for the three bHLHs in relation to anthocyanin accumulation were also investigated, specifically in the pericarp of the strongly pigmented cultivar Ziniangxi (ZNX) and of the non-red cultivar Yamulong (YML) (**Figure 6B**). In agreement with the fruit appearance (Supplementary Figure S3), significant accumulation of anthocyanin occurred during fruit maturation in the cultivar ZNX, while only minute anthocyanin amounts were detected in the pericarp of the cultivar YML at maturity. However, comparable levels of *LcbHLH1* and *LcbHLH2* expressions were observed in the pericarp of the two cultivars tested with no apparent trend following pigment accumulation during fruit

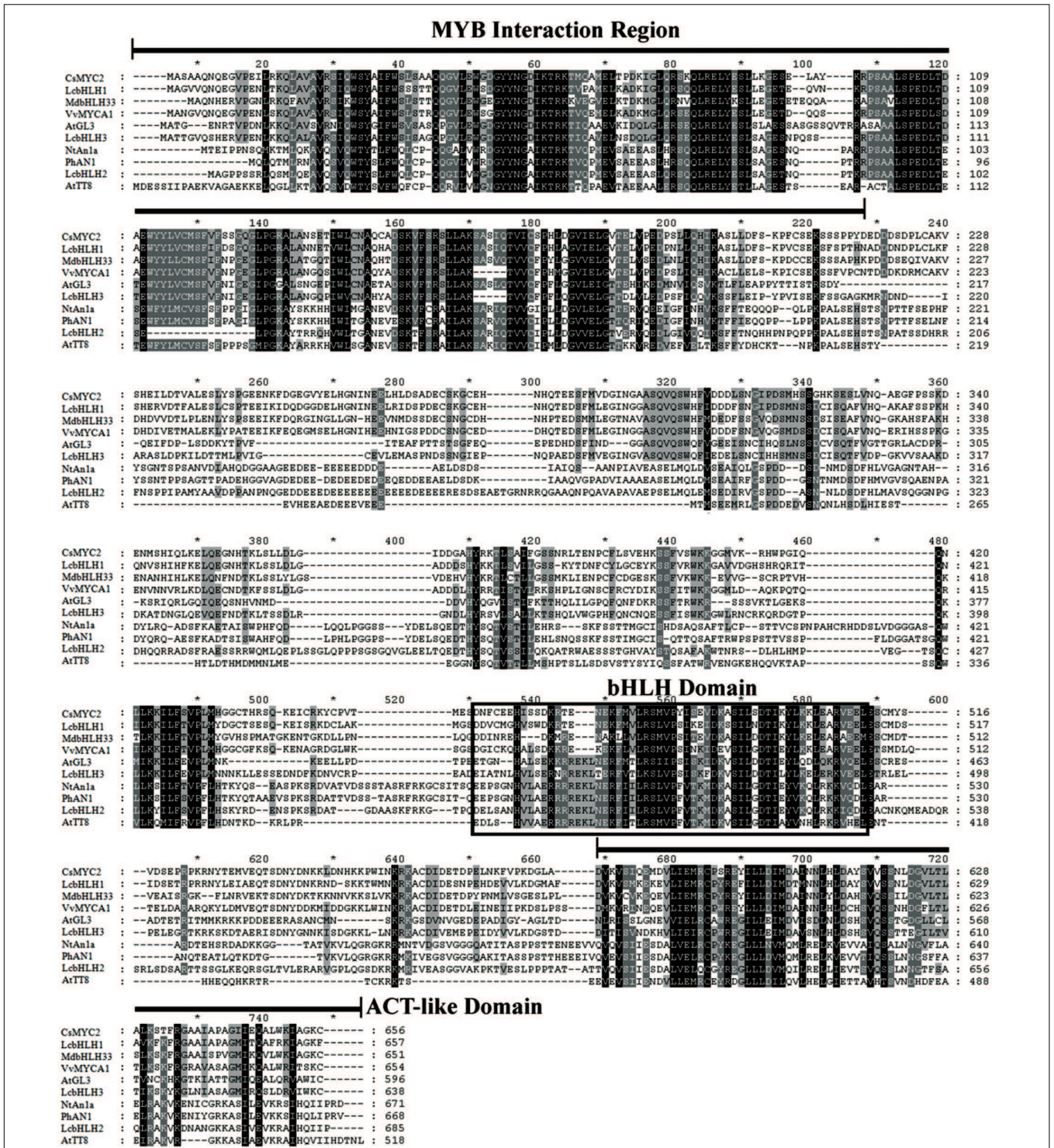

FIGURE 1 | Protein sequence alignment of three LcbHLH proteins and the known anthocyanin bHLH regulators in other species. Identical residues are shown in black and conserved residues in dark gray. MYB interaction region, bHLH domain and ACT-like domain are conserved among these bHLH transcription factors.

development. Except for the forth developmental stages of ZNX, the expression of *LcbHLH3* was low in the pericarp of both cultivars.

In the present study, the developmental transcript patterns of three bHLHs in relation to anthocyanin accumulation were also investigated in leaves of the above mention two cultivars

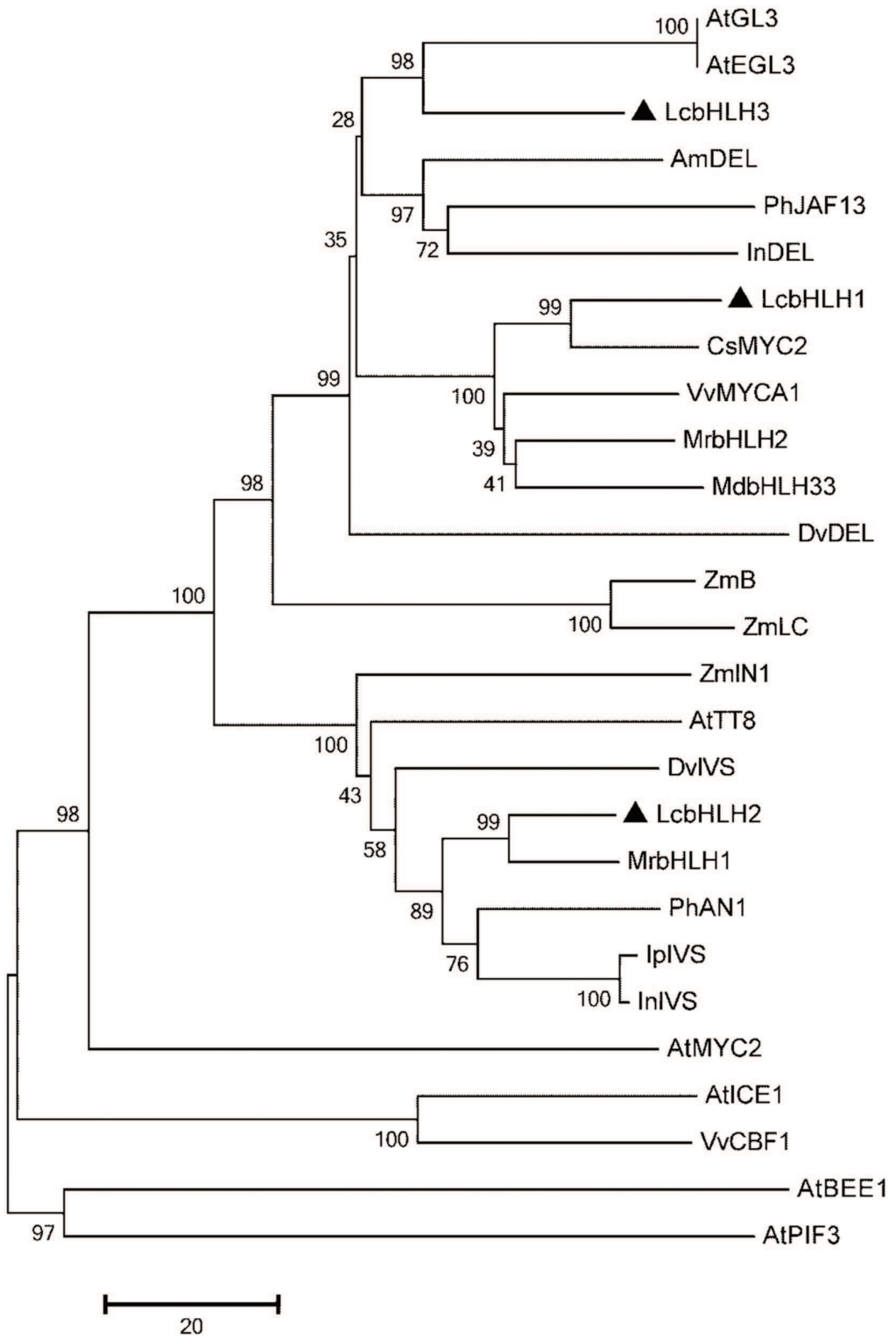

FIGURE 2 | Phylogenetic relationships between LcbHLH1-3 and anthocyanin-related bHLHs in other species. The tree was constructed using MEGA 5, neighboring-joining phylogeny testing, and 1,000 bootstrap replicates. The accession number of these proteins (or translated products) are as follows in the GenBank database:AtTT8, CAC14865.1; AtGL3, NP_680372; AtEGL3, NP_176552; MdbHLH33, ABB84474.1; PhJAF13, AAC39455; IpIVS, BAD18982.1; VvMYCA1, NP_001267954.1; CsMYC2, ABR68793.1; PhAN1, AAG25927; AmDEL, AAA32663; DvIVS, BAJ33515; DvDEL, BAJ33516; InDEL, BAE94393; ZmB, AGO65322.1; ZmLC, NP_001105339.1; InIVS, BAE94394; ZmIN1, AAB03841; MrbHLH1, JX629461; MrbHLH2, JX629462; AtMYC2, NP_174541.1; AtICE1, NM_113586.3; VvCBF1, AFI49627.1; AtPIF3, NM_179295.2; AtBEE1, AY138253.1.

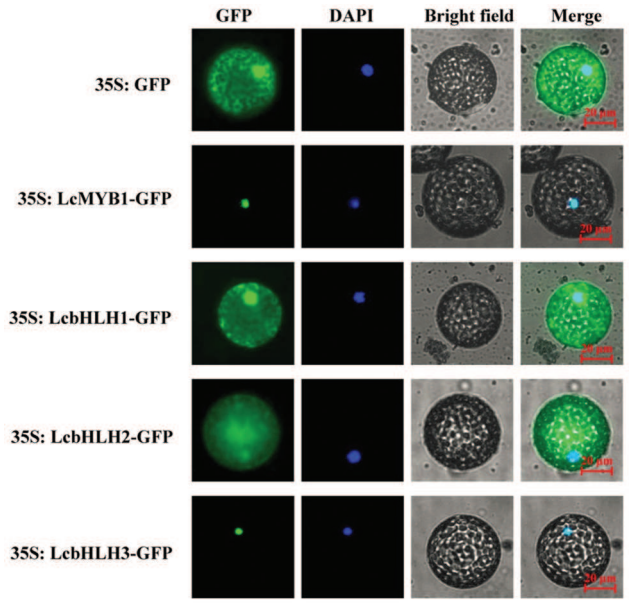

FIGURE 3 | Subcellular localization of LcMYB1 and LcbHLHs in *N. benthamiana* leaf protoplasts. Epidermal cells of *N. benthamiana* leaves were transiently transformed with LcMYB1–GFP and LcbHLHs–GFP constructs in *Agrobacterium tumefaciens* strain GV3101. GFP fluorescence was observed with a fluorescence microscope. Images were taken in a dark field for green fluorescence, while the outline of the cell and the merged were photographed in a bright field. Bars, 20 μm.

(**Figure 6C** and Supplementary Figure S4). The concentrations of anthocyanins were high in young leaves of ZNX, but decreased with leaf development. By contrast, little anthocyanin was detected in the leaves of the non-red cultivar YML throughout leaf development. *LcbHLH1* and *LcbHLH2* were highly expressed in the second developmental stage of the leaves of ZNX, while comparable expression levels were observed during the rest of development and between two cultivars. *LcbHLH3* displayed different transcript accumulation patterns. The expressions of *LcbHLH3* were much higher in pigmented leaves (young leaves of ZNX) than non-red leaves, i.e., mature leaves of ZNX and leaves of YML.

Transient Expression of Three *bHLHs* in Combination with *LcMYB1*

To further characterize the function of three litchi bHLH genes, the ORFs of them were cloned in the transient expression vector pEAQ-HT and transiently transformed into *N. tabacum* leaves via *Agrobacterium* infiltration. Significant anthocyanin accumulation was observed 4 days after infiltration in leaf patches with *LcMYB1* alone as well as co-infiltration with *LcMYB1* or *LcbHLHs*, while no anthocyanin was detected in leaves infiltrated with *LcbHLH1*, *LcbHLH2,* or *LcbHLH3* alone (**Figure 7**). Among the pigmented patches, leaves co-infiltrated with *LcMYB1* and *LcbHLH3* accumulated significantly higher anthocyanin levels than those infiltrated with *LcMYB1* alone and the co-infiltrations of *LcMYB1* and any of the other two bHLH factors.

The Biosynthesis of Anthocyanins in *LcMYB1* or/and *LcbHLH3* Overexpression Tobacco

Since *LcHLH3* co-transformed with *LcMYB1* display higher efficiency in inducing anthocyanin accumulation in tobacco leaves as compared to *LcMYB1-LcbHLH1*, we produced *LcMYB1-LcbHLH3* ectopic expression tobacco lines by crossing a 35S:*LcMYB1* transgenic line with a 35S:*LcbHLH3* line. Transformed tobacco lines ectopically expressing *LcMYB1*, *LcHLH3,* or *LcMYB1-LcbHLH3* were grown and used to further investigate the role of these genes in anthocyanin biosynthesis in tobacco. The lines over-expressing *LcMYB1-LcbHLH3* accumulated the highest amount of anthocyanin in the leaves, followed by the lines over-expressing *LcMYB1*, while no anthocyanin was detected in untransformed controls and plants expressing *LcbHLH3* (**Figures 8A,B**). Lines expressing the combination of *LcMYB1* and *LcbHLH3* accumulate about 10 times more anthocyanins than lines expressing *LcMYB1* alone.

Furthermore, the expression levels of the transgenes, *LcMYB1* and *LcbHLH3*, and ten anthocyanin biosynthetic genes, including three tobacco anthocyanin regulators, were investigated (**Figure 8C**) in the transgenic lines. Clear *LcMYB1* or/and *LcbHLH3* expression was detected in leaves of the *LcMYB1* or/and *LcbHLH3* transformant lines, while, as expected, no expression was detected in untransformed controls. This result also confirms the successful transformation of *LcMYB1* or/and *LcbHLH3*. The transcript levels for the two tobacco endogenous *bHLH* regulators, *NtAn1a* and *NtAn1b*, were dramatically up-regulated by the combined expression of *LcMYB1* and *LcHLH3*. Early structural genes including *NtPAL*, *NtCHS*, *NtCHI,* and *NtF3H* were down-regulated in *LcMYB1* or/and *LcbHLH3* overexpression leaves, while *NtDFR* and *NtANS* were up-regulated dramatically in leaves of *LcMYB1-LcbHLH3* transgenics as compared with lines transformed with *LcMYB1* only. The transcript levels of *NtDFR* and *NtANS* in leaves of *LcMYB1-LcbHLH3* transgenics were, respectively, about four and ten times higher than in *LcMYB1* transgenic leaves.

LcMYB1 and LcMYB1-LcbHLHs Activate the Promoters of Structural Genes

Transcription factors modulate the biosynthesis of flavonoids mainly activating the promoters of structural anthocyanin genes (Nesi et al., 2000; Bai et al., 2011; Liu et al., 2013). E-BOX and MYB-CORE *cis*-elements were believed to be the target of bHLH and MYB transcription factors (Hichri et al., 2011; Xu et al., 2015). Lots of E-BOX and MYB-CORE *cis*-elements in the promoter of litchi anthocyanin biosynthesis genes were found (Supplementary Figure S4). In the present study, a dual LUC assay was employed to investigate the downstream target gene of LcMYB1 and LcbHLHs. LcMYB1 or/and LcbHLHs were cloned into pEAQ-HT transient expressing vector as effectors and promoters of structural genes driving LUC gene served as reporters. Different combinations of effector and reporter were transiently expressed in tobacco leaves by *Agrobacterium* based infiltration. As shown in **Figure 9**, four (*LcF3H*, *LcF3′H*, *LcDFR,* and *LcUFGT* promoters) out of the seven investigated promoters

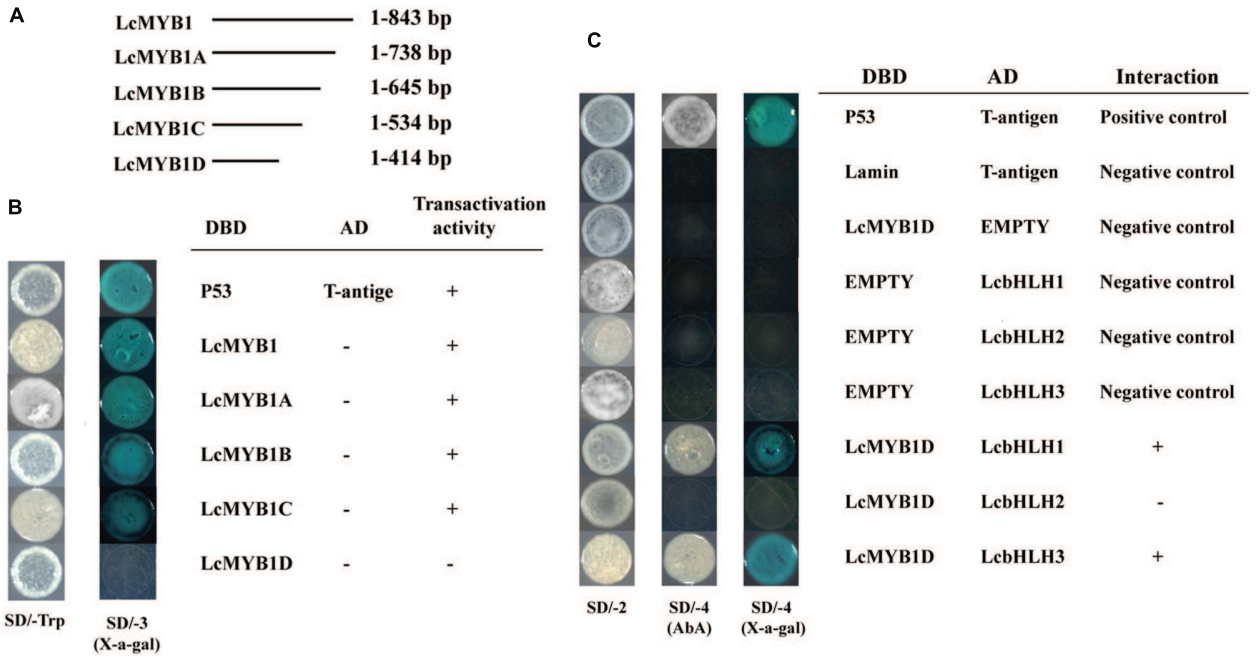

FIGURE 4 | Physical interactions between LcbHLH1-3 proteins and LcMYB1 detected in Y2H assays. (A) The coding regions of full length and partitial sequence of *LcMYB1* were cloned into the pGBKT7 (GAL4 DBD) vector to create the DBD-LcMYB1 and DBD-LcMYB1A-D constructs, respectively. **(B)** Transcriptional activation analysis of LcMYB1 and partitial sequence of LcMYB1. **(C)** All of the constructs together with the positive control (p-53+T-antigen) and negative control (pGBKT7) were transformed into yeast strain Gold Y2H. Yeast clones transformed with different constructs were grown on SD plates with or without tryptophan, histidine, and adenine but containing 125 μM Aureobasidin A for 3 days at 30°C. Transcription activation was monitored by the detection of yeast growth and a α-galactosidase (α-Gal) assay.

were activated by LcMYB1. LcbHLH1 alone did not activate any promoters, while LcbHLH3 clearly activated *LcANS* promoters. When *LcHLH1* and *LcHLH3* were co-transformed with *LcMYB1*, the activities of *LcCHS*, *LcCHI* and *LcANS* promoter were much higher as compared with transformed *LcMYB1* only. The activity of the *LcANS* promoter in *LcHLH3* co-transformed with *LcMYB1* was about six or fifty times higher, respectively, compared with *LcHLH1* co-transformed with *LcMYB1* and *LcMYB1* only.

DISCUSSION

Characteristics of Litchi bHLH Transcription Factors

MYBs and bHLHs that regulate the anthocyanin biosynthetic pathway have been extensively described in many plant species (Hichri et al., 2011; Jaakola, 2013; Xu et al., 2015). In litchi, LcMYB1 has been identified as the key regulator of anthocyanin biosynthesis (Lai et al., 2014). However, bHLH interaction partners of this MYB factor have so far not been described in litchi. In the present study, three putative LcbHLH transcription factors were isolated from litchi pericarp (**Figure 1**). The three transcription factors were quite different from each other, with the highest sequence similarity 47.9% between LcbHLH1 and LcbHLH3 at the amino acid level. Based on domain comparison and sequence similarity, these three putative LcbHLHs belong to the IIIf subgroup, which related to regulation of anthocyanin and proanthocyanidin biosynthesis and trichome development in plants (Heim et al., 2003). The three isolated putative LcbHLHs showed high similarity in the conserved motifs of bHLHs regulating pigmentation in other plant species (**Figure 2**).

More than one bHLH factor is known in most plants to regulate anthocyanin or proanthocyanidin biosynthesis, i.e., TT8, GL3, and EGL3 in *Arabidopsis* (Nesi et al., 2000; Payne et al., 2000; Zhang et al., 2003), JAF13 and PhAN1 in petunia (Quattrocchio et al., 1998; Spelt et al., 2002), NtAn1a and NtAn1b in tobacco (Bai et al., 2011), VvMYC1 and VvMYCA1 in grape (Hichri et al., 2010; Matus et al., 2010), MdbHLH3 and MdbHLH33 in apple (Espley et al., 2007). There is increasing evidence of specialization of function for the different bHLH proteins within a single species. In *Arabidopsis*, TT8 is involved in regulation of proanthocyanidin biosynthesis, while GL3 and EGL3 are required for seed coat mucilage production, trichomes and root hair spacing (Shirley et al., 1995; Payne et al., 2000; Zhang et al., 2003). In petunia, *JAF13* gene is homologous to *DELILA* (*DEL*) from snapdragon and *R* from maize which has been shown to regulate anthocyanin accumulation (Quattrocchio et al., 1998). *AN1,* another bHLH factor from petunia does not only control pigment synthesis but also vacuolar pH and seed coat development (Quattrocchio et al., 1993; Spelt et al., 2000).

Although all the three identified LcbHLHs contained MYB interaction region, only LcbHLH1 and LcbHLH3 localized

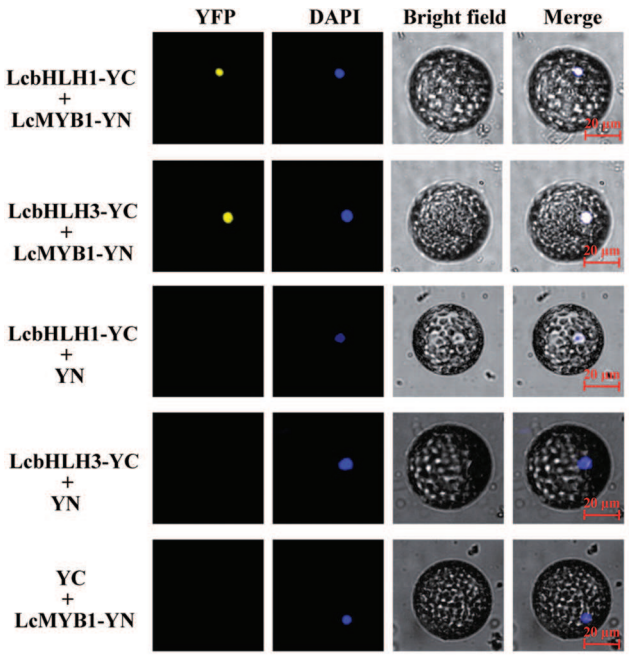

FIGURE 5 | Bimolecular fluorescence complementation visualization of the LcbHLH1 and LcbHLHs interaction in *N. benthamiana* leaf protoplasts. YFP indicates fluorescence of YFP; Merge is digital merge of bright field and fluorescent images. Bars, 20 μm.

in nucleus and displayed physical interaction with LcMYB1 (**Figures 4–6**). LcbHLH2 clustered with MrbHLH1, a key bHLH transcription factor regulating anthocyanin biosynthesis through interaction with MrMYB1 in bayberry (Liu et al., 2013). But, both yeast two-hybrid and BiFC assays showed no interaction between LcbHLH2 and LcMYB1 (**Figures 4** and **5**). These results suggest that LcbHLH1 and LcbHLH3 maybe, interaction partners of LcMYB1 and could play a role in regulating litchi anthocyanin biosynthesis, while LcbHLH2 is possibly not involved in this pathway.

The LcbHLH Interaction with LcMYB1 Regulated Anthocyanin Synthesis

The expression analysis of the three litchi bHLHs showed that none of them correlates with anthocyanin accumulation in different tissues and different developmental stages (**Figure 6**). This is consistent with what previously observed for *MdbHLH33*, *MdbHLH3*, and *VvMYC1*, which do not follow neither the accumulation of anthocyanins nor the expression pattern of the MYB factor (Espley et al., 2007; Hichri et al., 2010). Furthermore, transient expression of the three LcbHLHs did not induce anthocyanin accumulation in tobacco leaves (**Figure 7**) when not combined with a MYB factor. These results suggested that litchi bHLHs do not directly regulate the biosynthesis of anthocyanins and do not determine the pigment accumulation pattern.

In apple, Chinese bayberry, grape and peach, without the conjunct expression of bHLH partners, MYB genes do not induce anthocyanin when transiently expressed in tobacco leaves or grape cells (Espley et al., 2007; Hichri et al., 2010; Liu et al., 2013; Rahim et al., 2014). However, overexpression of *LcMYB1* alone efficiently induce anthocyanin accumulation in tobacco leaves. The exogenous *LcMYB1* induces indeed the expression of the tobacco endogenous *bHLH* transcription factor, *NtAn1b* (Lai et al., 2014). The study of the way of action of the kiwifruit AcMYB110 revealed different specificity to promote red pigmentation of tobacco leaves depending on the availability of endogenous bHLHs (Montefiori et al., 2015). These facts suggest the essential role of bHLH in anthocyanin biosynthesis.

In this study, we have tested the role of litchi bHLHs in regulating anthocyanin biosynthesis by co-infiltration with *LcMYB1*. Leaves transiently expressing *LcMYB1-LcbHLH1* or *LcMYB1-LcbHLH3* accumulated significant higher anthocyanins than leaves expressing just *LcMYB1* or *LcMYB1-LcbHLH2* (**Figure 7**). This provides further evidence for the involvement of LcbHLH1 and LcbHLH3 in litchi anthocyanin biosynthesis through interaction with LcMYB1. Similarly, transgenic tobacco (*Nicotiana tabacum*) overexpressing a combination of either potato StAN1 (MYB) with StJAF13 (bHLH) or StAN1 with StbHLH1 showed deeper purple pigmentation with respect to AN1 alone (D'Amelia et al., 2014).

The LcMYB1-LcbHLH Complex Enhanced Anthocyanin Accumulation by Activating Transcription of *ANS* and *DFR*

Significant accumulation of anthocyanin in the lines of *LcMYB1-LcbHLH3* was accompanied by dramatically up-regulation of two tobacco endogenous *bHLH* regulators, *NtAn1a* and *NtAn1b* (**Figure 8C**). Bai et al. (2011) indicated that NtAn1 and NtAn2 complex activates the promoters of two key structural genes of the anthocyanin pathway, *DFR* and *CHS*. In the present study, the accumulation of anthocyanin in an *LcMYB1-LcbHLH3* tobacco ectopic-expression line is associated with the upregulation of endogenous *bHLHs*. *NtAn1a* and *NtAn1b*. In tobacco, exogenous MYB requires NtAn1 to activate NtJAF13 then to regulate anthocyanin biosynthesis (Montefiori et al., 2015). These results suggest that the regulation of anthocyanin in tobacco might involve multiple bHLH in a hierarchic fashion.

In petunia, the transport of the bHLH protein AN1 factor to the nucleus is necessary for the activation of the transcription of the DFR gene and this is directly induced by the AN1 protein, as shown by the fact that it takes place in the presence of translation inhibitors (Spelt et al., 2000). The expression of the Dahlia *DvF3H*, *DvDFR*, and *DvANS* are repressed by the insertion of a transposon in the *bHLH* gene *DvIVS* (Ohno et al., 2011). In apple, MdbHLH3 binds to the promoters of anthocyanin biosynthesis genes *MdDFR* and *MdUFGT* and the regulatory gene *MdMYB1* to activate their expression (Xie et al., 2012). MrMYB1–MrbHLH1 complex activated *MrCHI*, *MrF3'H*, *MrDFR1*, *MrANS*, and *MrUFGT* promoters of Chinese bayberry (Liu et al., 2013). In the present study, however, the expressions of *NtCHS*, *NtCHI*, and *NtF3H* were almost diminished in the pigmented transformed control leaves (**Figure 8C**). These early structural genes leads to the formation of the dihydro-flavonols, but not necessarily related

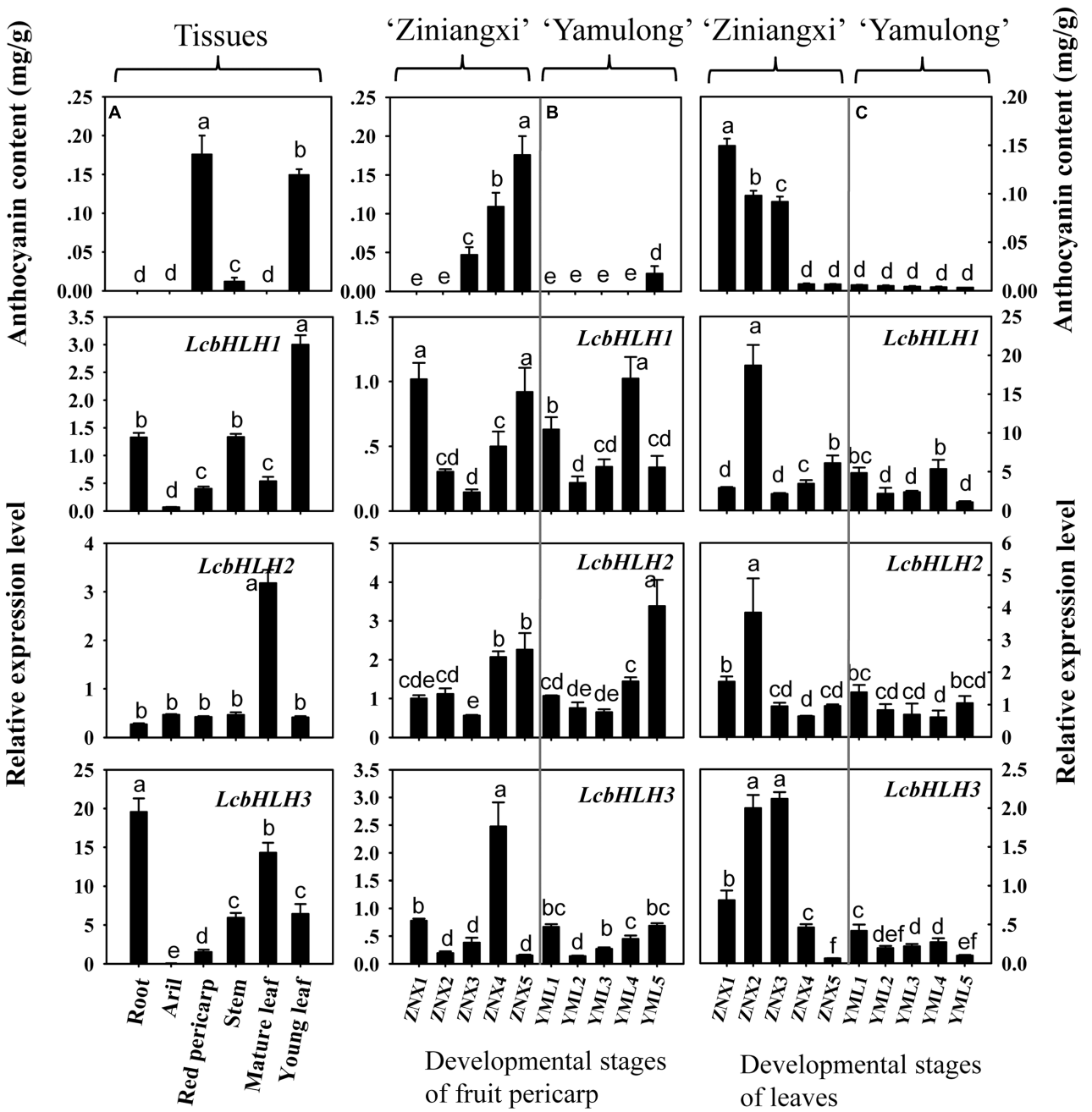

FIGURE 6 | Expression of three litchi bHLH in relation to anthocyanin accumulation. (A) The transcript patterns of three litchi bHLHs in relation to anthocyanin accumulation among tissues. **(B)** The developmental transcript patterns of three litchi bHLHs in relation to anthocyanin accumulation in the pericarp of 'Zinianxi' and 'Yamulong'. **(C)** The developmental transcript patterns of three litchi bHLHs in relation to anthocyanin accumulation in leaves of 'Zinianxi' and 'Yamulong'. The vertical bars represent the standard error of triplicate experiments. Different letters on the top of columns indicate significant difference at $p < 0.05$.

to the anthocyanin accumulation. This result consistent with previous reports that late structural genes but not early structural genes determined the anthocyanin accumulation (Niu et al., 2010; Liu et al., 2013; Lai et al., 2014). *LcMYB1* control the biosynthesis of anthocyanins in tobacco leaves by activating the expression of *NtDFR*, *NtANS,* and *NtUFGT* (Lai et al., 2014). In the present study, remarkable up regulation of these three late structural genes were notice in LcMYB1 transformed line, but only *NtDFR* and *NtANS* were upregulated in paralleling with higher anthocyanins in *LcMYB1-LcbHLH3* overexpression line as compared with *LcMYB1* overexpression line (**Figure 8C**). All this wealth of data suggests that the target genes of LcMYB1 or/and LcbHLH1 and LcbHLH3 are in litchi the homologous genes of the anthocyanin pathway.

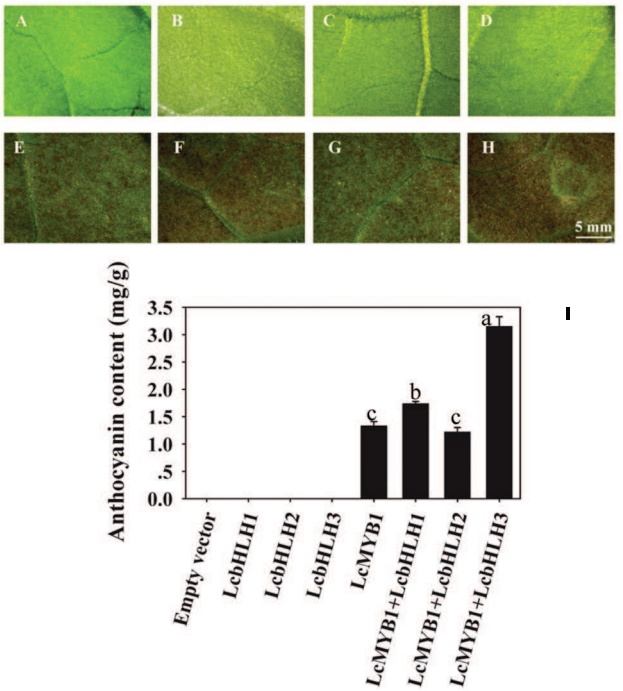

FIGURE 7 | Anthocyanin accumulation in tobacco leaves infiltrated with *LcMYB1* and co-infiltrated with *LcMYB1* and *LcbHLHs*. (A) pEAQ-HT empty vector; **(B)** pEAQ-LcbHLH1; **(C)** pEAQ-LcbHLH2; **(D)** pEAQ-LcbHLH3; **(E)** pEAQ-MYB1; **(F)** pEAQ-MYB1 with pEAQ-LcbHLH1; **(G)** pEAQ-MYB1 with pEAQ-LcbHLH2; **(H)** pEAQ-MYB1 with pEAQ-LcbHLH3. Pictures were taken at 4 days after infiltration. **(I)** Anthocyanin contents in different transiently transformed tobacco leaf patches. The vertical bars represent the standard error of triplicate experiments. Different letters on the top of columns indicate significant difference at $p < 0.05$.

To test this possibility, we isolated the promoters of anthocyanin biosynthesis structural genes in litchi and tested their activation by different combinations of factors. LcMYB1 activates the promoters of *LcF3H*, *LcF3′H*, *LcDFR,* and *LcUFGT*, while LcbHLH3 clearly activats the *LcANS* promoter (**Figure 9**). The activity of *LcDFR* and *LcANS* promoter was higher when they were cotransformed with the combination of regulators *LcMYB1-LcbHLH1* or *LcMYB1-LcbHLH3,* as compared to *LcMYB1* only. This result was consistent with the upregulation of *NtDFR* and *NtANS* in leaves of *LcMYB1-LcbHLH3* ectopic expression lines (**Figure 8**). In *Arabidopsis*, the TT8 protein is required for the expression of two flavonoid late biosynthetic genes, *DF*R and *BAN* (Nesi et al., 2000). No expression of *IpDFR* and *IpANS* was detected in seed coats of *ivs* mutants in *Ipomoea purpurea*, indicating they could be the target of the bHLH protein IVS (Park et al., 2007). We measured activity of the *ANS* promoter as induced by *LcMYB1-LcbHLH1* and *LcMYB1-LcbHLH3* in transient assay, while we could only detect minute activity of the same promoter upon expression of *LcMYB1*. *LcbHLHs* seems therefore to be required for the high expression of *LcANS*. In conclusion, these results indicated that LcMYB1-LcbHLH complex induces anthocyanin biosynthesis by activating transcription of *ANS* and *DFR*, late structural genes in anthocyanin biosynthesis pathway.

MATERIALS AND METHODS

Plant Materials

Five developmental stage fruits of red litchi cultivars 'Ziniangxi' (ZNX) and one non-red cultivar 'Yamulong' (YML) were used in this study. These trees were grown in the experimental orchard of Hainan academy of agricultural sciences (Haikou, China) received standard horticultural practices, and disease and insect control. Root, young stem, aril, young leaf, and mature leaf were collected from cultivar 'ZNX'. Pericarp disks of 'YML' were collected between May 28th, 2013 and June 17th, 2013 at 5 days intervals. Pericarp disks of 'ZNX' were collected between May 8th, 2013 and May 28th, 2013 at 5 days intervals. Different developmental leaves were sampled at 7 days interval from leaf flushing to mature as reflecting by net photosynthetic rate. All samples were immediately frozen in liquid nitrogen and stored at −80°C until use.

Tobacco (*N. tabacum*) was used for transient expression, *N. benthamiana* plants were used for subcellular localization and BiFC assays. Tobacco plants were grown in green houses at 28°C using natural light. *N. benthamiana* plants were grown in green houses at 25°C.

Anthocyanin Analysis

The total anthocyanin content was determined according to the method developed by Wei et al. (2011), which involves measuring the absorbance (520 nm) of extracts that have been diluted with pH 1.0 and 4.5 buffers.

RNA Extraction and cDNA Synthesis

Total RNA was extracted from different tissues of litchi and tobacco using the RNA_{OUT} kit (Tiandz, Beijing, China). Contaminating DNA was removed from RNA preparations using TURBO DNA-free^{TM} (Ambion, USA). cDNA was synthesized from total RNA (2 μg) using oligo (dT) primers according to the manufacturer's instructions of M-MLV (Invitrogen, USA) in 20 μL of total volume.

Gene Cloning and Sequence Analysis

The cDNAs were synthesized from the total RNA of the mature pericarp of cultivar 'ZNX' and used as the PCR templates. PCR-amplified products of appropriate length were cloned into T/A cloning vector pMD®20-T (TaKaRa, Japan) and then transformed into *Escherichia coli* DH5α Max Efficiency® Chemically Competent Cells (TaKaRa, Japan). Primers are listed in Supplementary Table S1. Plasmid DNA was isolated from positive *E. coli* cells and then sent to Beijing Genomics Institute for sequencing. Multiple sequence alignment was performed using ClustalX 1.83[2] and MEGA5 (Tamura et al., 2011).

[2]http://www.ebi.ac.uk

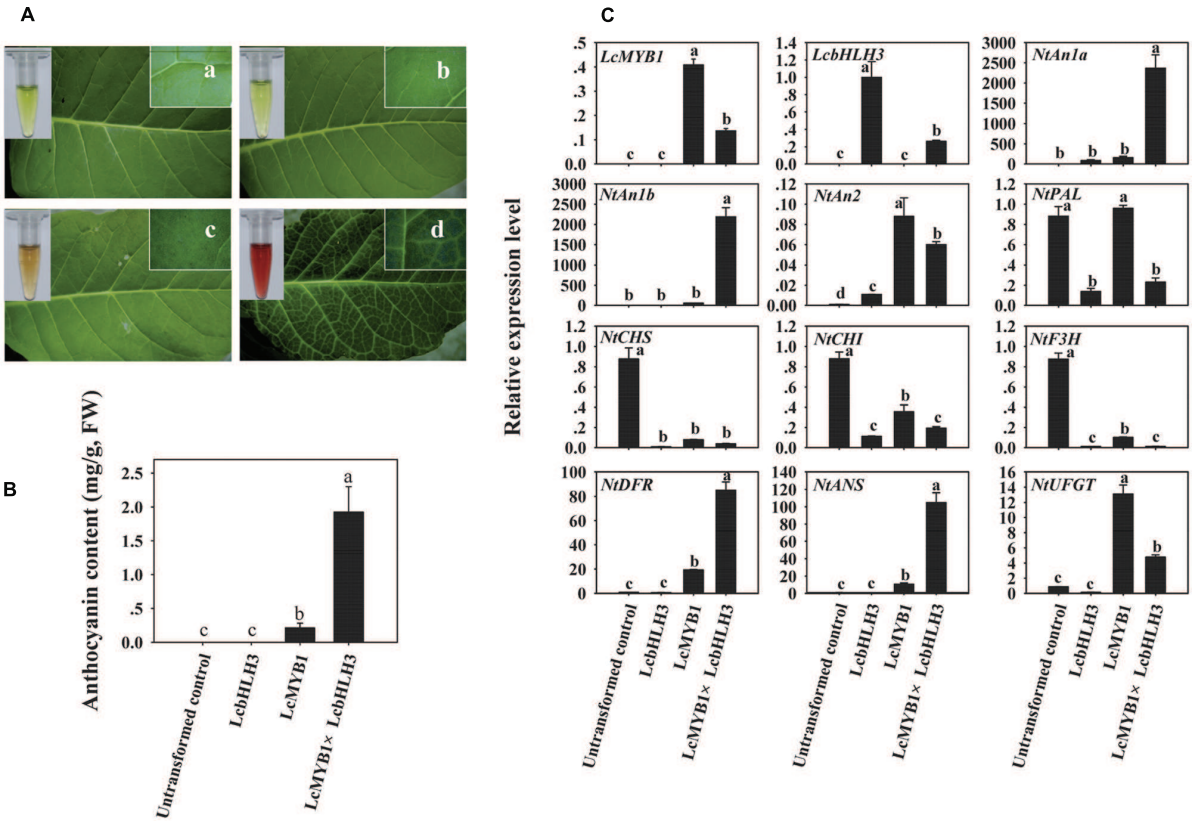

FIGURE 8 | The biosynthesis of anthocyanins in LcMYB1 or/and LcbHLH3 overexpression tobacco. (A) Color development in leaves of untransformed control and leaves transformation with LcMYB1 or/and LcbHLH3. **(B)** Anthocyanin contents in untransformed control and transgenic tobacco lines. **(C)** The expressions of exogenous litchi regulatory genes and tobacco endogenous regulatory and structural gene in the anthocyanin biosynthetic pathway in transgenic lines. The actin gene was used to normalize gene expression of the genes under identical conditions. The vertical bars represent the standard error of triplicate experiments. Different letters on the top of columns indicate significant difference at $p < 0.05$.

Real-Time Quantitative PCR

Total RNA was extracted from the pericarp of litchi and tobacco leaves and first strand cDNA was synthesized as described above. The transcription levels of both the litchi and tobacco anthocyanin biosynthetic genes were analyzed using quantitative real-time PCR (qRT-PCR) as described previously (Lai et al., 2014). The specific qRT-PCR primers were designed using a BatchPrimer3 program listed in Supplementary Table S2 (You et al., 2008). Using these gene-specific primers, each assay amplified a single product of the correct size and demonstrated an acceptable PCR efficiency (approximately 90%). qRT-PCR reactions were normalized to the Ct values for *LcACTIN* (HQ615689) and *LcGAPDH* (JF759907) in litchi (Zhong et al., 2011), and *NtACTIN* (GQ281246) for tobacco. The relative expression levels of the target genes were calculated using the formula $2^{-\Delta\Delta CT}$ (Livak and Schmittgen, 2001). All biological replicates were measured in triplicate.

Transient Assays and Stable Transformation of Tobacco

The plasmids used in the transient expression assay were constructed by ligating full-length *LcbHLH1-3* to pEAQ-HT using *Nru* I and *Xho* I. The primers used to amplify the encoding region were listed in Supplementary Table S3. The product was recombined with the linearized vector pEAQ-HT (In-Fusion^{TM} Advantage PCR Cloning Kits; Clontech). pEAQ-MYB1 was constructed previously (Lai et al., 2014). The constructs (pEAQ-LcbHLH1-3) were maintained in *Agrobacterium tumefaciens* strain GV3101. *Agrobacterium* cultures containing the different constructs were infiltrated into the abaxial leaf surface of *N. tabacum*, as described in Sainsbury et al. (2009). Control was infiltrated with empty vector (pEAQ-HT) at the same time. Digital photographs were taken 5 days after infiltration. Full-length of LcbHLH3 was amplified and then ligated with pBI121 vector. The resulting construct (pBI121- LcbHLH3) was introduced into *A. tumefaciens* strain EHA105. The recombinant strains were used to transform *N. tabacum* K326 using the leaf disk method (Horsch et al., 1985).

Subcellular Localization Analysis

The coding sequences of *LcMYB1* and *LcbHLH1-3* without the stop codon were amplified by PCR (primers are listed in Supplementary Table S4), and recombined into the pEAQ-HT-GFP vector using *Age* I in frame with the GFP sequence

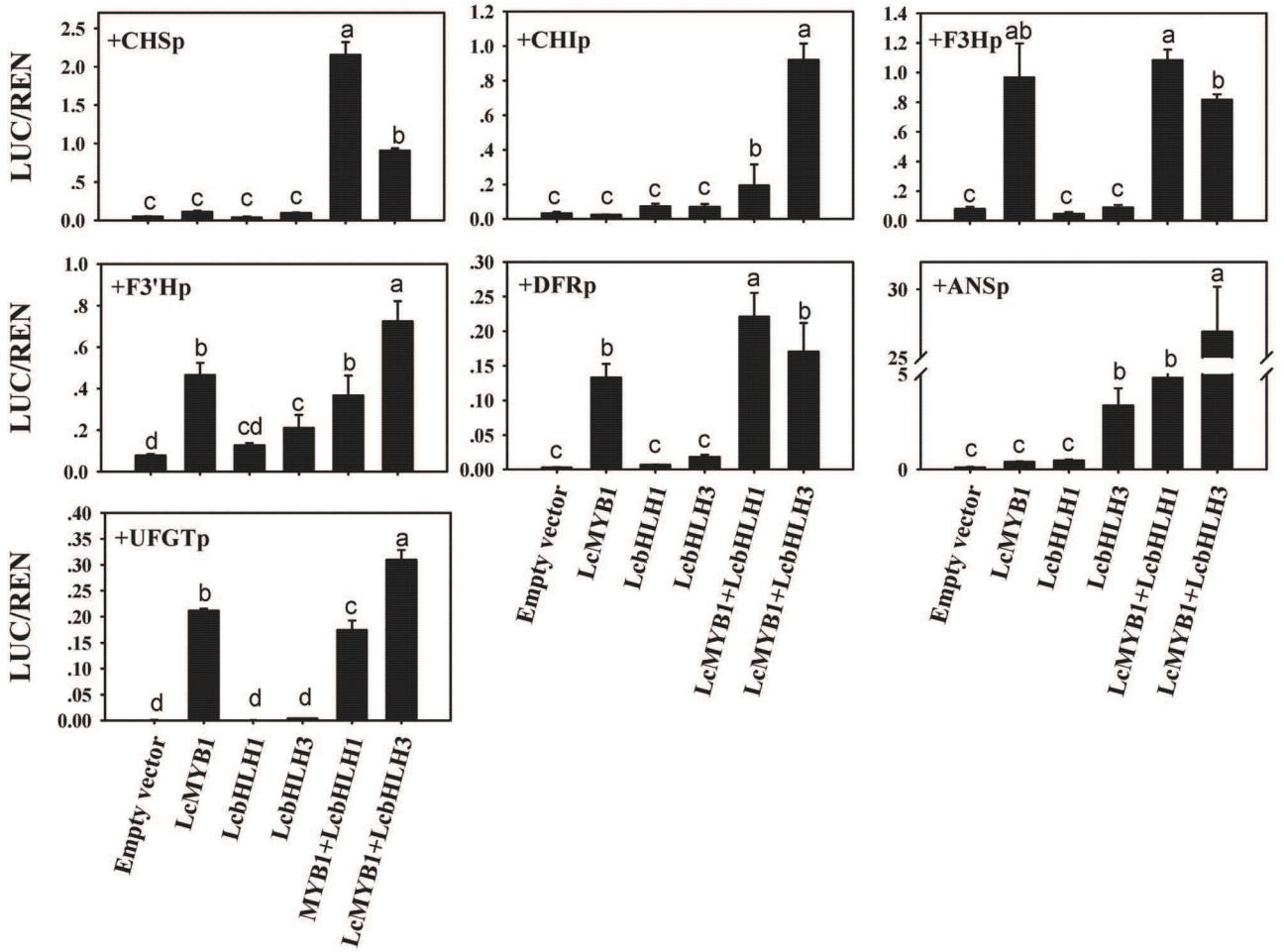

FIGURE 9 | *In vivo* interactions between litchi transcriptional factors and promoters of anthocyanin biosynthetic genes in litchi studied by dual luciferase assay in *N. benthamiana* leaves. *In vivo* associations of MYB, bHLHs and anthocyanin biosynthetic gene promoters as revealed by transient assays. The vertical bars represent the standard error of four replicate reactions. Different letters on the top of columns indicate significant difference at $p < 0.05$.

(Sainsbury et al., 2009). The fusion constructs and the control GFP vector were transformed into *Agrobacterium* strain GV3101 by freeze-thaw method. *Agrobacterium* cultures containing the 35S: LcMYB1-GFP, 35S: LcbHLH1-GFP, 35S: bHLH2-GFP, and 35S: LcbHLH3-GFP constructs were infiltrated into *N. benthamiana* leaves. Two days after infiltration, leaf protoplasts were isolated according to Schweiger and Schwenkert (2014). The protoplasts were incubated with 0.1 μg ml^{-1} DAPI for 10 min. GFP and DAPI fluorescence were observed with a fluorescence microscope (Zeiss Axio Observer D1). All transient expression assays were repeated at least three times.

Yeast Two-Hybrid Assay

Yeast two-hybrid assays were performed using the Matchmaker™ Gold Yeast Two-Hybrid System (Clontech). The coding regions of *LcbHLH1-3* and *LcMYB1* with different 3′-deletion were cloned into pGADT7 and pGBKT7 to fuse with the AD and DBD, respectively, to create different baits and preys (primers are shown in Supplementary Table S5). Full length of LcMYB1 showed autoactivation in yeast cells. Partial clones of *LcMYB1* (*LcMYB1D*) on the contrary did not show any transcriptional activation activity in yeast cells. Different pairs of bait and prey constructs were co-transformed into yeast strain Gold Y2H using the lithium acetate method, and yeast cells were grown on a (SD/–Leu/–Trp) according to the manufacturer's protocol (Clontech) for 3 days. Transformed colonies were then plated onto minimal medium quadruple dropout (SD medium with –Leu/–Trp/–His/–Ade) containing 125 μM Aureobasidin A and 4 mg ml^{-1} X-α-Gal at 30°C to test for possible interactions between LcbHLH1-LcbHLH3 and LcMYB1 according to their growth status and the activity of α-galactosidase.

BIFC Assays

NYFP (175-end) and CYFP (175-end) were amplified from pSAT5(A)-DEST-cEYFP and pSAT5(A)-DEST-cEYFP-N1 which were purchased from TAIR. pEAQ-NYFP-F CAAATTC GCGACCGGTATGGTGAGCAAGGGCGAGG and pEAQ-NYFP-R: AGTTAAAGGCCTCGAGTCAGTCCTCGATGTTGT

GG were used for amplify NYFP, pEAQ-CYFP-F: CAAA TTCGCGACCGGTGGCAGCGTGCAGCTCGCCGAC and pEAQ-CYFP-R: AGTTAAAGGCCTCGAGTCACTTGTACAGC TCGTCC were used for amplify CYFP. The products were recombined with the vector pEAQ-HT linearized using *Age* I and *Xho* I, and the obtained fragments were named pEAQ-NYFP and pEAQ-CYFP. The coding sequences of *LcMYB1* and *LcbHLH1-3* were amplified without stop codon by PCR (primers are listed in Supplementary Table S6) and then subcloned into pEAQ-NYFP and pEAQ-CYFP using *Age* I (In-Fusion^{TM} Advantage PCR Cloning Kits; Clontech), respectively. All constructed vectors were then transformed in *Agrobacterium* (strain GV3101). Two days after infiltration, leaf protoplasts were isolated as described above. YFP fluorescence was observed 2 days after infiltration with a fluorescence microscope. Expression of target genes alone was used as negative controls. All transient expression assays were repeated at least three times.

Dual Luciferase Assay of Transiently Transformed Tobacco Leaves

Specific primers were designed based on litchi whole genome sequence to amplify the promoters of anthocyanin biosynthetic genes *LcCHS*, *LcCHI*, *LcF3H*, *LcF3'H*, *LcANS*, *LcDFR,* and *LcUFGT* (primers are shown in Supplementary Table S7). Conserved *cis*-element motifs located in promoters were searched by online software New PLACE[3] (Higo et al., 1999). The promoters of anthocyanin biosynthetic genes were inserted into the pGreenII 0800-LUC vector at the 5′ end of a LUC gene (Hellens et al., 2005). All constructs were transformed into *Agrobacterium tumefaciens* GV3101. Activation of promoters by TF was measured as ratio of the enzyme activity of firefly LUC, driven by the promoter under investigation, and the REN, driven by CaMV:35S. Six to eight leaves old *N. benthamiana* plants were used for infiltration. Infiltrations, transient expression analysis, and enzyme activity determination of LUC and REN were conducted as described by Hellens et al. (2005).

[3] https://sogo.dna.affrc.go.jp/cgi-bin/sogo.cgi

AUTHOR CONTRIBUTIONS

BL performed most of the experiments and data analysis, and wrote the draft of the paper. L-ND, BH, RL, and W-BS carried out part of material collection, RNA extraction and data analysis. Y-HQ and J-TZ participated in the preparation of the manuscript. H-CW and G-BH conceived, designed and coordinated the studies. All authors have read and approved the final manuscript.

FUNDING

The project was supported by the China Litchi and Longan Industry Technology Research System (Project No. CARS-33), the National Natural Science Fund of China (Project No. 30971985), the Ministry of Agriculture, China, and the Key Laboratory of Innovation and Utilization for Germplasm Resources in Horticultural Crops in Southern China of Guangdong Higher Education Institutes, South China Agricultural University (No. KBL11008).

ACKNOWLEDGMENTS

We thank Francesca Quattrocchio for critical revision of the Manuscript (Swammerdam Institute of Life Sciences, University of Amsterdam, The Netherlands). We are grateful to Dr. George P. Lomonossoff (Department of Biological Chemistry, John Innes Centre) for providing pEAQ-HT vector and encouraging us to construct the BiFC vectors. Thank Dr. Roger P. Hellens (The New Zealand Institute of Plant and Food Research) for providing pGreenII 0800-LUC vector used in this study.

SUPPLEMENTARY MATERIAL

The Supplementary Material for this article can be found online at: http://journal.frontiersin.org/article/10.3389/fpls.2016.00166

REFERENCES

Bai, Y., Pattanaik, S., Patra, B., Werkman, J. R., Xie, C. H., and Yuan, L. (2011). Flavonoid-related basic helix-loop-helix regulators, NtAn1a and NtAn1b, of tobacco have originated from two ancestors and are functionally active. *Planta* 234, 363–375. doi: 10.1007/s00425-011-1407-y

Ban, Y., Honda, C., Hatsuyama, Y., Igarashi, M., Bessho, H., and Moriguchi, T. (2007). Isolation and functional analysis of a MYB transcription factor gene that is a key regulator for the development of red coloration in apple skin. *Plant Cell Physiol.* 48, 958–970. doi: 10.1093/pcp/pcm066

Borevitz, J. O., Xia, Y., Blount, J., Dixon, R. A., and Lamb, C. (2000). Activation tagging identifies a conserved MYB regulator of phenylpropanoid biosynthesis. *Plant Cell* 12, 2383–2394. doi: 10.2307/3871236

Broun, P. (2005). Transcriptional control of flavonoid biosynthesis: a complex network of conserved regulators involved in multiple aspects of differentiation in *Arabidopsis*. *Curr. Opin. Plant Biol.* 8, 272–279. doi: 10.1016/j.pbi.2005.03.006

Chagne, D., Carlisle, C. M., Blond, C., Volz, R. K., Whitworth, C. J., Oraguzie, N. C., et al. (2007). Mapping a candidate gene (MdMYB10) for red flesh and foliage colour in apple. *BMC Genomics* 8:212. doi: 10.1186/1471-2164-8-212

Chagne, D., Lin-Wang, K., Espley, R. V., Volz, R. K., How, N. M., Rouse, S., et al. (2013). An ancient duplication of apple MYB transcription factors is responsible for novel red fruit-flesh phenotypes. *Plant Physiol.* 161, 225–239. doi: 10.1104/pp.112.206771

D'Amelia, V., Aversano, R., Batelli, G., Caruso, I., Castellano, M. M., Castro-Sanz, A. B., et al. (2014). High AN1 variability and interaction with basic helix-loop-helix co-factors related to anthocyanin biosynthesis in potato leaves. *Plant J.* 80, 527–540. doi: 10.1111/tpj.12653

Espley, R. V., Hellens, R. P., Putterill, J., Stevenson, D. E., Kutty-Amma, S., and Allan, A. C. (2007). Red colouration in apple fruit is due to the activity of the MYB transcription factor, MdMYB10. *Plant J.* 49, 414–427. doi: 10.1111/j.1365-313X.2006.02964.x

Feller, A., Hernandez, J. M., and Grotewold, E. (2006). An ACT-like domain participates in the dimerization of several plant basic-helix-loop-helix transcription factors. *J. Biol. Chem.* 281, 28964–28974. doi: 10.1074/jbc.M603262200

Feng, S., Wang, Y., Yang, S., Xu, Y., and Chen, X. (2010). Anthocyanin biosynthesis in pears is regulated by a R2R3-MYB transcription factor PyMYB10. *Planta* 232, 245–255. doi: 10.1007/s00425-010-1170-5

Grotewold, E., Sainz, M. B., Tagliani, L., Hernandez, J. M., Bowen, B., and Chandler, V. L. (2000). Identification of the residues in the Myb domain of maize C1 that specify the interaction with the bHLH cofactor R. *Proc. Natl. Acad. Sci. U.S.A.* 97, 13579–13584. doi: 10.1073/pnas.250379897

Heim, M. A., Jakoby, M., Werber, M., Martin, C., Weisshaar, B., and Bailey, P. C. (2003). The basic helix-loop-helix transcription factor family in plants: a genome-wide study of protein structure and functional diversity. *Mol. Biol. Evol.* 20, 735–747. doi: 10.1093/molbev/msg088

Hellens, R. P., Allan, A. C., Friel, E. N., Bolitho, K., Grafton, K., Templeton, M. D., et al. (2005). Transient expression vectors for functional genomics, quantification of promoter activity and RNA silencing in plants. *Plant Methods* 1:13. doi: 10.1186/1746-4811-1-13

Hellens, R. P., Moreau, C., Lin-Wang, K., Schwinn, K. E., Thomson, S. J., Fiers, M. W. E. J., et al. (2010). Identification of Mendel's white flower character. *PLoS ONE* 5:e13230. doi: 10.1371/journal.pone.0013230

Hichri, I., Barrieu, F., Bogs, J., Kappel, C., Delrot, S., and Lauvergeat, V. (2011). Recent advances in the transcriptional regulation of the flavonoid biosynthetic pathway. *J. Exp. Bot.* 62, 2465–2483. doi: 10.1093/jxb/erq442

Hichri, I., Heppel, S. C., Pillet, J., Leon, C., Czemmel, S., Delrot, S., et al. (2010). The basic helix-loop-helix transcription factor MYC1 is involved in the regulation of the flavonoid biosynthesis pathway in grapevine. *Mol. Plant* 3, 509–523. doi: 10.1093/mp/ssp118

Higo, K., Ugawa, Y., Iwamoto, M., and Korenaga, T. (1999). Plant cis-acting regulatory DNA elements (PLACE) database: 1999. *Nucleic Acids Res.* 27, 297–300. doi: 10.1093/nar/27.1.297

Horsch, R., Fry, J., Hoffmann, N., Eichholtz, D., Rogers, S., and Fraley, R. (1985). A simple and general method for transferring genes into plants. *Science* 227, 1229–1231. doi: 10.1126/science.227.4691.1229

Jaakola, L. (2013). New insights into the regulation of anthocyanin biosynthesis in fruits. *Trends Plant Sci.* 18, 477–483. doi: 10.1016/j.tplants.2013.06.003

Kobayashi, S., Ishimaru, M., Hiraoka, K., and Honda, C. (2002). Myb-related genes of the Kyoho grape (*Vitis labruscana*) regulate anthocyanin biosynthesis. *Planta* 215, 924–933. doi: 10.1007/s00425-002-0830-5

Koes, R., Verweij, W., and Quattrocchio, F. (2005). Flavonoids: a colorful model for the regulation and evolution of biochemical pathways. *Trends Plant Sci.* 10, 236–242. doi: 10.1016/j.tplants.2005.03.002

Lai, B., Hu, B., Qin, Y., Zhao, J., Wang, H., and Hu, G. (2015). Transcriptomic analysis of *Litchi chinensis* pericarp during maturation with a focus on chlorophyll degradation and flavonoid biosynthesis. *BMC Genomics* 16:225. doi: 10.1186/s12864-015-1433-4

Lai, B., Li, X. J., Hu, B., Qin, Y. H., Huang, X. M., Wang, H. C., et al. (2014). LcMYB1 is a key determinant of differential anthocyanin accumulation among genotypes, tissues, developmental phases and ABA and light stimuli in *Litchi chinensis*. *PLoS ONE* 9:e86293. doi: 10.1371/journal.pone.0086293

Lee, H. S., and Wicker, L. (1991). Anthocyanin pigments in the skin of lychee fruit. *J. Food Sci.* 56, 466–468. doi: 10.1111/j.1365-2621.1991.tb05305.x

Liu, X. F., Yin, X. R., Allan, A. C., Lin-Wang, K., Shi, Y. N., Huang, Y. J., et al. (2013). The role of MrbHLH1 and MrMYB1 in regulating anthocyanin biosynthetic genes in tobacco and Chinese bayberry (*Myrica rubra*) during anthocyanin biosynthesis. *Plant Cell Tiss. Organ Cult.* 115, 285–298. doi: 10.1007/s11240-013-0361-8

Livak, K. J., and Schmittgen, T. D. (2001). Analysis of relative gene expression data using real-time quantitative PCR and the 2(-delta delta C(T)) Method. *Methods* 25, 402–408. doi: 10.1006/meth.2001.1262

Ludwig, S. R., Bowen, B., Beach, L., and Wessler, S. R. (1990). A regulatory gene as a novel visible marker for maize transformation. *Science* 247, 449–450. doi: 10.1126/science.247.4941.449

Ludwig, S. R., Habera, L. F., Dellaporta, S. L., and Wessler, S. R. (1989). Lc, a member of the maize R gene family responsible for tissue-specific anthocyanin production, encodes a protein similar to transcriptional activators and contains the myc-homology region. *Proc. Natl. Acad. Sci. U.S.A* 86, 7092–7096. doi: 10.1073/pnas.86.18.7092

Matus, J. T., Poupin, M. J., Canon, P., Bordeu, E., Alcalde, J. A., and Arce-Johnson, P. (2010). Isolation of WDR and bHLH genes related to flavonoid synthesis in grapevine (*Vitis vinifera* L.). *Plant Mol. Biol.* 72, 607–620. doi: 10.1007/s11103-010-9597-4

Montefiori, M., Brendolise, C., Dare, A. P., Lin-Wang, K., Davies, K. M., Hellens, R. P., et al. (2015). In the Solanaceae, a hierarchy of bHLHs confer distinct target specificity to the anthocyanin regulatory complex. *J. Exp. Bot.* 66, 1427–1436. doi: 10.1093/jxb/eru494

Nesi, N., Debeaujon, I., Jond, C., Pelletier, G., Caboche, M., and Lepiniec, L. (2000). The TT8 gene encodes a basic helix-loop-helix domain protein required for expression of DFR and BAN genes in *Arabidopsis* siliques. *Plant Cell* 12, 1863–1878. doi: 10.2307/3871198

Niu, S. S., Xu, C. J., Zhang, W. S., Zhang, B., Li, X., Lin-Wang, K., et al. (2010). Coordinated regulation of anthocyanin biosynthesis in Chinese bayberry (*Myrica rubra*) fruit by a R2R3 MYB transcription factor. *Planta* 231, 887–899. doi: 10.1007/s00425-009-1095-z

Ohno, S., Hosokawa, M., Hoshino, A., Kitamura, Y., Morita, Y., Park, K. II, et al. (2011). A bHLH transcription factor, DvIVS, is involved in regulation of anthocyanin synthesis in dahlia (*Dahlia variabilis*). *J. Exp. Bot.* 62, 5105–5116. doi: 10.1093/jxb/err216

Palapol, Y., Ketsa, S., Lin-Wang, K., Ferguson, I. B., and Allan, A. C. (2009). A MYB transcription factor regulates anthocyanin biosynthesis in mangosteen (*Garcinia mangostana* L.) fruit during ripening. *Planta* 229, 1323–1334. doi: 10.1007/s00425-009-0917-3

Park, K. I., Ishikawa, N., Morita, Y., Choi, J. D., Hoshino, A., and Iida, S. (2007). A bHLH regulatory gene in the common morning glory, Ipomoea purpurea, controls anthocyanin biosynthesis in flowers, proanthocyanidin and phytomelanin pigmentation in seeds, and seed trichome formation. *Plant J.* 49, 641–654. doi: 10.1111/j.1365-313X.2006.02988.x

Pattanaik, S., Xie, C. H., and Yuan, L. (2008). The interaction domains of the plant Myc-like bHLH transcription factors can regulate the transactivation strength. *Planta* 227, 707–715. doi: 10.1007/s00425-007-0676-y

Payne, C. T., Zhang, F., and Lloyd, A. M. (2000). GL3 encodes a bHLH protein that regulates trichome development in *Arabidopsis* through interaction with GL1 and TTG1. *Genetics* 156, 1349–1362.

Pires, N., and Dolan, L. (2010). Origin and diversification of basic-helix-loop-helix proteins in plants. *Mol. Biol. Evol.* 27, 862–874. doi: 10.1093/molbev/msp288

Quattrocchio, F., Wing, J. F., and Koes, R. E. (1993). Regulatory genes controlling anthocyanin pigmentation are functionally conserved among plant species and have distinct sets of target genes. *Plant Cell* 5, 1497–1512. doi: 10.2307/3869734

Quattrocchio, F., Wing, J. F., van der Woude, K., Mol, J. N., and Koes, R. (1998). Analysis of bHLH and MYB domain proteins: species-specific regulatory differences are caused by divergent evolution of target anthocyanin genes. *Plant J.* 13, 475–488. doi: 10.1046/j.1365-313X.1998.00046.x

Quattrocchio, F., Wing, J., van der Woude, K., Souer, E., de Vetten, N., Mol, J., et al. (1999). Molecular analysis of the anthocyanin2 gene of petunia and its role in the evolution of flower color. *Plant Cell* 11, 1433–1444. doi: 10.2307/3870973

Rahim, M. A., Busatto, N., and Trainotti, L. (2014). Regulation of anthocyanin biosynthesis in peach fruits. *Planta* 204, 913–929. doi: 10.1007/s00425-014-2078-2

Sainsbury, F., Thuenemann, E. C., and Lomonossoff, G. P. (2009). pEAQ: versatile expression vectors for easy and quick transient expression of heterologous proteins in plants. *Plant Biotechnol. J.* 7, 682–693. doi: 10.1111/j.1467-7652.2009.00434.x

Schweiger, R., and Schwenkert, S. (2014). Protein-protein interactions visualized by bimolecular fluorescence complementation in tobacco protoplasts and leaves. *J. Vis. Exp.* 85:e51327. doi: 10.3791/51327

Schwinn, K., Venail, J., Shang, Y., Mackay, S., Alm, V., Butelli, E., et al. (2006). A small family of MYB-regulatory genes controls floral pigmentation intensity and patterning in the genus *Antirrhinum*. *Plant Cell* 18, 831–851. doi: 10.1105/tpc.105.039255

Shirley, B. W., Kubasek, W. L., Storz, G., Bruggemann, E., Koornneef, M., Ausubel, F. M., et al. (1995). Analysis of *Arabidopsis* mutants deficient in flavonoid biosynthesis. *Plant J.* 8, 659–671. doi: 10.1046/j.1365-313X.1995.08050659.x

Spelt, C., Quattrocchio, F., Mol, J. N., and Koes, R. (2000). Anthocyanin1 of petunia encodes a basic helix-loop-helix protein that directly activates transcription of structural anthocyanin genes. *Plant Cell* 12, 1619–1632. doi: 10.1105/tpc.12.9.1619

Spelt, C., Quattrocchio, F., Mol, J., and Koes, R. (2002). ANTHOCYANIN1 of petunia controls pigment synthesis, vacuolar pH, and seed coat development by genetically distinct mechanisms. *Plant Cell* 14, 2121–2135. doi: 10.1105/tpc.003772

Tamura, K., Peterson, D., Peterson, N., Stecher, G., Nei, M., and Kumar, S. (2011). MEGA5: molecular evolutionary genetics analysis using maximum likelihood,

evolutionary distance, and maximum parsimony methods. *Mol. Biol. Evol.* 28, 2731–2739. doi: 10.1093/molbev/msr121

Wei, Y. Z., Hu, F. C., Hu, G. B., Li, X. J., Huang, X. M., and Wang, H. C. (2011). Differential expression of anthocyanin biosynthetic genes in relation to anthocyanin accumulation in the pericarp of *Litchi chinensis* Sonn. *PLoS ONE* 6:e19455. doi: 10.1371/journal.pone.0019455

Winkel, B. S. (2006). "The biosynthesis of flavonoids," in *The Science of Flavonoids*, ed. E. Grotewold (New York, NY: Springer), 233.

Xie, X. B., Li, S., Zhang, R. F., Zhao, J., Chen, Y. C., Zhao, Q., et al. (2012). The bHLH transcription factor MdbHLH3 promotes anthocyanin accumulation and fruit colouration in response to low temperature in apples. *Plant Cell Environ.* 35, 1884–1897. doi: 10.1111/j.1365-3040.2012.02523.x

Xu, W., Dubos, C., and Lepiniec, L. (2015). Transcriptional control of flavonoid biosynthesis by MYB-bHLH-WDR complexes. *Trends Plant Sci.* 20, 176–185. doi: 10.1016/j.tplants.2014.12.001

You, F. M., Huo, N., Gu, Y. Q., Luo, M. C., Ma, Y., Hane, D., et al. (2008). BatchPrimer3: a high throughput web application for PCR and sequencing primer design. *BMC Bioinformatics* 9:253. doi: 10.1186/1471-2105-9-253

Zhang, F., Gonzalez, A., Zhao, M., Payne, C. T., and Lloyd, A. (2003). A network of redundant bHLH proteins functions in all TTG1-dependent pathways of *Arabidopsis*. *Development* 130, 4859–4869. doi: 10.1242/dev.00681

Zhao, Z. C., Hu, G. B., Hu, F. C., Wang, H. C., Yang, Z. Y., and Lai, B. (2012). The UDP glucose:flavonoid-3-O-glucosyltransferase (UFGT) gene regulates anthocyanin biosynthesis in litchi (*Litchi chinesis* Sonn.) during fruit coloration. *Mol. Biol. Rep.* 39, 6409–6415. doi: 10.1007/s11033-011-1303-3

Zhong, H. Y., Chen, J. W., Li, C. Q., Chen, L., Wu, J. Y., Chen, J. Y., et al. (2011). Selection of reliable reference genes for expression studies by reverse transcription quantitative real-time PCR in litchi under different experimental conditions. *Plant Cell Rep.* 30, 641–653. doi: 10.1007/s00299-010-0992-8

Zimmermann, I. M., Heim, M. A., Weisshaar, B., and Uhrig, J. F. (2004). Comprehensive identification of *Arabidopsis thaliana* MYB transcription factors interacting with R/B-like BHLH proteins. *Plant J.* 40, 22–34. doi: 10.1111/j.1365-313X.2004.02183.x

Conflict of Interest Statement: The authors declare that the research was conducted in the absence of any commercial or financial relationships that could be construed as a potential conflict of interest.

frontiers in Plant Science

ORIGINAL RESEARCH
published: 08 April 2016
doi: 10.3389/fpls.2016.00365

Response of Potato Tuber Number and Spatial Distribution to Plant Density in Different Growing Seasons in Southwest China

*Shun-Lin Zheng[1], Liang-Jun Wang[2], Nian-Xin Wan[1], Lei Zhong[1], Shao-Meng Zhou[1], Wei He[3] and Ji-Chao Yuan[1]**

[1] Agronomy, Sichuan Agricultural University, Chengdu, China, [2] Agriculture Bureau of Dongpo County, Agrotechnical Station, Meishan, China, [3] Sichuan Academy of Agricultural Sciences, Crop Research Institute, Chengdu, China

The aim of this study was to explore the effects of different density treatments on potato spatial distribution and yield in spring and fall. Plant density influenced yield and composition, horizontal, and vertical distribution distances between potato tubers, and spatial distribution position of tuber weights. The results indicated that: (1) Spring potato yield had a convex quadratic curve relationship with density, and the highest value was observed at 15.75×10^4 tubers per hectare. However, the yield of fall potatoes showed a linear relationship with plant density, and the highest value was observed at 18×10^4 tubers per hectare; (2) Density had a greater influence on the tuber weight of spring potatoes and fruit number of single fall potatoes; (3) The number of potato tubers in the longitudinal concentration exhibited a negative linear relationship with density, whereas the average vertical distribution distance of tubers exhibited a positive incremental hyperbolic relationship. For spring and fall potato tubers, the maximum distances were 8.4152 and 6.3316 cm, and the minimum distances 8.7666 and 6.9366 cm, respectively; and (4) Based on the artificial neural network model of the spatial distribution of tuber weight, density mainly affected the number and spatial distribution of tubers over 80 g. Tubers over 80 g were mainly distributed longitudinally (6–10 cm) and transversely (12–20 cm) within the high density treatment, and the transverse distribution scope and number of tubers over 80 g were reduced significantly. Spring potato tubers over 80 g grown at the lowest density were mainly distributed between 12 and 20 cm, whereas those at the highest density were primarily distributed between 10 and 15 cm.

Keywords: potato, growing season, plant density, tuber yield, spatial distribution, artificial neural network model

OPEN ACCESS

Edited by:
Diego Rubiales, Consejo Superior de Investigaciones Cientificas, Spain

Reviewed by:
Grama Nanjappa Dhanapal, University of Agricultural Sciences, India
Margherita Irene Beruto, Istituto Regionale per la Floricoltura, Italy
Joelle Fustec, Ecole Superieure d'Agriculture, France

***Correspondence:**
Ji-Chao Yuan
yuanjichao5@163.com

Specialty section:
This article was submitted to Crop Science and Horticulture, a section of the journal Frontiers in Plant Science

Received: *15 November 2015*
Accepted: *08 March 2016*
Published: *08 April 2016*

Citation:
Zheng S-L, Wang L-J, Wan N-X, Zhong L, Zhou S-M, He W and Yuan J-C (2016) Response of Potato Tuber Number and Spatial Distribution to Plant Density in Different Growing Seasons in Southwest China. Front. Plant Sci. 7:365. doi: 10.3389/fpls.2016.00365

INTRODUCTION

With the increase in China's population and decrease in arable land, food security issues have become more prominent. Potato (*Solanum tuberosum* L.) is one of the most important staple food crops in China and plays important roles in coping with multiple crop indices, the output of cultivated land, and food security problems (Seyed and Asghar, 2011). In southwestern China, potatoes are planted in the spring and fall, leading to a relative high land output. The average potato yield in China is $\sim 1.5 \times 104$ kg hm^{-2}, whereas the average global yield is about 1.7×104 kg hm^{-2}. Theoretically, yield can reach 12×104 kg hm^{-2}, revealing that

there is potential to further improve potato production in China (Qu et al., 2005; Jia et al., 2011).

Increase in plant density is an effective way to improve potato yield, but certain differences exist among high densities and growing seasons (Vasilyev, 2014). Yu et al. (2009) showed that fall potato yield is positively correlated with density. Zhao et al. (2005) found that plant density has a downward parabolic relationship with potato yield, and delayed sowing dates require increased densities to obtain the maximum yield. Agricultural methods in China have become more mechanized in order to achieve higher efficiency and increase potato yields, but the rate of tuber injury during potato harvest is high. For instance, previous studies indicated that 70% of potato injuries are caused during harvest, and that the injury rates associated with potato harvest are ∼30% of the total output (Peters, 1996; Wang et al., 2014). These factors seriously influence the yield and commodity value of potato.

The design used to harvest potatoes is based on the horizontal and vertical distribution of tubers as well as the sowing depth (Zhang, 2014). Several factors affect the potato tuber distribution (Wurrt et al., 1993). For instance, stolon plays a decisive role in the size and distribution of tubers, and larger leaf areas and the accumulation of leaf dry matter are beneficial to the stolon formation (Liu et al., 2003). Moreover, larger canopy sizes can significantly promote tuber expansion (Yang et al., 1994). Previous studies have confirmed that the leaf area index (LAI) increases with the increasing plant density (Jin et al., 2013). However, high densities result in both decreased leaf area and photosynthetic rates. Furthermore, the crown and stolon number per plant increases with the increasing density, whereas the average potato weight decreases significantly (Xiao et al., 2003; Fu, 2012). These results implied that plant density increase results in individual competition, and individual growth inhibition eventually leads to differences in the spatial distribution of potato tubers. Previous studies on potato have focused on analyzing tuber size and number (Haverkort et al., 1990; Wurrt et al., 1997); however, little is known about the impact of planting density on tuber spatial distribution.

To address these issues, the present study aimed to investigate the differences between potato crops grown at different densities in spring and fall. In addition, this study investigated the spring and fall potato yield, the spatial distribution of tubers, and the relationship between density and tuber spatial distribution. The results of this study will provide information on the appropriate densities for mechanical harvest that increase potato yield.

MATERIALS AND METHODS

Site Description

The study was conducted at the experimental farm of Southwest Sichuan Agricultural University, Chengdu, Sichuan Province, southwest China (N30°67′, E 104°06′). Soil and weather data are shown in **Tables 1, 2**, respectively.

Experimental Materials and Design

Potato tubers (*S. tuberosum* cv. Chuanyu 117) were provided by the Crops Institute, Sichuan Academy of Agricultural Sciences, China. The study was conducted using the following plant densities: D1 (6×10^4 strains hm^{-2}), D2 (9×10^4 strains hm^{-2}), D3 (12×10^4 strains hm^{-2}), D4 (15×10^4 strains hm^{-2}), and D5 (18×10^4 strains hm^{-2}). A randomized block design with three replications was used in two growing seasons, spring and fall. The plot area was 14 m^2 (2 m × 7 m) with a 60 or 40-cm row space. Whole tubers (∼30–40 g) were planted at a depth of ∼10 cm. The amount of compound fertilizer used was ∼127.5 kg hm^{-2}, and field management was according to local practices. Irrigation was applied to maintain moisture at field capacity. Spring potato

TABLE 1 | Soil conditions in the two experimental sites.

Experimental site	Soil type	pH	Organic matter (g kg^{-1})	Total N content (g kg^{-1})	Total P content (g kg^{-1})	Total K content (g kg^{-1})	Available N (mg kg^{-1})	Available P (mg kg^{-1})	Available K (mg kg^{-1})
Spring site	PS	5.09	25.09	1.98	0. 83	14.20	136.82	163.33	107.00
Fall site	PS	5.92	24.54	1.85	0.92	14.12	191.94	126.99	91.29

PS, paddy soil; Soil type in both seasons was consistent, and the experimental sites were previously planted with rice.

TABLE 2 | Meteorological factors at each growing stage of spring and fall potatoes.

Growing season	Growth stage	Rain (mm)	AT (≥5 °C)	SD (h)	Day length (h)	DMT (°C)
Spring	SS-MS	139.0	1381.5	332.9	1025.03	17.3
	SS-TBS	7.9	513.0	149.9	411.45	15.5
	TBS-MS	131.1	868.5	183.0	613.58	18.5
	SS-MS	209.3	1239.7	146.7	873.20	16.1
Fall	SS-TBS	165.6	594.6	70.0	346.43	20.5
	TBS-MS	43.7	645.1	76.7	526.77	13.4

SS, seeding stage; TBS, tuber bulking stage; MS, maturity stage; AT, accumulated temperature; SD, sunshine duration; DMT, daily mean temperature.

TABLE 3 | Yield and yield components under different plant densities in the two growing seasons.

Growing season	Density (× 10^4 plant·hm^{-2})	Yield (t hm^{-2})	Effective plants (× 10^4 plant hm^{-2})	Tubers plant^{-1}	G tuber^{-1}
Spring	6	42.05c	5.52e	7.82a	103.22a
	9	44.27b	8.20d	7.75ab	73.87b
	12	47.71a	11.00c	7.00b	65.60c
	15	48.05a	13.94b	5.87c	62.18d
	18	47.63a	16.41a	6.08c	49.53e
Average		45.94	11.01	6.90	70.88
Fall	6	21.29d	5.84e	5.67a	62.77a
	9	22.52cd	8.73d	4.27b	56.53ab
	12	23.95bc	11.18c	4.40b	50.36b
	15	25.91b	13.65b	3.67b	54.75b
	18	28.17a	15.42a	3.87b	51.26b
Average		24.37	10.97	4.38	55.13

Data are presented as means of three replicates in each treatment. Different letters in each column represent significant differences at $p < 0.05$.

plants were harvested 5 months after sowing in December 2012, and fall potato plants were harvested 4 months after sowing in August 2013.

Sampling and Determination of Variables

The effective plant number was estimated based on the actual number plants at 14 days post emergence, and the effective unit area number based on the germination rate. Ten representative mature plants were selected from each plot to determine tuber weight, stems at the ridge surface level of mutilation, stem center, and ridge surface at the water level under different densities and position distribution models. The transverse distribution of the vertical tuber level was estimated from the stem to the furthest vertical distance, whereas the longitudinal distribution distance from the stem to the furthest horizontal distance at the bottom of the ridge surface to the tuber. The tuber weight was measured using an electronic scale. Twenty representative mature plants were selected from each experimental plot to determine yield and yield components under different densities and position distribution models. All statistical analyses were performed using Excel (Microsoft Corp., Redmond, WA, USA), Alphatruck 2.0 (Middlesex, UK), Sigmaplot 12.5 (Softonic International, Barcelona, Spain), and JMP 10 (SAS, Cary, NC, USA).

RESULTS

Influence of Density on Yield and Yield Components

Tuber number and tuber weight significantly decreased with the increasing plant density increased (**Table 3**), whereas the effective plant number increased. Differences between potato plant growing seasons and the effects of density on yield varied significantly. The variable coefficients of yield, fruit number, and tuber weight were 5.80, 13.18, and 28.34% for single spring potatoes, respectively, and 11.22, 17.85, and 11.22% for single fall potatoes, respectively. Spring potato tuber weight was significantly influenced by plant density, whereas fall potato tuber weight by single potato fruit number.

Spring potato yield and plant density exhibited a quadratic function relationship and the regression equation was: $y = 0.0665x^2 + 2.0942 + 31.5860$ ($R^2 = 0.9638^*$). The highest yield was measured at 15.75×10^4 tubers or plants hm^{-2}. However, fall potato yield and plant density exhibited a linear relationship, and the regression equation was: $y = 0.5717x + 17.5080$ ($R^2 = 0.9838^{**}$). The highest yield was measured of 0.5717×10^3 kg hm^{-2} was measured at 1.00×10^4 tubers or plants·hm^{-2}.

Correlation analysis (**Table 4**) revealed that the effective plant number was positively associated with yield, whereas the tuber number and weight values were negatively associated. No significant correlations were found between fall potato tuber weight and yield among plant densities. Furthermore, based on size, analysis showed that the effective plant number mostly affected yield, but the yield components of the two growing seasons differed slightly in the contribution rate. For spring potatoes, the contribution of weight was higher than that of potato number or effective strains, whereas for fall potatoes, the contribution of the effective plant number was higher than that of potato number or potato weight. During spring, the increased density maintained large tuber weights, and the increased density during fall mainly increased yield.

The Relationship between Density and Average Distribution of Potato Tuber Distance

A significant difference in potato tuber distribution was observed (**Table 5**), and the average distance transverse distribution coefficients of variation were 6.38 and 4.11% for spring and fall potatoes, respectively. The influence of density on the longitudinal distribution of the average distance of potato tubers

TABLE 4 | Contribution of yield components to yield.

Growing season	Yield components	Correlation coefficient	Direct effect	Contribution rate (%)
Spring	Effective plants	0.8484**	−0.1791	14.15
	Tuber number per plant	−0.7567**	−0.3408	24.02
	Single tuber weight	−0.8602**	−0.7717	61.83
	Effective plants	0.8946**	1.4000	77.20
Fall	Tuber number per plant	−0.7091**	0.2828	12.36
	Single tuber weight	−0.4511	0.3755	10.44

*** stands for each index contributed to yield reached extremely significant level.*

was relatively high. Moreover, the average distance of transverse distribution was essentially the same, whereas the effect of the transverse distribution on the average distance was greater. A general relationship between the average distribution of the longitudinal distance (Z) and density (x) fit well with the incremental hyperbolic function ($Z = a + b/x$). The equations were $Z = -9.8196/x + 8.4152$ ($R^2 = 0.8358^*$) for spring and $Z = -5.2716/x + 6.3316$ ($R^2 = 0.9547^{**}$) for fall. The equations suggested that the maximum distance between the vertical distribution of spring and fall potato tubers was on average 8.4152 and 6.3316 cm, respectively. The transverse distribution of the average distance (H) and density (x) were positively related to the decline of the hyperbolic function ($H = a + b/x$), and the equations were $H = 29.3939/x + 29.3939$ ($R^2 = 0.9638^{**}$) for spring and $H = 22.0697/x + 22.0697$ ($R^2 = 0.9670^{**}$) for fall. These equations showed that the minimum transverse distribution of the average distance of spring and fall potato tubers was 8.7666 and 6.9366 cm, respectively. Data indicated that the transverse distribution range was larger than the longitudinal distance of potato tubers. Furthermore, the transverse and vertical distance of spring potato tubers was larger than that of fall potatoes.

Cumulative Frequency of Tuber Number Distribution under Different Plant Densities

The vertical distribution distance increased with the increasing plant density, whereas the longitudinal distribution distance decreased (**Figure 1**). Moreover, the transverse distribution distance decreased significantly, and the tuber concentration increased over the two growing seasons. The longitudinal and transverse cumulative percentage (F) exponentially increased with the increasing distribution distance (u) in the two growing seasons, and the changes were in line with the following logistic Equation: $F = a/((u/c)b + 1)$ (**Table 6**).

After fitting the equations to spring and fall data (**Table 7**), the variation coefficients of the longitudinal distribution at a 50% tuber distribution distance were 5.80 and 4.42%, respectively. At a 90% tuber vertical distribution distance, the spring and fall variation coefficients were 9.74 and 3.74%, respectively. Moreover, at a 50% transverse tuber distribution distance, the spring and fall variation coefficients were 9.11 and 8.98%, respectively, and the variation coefficients at a 90% tuber transverse distribution distance were 15.26 and 10.94%, respectively. The results clearly indicated that the influence of distribution density on the tuber horizontal distance was greater. Furthermore, the tuber distance decreased with the increasing plant density when the two growing seasons reached 50 and 90% of the transverse distribution. Compared with the highest density, the minimum density of spring and fall potato distances associated with the tuber transverse distribution of 90% were 38.81 and 29.58% greater than that of the highest density, respectively.

TABLE 5 | Average longitudinal and transverse distance under different densities in the two growing seasons.

Density ($\times 10^4$ Density (plant hm^{-2})	Average longitudinal distance (cm)		Average transverse distance (cm)	
	Spring	Fall	Spring	Fall
6	6.90c	5.42d	13.63a	10.48a
9	7.20b	5.82c	12.09b	9.58b
12	7.32b	5.90b	11.41c	8.92c
15	7.86a	5.92b	10.31d	8.44cd
18	8.05a	6.05a	10.60d	7.93d
Average	7.47	5.82	11.61	9.07

Data are presented as means of three replicates in each treatment. Different letters in each column represent significant differences at $p < 0.05$.

Artificial Neural Network Model of the Tuber Weight Spatial Distribution

Due to ecological factors associated with spring and fall (**Table 2**), the average weight per tuber differed significantly. When plant density (x), tuber longitudinal distribution distance (z), and the transverse distribution of tuber distance (h) were used as variables, model training, and model validation of the tuber weight (Y) of the artificial neural network (ANN) were established. The results indicated that the two growing seasons better responded to spatial distribution models of tuber weight at different densities. The model training and validation decision coefficients (R^2) for the two growing seasons were over 0.86, and the root mean square error and mean absolute deviation were ∼10 g (**Table 8**).

The following equations were used to determine the spring potato tuber weight (Y) under spatial distribution models at different densities:

$$Y = -45.93H_1 - 58.65H_2 + 81.25H_3 - 25.92$$

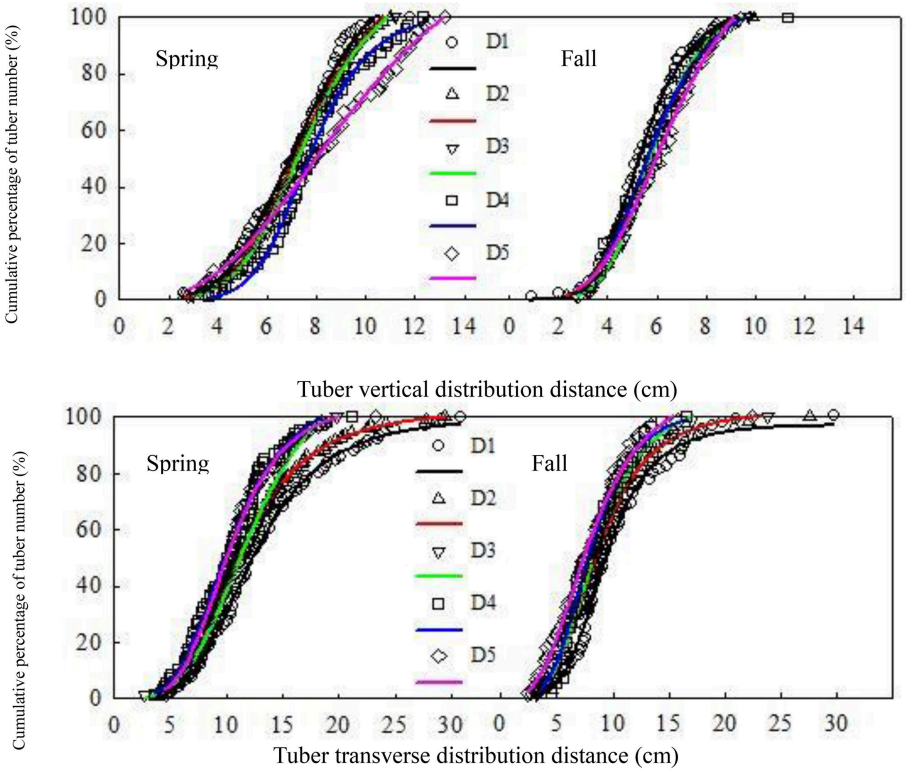

FIGURE 1 | Cumulative percentage of tuber number under different densities in the two growing seasons. Plant densities: D1, 6×10^4 strains hm^{-2}; D2, 9×10^4 strains hm^{-2}; D3, 12×10^4 strains hm^{-2}; D4, 15×10^4 strains hm^{-2}; and D5, 18×10^4 strains hm^{-2}.

$$H_1 = \tanh[0.5 \times (0.1051\,x + 0.2912\,z + 0.1131\,h - 6.7927)]$$
$$H_2 = \tanh[0.5 \times (0.0955\,x - 1.0442\,z + 0.4875\,h - 2.1808)]$$
$$H_3 = \tanh[0.5 \times (0.0492\,x + 0.0580\,z + 0.5001\,h - 5.1615)]$$

The following equations were used to determine the fall potato tuber weight (Y) under spatial distribution models at different densities:

$$Y = -89.35H_1 + 21.09H_2 + 92.12H_3 + 14.83$$
$$H_1 = \tanh[0.5 \times (0.0433\,x - 0.6260\,z + 0.2673\,h - 0.7287)]$$
$$H_2 = \tanh[0.5 \times (-0.1541\,x + 0.3231\,z + 0.2202\,h - 3.2938)]$$
$$H_3 = \tanh[0.5 \times (0.0479\,x - 0.2165\,z + 0.4430\,h - 2.9781)]$$

H_1, H_2, and H_3 represented the ANNs at three different weights in the hidden layer. Using these models, different space positions under different plant densities were predicted based on potato piece weights and potato piece weight distribution ranges.

A contour map was constructed using model predictions to estimate the longitudinal distance (**Figure 2A**). At 0–4-cm depth, tubers were mainly under 40 g in both growing seasons. Tubers over 80 g were mainly concentrated at 4–6-cm depth. In vertical distances greater than 10 cm, plant density was negatively associated with tuber size in both growing seasons. Regarding the transverse distance (**Figure 2B**), tuber weights in both growing seasons increased with the increasing distance of transverse distribution. At 0–5-cm depth, tubers were ∼20 g, whereas at 5–10-cm depth, they were 20–80 g. However, no significant differences between the various densities were identified. Furthermore, 80-g tubers exhibited a transverse distribution that differed from that of smaller tubers. In the spring, tubers greater than 80 g, which were planted at the lowest density, were mainly distributed at 12–20-cm depth. However, when planted at the highest density, the tubers were largely distributed at 10–15-cm depth. When the transverse distribution distance was greater than 20 cm, spring tubers were ∼40 g and fall tubers 20–60 g.

DISCUSSION

Ecological conditions that mainly affect yield are light, temperature, and water, but the level of influence is different (Song and Hou, 2003; Yao et al., 2009). Previous studies have shown that the size of the potato leaf area is closely related to plant light interception rate and dry matter yield (Men and Meng-Yun, 1995) and that plant growth and material accumulation determine the crop yield. Long photoperiod negatively affects the formation, enlargement, and number of tubers (Van Dam et al., 1996; Xiao and Guo, 2010), whereas short photoperiod length reduces photosynthesis (Qin et al., 2013). Low light conditions cause a series of shade avoidance

TABLE 6 | Cumulative percentage equation parameter values associated with potato tuber number and equations used to determine coefficients (R^2) under different plant densities.

Growing season	Density ($\times 10^4$ plant hm^{-2})	Tuber vertical distribution equation				Tuber transverse distribution equation			
		a	*b*	*c*	R^2	*a*	*b*	*c*	R^2
Spring	6	128.04	−4.32	7.67	0.9894**	100.10	−3.93	12.34	0.9975**
	9	121.23	−4.67	7.69	0.9977**	102.49	−3.78	11.24	0.9987**
	12	118.49	−4.90	7.73	0.9972**	124.03	−3.62	12.53	0.9936**
	15	102.72	−6.41	7.75	0.9959**	111.87	−3.75	10.46	0.9928**
	18	146.33	−2.84	10.04	0.9960**	106.27	−4.22	10.34	0.9933**
	6	106.26	−5.23	5.39	0.9979**	99.49	−4.07	9.15	0.9920**
Fall	9	112.68	−4.46	5.94	0.9961**	102.10	−3.88	8.62	0.9959**
	12	106.90	−5.57	5.87	0.9980**	106.92	−3.89	8.59	0.9784**
	15	109.59	−4.71	5.83	0.9631**	103.35	−4.19	7.98	0.9796**
	18	129.71	−3.92	6.71	0.9943**	114.10	−2.94	7.84	0.9918**

*** stands for the tuber number cumulative percentage to fit for equation reached extremely significant level, respectively.*

TABLE 7 | Potato tuber distribution distance of 50 and 90% at each plant density in the two growing seasons.

Growing season	Density ($\times 10^4$ plant hm^{-2})	50% tuber distribution distance (cm)		90% tuber distribution distance (cm)	
		Longitudinal	Transverse	Longitudinal	Transverse
Spring	6	6.92	12.33	9.36	21.53
	9	7.13	11.10	9.65	18.95
	12	7.25	11.24	9.78	16.39
	15	7.69	9.88	10.52	15.25
	18	7.97	10.05	11.84	15.51
	6	5.27	9.17	7.48	15.90
Fall	9	5.65	8.53	8.09	14.46
	12	5.74	8.31	7.93	13.20
	15	5.62	7.86	8.06	12.58
	18	5.96	7.20	8.27	12.27

responses such reductions in plant height, internode length, and branching number (Du et al., 2013). In contrast, high light and temperature conditions promote dry matter accumulation and transportation (Deng et al., 2012). During the seedling-tuber bulking of fall potato in southern China, high temperature, and humidity conditions suppress the normal plant vegetative growth and potato tuber formation, whereas low temperature and humidity conditions (**Table 2**) negatively affect tuber formation and enlargement, tuber number, and yield of fall potato. The average longitudinal and transverse distribution distance of spring potatoes is higher under low rainfall and loose soil texture conditions.

The plant growth and accumulation of dry matter distribution is different under different ecological conditions as well as the influence of density on yield and its components. Increase in plant density is beneficial for improving population structure and yield (Li et al., 2010, 2011). Comparison of the growing seasons showed that the ecological factors differed greatly, and that plant growth and yield formation were not consistent. Therefore, the influence of density on yield and its components resulted in specific differences (Yao et al., 2010; Xiao, 2013). The relationship between density and yield of spring potatoes fit a convex quadratic function, whereas an increasing linear relationship was observed between fall potato yield and density. The impact of density on the average spring potato weight was greater than that observed on fall potato weight, but the influence of the average individual junction on fall potato tubers was greater than that observed on spring potato tubers.

Several parameters played major roles in determining tuber size, including photosynthetic product quantity, tuber growth, and development via the regulation of the tuber number per unit area and the average tuber weight distribution. The results indicated that plant density could significantly increase the tuber number per unit area and decrease tuber weight. Tuber number was positively correlated with the average distribution and longitudinal distance, but negatively correlated with the transverse distribution of the average distance. The correlation coefficients for spring potatoes were 0.9404* and 0.9261*, respectively, whereas those for fall potatoes were 0.8769 and 0.8769**, respectively. These results indicated that density could

TABLE 8 | Artificial neural network model of the spatial distribution of potato tuber weight parameters during different growing seasons.

Growing season	R^2		MRSE (g)		Mean absolute deviation (g)		Sum frequency	
	Train	Validation	Train	Validation	Train	Validation	Train	Validation
Spring	0.8911	0.8933	11.7885	12.3637	9.6917	10.6256	100	51
Fall	0.9135	0.8677	11.3406	12.9161	9.3813	11.0060	100	50

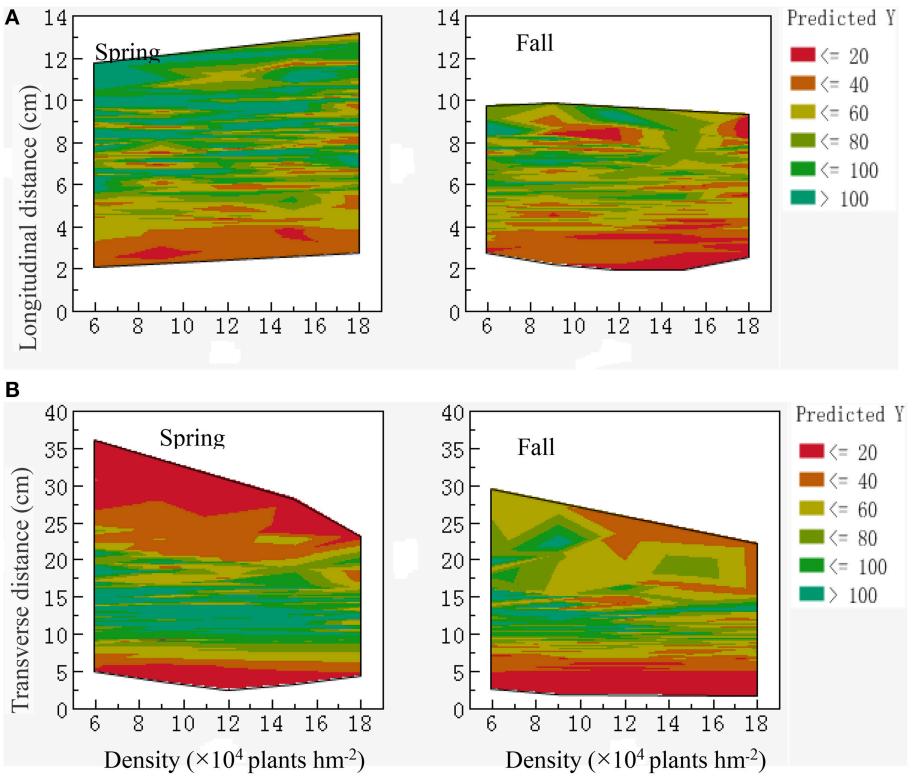

FIGURE 2 | Contour maps of potato tuber weight distribution model predictions under different plant densities. (A) Longitudinal distance (cm); **(B)** Transverse distance (cm).

significantly influence the spatial distribution of tuber distance by regulating the tuber number. Moreover, it reduced the concentration associated with the longitudinal tuber distance, and it increased that associated with the transverse tuber distance (**Figure 1**).

The factors associated with the decreased rate of large and medium tubers and increased rate of small tubers were largely influenced by high plant densities (Luo, 2011; Lei et al., 2013). The number of tubers over 80 g was significantly decreased with the increasing density, and the distribution range also reduced by the establishment of tuber weight spatial distribution under different density ANN models (Seyed et al., 2014). At different planting densities, longitudinal (0–6 cm) and transverse (0–12 cm) parameters were prioritized in tubers over 80 g. Moreover, tuber weight increased with the increasing distance, and the influence of density was not immediately apparent. Tubers over 80 g were mainly distributed horizontally (12–20 cm) and vertically (6–10 cm) in space. Under high-density conditions ($\geq 15 \times 10^4$ tubers or plant hm^{-2}), the transverse distribution and the tuber number ranges were significantly reduced. When the vertical distance was greater than 10 cm and the lateral distance was greater than 20 cm, tubers over 80 g were significantly reduced. Additionally, the tuber weight decreased with the increasing vertical and horizontal distances. These results illustrated that density mainly affected the tuber number and spatial distribution of tubers larger than 80 g.

CONCLUSION

In conclusion, increased density significantly increased potato yield, but the degree of influence associated with different growing seasons differed slightly. Therefore, the methods used to improve yield might vary based on the growing season. These values did not differ significantly with regard to plant density. In addition, the effective control of density on tuber number (based on the number per unit area and potato tuber size) could significantly affect the longitudinal and transverse distance concentrations, Thus, density changes within a certain range could be used to regulate the spatial distribution of potato tubers, and this could be accomplished by adjusting the

planting density or the mechanical harvesting parameters. This in turn would lead to the mechanization of potato production in southwestern China.

AUTHOR CONTRIBUTIONS

SZheng accomplished the whole experiment and article. LW did the field trail. NW, LZ, and SZhou helped SZheng did the index of potato, WH provided the potato, chuanyu 117, JY supported the fund to this article and directed the article accomplished.

ACKNOWLEDGMENTS

This research was supported by the National Sci-tech Support Plan (2012BAD06B0407) and the Sichuan Breeding Research Supporting Project (2011NZ0098-15-5).

REFERENCES

Deng, F., Wang, L., Liu, L., Liu, D. Y., Ren, W. J., and Yang W. Y. (2012). Effects of cultivation methods on dry matter production and yield of rice under different ecological conditions. *Acta Agron. Sin*. 10, 1930–1942. doi: 10.3724/SP.J.1006.2012.01930

Du, Y.-X., Ji, X., Zhang, J., et al. (2013). Research progress on the impacts of low light intensity on rice growth and development. *Chin. J. Eco Agric.* 11, 1307–1317 doi: 10.3724/SP.J.1011.2013.01307

Fu, Y. C. (2012). *Effects of Different Sizes of Pre-Elite Seed and Density on the Growth and Yield Formation of Potato*. Sichuan: Sichuan Agriculture University.

Haverkort, M., Van De Waart, K., and Bodlaender, B. A. (1990). Effect of pre-planting temperature and light treatments of seed tubers on potato yield and tuber size distribution. *Potato Res.* 33, 77–88 doi: 10.1007/BF02358132

Jia, J.-X., Yang, D.-Q., and Li, J.-D. (2011). Research and comparative analysis about potato production situation between China and continents in the world. *Agric. Eng.* 1, 84–86.

Jin, H., Liu, J., Song, B.-T., et al. (2013). Impact of plant density on the formation of potato minitubers derived from microtubers and tip-cuttings in plastic houses. *J. Integr. Agric.* 12, 1008–1017. doi: 10.1016/S2095-3119(13)60478-5

Lei, C.-Y., Zhang, Y.-X., Yi, G.-X., He, W.-J., Liu, D.-M., and Xing, D.-Y. (2013). Effects of density on main agronomic traits and yield of fall sowing potato in Jianghan plain. *Resour. Environ. Yangtze Basin* 26, 961–965.

Li, H.-X., Liu, Y.-X., Li, W.-B., et al. (2010). Effects of different planting densities on agronomic traits and yield of five Qingshu series potato varieties. *Guangxi Agric. Sci.* 41, 910–913.

Li, Y., Liu, S.-H., Ding, S.-C., et al. (2011). Impacts of entire potato size and planting density on growth and yield of potato. *Hunan Agric. Sci.* 11, 49–52.

Liu, K. L., Gao, J.-L., and Zhang, B.-L. (2003). The regular pattern of stolon and tuber formation in potato. *Chin. Potato J.* 17, 151–156.

Luo, W.-L. (2011). Effects of cultivation modes and planting density on potato Zhongshu 3 (*Solanum tubersum* L.) in winter season. *Fujian J. Agric. Sci.* 26, 961–965.

Men, F.-Y., and Meng-Yun, L. (1995). *Potato Cultivation Physiology [M]*. Beijing: China Agricultural Press.

Peters, R. (1996). Damage of potato tubers, a review. *Potato Res.* 39, 479–484. doi: 10.1007/BF02358463

Qin, Y.-Z., Chen, J., Xing, Z., et al. (2013). Effects of low temperature stress on photosynthesis in potato leaves. *J. Hunan Agric. Univ.* 39, 26–30. doi: 10.3724/SP.J.1238.2013.00026

Qu, D.-Y., Xie, K.-Y., Jin, L.-P., et al. (2005). Development of potato industry and food security in China. *Sci. Agric. Sin.* 38, 358–362.

Seyed, A., and Asghar, F. (2011). Population density and life-history parameters of the psyllid Bactericera nigricornis (Forster) on four commercial cultivars of potato. *Crop Prot.* 30, 844–848. doi: 10.1016/j.cropro.2011.03.003

Seyed, H. A., Ali, R. S, Mathias, N. A. et al. (2014). Modeling root length density of field grown potatoes under different irrigation strategies and soil textures using artificial neural networks. *Field Crops Res.* 162, 99–107 doi: 10.1016/j.fcr.2013.12.008

Song, X.-F., and Hou, Q. (2003). Influence of climate conditions on potato yield. *China Agric. Meteorol.* 2, 35–38.

Van Dam, J., Kooman, P. L, and Struik, P. C. (1996). Effects of temperature and photoperiod on early growth and final number of tubers in potato (*Solaum tuberosum* L.). *Potato Res.* 39, 51–62. doi: 10.1007/BF02358206

Vasilyev, A. A. (2014). Dependence of the yield and quality of potato tubers in the forest steppe zone of southern urals on the level of mineral nutrition and planting density. *Plant Ind.* 40, 422–425. doi: 10.3103/s1068367414060226

Wang, Y.-M., Sun, W., and Wang, G.-P. (2014). Research on mechanical damage to potato in harvesting. *J. Anhui Agric. Sci.* 42, 2837–2840.

Wurrt, D. C. E., Fwllowst, J. R., and Lynnand, J. R. (1993). The impact of some agronomic factors on the variability of potato tuber size distribution. *Potato Res.* 36, 237–245 doi: 10.1007/BF02360532

Wurrt, D. C. E., Hole, C. C., Fellows, J. R., et al. (1997). The effect of some environmental factors on potato tuber numbers. *Potato Res.* 40, 297–306 doi: 10.1007/BF02358011

Xiao, G.-L., and Guo, H.-C. (2010). Sensitivity of potato cultivars (*Solanum tuberosum* L.) to temperature and photoperiod and the relationship with some endogenous hormone. *Sci. Agric. Sin.* 7, 1500–1507. doi: 10.3864/j.issn.0578-1752.2010.07.023

Xiao, L., Hu, J.-F., Pan, G.-Y., et al. (2003). Potato yields of different density populations under single cropping condition. *Guizhou Agric. Sci.* 31, 46–47.

Xiao, T. (2013). *Effects of Temperature and Light on Plant Growth, Tuber Formation and Development of Potato Cultivars (Solatium tuberosum L.)*. Inner Mongolia: Inner Mongolia Agricultural University.

Yang, M.-J., Min-Fu, F., and Jiu-chang, L. (1994). The effects of potato canopies under dry land tillage up on expansion speed and yields of tubers. *Agric. Res. Arid Areas* 12, 105–110.

Yao, Y.-B., Wang, R.-Y., Deng, Z.-Y., et al. (2010). Effects of climate change on potato grow in semi-arid region of Loess Plateau, China. *Chin. J. Appl. Ecol.* 21, 379–385.

Yao, Y.-B., Zhang, X.-Y., Lu, H.-W., et al. (2009). Influence of meteorological conditions on potato tuber formation and yield in temperate and cool semi-humid regions of Northwest China. *Chin. J. Agrometeorol.* 30, 208—211.

Yu, W.-C., Chen, Z.-H., Liu, K.-R., et al. (2009). Effect of density on the yield and efficiency of fall potato. *Hubei Agric. Sci.* 48, 2082–2083.

Zhang, D.-X. (2014). *Design of a New Type of Potato Harvester*. Shandong: Shandong Agricultural University.

Zhao, P.-Y., Tuo, D.-B., Duan, Y., et al. (2005). Studies on suitable planting density and time of sowing of potato on dry land in Houshan Area. *Inner Mong. Acta Agric. Boreali Sin.* 20, 10–14.

Conflict of Interest Statement: The authors declare that the research was conducted in the absence of any commercial or financial relationships that could be construed as a potential conflict of interest.

frontiers in Plant Science

ORIGINAL RESEARCH
published: 08 January 2016
doi: 10.3389/fpls.2015.01225

Isolation and Screening of Bacteria for Their Diazotrophic Potential and Their Influence on Growth Promotion of Maize Seedlings in Greenhouses

*Medhin H. Kifle * and Mark D. Laing*

Discipline of Plant Pathology, School of Agricultural, Earth and Environmental Sciences University of KwaZulu-Natal, Pietermaritzburg, South Africa

Poor soil fertility is one of the major constraints for crop production. Nitrogen is the most limiting nutrient for increasing crop productivity. Therefore, there is a need to identify diazotrophic inoculants as an alternative or supplement to N-fertilizers for sustainable agriculture. In the current study, a number of free-living diazotrophic bacteria were isolated from soils collected from maize rhizosphere and from leaves and roots of maize within the KwaZulu-Natal Province, Republic of South Africa. Ninety-two isolates were selected for further screening because they were able to grow on N-free media containing different carbon sources. Isolates that were very slow to grow on N-free media were discarded. The isolates were screened *in vitro* for diazotrophic potential tests for ammonia production and acetylene reduction. Ethylene (C_2H_4) production was quantified and ranged from 4 to 73 nmoles of $C_2H_4 h^{-1}$ culture^{-1}. The top 20 isolates were re-screened on maize seedlings, and eight isolates significantly ($P = 0.001$) enhanced some growth parameters of maize above the un-inoculated control. Isolates that showed significant effect on at least two growth parameters were identified at species or genera level. In conclusion, selected diazotrophic isolates may be potentially beneficial but they should be tested more in greenhouse and field conditions with maize to confirm their potential for application as biofertilizers.

Keywords: diazotrophs, nitrogen fixation, plant growth promotion, acetylene reduction assay

OPEN ACCESS

Edited by:
Humberto Rodríguez Fuentes, Universidad Autónoma de Nuevo León, Mexico

Reviewed by:
Teresa Orlikowska, Research Institute of Horticulture, Poland
Katarzyna Turnau, Jagiellonian University, Poland

****Correspondence:***
Medhin H. Kifle
medhin7@yahoo.com

Specialty section:
This article was submitted to Crop Science and Horticulture, a section of the journal Frontiers in Plant Science

Received: *10 April 2015*
Accepted: *18 December 2015*
Published: *08 January 2016*

Citation:
Kifle MH and Laing MD (2016) Isolation and Screening of Bacteria for Their Diazotrophic Potential and Their Influence on Growth Promotion of Maize Seedlings in Greenhouses. Front. Plant Sci. 6:1225. doi: 10.3389/fpls.2015.01225

INTRODUCTION

Replacement of chemical fertilizers with biofertilizers is an attractive goal for sustainable agriculture. Nitrogen is the macro-nutrient that most frequently limits the growth and productivity of non-leguminous plants (Schepers et al., 1992) and is the most limiting factor in maize production (McCarty and Meisinger, 1997). A number of diazotrophic bacteria were previously found to interact with plants either in the rhizosphere or endophytes. Given the ability of diazotrophs to fix N, some strains may relieve N-deficiencies where there is inadequate application of N fertilizers. The genera *Bacillus*, *Burkholderia,* and *Enterobacter* are known to penetrate the roots of cereals and grow intercellularly as root endophytes, as well as in the rhizosphere (Reinhold-Hurek and Hurek, 1998; Wakelin and Ryder, 2004).

Some diazotrophic bacteria including those in the genera: *Rhanella*, *Pantoea*, *Rhizobium*, *Pseudomonas*, *Herbaspirillum*, *Enterobacter*, *Brevundimonas,* and *Burkholdera* were found to

be associated to maize plants (Montañez et al., 2012). Studies confirmed that the positive effect of some diazotrophic bacterial species on non-leguminous plant yields may not only be due to nitrogen fixation but other mechanisms may also contribute to the growth responses observed in non-leguminous plants (Caballero-Mellado et al., 1992; Vessey, 2003). For example, Abiala et al. (2015) isolated a *Bacillus* strain with multiple growth promoting characterstics from maize rhizosphere. It is also believed that some endophytic diazotrophic bacteria contribute substantial amounts of N to certain graminaceous crops (Barraquio et al., 1997). When some plant seeds were inoculated with diazotrophic bacteria, enhanced seed germination, biomass, increased nitrogen, and chlorophyll content were observed in seedlings (Riggs et al., 2001; Meena et al., 2012). Egamberdiyeva (2007) reported that *Pseudomonas alcaligenes* inoculation stimulated the growth and nutrient uptake of maize. Inoculation of *Bacillus megaterium* and *Bacillus mucilaginous* increased the nutritional assimilation of maize plant (Wu et al., 2005).

In vitro screening techniques have been employed to select effective strains of bacteria with multiple plant growth-promotions (Ahmad et al., 2006, 2008; Çakmakçi et al., 2007). Although lack of consistency in correlation between the results obtained *in vitro* and *in vivo* have been reported (Khalid et al., 2004; Yobo et al., 2004), these techniques are simple and efficient for screening large numbers of isolates (Campbell, 1989). Combination of *in vitro* and *in vivo* screening may lead to identification of effective strains for sustainable agriculture. The current study was therefore aimed at isolating diazotrophic bacteria, their partial characterization and for preliminary screening of some growth parameters on maize seedlings in greenhouse experiment.

MATERIALS AND METHODS

Bacterial Isolation

Diazotrophic bacteria were isolated from rhizospheres, roots and leaves of maize and wheat plants collected from Cedara (Agricultural research collage, Hawick), Greytown, and Ukulinga (University of KwaZulu-Natal research farm, Pietermaritzburg), all within the KwaZulu-Natal province, Republic of South Africa. Roots and leaves were surface sterilized with 3.5% sodium hypochlorite for 5 min and subsequently rinsed three times with sterile distilled water, using a modified protocol of Kloepper et al. (1991). Roots and leaves were cut into pieces and grounded with 10 mL of distilled water. A modified protocol of Döbereiner (1988) (N-free semi-solid media) was used to isolate rhizospheric, rhizoplane, and endophytic diazotrophs. Pure cultures of diazotrophic bacteria were then isolated by serial dilution, and plated onto N-free (NF) media containing of either 20g $l^{-1}$of mannitol, sucrose, or malate as the carbon source; 0.2 g L^{-1} K_2HPO_4; 0.2 g L^{-1}NaCl; 0.2 g L^{-1}; $MgSO_4.7H_2O$; 0.1 g $L^{-1;}$ K_2SO_4; 5.0 g L^{-1} $CaCO_3$; 20 g L^{-1} agar (Merck) for solid agar media, or with 5 g of agar per liter for a semi-solid media. These bacteria were incubated at 30°C for 4 days.

Soil samples were collected from the rhizosphere of maize and wheat from different sites by uprooting the root system and placing them in plastic bags for transport to the laboratory. They were stored at 4°C for subsequent analysis. Excess soil was shaken off and the soil adhering to the plant roots was collected from each soil sample. Ten grams of each soil sample were transferred to a 250 mL-Erlenmeyer flask containing 90 mL sterile distilled water and shaken at 150 rpm in an orbital shaker incubator for 30 min. Plates with NF medium with mannitol as a carbon source for diazotrophic bacteria were inoculated with 0.1 mL of suspensions obtained from the above dilution procedure (three replicates per dilution). The pH was adjusted to 6.5 using 98% sulphuric acid, and 50% sodium hydroxide. After 5 days of incubation, colonies were transferred onto fresh N-free media, and after 2 days were streaked out onto tryptone soy agar (TSA; Merck) plates. Bacterial isolates were selected by size and shape of colony and by their ability to grow on N-free media. These colonies were sub-cultured onto TSA and incubated at 30°C, purified and stored in 15% glycerol at −80°C.

Ammonia Production Test

Ammonia production was analyzed using the qualitative method of Ahmad et al. (2008). Bacterial isolates were tested for the production of ammonia in peptone water. Freshly grown cultures were inoculated in 10 mL peptone water in each tube and incubated for 48–72 h at 28 ± 2°C. Nessler's reagent (0.5 mL) was added in each tube. Development of a brown to yellow color was a positive test for ammonia production.

Acetylene Reduction Assay (ARA)

The basis for the assay is the fact that nitrogenase, the enzyme complex in diazotrophic microorganisms that reduces nitrogen to ammonia, also reduces acetylene to ethylene. The diazotrophic nature of all the recovered isolates was determined by ARA. Ethylene was quantified by gas chromatography (GC) and the results were expressed in nano moles of C_2H_4 produced h^{-1} $culture^{-1}$. One milliliter of pure culture grown in tryptone soy broth (TSB) for 24 h were inoculated onto 10 mL of nitrogen-free semi-liquid medium, with 0.5% mannitol as a carbon source, solidified by 0.3% gellan gum in 20 mL serum bottles and closed with a red rubber septum (SIGMA-ALDRICH, William Freeman and Co., Ltd.) and incubated for 72 h at 28°C. Bottles that showed bacterial growth were assayed for acetylene reduction. Ten percent of the atmosphere in the bottles was replaced with acetylene (C_2H_2), whereas bottles without acetylene were used as the control. After 2 h, at 24°C, 0.25 mL gas samples were taken from each vial and analyzed for amount of ethylene formed using a gas chromatography. These processes were repeated three times from same vial and average were taken for the statistical analysis. A gas chromatograph (Hewlett-Packard 5830A) fitted with a 2–2.1 mm, 80–100 mesh, Poropak R column was used and the oven temperature was adjusted to 70°C. Injection and flame-ionization detector temperatures were adjusted to 150°C. Nitrogen carrier gas flow rate was adjusted to 50 mL min^{-1}.

Source of Seeds

Seeds of a white maize cultivar, Mac are Medium Pearl (an open pollinated variety), were purchased from McDonalds Seeds® (MacDonald's Seeds (Ltd).P.O. Box 40, Mkondeni, 3212,

Pietermaritzburg, Republic of South Africa) and were used throughout the experiment.

Inoculum Preparation

Bacterial isolates were grown in 100 mL Erlenmeyer flasks each containing a 25 mL tryptic soy broth (TSB; Merck) for 3 d at 28 ± 2°C in a shaker at 150 rpm. Flasks were inoculated with bacteria previously grown in TSA for 48 h. After 3 d bacteria were harvested by centrifugation using a Beckman J2-HS Centrifuge (Beckman Coulter Inc. 4300 N Harbor Boulevard, Box 3100, Fullerton, California, 92834-300, USA) at 9000 rpm for 15 min. The broth was decanted and bacterial pellets were re-suspended in sterile distilled water. Bacterial cells were then counted using a plate dilution technique on TSA plates, and adjusted to a concentration of 10^8colony forming unit (cfu) mL^{-1} of water.

Seed Treatment

Twenty out of 92 bacterial isolates which produced relatively high C_2H_4 levels were selected for further greenhouse screening on maize seedlings. Final cell pellets were diluted with sterile distilled water and cell numbers were adjusted to 2.4×10^8 cfu mL^{-1} for each of the bacterial isolates, as determined by serial dilution and plating. Two grams of a sticker, gum arabic, were dissolved in 100 mL of bacterial suspension, stirred, and allowed to stand for 1 h. This allowed the substance to dissolve and form a homogeneous suspension. Seed coating took place in a plastic bag. The bag was filled with 200 g seeds. The bacterial sticker suspension was added at a rate of 0.1 mL g^{-1} of seeds in order to increase the number of bacteria stuck onto each seed. The bag was closed in such a way to trap air as much as possible. The bag was shaken for 2 min, until all the seeds were uniformly wetted with the sticker suspension. The bag was opened and the seed spreads onto paper towels and air-dried overnight. Treated maize seeds were planted on pine bark artificial growing medium. Composition of the composted pine bark growing medium analyzed by KwaZulu-Natal Agriculture and Environmental Affairs (KZN Agriculture and Environmental Affairs, Private Bag X9059, Pietermaritzburg, 3200, Republic of South Africa) is as follows: 12.39 C (%); 0.11 S (%); 0.43 N (%); 0.61 Ca (%); 0.10 Mg(%); 0.28 K (%); 0.18 P (%); 25.07 Moisture (%); 405.0 Na (mg kg^{-1}); 73.0 Zn (mg kg^{-1}); 16.7 Cu (mg kg^{-1}); 802Mn (mg kg^{-1}); 12293 Fe (mg kg^{-1}); 7120 Al (mg kg^{-1}).

Measurements of Stomatal Conductance and Chlorophyll Content Index

Greenhouse measurements of stomatal conductance and leaf chlorophyll were made on 8 weeks old seedlings. Leaf stomatal conductance was measured with a portable porometer (SC-1 Leaf Porometer, Decagon Devices, Inc., 2365 NE Hopkins Court, Pullman, WA 99163, USA). Stomatal conductance readings were made between 9:00 am and 3:00 pm on sunny days on 10 leaves of each pot of nine plants per treatment. Chlorophyll was measured using a portable, handheld device called chlorophyll meter (CCM-200 Plus, Opti-Science Inc., 8 Winn Avenue, Hudson, NH, USA, 03051; that estimates the chlorophyll content of leaves). Measurements were made on eight leaves of each pot of nine plants per treatment.

DNA Extraction and 16S rRNA Sequence Analysis

One mL of 24 h bacterial culture was centrifuged at 14,000 relative centrifugal force (rcf) for 5 min. The pellet was suspended in 25 µL of (10 mM) Tris and 1 mL of buffer was added and incubated at 60°C for 1 h. One milliliter of CTAB buffer was added and gently mixed. Then the bacterial-buffer suspension were divided into two in 1.5 mL tubes, and 500 µL of chloroform-iso-amyl alcohol was added and mixed gently, and the resultant mixture was centrifuged at 14,000 rcf for 10 min. By avoiding the layer of impurities, 900 µl of clear supernatant was removed as the sample. To this, 600 µl of propan-2-ol was added and refrigerated at −20°C for 1 h. It was centrifuged for 15 min at 4000 rcf and the supernatant was discarded. The pellet were washed with 50 µl of 70% ethanol solution and dried in a laminar flow with lid of the tube being left open for 30 min. The pellet was then suspended in 50 µL of 10 mM Tris (pH 8) or 0.5 X TE buffer. At this point the DNA purity and quality were checked on the nano drop UV spectrophotometer equipment (nano drop 1000, Inqaba Biotech, P.O.Box 1435, Hatfield 0028, Pretoria, South Africa) and a 5 µL sample was run on 0.8% agarose gel [SeakemLE Agarose, Whitehead Scientific (Pty) Ltd www.whitesci.co.za] stained with SYBRSafe nucleic acid stain (Invitrogen) stained with SYBRSafe nucleic acid stain (Invitrogen), with a GeneRuler 1 kb DNA Ladder Plus molecular weight marker (Thermo Fisher Scientific Inc., 81 Wyman street, Waltham, MA 02454, US) to confirm the presence, size and quality of genomic DNA. Once the purity of the DNA was checked, it was sent to the Central Analytic Facility, Stellenbosch University, South Africa for sequencing and BLAST identification. The BLAST identifications were then confirmed by matrix assisted laser desorption ionization-time of flight (Maldi-TOF) classification [Brucker Daltonik Maldi-TOF Biotyper (www.bruker.com)].

Bruker Daltonik Maldi Biotyper Classification

Bacterial cultures were sub-cultured on 10% TSA for 24 h at 30°C. A single bacterial colony were taken and placed into a 2 mL eppendorf tube with 300 µL of ultra-pure water, and 900 µL of pure ethanol were added, mixed and the suspension was centrifuged at 14,000 rcf for 2 min. A small pellet of bacterial cells was visible at the bottom of the tube. The liquid was removed, and the pellet was briefly re-spun followed by the removal of residual ethanol. It was then re-suspended in 10 µL of 70% formic acid, and 10 µL of aceto-nitrile was added, and the sample was vortexed briefly. The mixture was centrifuged for 2 min at 14,000 rcf, and the supernatant transferred into a clean micro-tube. The sample to be analyzed was warmed to room temperature, and a 1 µL sample was spotted onto a steel target plate (Bruker Daltonics Inc., Billerica, MA, USA) and gently mixed with 2 µL of matrix solution.

TABLE 1 | Nitrogenase activity of the bacterial isolates measured by acetylene reduction assay (ARA).

Isolates	nmol of $C_2H_4h^{-1}$ culture^{-1}		Isolates	nmol of $C_2H_4h^{-1}$ culture^{-1}		Isolates	nmol of $C_2H_4h^{-1}$ culture^{-1}	
Broth	0.32	a	M12	21.86	cdefghijklmn	Bt12	29.01	ghijklmnop
Bt14	4.81	ab	StB12	21.91	cdefghijklmn	Bt7	29.46	ghijklmnop
M11	6.20	ab	V1	21.91	cdefghijklmn	StB8	29.87	ghijklmnop
Mr2	6.24	ab	Br2	21.96	cdefghijklmn	G3	31.78	hijklmnopq
SB1	6.46	ab	Bt1	21.96	cdefghijklmn	V3	31.99	ijklmnopq
Mr63	6.51	ab	RB1	21.96	cdefghijklmn	Mr27	32.27	ijklmnopq
Bt10	7.29	abc	Bt15	22.01	cdefghijklmn	V14	32.39	ijklmnopqr
Bt3	7.32	abc	RB6	22.01	cdefghijklmn	Mr57	32.77	jklmnopqr
Mr141	7.61	abc	V12	22.01	cdefghijklmn	Mr34	33.04	klmnopqr
Mr20	7.90	abc	Mr148	22.02	cdefghijklmn	Bt4	33.26	klmnopqr
Mr25	9.10	abcd	RB2	22.06	cdefghijklmn	Bt5	33.49	lmnopqr
Mr8	9.76	abcde	StB7	22.06	cdefghijklmn	V20	33.58	lmnopqr
StB3	10.46	abcde	LB7	22.11	cdefghijklmn	Bt11	33.69	lmnopqr
V15	10.96	abcde	Bt9	22.15	cdefghijklmn	Mr21	33.94	mnopqrs
Mr53	12.26	abcdef	Bt6	22.20	cdefghijklmn	StB13	35.09	nopqrst
Mr35	12.29	abcdef	Bt8	22.20	cdefghijklmn	V10	35.33	nopqrst
E9	12.66	abcdef	V2	22.20	cdefghijklmn	Mr150	35.54	nopqrstu
Mr38	15.40	bcdefg	StB17	22.30	cdefghijklmn	Mr131	37.13	nopqrstu
Mr58	15.96	bcdefg	V6	22.40	cdefghijklmn	StB1	37.23	nopqrstu
Mr6	16.44	bcdefgh	M9	22.41	cdefghijklmn	Mr37	38.82	opqrstuv
V5	17.02	bcdefghi	V7	22.45	cdefghijklmn	a2	42.00	pqrstuv
Mr16	17.22	bcdefghi	LB9	22.55	cdefghijklmn	a3	45.10	qrstuv
V4	17.25	bcdefghij	X	22.80	cdefghijklmn	B1	45.84	qrstuv
Mr19	17.32	bcdefghij	D6	24.19	defghijklmno	a61	46.69	qrstuv
Mr13	17.38	bcdefghij	Mr17	24.19	defghijklmno	a5	47.28	rstuv
Mr7	17.53	bcdefghij	Mr22	24.73	efghijklmno	LB5	48.36	stuv
Mr121	17.76	bcdefghijk	Mr9	25.09	efghijklmno	L1	48.75	tuv
Mr55	18.22	bcdefghijkl	V18	25.20	efghijklmno	a6	49.88	uv
LB2	18.75	bcdefghijklm	V17	27.48	fghijklmnop	StB5	52.37	v
V13	19.05	bcdefghijklm	V19	28.40	ghijklmnop	V16	65.15	w
Bt2	21.86	cdefghijklmn	V11	28.82	ghijklmnop	V9	73.20	w
CV%	30.4							
DMRT	12.035							
Sed	6.101							
F-test	9.662							
P-value	<0.001							

Means with the same letter are not significantly different at $P \leq 0.05$. Each treatment was replicated three times ($n = 3$). Each treatment vial was sampled three times.

Experimental Design

Maize seedlings treated with bacterial isolates were watered every day with 500 mL nutrient solution containing: 0.11 mL L^{-1} H_3PO_4; 0.13 g L^{-1} KOH; 0.14 g L^{-1} K_2SO_4; 0.74 g L^{-1} $CaCl_2.2H_2O$; 0.10 g L^{-1} $MgSO_4.7H_2O$; and 0.02 g L^{-1} of micronutrients (MICROPLEX®; Ocean Agriculture (Pty) Ltd, P.O. Box 741, Mulders drift, 1747, South Africa). There were two controls: one was untreated and supplemented with a soluble fertilizer NPK (3:1:3 [38] complete) which was parched from Ocean Agriculture (Pty) Ltd, P.O. Box 741, Mulders drift, 1747, South Africa at a rate of 1 gL^{-1} and the second was untreated control and supplemented with MICROPLEX® nutrient solution. Each treatment consisted of three pots with a top diameter of 200 mm that held 2 kg of composted pine bark. Each pot was seeded with five seeds. The seedlings were thinned to three plants per pot. Pots with each of the 20 isolates were watered every day with an equal amount of a nutrient solution containing phosphorus and potassium of levels adjusted to the full recommended amounts. The experiment was arranged in a randomized complete block design (RCBD), replicated three times. Two months after planting, chlorophyll and stomatal conductance were measured and plants were harvested and dry weight was taken after the biomass was dried in an oven for 72 h at 70°C.

Statistical Analysis

Experiments were repeated twice, unless otherwise stated. Data were analyzed using GenStat executable release 14th edition

TABLE 2 | Influence of maize seeds inoculation with diazotrophic bacteria on some growth parameters of 2 months seedlings in greenhouse experiment.

Bacterial isolates	Chlorophyll content index		%Over control	Dry weight(g)		%Over control	Stomatal conductance (m mol m^{-2} s^{-1})		%Over control
Control	4.45	a	–	2.77	a	–	54.2 (1.733)	a	–
Mr21	5.08	ab	14.16	3.63	ab	31.05	121.6 (2.085)	abc	124.35
Mr131	5.24	abc	17.75	3.62	ab	30.69	122.5 (2.086)	abc	126.01
Bt11	5.38	abcd	20.90	3.63	ab	31.05	122.5 (2.087)	abc	126.01
Mr150	5.59	abcde	25.62	4.13	abcd	49.10	142.0 (2.152)	abcd	161.99
StB1	5.83	abcde	31.01	5.17	bcd	86.64	137.7 (2.127)	abc	154.06
StB13	5.95	abcdef	33.71	3.79	abc	36.82	130.3 (2.115)	abc	140.41
Mr37	6.08	abcdef	36.63	3.72	abc	34.30	147.3 (2.165)	abcd	171.77
V20	6.11	abcdef	37.30	5.85	cd	111.19	147.6 (2.169)	abcd	172.32
V10	6.21	abcdefg	39.55	5.79	cd	109.03	134.6 (2.129)	abc	148.34
A61	6.28	bcdefg	41.12	6.23	d	124.91	206.5 (2.295)	cde	281.00
A2	6.37	bcdefg	43.15	5.84	cd	110.83	198.3 (2.274)	cde	265.87
B1	6.52	bcdefg	46.52	3.80	abc	37.18	244.1 (2.383)	de	350.37
A6	6.71	bcdefg	50.79	3.41	ab	23.10	218.1 (2.335)	cde	302.40
A5	7.03	cdefg	57.98	2.42	a	−12.64	188.8 (2.253)	bcde	248.34
A3	7.06	cdefg	58.65	5.26	bcd	89.89	219.3 (2.341)	cde	304.61
LB5	7.11	defg	59.78	5.51	bcd	98.92	203.4 (2.278)	cde	275.28
L1	7.26	efg	63.15	5.85	cd	111.19	206.2 (2.281)	cde	280.44
V16	7.70	fg	73.03	5.99	d	116.25	265.0 (2.423)	e	388.93
V9	7.72	fg	73.48	2.80	a	1.08	253.3 (2.404)	e	367.34
StB5	8.03	g	80.45	3.48	ab	25.63	244.7 (2.386)	de	351.48
NPK	13.62	h	206.07	9.90	e	257.40	517.5 (2.712)	f	854.80
CV%	14			23.9			23.20 (4.2)		
DMRT	1.544			1.833			90.41 (0.198)		
SED	0.765			0.908			43.00 (0.093)		
P	<0.001			<0.001			<0.001		

Means with the same letters in the same column are not significantly different at P < 0.05; values in parentheses are transformed data using log base 10 for the stomatal conductance. Means were calculated from n = 3 for dry weight, n = 24 for chlorophyll content index, and n = 30 for stomatal conductance.

statistical analysis software. Significant differences between treatments were determined using Duncan's multiple range test at 5% significant level.

RESULTS

Isolation and Preliminary Screening of Bacterial Diazotrophs

There were differences between diazotrophic isolates, in their ability to grow on semi-solid N-free medium, and using D-mannitol, D-malate or sucrose as carbon sources. Bacterial growth were considered slow when the mass doubling time was longer than 10–12 h and considered well when the mass doubling time was less than 10 h. All these isolates were able to grow well on the N-free semi-liquid medium when sucrose was used as the carbon source, and generated ammonia in peptone water. About 20% of the bacterial isolates grew well on N-free media with D-mannitol, sucrose, or malate as growth substrates. Approximately, 80% of the bacterial isolates showed slow growth on N-free medium with D-mannitol or malate.

Acetylene Reduction Assay (ARA)

All the isolates exhibited nitrogenase activity, but the level of activity varied with different isolates (**Table 1**). Approximately 17% of the isolates produced very little amount C_2H_4, no more than the control; 66% of the isolates produced significantly ($P < 0.001$) more C_2H_4 compared to the control (N-free semi-liquid medium). The 20 isolates which produced relatively high levels of C_2H_4 were further screened in the greenhouse.

Effect of Diazotrophic Inoculation on Chlorophyll Content Index, Dry Weight and Stomatal Conductance

Of the 20 diazotrophic isolates, about 50% showed significantly higher ($P < 0.001$) chlorophyll content index, stomatal conductance and dry weight, relative to the untreated control (**Table 2**). The rest of these isolates had no effect ($P < 0.05$) on the above parameters. Plants of the untreated control showed the lowest stomatal conductance, chlorophyll level and dry weight and plants of the 100% NPK fertilized (NPK control) the highest (**Table 2**). Isolate StB5 had the highest chlorophyll content index

TABLE 3 | Affiliation of the isolates in the GenBank and the identification of the closest type strain based on the 16S rRNA gene sequencing and Bruker Daltonik MALDI-TOF Biotyper classification.

Isolates	16S rRNA similarities (highest match)	BrukerMALDI biotype (highest score)
V16	*Bacillus megaterium* Strain As-30 (97%)	*Bacillus* sp. (1.722)
A5	*Burkholderia* sp. IBP-VNS127 (99%)	*Burkholderia* sp. (1.867)
V9	*Burkholderia ambifaria* (99%)	*Burkholderia ambifaria* (2.462)
L1	*Enterobacter cloacae* Strain G35-1(98%)	*Enterobacter cloacae (2.327)*
A2	*Klebsiella variicola* (99%)	*Klebsiella variicola* (2.243)
LB5	*Pantoea ananatis* (97%)	*Pantoea ananatis* (2.268)
A3	*Pseudomonas nitroreducens* Strain R5-791 (99%)	*Pseudomonas* sp. (1.901)
A6	*Pseudomonas nitroreducens* (99%)	*Pseudomonas* sp. (1.96)
B1	*Pseudomonas nitroreducens* (99%)	*Pseudomonas nitroreducens* (2.034)
StB5	*Pseudomonas nitroreducens* Strain R5-791 (99%)	*Pseudomonas* sp. (1.989)
A61	*Pseudomonas nitroreducens* (99%)	*Pseudomonas* sp. (1.882)

and stomatal conductance but its dry weight was not significantly higher than in the non-inoculated control. The highest dry weight was obtained in the seedlings inoculated with V16 and L1; their chlorophyll content index and stomatal conductance were significantly higher than in control plants.

Identification of Diazotrophic Isolates

Comparative analyses of nucleotide sequences of amplified 16S rRNA fragments, using a BLAST approach, revealed that some of the isolates with 99% sequence accuracy. Isolates StB5, A3, A6, B1, and A61 demonstrated this accuracy with *Pseudomonas nitroreducens*, A5 with *Burkholderia* sp., V9 with *Burkholderia ambifaria,* and A2 with *Klebsiella variicola*. Isolate L1 showed 98% similarity with *Enterobacter cloacae*; V16 (97%) with *B. megaterium* and LB5 (97%) with *Pantoea ananatis* (**Table 3**). With laser desorption ionization-time of flight (Maldi-TOF) classification system, a score of $\geq$2.000 indicates species level identification, a score of 1.700–1.999 indicates identification to the genus level, and a score of $<$1.700 is interpreted as no identification. Isolates StB5, A3, A6, and A61 were identified as *Pseudomonas* sp with MALDI-TOF scores of 1.98, 1.90, 1.96, and 1.88, respectively. Isolate B1 (2.03) as *P. nitroreducens*, V9 (2.46) as *Burkholderia ambiferia* and A5 (1.86) were identified as *Burkholderia* sp, isolate L1 (2.33) as *E. cloacae*, isolate V16 (1.72) as *Bacillus* sp, A2 (2.24) as *K. variicola* and isolate LB5 (2.27) as *Pantoea ananatis*. An independent identification of these isolates, based on 16S rRNA gene and Maldi-TOF biotyper, confirmed their identity to species and genera level.

DISCUSSION

Isolation and screening for potential diazotrophic bacteria are crucial steps in research on biofertilizers. In order to discover efficient nitrogen fixing bacteria, there is a need to develop simple, inexpensive and quick procedures with repeatable and reliable results (Döbereiner, 1988). Such as an *in vitro* screening procedure (growth on N-free semi-solid media, ARA, and the ammonia production test) and the combinations of which provides rapid and repeatable results. All the isolates proved to be nitrogen fixers. Though it is difficult to compare the nitrogenase activity of bacterial strains studied in this work with the results obtained by others, a study by Różycki et al. (1999) showed similar results of nitrogenase activity by some of diazotrophic isolates belonging to the genera *Pseudomonas* and *Bacillus*.

About 50% of the best isolates used in this study were identified as *Pseudomonas*. In another study, the genera of *Pseudomonas* and *Enterobacter* were reported to be dominant in maize cultivars (Rodríguez-Blanco et al., 2015). Moreover, Berge et al. (1991) reported that an *E. cloacae was* the most abundant diazotrophic bacterium in the rhizosphere of maize-growing soils in France. *Klebsiella* and *Burkholderia* were also dominant genera both in roots and rhizosphere of maize (Arruda et al., 2013). Estrada et al. (2002) isolated a strain of endophytic, N_2-fixing *Burkholderia* sp. associated with maize in Mexico. Similarly, Perin et al. (2006) isolated *Burkholderia* sp. from the rhizosphere of maize. The predominance of these genera both in the soil and in the root zone may be due to low nutritional requirements, its capacity to utilize numerous complex of organic substrates (Krotzky and Werner, 1987) and high tolerance to low pH (Eckford et al., 2002).

In this study, some of the bacterial isolates with high nitrogenase activity were found to improve chlorophyll content, stomatal conductance and dry weight in maize. All the tested isolates showed increases (124.4–351.5%) in stomatal conductance, nine isolates showed (86.6–24.9%) increases in dry weight, and 11 of the isolates (41.12–80.45%) increases in chlorophyll content index over the control. Diazotrophic microbes isolated either from soil or endophytes increased sweet corn biomass both in greenhouse and field trials (Mehnaz and Lazarovits, 2006; Mehnaz et al., 2010). In another study, interaction of diazotrophic plant growth promoting rhizobacteria with sugar cane, cotton, wheat, rice, and maize significantly increased the vegetative growth and grain yield (Kennedy et al., 2004). Likewise, maize plants inoculated with endophytic diazotrophs such as (*Herbaspirillum* sp, *Psuedomonas* sp., and *Burkholderia vietnamienis*) gained greater early biomass and

higher rates of net CO_2 assimilation than the un-inoculated control (Knoth et al., 2013). Furthermore, dry matter of maize increased by 25–54% after inoculation with strains *Achromobacter* sp., *Burkholdria* sp. and *Arthrobacter* sp. (Arruda et al., 2013). In this study, inoculation of maize seeds with *Burkholderia ambifaria* (V9), *Bacillus* sp. (V16), *P. nitroreducens* (B1), Pseudomonas spp. (A3, A6, A61, StB5), *E. cloacae (L1), P. ananatis (LB5), and Klebsiella variicola (A2)* enhanced stomatal conductance and chlorophyll content index compared to the control. The increases could be a result of increased leaf N through nitrogen fixation by these diazotrophs. Nitrogen fixed by diazotrophic bacteria may not fully replace chemical fertilizers however; use of diazotrophic bacterial inoculants may be an important factor for sustainable agriculture.

CONCLUSION

It can be concluded that the selected diazotrophic isolates may be potentially beneficial biofertilizers and should be tested more in field conditions to confirm their potential to use as biofertilizers inoculants.

ACKNOWLEDGMENTS

We wish to acknowledge Matthew and Heather from microbiology department, UKZN, PMB campus, South Africa, for their assistance with the use of MALDI Biotyper and Mrs Susan Van der Merwe for her technical assistance with the greenhouse.

REFERENCES

Abiala, M., Odebode, A., Hsu, S., and Blackwood, C. (2015). Phytobeneficial properties of bacteria isolated from the rhizosphere of maize in southwestern nigerian soils. *Appl. Environ. Microbiol.* 81, 4736–4743. doi: 10.1128/AEM.00570-15

Ahmad, F., Ahmad, I., Aqil, F., Ahmed Wani, A., and Sousche, Y. S. (2006). Plant growth promoting potential of free−living diazotrophs and other rhizobacteria isolated from northern indian soil. *Biotechnol. J.* 1, 1112–1123. doi: 10.1002/biot.200600132

Ahmad, F., Ahmad, I., and Khan, M. (2008). Screening of free-living rhizospheric bacteria for their multiple plant growth promoting activities. *Microbiol. Res.* 163, 173–181. doi: 10.1016/j.micres.2006.04.001

Arruda, L., Beneduzi, A., Martins, A., Lisboa, B., Lopes, C., Bertolo, F., et al. (2013). Screening of rhizobacteria isolated from maize (*zea mays* L) in Rio grande do sul state (south Brazil) and analysis of their potential to improve plant growth. *Appl. Soil Ecol.* 63, 15–22. doi: 10.1016/j.apsoil.2012.09.001

Barraquio, W., Revilla, L., and Ladha, J. (1997). Isolation of endophytic diazotrophic bacteria from wetland rice. *Plant Soil* 194, 5–24. doi: 10.1023/a:1004246904803

Berge, O., Heulin, T., and Balandreau, J. (1991). Diversity of diazotroph populations in the rhizosphere of maize (*Zea mays* L) growing on different French soils. *Biol. Fertil. Soils* 11, 210–215. doi: 10.1007/bf00335769

Caballero-Mellado, J., Carcano-Montiel, M., and Mascarua-Esparza, M. (1992). Field inoculation of wheat (*Triticum aestivum*) with *Azospirillum brasilense* under temperate climate. *Symbiosis*13, 243–253.

Çakmakçi, R., Erat, M., Erdogan, U., and Dönmez, M. F. (2007). The influence of plant growth–promoting rhizobacteria on growth and enzyme activities in wheat and spinach plants. *J. Plant Nutr. Soil Sci.* 170, 288–295. doi: 10.1002/jpln.200625105

Campbell, R. (1989). *Biological Control of Microbial Plant Pathogens*. Cambridge, UK: Cambridge University Press.

Döbereiner, J. (1988). Isolation and identification of root associated diazotrophs. *Plant Soil* 110, 207–212.

Eckford, R., Cook, F. D., Saul, D., Aislabie, J., and Foght, J. (2002). Free-living heterotrophic nitrogen-fixing bacteria isolated from fuel-contaminated Antarctic soils. *Appl. Environ. Microbiol.* 68, 5181–5185. doi: 10.1128/AEM.68.10.5181-5185

Egamberdiyeva, D. (2007). The effect of plant growth promoting bacteria on growth and nutrient uptake of maize in two different soils. *Appl. Soil Ecol.* 36, 184–189. doi: 10.1016/j.apsoil.2007.02.005

Estrada, P., Mavingui, P., Cournoyer, B., Fontaine, F., Balandreau, J., and Caballero-Mellado, J. (2002). An N_2-fixing endophytic *Burkholderia* sp. associated with maize plants cultivated in Mexico. *Can. J. Microbiol.* 48, 285–294. doi: 10.1139/w02-023

Kennedy, I. R., Choudhury, A., and Kecskés, M. L. (2004). Non-symbiotic bacterial diazotrophs in crop-farming systems: can their potential for plant growth promotion be better exploited? *Soil Biol. Biochem.* 36, 1229–1244. doi: 10.1016/j.soilbio.2004.04.006

Khalid, A., Arshad, M., and Zahir, Z. (2004). Screening plant growth−promoting rhizobacteria for improving growth and yield of wheat. *J. Appl. Microbiol.* 96, 473–480. doi: 10.1046/j.1365-2672.2003.02161.x

Kloepper, J. W., Zablotowicz, R. M., Tipping, E. M., and Lifshitz, R. (1991). "Plant growth promotion mediated by bacterial rhizosphere colonizers," in *The Rhizosphere and Plant Growth*, eds L. Keister and P. B. Cregan (Dordrecht: Kluwer Academic Publishers), 315–326.

Knoth, J. L., Kim, S. H., Ettl, G. J., and Doty, S. L. (2013). Effects of cross host species inoculation of nitrogen-fixing endophytes on growth and leaf physiology of maize. *GCB Bioenergy* 5, 408–418. doi: 10.1111/gcbb.12006

Krotzky, A., and Werner, D. (1987). Nitrogen fixation in *Pseudomonas stutzeri*. *Arch. Microbiol.* 147, 48–57. doi: 10.1007/BF00492904

McCarty, G., and Meisinger, J. (1997). Effects of n fertilizer treatments on biologically active N pools in soils under plow and no tillage. *Biol. Fertil. Soils* 24, 406–412. doi: 10.1007/s003740050265

Meena, H., Sharma, G., Golada, S. L., and Jain, H. (2012). Yield and quality of sweet corn (*Zea mays* (L.) ssp. Saccharata) as affected by nitrogen levels, *Azotobacter* culture and nitrogen sources. *Res. Crops* 13, 486–492.

Mehnaz, S., Kowalik, T., Reynolds, B., and Lazarovits, G. (2010). Growth promoting effects of corn (*zea mays*) bacterial isolates under greenhouse and field conditions. *Soil Biol. Biochem.* 42, 1848–1856. doi: 10.1016/j.soilbio.2010.07.003

Mehnaz, S., and Lazarovits, G. (2006). Inoculation effects of *Pseudomonas putida*, *Gluconacetobacter azotocaptans*, and *Azospirillum lipoferum* on corn plant growth under greenhouse conditions. *Microb. Ecol.* 51, 326–335. doi: 10.1007/s00248-006-9039-7

Montañez, A., Blanco, A. R., Barlocco, C., Beracochea, M., and Sicardi, M. (2012). Characterization of cultivable putative endophytic plant growth promoting bacteria associated with maize cultivars (*zeamays* l.) and their inoculation effects *in vitro*. *Appl. Soil Ecol.* 58, 21–28. doi: 10.1016/j.apsoil.2012.02.009

Perin, L., Martínez-Aguilar, L., Paredes-Valdez, G., Baldani, J., Estrada-de Los Santos, P., Reis, V., et al. (2006). Burkholderia silvatlantica sp. nov., a diazotrophic bacterium associated with sugar cane and maize. *Int. J. Syst. Evol. Microbiol.* 56, 1931–1937. doi: 10.1099/ijs.0.64362-0

Reinhold-Hurek, B., and Hurek, T. (1998). Life in grasses: diazotrophic endophytes. *Trends Microbiol.* 6, 139–144. doi: 10.1016/S0966-842X(98)01229-3

Riggs, P. J., Chelius, M. K., Iniguez, A. L., Kaeppler, S. M., and Triplett, E. W. (2001). Enhanced maize productivity by inoculation with diazotrophic bacteria. *Funct. Plant Biol.* 28, 829–836. doi: 10.1071/PP01045

Rodríguez-Blanco, A., Sicardi, M., and Frioni, L. (2015). Plant genotype and nitrogen fertilization effects on abundance and diversity of diazotrophic bacteria associated with maize (*zea mays* l). *Biol. Fertil. Soils* 51, 391–402. doi: 10.1007/s00374-014-0986-8

Różycki, H., Dahm, H., Strzelczyk, E., and Li, C. Y. (1999). Diazotrophic bacteria in root-free soil and in the root zone of pine (*Pinus sylvestris* L) and oak (*Quercus robur* L). *Appl. Soil Ecol.* 12, 239–250. doi: 10.1016/S0929-1393(99)00008-6

Schepers, J., Francis, D., Vigil, M., and Below, F. (1992). Comparison of corn leaf nitrogen concentration and chlorophyll meter readings. *Commun. Soil Sci. Plant Anal.* 23, 2173–2187. doi: 10.1080/00103629209368733

Vessey, J. K. (2003). Plant growth promoting rhizobacteria as biofertilizers. *Plant Soil* 255, 571–586. doi: 10.1023/A:1026037216893

Wakelin, S. A., and Ryder, M. H. (2004). Plant growth-promoting inoculants in australian agriculture. *Crop Manag.* 3, 1–5. doi: 10.1094/cm-2004-0301-01-rv

Wu, S., Cao, Z., Li, Z., Cheung, K., and Wong, M. (2005). Effects of biofertilizer containing N-fixer, P and K solubilizers and AM fungi on maize growth: a greenhouse trial. *Geoderma* 125, 155–166. doi: 10.1016/j.geoderma.2004.07.003

Yobo, K., Laing, M., Hunter, C., and Morris, M. (2004). Biological control of Rhizoctonia solani by two Trichoderma species isolated from south african composted soil. *S. Afr. J. Plant Soil* 21, 139–144. doi: 10.1080/02571862.2004.10635039

Conflict of Interest Statement: The authors declare that the research was conducted in the absence of any commercial or financial relationships that could be construed as a potential conflict of interest.

Advantages of publishing in Frontiers

OPEN ACCESS
Articles are free to read, for greatest visibility

COLLABORATIVE PEER-REVIEW
Designed to be rigorous – yet also collaborative, fair and constructive

FAST PUBLICATION
Average 85 days from submission to publication (across all journals)

COPYRIGHT TO AUTHORS
No limit to article distribution and re-use

TRANSPARENT
Editors and reviewers acknowledged by name on published articles

SUPPORT
By our Swiss-based editorial team

IMPACT METRICS
Advanced metrics track your article's impact

GLOBAL SPREAD
5'100'000+ monthly article views and downloads

LOOP RESEARCH NETWORK
Our network increases readership for your article

Frontiers
EPFL Innovation Park, Building I • 1015 Lausanne • Switzerland
Tel +41 21 510 17 00 • Fax +41 21 510 17 01 • info@frontiersin.org
www.frontiersin.org

Find us on